PHASE TRANSFER CATALYSIS: CATALYST SCREENING, REACTION DEVELOPMENT, AND MECHANISM ANALYSIS

BY

ROBERT CARL WEINTRAUB

THESIS

Submitted in partial fulfillment of the requirements
for the degree of Master of Science in Chemistry
in the Graduate College of the
University of Illinois at Urbana-Champaign, 2012

Urbana, Illinois

Advisor:
Professor Scott E. Denmark

Abstract

The asymmetric alkylation of a glycine Schiff base in addition to the development of a [2,3]-Wittig rearrangement under phase transfer catalysis (PTC) reaction conditions was investigated. Supplementing these studies, a deeper understanding of the PTC mechanism was sought for the alkylation of phenol.

In regards to the asymmetric PTC (APTC) alkylation, a small library of catalysts derived from *Cinchona* alkaloids was examined for selectivity and activity. An array of substituent modifications were tested, examining the role of steric and electronics on catalyst activity. Catalysts that contained large substituents attached to the quinuclidinium core were found to be the most selective and those in which the hydroxyl group was protected generally afforded faster catalysts. The removal or augmentation of the dipole of the hydroxyl group position significantly impacted catalyst activity.

For the development of an APTC [2,3]-Wittig rearrangement, substituted α-allyloxy-phenylacetonitrile substrates were employed. Under liquid-liquid PTC reaction conditions, these substrates were found to rearrange and afford phenyl ketone products. Initial rearrangement products that contained enolizable hydrogens were found to isomerize under the reaction conditions. The use of terminally disubstituted allkyloxy substituents led to the formation of ketones containing adjacent carbon-centered quaternary stereocenters as stable rearrangement products. When a [5,5,5]-pyrolizidinium type of chiral, non-racemic catalyst was employed with a prochiral substrate, an enantioenriched rearrangement product was obtained, albeit in low selectivity (er 55:45).

The mechanistic analysis of the base-mediated PTC alkylation of phenol has revealed startling insights. A series of symmetrical, tetraalkylammonium salts were examined for their

catalytic and intrinsic reactivity. Tetraalkylammonium phenolate salts were prepared from the corresponding ammonium bromides and their activity was evaluated for the *n*-butylation of phenol. Small differences in intrinsic reactivity were observed with alkyl lengths greater than C_2. In contrast, under phase transfer catalysis conditions large differences in alkylation rate were observed among C_2, C_3 and C_4 tetraalkylammonium catalysts. Consequently, the intrinsic reaction rate plays only a minor role in the reactivity of tetraalkylammonium catalysts using a phase transfer process. Benzyl bromide titration of the organic under PTC reaction conditions revealed the presence of potassium phenoxide complexed with the tetraalkylammonium phenoxide. The relative amounts of complexed potassium phenoxide was found to have a negligible impact on the catalytic activity.

Acknowledgements

I would like to thank all my current and former colleagues in the Denmark research group with whom I have had the pleasure of working with for these past several years. Special thanks are deserved for my mentors, Dr. Son Nguyen, Dr. Min Xie, and Dr. Nathan Werner, because without your guidance and patience none of this would have been possible. Utmost praise is due for Susan Lightly, because ice hockey is not that same unless the person next to you is screaming awful things to the opposing teams' goalies.

To my advisor, Scott Denmark, I am and will be in awe how one person can accumulate such a wide and deep understanding of organic chemistry. Your patient guidance and unwillingness to accept any explanation that was not carefully thought out will forever shape my character as a chemist. Part of me will miss being in a 'low energy conformation' (i.e. leaning back in my chair, feet up) and reading papers late into the night to explain one data point.

Finally, to my parents, without your motivation this endeavor would have ended a long time ago. Thank you.

Table of Contents

CHAPTER 1: *Phase Transfer Catalysis Fundamentals*

1.1. Introduction

1.1.1. What is Phase Transfer Catalysis?

Phase transfer catalysis (PTC) as a reaction protocol is defined by the separation of reactants and reagents between two or more different immiscible phases in which the transport of the reactants and reagents is facilitated by a phase-transfer agent.[1] Often, this agent is referred to as the phase transfer catalyst, or simply catalyst. Generally, this process involves the transport of ions between phases facilitated by the formation of a catalyst-reagent ion pair. After the intermediate ion-pair has crossed the phase boundary, this reactive ion-pair can participate in a number of different chemical reactions. Finally, the catalyst must be regenerated after its transport of the reactant/reagent to complete the catalytic cycle.

PTC reactions are performed as a combination of phases; the most common are liquid-liquid and liquid-solid phase reactions. In the case of liquid-liquid PTC reactions, one phase is generally a non-polar organic solvent and the other phase is a polar solvent, typically an aqueous solution. Most often, a reagent is transferred from the aqueous phase into the organic phase. Solid-liquid PTC reactions are similar in most respects with the exception that one phase remains a solid. The majority of PTC processes involve reactions of interest taking place in the organic phase, although in certain cases this trend may be inverted and the desired reaction will proceed in the aqueous or solid phase.[2]

1.1.2. Advantages of a PTC Process

PTC reactions has enjoyed much commercial success in recent decades and as of the early 1990's over 500 applications of PTC have been implemented within the chemical industry.[3] PTC represents an attractive alternative to traditional chemical reactions conducted in a homogeneous medium, primarily because of its generality with regard to reaction scope. In addition to its generality, PTC processes offer the advantage of mild reactions conditions, readily available raw materials, solvent flexibility, and facile product isolation. Often the main obstacles to the implementation of a successful PTC process are the choice of catalyst and the time required for process optimization at large scale.[4] Advances in recent decades have demonstrated that PTC processes can be applied to asymmetric transformations as well (See Section 1.2).[5]

1.1.3. Examples of PTC Reactions

The concept of PTC was first described by Starks in which various alkyl halides in an organic solvent underwent S_N2 displacement reactions by cyanide ions in aqueous solution catalyzed by a quaternary ammonium or phosphonium salt.[6] These catalysts allowed for the transport of anion, normally insoluble in an organic solvent, to react with a suitable electrophile in the organic phase. This catalyst-reagent ion pair is sufficiently reactive to displace an alkyl halide. Starks also investigated olefin oxidation, olefin cyclopropanation, hydrogen/deuterium exchange, ketone reduction, and hydrolysis reaction through similar PTC processes.

Some of the more widely applicable reaction classes that are susceptible to PTC include S_N2 displacements, alkylations, oxidations, reductions, polymerizations, hydrogenation, and hydrogen/deuterium exchange.[7] Some of the oxidizing agents that have been applied to PTC include, permaganate, hypochlorite, peroxide, oxygen, and periodate.[8,9] Common PTC reducing

agents have included borohydride, aluminohydride, and formate anions. Examples of S_N2 displacements include the use of cyanide, halide, alkoxide, and carboxylate anions. PTC alkylations have been employed for the formation of C-C, C-N, and C-S bond with a variety of organic substrates.

In addition to the wide scope of reagents employed in PTC processes, the catalyst used for a particular reaction has shown similar chemical diversity. The catalyst used can be either soluble in one of the two phases or insoluble. Soluble catalysts include quaternary ammonium and phosphonium salts, polyethylene glycol and its derivatives, crown ethers and cryptands, and polymeric analogs. Insoluble catalysts include polymer-bound derivatives of soluble catalysts, or species which show negligible solubility in either phase and exist as a separate third phase. No one class of catalyst can be applied to all reactions amenable to PTC processes. For this manuscript, only quaternary ammonium salt catalysts will be discussed.

1.2. Mechanisms of Phase Transfer Catalysis

1.2.1. Extraction Mechanism

Two competing mechanisms are thought to exist for PTC processes.[10,11] The extraction mechanism, first proposed by Starks in the early 1970's, postulates that the phase-transfer catalyst can transport counterions between the aqueous and organic phases.[6] For example, in the PTC cyanide displacement of 1-bromooctane with a tetraalkylammnonium (R_4N^+) and/or phosphonium salts (R_4P^+), Q^+ (Figure 1). First, the phase-transfer catalyst exchanges its native counterion for a cyanide anion in the aqueous phase. Second, the newly formed ion pair, Q^+CN^-, must then be extracted into the organic phase by crossing the interface where the equilibrium of this transfer is determined by the properties of the ion pair. The Q^+CN^- ion pair is then poised to

react with 1-bromooctane in the organic phase, and this step is referred to as the intrinsic reaction. In this case the intrinsic reaction regenerates the catalyst, but the original ion pair, Q^+Br^-, must be extracted back into the aqueous phase to complete the catalytic cycle. The sequences of steps that transport cyanide into the organic phase are referred to as transfer steps.

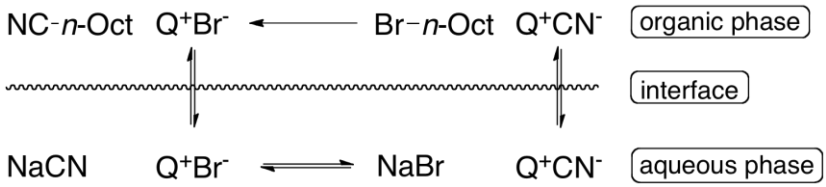

Figure 1. Starks extraction mechanism.

Starks' extraction mechanism can be reduced to a series of equilibrium constants in and between the phases of a PTC reaction, specifically a liquid-liquid process (Figure 2). First, there is the ion exchange of Q^+X^-, where X^- is a generic anion, with the aqueous phase anion, Y^- ($K_1 = k_1/k_{-1}$). Second, the newly formed quaternary ammonium ion pair, Q^+Y^-, must partition between the aqueous and organic phases ($K_2 = k_2/k_{-2}$). Third, the intrinsic reaction occurs within the organic phase (k_3) and this reaction is irreversible. Fourth, the quaternary ammonium ion pair product from the intrinsic reaction, Q^+X^-, must again partition between the aqueous and organic phases to complete the catalytic cycle ($K_4 = k_4/k_{-4}$). This last step is important and can be significant affected by the choice of the X^- anion. For instance, quaternary ammonium iodides are sufficiently lipophilic such that transport back to the aqueous phase is often the rate-determining step of the catalytic cycle. For this reason quaternary ammonium iodides are viewed as ineffective phase transfer catalysts.[12,13] Each rate constant ($k_1 - k_4$) is a product of the intrinsic mass transfer rate constant, k^0_n, and the interfacial surface area. The intrinsic mass transfer rate constant is a function of the structure of Q^+ with respect to the two solvents employed. Often the rate-determining step of an extraction mechanism is the intrinsic reaction

because the transfer steps (K_1, K_2, and K_4) are rapid. In most cases the organic phase concentration of Q^+Y^- remains constant for the course of the reaction, in which case steady-state kinetics can be applied.

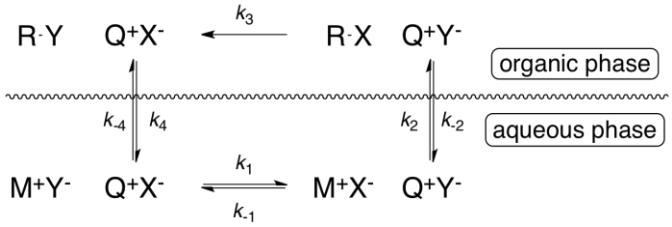

Figure 2. Extraction mechanism with mass transfer steps.

The extraction mechanism becomes more complicated for a base-mediated PTC reaction (Figure 3). In theses reactions an organic substrate, such as phenol, is deprotonated in the aqueous phase or interfacial layer. The resulting anion can then exchange with Q^+X^- to form Q^+R^-, where R^- = PhO^- in this instance. The intermediate, Q^+R^-, can then transverse into the organic phase where the intrinsic reaction takes place. A base-mediate PTC reaction adds two important equilibriums to the mechanism, the partition of substrate between the aqueous and organic phases ($K_5 = k_5/k_{-5}$) and the acid-base equilibrium between substrate and base ($K_6 = k_6/k_{-6}$). Both equilibriums are highly dependent on the lipophilicity and acidity of the substrate. While substrate lipophilicity can sometimes be overcome by modification to the mechanism (see section 1.2.3.), changes in substrate acidity are often responsible for a change in PTC reaction mechanism. An increase in substrate pK_a can turn an extraction mechanism into an interfacial mechanism.

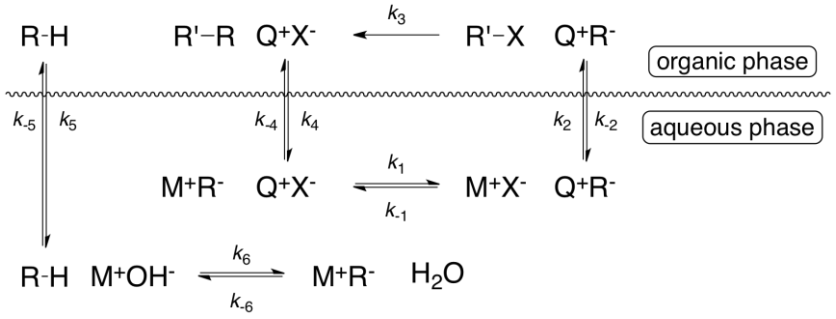

Figure 3. Base-mediated, extraction PTC mechanism.

1.2.2. Interfacial Mechanism

The second mechanism is referred to as the Makosza interfacial mechanism.[14] This mechanism is postulated from the observation that highly lipophilic tetraalkylammonium salts showed limited or no aqueous solubility yet still remained highly active catalysts.[15] As an example, the PTC alkylation of phenylacetonitrile with benzyl bromide and aqueous hydroxide base illustrates the Makosza interfacial mechanism (Figure 4). Unlike the Starks extraction mechanism, Q^+, does not enter the aqueous phase. First, phenylacetonitrile migrates to the interfacial layer where it undergoes depro tonation by a hydroxide anion, which is also present in the interface. The resulting nitrile anion is formed in the interface layer. This intermediate is too polar to be extracted into the organic phase and too basic to persist in the aqueous phase. Concurrently, Q^+Br^- will exist in equilibrium between the organic phase and interfacial layer. Once at the interface, Q^+Br^- can undergo an ion exchange with the nitrile anion. The resulting ion pair is now sufficiently lipophilic to be extracted into the organic phase and participate in the intrinsic reaction, in this case an alkylation with benzyl bromide.

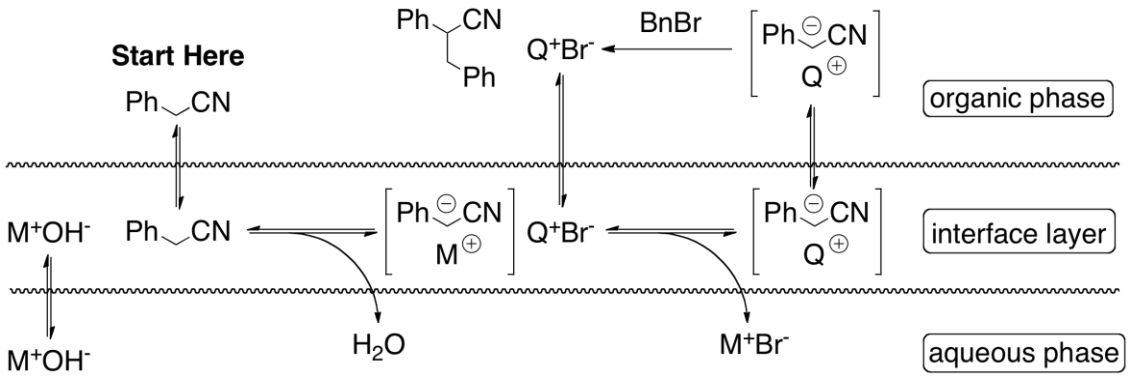

Figure 4. Makosza interfacial mechanism for phenylacetonitrile alkylation.

Given the several phase equilibria which transverse the interfacial layer, the rate determining step of a particular interfacial PTC process often involves an intermediate at the interphase. Therefore, an interfacial PTC mechanism is strongly dependent on the interfacial surface area between the bulk phases. For this reason, efficient agitation methods (e.g. stirring speed) are necessary for a PTC reaction operating under an interfacial mechanism.

1.2.3. Mechanism Modifications

To summarize, in the extraction mechanism the catalyst can cross the interfacial layer and exist in both the aqueous an organic phase, whereas in the interfacial mechanism the catalyst cannot penetrate beyond the interfacial layer. In the modified interfacial mechanism the organic acid, hydroxide base, and the Q^+X^- can exist in the interfacial layer (Figure 5). Both Q^+X^- and M^+OH^- base undergo ion exchange at the interface similar to the extraction mechanism, wherein this step occurs in the aqueous phase. The organic acid in the interfacial layer is not deprotonated by a metal hydroxide but rather by Q^+OH^- present in the interfacial layer to generate the carbanion intermediate, Q^+R^-. The Q^+R^- intermediate is extracted back into the organic phase where the intrinsic reaction takes place, similar to original interfacial mechanism.

Also, as was the case in the original interfacial mechanism, the Q^+ species does not enter the aqueous phase.

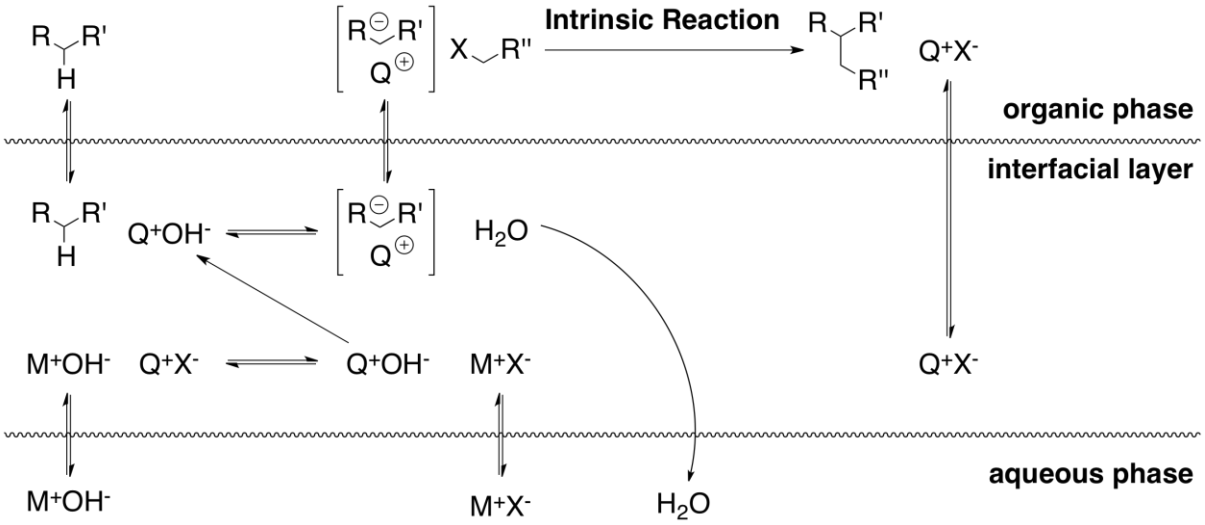

Figure 5. Modified interfacial mechanism.

A similar modification exists for the extraction mechanism, the Brandstrom-Montanari modification. Like the modified interfacial mechanism the catalyst species, Q^+, does not enter the aqueous phase. Instead the reagent from the aqueous phase partitions into the interfacial layer where the catalyst will undergo ion exchange and transport the aqueous reagent to the organic phase. However, no experimental evidence exists to support this modified mechanism.[16]

These mechanisms illustrate the variables that may affect a PTC reaction. Reaction variables such as the catalyst structure, reactant and reagent structure, solvent, temperature, agitation (e.g. stirring speed, reaction vessel, stirrer paddle shape), and the organic/aqueous volume ratio can all affect the multitude of kinetic steps in a PTC reaction. Because many of the transfer steps involve the catalyst, its structure is critical to developing an efficient PTC process.

1.3. Asymmetric Phase Transfer Catalysis

Phase transfer catalyzed processes that can afford enantioenriched products by the action of chiral, nonracemic catalyst are referred to as asymmetric phase-transfer catalysis (APTC) reactions. Given the immense range of reaction classes that are amenable to PTC, the development of general asymmetric variants would be desirable. For the large-scale synthesis of enantioenriched therapeutic compounds, APTC can offer an alternative to classical chiral resolutions and transition metal-catalyzed reactions. To date, investigations into APTC have been primarily focused on improving enantioselectivity and expanding reaction scope.[17,18,19,20,21,22,23,24]

1.3.1. Early Examples

Because quaternary ammonium salts form the vast majority of catalysts, the first APTC reactions employed catalysts derived from chiral amines. Hiyama *et al.* reported the first APTC for an enantioselective oxirane synthesis employing quaternary ammonium salts derived from enantiomerically pure ephedrine.[25] Further examples of APTC nucleophilic displacements were developed over the next decade that employed chiral, nonracemic quaternary ammonium salts derived from ephedrine[26], amino alcohols[27], and *Cinchona* alkaloids.[28] However, these early examples afforded products with low to moderate levels of enantioenrichment with limited catalyst optimization. Amongst the chiral quaternary ammonium salts employed in the initial development of APTC, those derived from *Cinchona* alkaloids have seen the most development in recent years.

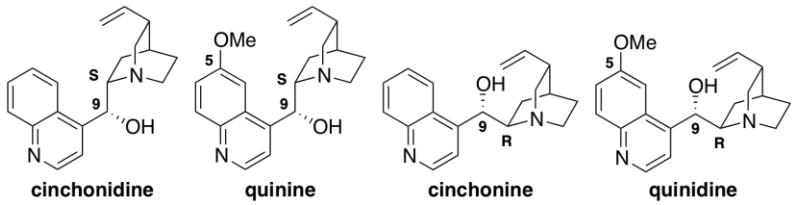

Figure 6. Cinchona alkaloids.

Cinchona alkaloids have a long history as therapeutic agents and as catalysts in asymmetric synthesis.[29,3031] The diverse array of functional groups present in the *Cinchona* alkaloids, a tertiary amine (quinuclidine), a heteroaromatic nitrogen (quinoline), a monosubstituted alkene, and a secondary hydroxyl group permit an immense range chemical manipulations to the core structure (Figure 6). Perhaps most importantly, these alkaloids are readily available and in the optically enriched form. The application of *Cinchona* alkaloids in chemical synthesis will often involve a manipulation at one or more of the functional groups previously mentioned. Examples of reactions catalyzed by *Cinchona* alkaloids include asymmetric reductions, oxidations, and carbon-carbon or carbon-heteroatom couplings in both transition metal catalyzed and organocatalytic variants. Outside the realm of APTC, *Cinchona* alkaloids have gained the most visibility and utility as ligands for transition metal catalyzed asymmetric dihydroxylations and as organocatalysts for the aldol and Michael reactions.[32,33,34] The scope of reactions employing *Cinchona* alkaloids has proven applicable to a wide variety of substrates, with high levels of selectivity, and low catalyst loadings. It is this versatility in substrate and reaction scope, combined with a diverse library of catalyst analogs that elevates the *Cinchona* alkaloid scaffold to the class of 'privileged' chiral catalysts.[35] Some of the more widely employed catalysts derived from *Cinchona* alkaloids are shown below (Figure 7) but will be discussed in more detail later (See Chapter 2).

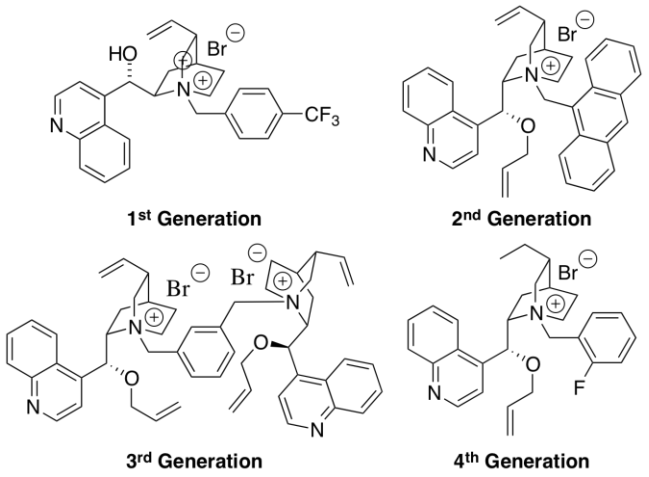

Figure 7. Generations of catalysts derived from *Cinchona* alkaloids.

1.3.2. Other Chiral Catalyst Scaffolds

Highly selective APTC catalysts have utilized scaffolds other than the *Cinchona* alkaloid-derived ones. C_2-Symmetric chiral binaphthyl and spiro, two-center, and crown ethers motifs have all been applied to APTC reaction with high levels of selectivity. For brevity, only the most selective catalysts that have been applied to the APTC glycine Sciff base alkylation will be mentioned.

Maruoka *et al.* was first to incorporate the BINOL scaffold into a selective catalyst (Figure 8).[36,37,38] Unfortunately, these catalysts are sluggish under normal reaction conditions due to their high lipophilicity. With the aid of crown ethers, catalyst activity improved, which the authors speculated arises from the ability of the crown ether to extract KOH into the organic phase. By replacing two of the quaternary ammonium aromatic substituents with alkyl chains, catalytic activity is improved such that a cocatalyst is unnecessary, and high levels of selectivity are preserved.[39]

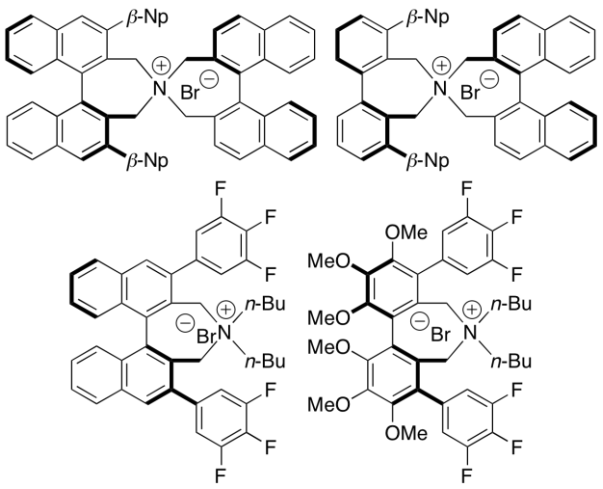

Figure 8. *C*$_2$-Symmetric binaphthyl and biphenyl catalysts.

Employing a configurationally labile biphenyl backbone, a similar catalyst scaffold has been developed by Lygo *et al.* that derived its chirality from a chiral amine component.[40] A number chiral, non-racemic, secondary amines were used in the final step of the catalyst synthesize to create a small library of catalysts that were then screened for the APTC alkylation of a glycine imine. Moderate to very high levels of enantioselectivity (er 35:65 to 95.5:4.5) were afforded with this class of catalyst (Scheme 1).

Scheme 1

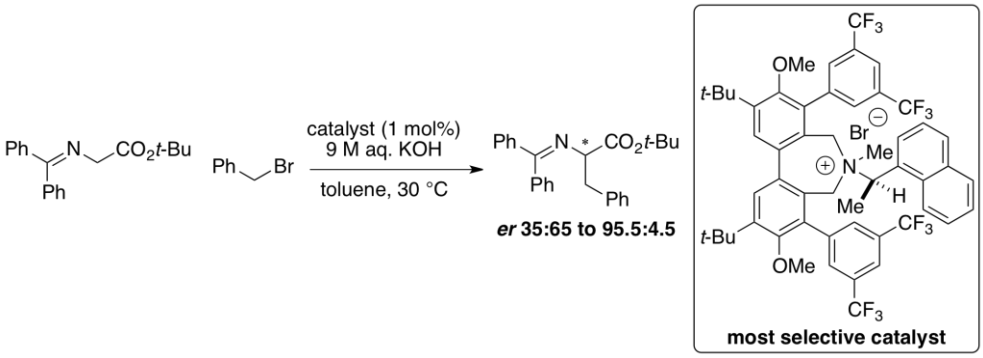

Additional *C*$_2$-symmetric catalysts have been developed that do not incorporate the BINOL or biphenyl backbone and contain two quaternary ammonium centers (Figure 9). One such catalyst constructed by Shibasaki *et al.* was synthesized from enantioenriched diethyl-

tartrate.[41,42] Applied to the APTC alkylation of a glycine imine, these catalyst have afford products of only moderate to good levels of enantioselectivity. A similar tartrate-derived catalyst has been examined by MacFarland *et al.* that also employed a dual quaternary ammonium center motif.[43,44] Despite extensive modification, only low levels of enantioselectivity were obtained from these novel catalysts. An unusual spirobenzopyrrolidine based catalyst was pioneered by Sasai, but suffered from the same lack of selectivity.[45]

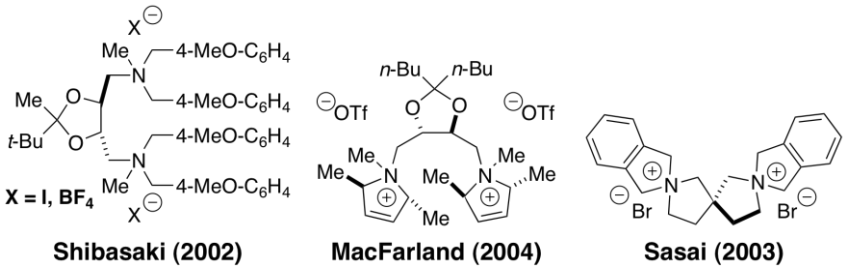

Figure 9. C_2-Symmetric, Two-center Catalysts.

CHAPTER 2: *Catalyst Screening with Cinchona-Alkaloid Derived Catalysts for APTC Alkylation*

2.1. Introduction

Cinchona alkaloid-derived catalysts have enjoyed much success within the realm of APTC and other catalytic asymmetric reactions.[46,47,48] Despite such applicability, the vast majority of studies dealing with development of the *Cinchona* alkaloid-derived catalysts has focused on expanding reaction scope and improving selectivity. Little attention has been paid to study of catalyst activity, and catalyst design has proceeded on primarily an empirical basis.

The following section will discuss the four main generations of catalyst design with *Cinchona* alkaloids. The first generation of catalysts contain modifications to the quinuclidine nitrogen in the form of benzyl derivatives. The second catalyst generation arises from modifications made to the hydroxyl group and use of a large π-surface area, such as anthracene, for the quinuclidine substituent. Third generation catalysts employ a dimeric structure containing a linker substituent attached to the quinuclidine nitrogen. The fourth generation of *Cinchona* alkaloid catalysts contains electronic substituents to the benzyl group appended to the quinuclidine nitrogen.

2.1.1 First Generation Catalysts

The first major utilization of *Cinchona* alkaloids as a catalyst scaffold for APTC was carried out by the Merck process development group for the alkylation of a substituted indanone substrate (Scheme 2).[49] Prior to this work, only moderate levels of enantioselectivity had been reported for APTC alkylations. A preliminary Hammett study of several *N*-benzyl substituents revealed that electron withdrawing groups afforded higher levels of enantioselectivity, with the –

CF_3 substituent yielding the best selectivity. The authors hypothesize that a π-stacking interaction is the primary interaction for asymmetric induction in the catalyst-enolate ion pair. Detailed mechanistic studies were later conducted for this APTC alkylation revealed that the reaction was half-order in catalyst.[50] Further experiments revealed the catalyst formed a lipophilic, catalyst dimer intermediate due to its unmodified hydroxyl group.

Scheme 2

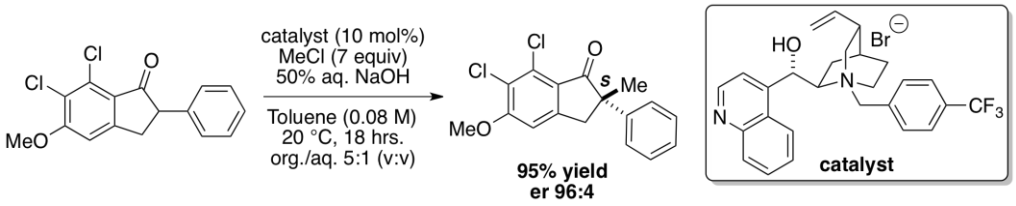

Later work by O'Donnell *et al.* demonstrated that the APTC alkylation of *N*-(diphenylmethylene)glycine *tert*-butyl ester, **1**, with 1st generation catalysts afforded good levels of enantioselectivity (Scheme 3).[51] Among the *Cinchona* alkaloids examined, cinchonine and cinchonidine derived catalysts afforded the *R* and *S* configurations of the alkylation product as the major enantiomer, respectively. It was also observed that the cinchonidine based catalyst were more selective than the corresponding quinine-derived catalyst (er 78:22 compared to er 60:40, respectively).

Scheme 3

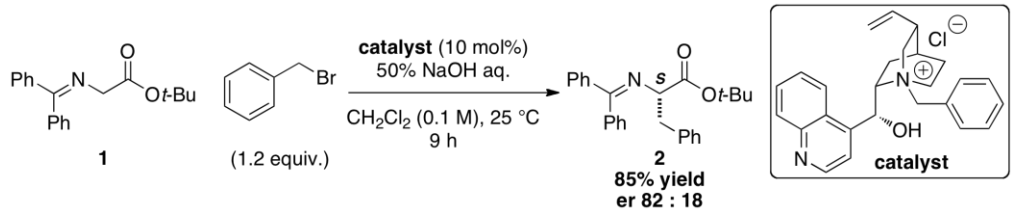

The use of **1** as an APTC alkylation substrate was undertaken for several reasons. First, the substrate is relatively acidic (pK_a 18.7, DMSO, ethyl ester analogue) and therefore can be deprotonated under most base-mediated PTC reaction conditions.[52] Second, **1** selectively forms

monoalkylated products. A dramatic decrease in acidity of **2** (pK_a 23.2, DMSO, ethyl ester analogue) results from $A_{1,3}$-strain in the enolate intermediate derived from **2** (Scheme 4). And third, alkylation products derived from **1** can be easily converted to novel, synthetically useful α-amino acids. These advantages have ensured the continued use of **1** as a model substrate for APTC alkylations.

Scheme 4

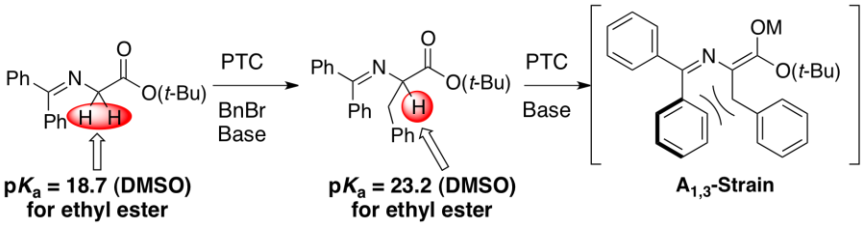

A subsequent study by O'Donnell *et al.*, investigated the fate of the phase-transfer catalyst during the reaction.[53] Contrary to the previous assertion by Dolling *et al.* that invoked a dimer intermediate, O'Donnell reasoned that the hydroxyl group is alkylated *in situ* to form the *O*-alkylated, active catalyst. This notion was supported by the observation that the catalysts *N*-benzylcinchonidinim bromide and *O*-benzyl-*N*-benzylcinchonidinium bromide afforded **2** with nearly identical levels of enantioselectivity.

To further elucidate the nature of the active catalyst in the reaction, enantiopure **2** was subjected to the reaction conditions in the absence of a catalyst, and in the presence of the following catalysts tetrabutylammonium bromide (TBAB), *N*-benzylcinchonidinium bromide, *N*-benzylcinchonidinim bromide with benzyl bromide, and *O*-benzyl-*N*-benzylcinchonidinium bromide to test for racemization. With no catalyst, TBAB, *N*-benzylcinchonidinium bromide with benzyl bromide, and *O*-benzyl-*N*-benzylcinchonidinium bromide no racemization was observed. However with *N*-benzylcinchonidinium bromide alone, a 70% loss of enantiopurity was observed after ten hours. The authors proposed that during the course of the reaction the

unprotected hydroxyl group becomes deprotonated to form a zwitterionic quaternary ammonium alkoxide. In the presence of sufficient quantities of benzyl bromide, this species becomes alkylated *in situ* to form *O*-benzyl-*N*-benzylcinchonidinium. If no benzyl bromide was present, then this zwitterion intermediate could deprotonate **2**, leading to racemization under the reaction conditions. The zwitterion can also slowly form the oxirane through a ring expansion process, leading to an inactive catalyst (Scheme 5). As a result of this study, the use of *Cinchona* catalysts for APTC containing an unmodified hydroxyl group has been rendered obsolete.

Scheme 5

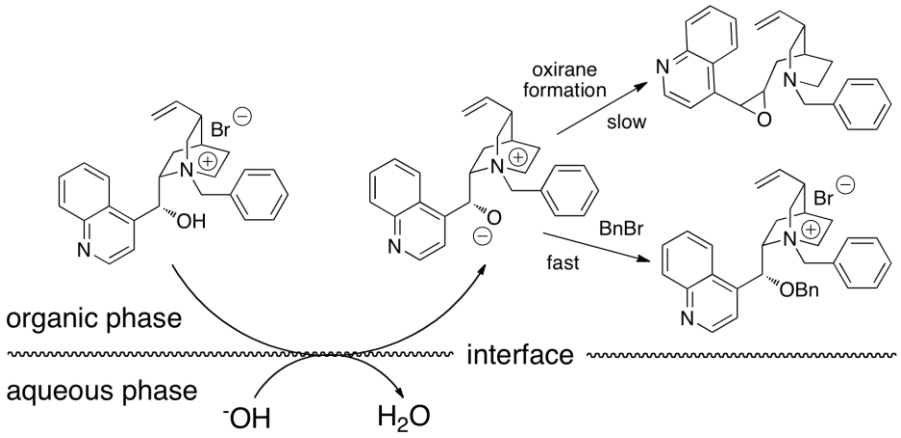

2.1.2 Second Generation Catalysts

Investigations by Lygo and Wainwright first observed that augmenting the steric bulk of the quinuclidine arylmethylene substituent afforded a catalyst with remarkable selectivity (Scheme 6).[54] The use of a 9-substituted anthracene as the aryl group afforded **2** in excellent enantioselectivity (er 95.5:4.5). It was also observed that the background reaction was inhibited when aqueous potassium hydroxide was used in place of aqueous sodium hydroxide. A variety of other electrophiles afforded good levels of enantioselectivity (er 86:14 to 94.5:5.5).

Scheme 6

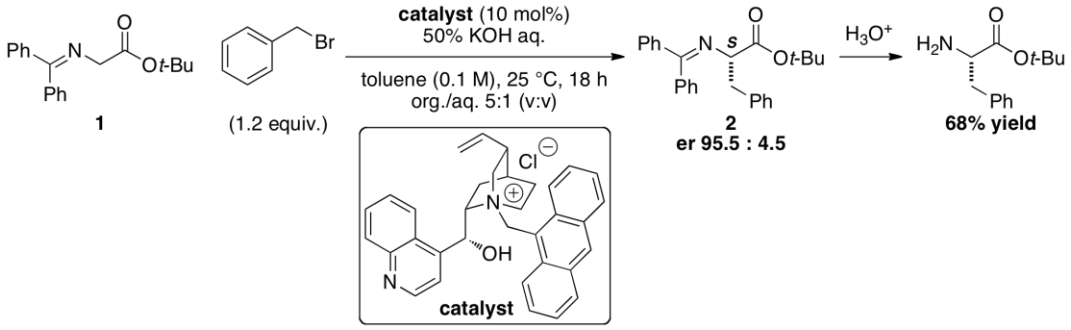

The catalyst structure was further optimized by Corey *et al.* with the introduction of an *O*-allyl substituent at *C*(9).[55,56] In contrast to previous APTC alkylations of **1** that employed a liquid-liquid PTC conditions, low temperature (-78 °C) solid-liquid PTC conditions were employed to afford **2** in excellent enantioselectivity (er 97:3, Scheme 7). The authors proposed a stereochemical model that reasoned that the 9-anthracenylmethyl substituent provides conformational rigidity in the catalyst-substrate ion-pair during the stereodetermining step of the reaction. In contrast to Dolling's stereochemical rationalization that invoked a π-stacking interaction, the authors do not suggest such interaction occurs.

Scheme 7

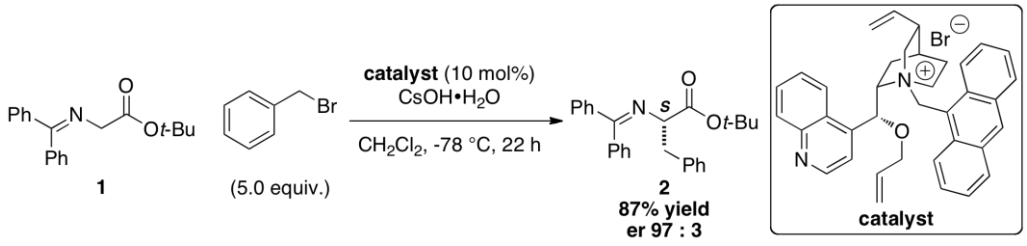

Lygo et al. undertook a preliminary structure selectivity study with the second generation of *Cinchona* catalysts.[57] In this study the quinuclidine core was kept intact with the sites of modification restricted to the quinoline region, the C(9) hydroxyl, and the arylmethylene substituent appended to the quinuclidine nitrogen. Previous work had shown that modifications to the quinuclidine vinyl group had little effect on catalyst selectivity and so it was removed prior

to catalyst modification. 19 catalysts were screened for selectivity in the APTC alkylation of **1** (Figure 10).

Results from this catalyst screen showed that the original quinoline group provided a more selective catalyst. Substitution of the quinoline nitrogen for a carbon atom afforded a less selective catalyst (er 78:22 versus 68:32). At the quinuclidine region, $\mathbf{R^3}$, alkyl substituents showed minimal enantioselectivity. Incorporation of 4-nitrobenzyl and 4-methoxybenzyl substituents led to catalysts that are less selective than a benzyl substituent. The *C*(9) oxygen substituents, $\mathbf{R^1}$, showed the least influence on catalyst enantioselectivity. The configuration of the substituent at *C*(9) was left unexamined.

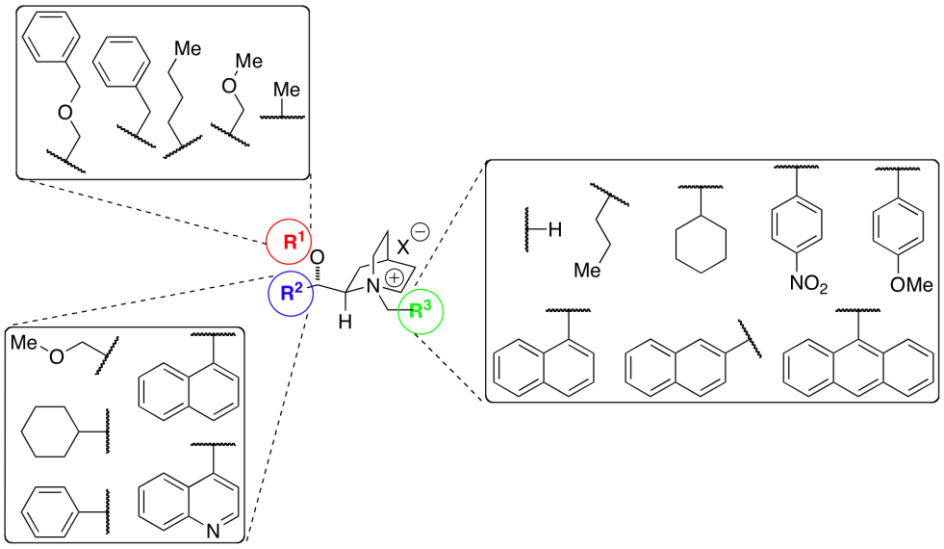

Figure 10. Second generation cinchonidine based catalyst library.

2.1.3 Third Generation Catalysts

Drawing inspiration from the dimeric *Cinchona* alkaloid ligands utilized successfully in the Sharpless asymmetric dihydroxylation,[32,33] a third generation of *Cinchona* alkaloid based catalysts were developed that incorporate a dimeric catalyst structure. Unlike the Sharpless ligands that require a tertiary amine for activity and are linked at the *C*(9) oxygen, the dimeric

phase transfer catalysts are linked at the quinuclidine nitrogen. Jew and Park demonstrated the α,α'-bis[*O*-allylcinchonidinium)-*m*-xylene dibromide catalyst afford high levels of enantioselectivity for the APTC alkylation of **1** (Scheme 8).[58] The *p*-xylene dimer shows similar enantioselectivity to previously employed monomeric catalysts, whereas a reduction in selectivity is observed with the *o*-xylene dimer, presumably due to unfavorable steric interactions. Trimeric catalysts were also tested under similar reaction conditions with substrate 1 to afford alkylation products with similar levels of enantioenrichment (er 97:3).[59]

Scheme 8

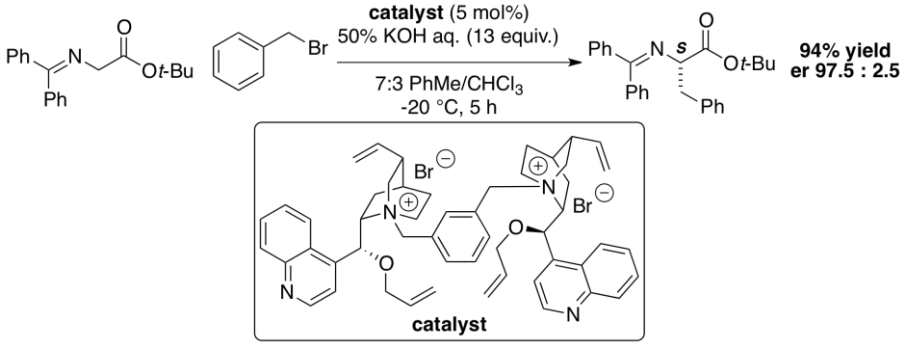

2.1.4 Fourth Generation Catalysts

The first three generations of *Cinchona* alkaloid based catalysts deal primarily with steric modification to the quinuclidine substituent and secondarily with modification to the hydroxyl group. The effect of varying the electronic properties of the substituent on the quinucldine nitrogen was briefly investigated by Dolling *et al.*, who found that that increased π-acidity of the quinuclidine substituent afforded increased enantioselectivity in an APTC alkylation of an indanone derivative.[49,50] Studies undertaken by Jew and Park had shown that incorporation of a fluorine atom in the *ortho* position of the quinuclidine benzyl substituent led to a significant increase in selectivity.[60] Monofluoro analogs at the *meta* and *para* positions were no more

selective than the non-fluorinated catalyst and the incorporation of two additional fluorines at the meta and para positions led to a synergistic increase in selectivity (Scheme 9).

Scheme 9

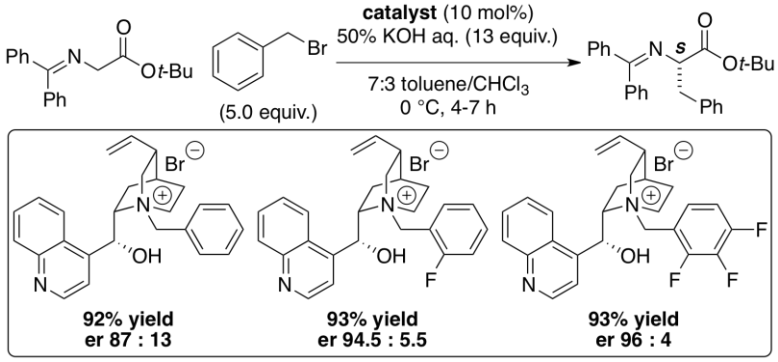

The arylfluorine substituent is proposed to provide for a more conformationally rigid catalyst by means of a hydrogen bonding interaction between the fluorine and hydroxyl group. On the basis of this hypothesis, additional analogs were synthesized with varying electronegative functional groups. Both the 2-cyanobenzyl and *N*-(1-oxy-2-pyridinylmethyl) derivatives afford catalysts with high levels of enantioselectivity similar to those observed with the 2-fluorobenzyl analog (Figure 11).[61] It is speculated that a water molecule from the reaction mixture remains hydrogen bound in a cavity between the *O*-allyl and fluoro/*N*-oxy/cyano benzyl substituent. However, there is some debate as to whether arylfluorines can even participate in hydrogen bonding.[62]

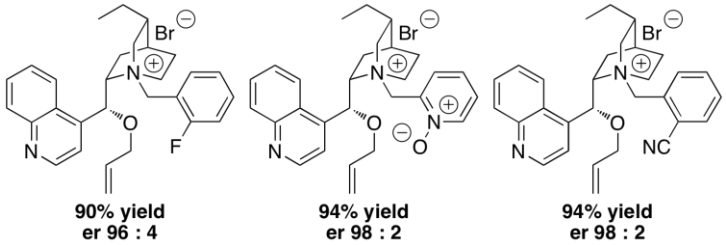

Figure 11. Electronic modifications to fourth generation catalysts.

2.1.5 Objectives

Despite the numerous examples of modified *Cinchona* alkaloids in APTC, no systematic study has been conducted to examine to effect of substituents on catalyst selectivity and reactivity. Of the many modifications to the *Cinchona* alkaloid scaffold in APTC, few studies have probed the importance of the C(9) oxygen-bearing center.[63] Variables such as the configuration, substituents on the oxygen, the replacement of the oxygen atom, or the removal of that heteroatom remain to be investigated.

The aim of this study was to examine the steric and electronic contributions of the arylmethylene substituent appended to the quinuclidinium nitrogen (substituent X). Specifically, the aromatic groups that would be surveyed are 9-anthracenyl, 2-naphthyl, 1-naphthyl, phenyl, and 3,5-bis(trifluoromethyl)phenyl. Eight different substituents were proposed for the *C*(9) position on cinchonidine to examine the effect of sterics, dipole strength, and configuration (substituent Y). To that end, hydroxy, *epi*-hydroxy, benzyloxy, allyloxy, methoxy, *epi*-methoxy, fluoro, and hydro group would be screened for substituent Y. The substitution of the native hydroxyl group with a fluoro substituent would determine what effect dipole strength and hydrogen bonding have on catalyst activity and selectivity. Additionally, removal of the dipole at *C*(9) would also provide similar answers. Altogether, 40 catalysts were to be screened for activity and selectivity for the APTC benzylation of **1** (Figure 12).

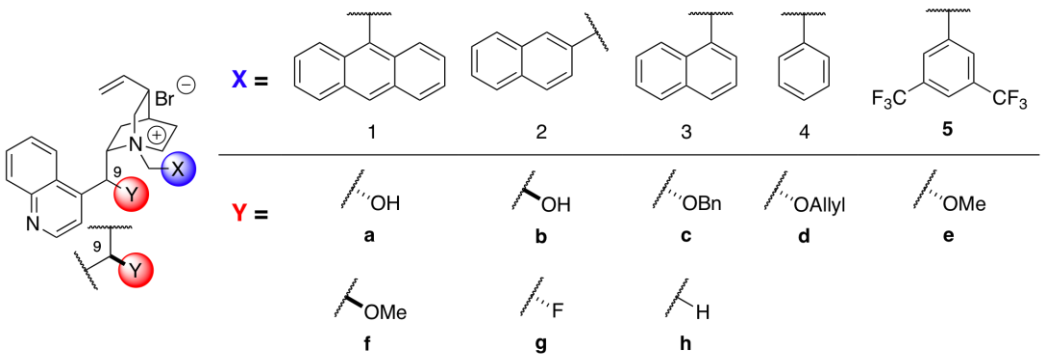

Figure 12. Proposed *Cinchona* catalyst library.

2.2 Catalyst Synthesis

2.2.1 Retrosynthesis

Cinchona alkaloid based catalysts for APTC have been synthesized by first generating the quaternary ammonium salt by alkylation of the quinuclidine nitrogen followed by modification to the *C*(9) hydroxyl group, often under PTC reaction conditions. If the alkylating reagent for both the hydroxyl and tertiary amine groups is the same, then both alkylations could be performed in one pot.

Following the previously described catalyst syntheses of O'Donnell, Lygo, Wainwright, and Corey afford catalysts in low yields and complex product mixtures, which required difficult separations. Shortly thereafter, a new strategy was implemented wherein the hydroxyl group would be modified first followed by alkylation of the quinuclidine nitrogen (Scheme 10). This strategy has an advantage over previous methods by introducing the *C*(9) functionality prior to *N*-alkylation, thus yielding a more stable catalyst precursor. Additionally, this route is more amenable to a library synthesis. Generally, the quinuclidine alkylation is robust and performed under neutral conditions, thus rendering it ideal for the last step of the catalyst synthesis. This strategy allowed for the efficient synthesis of 39 catalysts from only 8 precursors.

Scheme 10

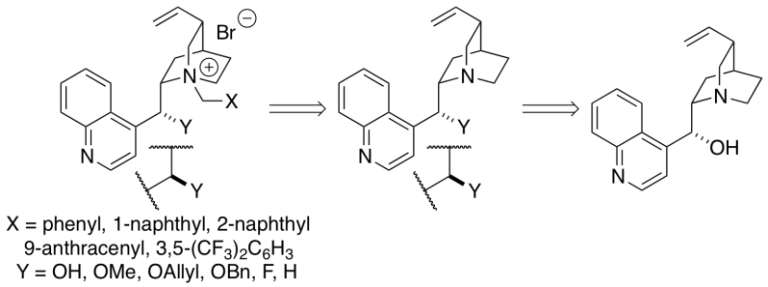

2.2.2 *C*(9) *Epi*-cinchonidine

Epi-cinchonidine was synthesized by means of a Mitsunobu reaction, following conditions reported by Lectka *et al.*.[64] On small scale, this procedure was found to be effective, but upon scale-up, a complex product mixture was obtained. Subsequent optimization found that the addition of three equivalents of the carboxylic acid led to a formation of a single product in 85% yield (Scheme 11).

Scheme 11

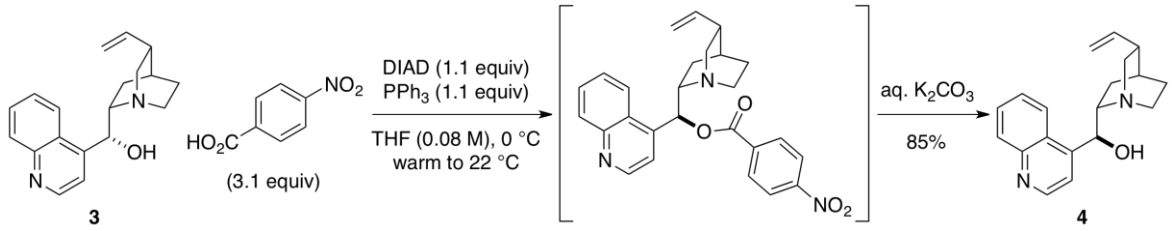

Prior to the hydrolysis of the benzoyl ester, the cinchonidine reactant was not observed in the crude product by thin-layer chromatography (TLC). Yet after hydrolysis with saturated aqueous potassium carbonate, significant amount of cinchonidine were observed in the reaction product by ^{1}H-NMR spectroscopy. Mechanistically, the Mitsunobu reaction proceeds through an S_N2 displacement of an oxyphosphonium ion to afford stereoinverted products. To obtain a stereoretentive product, a double S_N2 displacement must be operative through the intermediacy

of an azirdinium ion. In the presence of one equivalent of carboxylic acid, the quinuclidine nitrogen competes with the carboxylate anion for displacement of the oxyphosphonium ion. The aziridinium ion can then be opened by the carboxylate anion to afford the stereoretentive benzoate (Scheme 12). A stoichiometric excess of 4-nitrobenzoic acid (3 equivalents) ensures the quinuclidine nitrogen remains protonated, preventing aziridinium ion formation.

Scheme 12

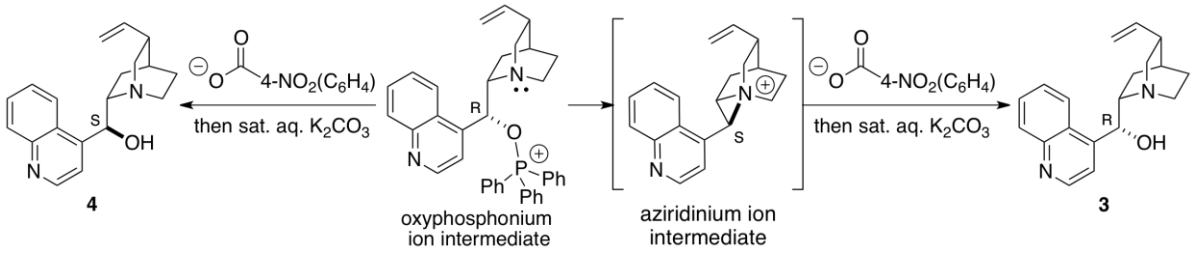

2.2.3 Ether Analogs of Cinchonidine

The alkyloxy *Cinchona* catalyst analogues were synthesized by mean of a Williamson ether synthesis with the respective alkyl halide (Scheme 13). All ether analogs were obtained in moderate to good yields (61-86% yield). Despite employing only a minimal excess of alkyl halide and low reaction temperatures, trace amounts of the undesired quaternary ammonium salt were observed in all cases.

Scheme 13

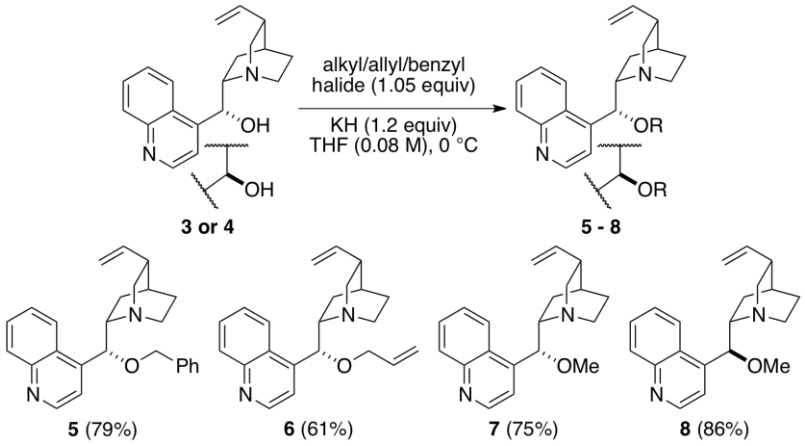

2.2.4 Deoxyfluorocinchonidine Synthesis

The initial efforts towards the synthesis of deoxyfluorocinchonidine followed the synthesis reported by Hoffmann *et al*., wherein *O*-mesyl-cinchonidine was displaced by fluoride with a TBAF/THF solution.[65] Unfortunately, this method resulted in low yields and a complex product mixture. However, a later procedure reported by Gilmour demonstrated improved yields starting from cinchonidine and employed the fluorinating agent, diethylaminosulfur trifluoride (DAST).[66] Application of this synthetic protocol proved successful, although at somewhat lower yields than reported (Scheme 14).

Scheme 14

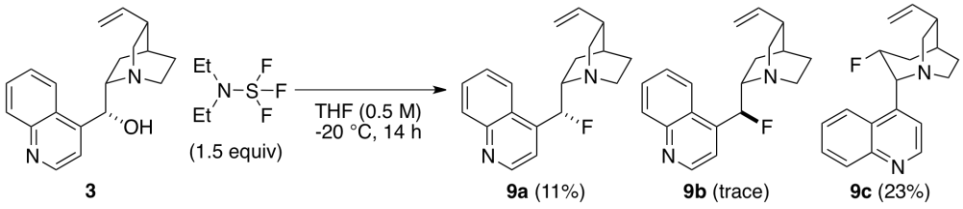

The synthesis of deoxyfluorocinchonidine was complicated by the formation of several side products. The DAST mediated fluorination of cinchonidine afforded the stereoinversion product, **9b**, the [3,2,2] ring-expanded product, **9c**, decomposition products that showed no

incorporation of fluorine, in addition to the desired product, **9a**. Interestingly, the product ratio was significantly dependent on the reaction temperature. At lower reaction temperatures (-60 °C), **9c** was formed almost exclusively, while at higher temperatures (0 °C), product decomposition was observed. These results, in addition to the reported mechanism of DAST fluorinations, supported the presence of an aziridinium ion intermediate (Scheme 15).[67] The near exclusive formation of **9c** at low temperatures suggests that ring expansion by fluorine displacement is the kinetically favored pathway. Similar functionalized substrates have been shown to proceed through an aziridinium ion intermediate under DAST fluorination.[68] Given the structural similarity of **9a** and **9b**, laborious chromatographic purification was required for the isolation of **9a**.

Scheme 15

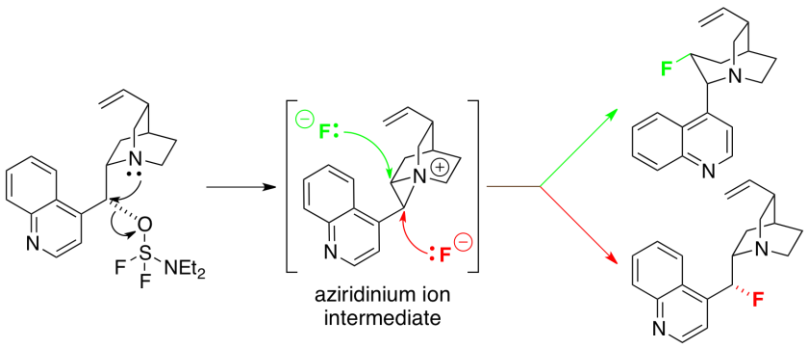

2.2.5 Deoxycinchonidine Synthesis

A synthesis of deoxycinchonidine was reported by Stenberg and Travecedo through an acid-catalyzed photochemical reduction.[69] This method utilized ultraviolet irradiation and suffered from low yield (49%), and as a result a more general synthesis was sought. Accordingly, deoxycinchonidine was synthesized by means of a Barton-McCombie radical deoxygenation from the precursor thionocarbonate in excellent yield (Scheme 16).[70,71]

Scheme 16

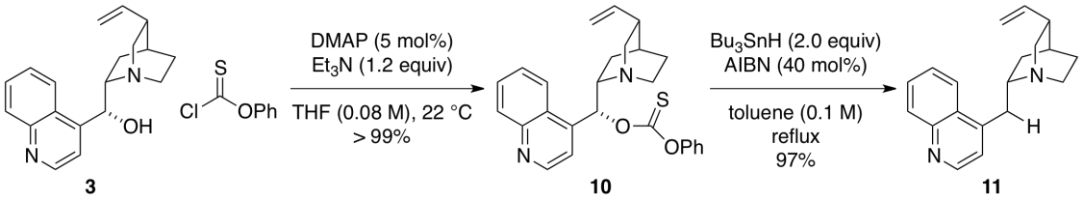

2.2.6 Alkylation of the Quinuclidine Nitrogen

Typically the S_N2 alkylation of the quinuclidine nitrogen of *Cinchona* alkaloids and its derivatives is performed in either toluene or 2-propanol, either at reflux or room temperature. This approach was reproduced early during quaternization attempts of cinchonidine, but often resulted in impure product mixtures. Given that S_N2 reactions are typically accelerated in polar aprotic media, this alkylation reaction was tested in acetonitrile.[72] The desired quaternary ammonium salts were obtained in good to excellent yields in nearly all cases (Scheme 17). The catalysts were purified by means of recrystallization or silica gel chromatography.

Scheme 17

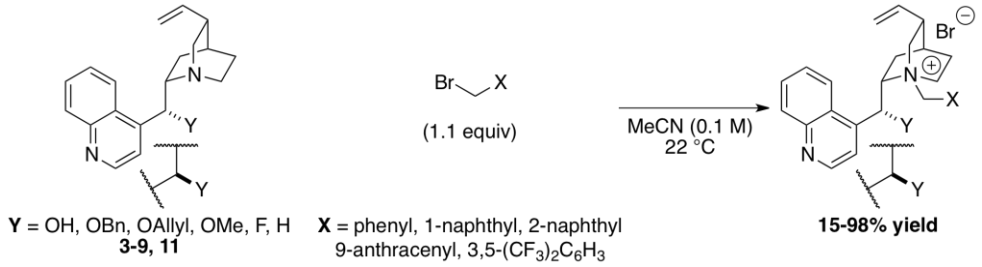

Table 1. Catalyst Library Synthesis

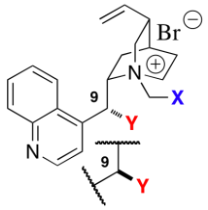

X = / Y =	1	2	3	4	5
OH **a**	**1a** (86%)[a]	**2a** (88%)	**3a** (90%)	**4a** (97%)	**5a** (87%)
OH **b**	**1b** (88%)	**2b** (71%)	**3b** (81%)	**4b** (87%)	**5b** (98%)
OBn **c**	**1c** (82%)	**2c** (93%)	**3c** (92%)	**4c** (93%)	**5c** (92%)
OAllyl **d**	**1d** (72%)	**2d** (64%)	**3d** (84%)	**4d** (73%)	**5d** (85%)
OMe **e**	**1e** (75%)	**2e** (83%)	**3e** (90%)	**4e** (73%)	**5e** (67%)
OMe **f**	**1f** (90%)	**2f** (74%)	**3f** (72%)	**4f** (97%)	**5f** (93%)
F **g**	**1g** (88%)	**2g** (72%)	**3g** (52%)	**4g** (82%)	**5g** (76%)
H **h**	**1h** (15%)	**2h** (87%)	**3h** (87%)	**4h** (84%)	**5h** (N/A)

[a]Catalyst yield

In most cases the alkylation of the quinuclidine nitrogen with an arylmethylene bromide proceeded in good to excellent yields. The exception to this trend was observed with the alkylation of deoxycinchonidine (Table 1, row h). Several deoxycinchonidinium catalysts proved to be unstable to workup or purification conditions. Notably, catalyst **5h** was unable to be isolated with sufficient purity and was therefore removed from the catalyst library. Chromatographic purification of several deoxycinchonidinium catalysts afforded a side product with an extra olefinic signal in the ^{1}H-NMR spectrum, suggesting an elimination mechanism to the ring-expanded product. In cases where chromatographic separation led to decomposition, the catalysts was precipitated with ether and washed repeatedly prior to use.

2.3 Results

2.3.1 APTC Reaction Conditions

For this catalyst survey, the asymmetric alkylation reaction of interest was the benzylation of **1** under liquid-liquid PTC conditions. To gain insight into catalyst activity, the formation of **2** was monitored with the aid of an internal standard, 1,1-diphenyl-1-heptene (Scheme 18).[73] First, all the organic components were combined and then allowed to cool to 2-4 °C. To start the reaction, pre-cooled aqueous base was then added. Catalyst activity and selectivity were determined by high-performance liquid chromatographic (HPLC) analysis from aliquots of the organic phase.

Scheme 18

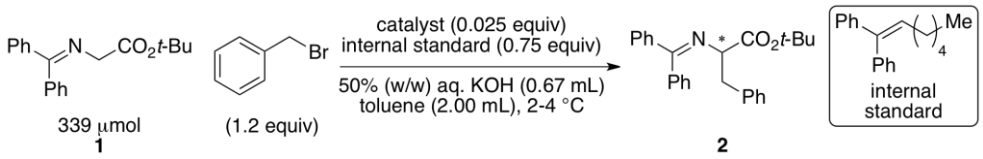

The APTC alkylation rate of **1** was found to be significantly dependent on the stirring speed of the reaction due to the change in interfacial surface area. This finding suggests an interfacial mechanism is operative for the APTC alkylation of **1**. To ensure reproducible interfacial surface area during the reaction, magnetic stir bars of a consistent size and shape (1.5 cm length, egg-shapped) were employed. Additionally, the solvent volumes were adjusted such that the stir bar lay between the phase boundaries in order to provide satisfactory mixing between the aqueous and organic phases. All stir plates were set to the maximum stirring speed and after calibration were found to rotate at 1500 rpm or higher.[74]

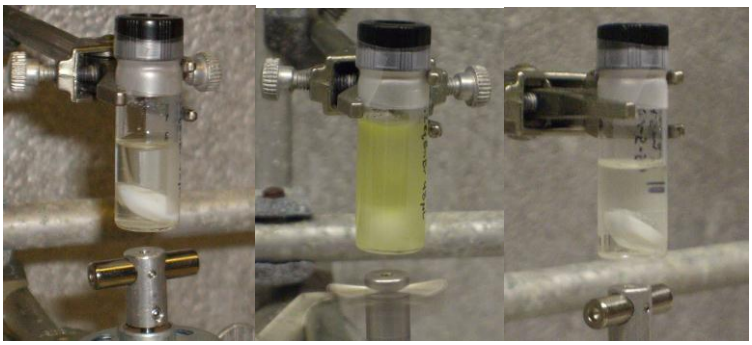

Figure 13. APTC reaction from beginning to completion.
From left to right: reaction immediately after the addition of base; stirring with base; reaction after completion

The decision to perform the APTC reaction at 2-4 °C was done primarily to ensure reproducible alkylation rate data, rather than for the sake of enantioselectivity. A catalyst loading of 0.025 equivalents was employed because of the limited solubility of quaternary ammonium salts in organic solvents. The comparison of catalyst activity would be complicated if all catalysts were present in varying concentrations. Potassium hydroxide was used instead of sodium hydroxide because the later was found to promote a significant background reaction.

Each catalyst was run in duplicate for both activity and selectivity measurements. Catalyst activity was determined by the percent conversion to product. For each run these percent conversion values were fitted to either an exponential decay or logistic decay function

with the aid of OriginLab Pro™ software. A reaction half-life was then calculated from each fitting function and reported in minutes. Generally, a logistic decay function was required for catalysts that displayed an induction period. Catalyst selectivity was determined as the mean enantiomeric ratio of **2** on a chiral stationary phase (CSP) HPLC from duplicate runs. The absolute configuration of the major enantiomer formed was established to be *S* by comparison of the optical rotation of **2** with known values.[75]

2.3.2 Reaction Half-Life Results

The calculated half-life values shown below were calculated from percent conversion to alkylated product plots for each catalyst in duplicate and then fitted to an exponential decay functon (Figure 14). Each column in the table represents a different *N*-quinuclidine substituent, X, and each row represents a different substituent at C(9), Y. While most catalysts were soluble in the organic phase when dissolved at room temperature, a number of them showed a minor amount of precipitation after equilibration at the reaction temperature. However, some catalysts (**2a**, **2b**, **4c**, **1g**, **2g**, **1h**, **2h**, **3h**, **4h**) were observed to be only partially soluble even at room temperature.

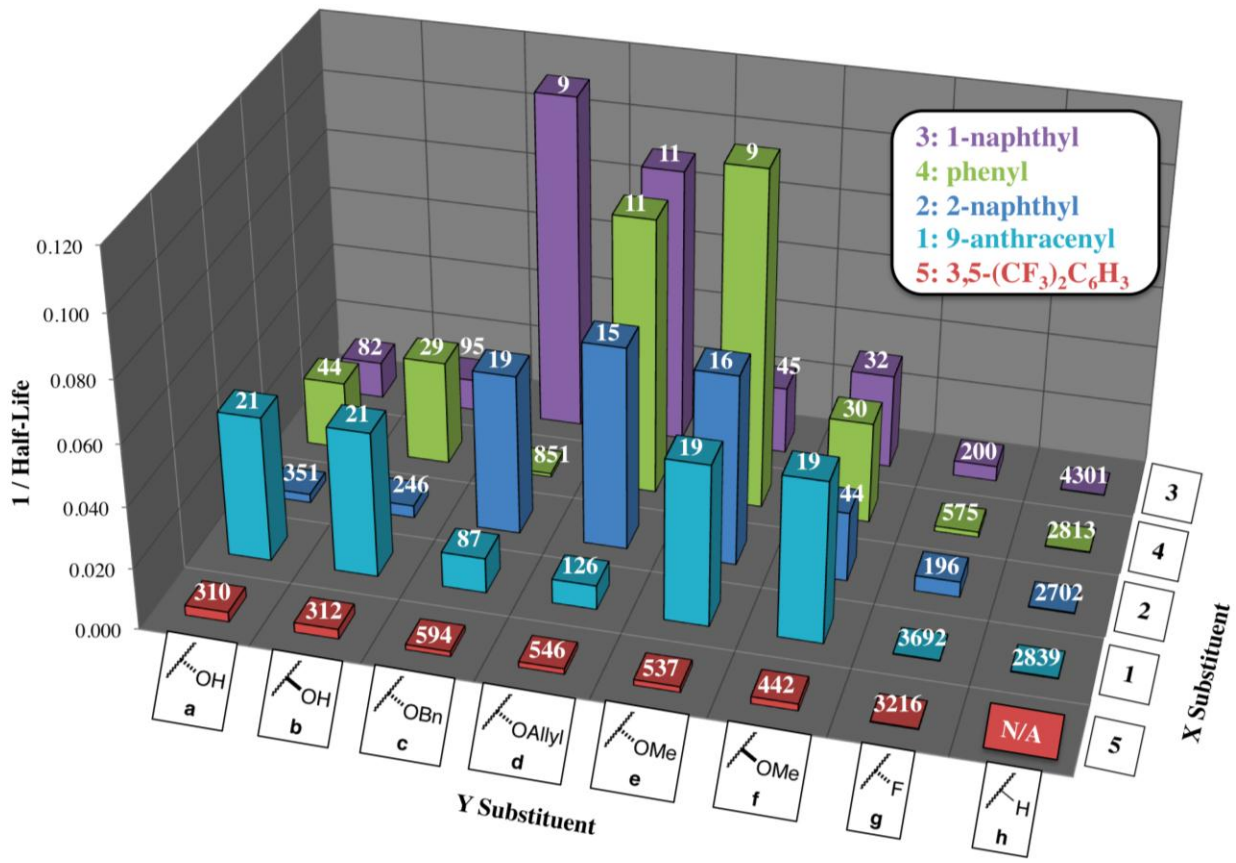

Figure 14. Reaction half life, $t_{1/2}$ (min.).

A significant dependence of reaction rate on the π-acidity of substituent X was observed in this survey. For nearly every Y substituent examined, catalysts bearing a $(CF_3)_2C_6H_3$ group showed significantly less activity compared to other catalysts. With the exception of the deoxycinchonidinium catalysts (series **h**), the reaction half-life was ten-fold higher with X = 3,5-$(CF_3)_2C_6H_3$.

An induction period was observed for some of the hydroxy catalysts (**1a**, **2a**, **3a**, **4a**), yet surprisingly not observed with the respective *epi*-hydroxy catalysts (**1b**, **2b**, **3b**, **4b**). A clear difference in reaction rate was observed between the hydroxy (series **a**) and benzyloxy (series **c**) catalysts. In several instances benzyloxy catalysts showed less activity than their hydroxyl catalyst analog (**1c**, **4c**, **5c**) while the other benzyloxy catalysts (**2c**, **3c**) had significantly

enhanced activity. Inversion of configuration at *C*(9) for both the hydroxyl substituent (series a and b) and the methoxy substituent (series **e** and **f**) showed little difference on reaction rate.

Substitution of hydroxy group at *C*(9) with a fluoro substituent generally afforded less active catalysts (**1g**, **3g**, **4g**, **5g**). In one instance, a deoxyfluorocinchonidinium catalyst (**2g**) was observed as a more active catalyst than its hydroxyl analog. Both catalysts **2a** and **2g** displayed limited solubility in the organic phase, and one cannot compare their relative activities with certainty since their effective concentrations in the reaction mixture are unknown. Moreover, it can be seen that removing the heteroatom entirely will result in a sluggish catalyst. Reactions with the deoxycinchonidinium catalysts had half-lives two to three orders of magnitude larger than their hydroxyl or ether counterparts. Additionally, these catalysts consistently failed to catalyze the APTC alkylation to full conversion.

2.3.3 Catalyst Selectivity Results

In cases where the reaction did not reach full conversion (<70%), the alkylation product was isolated by chromatographic purification and then subsequently analyzed by CSP-HPLC. The results of this enantioselectivity survey are shown below and represent the average value over two or more reactions (Figure 15).

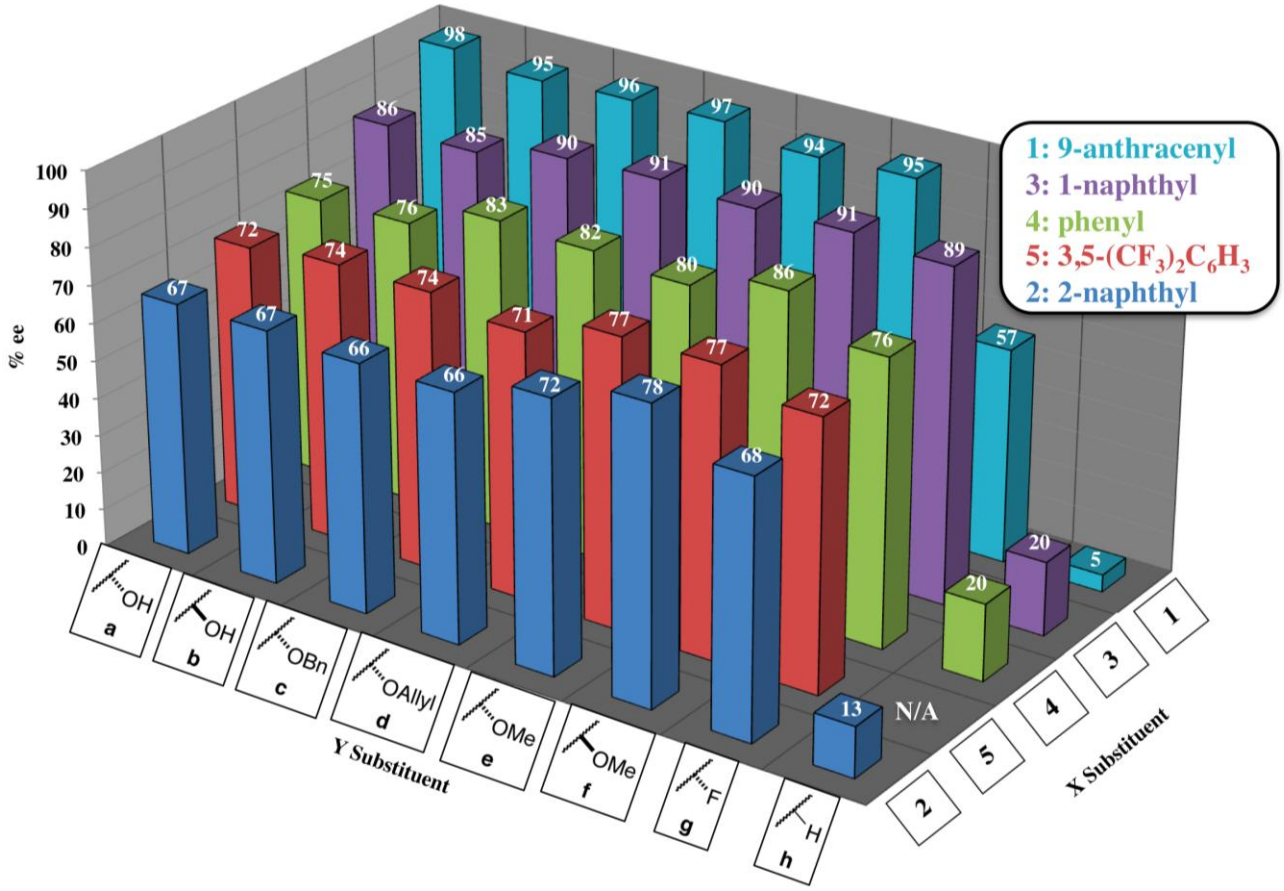

Figure 15. Catalyst selectivity screen.

The product enantiomeric ratio was most dependent on the X substituent. The highest enantioselectivities were observed for series **1** (X = 9-anthracenyl) and decreasing in selectivity to series **3** (X = 1-naphthyl), series **4** (X = phenyl), series **5** (X = 3,5-$(CF_3)_2C_6H_3$), and with lowest enantioselectivities observed with series **2** (X = 2-naphthyl). The increased selectivity of the 1-naphthyl substituent versus its isomeric 2-naphthyl analog reaffirms a similar finding by Lygo (er 76:24 versus 70:30, respectively).[40] An important result of this study was the effect on catalyst selectivity by the substituent configuration at *C*(9). Not only do both the *C*(9)-hydroxy (series **a**) and *C*(9)-*epi*-hydroxy (series **b**) afford the same major enantiomer, but both catalyst series have nearly identical enantiomeric ratios. Similar results were obtained for the methoxy

(series **e**) and *C*(9)-*epi*-methoxy (series **f**) catalyst series. Although, the *C*(9)-*epi*-methoxy catalysts were observed to be somewhat more selective. No significant differences in selectivity were observed among the ether analogs although generally the *O*-alkylated catalysts were slightly more selective than their hydroxy analogs.

The deoxyfluoro catalysts (series **g**) afforded catalysts of similar selectivity compared to the parent hydroxy catalysts (series **a**). Catalyst **1g** remained an outlier to this trend, but given its low activity, its decomposition to a less selective species cannot be ruled out. Removal of the dipole at *C*(9) with the deoxycinchonidium catalysts (series **h**) resulted in a near complete loss in product enantioselectivity.

2.4 Discussion

2.4.1 Catalyst Reactivity

Among the X substituents the primary trend observed is a pronounced reduction in catalyst activity for series **5** (X = 3,5-$(CF_3)_2C_6H_3$). The steric bulk of the X substituent showed little effect on catalyst activity. The increased π-acidity of the 3,5-bis(trifluoromethyl)benzyl substituent may explain the slower reaction rate due to a tighter enolate-catalyst ion pair. The incorporation of electron withdrawing substituents to the catalyst may increase the coulombic interaction between the ammonium-enolate ion-pair. A stronger coulombic interaction would raise the activation barrier to the ammonium-enolate alkylation transition state. This tight ion pair may shift the reaction to the intrinsic rate limited regime if the interaction energy between substrate and catalyst is sufficiently large.

Catalyst activity was most dependent on the Y substituent. One of the most surprising results of this survey was the significant difference in reaction rate between the hydroxy (series

a) and benzyloxy (series **c**) catalysts. Previous reports suggested that the *C*(9)-hydroxyl catalyst is transformed to its *O*-benzylated analog *in situ* based on similar enantioselectivity values.[53] This rate difference excludes the possibility that the *C*(9)-benzyloxy catalyst is solely responsibly for the observed rates within the hydroxy catalyst series. Additionally, most of the *C*(9)-hydroxyl catalysts showed an induction period. This induction period may be the result of *in situ* O-alkylation by benzyl bromide, but it does not account for why some catalysts showed increased activity as the benzyloxy analog (**2c**, **3c**) and other catalysts (**1c**, **4c**, **5c**) showed diminished activity as the benzyloxy appended structure.

A more likely explanation of this induction period can be found in Dolling's study in the APTC alkylation of a substituted indanone substrate with *Cinchona* alkaloid based catalyst.[50] The authors observed that the hydroxy cinchoninium catalysts had poor solubility in the organic solvent, yet after the addition of aqueous base significant amounts of the catalyst could be detected in the organic phase. Further tritration and elemental analysis studies led the authors to conclude that the catalyst forms a pseudo-dimer species (monobromide and monoalkoxide) in the presence of aqueous base. This induction period can be explained by the formation of a dimer species, which exhibits increased organic phase solubility. Interestingly, none of the *epi*-hydroxy catalysts showed any noticeable induction period. This finding would suggest that the rate of dimer formation is dependent on the diastereomeric configuration of the hydroxyl group.

The reduction in catalytic activity for catalysts bearing electron deficient substituents, due to an increase in coulombic interaction, may be a likely explanation for the lack of activity within the deoxyfluoro catalyst analogues (series **g**). Across most X substituents, the deoxyfluoro catalysts were less active than their hydroxy counterparts. The exception, catalyst **2a**, was likely due to solubility factors. The absence of an induction period with the deoxyfluoro

catalysts provides further support of a functionalization of the hydroxy group during the course of the alkylation reaction. The drastic drop in catalytic activity going from **1a** to **1g** (two orders of magnitude) is more indicative of catalyst decomposition rather than the reactivity of the ammonium-enolate ion-pair. It is unknown why catalyst **1g** would be more susceptible to decomposition than the rest of series **g**.

The near total loss of catalytic activity for the deoxycinchonidinium catalyst (series **h**) mainly stems from obstacles encountered during their synthesis. Given their facile decomposition under the relatively mild conditions of reaction workup, the likelihood these catalysts would persist under a base-mediated PTC reaction conditions is marginal. The mechanism for catalyst decomposition within series **h** is a Hoffmann elimination (Scheme 19). According to the mechanism, the initial decomposition product may be alkylated at the tertiary amine. The product of such an alkylation could function as a phase transfer catalyst. Without any knowledge on the rate of catalyst decomposition under the reaction conditions, it is difficult to determine what catalyst structure is responsible for the diminished reactivity of series h. Another possible explanation would be that the starting deoxycinchonidinium catalyst is immediately decomposed upon addition of base. The inactivated catalyst could then undergo a slow alkylation under the PTC reaction conditions with benzyl bromide to afford an active catalyst. This alkylation would likely proceed at a diminished rate considering it would take place in a toluene solvent at 0 °C. Therefore, the lack of catalytic activity would be the result of a very low loading of active catalyst.

Scheme 19

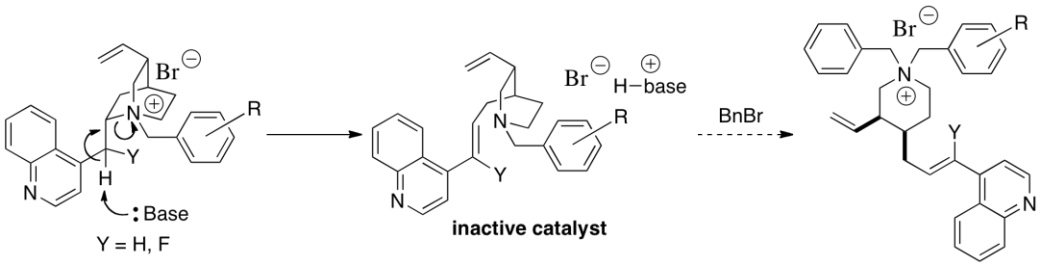

2.4.2 Catalyst Selectivity

In contrast to reaction rate, which was dependent on the Y substituent, catalyst enantioselectivity was found to be dependent on the structure of the X substituent. Most of the catalyst enantioselectivity trends are consistent with the tetrahedron stereochemical model as proposed by Park and Jew (Figure 16).[76] The highest enantioselectivities were observed with catalyst series **1** (X = 9-anthracenyl) whereas the lowest enantioselectivities were observed for catalyst series **2** (X = 2-naphthyl). Catalyst series **4** (X = phenyl) was shown to be more selective than both series **2** and series **5** (X = 3,5-$(CF_3)_2C_6H_3$) despite having less steric bulk. This finding suggests that not only the size but also the relative orientation of the X substituent is critical to the enantiomeric ratio of the product. Contrary to previous studies by Dolling et. al. who proposed a π-π stacking interaction in the catalyst-substrate ion pair, increasing the π-acidity of position X did not result in a more enantioselective catalyst; the unmodified benzyl substituent was more selective in every case.[49]

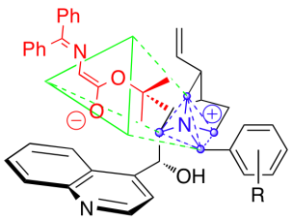

Figure 16. Jew and Park tetrahedron stereochemical model.

Whereas the Y substituent did not provide significant influence on product selectivity, its structure and configuration has provided several insights into the mechanism of asymmetric induction. Earlier work by Dehmlow had shown that inverting the *C*(9) hydroxyl group configuration led to a reversal in product configuration in the APTC epoxidation of naphthoquinones.[63] The insignificant differences in enantioselectivites between the epimeric hydroxy and methoxy series demonstrated that the configuration of the substituent at *C*(9) does not significantly alter the geometry of the catalyst-enolate ion pair. The slight increase in selectivity of the ether catalysts (series **c**, **d**, **e**, and **f**) compared to the *C*(9)-hydroxy and the *C*(9)-deoxyfluoro (series **g**) catalyst would indicate that any additional steric bulk at that position is beneficial to selectivity.

The remarkably similar enantioselectivity values between the *C*(9)-hydroxy and *C*(9)-deoxyfluoro catalyst series (excluding **1g**) suggests that increasing the electronegativity or altering the hydrogen bonding aptitude of substituent Y has only a minor influence on the stereodetermining step. More importantly, a hydrogen bonding interaction originating from the *C*(9) hydroxyl group was not necessary for asymmetric induction. The lack of selectivity with the deoxycinchonidinium catalysts (series **h**) can be attributed to catalyst decomposition. The initial product formed from the elimination can be subsequently *N*-alkylated with the excess benzyl bromide present in the reaction mixture. Although this newly formed quaternary ammonium salt is still chiral, the stereocenters are far removed from the charged center and would provide less influence on the stereodeterming step. The use of a less reactive electrophile would inhibit the formation of the less desired *N*-alkylation product and could result in a more accurate enantioselectivity value of the initial catalyst.

2.5 Conclusion

2.5.1 Summary

A library of 39 catalysts was examined for activity and selectivity for the APTC alkylation of **1**. The catalysts were synthesized cinchonidine by formation of a quaternary ammonium ion at the quinuclidine nitrogen. Catalyst modification was limited to two regions of the *Cinchona* alkaloid scaffold, the *C*(9) hydroxyl group (Y substituent) and the arylmethylene group appended to the quinuclidine nitrogen (X substituent). Five different aromatic groups were screened at the X substituent, and eight different groups were tested at the Y substituent.

In regards to catalyst activity, the *C*(9) substituent was observed to contribute most significantly to reaction half-life. Ether substituents were found to afford the most active catalysts with the configuration at *C*(9) having an insignificant effect on activity. Installation of a fluoro group or removal of the heteroatom at *C*(9) consistently afforded less active catalysts. However, it is unclear whether the increased reaction half-life is due to poor catalyst activity or stability to the reaction conditions. Less active catalysts were also observed when electron-withdrawing groups were incorporated at the X substituent.

Catalyst selectivity was found to be primarily influenced by the structure of the X substituent, with the 9-anthracenyl series affording the most selective catalysts. Inversion of the stereocenter at *C*(9) led to the same major enantiomer of **2** with negligible differences in enantioselectivity. In most cases substitution of a fluoro for a hydroxyl at *C*(9) resulted in catalysts of comparable selectivity. The removal of the *C*(9)-heteroatom led to a substantial loss of selectivity. Combined with the low activity of the deoxycinchonidinium catalyst series, this loss of selectivity is likely related to rapid catalyst decomposition.

2.5.2 Future Directions

Future studies will focus on expanding the catalyst library by introducing modifications to the *Cinchona* alkaloid scaffold. Synthetic targets include heteroatom analogs at the *C*(9) position on the *Cinchona* scaffold. The introduction of two heteroatoms at this position would significantly affect the catalyst's dipole as well as remove a possible catalyst decomposition pathway (Figure 17). Additionally, other X substituents may be introduced similar to those employed for Jew and Park's fourth generation catalyst series.[60,61] Although the selectivity of the 4th generation *Cinchona* alkaloid based catalyst are well known, no investigation into the relative activity of these catalysts has been conducted.

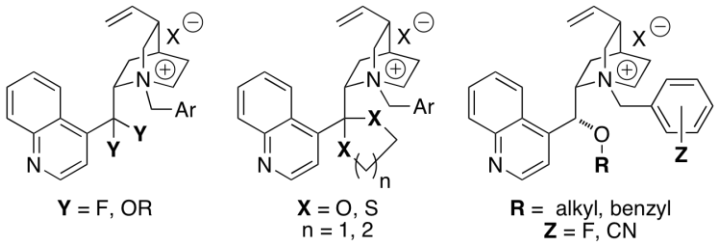

Figure 17. Future catalyst structures.

The presence of two heteroatoms at *C*(9) can also provide significantly more dipole enhancements as well as steric bulk compared to a single heteroatom substituent. Without a hydrogen present a *C*(9) Hoffmann degradation would be less likely and could potentially result in more stable catalysts. Other degradation pathways can still exist, in which the position adjacent to the quaternary ammonium and *C*(9) is deprotonated under sufficiently basic conditions to afford configurationally labile scaffold or eliminate one of the heteroatom substituents (Figure 18).

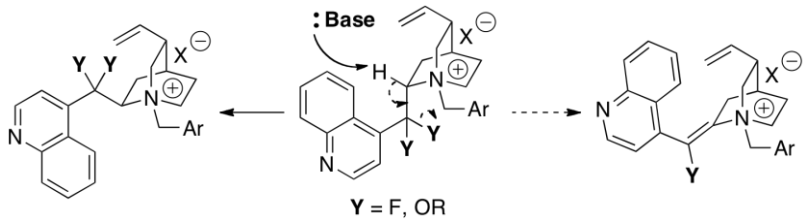

Figure 18. Other decompostion mechanisms.

Efforts are underway to develop a deeper understanding of the stereodetermining step. These studies will provide a more detailed stereochemical model, which can allow for the development of more selective catalysts. An experimental determination of the *E/Z* geometry of the intermediate enolate formed under the standard reaction conditions could provide a better stereochemical model. Previous studies only dealt with the enolate geometry computationally, which suggested a more favorable *E* configuration.[77] A recent study by Porco *et al.* examined the conformation of an enolate/dimeric *Cinchona* catalyst ion pair through NOESY and ROESY NMR spectroscopy in conjunction with molecular docking software, for an asymmetric dearomatization/alkylation reaction.[78] To date, no such spectroscopic study has been conducted for the APTC alkylation reaction with monomeric *Cinchona* alkaloid-derived catalysts. The incorporation of Porco's methods into this study may provide useful insight into the stereodetermining step.

CHAPTER 3: *Asymmetric Phase Transfer Catalyzed [2,3]-Wittig Rearrangement*

3.1. Introduction

3.1.1 Background

The [2,3]-Wittig rearrangement is a well-established reaction within the synthetic chemist's toolbox.[79,80,81,82] The [2,3]-Wittig rearrangement falls under a class of transformations referred to as sigmatropic reactions, which is defined as "the migration of a σ bond flanked by one or more π electron systems, … in an uncatalyzed intramolecular process."[83] Examples of the sigmatropic rearrangements include the [1,5]-hydride shift,[84] the Claisen rearrangement,[85,86,87] and the Cope rearrangement.[85,88,89] Specifically, the [2,3]-Wittig rearrangement can be classified as an anionic sigmatropic reaction (i.e. rearrangement starting material is anionic) which includes reactions such as the Sommelet-Hauser[90,91] and sulfonium ylide[92] rearrangements.

The general transformation of a [2,3] sigmatropic rearrangement is the migration of stabilized carbanion across a π-system, typically an allyl or a benzyl group (Figure 20). When X = O, the rearrangement is called a Wittig rearrangement and for X = N, an aza-Wittig rearrangement. Mechanistically, both [1,2] and [2,3] sigmatropic rearrangement products can be obtained. In nearly all cases, a carbanion stabilizing group, **G**, is required for the rearrangement to occur. The activation energy of the [2,3]-Wittig rearrangment is proportional to the HOMO-LUMO energy gap between the carbanion and π-system, respectively. Less stable carbanions will react faster than their more stabilized counterparts due to an increase in the HOMO energy level.

Scheme 20

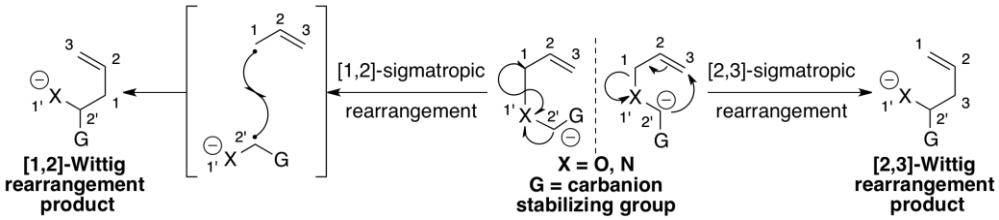

Wittig and Löhmann were first to report this class of pericyclic reaction for the [1,2]-sigmatropic rearrangement of several benzylic ethers.[93,94] Stevens *et al.* observed that the treatment of allyl flourenyl ethers in presence of organolithium bases or sodium alkoxide bases afforded a mixture of both [1,2] and [2,3] rearrangement products (Scheme 21).[95] For the purposes of this report, only the [2,3]-Wittig rearrangement and its asymmetric variants will be discussed in this chapter

Scheme 21

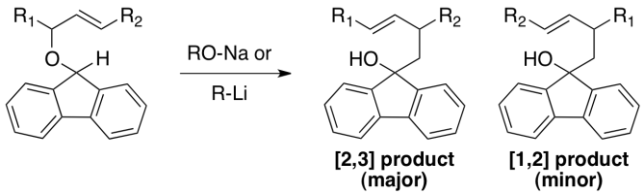

Both [1,2] and [2,3]-Wittig rearrangement pathways can be operative depending on the substrate structure and reaction temperature. Generally, it has been observed that the [1,2] pathway can be inhibited at lower reaction temperatures (Scheme 22).[96] Another factor to consider are the various resonance structures of the intermediate carbanion. Rautenstrauch reported that for the lithiation of bis(prenyl) ether, [1,2], [2,3], [3,4], and [1,4]-rearrangement pathways are possible, but the [2,3]-rearrangement is the dominant pathway (Scheme 23).[96] Alternative rearrangement pathways become more of an issue when substrates contain similar π-systems in close proximity. A related issue to consider is the possibility of additional

sigmatropic rearrangements resulting from the initial rearrangement product. With a suitable substrate, the [2,3]-Wittig rearrangement can be followed by one or a series of sigmatropic rearrangements, such as a Claisen or a Cope rearrangement (Scheme 24).[97,98]

Scheme 22

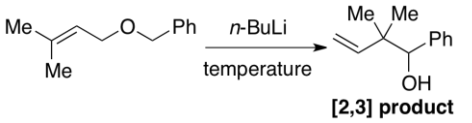

T (°C)	[2,3] : [1,2]
-25	7.5 : 1
25	6 : 1

Scheme 23

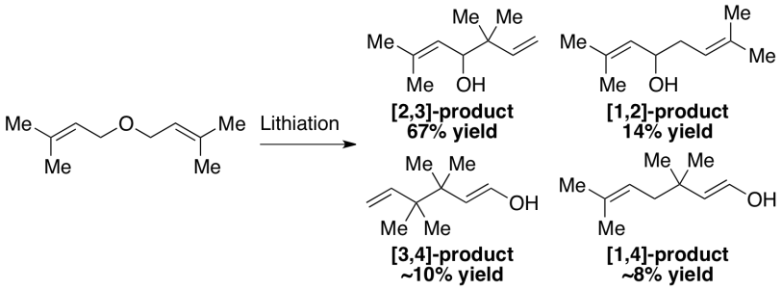

Scheme 24

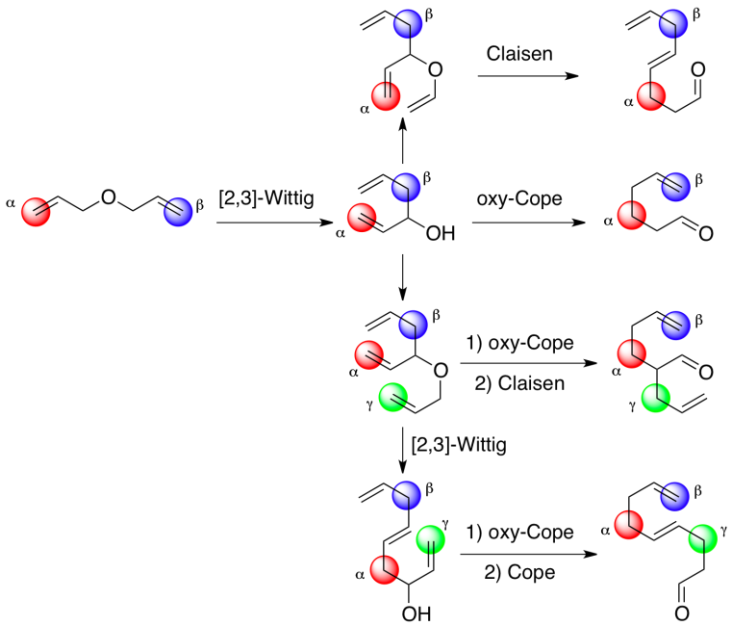

The [2,3]-Wittig rearrangement proceeds by means of a six-electron, five-membered, cyclic transition state in a concerted mechanism. The transition state of the [2,3]-Wittig rearrangement is often represented as one of three different conformations, **A**-**C** (Figure 19).[79,80] Substituent **G** represents the various carbanion stabilizing functional groups and its structure can have a significant impact on the transition state. Generally with monosubstituted alkenes, the [2,3]-Wittig rearrangement affords the (*E*)-olefin as the major isomer. The highest selectivities are observed when **G** is a phenyl or alkynyl group (Scheme 25).[99]

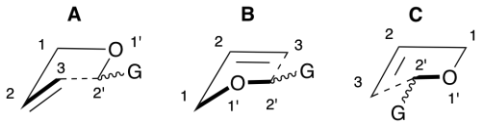

Figure 19. [2,3]-Wittig rearrangement transition state conformations.

Scheme 25

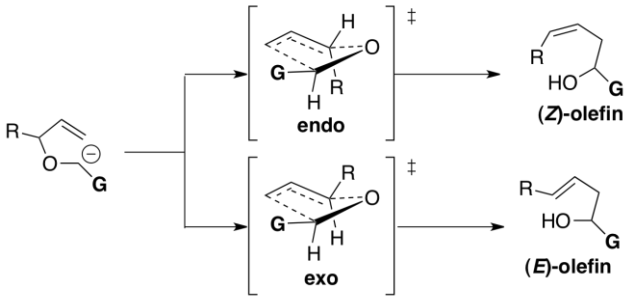

G =	*E*:*Z* Olefin
-Ph	100:1
-C≡C-R (R = H, Me, $SiMe_3$)	98-93:2-7
-CR=CH_2 (R = H, Me)	98:2
-CO_2H	74:26
-CO_2Me	78:22

To selectively access the (*Z*)-olefin as the major, other reaction conditions are required. Experiments conducted by Still and Mitra showed that allyl stannylmethyl ethers serve as excellent carbanion precursors via a tin-lithium exchange to afford the (*Z*)-olefin [2,3]-Wittig product with good to excellent selectivity depending of the substrate substituents (Scheme 26).[100] The organolithium compound resulting from the tin-lithium exchange lacks a stabilizing group, and in its absence the HOMO energy level is raised for the carbanion intermediate. This increase

in the HOMO energy level of the carbanion decreases the HOMO-LUMO energy gap, and therefore significantly enhances its reactivity to afford (Z)-olefin rearrangement products.

Scheme 26

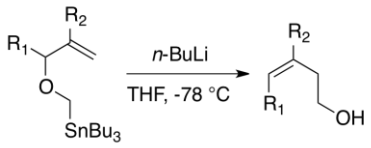

R_1 =	R_2 =	*E* : *Z*
n-C_7H_{15}	H	40 : 60
n-Bu	Me	0 : 100

This high level of stereoselectivity for [2,3]-Wittig rearrangements can be maintained when additional substituents are appended, such as with disubstituted alkene substrates. This high degree of stereocontrol is illustrated in transitions state structures, **T_1-T_4** (Scheme 27). The formation of *cis* or *trans* products with respect to the hydroxy group, is primarily determined by the olefin geometry of the starting material, and the level of diastereoselectivity is greatly impacted by the structure of substituent **G**.

Scheme 27

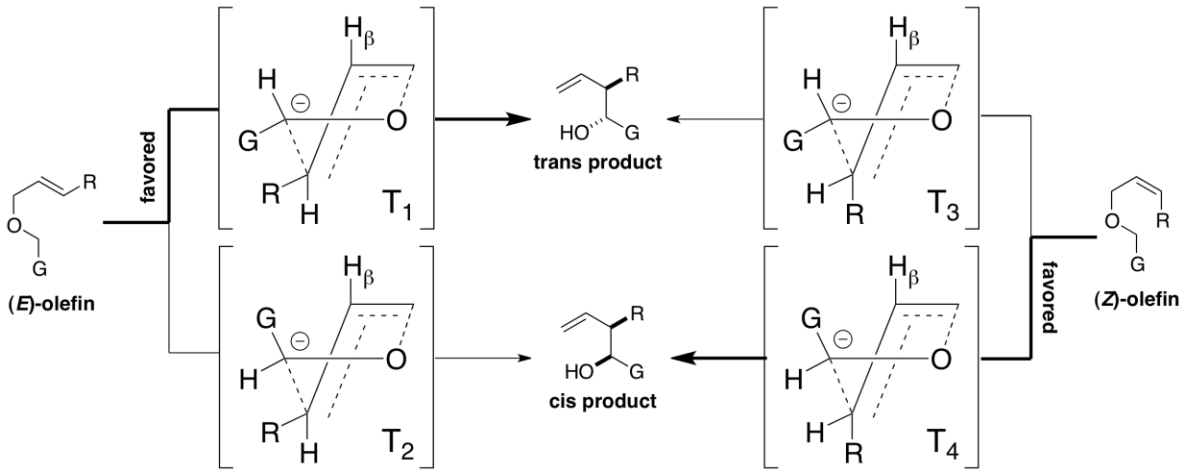

When the [2,3]-Wittig rearrangement substrate is an (*E*)-olefin, **T_1** becomes the favored conformation due to a 1,3-psuedo axial interaction between **H_β** and **G**, thus affording the *trans* product. If a (*Z*)-olefin is employed as the substrate, **T_4** is favored due to a minimization of steric

repulsion between substituent **R** and **G**, thus affording the *cis* product. Generally, (*Z*)-olefin substrates afford more diastereoenriched rearrangement products than their (*E*)-olefin counterparts. The basis for this observation for this observation can be found in $\mathbf{T_3}$ and $\mathbf{T_4}$. If another substituent were appended to the allylic position (to the right of $\mathbf{H_\beta}$) of the substrate, it would result in a $A_{1,3}$ strain interaction with substituent **R**. The stereochemical preferences described previously have dealt primarily with benzylic, allylic, and propargylic substrates (**G** = phenyl, alkenyl, alkynyl). A notable exception to this diastereomeric selectivity can occur with α-allyloxy appended esters, acids, and amides (**G** = CO_2H, CO_2R, and $CONR_2$).[101,102] In these instances, the gauche interactions between **G** and **R** could have more influence and may overcome the pseudo-1,3-diaxial interaction between $\mathbf{H_\beta}$ and **G**. As a result (*E*)-α-allyloxy acids, esters, and amides can afford *cis* products as the major diastereomer.

The asymmetric [2,3]-Wittig rearrangement (AWR) has also been developed successfully and can be organized into four different classes, which include the transition, asymmetric induction, chiral base-induced, and the configurationally defined carbanion type of AWR.[80] For the asymmetric transition class, asymmetry is introduced with the use of a chiral, non-racemic allylic alcohol. Generally this configurationally defined stereocenter is directly involved within the transition state. The second class is referred to as asymmetric induction, which is accomplished by means of a chiral auxillary and is not directly involved in the transition state. The third class of asymmetric variants involves a chiral base induction, typically through the use of chiral, non-racemic lithium amide bases. The fourth class incorporates the use a configurationally defined carbanion, such as those generated via a tin-lithium exchange from a configurationally defined organostannane. Focus will be given to the third class of AWR because the asymmetric induction is derived from reagent control.

The first example of a reagent-controlled AWR was performed by Marshall and Lebreton for the ring contraction of a macrocyclic ether in the total synthesis of (+)-Aristolactone.[103] In this instance, chiral, non-racemic lithium amide bases was employed to afford both enantiomers of the [2,3]-Wittig rearrangement product in good yield and enantioselectivity (er 85.5:14.5 to 86.5:13.5). However, these chiral bases were unselective with acyclic substrates.[104] Later work with this ligand by Marshall and Wang with α-propargyloxyacetic acids underwent the AWR to afford the allenyl alcohol product with low levels of enantioselectivity (er 67:33 to 74:26).[105] Further success with acyclic substrates for the AWR was realized by Kang et al. for allyl propargyl ethers with *sec*-butyllithium and an excess of (-)-α-isosparteine.[106] Good diasteroselectives and low to moderate levels of enantioselectivity (er 64.5:35.5 to 85.5:14.5) were obtained when the reaction was performed at low temperature (-78 °C) in hexane. Manabe had also reported the use of a chiral lithium amide base complex for the AWR of dipropargyl ethers to generate enantioenriched allenyl proparyl alcohols with moderate levels of enantioselectivity (er 73:27 to 81:19).[107] High levels of enantioselectivity were established with acyclic substrate by Jefferson et al. in the AWR with allyl benzylic ethers of tricarbonylchromium complexes.[108] Employing a bidentate lithium amide complex, the selected substrates underwent the AWR in low to good yields with good to excellent levels of enantioselectivity (er 92:8 to 99.5:0.5). Work by Nakai *et al.* also observed good enantioselectivities (er ≤ 94.5:5.5) with acyclic substrate when using a chiral bis(oxazoline) ligand.[109]

Scheme 28

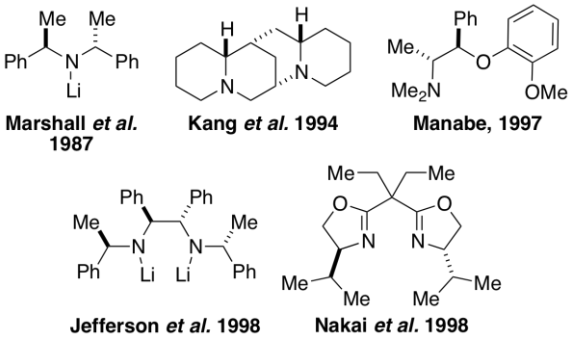

The first catalytic AWR was conducted by Kimachi and Kawaski.[110] In this study, a benzyl allyl ether was treated with *n*-butyllithium in the presence of a substoichiometric amount of (-)-sparteine to afford product in modest yield (44%) and a moderate level of enantioselectivity (er 74:26). Nakai *et al.* explored the catalytic AWR utilizing benzyl allyl ethers, propargyl allyl ethers, *tert*-butylithium, and 0.2 equivalents of a chiral bis(oxazoline) ligand, but afford products with low enantioenrichment (er 65:35–67:33).[111] Maezaki et al. obtained excellent asymmetric induction for a catalytic AWR of an allyl benzyl ether substrate, employing a bis(oxazoline) ligand (Scheme 29).[112] The benzylic alcohol product derived from this rearrangement was obtained in low to moderate yields (23-52%) but with consistently high levels of enantioselectivity (er >97.5:2.5). While this most recent example may suggest the catalytic AWR is well-developed, it employs harsh conditions (alkyllithium bases) at cryogenic temperatures with relatively large quantities of a chiral ligand.

Scheme 29

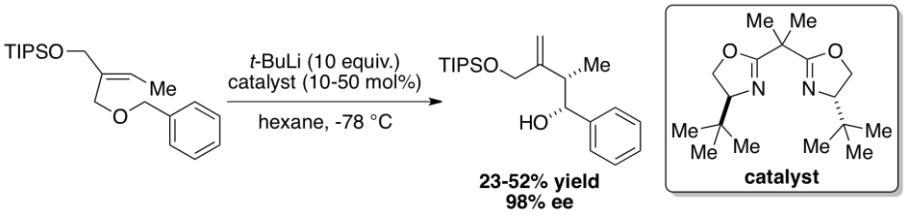

To date only one example of a PTC [2,3]-Wittig rearrangement has been reported. Yamamoto *et al.* observed the rearrangement of several allyl fluorenyl ethers in presence of solid potassium hydroxide and either a quaternary ammonium/phosphonium salt or crown ether as a catalyst (Scheme 30).[113] When more substituted ethers were employed a significant amount of the [1,2]-rearrangement product was obtained, but its formation could be suppressed at lower reaction temperatures. The authors note that aqueous potassium hydroxide, in addition to solid potassium carbonate, bicarbonate, and fluoride were unable to promote the rearrangement. Benzyl allyl ether was found to be completely resistant to rearrangement with all bases examined.

Scheme 30

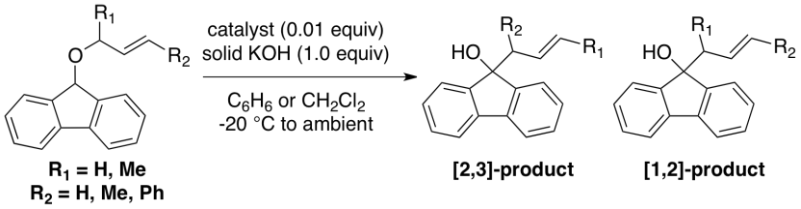

Base-mediated PTC reaction conditions have the potential to generate carbanions of relatively weak C-H acids that are typically associated with traditional [2,3]-Wittig rearrangement substrates and would normally require strong bases for rearrangement, such as organolithiums. For instance, deuterium exchange studies conducted by Rabinovitz *et al.* observed that allyl benzene (pK_a = 34, DMSO) could incorporate a deuterium label and isomerized to β-methyl-styrene when treated with aqueous sodium hydroxide (18.3 M NaOD in D_2O) and toluene in the presence of a catalyst.[114,115] Deuterium was exclusively incorporated at the allylic position of β-methyl-styrene. This finding demonstrated that while carbanion formation from weak C-H acids may occur under PTC conditions, the resulting carbanion was sufficiently reactive such that isomerization was preferred kinetically, even in the presence of an

aqueous solvent. These reports were encouraging for the development of a general PTC [2,3]-Wittig rearrangement.

3.1.2 Objectives

All [2,3]-Wittig rearrangements involve the intermediacy of a carbanion that is typically generated from reactive bases such as alkyllithiums and lithium amides and at cryogenic temperatures. It has been well established that base-mediated PTC is an attractive and efficient method for the generation of carbanions intermediates without the need for reactive bases and employing milder reagents and temperatures (See Chapter 1.1). In particular, the alkylation of PTC-generated carbanions has been applicable to a wide array of substrates, with large range of C-H acidities, and with highly stereoselective variants.[116] It should be possible to develop a base-mediate PTC process for the [2,3]-Wittig rearrangement and potentially other sigmatropic rearrangements. If such carbanions could react with a suitable π-system, a new class of PTC reactions would be open to development.

The [2,3]-Wittig rearrangement was selected amongst other sigmatropic rearrangements because it has employed substrates amenable to other base-mediated PTC reactions (e.g. alkylation), and had the potential to form two contiguous stereocenters. A variety of carbanion stabilizing groups, **G**, would be tested including substrates such as cyanides, carboxylic acids, esters, amides, phosphonates, and sulfonates (Scheme 31). The primary objective of this investigation will be to develop a base-mediated PTC [2,3]-Wittig rearrangement under liquid-liquid reaction conditions. Employing aqueous bases, this PTC rearrangement should have a general substrate scope and afford a minimal amount of side products. Should this PTC rearrangement be found to proceed effectively, a secondary objective will be to develop a first-

in-class APTC [2,3]-Wittig rearrangement with the aid of a chiral, non-racemic quaternary ammonium salt.

Scheme 31

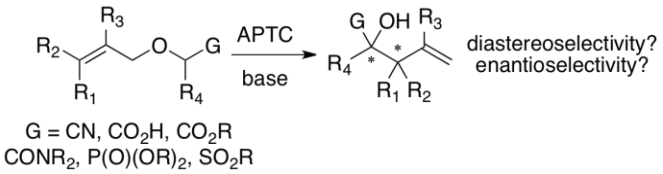

Previous studies have shown substrates such as phenylacetonitrile can be alkylated through the use of base-mediated PTC conditions.[117,118] Additionally, the introduction of an terminally substituted allyloxy group on the methylene carbon position of phenylacetonitrile would afford a substrate capable of [2,3]-Wittig rearrangement.[119,120,121] These reports demonstrate that under homogeneous reaction conditions, the initial [2,3]-Wittig rearrangement product, a cyanohydrin, collapses down to form a ketone under the basic reaction conditions (Scheme 32). A propargyloxy group could also be appended to the same position to afford aromatic allenyl ketones in a stereoselective fashion.[120] Consequently, this class of substrates may only form one stereocenter that is adjacent to a ketone. Substitution of the cyano group with other carbanion-stabilizing groups (e.g. esters, amides, phosphonates) offers the possibility of forming two contiguous stereocenters in a diastereoselective and enantioselective fashion.

Scheme 32

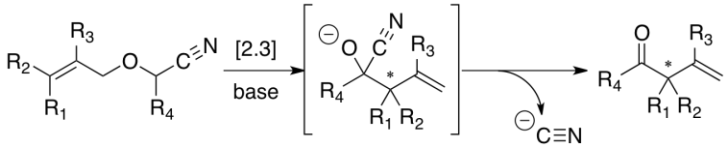

A tertiary objective of this study will be to test higher pK_a C-H acid substrates such as allyl-propargyl, bis(allyl), allyl-benzyl, and benzyl-propargyl ethers. Classical [2,3]-Wittig

rearrangement reaction conditions require the use of lithium amide, aryllithium, or alkyllithium bases. These harsh reaction conditions limit the scope of applicable substrates, making a PTC process a viable alternative.

3.2 Substrate Synthesis

3.2.1 Synthetic Routes Based on Phenylacetonitrile Derivatives

Several obstacles were encountered en route to the desired α-allyloxy-phenylacetonitrile derivatives required to test the feasibility of this reaction. Initially, it was proposed this material could be generated from an α-bromo-phenylacetronitrile and the appropriate alcohol by means of the Williamson ether synthesis.[122,123,124] This route was unsuccessful because the stoichiometric formation of the alkali metal alkoxide led to deprotonation of α-bromo-phenylacetonitrile rather than a displacement of the bromide and afforded a complex mixture of products (Scheme 33). The α-tosyl-phenylacetonitrile was also prepared as a substrate precursor, but several *O*-alkylation conditions tested were unable to afford the desired cyano ether product. A minor amount of the α-crotyloxy-phenylacetonitrile was prepared by heating α-tosyl-phenylacetonitrile in neat crotyl alcohol. However, this method required laborious chromatographic purification, and other alcohols that were tested afforded a complex mixture of products.

Scheme 33

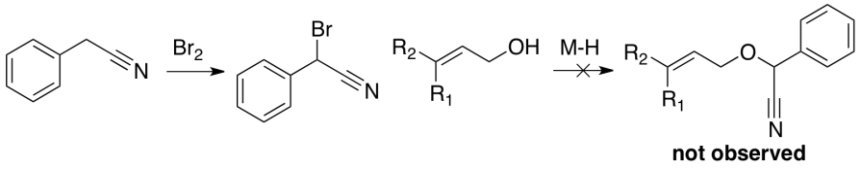

A two-step route for the preparation of α-allyloxy-phenylacetonitrile derivatives from phenylacetonitrile and an allylic alcohol was not viable. Given the acidity of the methine

position of the brominated phenylacetonitrile-derived precursor, alternative synthetic routes were investigated. One option was to perform an *O*-alkylation of a cyanohydrin intermediate, and another option was to perform a cyanide displacement of an acetal with Lewis acid catalysis (Scheme 34).

Scheme 34

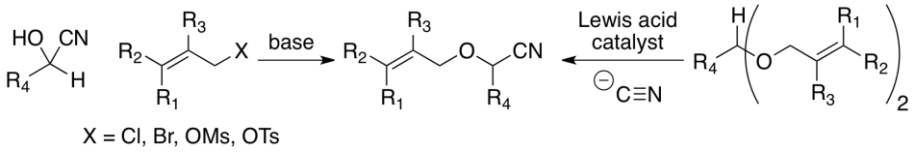

The preparation of α-allyloxy-phenylacetonitrile derivatives was attempted by means of a PTC method with benzaldehyde, aqueous potassium cyanide, allyl bromide, and a catalyst, triethylbenzylammonium chloride.[125] When 3-bromo-2-methyl-2-propene was used as the alkylating agent, only a trace amount of the desired product was observed with the majority of the product determined to be the substituted allyl cyanide. Other conditions developed by Cazes and Julia for the synthesis of substituted cyanoethers have been reported, and these routes have yet to be fully investigated (Scheme 35).[126,127]

Scheme 35

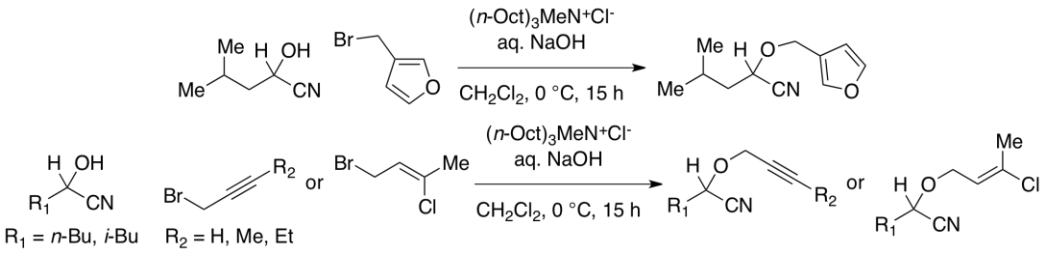

3.2.2 Current Synthetic Route

A recent disclosure by Oriyama and Iwanami reported the preparation of α-allyloxy-phenylacetonitrile from benzaldehyde, trimethylsilyl allyl ether, trimethylsilyl cyanide, and a

substoichiometric amount of ferric chloride in one-pot.[128] Replication of this procedure with trimethylsilyl allyl ether afforded the desired product in good yield and purity (Scheme 36). Unfortunately, the use of more substituted TMS-protected allyl alcohols did not afford the desired product. The use of crotyl, prenyl, and cinnamyl derivatives resulted in a complex product mixture in each case.

Scheme 36

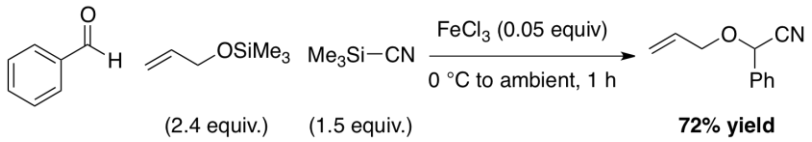

Because these substrates were required only for a proof of concept experiment, extensive experimentation to indentify the cause of this failure was not performed. Instead of troubleshooting the one-pot method described previously, the synthesis was split into two separate reactions, acetalization followed by displacement with cyanide.

Crotyl (R_1=H, R_2=Me), prenyl (R_1=Me, R_2=Me), cinnamyl (R_1=H, R_2=Ph), and (*E*)-α-methyl-cinnamyl alcohol (R_1=Me, R_2=Ph) were *O*-silylated by heating in neat hexamethyldisilazane to afford the desired products in good to excellent yields after distillation (Scheme 37). The crotyl, prenyl, and cinnamyl alcohols were commercially available and used directly without further purification.

Scheme 37

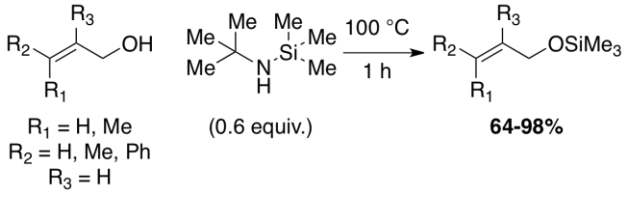

To prepare α-methyl-cinnamyl alcohol, acetophenone was treated with triethylphosphonoacetate in the presence of *n*-BuLi in a Horner-Wadsworth-Emmons olefination.[129] Chromatographic purification afforded a 5:1 ratio of *E*:*Z* olefin isomers of the α,β-unsaturated ester product in 79% overall yield (Scheme 38). Each ester was subsequently reduced with diisobutylaluminum hydride (DIBAL-H) to afford both the *E* and *Z* allylic alcohols in 50% and 76% yield, respectively.[129] Later experiments found this reduction could be performed with lithium aluminum hydride at 0 °C to selectively afford the 1,2-reduction product in 89% yield starting from the (*E*)-olefin (Scheme 39).

Scheme 38

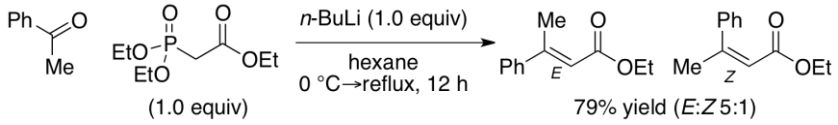

Scheme 39

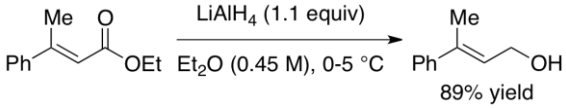

Only the prenyl and (*E*)-α-methyl-cinnamyl silyl ethers were carried forward to the target α-allyloxy-phenylacetonitrile substrate by means of the two step acetalization/cyanation route. Employing Noyori acetalization conditions, both TMS-ethers were combined with benzaldehyde and a substoichiometric amount of trimethylsilyl trifluoromethanesulfonate to afford the desired acetal in good and moderate yields (Scheme 40).[130] Unfortunately, this procedure has thus far been irreproducible. The source of problem is unknown at this time, and other acetalization methods are currently under investigation.

Scheme 40

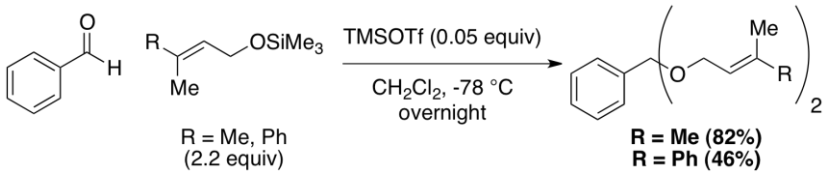

From here the acetal was treated with one equivalent of cyanide in the presence of a Lewis acid catalyst to afford a cyanoether product.[131] Several Lewis acids were examined and stannous chloride was found to be the most effective catalyst. Employing a slight excess of trimethylsilyl cyanide as the cyanide source, the target α-allyloxy-phenylacetonitrile analogues were prepared in moderate to low yields (Scheme 41).

Scheme 41

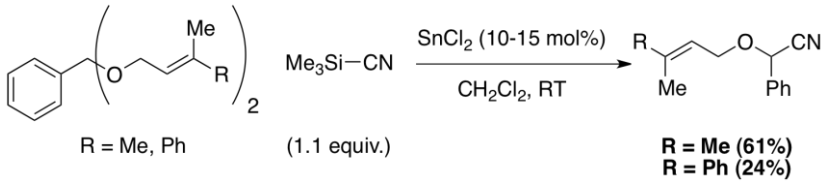

Although this route was ultimately successful in providing adequate amounts of substrate for proof of concept experiments, a more general and efficient synthesis would be required for examining the substrate scope of the PTC [2,3]-Wittig arrangement. Ideally, such a synthetic route would be based on the use of allylic alcohol precursors, given their potentially large structural diversity and ease of preparation. Transition metal-catalyzed diazo insertion into an O-H bond was briefly investigated although ultimately unsuccessful, likely due to competeing reactivity of the alkene functional group.[132,133] Unless the reproducibility issue of the acetalization reaction can be overcome, the most promising route for the preparation of the cyanoethers would be a base-mediated alkylation of a cyanohydrin.

3.3 Results and Discussion

3.3.1 Achiral [2,3]-Wittig Rearrangement Substrates

Once sufficient amounts of the α-allyloxy-phenylacetonitriles were prepared, a proof of concept experiment was performed under base-mediated PTC reaction conditions utilizing tetrabutylammonium bromide (TBAB) as the phase transfer catalyst. Employing an aqueous potassium hydroxide/toluene biphase, the starting material was consumed within 20 minutes at ambient temperature after the addition of base (Scheme 42). In the absence of TBAB, no reaction was observed after stirring overnight at ambient temperature.

Scheme 42

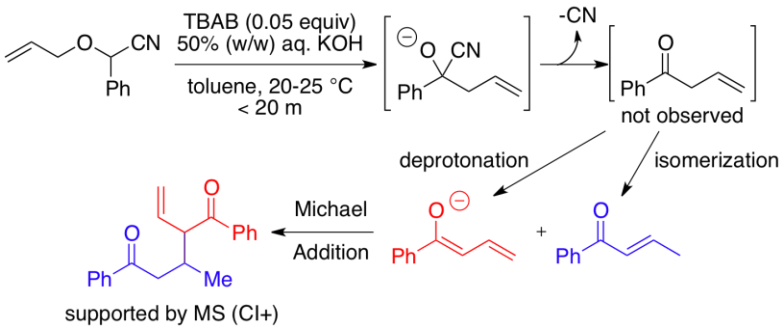

Isolation and purification of the crude product led to an interesting observation. The ^{13}C-NMR spectroscopic data from the purified material indicated the presence of two ketone functional groups, and the ^{1}H-NMR spectroscopic data contained far too many ^{1}H absorbences to support a phenyl allyl ketone structure. Both the thin-layer (TLC) and gas chromatography (GC) data supported the formation of a single compound, or at the least the formation of a mixture of inseparable isomers. The most interesting result came for the chemical ionization (CI+) mass spectrometry data, which supported the formation of a Michael addition product (293.1 *m/z* [M-H^{+}]). This observation can be explained by the formation of an enolizable ketone as the initial product of the reaction. The allyl ketone may form an enolate intermediate under the reaction

conditions, and any enolate that is subsequently isomerized to an α,β-unsaturated ketone could participate in a Michael addition with the enolate. Ultimately, this proof of concept experiment had demonstrated that the facile deprotonation of the initial [2,3]-Wittig rearrangement product led to rapid, undesired side reaction.

The use of a crotyloxy analogue (Scheme 32, R_2=Me, R_4=Ph) suffered the same pitfall as the rearrangement of α-allyloxy-phenylacetonitrile. The initial [2,3]-Wittig rearrangement product was observed to isomerize to an α,β-unsaturated ketone under the base-mediatied PTC reaction conditions (Scheme 43). This product structure was supported by two methyl signals in the ^{1}H-NMR spectrum, one doublet and one singlet. With this result in hand, it was deemed unnecessary to examine the cinnamyloxy derivative (Scheme 32, R_2=Ph, R_4=Ph) given the likelihood of isomerization.

Scheme 43

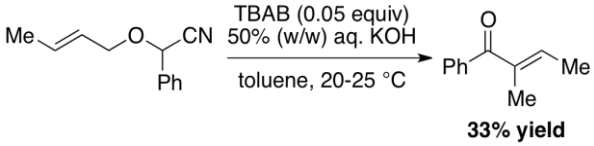

33% yield

While disappointing, the observation of a rapid isomerization under the reaction conditions is not surprising. Given the C-H acidity of the initial [2,3]-Wittig rearrangement product (pK_a <25, DMSO), the thermodynamic stability provided by the formation of a trisubstituted alkene over a monosubstituted one, and the extension of the conjugated π-system, it would have been more surprising had the product not isomerized under the reaction conditions. This isomerization had unfortunate side effect of destroying the one stereocenter formed in the sigmatropic rearrangement, thus limiting the choice of substrate to terminally disubstituted allyloxy analogues for an APTC reaction.

When two methyl groups were appended to alkene terminus of α-allyloxy-phenylacetonitrile and then subjected to base-mediated PTC reaction conditions, the desired [2,3]-Wittig rearrangement product was afforded in 66% yield (Scheme 44). The ^{1}H-NMR spectrum of the product after chromatographic purification contained ^{1}H absorbencies suggestive of a trace amount of the [1,2]-Wittig rearrangement product. Replication of this reaction with the same substrate on larger scale would be required in order to confirm this finding. These proof of concept experiments demonstrated that under base-mediated PTC reaction conditions, carbanions derived from alpha-allyloxy-phenylacetonitrile and its analogues will successfully undergo a [2,3]-Wittig sigmatropic rearrangement.

Scheme 44

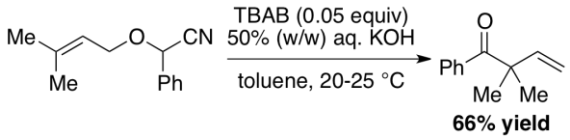

3.3.2 Preliminary APTC [2,3]-Wittig Rearrangement

With the feasibility of the PTC [2,3]-Wittig rearrangement established, the secondary objective of this study, the development of an APTC [2,3]-Wittig rearrangement was initiated. For this study, substrates would have to be limited to terminally disubstituted allyl groups to yield quaternary stereocenters adjacent to ketones. Using the dimethyl, terminally, disubstituted substrate as a starting point, a methyl group was replaced with a phenyl ring to generate the (*E*)-olefin configuration and a prochiral substrate. Initially, TBAB was first used as a catalyst, both to generate racemate and to provide a rough estimate of reaction time at lower temperatures (0 °C). The first chiral, non-racemic quaternary ammonium salt catalyst tested was Corey's catalyst (See Chapter 2, catalyst **1d**). However, after two additions of 0.1 equivalents of catalyst and two days

of stirring at ambient temperature, no starting material was observed to undergo the rearrangement. When a [5,5,5]-pyrolizindium catalyst was employed for the rearrangement, the starting material was consumed in less than an hour at 0 °C to afford the desired product in 49% yield and an enantiomeric ratio of 55:45 (Scheme 45).[73,134] This was the first example of asymmetric induction for a [2,3]-Wittig rearrangement under PTC reaction conditions! The absolute configuration of the product was not determined.

Scheme 45

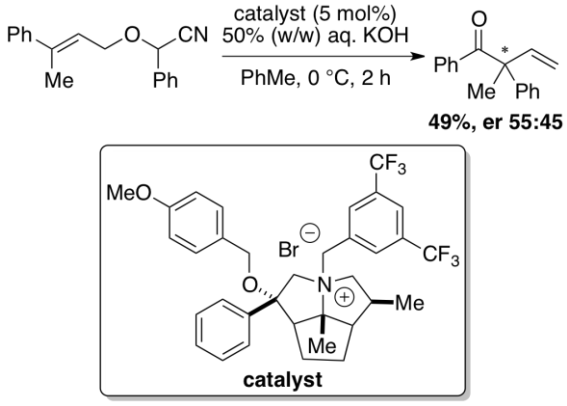

The absence of catalytic activity with a *Cinchona* alkaloid derived catalyst was surprising. It is unclear at this time whether this result is due to the decomposition of the catalyst or it is simply unable to promote the rearrangement. One possibility, is that the formation of the ammonium•carbanion ion pair leads to an unfavorable conformation of the reactant carbanion and therefore unable to participate in a [2,3]-Wittig rearrangement. If a quaternary ammonium hydroxide intermediate is indeed responsible for the generation of the reactive carbanion, then another possibility exists that the hydroxide ion-pair derived from Corey's catalyst is simply unstable. Because only one chiral, non-racemic catalyst has been found to promote asymmetric induction, the degree to which enantioselectivity could be further improved is unknown. Given

the unimolecular nature of the [2,3]-Wittig rearrangement, it is possible that an entirely different catalyst scaffold would be required for a high level of enantioselectivity.

3.4 Conclusion

3.4.1 Summary

This preliminary investigation into the [2,3]-Wittig rearrangement has demonstrated that α-allyloxy-phenylacetonitrile and its more substituted analogues are capable of undergoing rearrangement under PTC reaction conditions. Further, the choice of substrate was critical to the structure of the product. The initial rearrangement products that possessed enolizable hydrogens were found to isomerize under the base-mediated reactions conditions to an α-β-unsaturated ketone. Therefore, all potential APTC substrates could only afford quaternary stereocenters adjacent to ketones. A proof of concept APTC [2,3]-Wittig rearrangement was conducted with a [5,5,5]-pyrolizindium catalyst but only afforded low levels of enantioselectivity.

3.4.2 Future Directions

Preliminary investigations have begun to expand this new reactivity to other substrates. α-Allyloxy-*t*-butyl acetate has been tested under similar PTC reaction conditions, however no [2,3]-Wittig rearrangement product was detected (Scheme 46). While this was a disappointing result it was not entirely unexpected. Earlier experiments by Nakai *et al.* had shown that the [2,3]-Wittig rearrangement pathway could not be obtained with α-allyloxy-esters in a LDA/THF system alone.[135] It was found that only after the addition of hexamethylphosphoramide (HMPA, 25% by vol.) could the [2,3]-Wittig rearrangement proceed to afford the desired hydroxy ester. That same study also observed that carboxylic acids and amides proceeded through a [2,3]-

Wittig rearrangement without the addition of HMPA. The authors propose that lithium coordination to the enolate minimizes the carbanion reactivity of ester substrate. Other methods exist for the preparation of [2,3]-Wittig rearrangement products from ester substrates, although with a limited substrate scope.[136]

Scheme 46

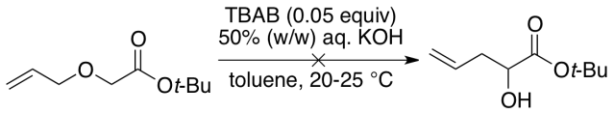

If the base-mediated PTC method could be extended successfully to the ester substrate class, it would represent an attractive alternative to traditional reaction conditions. It is likely that alternative PTC reaction conditions (*e.g.* solvent, catalyst, base) would be required for a successful rearrangement of the ester substrate class.

CHAPTER 4: *Phase Transfer Catalyzed Phenol Alkylation*

4.1. Introduction

The past several decades have seen tremendous advances in the realm of phase transfer catalysis (PTC).[1,5,12,14] One type of PTC reaction that has shown considerable importance is base-mediated reactions. Since the initial developments of PTC processes, base-mediated PTC has become the most widely employed class of PTC reactions. Base-mediated PTC reactions are used for the deprotonation of acidic organic reactants to generate reactive anions, which can then undergo a multitude of nucleophilic displacements within the organic solvent. Roughly 60% of all commercial PTC processes incorporate the hydroxide ion as a reagent.[137]

A wide range of acidic substrate are accessible for a base-mediated PTC reaction, and may include functional groups such as O-H acids (e.g. carboxylic acids, alcohols, phenols), N-H acids (e.g. amines, amides), and C-H acids (e.g. ketones, esters, alkyl nitriles) to name a few. Among the most useful base-mediated PTC reactions are alkylations, through formation of C-O, C-N, and C-C covalent bonds. Although homogeneous reaction conditions have traditionally been used to access these reactive anion intermediates, in many cases strong bases (pK_a >35, DMSO) are required. Perhaps the greatest advantage of a base-mediated PTC process is the use of inexpensive, relatively less reactive bases, such as alkali metal hydroxide and carbonate bases as aqueous solutions or solids.

Although the substrate and reaction scope of base-mediated PTC reactions is well-developed, some more fundamental questions remain. For instance, how does the intrinsic reactivity of a quaternary ammonium-carbanion intermediate under PTC reaction conditions compare to the reactivity of an alkali metal-carbanion under homogeneous reaction conditions. The latter has been extensively studied and has shown a large dependence on solvent polarity

and choice of cation.[138] Are the same factors responsible for reactivity under homogeneous reaction conditions applicable to the catalytic activity in a PTC process? Given the large structural diversity of quaternary ammonium cations, the exact role of the catalyst structure on intrinsic reactivity of the ion-pair intermediate under PTC reaction conditions remains obscure.

4.1.1 Mechanism

With respect to the kinetics of a PTC reaction, catalyst activity is controlled by three factors (1) the reaction rate in the organic phase, (2) the mass transfer steps between the organic and aqueous phases and (3) the distribution equilibrium of the tetraalkylammonium species between two phases.[139] Base-mediated PTC reactions operate in a mechanistic continuum that is significantly dependent on the pK_a of the organic substrate and the lipophilicity of the catalyst species. More acidic substrates (pK_a <18 (DMSO)) often react by means of an extractive mechanism, whereas more basic substrates proceed through an interfacial mechanism (See Chapter 1). Should a catalyst species be sufficiently lipophilic such that its aqueous phase concentration is negligible, interfacial transport steps must be invoked to account for any observed catalytic activity. It is important to note that just because mass transport through an interfacial layer is part of a kinetic rate expression in a PTC reaction, it does not imply that the reaction proceeds through an interfacial mechanism. For an interfacial mechanism to be operative, the rate-determining step must be one of the transport steps to or from the interfacial layer.

Regardless of which mechanism is dominant, because base-mediated PTC reactions involve an additional anionic species, generally hydroxide (OH^-), the kinetics analysis becomes complicated due to additional transfer steps (Figure 20). In the context of Starks' extraction

mechanism, hydroxide stays in the aqueous phase where it can deprotonate the organic substrate (R-H) to generate reactive anion intermediate (M^+R^-), and the catalyst (Q^+X^-) can partition between both phases. The intermediate M^+R^- can then undergo ion exchange with Q^+X^- to generate the catalyst•anion reactive intermediate (Q^+R^-) in the bulk aqueous phase. If Q^+R^- is sufficiently lipophilic, then it will partition into the organic phase where it can react with a suitable electrophile (R'-X).

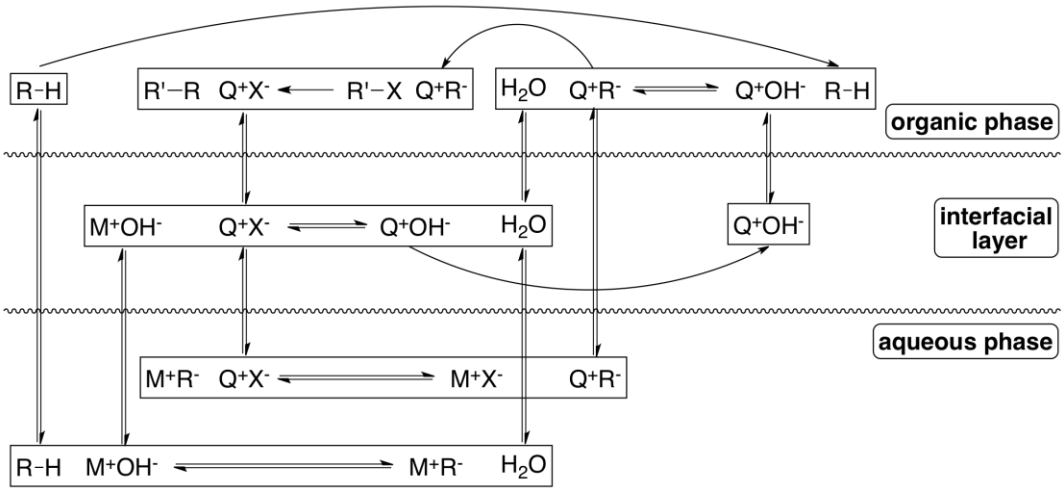

Figure 20. Base-mediated PTC extraction mechanism with hydroxide base.

A modification of this mechanism was proposed by Brändström and Montanari, in which Q^+X^- or R-H is unable to partition into the aqueous phase, but can exist in the interfacial layer of the organic/aqueous biphase.[140,141] At the interphase, Q^+X^- can undergo ion exchange with the hydroxide base (M^+OH^-) also present to generate a catalyst□hydroxide species (Q^+OH^-). The now more lipophlic base, Q^+OH^-, can deprotonate the R-H at the interphase (not shown) or migrate to the organic phase for the deprotonation. The product of either deprotonation, Q^+R^-, may then migrate into the organic phase and participate in the intrinsic reaction with R'-X to generate the final product (R'-R).

An interfacial mechanism can arise in one of two ways for a base-mediated PTC reaction. For PTC process with a visible and distinct biphase, the reaction rate is typically limited by the transport of Q^+R^- out of the interfacial layer. The interfacial mechanism can also arise from the formation of a third liquid phase (TLP) depending on the reactants, catalyst, and conditions employed. The former scenario will not be discussed here because it has already been extensively studied for a range of reactions.[142,143,144,145,146,147] The latter scenario is more interesting because it can manifest from PTC reactions normally operating under an extraction mechanism by a relatively minor change in reaction conditions (e.g. catalyst loading, temperature).[148]

4.1.2 Background

Despite the complexity of transfer steps in a base-mediated PTC process, a more fundamental question persists. How does the intrinsic reactivity of Q^+R^- affect the overall catalytic activity of Q^+X^- in a PTC process? To investigate this question, a suitable model, base-mediated PTC reaction would be developed, one that would also been amenable to homogeneous reaction conditions. In this regard, the alkylation of phenol was chosen for this study. This subset of PTC alkylation has been well studied in regards to reaction conditions, scope of electrophile, and the phenol substrate derivatives.[137,149] Depending on the reaction conditions and catalyst employed, the PTC alkylation of phenol can proceed by means of an extraction or interfacial mechanism.[148]

The first examples of a PTC alkylation of phenol was reported by McKillop *et al.* that subjected many different phenols and several naphthols with several alkylating agents, mainly methylating agents, in the presence of a substoichiometric amount of tri(*n*-

butyl)benzylammonium bromide (Scheme 47).[150] Wang and Yang conducted more detailed PTC alkylation studies for the allylation of 2,4,6-tribromophenol for the purpose of optimizing the synthesis of a monomer in the development of poly-bromominated polymers (Scheme 48).[151]

Scheme 47

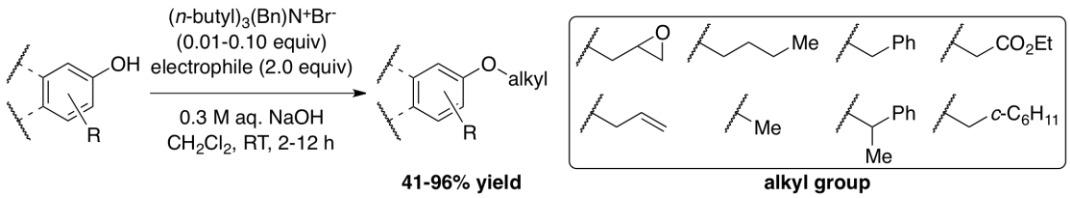

Scheme 48

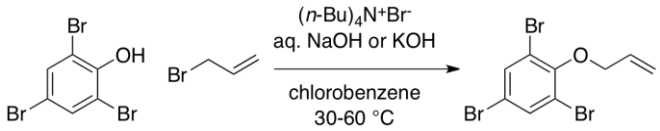

This mechanistic study found that potassium hydroxide was a better aqueous base, more polar, organic solvents afforded higher reactivities, and above an impellor speed of 600 rpm, stirring rate did not affect the reaction rate. The reaction was observed to be first order in catalyst, tetra(n-butyl)ammonium bromide (TBAB), and allyl bromide. Similar alkylation rates were observed for tri(n-butyl)benzylammonium bromide as well. A later kinetic modeling study by the same authors, determined the intrinsic alkylation rate of the quaternary ammonium□phenoxide ion-pair.[152] With this information in hand, it was possible to computationally model this particular PTC alkylation based on the mass transfer and distribution coefficients of the ammonium species present in the reaction. There was excellent agreement between the model and experimental data.

The reactivity of phenoxides has been extensively investigated under homogeneous reaction conditions, both in the context of total synthesis and the initial development of a linear

free energy relationship (LFER).[153,154,155,156,157] One of the earliest studies that examined the reactivity of ammonium phenoxides was undertaken by Ugelstad *et al.* for the alkylation of butyl halides under homogeneous reaction conditions (Scheme 49).[158] The substitution of a potassium cation by a tetra(*n*-butyl)ammonium cation was found to increase the rate of alkylation by several orders of magnitude more, and the reaction rate of the ammonium phenoxide was significantly less sensitive to the polarity of the solvent compared to the potassium salt.

Scheme 49

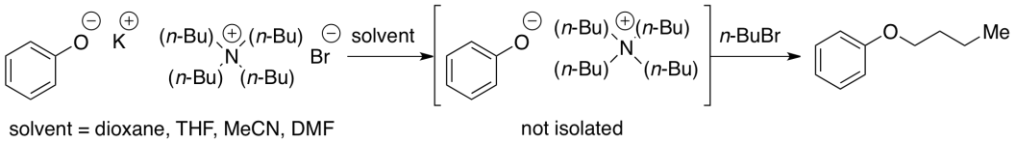

The augmented reactivity of the quaternary ammonium phenoxide is rationalized by the greater ionic radius of the tetra(*n*-butyl)ammonium cation (~4.37 Å)[159] compared to the potassium ion (1.33 Å).[160] This increase in charge separation allows for greater localization of charge density on the phenoxide oxygen, thus leading to enhanced nucleophilicity.[161] Computational studies have determined that the interaction energy for tetrabutylammonium phenoxides (2.5 kcal/mol) is significantly lower than for sodium phenoxide (4.5 kcal/mol), further supporting the observation that ammonium ion-pairs are more reactive than their alkali metal counterparts.[162]

Although the PTC alkylation of phenol was chosen as the model reaction, the first detailed investigation that aimed to elucidate the role of catalyst structure on a PTC nucleophilic displacement was undertaken by Landini *et al*. with inorganic anions.[163] The authors examined the rates of displacement of six anions (e.g. halides, cyanides, azides) with *n*-octyl methanesulfonate in the presence of eleven different quaternary ammonium salts and two phosphonium salts in a chlorobenzene/water biphase (Scheme 50). Stirring speeds above 300

rpm were found to have no influence on the reaction rate and suggested that an extraction mechanism was operative.

Scheme 50

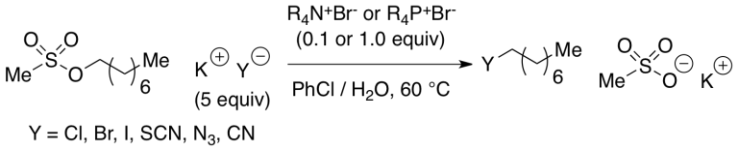

In addition to studying the reaction under PTC conditions, intrinsic reaction rates for eight different quaternary ammonium•anions were determined under homogeneous conditions. Furthermore, when these homogeneous reaction rate studies were conducted with wet solvent, the specific water content of which was determined from Karl-Fisher titration under the respective PTC reaction conditions, the intrinsic reactivities were found to closely resemble that of the PTC reaction rates. This finding led the authors to conclude that the level hydration of the ion-pair intermediate significantly influences the intrinsic reaction rate of a PTC process. A later study by the same authors sought to answer what effect the level of hydration of the anionic nucleophile would have on the intrinsic reactivity of the quaternary ammonium ion-pair.[164] Their investigation revealed that decreasing the level of hydration led to reaction rates approaching that of the rates under anhydrous homogeneous reaction conditions. Specifically in the displacement of *n*-octyl methanesulphonate with tetra(*n*-hexyl)ammonium phenoxide•nH$_2$O, a factor of 75 rate enhancement was observed upon increasing the aqueous sodium hydroxide base concentration from 15% to 50% and a reduction in the hydration state from n = 4.0 to n = 1.5. Additional experiments on the rate of the Hoffman elimination for quaternary ammonium ions have demonstrated that the effect on intrinsic reactivity by the level of hydration is significantly enhanced for anionic nucleophiles with high charge density, such as hydroxide and fluoride.[165]

A more thorough study emphasizing the effect of catalyst structure on the alkylation of thiophenol with 1-bromooctane was undertaken by Herriott and Picker (Scheme 51).[166] In their investigation, the activities of nearly two dozen phase transfer catalysts were determined. The authors observed that catalysts with longer alkyl groups led to increased reactivity.

Scheme 51

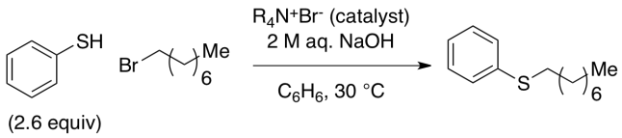

With the catalysts examined in this study, no alkylation rate ceiling (i.e. activity plateau) was observed. Attempts were made to determine the intrinsic reactivity of the ion pair intermediate with the homogeneous alkylation rate of tetra(*n*-butyl)ammonium thiophenoxide. Unfortunately, the authors were unable to obtain reproducible alkylation rates and could not conclude to what degree the reactivity of the catalyst•thiophenoxide ion-pair played in the catalytic reactivity.

Landini and Maia reported the most comprehensive comparison between the intrinsic reactivity of a quaternary ammonium ion-pair and its activity as a catalyst under PTC reaction conditions.[167] In the displacement of *n*-octylmethane sulphonate with chloride anion or the displacement of *n*-butyl bromide with 4-nitro-phenoxide anion under PTC reaction conditions, the authors observed significant rate constant differences between the organic solvents (chlorobenzene and 4-methyl-2-pentanone) and the quaternary ammonium cation employed ($Me(n\text{-}Bu)_3N^+$, $(n\text{-}Bu)_4N^+$, $(n\text{-}Hex)_4N^+$) (Scheme 52).

Scheme 52

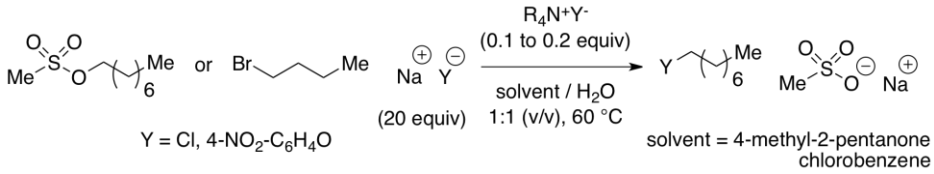

In the chlorobenzene/water biphase, the rate constant increased by a factor of a 100 with the chloride anion and nearly a factor of 14 for the 4-nitro-phenoxide anion going from Me(*n*-Bu)$_3$N$^+$ to (*n*-hexyl)$_4$N$^+$. For the 4-methyl-2-pentanone/water biphase, a 20-fold rate constant enhancement was observed with the chloride anion and virtually no enhancement was observed with the 4-nitro-phenoxide anion with the same quaternary ammonium catalysts. The authors rationalized this observation based on the partition coefficient of the quaternary ammonium nitrophenoxide in 4-methyl-2-pentanone, which was found to be very soluble in the more polar ketone solvent, in contrast to chlorobenzene. The intrinsic reactivity of the ion-pair was examined under homogeneous reaction conditions for the displacement of *n*-butyl bromide with the respective quaternary ammonium halide (I^-, Br^-, and Cl^-) in a chlorobenzene, methyl-*tert*-amyl ether, and 4-methyl-2-pentanone solvents. A 1.7 to 30-fold rate constant enhancement was observed in comparison to the analogous reaction conducted in the biphase. In general, a much wider range in rates was observed under anhydrous, homogeneous reaction conditions, in which chloride anions were found to be the most reactive.

4.1.3 Characterization of the Quaternary Ammonium Phenoxide

To perform an accurate kinetic analysis between homogeneous and PTC reaction conditions so that a comparison between intrinsic reactivity and catalytic activity could be made, a suitable procedure for the preparation of quaternary ammonium phenoxides would be required.

Nielsen and Hammerich found that treatment of tetra(*n*-butyl)ammonium hydroxide with two equivalents of phenol, followed by azeotropic removal of water with cyclohexane, afforded the homo-hydrogen bonded quaternary ammonium phenoxide dimer, $(n\text{-Bu})_4N^+[(PhOH)OPh]^-$ (Scheme 53, left).[168] Reetz *et al.* reported the X-Ray crystal structure of $(n\text{-Bu})_4N^+[(PhOH)OPh]^-$ and prepared the complex by a similar protocol, wherein water was removed under high-vacuum over phosphorus pentoxide (Scheme 53, right).[169] The ion-pair distance between the phenoxide oxygen and the α-carbon adjacent to the ammonium center was measured as 3.340 Å (Figure 21).[170]

These higher order aggregates are less prone to decomposition when paired with quaternary ammonium salt due to the decreased basicity (i.e. nucleophilicity) of phenoxide anion in the homo-hydrogen bonded complex.[154] Landini *et al.* have demonstrated that quaternary ammonium hydroxide ion-pairs are capable of undergoing a Hoffman elimination pathway (i.e. deprotonation of the β-hydrogen with respect to the ammonium center).[171] In the absence of hydrogen bond donors (e.g. H_2O), the phenoxide anion may react with its quaternary ammonium counterion.

Scheme 53

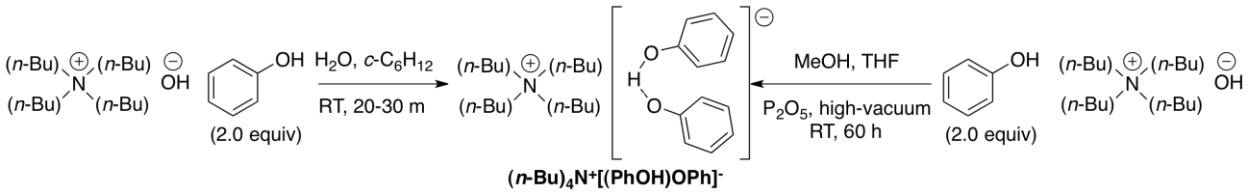

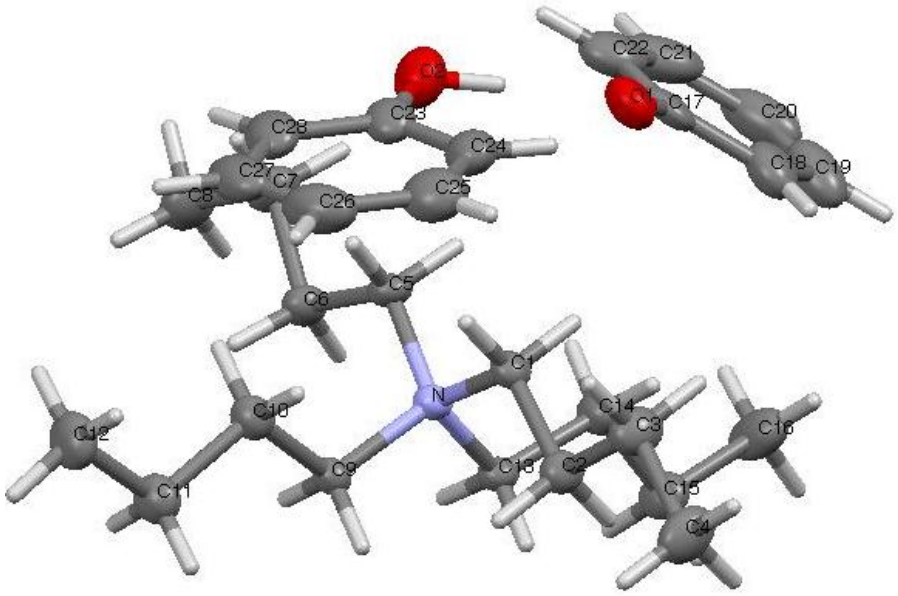

Figure 21. X-Ray crystal structure for $(n\text{-Bu})_4N^+[(PhOH)OPh]^-$.

Limited solution phase characterization studies on quaternary ammonium borohydride ion-pairs have been conducted by Pochapsky *et al.*[172,173] Employing nuclear Overhauser effects (NOE) on tetra(*n*-butyl)ammonium borohydride in a $CDCl_3$ solvent, the authors observed a significant enhancement at the α-CH (18.0%) and β-CH (8.1%). No concentration dependence was observed over a 0.02 to 0.60 M range, indicating that aggregate formation (if any) had an insignificant effect on the proximity of the borohydride anion to the ammonium center. Combined with CPK modeling (i.e. space-filling) calculations, the authors estimated the nitrogen-boron distance at ~3 Å.

4.1.4 Objectives

The objective of this study was to develop a quantitative structure activity relationship (QSAR) for the PTC alkylation of phenol with linear, symmetric quaternary ammonium salts. Six ammonium cations would be examined, Me_4N^+, Et_4N^+, $(n\text{-Pr})_4N^+$, $(n\text{-Bu})_4N^+$, $(n\text{-Hex})_4N^+$,

and (n-Oct)$_4$N$^+$. These particular ammonium cations were chosen for this study because they were readily available as their bromide salts and spanned a large range of relative lipophilicity. For each ammonium cation, the relative contribution of anion activation and anion transport to PTC reaction rate would be determined. To do so, the reactivity of the ammonium phenoxide under homogeneous reaction conditions and the activity of the same ammonium salts under PTC reaction conditions would be determined. This investigation would serve to answer a fundamental question, namely, what role does charge separation (i.e. nucleophile activation) play in PTC reaction rate.

4.2 **Results**

The synthesis and alkylation kinetic studies of the quaternary ammonium, homo-hydrogen bonded phenoxides were performed by a Nathan D. Gould.[174]

4.2.1 Synthesis of the Quaternary Ammonium Phenoxides

The requisite quaternary ammonium hydroxides were prepared from the commercially available bromide salts by ion exchange, closely following the protocol of Harlow, Noble, and Wild, with the exception that anhydrous methanol was used as the solvent rather than isopropanol.[175] Multiple passes (3 to 6) through an Amberlyst^{TM} A-26 resin were required to fully exchange the halide for hydroxide.[176] The resulting quaternary ammonium hydroxide solutions in methanol were titrated for total base to a phenolphthalein endpoint (3-6 determinations) and titrated for residual halide with an ion selective electrode (2-3 determinations).[177] The extent of exchange was greater than 97% in all cases, and the methanolic

salt solutions could be stored at -20 °C for an extended period (~1 month) with no change in effective base concentration.

The quaternary ammonium hydroxide solutions were then combined with a solution of phenol in dioxane to afford a quaternary ammonium phenoxides. Removal of water from these solutions was accomplished by three azeotropic concentrations with additional dioxane which then afforded finely powdered solids that could be handled in a glove box (Scheme 54). The stoichiometry of the phenoxide complexes was confirmed by treating the salts with a stoichiometric excess of benzyl bromide in acetonitrile. The ratio of benzyl phenyl ether to phenol was found to be 1:1 (± 0.04) by GC analysis in all cases. Thus, the salts corresponded to the homo-hydrogen bonded complexes of the ammonium phenoxides, $R_4N^+[(PhOH)OPh]^-$.

Scheme 54

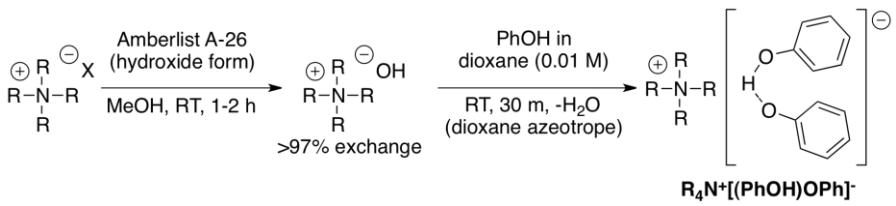

4.2.2 Kinetic Analysis of Phenoxide Alkylation under Homogeneous Reaction Conditions

The intrinsic reactivity of the $R_4N^+[(PhOH)OPh]^-$ ion-pair was determined by employing conditions directly analogous to the most comprehensive set of data available, namely, reaction with a slight excess of 1-bromobutane in acetonitrile at 0.016 M.[158] The least polar, water immiscible, aprotic solvent that was tested and could completely dissolve the ammonium phenoxides was diisopropyl ketone (DIPK).[178] Initial-rate kinetic data was collected for each ammonium phenoxide as well as the corresponding sodium and potassium homo-hydrogen bonded dimers in each solvent (Scheme 55).[179]

Scheme 55

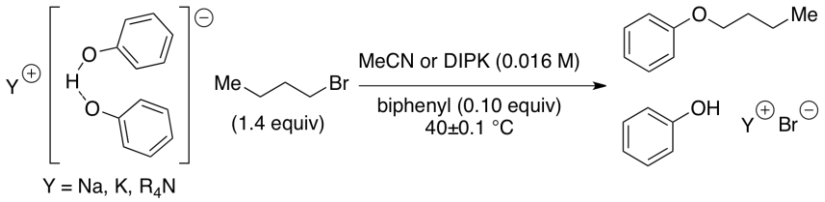

The reactions were monitored to typically 5-10% conversion and reaction rate was expressed as the mean of triplicate reactions in terms of the change in *n*-butyl phenyl ether concentration (mol/L) with respect to time (s).[180] The error bars in the summary plot represent one standard deviation in reaction rate (Figure 22). The alkylation rate for $Na^{+}[(PhOH)OPh]^{-}$ was 5.09 x 10^{-8} (mol*L^{-1}*s^{-1}) and was not shown on the plot.

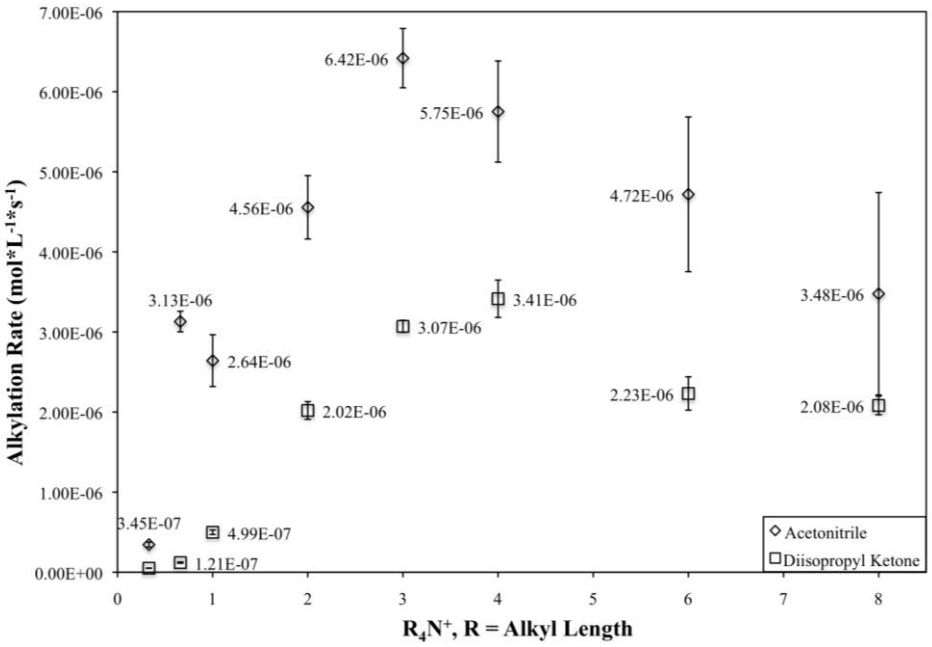

Figure 22. Stoichiometric ammonium phenoxide reactivity.

Reactions performed in acetonitrile were between a factor of 1.5 to 5 faster than those in DIPK in every case, with the quaternary ammonium cations examined. Overall, the reaction rates were more reproducible in DIPK than acetonitrile, potentially as a consequence of the difficulty of removing all adventitious water from the acetonitrile. The homogeneous, phenoxide alkylation

survey showed a strong solvent dependence on the rate of the reaction when the cation employed was an alkali metal (Na^+ and K^+) or Me_4N^+. For acetonitrile, the alkylation rate increased by a factor of 9 going from sodium phenoxide ($Na^+[(PhOH)OPh]^-$) to a potassium phenoxide ($K^+[(PhOH)OPh]^-$). Whereas with DIPK, the rate increase going from sodium to potassium was slightly greater than a factor of two. The alkylation rate of $K^+[(PhOH)OPh]^-$ was 18% higher than that of $Me_4N^+[(PhOH)OPh]^-$ in acetonitrile. In contrast, the rate for $Me_4N^+[(PhOH)OPh]^-$ was higher than potassium by more than a factor of 4 in DIPK.

In comparison of both solvents, DIPK showed a wider range in rate (a factor of 67), whereas acetonitrile displayed a narrower range in reactivity (a factor of 18.6). The highest reaction rate in acetonitrile was observed for the $(n\text{-Pr})_4N^+$ and was faster than the most active cation in DIPK, $(n\text{-Bu})_4N^+$, by nearly a factor of two. For quaternary ammonium cations larger than Me_4N^+, the range in rate for acetonitrile varied by a factor of 1.8, and for DIPK the reactivity range varied by a factor of 1.7. This finding was surprising given the difference in ionic radius between the Et_4N^+ and $(n\text{-Oct})_4N^+$ cation. Furthermore, the alkylation rates for Et_4N^+ and $(n\text{-Oct})_4N^+$ in DIPK were remarkably similar at 2.02×10^{-6} versus 2.08×10^{-6} ($mol*L^{-1}*s^{-1}$), respectively.

4.2.3 Kinetic Analysis of Phenoxide Alkylation under PTC Reaction Conditions

The PTC alkylation of phenol with *n*-butyl bromide was then conducted as a comparison to the stoichiometric, homogeneous ammonium phenoxide alkylation rates (Scheme 56). The same series of quaternary ammonium cations that were employed for the homogeneous reaction study were surveyed under PTC reaction conditions starting from the quaternary ammonium bromide. Both phases appeared homogeneous prior to and after the addition of *n*-butyl bromide

at ambient (~20 °C) and elevated temperature (40 °C). This eliminated the possibility of any solid to liquid transfer steps. Biphenyl was employed as an internal standard to monitor the initial rate for the formation of *n*-butyl phenyl ether by GC analysis.

Scheme 56

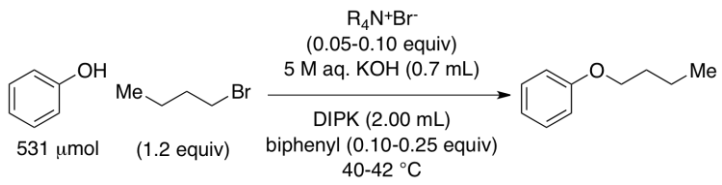

Employing these reactions conditions, the background reaction was very slow; only 5% conversion to product was observed after five days.[181] Several aqueous base concentrations were tested (10 M and 50% (w/w) aq. NaOH and KOH), and it was observed that 5 M aq. KOH afforded the most reproducible results. Higher aqueous base concentrations led to the formation of a white precipitate and alkylation rates that were too rapid to reliably monitor. All of the catalysts were screened at 0.05 equivalent loading and at 0.10 equivalent loading for tetra(*n*-propy)ammonium bromide (TPAB), tetra(*n*-butyl)ammonium bromide (TBAB), tetra(*n*-hexyl)ammonium bromide (THAB), and tetra(*n*-octyl)ammonium bromide (TOAB).

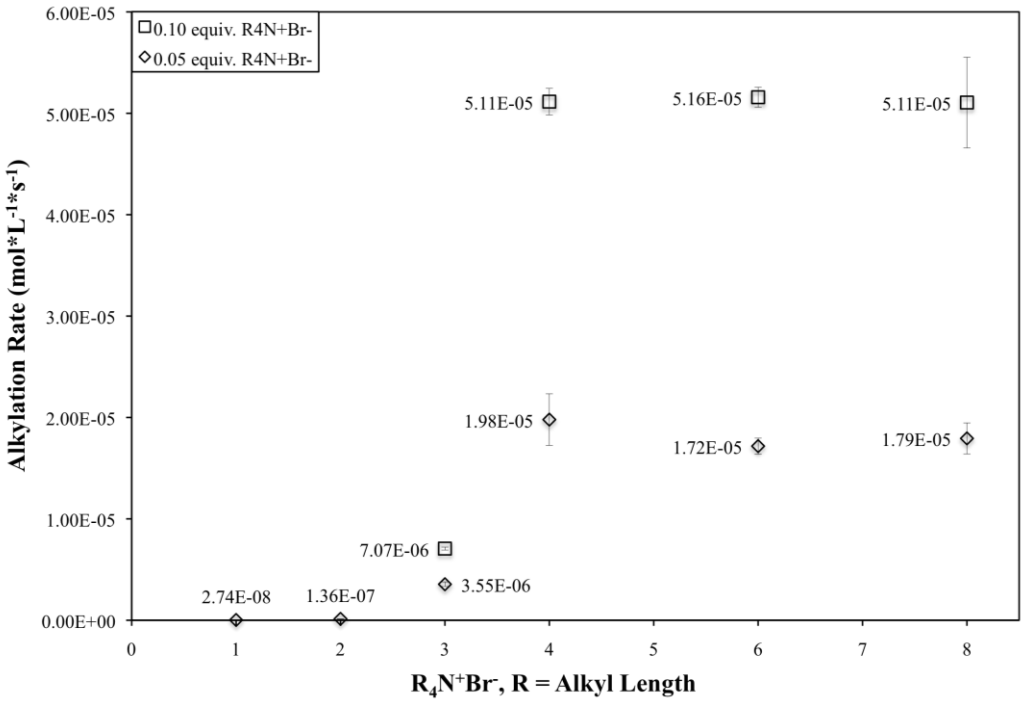

Figure 23. Catalyst survey for PTC phenol alkylation.

Tetramethylammonium bromide (TMAB) was found to be an inactive catalyst at 0.05 equivalent loading and afforded an alkylation rate no greater than the background rate. At the same catalyst loading, tetraethylammonium bromide (TEAB) was able to catalyze the reaction 4.6 times faster than background and TPAB catalyzed the reaction 167 times faster than background. Another significant jump in catalytic activity was observed with TBAB, which afforded a 660 fold rate increase over background and the represented the maximum rate for the catalyst series. For catalysts more lipophilic than TBAB, only a small change in catalytic activity was seen at 0.05 equivalents and virtually no difference was seen at 0.10 equivalents of catalyst.

Carrying out the alkylation with 0.10 equivalents insteads of 0.05 equivalents of TPAB afforded a two fold increase in alkylation rate, consistent with intrinsic-rate limited PTC reaction that is first order in catalyst. However, for TBAB, THAB, and TOAB a 2.6, 3.0, and 2.9 factor increase, respectively, in alkylation rate was observed upon doubling the catalyst loading. These

increases in alkylation rates suggest the presence of higher order ammonium and potassium phenoxide aggregates in the organic phase. The emergence of an interfacial mechanism may also be responsible for the alkylation rate augmentation.

The range in catalytic activity (a factor of 660) was approximately an order of magnitude greater than the range in reactivity observed for $R_4N^+[(PhOH)OPh]^-$ observed under homogeneous reaction conditions (a factor of 67). A relatively large difference in catalytic activity was observed with TEAB and TPAB under PTC reaction conditions, in contrast to the homogeneous reaction conditions that displayed similar reactivities with the same ammonium cations. As was the case in the reactions of the ammonium phenoxides under homogeneous reaction conditions in DIPK, a maximum rate was observed with the $(n\text{-Bu})_4N^+$ cation. However, in DIPK under homogeneous reaction conditions the reactivity went down after $(n\text{-Bu})_4N^+$, whereas under PTC reactions conditions the activity stayed nearly constant after TBAB. The catalyst survey under PTC reaction conditions clearly demonstrates that the intrinsic reactivity of $R_4N^+[(PhOH)OPh]^-$ has little effect on the catalytic activity.

4.2.4 Order in Electrophile for the PTC Phenol Alkylation

It was first hypothesized that the leveling off in catalytic activity after TBAB under PTC reaction conditions was the result of a change in reaction mechanism. Specifically, it was proposed that the PTC reaction deviated from an intrinsic-rate limited process, either with small or large alkyl chains on the quaternary ammonium cation. To test for the possibility of a change in reaction mechanism, the order in electrophile was determined. The PTC reactions with TPAB and TOAB were repeated using a range of *n*-butyl bromide equivalents spanning an order of magnitude (0.5, 1.0, 2.0, and 5.0 equivalents with respect to phenol) (Figure 24). If a change in

reaction mechanism were operative (i.e. a change from intrinsic rate to transport rate limiting), then a different order in electrophile would be observed for the two catalysts. If one of the catalysts led to a transport rate-limited PTC reaction, then a zero order in *n*-butyl bromide would be expected.

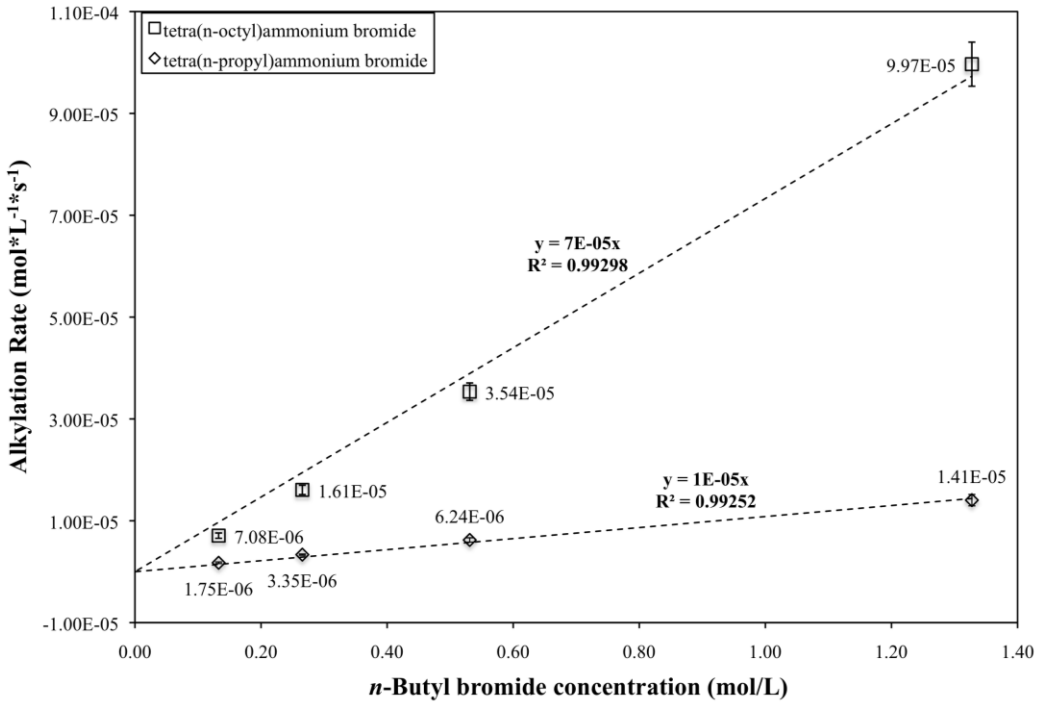

Figure 24. Variable n-butyl bromide equivalents.

A direct, linear relationship of *n*-butyl bromide concentration on alkylation rate was observed for both catalysts. With TPAB, the alkylation rate increased a factor of 8 over the range of *n*-butyl bromide concentrations, and with TOAB over the same range; the alkylation rate increased a factor of 14. For a reaction that is first order in electrophile, the initial alkylation rate should only increase by a factor of 10. It is possible that increasing the quantity of *n*-butyl bromide in the reaction may change the polarity of the bulk organic solvent, thereby affecting the intrinsic reactivity of the tetraalkylammonium phenoxide ion-pair. Neither catalyst demonstrated a zero order in *n*-butyl bromide, and this finding supported an intrinsic reaction rate-limiting

PTC reaction. In essence, the rate-determining step of this PTC reaction is the alkylation of the ammonium phenoxide in the organic phase.

4.2.5 Effect of Variable Stirring Speed on PTC Alkylation Rate

To determine whether an extraction mechanism or interfacial mechanism was operative, a variable stirring speed experiment was conducted with TBAB as the catalyst (Scheme 57). The PTC reaction had to be run at ambient temperature because of the design of the electric motor. The stirring speed was varied from 500 rpm to 2000 rpm, and no stirring speed dependence on the reaction rate was observed above 500 rpm (Figure 25). Therefore, this result supports an extraction mechanism and an intrinsic reaction rate-limited PTC reaction.

Scheme 57

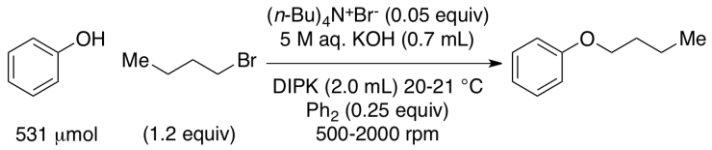

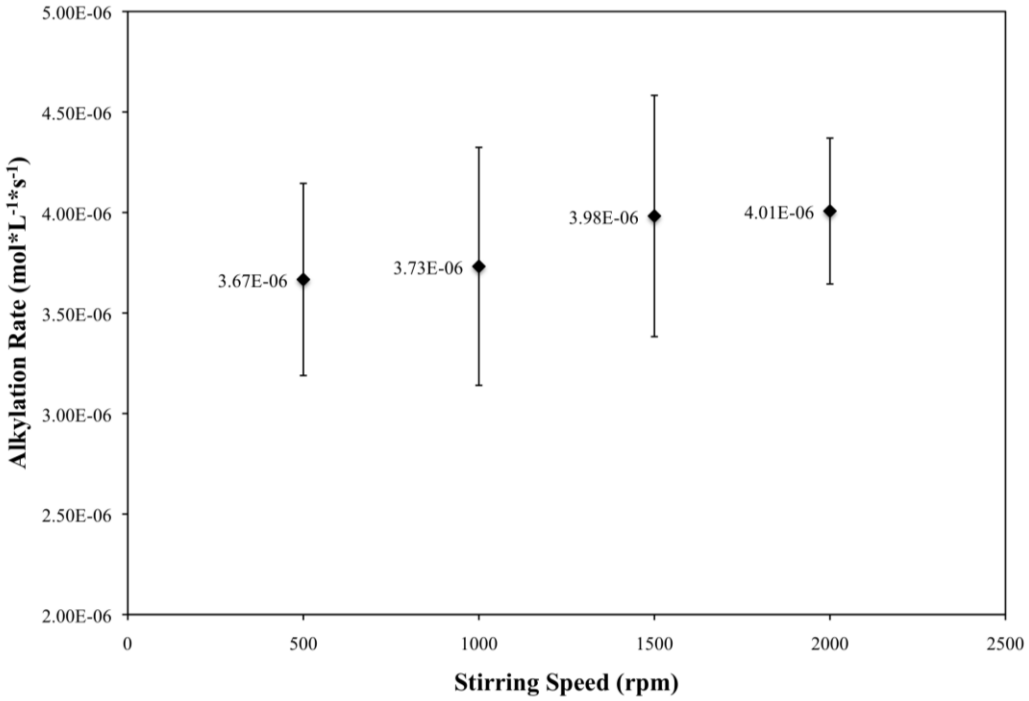

Figure 25. Variable stirring speed under PTC reaction conditions.

4.2.6 UV-vis Spectroscopy of the Aqueous Phase

The results of the previous studies had supported that an extraction mechanism was operative in this PTC reaction, with the rate-determining step being the intrinsic reaction in the organic phase. It was postulated that the concentration of the quaternary ammonium phenoxide intermediate, [$R_4N^+PhO^-$], approaches its theoretical maximum with TBAB, THAB, and TOAB. To test this hypothesis several experiments were conducted to quantify the amount of this reactive species in the organic phase. Given that the reaction of interest was the alkylation of phenol, it was reasoned that the partition of phenol could be analyzed by UV-vis spectroscopy. Unfortunately, DIPK is a UV-active solvent and masked the UV absorption of phenoxide anion. Instead, the change in phenoxide concentration of the aqueous phase would be used to calculate the amount of phenoxide transferred to the organic phase by difference (Scheme 58).

Scheme 58

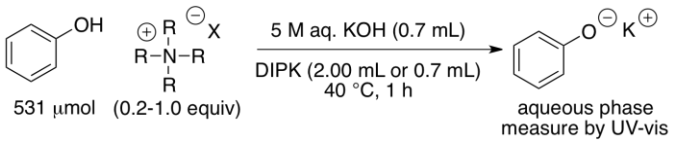

The same tetraalkyl ammonium bromide catalysts were surveyed for the amount of phenoxide transferred to the organic phase at 0.2 and 1.0 equivalents (Figure 26). With 1.0 equivalent of catalyst the organic phase volume was reduced to 0.7 mL, the same as the aqueous phase volume. No measurement was made with 0.2 equivalents of TMAB, a hydrophilic ammonium salt, due to the likelihood of an insignificant change in aqueous phase concentration.

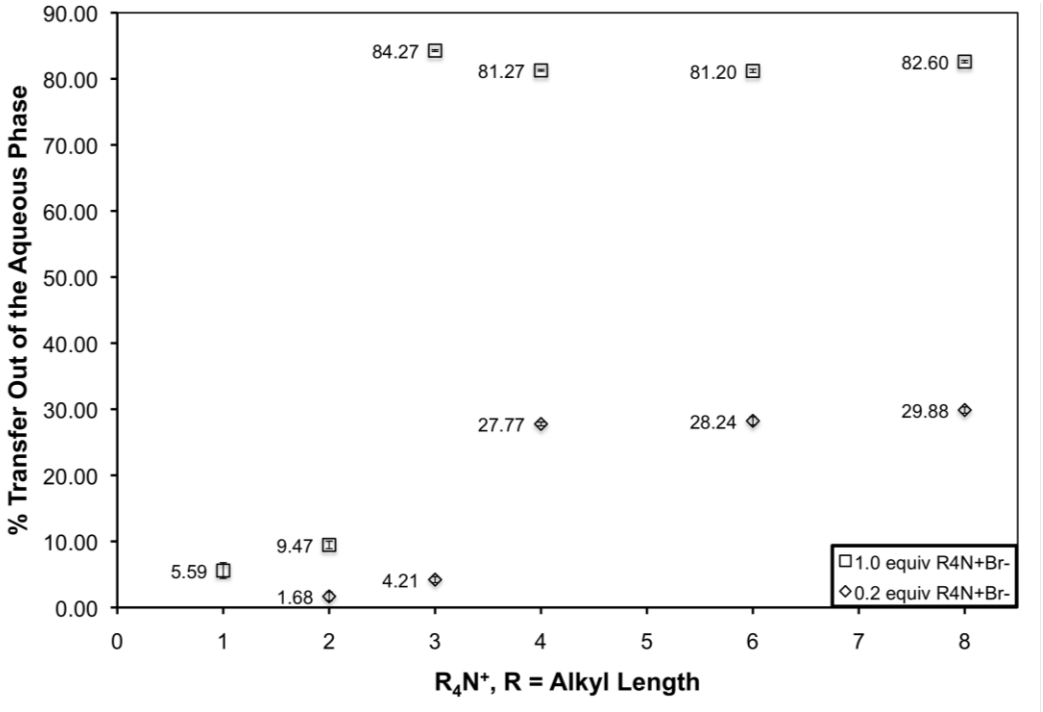

Figure 26. UV-vis data for the transfer of aqueous phase phenoxide.

The results from the UV-vis absorbtion survey show that at 1.0 equivalent loading the more lipophilic salts, TPAB, TBAB, THAB, and TOAB, transferred a large amount of phenoxide out of the aqueous phase. The less lipophilic salts, TMAB and TEAB, would transfer

a much smaller amount (c.a. 5-10%). At 1.0 equivalent of TPAB, an amber colored third liquid phase (TLP) was observed that formed between the aqueous and organic phases (Figure 27). An analysis of the TLP by UV-vis spectroscopy found that the phenoxide concentration was a little more than twice the starting aqueous phase concentration.[182]

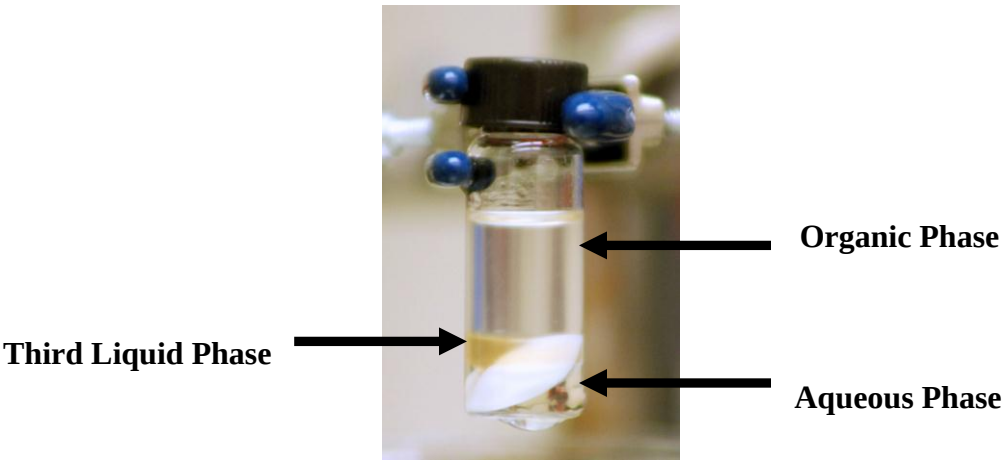

Figure 27. Third liquid phase visible with 1.0 equivalent of TPAB.

At 0.2 equivalent catalyst loading, a large difference in phenoxide transport was observed between TEAB and TBAB (a factor of 16.5). The largest change was found going from TPAB to TBAB, which afforded nearly a 7-fold increase in the transport of phenoxide out of the aqueous phase. At 0.2 equivalents of TPAB, the amount of transferred phenoxide was drastically reduced and no TLP was observed. Taking into account the relatively large alkylation rate observed for TPAB (a factor of 120 over background), this finding suggests that the observed TLP is rich in both ammonium and phenoxide ions. The critical catalyst concentration required for the formation of TLP with TPAB was not determined.

The second important finding from the catalyst survey with UV-vis spectroscopy was that the amount of phenol transferred to the organic phase with TBAB, THAB, and TOAB, was 27.2%, 27.6%, and 29.3% when only 0.2 equivalents of the ammonium salts were employed,

respectively. This corresponds to a greater than 100% transfer of phenoxide per molecule of tetraalkylammonium salt. This striking and unexpected finding stimulated a more direct and refined analysis of the composition of the phenoxide species in the organic phase.

4.2.7 Benzyl Bromide Titrations of the Organic Phase

The first stage in this study was to quantitatively determine the composition of the organic phase. Direct analysis of the organic phase was accomplished by quenching reaction aliquots with an excess of benzyl bromide so that the active phenoxide concentration could be determined by measuring the amount of benzyl phenyl ether formed. The quenched reaction aliquots were analyzed by gas chromatography with the aid of a biphenyl internal standard. The same set of tetraalkylammonium salts were surveyed at 0.1 equivalents with respect to phenol (Figure 28).

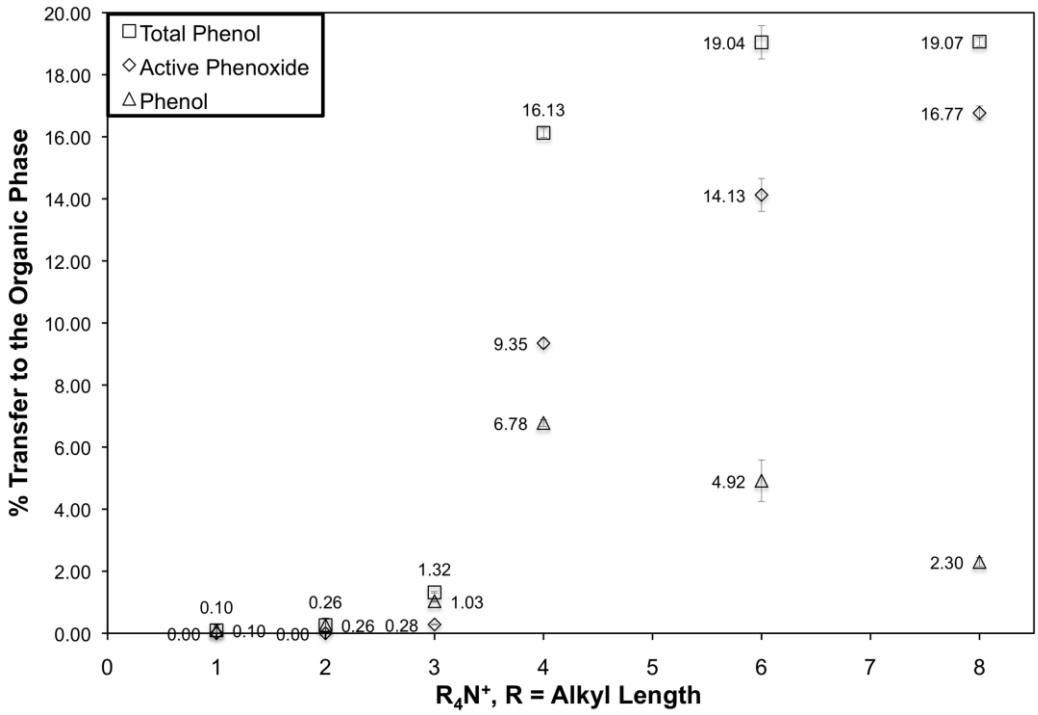

Figure 28. Benzyl bromide titration of organic phase using 0.1 equiv of $R_4N^+Br^-$.

At 0.10 equivalent catalyst loading, both TMAB and TEAB had no active phenoxide present in the organic phase and only a minimal amount of phenol had transferred. This finding was expected given their respectively sluggish alkylation rates. With TPAB a small amount of active phenoxide was present in the organic phase, but with substantial greater proportion of phenol. The active phenoxide content with TPAB was lower than expected given its relatively large PTC initial alkylation rate. A significant amount of active phenoxide was present in the organic phase for TBAB, THAB, and TOAB with a 9.35, 14.13, and 16.77%, respectively. The amount of active phenoxide was found to increase with increasing the alkyl chain length of the catalyst, and the greater than 10% transfer of active phenoxide to the organic phase suggests the presence of potassium phenoxide complexed with the ammonium phenoxide.

A notable feature of this catalyst survey was the presence of phenol in the organic phase. This was unusual because hydroxide base was chosen as the aqueous phase, and the acid/base equilibrium should heavily favor (by several pK_a units) the formation of potassium phenoxide over phenol. Even more interesting was that the concentration of organic phase phenol was unique to each ammonium salt examined, and therefore not simply a consequence of the employed base and organic solvent. For TBAB, THAB, and TOAB the amount of transferred phenol was found to be 6.78, 4.92, and 2.30%, respectively. The less lipophilic ammonium salts showed a lesser amount of phenol in the organic phase. What was unexpected was the difference in phenol and active phenoxide content between the lipophilic catalysts, given their similar alkylation rates. The amount of transferred phenol was found to decrease with increasing alkyl chain length of the catalyst.

Attempts to quantify the amount of potassium phenoxide associated with [$R_4N^+PhO^-$] in the organic phase have been limited. An experiment that employed 0.10 equivalents of TOAB,

provided a sample for direct analysis of the organic phase. After quenching the organic phase phenoxide with an excess of benzyl bromide, analysis by inductively coupled plasma-optical emission spectroscopy (ICP-OES) found that the concentration of potassium in the organic phase was 590 ppm (590 mg/L). This value corresponds to a 6.82% transfer of potassium phenoxide to the organic phase based on the initial amount of phenol. Given that there was a 16.77% transport of active phenoxide to the organic phase with TOAB, this leads to a 9.95% transport of $[R_4N^+PhO^-]$ to the organic phase, and that 99.5% of the quaternary ammonium cation forms an ion pair with phenoxide.

4.3 Discussion

4.3.1 Homogeneous vs. PTC

Comparison of both the stoichiometric and catalytic series, the quaternary ammonium cations reveals significant differences in reactivity and activity. Under homogeneous reaction conditions, the quaternary ammonium cations, Et_4N^+, $(n\text{-Pr})_4N^+$, $(n\text{-Bu})_4N^+$, $(n\text{-Hex})_4N^+$, and $(n\text{-Oct})_4N^+$, displayed a narrow reactivity range, with a 1.6 to 1.7 factor difference in rate for acetonitrile and DIPK, respectively. This outcome was in stark contrast to the PTC reaction conditions that displayed an activity range of just over two orders of magnitude for the same ammonium cations. It was clear that the intrinsic reactivity of the ammonium phenoxide ion pair does not correlate well with its activity as a catalyst under PTC reaction conditions.

The finding that Me_4N^+ had a significant reactivity under homogeneous reaction conditions, but no catalytic activity, is consistent with an extraction mechanism, wherein reaction rate is reflected by the concentration of $[R_4N^+PhO^-]$ in the organic phase. This finding was further supported by the extraction constants for several linear, tetraalkylammonium picrate

(ArO^-) salts in a dichloromethane/water biphase (Eq 1).[183] The extraction constant (K) for [$Me_4N^+ArO^-$] was measured at 1.5 and was found to increase by approximately two orders of magnitude for each extension of the alkyl chain, Et_4N^+ (K = 220) through (n-Pent)$_4N^+$ (K = $2.45*10^8$).

Equation 1

$$\text{Extraction Constant, } K = [R_4N^+ArO^-]_{org.} / [R_4N^+ArO^-]_{aq.}$$

4.3.2 Determination of the PTC Rate Constant

A PTC rate constant can be calculated from the initial alkylation rate (Eq 2). Because only the initial alkylation rates were collected, the concentration of *n*-butyl bromide can be treated as a constant and will not be factored into any calculations. These PTC rates constants were then compared to the rate constants collected under homogeneous reaction conditions. The effective concentration of the ammonium phenoxide was expressed one of two ways, (1) that all of the ammonium salt partitions into the organic phase and the ammonium phenoxide concentration reflects the concentration of the catalyst loading, or (2) the ammonium phenoxide concentration was calculated based on the amount of active phenoxide as was determined by the benzyl bromide titrations. While the 100% transfer of the tetraalkylammonium species for every catalyst is unlikely, it will be presented as a comparison to the homogeneous rate constants. Notably, the benzyl bromide titration data is an expression of the active phenoxide (tetraalkylammonium phenoxide and potassium phenoxide) in the organic phase. The red and green data points are representative of a 100% transfer of the tetraalkylammonium salt, and the blue squares factor in the organic phase active phenoxide content as determined by benzyl

bromide titration (Figure 29). The homogeneous rate constants are expressed as purple data points.

Equation 2

Alkylation Rate (mol*L^{-1}*s^{-1}) = Rate constant, k (s^{-1})*[$R_4N^+PhO^-$](mol/L)*[*n*-BuBr](mol/L)

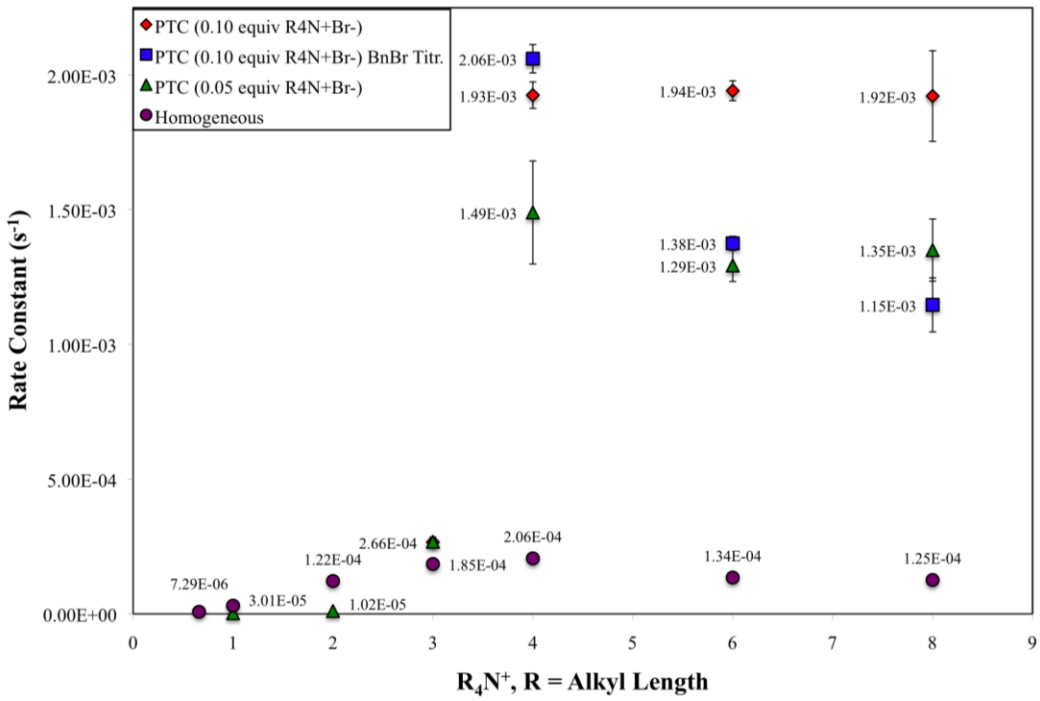

Figure 29. Rate constant comparison between homogeneous and PTC conditions.

For ammonium cations larger than $(n\text{-Pr})_4N^+$ at both 0.05 and 0.10 equivalents loading, the calculated rate constants under PTC reaction conditions were approximately an order of magnitude larger than the homogeneous ones for the same ammonium cations. Only the TMAB and TEAB displayed rate constants lower than that of the homogeneous rate constants. Under PTC reaction conditions, a wide range in rate constant values was calculated for TPAB. At 0.05 and 0.10 equiv loading, its rate constant was similar to the homogeneous series. However, when the effective active phenoxide concentration was taken into account, the rate constant increases 35-fold to $9.39*10^{-3}$ (s^{-1}) for TPAB at 0.10 equivalents loading (not shown in Figure 29). This

large jump in rate constant is likely due to the formation of a TLP (See section 4.3.4.). When the benzyl bromide titration data was incorporated into the calculation of the ammonium phenoxide present in the organic phase, a different trend emerges for TBAB, THAB, and TOAB. The rates constants are still an order of magnitude larger than their homogeneous counterparts, but the rate constant for TBAB is roughly double than that of the TOAB rate constant.

While the rate constants between homogeneous and PTC reaction conditions have been compared, the tetraalkylammonium phenoxides employed under homogeneous conditions were actually a homo-hydrogen bonded dimer with phenol. In this regard, the observed alkylation rates cannot accurately reflect the intrinsic reactivity of an unstabilized, tetraalkylammonium phenoxide. It has been previously demonstrated by experiment that hydration of the anionic nucleophile, which is ion-paired with a quaternary ammonium cation, inhibits catalytic activity under PTC reaction conditions.[163,164,165] These experimental observations are supported by computational studies conducted by Benjamin *et al.*[184] Using *ab initio* calculations in a polarizable continuum solvent model, the activation energy was found to depend significantly on the level of hydration of the anionic nucleophile. The source of this difference in rate constants between homogeneous and PTC system is currently under investigation.

4.3.3 Composition of the Organic Phase

Although the UV-vis spectroscopy data was not able to quantitatively determine the composition of reactive species in the organic phase, it did bring to light the superstoichiometric transfer of phenoxide out of the aqueous phase with respect to the amount of catalyst employed. For TBAB, THAB, and TOAB, ~50% more phenoxide was transferred to the organic phase than the theoretical maximum. It is tempting to attribute this observation to the formation of an

aggregated species. However, no spectroscopic evidence exists that would suggest this association of phenolic species and quaternary ammonium cations has any sort of geometric order.

The benzyl bromide titration survey sought to quantify the amount of phenolic compounds present in the organic phase as a function of the quaternary ammonium cation lipophilicity. Surprisingly, the organic phase contained a significant quantity of phenol, particularly with the more lipophilic catalysts, and that the ratio of active phenoxide to phenol was unique to a particular ammonium salt. These findings are striking for two reasons. First, in a strongly basic aqueous medium the equilibrium between phenol and phenoxide strongly favors phenoxide given the difference in pK_a between water and phenol (15.7 and 9.95, (H_2O, respectively)). The observation that any phenol was left protonated was surprising. Second, despite the unique phenol/phenoxide ratios with TBAB, THAB, and TOAB, their PTC alkylation rates are remarkably similar. This observation implies that under PTC reaction conditions the composition of the organic phase phenolic species was inconsequential to the activity of the ammonium phenoxide present. The most important factor was the effective concentration of the [$R_4N^+PhO^-$] ion-pair intermediate in the organic phase for the determination of catalytic activity.

To account for this transport of phenol in such a strongly basic medium, a hydrogen bonding interaction must be invoked. Dehmlow *et al.* and Sasson *et al.* had observed that quaternary tetraalkylammonium alkoxides derived from diols exhibited a greater organic phase concentration in contrast to alcohols containing a single hydroxyl group.[185,186] These partition studies were conducted in excess base and it was thought that a dianion formed from the diol would be too polar for transport into the organic phase. This observation was rationalized by the formation of an intramolecular hydrogen bond between the tetraalkylammonium alkoxide and

the other alcohol functional group contained within the diol. Such a hydrogen bonding interaction between phenol and phenoxide is likely responsible for the organic phase phenol.

Interestingly, the amount of phenol present in the organic phase was found to be inversely proportional to the lipophilicity of the tetraalkylammonium salt, whereas the amount of active phenoxide in the organic phase was found to be directly proportional to the lipophilicity of the tetraalkylammonium salt. This observation would appear counterintuitive to our understanding of intermolecular forces. According to these results, the most lipophilic ammonium salt is able to transport the most potassium phenoxide, a highly polar ion pair. This is in contrast to a slightly less lipophilic ammonium salt, TBAB, that has 55% the active phenoxide content of TOAB but nearly three fold the amount of organic phase phenol compared to TOAB.

To understand the role of the organic phase phenoxide in the rate of alkylation, a closer examination of the mechanism of tetraalkylammonium phenoxide transport is required. As a tetraalkylammonium cation approaches the interphase boundary separating the bulk aqueous and organic phase, its alkyl chains may orient toward the bulk organic phase due to hydrophobic interactions with the aqueous phase. This conformation change allows for an increase in polar surface area of the ammonium center. At the interfacial boundary the tetraalkylammonium phenoxide forms first, and with this increased accessibility, an additional potassium phenoxide may complex with the ammonium phenoxide to form a quadrapolar complex/dimeric ion pair (Figure 30). This dimer is highly charged, and without sufficient lipophilicity provided by the tetraalkylammonium alkyl chains it is unable to partition into the bulk organic phase. On the basis of the benzyl bromide titration data, the $(n\text{-Bu})_4N^+$ cation is not sufficiently lipophilic to

transport the dimer to the organic phase compared to the $(n\text{-Oct})_4N^+$ cation that can complex a significant amount potassium phenoxide.

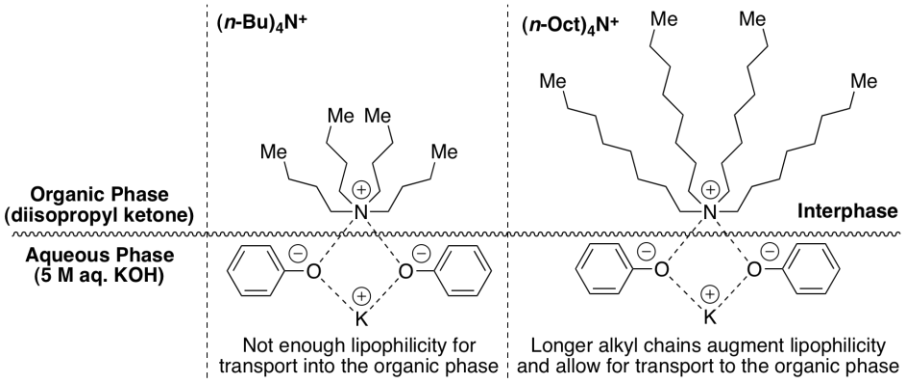

Figure 30. Proposed tetrameric ion-pair complex.

These same interactions may also explain the inverse relationship between organic phase phenol content and ammonium lipophilicity. Since the dimeric complex with $(n\text{-Bu})_4N^+$ is insufficiently lipophilic for transport, phenol may displace a potassium phenoxide from the complex at the interfacial boundary. The newly formed homo-hydrogen bonded complex is less polar than the former quadrapole complex and sufficiently lipophilic for partition into the organic phase. In the case of $(n\text{-Oct})_4N^+$ the dimeric ion-pair readily moves into the organic phase before phenol can displace a potassium phenoxide. With the increased alkyl chain length of $(n\text{-Oct})_4N^+$ this complex may also be sterically inaccessible for formation of a homo-hydrogen bonded complex.

The formation of dimeric, tetraalkylammonium ion-pair complexes has been previously observed in organic solvents. Sawada *et al.* examined the distribution between monomeric and dimeric tetraalkylammonium-anion ion-pairs in a wide range of solvent polarities in addition to anion structure.[187,188] The authors observed that symmetrical tetraalkylammonium salts had a greater tendency to form dimers in solution. The latter study found that the dimerization constant

for tetraalkylammonium salts was inversely proportionally to the polarity of the medium and was also significantly affected by the choice of anion. For instance, picrate anions displayed less solvent dependency on complex formation compared to other inorganic anions (e.g. halides, perchlorate). A similar study by Odashima *et al.* looked at the complex formation between tetraalkylammonium salts and neutral phenols.[189] The authors found that complex stability was greatly dependent on the hydrogen bonding interaction between the phenolic O-H and the native anion of the ammonium salt, X^-. The alkyl length of the tetraalkylammonium salt showed a minimal effect on the complex stability. The intrinsic reactivity of these tetraalkylammonium anion complexes remains to be elucidated.

4.3.4 The Third Liquid Phase

The $(n\text{-Pr})_4N^+$ cation did not conform to the trends observed with the other cations. In view of its intrinsic reactivity and catalytic activity compared to its partition of phenolic intermediates between both phases. The low concentration of organic phase reactive intermediates would suggest that this tetraalkylammonium cation is hydrophilic and should display poor catalyst activity. Despite this finding, the catalytic activity of TPAB was more in common with activity of the lipophilic catalysts, TBAB, THAB, and TOAB. The intrinsic reactivity of $(n\text{-Pr})_4N^+$ excludes the possibility that the $[(n\text{-Pr})_4N^+PhO^-]$ intermediate is simply more reactive under PTC reaction conditions.

The UV-vis survey of catalysts provided a possible explanation for the augmented catalytic activity of TPAB, namely the formation of a TLP. Earlier studies have concluded that the TLP in a PTC process is a catalyst rich phase, and therefore the presence of a TLP would explain the enhanced alkylation rate for an intrinsic reaction that was first order in

catalyst.[148,190,191,192,193] A TLP was observed when a full equivalent of TPAB with respect to phenol was introduced. However, no TLP was visually evident when substoichiometric amounts of TPAB were implemented. This lack of an observable TLP does not exclude the possibility of its existence however. Sasson *et al.* were able to observe the formation of a TLP in the elimination of phenethyl bromide to styrene under PTC reaction conditions.[191] A closer examination of their TLP revealed its physical characteristics as a membrane surrounding an aqueous droplet. If such a TLP were formed in reaction with a low ammonium salt content, it would be reasonable to assume that the total volume of the TLP is so low as to prevent coalescence of TLP droplets into a visible layer.

4.4 Conclusion

4.4.1 Summary

This survey of linear, symmetrical, tetraalkylammonium salts has shown that the intrinsic reactivity of the tetraalkylammonium phenoxide ion pair is greatly overshadowed by its effective concentration in the organic phase, the medium in which the intrinsic reaction takes place. Under PTC reaction conditions, the highest initial alkylation rate was observed for tetraalkylammonium salts with alkyl chains *n*-butyl and longer. Further kinetic studies concluded that the leveling off in catalytic activity was not the result of a change in reaction mechanism, but rather a change in the rate-determining step of the catalytic cycle. Subsequent experiments confirmed that the tetraalkylammonium phenoxide ion pair exists as a complex of phenolic species within the organic phase, and it was shown that ratio of complex components had no effect on catalytic activity. Preliminary measurements of the amount of potassium phenoxide in the organic phase indicate that the near theoretical maximum of tetraalkylammonium phenoxide

was transported into the organic phase with the remaining active phenoxide complexed to the tetraalkylammonium phenoxide.

CHAPTER 5: *Experimental and Supporting Information*

5.1 General Experimental

All reactions were performed in oven-dried (145 °C) or flame-dried glassware under an inert atmosphere of dry argon. Reaction solvents THF (Fisher, HPLC grade), Et_2O (Fisher, BHT stabilized ACS grade) and methylene chloride (Fisher, unstabilized HPLC grade) were dried by percolation through two columns packed with neutral alumina under a positive pressure of argon. Reaction solvents hexane (Fisher, OPTIMA grade) and toluene (Fisher, ACS grade) were dried by percolation through a column packed with neutral alumina and a column packed with Q5 reactant, a supported copper catalyst for scavenging oxygen, under a positive pressure of argon. Reactions were carried out at the temperature indicated (external temperature) as measured by a thermocouple device unless otherwise indicated.

Column chromatography was performed using Merck grade 9385, 60 Å silica gel and column diameter (∅) was expressed in mm. Visualization was accomplished by UV light, permanganate ($KMnO_4$), or iodine (I_2) as indicated. Analytical and preparative thin-layer chromatography was performed on Merck silica gel plates with F-254 indicator. Chromatography solvents EtOAc (Honeywell, HPLC grade), CH_2Cl_2 (Sigma-Aldrich, ACS grade), TBME (Sigma-Aldrich, ACS grade), and MeOH (Fisher, Optima grade) were used as supplied.

^{1}H NMR, ^{13}C NMR, ^{19}F NMR spectra were acquired at 500 MHz, 126 MHz, and 376 MHz, respectively, and referenced to residual solvent [$CHCl_3$ at 7.26 (^{1}H) and 77.00 (^{13}C) or MeOH 3.31 (^{1}H), 49.00 (^{13}C) or DMSO at 2.50 (^{1}H) and 39.5 (^{13}C) ppm]. Chemical shifts are reported in ppm; multiplicities are indicated by s (singlet), d (doublet), t (triplet), q (quartet), p, (pentet), m (multiplet) and br (broad). Coupling constants, *J*, are reported in Hertz. Mass Spectrometry was performed by the University of Illinois Mass Spectrometer Center. ESI mass spectra were performed on a Waters Q-Tof Ultima or a Waters ZMD Quadrupole instrument. Data are reported in the form of *m/z* (intensity relative to base peak = 100). Melting points were obtained in vacuum-sealed glass tubes using a Thomas-Hoover Uni-Melt™ melting point apparatus and are corrected.

Analytical high performance liquid chromatography (HPLC) was performed using a Hewlett Packard 1090L Chromatograph equipped with a variable wavelength diode array

detector and an autosampler. The chromatograph was equipped with a reverse phase Agilent Zorbax 300SB-C8 column (5 μm, 4. 6x 200mm, lamp current = 1).

HPLC Method 1: Linear Gradient; flow rate = 1.0 mL/min, l = 254 nm, solvent = CH_3CN/H_2O (30:70) to CH_3CN/H_2O (90:10) over 10 min, then isocratic for 7 min. A 3 min re-equilibration time was utilized between runs. The water eluent contained 0.1% v/v acetic acid.

Chiral stationary phase HPLC (CSP-HPLC) Method 2: *R,R*-Welk-O, 1.0 mL/min, IPA/hexanes 5:95.

Analytical capillary gas chromatography (GC) was performed using a gas chromatograph fitted with a flame ionization detector (H_2 carrier gas, 1 mL/min). Retention times (t_R) and integrated ratios were obtained using Agilent Chemstation Software. Sample injections were made using a PH 6890 Series Autosample Injector.

GC Method 1: Injections were made onto a Hewlett-Packard HP-1, 30-m x 0.320 mm column. The detector temperature was 300 °C. The column temperatures was maintained at 100 °C isotherm over 3 minutes then ramped to 200 °C over 5 minutes (20 °C/min.).

GC Method 2: Injections were made onto a Hewlett-Packard HP-1, 30-m x 0.320 mm column. The detector temperature was 300 °C. The column temperatures was maintained at 100 °C isotherm over 3 minutes, ramped to 200 °C over 5 min (20 °C/min.), and then held at 200 °C for 2 minutes.

Analytical supercritical fluid chromatography (SFC) was performed on an Agilent 1100 HPLC equipped with an Aurora Systems A-5 supercritical CO_2 adapter for supercritical fluid chromatography and a UV detector (220 nm) using Daicel Chiralcel OJ column.

SFC Method 1: 15μL injection, 2.5 mL/min gradient elution 1% to 10% MeOH over 10 min, hold 10% MeOH for 5 min, and then to 5% MeOH over 1 min and hold for 4 min. Max pressure 350 bar.

Fitting of kinetic data was done with OriginPro 8 SR4 version 8.0951 (B951). Interpolation of kinetic plots was done with Microsoft Excel 2008.

The variable stirring speed motor was constructed with the help of University of Illinois at Urbana-Champaign, School of Chemical Sciences electronics shop (special thanks to Ben Fisher). The speeds were calibrated with the aid of a phototachometer measured at the rotating magnetic with no coupled magnetic stir-bar.

Cinchonidine and diisopropyl ketone (DIPK) were purchased from Acros Organics. 3,5-bis(trifluoromethyl)benzyl bromide was purchased from Alfa-Aesar. Benzyl bromide, allyl bromide, methyl iodide, diethylaminosulfur trifluoride (DAST), thiophosgene, Tributyltinhydride, benzaldehyde, trimethylsilyl allyl ether, and trimethylsilyl cyanide were purchased from Aldrich. 9-bromomethylanthracene[194], 2-bromomethylnaphthalene[195], 1-bromomethylnaphthalene[2], *N*-(diphenylmethylene)glycine*tert*-butyl ester,[196,197] phenylchlorothionoformate,[198] and α-tosyl-phenylacetonitrile[199] were prepared as described in the literature. DIPK was distilled over P_2O_5 under argon (b.p. 124-125 °C) prior to use. Tetramethylammonium bromide was purchased from Aldrich, recrystallized from refluxing ethanol, dried under high vacuum, and then stored in an argon glove box. Tetraethylammonium bromide (98%) was purchased from Aldrich, recrystallized from refluxing methanol, drieded under high vacuum, and then strored in an argon glove box. Tetra(*n*-propyl)ammonium bromide (98%) and tetra(*n*-butyl)ammonium bromide (>99%) were purchased from Aldrich, ground to a powder with a mortar and pestle, dried overnight a 100 °C under high vacuum, and then stored in an argon glove box. Tetra(*n*-hexyl)ammonium bromide (99%) and tetra(*n*-octyl)ammonium bromide (98%) were purchased from Aldrich and were used as supplied.

5.2 Chapter 2

5.2.1. Catalyst Synthesis

General Procedure I. *N*-Quaternization of Cinchona Alkaloids

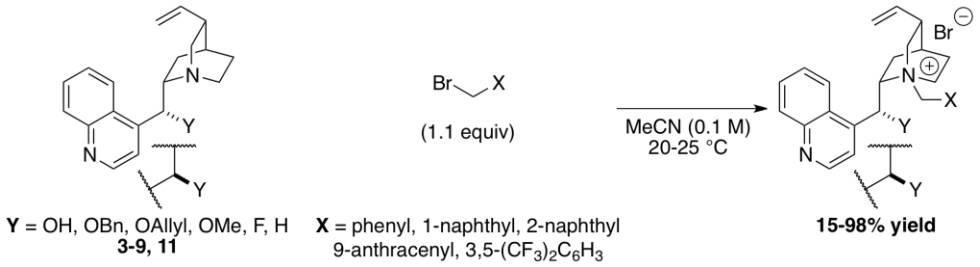

The cinchona alkaloid was placed in a single-neck, round-bottomed flask containing a magnetic stir bar and the arylmethylene bromide was then added (1.1 equiv). The flask was then purged with dry argon and the contents were dissolved in MeCN (0.1 M). The reaction mixture was allowed to stir until the starting material was consumed. Reactions were typically monitored by ^{1}H NMR spectroscopy of reaction aliquots (~100 μL). Solvent was removed on a rotavap (20 mm Hg, 25 °C) and the residue was purified either by washing, chromatography or recrystallization.

Preparation of *epi*-Cinchonidine (4)

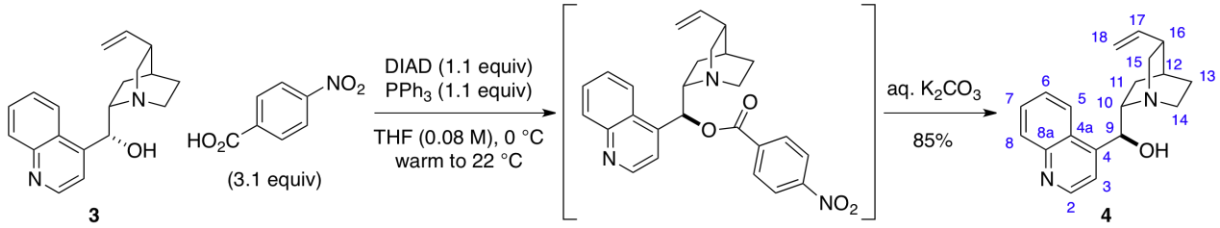

Cinchonidine (**3**) (2.94 g, 10.0 mmol), triphenylphosphine (2.89 g, 11.0 mmol, 1.1 equiv), and 4-nitrobenzoic acid (5.18 g, 31.0 mmol, 3.1 equiv) were dissolved in THF (125 mL, 0.08 M) in a 250-mL, three-neck round-bottomed flask fitted with an argon inlet, septum, and thermocouple. The suspension was cooled to 0 °C (internal) in an ice-bath over 1 h, whereupon diisopropyl azodicarboxylate (2.17 mL, 11.0 mmol, 1.1 equiv) was then added slowly over the course of several minutes. The reaction mixture was stirred for an additional hour at 0 °C then was allowed to warm to 22 °C over 1 h. The reaction mixture was diluted with Et_2O (50 mL), then was transferred to a 250-mL separatory funnel and was extracted with 1 N HCl aq. (3 x 50 mL). The combined aqueous extracts were basified with solid K_2CO_3 to pH 9-11. This aqueous phase was extracted with Et_2O (3 x 50 mL) then CH_2Cl_2 (50 mL). The combined organic extracts were dried over Na_2SO_4 and then the solvent was removed on a rotavap (20 mm Hg, 25 °C) to afford 2.50 g (85%) of **4** as a light-yellow solid. The entire product was further purified by recrystallization from boiling *i*-PrOH (~150 mL) to afford **4** as a white, crystalline solid.

Data for **4**:

mp: 203-205 °C

^{1}H-NMR: (500 MHz, $CDCl_3$)

8.82 (d, *J* = 4.6 Hz, 1H, HC(2)), 8.24 (d, *J* = 8.2 Hz, 1H, HC(8)), 8.06 (dd, *J* = 8.5, 0.6 Hz, 1H, HC(5)), 7.77 (ddd, *J* = 8.4, 6.9, 1.3 Hz, 1H, HC(6)), 7.72 (d, *J* = 4.6 Hz, 1H, HC(3)), 7.66 (ddd, *J* = 8.3, 6.9, 1.3 Hz, 1H, HC(7)), 5.75 (ddd, *J* = 17.7, 10.4, 7.6 Hz, 1H, HC(17)), 5.64 (d, *J* = 3.9 Hz, 1H, HC(9)), 5.01 - 4.82 (m, 3H, HC(18)), 3.61 (dddd, *J* = 13.2, 10.6, 5.0, 2.5 Hz, 1H, HC(14)), 3.18- 3.01 (m, 2H, HC(10), HC(15)), 2.73 - 2.57 (m, 2H, HC(14), HC(15)), 2.33 (d, *J* = 1.3 Hz, 1H, HC(16)), 1.94 - 1.72 (m, 3H, HC(11), HC(12), HC(13)), 1.63 - 1.40 (m, 2H, HC(11), HC(13)).

^{13}C-NMR: (126 MHz, $CDCl_3$)

149.99, 149.61, 148.06, 141.77, 130.10, 128.95, 126.52, 125.61, 122.94, 118.19, 114.27, 71.76, 60.34, 56.95, 43.16, 39.90, 27.88, 27.58, 21.45.

Analysis: $C_{19}H_{22}N_2O$ (294.39)

Calcd:	C, 77.52;	H, 7.53;	N, 9.52
Found:	C, 77.38;	H, 7.67;	N, 9.47

LRMS: (ESI^+, Q-tof)

295.2 (100, M-Br+)

HRMS: $C_{19}H_{23}N_2O^+$ (ESI^+, Q-tof)

Calcd:	295.1810
Found:	295.1814

TLC: R_f 0.11 (CH_2Cl_2/MeOH, 10:1) [silica gel, I_2]

Preparation of *O*-Benzylcinchonidine (5)

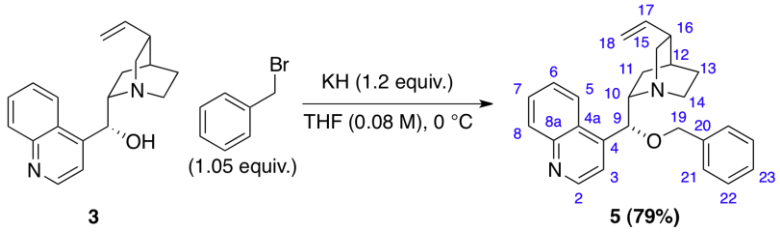

Potassium hydride (164 mg, 4.08 mmol, 1.2 equiv) was placed in a 100-mL, single-neck,, round-bottomed flask fitted with an argon inlet adapter and septum in a glove box. This flask was then removed from the glove box and a solution of **3** (1.00 g, 3.40 mmol) in THF (43 mL, 0.08 M) was then added *via* syringe under argon. The reaction mixture was stirred for 15 min at 22 °C until it became a light orange solution and no further gas evolution was observed. The reaction mixture was cooled to 0 °C (external) on an ice bath over 2 h. Benzyl bromide (420 µL, 3.57 mmol, 1.05 equiv) was then added *via* syringe and the mixture was stirred for 4 h at 0 °C.

The reaction mixture was quenched with sat. aq. NH_4Cl solution (~2 mL), and then was diluted with Et_2O (30 mL). The quenched reaction mixture was transferred to a 125-mL separatory funnel and then was extracted with 1 N aq. HCl solution (3 x 30 mL). The combined aqueous extracts were washed with Et_2O (3 x 30 mL) then were basified with solid K_2CO_3 until a white suspension persisted with a pH of 9-11. The aqueous suspension was diluted with H_2O (20 mL) and then was extracted with CH_2Cl_2 (3 x 30 mL). The combined organic extracts were washed with brine (30 mL), dried over $MgSO_4$, and then concentrated on a rotavap (20 mm Hg, 25 °C) to afford 1.41 g of crude **5** as a light-amber oil.

The product was purified by silica gel flash chromatography (50 g SiO_2, ∅ = 30, 20:1 to 5:1, EtOAc/MeOH gradient elution) to afford 1.03 g (79%) of **5** as an off-white amorphous solid.

Data for **5:**

^{1}H-NMR: (500 MHz, $CDCl_3$)

8.96 (d, *J* = 4.6 Hz, 1H, HC(2)), 8.87 (dd, *J* = 9.7, 3.7 Hz, 1H, HC(8)), 8.30 (d, *J* = 7.7 Hz, 1H, HC(5)), 7.89 - 7.79 (m, 2H, HC(6), HC(7)), 7.67 (d, *J* = 4.5 Hz, 1H, HC(3)), 7.42 - 7.28 (m, 5H, HC(21), HC(22), HC(23)), 6.69 (d, *J* = 5.7 Hz, 1H, HC(9)), 5.57 (ddd, *J* = 17.1, 10.7, 6.6 Hz, 1H, HC(17)), 5.09 - 5.00 (m, 2H, HC(18)), 4.74 (d, *J* = 11.0 Hz, 1H, HC(19)), 4.53 (d, *J* = 11.0 Hz, 1H, HC(19)), 4.08 (ddd, *J* = 10.8, 7.1, 2.5 Hz, 1H, HC(14)), 3.57 - 3.47 (m, 1H, HC(15)), 3.42

(t, J = 9.0 Hz, 1H, HC(10)), 3.26 - 3.12 (m, 2H, HC(14), HC(15)), 2.73 (d, J = 1.7 Hz, 1H, HC(16)), 2.30 - 2.19 (m, 1H, HC(11)), 2.14 - 2.02 (m, 2H, HC(12), HC(13)), 1.93 - 1.80 (m, 1H, HC(13)), 1.53 (t, J = 12.0 Hz, 1H, HC(11)).

^{13}C-NMR: (126 MHz, $CDCl_3$)

150.17, 148.60, 146.38, 141.84, 137.81, 130.52, 129.09, 128.42, 127.73, 127.64, 126.69, 126.52, 123.21, 118.59, 114.25, 71.31, 60.80, 57.03, 43.15, 39.99, 27.92, 27.73.

Analysis: $C_{26}H_{28}N_2O$ (384.51)

Calc:	C, 81.21;	H, 7.34;	N, 7.29
Found:	C, 81.24;	H, 7.57;	N, 7.30

LRMS: (ESI^+, Q-tof)

385.2 (100, $M+H^+$)

HRMS: $C_{26}H_{29}N_2O^+$ (ESI^+, Q-tof)

Calcd:	385.2280
Found:	385.2278

TLC: R_f 0.38 (CH_2Cl_2/MeOH, 10:1) [silica gel, I_2]

Preparation of *O*-Allylcinchonidine (6)

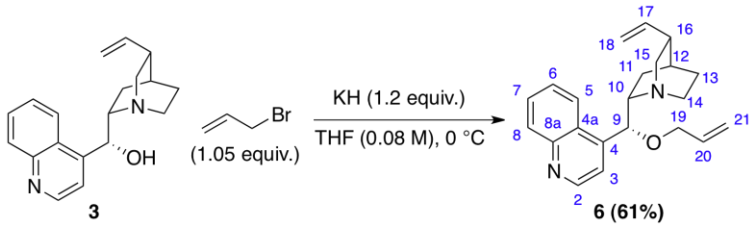

Potassium hydride (164 mg, 4.08 mmol, 1.2 equiv) was placed in a 100-mL, single-neck,, round-bottomed flask fitted with an argon inlet adapter and septum in a glove box. This flask was then removed from the glove box and a solution of **3** (1.00 g, 3.40 mmol) in THF (43 mL, 0.08 M) was then added *via* syringe under argon. The reaction mixture was stirred for 15 min at 22 °C until it became a light orange solution and no further gas evolution was observed. The reaction mixture was cooled to 0 °C (external) on an ice bath over 2 h. Allyl bromide (310 µL, 3.57 mmol, 1.05 equiv) was then added *via* syringe and the mixture was stirred for 4 h at 0 °C.

The reaction mixture was quenched with sat. aq. NH_4Cl solution (~2 mL), and then was diluted with Et_2O (30 mL). The quenched reaction mixture was transferred to a 125-mL separatory funnel and then was extracted with 1 N aq. HCl solution (3 x 30 mL). The combined aqueous extracts were washed with Et_2O (3 x 30 mL) then were basified with solid K_2CO_3 until a white suspension persisted with a pH of 9-11. The aqueous suspension was diluted with H_2O (20 mL) and then was extracted with CH_2Cl_2 (3 x 30 mL). The combined organic extracts were washed with brine (30 mL), dried over $MgSO_4$, and then concentrated on a rotavap (20 mm Hg, 25 °C) to afford 1.13 g (99+%) of crude **6** as a light-brown oil.

The product was purified by silica gel flash chromatography (40 g SiO_2, ∅ = 30, 20:1 to 10:1, EtOAc/MeOH) to afford 1.03 g (79%) of **6** as a light-amber oil.

Data for **6**:

^{1}H-NMR: (500 MHz, $CDCl_3$)

8.90 (d, *J* = 4.4 Hz, 1 H, HC(2)), 8.13 (dd, *J* = 13.3, 8.5 Hz, 2 H, HC(5), HC(8)), 7.72 (ddd, *J* = 8.3, 6.9, 1.3 Hz, 1 H, HC(7)), 7.57 (ddd, *J* = 8.2, 6.9, 1.2 Hz, 1 H, HC(6)), 7.49 (d, *J* = 4.4 Hz, 1 H, HC(3)), 5.93 (ddt, *J* = 17.1, 10.6, 5.4 Hz, 1 H, HC(20)), 5.77 - 5.65 (m, 1 H, HC(17)), 5.36 - 5.21 (m, 2 H, HC(9), HC(21)), 5.21 - 5.13 (m, 1 H, HC(21)), 4.99 - 4.84 (m, 2 H, HC(18)), 3.95 (ddt, *J* = 12.8, 5.1, 1.4 Hz, 1 H, HC(19)), 3.87 (dd, *J* = 12.8, 5.7 Hz, 1 H, HC(19)), 3.44 (s, 1 H, HC(14)),

3.10 (dd, *J* = 13.5, 10.1 Hz, 2 H, HC(10), HC(15)), 2.71 (dd, *J* = 17.0, 7.3 Hz, 1 H, HC(14)), 2.63 (d, *J* = 13.4 Hz, 1 H, HC(15)), 2.27 (s, 1 H, HC(16)), 1.88 - 1.74 (m, 3 H, HC(11), HC(12), HC(13)), 1.53 (ddd, *J* = 15.4, 12.7, 8.7 Hz, 2 H, HC(11), HC(13)).

^{13}C-NMR: (126 MHz, $CDCl_3$)

150.14, 148.54, 146.31, 141.73, 134.31, 130.49, 129.05, 126.68, 126.41, 123.12, 118.39, 116.95, 114.27, 70.14, 60.65, 57.09, 43.27, 39.98, 27.93, 27.69, 22.04.

Analysis: $C_{22}H_{26}N_2O$ (334.45)

Calc:	C, 79.00;	H, 7.84;	N, 8.38
Found:	C, 78.76;	H, 8.21;	N, 8.11

LRMS: (ESI^+, Q-tof)

335.2 (100, $M+H^+$)

HRMS: $C_{22}H_{27}N_2O^+$ (ESI^+, Q-tof)

Calcd:	335.2123
Found:	335.2117

TLC: R_f 0.34 (CH_2Cl_2/MeOH, 10:1) [silica gel, I_2]

Preparation of *O*-Methylcinchonidine (7)

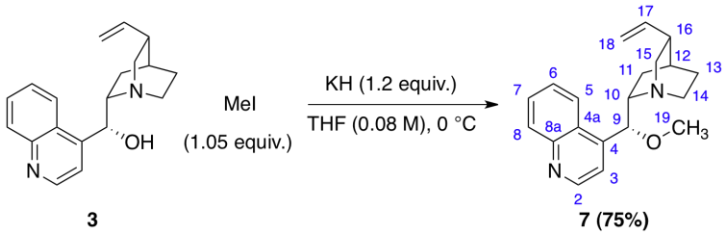

Potassium hydride (164 mg, 4.08 mmol, 1.2 equiv) was placed in a 100-mL, single-neck,, round-bottomed flask fitted with an argon inlet adapter and septum in a glove box. This flask was then removed from the glove box and a solution of **3** (1.00 g, 3.40 mmol) in THF (43 mL, 0.08 M) was then added *via* syringe under argon. The reaction mixture was stirred for 15 min at 22 °C until it became a light orange solution and no further gas evolution was observed. The reaction mixture was cooled to 0 °C (external) on an ice bath over 2 h. Methyl iodide (220 µL, 3.57 mmol, 1.05 equiv) was then added *via* syringe and the mixture was stirred for 4 h at 0 °C.

The reaction mixture was quenched with sat. aq. NH_4Cl solution (~2 mL), and then was diluted with Et_2O (30 mL). The quenched reaction mixture was transferred to a 125-mL separatory funnel and then was extracted with 1 N aq. HCl solution (3 x 30 mL). The combined aqueous extracts were washed with Et_2O (3 x 30 mL) then were basified with solid K_2CO_3 until a white suspension persisted with a pH of 9-11. The aqueous suspension was diluted with H_2O (20 mL) and then was extracted with CH_2Cl_2 (3 x 30 mL). The combined organic extracts were washed with brine (30 mL), dried over $MgSO_4$, and then concentrated on a rotavap (20 mm Hg, 25 °C) to afford 1.17 g of crude **7** as a light-yellow, crystalline solid.

The product was purified by silica gel flash chromatography (40 g SiO_2, ∅ = 30, 20:1 to 10:1, CH_2Cl_2/MeOH) to afford 781 mg (75%) of **7** as a white, crystalline solid. The entire product was further purified by recrystallization from boiling hexane.

Data for **7**:

m.p.: 125-126 °C

^{1}H-NMR: (500 MHz, $CDCl_3$)

8.90 (d, *J* = 4.4 Hz, 1 H, HC(2)), 8.12 (dd, *J* = 21.0, 8.4 Hz, 2 H, HC(5), HC(8)), 7.72 (ddd, *J* = 8.3, 6.9, 1.3 Hz, 1 H, HC(7)), 7.57 (ddd, *J* = 8.3, 6.9, 1.2 Hz, 1 H, HC(6)), 7.46 (d, *J* = 4.4 Hz, 1 H, HC(3)), 5.71 (ddd, *J* = 17.7, 10.3, 7.7 Hz, 1 H,

HC(17)), 5.07 (s, 1 H, HC(9)), 4.91 (ddt, *J* = 20.2, 10.3, 1.4 Hz, 2 H, HC(18)), 3.39 (t, *J* = 9.0 Hz, 1 H, HC(14)), 3.30 (s, 3 H, HC(19)), 3.09 (dd, *J* = 13.5, 10.2 Hz, 2 H, HC(10), HC(15)), 2.75 - 2.65 (m, 1 H, HC(14)), 2.65 - 2.55 (m, 1 H, HC(15)), 2.25 (s, 1 H, HC(16)), 1.84 - 1.69 (m, 3 H, HC(11), HC(12), HC(13)), 1.51 (ddd, *J* = 16.8, 12.5, 7.7 Hz, 2 H, HC(11), HC(13)).

^{13}C-NMR: (126 MHz, $CDCl_3$)

150.14, 148.56, 146.07, 141.67, 130.49, 129.04, 126.69, 126.52, 123.16, 118.34, 114.34, 82.83, 60.57, 57.18, 56.96, 43.21, 39.92, 27.88, 27.59, 21.90.

Analysis: $C_{20}H_{24}N_2O$ (308.42)

Calcd:	C, 77.89;	H, 7.84;	N, 9.08
Found:	C, 77.96;	H, 7.95;	N, 9.17

LRMS: (ESI^+, Q-tof)

309.2 (100, $M+H^+$)

HRMS: $C_{20}H_{25}N_2O^+$ (ESI^+, Q-tof)

Calcd:	309.1967
Found:	309.1960

TLC: R_f 0.29 (CH_2Cl_2/MeOH, 10:1) [silica gel, I_2]

Preparation of *O*-Methyl-*epi*-cinchonidine (8)

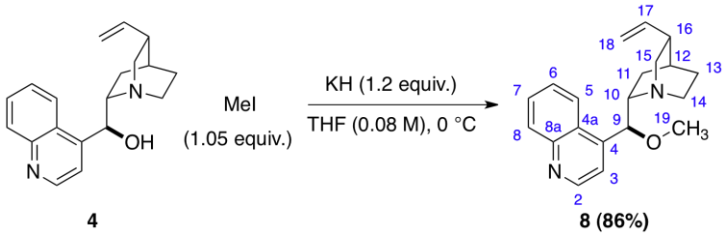

Potassium hydride (120 mg, 3.00 mmol, 1.2 equiv) was placed in a 50-mL, single-neck, round-bottomed flask fitted with an argon inlet adapter and septum in a glove box. This flask was then removed from the glove box and a solution of **4** (736 mg, 2.50 mmol) in THF (31.0 mL, 0.08 M) was then added *via* syringe under argon. The reaction mixture was stirred for 15 min at 22 °C until it became a light orange solution and no further gas evolution was observed. The reaction mixture was cooled to 0 °C (external) on an ice bath over 2 h. Methyl iodide (164 µL, 2.63 mmol, 1.05 equiv) was then added *via* syringe and the mixture was stirred for 4 h at 0 °C.

The reaction mixture was quenched with sat. aq. NH_4Cl solution (~2 mL), and then was diluted with Et_2O (30 mL). The quenched reaction mixture was transferred to a 125-mL separatory funnel and then was extracted with 1 N aq. HCl solution (3 x 30 mL). The combined aqueous extracts were washed with Et_2O (3 x 30 mL) then were basified with solid K_2CO_3 until a white suspension persisted with a pH of 9-11. The aqueous suspension was diluted with H_2O (20 mL) and then was extracted with CH_2Cl_2 (3 x 30 mL). The combined organic extracts were washed with brine (30 mL), dried over $MgSO_4$, and then concentrated on a rotavap (20 mm Hg, 25 °C) to afford 1.04 g of crude **8** as a light-yellow, crystalline solid.

The product was purified by silica gel flash chromatography (50 g SiO_2, ∅ = 30, 20:1 to 5:1, CH_2Cl_2/MeOH, gradient elution) to afford 665 mg (86%) of **8** as a white, crystalline solid. The entire product was further purified by recrystallization from boiling hexane.

Data for **8**:

m.p.: 125-126 °C

^{1}H-NMR: (500 MHz, $CDCl_3$)

8.90 (d, *J* = 4.4 Hz, 1 H, HC(2)), 8.18 - 8.06 (m, 2 H, HC(5), HC(8)), 7.72 (ddd, *J* = 8.3, 6.9, 1.3 Hz, 1 H, HC(7)), 7.57 (ddd, *J* = 8.3, 6.9, 1.2 Hz, 1 H, HC(6)), 7.46 (d, *J* = 4.4 Hz, 1 H, HC(3)), 5.76 - 5.66 (m, 1 H, HC(17)), 5.07 (s, 1 H, HC(9)),

4.91 (ddt, J = 20.2, 10.3, 1.4 Hz, 2 H, HC(18)), 3.43 - 3.33 (m, 1 H, HC(14)), 3.30 (s, 3 H, HC(19)), 3.08 (dt, J = 18.9, 9.6 Hz, 2 H, HC(10), HC(15)), 2.75 - 2.64 (m, 1 H, HC(14)), 2.64 - 2.57 (m, 1 H, HC(15)), 2.26 (s, 1 H, HC(16)), 1.83 - 1.69 (m, 3 H, HC(11), HC(12), HC(13)), 1.51 (ddd, J = 16.4, 12.1, 7.7 Hz, 2 H, HC(11), HC(13)3).

^{13}C-NMR: (126 MHz, $CDCl_3$)

150.14, 148.51, 146.25, 141.85, 130.46, 129.00, 126.61, 126.51, 123.10, 118.33, 114.20, 83.09, 60.55, 57.17, 57.03, 43.16, 40.03, 27.87, 27.67, 21.98.

analysis: $C_{20}H_{24}N_2O$ (308.42)

Calcd:	C, 77.89;	H, 7.84;	N, 9.08
Found:	C, 77.90;	H, 7.95;	N, 9.14

LRMS: (ESI^+, Q-tof)

309.2 (100, $M+H^+$)

HRMS: $C_{20}H_{25}N_2O^+$ (ESI^+, Q-tof)

Calcd:	309.1967
Found:	309.1965

TLC: R_f 0.30 (CH_2Cl_2/MeOH, 10:1) [silica gel, I_2]

Preparation of Deoxyfluorocinchondine (9)

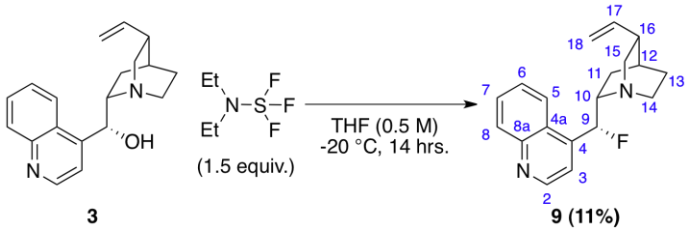

Cinchonidine (**3**) (2.36 g, 8.00 mmol) was placed in a 50-mL, single-neck,, PTFE round-bottomed flask fitted with a septum and was then suspended in THF (16.0 mL, 0.50 M). The suspension was cooled to -20 °C (external) with a refrigerator unit in an *i*-PrOH bath over 2-3 h. Diethylaminosulfur trifluoride (1.58 mL, 12.0 mmol, 1.50 equiv) was then added slowly over several minutes *via* a polypropylene syringe under an argon atmosphere, and the mixture was then stirred for 14 h at -20 °C. The reaction was quenched by transferring the brown solution to a 250-mL separatory funnel containing a sat. aq. $NaHCO_3$ solution (60 mL) which was then extracted with CH_2Cl_2 (3 x 60 mL). The combined organic extracts were washed with brine (60 mL), dried over $MgSO_4$, and then were concentrated on a rotavap (20 mm Hg, 25 °C) to afford 2.75 g (116%) of **9** as an orange-amber, viscous oil.

The crude product was purified by three successive chromatographic separations on silica gel. The first column (100 g SiO_2, ∅ = 40, 20:1 to 5:1, CH_2Cl_2/MeOH gradient elution) afforded 1.42 g (60%) of crude **9** as a brown-amber oil. The second column (40 g SiO_2, ∅ = 30, 20:1 to 5:1, EtOAc/MeOH gradient elution) afforded 521 mg (22%) of crude **9** as a yellow oil. The third column (50 g SiO_2, ∅ = 30, 10:1 to 8:1, TBME/MeOH) afforded 253 mg (11%) of **9** as a white, crystalline solid. The entire product was further purified by recrystallization from boiling pentane.

Data for **9**:

m.p.: 78-81 °C

^{1}H-NMR: (500 MHz, CD_3OD)

8.89 (d, *J* = 4.6 Hz, 1H, HC(2)), 8.11 (d, *J* = 8.3 Hz, 1H, HC(8)), 8.06 (d, *J* = 8.4 Hz, 1H, HC(5)), 7.83 (ddd, *J* = 8.4, 6.9, 1.3 Hz, 1H, HC(7)), 7.71 (ddd, *J* = 8.3, 6.9, 1.2 Hz, 1H, HC(6)), 7.66 (d, *J* = 4.6 Hz, 1H, HC(3)), 6.48 (dd, *J* = 48.5, 2.2 Hz, 1H, HC(9)), 5.78 (ddd, *J* = 17.6, 10.4, 7.5 Hz, 1H, HC(17)), 4.96 (ddt, *J* =

31.6, 10.4, 1.4 Hz, 2H, HC(18)), 3.49 - 3.37 (m, 1H, HC(14)), 3.18 (dd, *J* = 13.7, 10.2 Hz, 2H, HC(10), HC(15)), 2.89 - 2.78 (m, 1H, HC(14)), 2.73 (ddd, *J* = 13.7, 5.1, 2.5 Hz, 1H, HC(15)), 2.40 (s, 1H, HC(16)), 1.89 - 1.77 (m, 3H, HC(11), HC(12), HC(13)), 1.66 (ddd, *J* = 14.6, 9.1, 3.2 Hz, 1H, HC(13)), 1.54 (td, *J* = 10.4, 5.1 Hz, 1H, HC(11)).

^{13}C-NMR: (126 MHz, CD_3OD)

150.89, 148.81, 145.79 (d, *J* = 20.5 Hz), 142.31, 131.13, 130.33, 128.78, 125.91 (d, *J* = 5.3 Hz), 124.09, 118.93 (d, *J* = 11.6 Hz), 115.15, 93.76 (d, *J* = 178.9 Hz), 60.81 (d, *J* = 21.9 Hz), 57.27, 44.22 (d, *J* = 5.4 Hz), 40.66, 29.03, 27.99, 21.27 (d, *J* = 5.8 Hz).

^{19}F-NMR: (376 MHz, CD_3OD)

-199.29 (dd, $J_{H\text{-}F}$ = 48.4, 27.4 Hz).

analysis: $C_{19}H_{21}FN_2$ (296.38)

Calcd:	C, 77.00;	H, 7.14;	N, 9.45
Found:	C, 77.04;	H, 7.33;	N, 9.47

LRMS: (ESI^+, Q-tof)

297.2 (100, $M+H^+$)

HRMS: $C_{19}H_{22}FN_2^+$ (ESI^+, Q-tof)

Calcd: 297.1767

Found: 297.1776

TLC: R_f 0.42 (CH_2Cl_2/MeOH, 10:1) [silica gel, I_2]

Preparation of Cinchonan-9-ol, 9-(phenol thiocarbonate) (10)

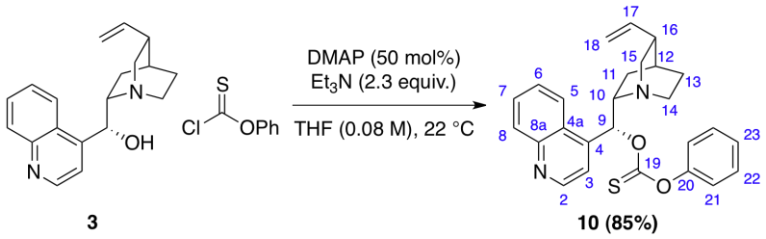

Cinchonidine (**3**) (1.77 g, 6.00 mmol) and 4-dimethylaminopyridine (367 mg, 3.00 mmol, 0.50 equiv) were added to a 100-mL, single-neck, round-bottomed flask fitted with an argon inlet adapater and septum and followed by THF (67.0 mL, 0.09 M). Triethylamine (1.92 mL, 13.8 mmol, 2.30 equiv) was then added and the mixture was stirred until it became homogeneous. Phenyl chlorothionoformate (1.67 mL, 12.0 mmol, 2.0 equiv) was then added *via* syringe to afford a suspension with a yellow precipitate and the reaction mixture was stirred at room temperature for 3 h. The reaction mixture was transferred to 125-mL separatory funnel followed by the addition of a sat. aq. $NaHCO_3$ solution (70 mL) and the suspension was extracted with EtOAc (3 x 70 mL). The combined organic extracts were washed with brine (70 mL), dried over Na_2SO_4, and concentrated on a rotavap (20 mm Hg, 30 - 35 °C) to afford 6.07 g of crude **10** as a dark-brown liquid.

The product was purified by silica gel flash chromatography (100 g SiO_2, ∅ = 40, 20:1 to 10:1, EtOAc/MeOH) to afford 2.18 g (85%) of **10** as a brown, amorphous solid.

Data for **10**:

^{1}H-NMR: (500 MHz, $CDCl_3$)

8.94 (d, *J* = 4.5 Hz, 1 H, HC(2)), 8.20 (d, *J* = 8.2 Hz, 1 H, HC(8)), 8.16 (dd, *J* = 8.5, 0.8 Hz, 1 H, HC(5)), 7.74 (ddd, *J* = 8.3, 6.9, 1.3 Hz, 1 H, HC(6)), 7.61 (ddd, *J* = 8.3, 6.9, 1.3 Hz, 1 H, HC(7)), 7.48 (d, *J* = 4.5 Hz, 1 H, HC(3)), 7.42 - 7.35 (m, 2 H, HC(22)), 7.31 - 7.23 (m, 1 H, HC(23)), 7.09 - 7.00 (m, 3 H, HC(9), HC(21)), 5.81 (ddd, *J* = 17.6, 10.4, 7.5 Hz, 1 H, HC(17)), 4.99 (ddt, *J* = 10.3, 6.4, 1.4 Hz, 2 H, HC(18)), 3.43 (dd, *J* = 16.9, 7.8 Hz, 1 H, HC(10)), 3.28 - 3.16 (m, 1 H, HC(14)), 3.07 (dd, *J* = 13.9, 10.1 Hz, 1 H, HC(15)), 2.78 - 2.67 (m, 1 H, HC(14)), 2.60 (ddd, *J* = 13.7, 4.5, 2.4 Hz, 1 H, HC(15)), 2.30 (s, 1 H, HC(16)), 1.96 - 1.85 (m, 2 H, HC(11), HC(12)), 1.85 - 1.76 (m, 1 H, HC(13)), 1.76 - 1.68 (m, 1 H,

HC(11)), 1.64 - 1.52 (m, 1 H, HC(13)).

^{13}C-NMR: (126 MHz, $CDCl_3$)

193.94, 153.33, 149.95, 148.59, 143.98, 141.51, 130.51, 129.53, 129.28, 126.99, 126.67, 125.81, 123.41, 121.76, 118.67, 114.56, 84.01, 60.24, 56.80, 42.80, 39.66, 27.58, 23.79

LRMS: (ESI^+, ZMD)

277.2 (47), 431.1 (100, $M+H^+$)

Preparation of Deoxycinchonidine (11)

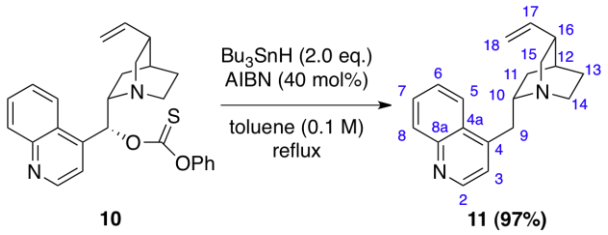

Azodiisobutyrodinitrile (333 mg, 2.00 mmol, 0.40 equiv) and a solution of **10** (2.15 g, 5.00 mmol) in toluene (50 mL, 0.10 M) were combined in a 100-mL, single-neck, round-bottomed flask fitted with a condenser and argon inlet. Tributyltinhydride (2.73 mL, 10.0 mmol, 2.00 equiv) was then added *via* syringe and the reaction mixture was stirred at reflux for 1 h. The reaction mixture was allowed to cool to 22 °C and was then concentrated on a rotavap (20 mm Hg, 35-40 °C) to afford a yellow liquid.

The product was purified by silica gel flash chromatography [50 g SiO_2, ∅ = 30, 10:1, EOAc : (10% aq. NH_4OH in MeOH)] to afford 1.38 g (97%) of **11** as a light-brown, crystalline solid. The product was further purified by recrystallization from concentrated pentane solution and cooling overnight in a freezer to afford an off-white, crystalline solid.

Data for **11:**

m.p.: 58 – 59 °C

^{1}H-NMR: (500 MHz, $CDCl_3$)

8.81 (d, *J* = 4.4 Hz, 1 H, HC(2)), 8.09 (dd, *J* = 19.7, 8.4 Hz, 2 H, HC(5), HC(8)), 7.74 - 7.66 (m, 1 H, HC(7)), 7.61 - 7.52 (m, 1 H, HC(6)), 7.28 (d, *J* = 4.4 Hz, 1 H, HC(3)), 5.79 (ddd, *J* = 17.8, 10.3, 7.6 Hz, 1 H, HC(17)), 4.97 (ddd, *J* = 13.7, 11.3, 1.2 Hz, 2 H, HC(18)), 3.41 (dd, *J* = 13.8, 5.8 Hz, 1 H, HC(9)), 3.28 - 3.15 (m, 3 H, HC(10), HC(14), HC(15)), 3.08 (dd, *J* = 13.8, 8.5 Hz, 1 H, HC(9)), 2.85 - 2.74 (m, 1 H, HC(14)), 2.70 (ddd, *J* = 13.8, 4.9, 2.4 Hz, 1 H, HC(15)), 2.33 - 2.22 (m, 1 H, HC(16)), 1.87 - 1.72 (m, 2 H, HC(11), HC(13)), 1.71 - 1.62 (m, 1 H, HC(12)), 1.62 - 1.51 (m, 1 H, HC(11)), 1.17 (dd, *J* = 13.2, 6.6 Hz, 1 H, HC(13)).

^{13}C-NMR: (126 MHz, $CDCl_3$)

150.04, 148.37, 145.40, 141.77, 130.31, 128.95, 127.76, 126.38, 123.44, 121.52, 114.29, 56.25, 56.05, 41.06, 39.54, 38.18, 28.87, 27.96, 27.90.

analysis: $C_{19}H_{22}N_2O$ (278.39)

	Calcd:	C, 81.97;	H, 7.97;	N, 10.06
	Found:	C, 82.13;	H, 8.11;	N, 10.13

LRMS: (ESI^+, Q-tof)

279.2 (100, $M+H^+$)

HRMS: $C_{19}H_{23}N_2O^+$ (ESI^+, Q-tof)

Calcd: 279.1861

Found: 279.1864

TLC: R_f 0.28 (CH_2Cl_2/MeOH, 10:1) [silica gel, I_2]

Preparation of Cinchonidinium Salts in Series A

Preparation of *N*-9-Anthracenylmethylcinchonidinium Bromide (1a)

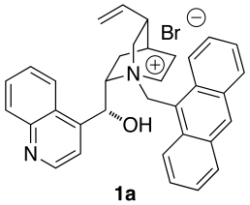

1a

Following General Procedure I, cinchonidine (1.31 g, 4.4 mmol), MeCN (25 mL), and 9-bromomethylanthracene (1.32 g, 4.84 mmol, 1.1 equiv) were combined in a 50-mL, single-neck, round-bottomed flask fitted with an argon inlet, wrapped in aluminum foil and the mixture was stirred overnight. Care was taken to avoid light exposure. The solvent was removed on a rotavap (20 mm Hg, 25 °C) and yellow solid residue was triturated with Et_2O (25-mL) and filtered to afford 2.16 g (86%) of **1a** as a light-yellow, crystalline solid. The entire product was further purified by recrystallization from a concentrated CH_2Cl_2 solution by slow diffusion of Et_2O in a chamber.

Data for **1a**:

m.p.: 154 °C (decomp.)

^{1}H-NMR: (500 MHz, CD_3OD)

9.01 (d, *J* = 4.6 Hz, 1 H), 8.86 - 8.77 (m, 2 H), 8.66 - 8.56 (m, 2 H), 8.22 (d, *J* = 8.5 Hz, 2 H), 8.20 - 8.14 (m, 1 H), 8.08 (d, *J* = 4.5 Hz, 1 H), 7.96 - 7.88 (m, 2 H), 7.83 - 7.75 (m, 2 H), 7.63 (ddd, *J* = 8.4, 6.6, 4.1 Hz, 2 H), 7.11 (d, *J* = 1.8 Hz, 1 H), 6.50 (d, *J* = 14.0 Hz, 1 H), 5.93 (d, *J* = 14.0 Hz, 1 H), 5.71 (ddd, *J* = 17.4, 10.4, 7.2 Hz, 1 H), 5.01 (dd, *J* = 26.2, 13.8 Hz, 2 H), 4.74 - 4.63 (m, 1 H), 4.48 (t, *J* = 9.0 Hz, 1 H), 3.86 (ddd, *J* = 12.5, 4.9, 3.2 Hz, 1 H), 3.24 (dd, *J* = 12.4, 10.9 Hz, 1 H), 2.80 (td, *J* = 11.7, 4.6 Hz, 1 H), 2.45 (s, 1 H), 2.30 (dd, *J* = 13.4, 8.2 Hz, 1 H), 2.18 - 2.07 (m, 1 H), 1.93 (d, *J* = 2.7 Hz, 1 H), 1.62 - 1.50 (m, 1 H), 1.50 - 1.39 (m, 1 H).

^{13}C-NMR: (126 MHz, CD_3OD)

151.03, 148.72, 147.83, 138.79, 134.80, 134.71, 133.72, 133.04, 133.00, 131.35, 131.16, 131.08, 130.29, 129.29, 126.59, 126.32, 125.60, 125.12, 124.51, 121.55, 121.52, 119.25, 117.63, 69.95, 67.24, 63.74, 56.84, 53.37, 39.66, 27.29, 26.26,

23.04.

LRMS: (ESI$^+$, Q-tof)

191.1 (35), 295.2 (25), 485.3 m/z (100, M-Br+)

HRMS: $C_{34}H_{33}N_2O^+$ (ESI$^+$, Q-tof)

Calcd: 485.2593

Found: 485.2598

TLC: R_f 0.31 (CH_2Cl_2/MeOH, 5:1) [silica gel, I_2]

Preparation of *N*-(2-Naphthylmethyl)cinchonidinium Bromide (2a)

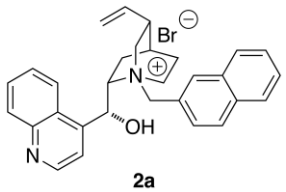

2a

Following General Procedure I, cinchonidine (1.47 g, 5 mmol), MeCN (50 mL), and 2-bromomethylnaphthalene (2.35 g, 10.5 mmol, 2.1 equiv) were combined in a 100-mL, single-neck, round-bottomed flask and the mixture was stirred overnight. The solvent was removed on a rotavap (20 mm Hg, 25 °C) and the remaining off-white solid was triturated in Et_2O (3 x 25 mL) then was filtered three times separately to afford 2.27 g (88%) of **2a** as a white, crystalline solid.

Data for **2a**:

m.p.: 236 °C (decomp.)

^{1}H-NMR: (500 MHz, d_6-DMSO)

9.00 (d, J = 4.4 Hz, 1 H), 8.37 - 8.28 (m, 2 H), 8.12 (dd, J = 7.9, 6.0 Hz, 2 H), 8.08 - 8.01 (m, 2 H), 7.89 - 7.80 (m, 3 H), 7.79 - 7.72 (m, 1 H), 7.69 - 7.61 (m, 2 H), 6.78 (d, J = 4.3 Hz, 1 H), 6.62 (s, 1 H), 5.69 (ddd, J = 17.2, 10.5, 6.5 Hz, 1 H), 5.31 (d, J = 12.4 Hz, 1 H), 5.17 (dd, J = 14.5, 13.3 Hz, 2 H), 4.96 (d, J = 10.5 Hz, 1 H), 4.35 (t, J = 10.6 Hz, 1 H), 3.98 (t, J = 8.9 Hz, 1 H), 3.81 (dd, J = 8.9, 3.7 Hz, 1 H), 3.46 - 3.34 (m, 2 H), 2.64 (s, 1 H), 2.11 (dt, J = 22.9, 10.9 Hz, 2 H), 1.99 (d, J = 2.3 Hz, 1 H), 1.79 (t, J = 10.4 Hz, 1 H), 1.31 (dd, J = 12.9, 10.3 Hz, 1 H).

^{13}C-NMR: (126 MHz, d_6-DMSO)

150.17, 147.62, 145.26, 138.13, 133.91, 133.27, 132.55, 130.15, 129.88, 129.45,

128.38, 128.33, 127.65, 127.54, 127.17, 126.83, 125.41, 124.30, 123.64, 120.06, 116.36, 67.57, 64.20, 62.92, 59.29, 50.67, 36.93, 25.87, 24.25, 20.92.

LRMS: (ESI^+, Q-tof)

295.2 (10), 435.2 (100, M-Br+)

HRMS: $C_{30}H_{31}N_2O^+$ (ESI^+, Q-tof)

Calcd: 435.2436

Found: 435.2439

TLC: R_f 0.25 (CH_2Cl_2/MeOH, 5:1) [silica gel, I_2]

Preparation of *N*-(1-Naphthylmethyl)cinchonidinium Bromide (3a)

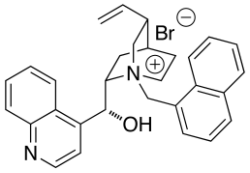

3a

Following General Procedure I, cinchonidine (1.47 g, 5.00 mmol), MeCN (50.0 mL), and 1-bromomethylnaphthalene (1.22 g, 5.50 mmol, 1.1 equiv) were combined in a 100-mL, single-neck, round-bottomed flask fitted with an argon inlet and the reaction mixture was stirred overnight. The solvent was removed on a rotavap (20 mm Hg, 25 °C) and remaining solid was triturated with Et_2O (50 mL) then was filtered to afford 2.33 g (90%) of **3a** as a white, crystalline solid. The entire crude product was further purified by recrystallization from a concentrated CH_2Cl_2 solution by slow diffusion of Et_2O in a chamber.

Data for **3a**:

m.p.: 200 °C (decomp.)

^{1}H-NMR: (500 MHz, CD_3OD)

8.98 (d, *J* = 4.6 Hz, 1 H), 8.40 (d, *J* = 8.2 Hz, 2 H), 8.20 - 8.11 (m, 2 H), 8.09 - 7.99 (m, 3 H), 7.87 (dtd, *J* = 16.5, 6.9, 1.2 Hz, 2 H), 7.79 - 7.73 (m, 1 H), 7.73 - 7.67 (m, 1 H), 7.65 (t, *J* = 7.5 Hz, 1 H), 6.87 (s, 1 H), 5.91 (d, *J* = 13.1 Hz, 1 H), 5.70 (ddd, *J* = 17.3, 10.5, 6.8 Hz, 1 H), 5.37 (d, *J* = 13.1 Hz, 1 H), 5.14 (d, *J* = 17.2 Hz, 1 H), 5.00 (d, *J* = 10.5 Hz, 1 H), 4.68 - 4.57 (m, 1 H), 4.22 (t, *J* = 9.1 Hz, 1 H), 3.88 - 3.78 (m, 1 H), 3.56 (dd, *J* = 12.5, 10.8 Hz, 1 H), 3.16 (td, *J* = 11.4, 3.7

Hz, 1 H), 2.65 (s, 1 H), 2.35 - 2.25 (m, 1 H), 2.24 - 2.14 (m, 1 H), 2.04 (s, 1 H), 1.80 - 1.69 (m, 1 H), 1.42 (td, *J* = 10.2, 3.2 Hz, 1 H).

^{13}C-NMR: (126 MHz, $CDCl_3$)

149.28, 146.89, 144.85, 135.77, 134.29, 133.01, 132.77, 130.27, 129.31, 128.64, 128.06, 127.41, 126.88, 125.70, 124.74, 124.11, 123.45, 123.25, 122.09, 119.48, 117.78, 65.92, 65.80, 59.49, 57.22, 50.99, 37.89, 25.93, 25.31, 22.81

LRMS: (ESI^+, Q-tof)

435.2 (100, M-Br^+)

HRMS: $C_{30}H_{31}N_2O^+$ (ESI^+, Q-tof)
Calcd: 435.2436

Found: 435.2436

TLC: R_f 0.31 (CH_2Cl_2/MeOH, 5:1) [silica gel, I_2]

Preparation of *N*-(Benzyl)cinchonidinium Bromide (4a)

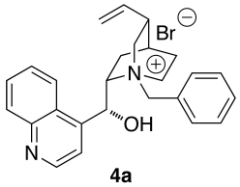

4a

Following General Procedure I, cinchonidine (1.47 g, 5.00 mmol), MeCN (50.0 mL), and benzyl bromide (650 µL, 5.50 mmol, 1.1 equiv) were combined in a 100-mL, single-neck, round-bottomed flask fitted with an argon inlet and the mixture was stirred overnight. The reaction mixture was filtered and the filter cake washed several times with MeCN (50 mL). The filtrate was concentrated on a rotavap (20 mm Hg, 25 °C) and the solid residue triturated with Et_2O (50 mL) then filtered. Both filter cakes were combined to afford 2.25 g (97%) of **4a** as a white, crystalline solid. The entire crude product was further purified by recrystallization from a concentrated CH_2Cl_2 solution by slow diffusion of Et_2O in a chamber.

Data for **4a**:

m.p.: 164 °C (decomp.)

^{1}H-NMR: (500 MHz, CD_3OD)

8.95 (d, *J* = 4.6 Hz, 1 H), 8.28 (d, *J* = 8.2 Hz, 1 H), 8.13 (d, *J* = 8.2 Hz, 1 H), 7.97 (d, *J* = 4.6 Hz, 1 H), 7.90 - 7.84 (m, 1 H), 7.84 - 7.77 (m, 1 H), 7.74 (dd, *J* = 6.5,

2.9 Hz, 2 H), 7.62 - 7.55 (m, 3 H), 6.66 (s, 1 H), 5.69 (ddd, *J* = 17.3, 10.5, 6.8 Hz, 1 H), 5.17 (dd, *J* = 21.7, 14.8 Hz, 2 H), 5.00 (d, *J* = 11.9 Hz, 2 H), 4.50 - 4.40 (m, 1 H), 4.00 (t, *J* = 9.1 Hz, 1 H), 3.66 (ddd, *J* = 12.7, 4.7, 3.3 Hz, 1 H), 3.48 (dd, *J* = 12.7, 10.8 Hz, 1 H), 3.41 (td, *J* = 11.3, 3.8 Hz, 1 H), 2.72 (s, 1 H), 2.33 - 2.19 (m, 2 H), 2.08 (d, *J* = 2.8 Hz, 1 H), 1.88 (ddd, *J* = 15.1, 5.2, 2.6 Hz, 1 H), 1.42 (ddd, *J* = 13.4, 6.5, 3.4 Hz, 1 H).

^{13}C-NMR: (126 MHz, $CDCl_3$)

149.42, 147.14, 144.42, 135.97, 134.02, 129.92, 129.58, 128.62, 128.34, 127.28, 126.90, 123.57, 122.88, 119.76, 117.77, 66.96, 65.06, 62.16, 60.04, 50.28, 37.79, 26.44, 25.08, 22.36

LRMS: (ESI^+, Q-tof)

385.2 (100, M-Br^+)

HRMS: $C_{26}H_{29}N_2O^+$ (ESI^+, Q-tof)

Calcd: 385.2280

Found: 385.2282

TLC: R_f 0.27 (CH_2Cl_2/MeOH, 5:1) [silica gel, I_2]

Preparation of *N*-(3,5-Bis-trifluoromethylbenzyl)cinchonidinium Bromide (5a)

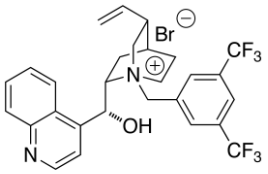

5a

Following General Procedure I, cinchonidine 589 mg (2.00 mmol), MeCN (20.0 mL), and bis-(3,5-trifluoromethyl)benzyl bromide (404 µL, 2.20 mmol, 1.1 equiv) were combined in a 50-mL, single-neck, round-bottomed flask fitted with an argon inlet and the mixture was stirred for 72 hours. The solvent was removed on a rotavap (20 mm Hg, 25 °C) and the solid residue was triturated with Et_2O (30 mL) then filtered to afford 1.04 g (87%) of **5a** as a white, crystalline solid. The product was further purified by recrystallization from a concentrated CH_2Cl_2 solution by slow diffusion of Et_2O in a hamber.

Data for **5a**:

m.p.: 173 °C (decomp.)

^{1}H-NMR: (500 MHz, CD_3OD)

8.95 (d, *J* = 4.6 Hz, 1 H), 8.45 (s, 2 H), 8.33 (d, *J* = 8.1 Hz, 1 H), 8.24 (s, 1 H), 8.13 (dd, *J* = 8.4, 1.0 Hz, 1 H), 7.96 (d, *J* = 4.5 Hz, 1 H), 7.85 (dddd, *J* = 16.5, 8.2, 6.9, 1.3 Hz, 2 H), 6.66 (s, 1 H), 5.69 (ddd, *J* = 17.3, 10.5, 6.8 Hz, 1 H), 5.34 (dd, *J* = 63.7, 12.6 Hz, 2 H), 5.17 (d, *J* = 17.2 Hz, 1 H), 5.01 (d, *J* = 10.5 Hz, 1 H), 4.64 - 4.52 (m, 1 H), 4.05 (t, *J* = 8.4 Hz, 1 H), 3.83 - 3.70 (m, 1 H), 3.47 (dd, *J* = 12.3, 10.8 Hz, 1 H), 3.39 (td, *J* = 11.3, 3.8 Hz, 1 H), 2.74 (s, 1 H), 2.38 - 2.20 (m, 2 H), 2.10 (d, *J* = 2.4 Hz, 1 H), 1.96 - 1.84 (m, 1 H), 1.50 - 1.38 (m, 1 H).

^{13}C-NMR: (126 MHz, CD_3OD)

151.06, 148.76, 147.28, 138.52, 135.45, 133.68 (q, $J_{C\text{-}F}$ = 33.8 Hz), 132.03, 131.22, 130.41, 129.25, 126.06, 125.50 (m), 124.10, 123.43, 121.31, 117.69, 70.34, 66.32, 63.43, 61.93, 53.02, 39.13, 27.92, 25.86, 22.51.

LRMS: (ESI^+, Q-tof)

521.2 (100, M-Br^+)

HRMS: $C_{28}H_{27}N_2OF_6^+$ (ESI^+, Q-tof)

Calcd: 521.2028

Found: 521.2029

TLC: R_f 0.28 (CH_2Cl_2/MeOH, 5:1) [silica gel, I_2]

Preparation of Cinchonidinium Salts in Series B

Preparation of *N*-(9-Anthracenylmethyl)-*epi*-cinchonidinium Bromide (1b)

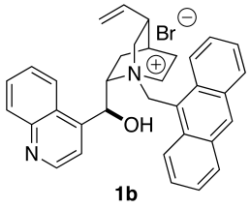

1b

Following General Procedure I, epi-cinchonidine (100 mg, 0.340 mmol), MeCN (3.4 mL), and 9-bromomethylanthracene (101 mg, 0.374 mmol, 1.10 equiv) were combined in a 10-mL, single-neck, round-bottomed flask fitted with an argon inlet, wrapped in aluminum foil and the mixture was stirred overnight. Care was taken to avoid light exposure. The reaction mixture was diluted with CH_2Cl_2 (~5 mL) then was loaded directly on a silica gel column (15 g SiO_2, ∅ = 20, 100:0 to 10:1, CH_2Cl_2/MeOH gradient elution) to afford 169 mg (88%) of **1b** as a light-yellow, crystalline solid. The entire product was further purified by recrystallization from a concentrated CH_2Cl_2 solution by slow diffusion of Et_2O in a chamber.

Data for **1b**:

mp: 154-162 °C (decomp.)

^{1}H-NMR: (500 MHz, CD_3OD)

9.01 (d, *J* = 4.6 Hz, 1 H), 8.85 (s, 1 H), 8.80 (d, *J* = 9.0 Hz, 1 H), 8.63 (d, *J* = 9.0 Hz, 1 H), 8.61 - 8.56 (m, 1 H), 8.23 (d, *J* = 8.5 Hz, 2 H), 8.20 - 8.15 (m, 1 H), 8.08 (d, *J* = 4.5 Hz, 1 H), 7.95 - 7.88 (m, 2 H), 7.80 (dtd, *J* = 7.7, 6.2, 1.1 Hz, 2 H), 7.67 - 7.59 (m, 2 H), 7.11 (d, *J* = 1.9 Hz, 1 H), 6.51 (d, *J* = 14.0 Hz, 1 H), 5.93 (d, *J* = 14.0 Hz, 1 H), 5.70 (ddd, *J* = 17.4, 10.4, 7.2 Hz, 1 H), 5.01 (dd, *J* = 23.7, 13.8 Hz, 2 H), 4.74 - 4.64 (m, 1 H), 4.46 (t, *J* = 9.0 Hz, 1 H), 3.85 (ddd, *J* = 12.5, 4.9, 3.2 Hz, 1 H), 3.24 (dd, *J* = 12.4, 10.9 Hz, 1 H), 2.81 (td, *J* = 11.3, 4.2 Hz, 1 H), 2.45 (s, 1 H), 2.30 (dd, *J* = 13.6, 8.1 Hz, 1 H), 2.19 - 2.08 (m, 1 H), 1.93 (d, *J* = 2.7 Hz, 1 H), 1.62 - 1.52 (m, 1 H), 1.47 (ddd, *J* = 13.3, 8.3, 3.3 Hz, 1 H).

^{13}C-NMR: (126 MHz, CD_3OD)

151.10, 148.88, 147.65, 138.76, 134.82, 134.73, 133.74, 133.07, 133.03, 131.28, 131.17, 131.09, 130.44, 129.30, 129.25, 129.22, 126.60, 126.56, 126.32, 125.50, 125.07, 124.38, 121.50, 119.23, 117.61, 70.06, 67.24, 63.80, 56.89, 53.42, 39.66,

27.29, 26.27, 23.04

LRMS: (ESI$^+$, Q-tof)

485.2 (100, M-Br$^+$)

HRMS: $C_{34}H_{33}N_2O^+$ (ESI$^+$, Q-tof)

Calcd: 485.2593

Found: 485.2594

TLC: R_f 0.58 (CH_2Cl_2/MeOH, 5:1) [silica gel, I_2]

Preparation of *N*-(2-Naphthylmethyl)-*epi*-cinchonidinium Bromide (2b)

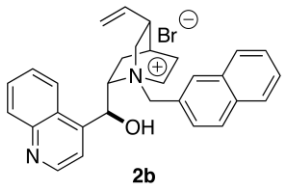

2b

Following General Procedure I, epi-cinchonidine (100 mg, 0.340 mmol), MeCN (3.4 mL), and 2-bromomethylnaphthalene (83.0 mg, 0.374 mmol, 1.1 equiv) were combined in a 10-mL, single-neck, round-bottomed flask fitted with an argon inlet and the mixture was stirred overnight. Reaction was diluted with CH_2Cl_2 (~5 mL) and MeOH (several drops) then was loaded directly on a silica gel column (15 g SiO_2, ∅ = 20, 100:0 to 10:1, CH_2Cl_2/MeOH gradient eleution) to afford 125 mg (71%) of **2b** as a pale-yellow, crystalline solid.

Data for **2b**

m.p.: 198-210 °C (decomp.)

^{1}H-NMR: (500 MHz, d_6-DMSO)

9.00 (d, *J* = 4.5 Hz, 1 H), 8.37 - 8.29 (m, 2 H), 8.15 - 8.08 (m, 2 H), 8.08 - 8.00 (m, 2 H), 7.85 (ddd, *J* = 11.4, 8.3, 2.5 Hz, 3 H), 7.76 (ddd, *J* = 8.2, 6.9, 1.2 Hz, 1 H), 7.69 - 7.60 (m, 2 H), 6.82 (d, *J* = 4.3 Hz, 1 H), 6.62 (d, *J* = 2.9 Hz, 1 H), 5.69 (ddd, *J* = 17.2, 10.6, 6.5 Hz, 1 H), 5.33 (d, *J* = 12.4 Hz, 1 H), 5.17 (t, *J* = 14.5 Hz, 2 H), 4.96 (d, *J* = 10.5 Hz, 1 H), 4.36 (t, *J* = 10.6 Hz, 1 H), 3.98 (t, *J* = 8.9 Hz, 1 H), 3.86 - 3.76 (m, 1 H), 3.39 (ddd, *J* = 18.8, 12.1, 7.8 Hz, 2 H), 2.65 (d, *J* = 3.7 Hz, 1 H), 2.19 - 2.02 (m, 2 H), 1.99 (d, *J* = 2.5 Hz, 1 H), 1.79 (t, *J* = 9.3 Hz, 1 H), 1.31 (dd, *J* = 12.9, 10.2 Hz, 1 H).

^{13}C-NMR: (126 MHz, d_6-DMSO)

150.11, 147.60, 145.21, 138.08, 133.86, 133.24, 132.51, 130.10, 129.84, 129.38, 128.33, 128.28, 127.60, 127.49, 127.12, 126.77, 125.38, 124.28, 123.59, 120.03, 116.31, 67.58, 64.14, 62.88, 59.33, 50.64, 36.90, 25.85, 24.22, 20.90, 19.27.

LRMS: (ESI^+, Q-tof)

435.2 (100, M-Br^+)

HRMS: $C_{30}H_{31}N_2O^+$ (ESI^+, Q-tof)

Calcd: 435.2436

Found: 435.2432

TLC: R_f 0.51 (CH_2Cl_2/MeOH, 5:1) [silica gel, I_2]

Preparation of *N*-(1-Naphthylmethyl)-*epi*-cinchonidinium Bromide (3b)

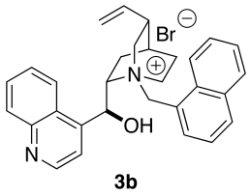

3b

Following General Procedure I, *epi*-cinchonidine (100 mg, 0.340 mmol), MeCN (3.4 mL), and 1-bromomethylnaphthalene (83.0 mg, 0.374 mmol, 1.1 equiv) were combined in a 10-mL, single-neck, round-bottomed flask fitted with an argon inlet and the mixture was stirred overnight. The reaction mixture was diluted with CH_2Cl_2 (~5 mL) and then was loaded directly on a silica gel column (15 g SiO_2, d = 20, 100:0 to 10:1, CH_2Cl_2/MeOH gradient eleution) to afford 141 mg (81%) of **3b** as a white, crystalline solid.

Data for **3b**:

m.p.: 189-197 °C (decomp.)

^{1}H-NMR: (500 MHz, CD_3OD)

8.98 (d, J = 4.5 Hz, 1 H), 8.41 (dd, J = 8.0, 4.6 Hz, 2 H), 8.21 - 8.10 (m, 2 H), 8.10 - 7.99 (m, 3 H), 7.93 - 7.80 (m, 2 H), 7.76 (t, J = 7.6 Hz, 1 H), 7.72 - 7.67 (m, 1 H), 7.64 (t, J = 7.5 Hz, 1 H), 6.87 (s, 1 H), 5.91 (d, J = 13.1 Hz, 1 H), 5.70 (ddd, J = 17.2, 10.5, 6.8 Hz, 1 H), 5.39 (d, J = 13.1 Hz, 1 H), 5.14 (d, J = 17.2 Hz, 1 H), 5.00 (d, J = 10.5 Hz, 1 H), 4.63 (t, J = 10.2 Hz, 1 H), 4.22 (t, J = 8.9 Hz, 1

H), 3.89 - 3.79 (m, 1 H), 3.61 - 3.51 (m, 1 H), 3.16 (td, *J* = 11.3, 3.8 Hz, 1 H), 2.65 (s, 1 H), 2.35 - 2.24 (m, 1 H), 2.24 - 2.13 (m, 1 H), 2.04 (s, 1 H), 1.81 - 1.68 (m, 1 H), 1.42 (td, *J* = 10.0, 2.8 Hz, 1 H).

^{13}C-NMR: (126 MHz, CD_3OD)

151.07, 148.81, 147.54, 138.73, 135.81, 135.65, 134.80, 133.10, 131.20, 130.64, 130.42, 129.18, 128.96, 127.60, 126.41, 126.16, 124.53, 124.14, 121.35, 117.52, 69.68, 66.74, 62.70, 61.28, 53.30, 39.36, 27.64, 26.08, 22.74.

LRMS: (ESI^+, Q-tof)

435.2 (100, M-Br^+)

HRMS: $C_{30}H_{31}N_2O^+$ (ESI^+, Q-tof)

Calcd: 435.2436

Found: 435.2444

TLC: R_f 0.55 (CH_2Cl_2/MeOH, 5:1) [silica gel, I_2]

Preparation of *N*-(Benzyl)-*epi*-cinchonidinium Bromide (4b)

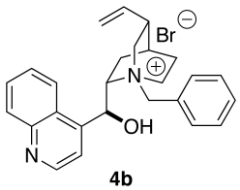

4b

Following General Procedure I, *epi*-cinchonidine (100 mg, 0.340 mmol), MeCN (3.4 mL), and benzyl bromide (44.0 μL, 0.374 mmol, 1.10 equiv) were combined in a 10-mL, single-neck, round-bottomed flask fitted with an argon inlet and the mixture was stirred overnight. The reaction mixture was diluted with CH_2Cl_2 (~5 mL) and then was loaded directly on a silica gel column (15 g SiO_2, ∅ = 20, 100:0 to 10:1, CH_2Cl_2/MeOH gradient eleution) to afford 137 mg (87%) of **4b** as a white, crystalline solid.

Data for **4b**:

m.p.: 165-169 °C (decomp.)

^{1}H-NMR: (500 MHz, CD_3OD)

8.95 (d, *J* = 4.6 Hz, 1 H), 8.29 (d, *J* = 7.9 Hz, 1 H), 8.13 (dd, *J* = 8.4, 0.9 Hz, 1 H), 7.97 (d, *J* = 4.4 Hz, 1 H), 7.84 (dtd, *J* = 16.5, 7.0, 1.2 Hz, 2 H), 7.75 (dd, *J* = 6.4,

2.9 Hz, 2 H), 7.59 (dd, *J* = 4.7, 1.8 Hz, 3 H), 6.66 (s, 1 H), 5.69 (ddd, *J* = 17.2, 10.5, 6.8 Hz, 1 H), 5.17 (dd, *J* = 22.4, 14.8 Hz, 2 H), 5.01 (t, *J* = 11.5 Hz, 2 H), 4.46 (t, *J* = 10.5 Hz, 1 H), 4.01 (t, *J* = 9.1 Hz, 1 H), 3.68 (ddd, *J* = 12.7, 4.5, 3.1 Hz, 1 H), 3.48 (dd, *J* = 12.6, 10.9 Hz, 1 H), 3.41 (td, *J* = 11.2, 3.5 Hz, 1 H), 2.72 (s, 1 H), 2.26 (ddd, *J* = 25.9, 14.7, 6.5 Hz, 2 H), 2.07 (s, 1 H), 1.94 - 1.81 (m, 1 H), 1.42 (td, *J* = 10.1, 2.8 Hz, 1 H).

^{13}C-NMR: (126 MHz, CD_3OD)

151.04, 148.78, 147.52, 138.73, 134.90, 131.76, 131.15, 130.40, 129.15, 128.72, 126.11, 124.08, 121.32, 117.50, 69.70, 66.32, 65.26, 62.10, 52.75, 39.13, 28.04, 25.95, 22.51.

LRMS: (ESI^+, Q-tof)

295.2 (40), 385.2 m/z (100, M-Br^+)

HRMS: $C_{26}H_{29}N_2O^+$ (ESI^+, Q-tof)

Calcd: 385.2280

Found: 385.2285

TLC: R_f 0.51 (CH_2Cl_2/MeOH, 5:1) [silica gel, I_2]

Preparation of *N*-(3,5-Bis-trifluoromethylbenzyl)-*epi*-cinchonidinium Bromide (5b)

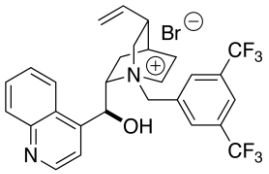

5b

Following General Procedure I, *epi*-cinchonidine (100 mg, 0.340 mmol), MeCN (3.4 mL), and bis-(3,5-trifluormethyl)-benzyl bromide (69.0 μL, 0.374 mmol, 1.10 equiv) were combined in a 10-mL, single-neck, round-bottomed flask fitted with an argon inlet and the mixture was stirred overnight. The reaction mixture was diluted with CH_2Cl_2 (~5 mL) and then was loaded directly on a silica gel column (15 g SiO_2, ∅ = 20, 100:0 to 10:1, CH_2Cl_2/MeOH gradient eleution) to afford 200 mg (98%) of **5b** as a white, crystalline solid.

Data for **5b**:

m.p.: 200-212 °C (decomp.)

^{1}H-NMR: (500 MHz, CD_3OD)

8.96 (d, *J* = 4.6 Hz, 1 H), 8.45 (s, 2H), 8.32 (d, *J* = 8.5 Hz, 1 H), 8.25 (s, 1 H), 8.14 (dd, *J* = 8.4, 1.0 Hz, 1 H), 7.96 (d, *J* = 4.4 Hz, 1 H), 7.85 (dddd, *J* = 24.2, 8.2, 6.9, 1.3 Hz, 2H), 6.66 (s, 1 H), 5.69 (ddd, *J* = 17.3, 10.5, 6.8 Hz, 1 H), 5.40 (d, *J* = 12.6 Hz, 1 H), 5.27 (d, *J* = 12.6 Hz, 1 H), 5.17 (d, *J* = 17.2 Hz, 1 H), 5.01 (d, *J* = 10.5 Hz, 1 H), 4.63 - 4.52 (m, 1 H), 4.05 (t, *J* = 9.1 Hz, 1 H), 3.81 - 3.69 (m, 1 H), 3.48 (dd, *J* = 12.3, 10.8 Hz, 1 H), 3.39 (td, *J* = 11.3, 4.2 Hz, 1 H), 2.74 (s, 1 H), 2.37 - 2.21 (m, 2H), 2.10 (d, *J* = 2.3 Hz, 1 H), 1.97 - 1.85 (m, 1 H), 1.45 (td, *J* = 10.3, 3.3 Hz, 1 H).

^{13}C-NMR: (126 MHz, CD_3OD)

151.07, 148.80, 147.24, 138.51, 135.43, 133.71 (q, $J_{C\text{-}F}$ = 33.7 Hz), 132.02, 131.21, 130.45, 129.23, 126.07, 125.59, 124.05, 123.42, 121.30, 117.70, 70.39, 66.34, 63.48, 62.00, 53.04, 39.14, 27.92, 25.87, 22.51.

LRMS: (ESI^+, Q-tof)

261.1 (15), 521.2 (100, $M\text{-}Br^+$)

HRMS: $C_{28}H_{27}N_2OF_6^+$ (ESI^+, Q-tof)

Calcd: 521.2028

Found: 521.2023

TLC: R_f 0.55 (CH_2Cl_2/MeOH, 5:1) [silica gel, I_2]

Preparation of Cinchonidinium Salts in Series C

Preparation of *O*-Benzyl-*N*-(9-Anthracenylmethyl)cinchonidinium Bromide (1c)

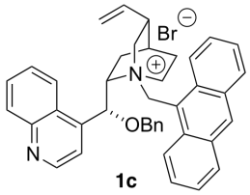

1c

Following General Procedure I, a solution *O*-benzyl-cinchonidine (100 mg, 0.260 mmol) in MeCN (2.60 mL, 0.1 M) was combined with 9-bromomethylanthracene (82.0 mg, 0.286 mmol, 1.1 equiv) in a 5-mL, single-neck, round-bottomed flask fitted with an argon inlet, wrapped in aluminum foil and the mixture was stirred overnight. Care was taken to avoid light exposure. The reaction mixture was diluted with CH_2Cl_2 (~5 mL) and then was loaded directly on a silica gel column (15 g SiO_2, ∅ = 20, 100:0 to 2.5:1, TBME/MeOH, gradient elution) to afford 140 mg (82%) of **1c** as a light-yellow, crystalline solid. The entire product was further purified by recrystallization from a concentrated CH_2Cl_2 solution via Et_2O slow diffusion in a chamber.

Data for **1c**:

m.p.: 185-188 °C (decomp.)

^{1}H-NMR: (500 MHz, CD_3OD)

9.08 (d, *J* = 4.5 Hz, 1 H), 8.87 (s, 1 H), 8.69 (d, *J* = 9.0 Hz, 1 H), 8.59 (s, 1 H), 8.28 - 8.16 (m, 3 H), 8.09 (dd, *J* = 10.3, 6.8 Hz, 2 H), 8.01 - 7.90 (m, 2 H), 7.79 (ddd, *J* = 8.9, 6.6, 1.2 Hz, 1 H), 7.72 (d, *J* = 7.3 Hz, 2 H), 7.66 - 7.47 (m, 5 H), 7.41 - 7.32 (m, 1 H), 7.06 (s, 1 H), 6.27 (d, *J* = 13.7 Hz, 1 H), 5.87 (d, *J* = 13.9 Hz, 1 H), 5.67 (ddd, *J* = 17.4, 10.2, 7.4 Hz, 1 H), 4.99 (ddd, *J* = 17.6, 14.9, 8.0 Hz, 4 H), 4.47 (t, *J* = 8.8 Hz, 1 H), 4.43 - 4.34 (m, 1 H), 3.69 (ddd, *J* = 12.6, 5.6, 3.0 Hz, 1 H), 3.21 - 3.09 (m, 1 H), 2.85 (td, *J* = 11.4, 5.6 Hz, 1 H), 2.61 - 2.50 (m, 1 H), 2.40 (s, 1 H), 2.19 - 2.07 (m, 1 H), 1.97 (d, *J* = 2.8 Hz, 1 H), 1.71 - 1.50 (m, 2H).

^{13}C-NMR: (126 MHz, CD_3OD)

150.46, 148.26, 144.28, 138.46, 138.11, 134.78, 134.43, 133.91, 133.02, 132.96, 132.15, 131.21, 131.15, 130.29, 129.86, 129.77, 129.45, 129.31, 129.17, 126.63,

126.44, 125.33, 124.75, 118.74, 117.82, 79.47, 72.73, 70.28, 63.31, 57.62, 53.82, 39.48, 27.33, 26.17, 23.31.

LRMS: (ESI^+, Q-tof)

575.3 (100, M-Br^+)

HRMS: $C_{41}H_{39}N_2O^+$ (ESI^+, Q-tof)

Calcd: 575.3062

Found: 575.3059

TLC: R_f 0.24 (CH_2Cl_2/MeOH, 10:1) [silica gel, I_2]

Preparation of *O*-Benzyl-*N*-(2-Naphthylmethyl)cinchonidinium Bromide (2c)

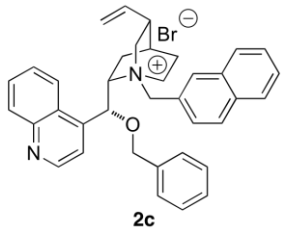

2c

Following General Procedure I, a solution of *O*-benzyl-cinchonidine (100 mg, 0.260 mmol) in MeCN (2.60 mL, 0.1 M) was combined with 2-bromomethylnaphthalene (63.0 mg, 0.286 mmol, 1.10 equiv) in a 5-mL, single-neck, round-bottomed flask fitted with an argon inlet and the mixture was stirred overnight. The reaction mixture was diluted with CH_2Cl_2 (~5 mL) and then was loaded directly on a silica gel column (15 g SiO_2, ∅ = 20, 100:0 to 10:1, CH_2Cl_2/MeOH, gradient elution) to afford 146 mg (93%) of **2c** as a pale-yellow, crystalline solid. The entire product was further purified by recrystallization from a CH_2Cl_2 solution via Et_2O slow diffusion in a chamber.

Data for **2c**:

m.p.: 167-175 °C (decomp.)

^{1}H-NMR: (500 MHz, CD_3OD)

9.03 (d, J = 4.4 Hz, 1 H), 8.26 (d, J = 7.6 Hz, 1 H), 8.20 (d, J = 8.4 Hz, 1 H), 8.08 - 7.95 (m, 5 H), 7.95 - 7.87 (t, J = 7.5 Hz, 1 H), 7.83 (t, J = 7.4 Hz, 1 H), 7.63 (ddd, J = 21.1, 11.3, 6.2 Hz, 4 H), 7.58 - 7.49 (m, 3 H), 7.45 (t, J = 7.3 Hz, 1 H), 6.51 (s, 1 H), 5.68 (ddd, J = 17.3, 10.4, 6.9 Hz, 1 H), 5.11 (d, J = 17.2 Hz, 1 H), 5.00 (d, J = 10.5 Hz, 1 H), 4.93 (dd, J = 13.9, 12.1 Hz, 2 H), 4.80 (d, J = 12.3 Hz,

1 H), 4.67 (d, *J* = 11.5 Hz, 1 H), 4.20 (dd, *J* = 14.5, 7.2 Hz, 1 H), 4.01 (t, *J* = 9.0 Hz, 1 H), 3.63 (ddd, *J* = 12.6, 5.0, 3.0 Hz, 1 H), 3.57 - 3.46 (m, 1 H), 3.40 (td, *J* = 11.3, 4.8 Hz, 1 H), 2.65 (s, 1 H), 2.47 (dd, *J* = 13.1, 7.9 Hz, 1 H), 2.20 (dd, *J* = 18.9, 8.0 Hz, 1 H), 2.07 (d, *J* = 2.6 Hz, 1 H), 1.83 (t, *J* = 9.6 Hz, 1 H), 1.59 (dd, *J* = 13.2, 10.7 Hz, 1 H).

^{13}C-NMR: (126 MHz, CD_3OD)

151.11, 149.29, 142.99, 138.50, 137.75, 135.37, 135.35, 134.44, 131.45, 130.72, 130.55, 130.49, 130.32, 130.12, 130.10, 129.47, 129.45, 129.02, 128.85, 128.26, 126.95, 125.47, 123.85, 121.75, 117.67, 79.46, 72.48, 69.59, 65.56, 62.24, 52.88, 38.95, 27.97, 25.84, 22.82.

LRMS: (ESI^+, Q-tof)

525.3 (100, M-Br^+)

HRMS: $C_{37}H_{37}N_2O^+$ (ESI^+, Q-tof)

Calcd: 525.2906

Found: 525.2910

TLC: R_f 0.28 (CH_2Cl_2/MeOH, 10:1) [silica gel, I_2]

Preparation of *O*-Benzyl-l-*N*-(1-Naphthylmethyl)cinchonidinium Bromide (3c)

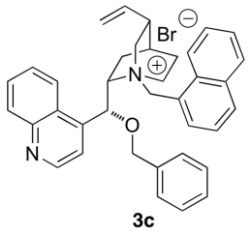

3c

Following General Procedure I, a solution of *O*-benzyl-cinchonidine (100 mg, 0.260 mmol) in MeCN (2.6 mL, 0.1 M) was combined with 1-bromomethylnaphthalene (63.0 mg, 0.286 mmol, 1.10 equiv) in a 5-mL, single-neck, round-bottomed flask fitted with an argon inlet and the mixture was stirred overnight. The reaction mixture was diluted with CH_2Cl_2 (~5 mL) and then was loaded directly on a silica gel column (15 g SiO_2, ∅ = 20, 100:0 to 10:1, CH_2Cl_2/MeOH, gradient elution) to afford 144 mg (92%) of **3c** as a pale-yellow, crystalline solid. The entire product was further purified by recrystallization from a concentrated CH_2Cl_2 solution via Et_2O slow diffusion in a chamber.

Data for **3c**:

m.p.: 164-173 °C (decomp.)

^{1}H-NMR: (500 MHz, CD_3OD)

9.05 (d, *J* = 4.5 Hz, 1 H), 8.43 (d, *J* = 5.2 Hz, 1 H), 8.21 (d, *J* = 7.8 Hz, 1 H), 8.14 (d, *J* = 8.2 Hz, 1 H), 8.03 (dd, *J* = 11.0, 5.8 Hz, 3 H), 7.98 - 7.80 (m, 3 H), 7.67 (dd, *J* = 13.4, 7.5 Hz, 3 H), 7.60 (t, *J* = 7.5 Hz, 1 H), 7.51 (ddd, *J* = 23.2, 14.8, 7.3 Hz, 4 H), 6.75 (s, 1 H), 5.68 (ddd, *J* = 17.3, 10.4, 7.0 Hz, 1 H), 5.49 (d, *J* = 12.9 Hz, 1 H), 5.30 (d, *J* = 13.0 Hz, 1 H), 5.09 (d, *J* = 17.1 Hz, 1 H), 4.97 (dd, *J* = 22.8, 10.9 Hz, 2 H), 4.81 (d, *J* = 11.3 Hz, 1 H), 4.33 - 4.16 (m, 2 H), 3.79 - 3.67 (m, 1 H), 3.44 (t, *J* = 11.7 Hz, 1 H), 3.15 (td, *J* = 11.2, 4.8 Hz, 1 H), 2.59 (s, 1 H), 2.55 - 2.42 (m, 1 H), 2.16 (dd, *J* = 19.2, 7.9 Hz, 1 H), 2.05 (d, *J* = 2.5 Hz, 1 H), 1.73 (t, *J* = 9.4 Hz, 1 H), 1.59 (dd, *J* = 13.0, 10.6 Hz, 1 H).

^{13}C-NMR: (126 MHz, CD_3OD)

151.10, 149.35, 142.89, 138.47, 137.98, 135.76, 134.53, 133.23, 131.50, 130.70, 130.65, 130.26, 129.94, 129.84, 129.50, 128.91, 127.57, 127.00, 126.36, 124.38, 124.16, 124.08, 121.78, 117.72, 79.46, 72.62, 69.90, 62.63, 61.89, 53.44, 39.17, 27.65, 25.96, 23.07.

LRMS: (ESI^+, Q-tof)

525.3 (100, $M\text{-}Br^+$)

HRMS: $C_{37}H_{37}N_2O^+$ (ESI^+, Q-tof)

Calcd: 525.2906

Found: 525.2914

TLC: R_f 0.31 (CH_2Cl_2/MeOH, 10:1) [silica gel, I_2]

Prepartion of *O*-Benzyl-*N*-(Benzyl)cinchonidinium Bromide (4c)

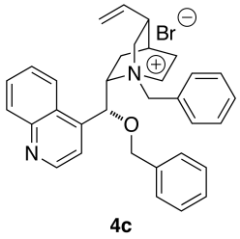

4c

Following General Procedure I, a solution of *O*-benzyl-cinchonidine (100 mg, 0.260 mmol) in MeCN (2.6 mL, 0.1 M) was combined with beznyl bromide (34 μL, 0.286 mmol, 1.1 equiv) in a 5-mL, single-neck, round-bottomed flask fitted with an argon inlet and the mixture was stirred overnight. The reaction mixture was diluted with CH_2Cl_2 (~5 mL) and then was loaded directly on a silica gel column (15 g SiO_2, ∅ = 20, 100:0 to 10:1, CH_2Cl_2/MeOH, gradient elution) to afford 134 mg (93%) of **4c** as a white, crystalline solid. The entire product was further purified by recrystallization from a concentrated CH_2Cl_2 solution via Et_2O slow diffusion in a chamber.

Data for **4c**:

m.p.: 201 - 205 °C(decomp.)

^{1}H-NMR: (500 MHz, CD_3OD)

9.02 (d, *J* = 4.5 Hz, 1 H), 8.25 (d, *J* = 7.6 Hz, 1 H), 8.19 (dd, *J* = 8.4, 0.9 Hz, 1 H), 7.95 (d, *J* = 4.5 Hz, 1 H), 7.91 (ddd, *J* = 8.3, 6.9, 1.2 Hz, 1 H), 7.85 (ddd, *J* = 8.2, 7.0, 1.2 Hz, 1 H), 7.61 - 7.45 (m, 9 H), 7.44 - 7.38 (m, 1 H), 6.46 (s, 1 H), 5.67 (ddd, *J* = 17.3, 10.5, 6.9 Hz, 1 H), 5.11 (d, *J* = 17.2 Hz, 1 H), 4.99 (d, *J* = 10.5 Hz, 1 H), 4.90 - 4.76 (m, 2 H), 4.65 (dd, *J* = 11.8, 7.1 Hz, 2 H), 4.17 - 4.06 (m, 1 H), 3.97 (dd, *J* = 9.8, 8.4 Hz, 1 H), 3.57 (ddd, *J* = 12.8, 5.3, 3.1 Hz, 1 H), 3.43 (dd, *J* = 12.8, 10.7 Hz, 1 H), 3.32 (dd, *J* = 16.6, 10.6 Hz, 1 H), 2.72 - 2.61 (m, 1 H), 2.49 - 2.38 (m, 1 H), 2.24 - 2.12 (m, 1 H), 2.07 (dd, *J* = 6.0, 2.9 Hz, 1 H), 1.84 (ddd, *J* = 14.4, 4.7, 2.3 Hz, 1 H), 1.61 - 1.49 (m, 1 H).

^{13}C-NMR: (126 MHz, CD_3OD)

151.09, 149.26, 142.99, 138.51, 137.69, 134.83, 131.83, 131.46, 130.65, 130.41, 130.37, 130.24, 130.04, 129.50, 128.25, 126.93, 123.95, 121.75, 117.66, 73.17, 72.41, 69.59, 65.33, 61.98, 52.70, 38.91, 27.99, 25.79, 22.80.

LRMS: (ESI$^+$, Q-tof)

475.3 (100, M-Br$^+$)

HRMS: $C_{33}H_{35}N_2O^+$ (ESI$^+$, Q-tof)

Calcd: 475.2749

Found: 475.2756

TLC: R_f 0.26 (CH_2Cl_2/MeOH, 10:1) [silica gel, I_2]

Preparation of *O*-Benzyl-*N*-(3,5-Bis-trifluoromethylbenzyl)cinchonidinium Bromide (5c)

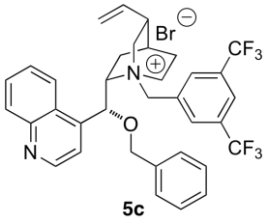

5c

Following General Procedure I, a solution of *O*-benzyl-cinchonidine (100 mg, 0.260 mmol) in MeCN (2.60 mL, 0.1 M) was combined with beznyl bromide (34.0 μL, 0.286 mmol, 1.10 equiv) in a 5-mL, single-neck, round-bottomed flask fitted with an argon inlet and the mixture was stirred overnight. The reaction mixture was diluted with CH_2Cl_2 (~5 mL) and then was loaded directly on a silica gel column (15 g SiO_2, ∅ = 20, 100:0 to 10:1, CH_2Cl_2/MeOH, gradient elution) to afford 166 mg (92%) of **5c** as a white, crystalline solid. The entire product was further purified by trituration in hexane then filtered.

Data for **5c**:

m.p.: 164-170 °C (decomp.)

^{1}H-NMR: (500 MHz, CD_3OD)

9.02 (d, *J* = 4.5 Hz, 1 H), 8.31 (d, *J* = 7.8 Hz, 1 H), 8.24 (s, 1 H), 8.21 - 8.12 (m, 3 H), 7.96 (d, *J* = 4.5 Hz, 1 H), 7.92 (t, *J* = 7.2 Hz, 1 H), 7.87 (dd, *J* = 11.2, 3.9 Hz, 1 H), 7.60 (d, *J* = 7.2 Hz, 2 H), 7.48 (t, *J* = 7.5 Hz, 2 H), 7.41 (t, *J* = 7.4 Hz, 1 H), 6.46 (s, 1 H), 5.67 (ddd, *J* = 17.3, 10.5, 6.9 Hz, 1 H), 5.12 (t, *J* = 14.8 Hz, 2 H), 5.00 (d, *J* = 10.5 Hz, 1 H), 4.88 (d, *J* = 11.5 Hz, 1 H), 4.75 (d, *J* = 12.5 Hz, 1 H), 4.68 (d, *J* = 11.4 Hz, 1 H), 4.19 (dd, *J* = 12.4, 8.7 Hz, 1 H), 4.02 (t, *J* = 9.0 Hz, 1 H), 3.68 (ddd, *J* = 12.3, 4.7, 3.2 Hz, 1 H), 3.47 - 3.37 (m, 1 H), 3.36 - 3.21 (m, 1 H), 2.70 (s, 1 H), 2.53 - 2.41 (m, 1 H), 2.28 - 2.15 (m, 1 H), 2.10 (d, *J* = 2.6 Hz, 1

H), 1.87 (t, J = 9.5 Hz, 1 H), 1.58 (dd, J = 13.2, 10.6 Hz, 1 H).

^{13}C-NMR: (126 MHz, CD_3OD)

151.11, 149.27, 142.81, 138.25, 137.86, 135.29, 133.68 (q, $J_{C\text{-}F}$ = 33.8 Hz), 131.46 (d, $J_{C\text{-}F}$ = 4.3 Hz), 130.71, 130.41, 130.23, 130.09, 129.59, 126.87, 125.76 (d, $J_{C\text{-}F}$ = 3.7 Hz), 125.52, 123.95, 123.35, 121.68, 117.86, 73.37 (d, $J_{C\text{-}F}$ = 11.2 Hz), 72.52, 70.28, 63.61, 61.91, 52.97, 38.90, 27.85, 25.74, 22.79.

LRMS: (ESI^+, Q-tof)

611.2 (100, M-Br^+)

HRMS: $C_{35}H_{33}N_2OF_6^+$ (ESI^+, Q-tof)

Calcd: 611.2497

Found: 611.2499

TLC: R_f 0.29 (CH_2Cl_2/MeOH, 10:1) [silica gel, I_2]

Preparation of Cinchonidinium Salts in Series D

Preparation of *O*-Allyl-*N*-(9-Anthracenylmethyl)cinchonidinium Bromide (1d)

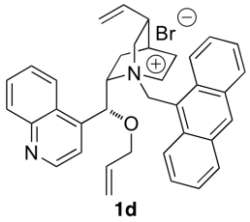

1d

Following General Procedure I, a solution of *O*-allyl-cinchonidine (103 mg, 0.308 mmol) in MeCN (3.20 mL, 0.1 M) was combined with 9-bromomethylanthracene (92.0 mg, 0.339 mmol, 1.10 equiv) in a 10-mL, single-neck, round-bottomed flask fitted with an argon inlet, wrapped in aluminum foil and the mixture was stirred overnight. Care was taken to avoid light exposure. The reaction mixture was diluted with CH_2Cl_2 (~5 mL) and then was loaded directly on a silica gel column (30 g SiO_2, ∅=30, 100:0 to 5:1, CH_2Cl_2/MeOH, gradient elution) to afford 135 mg (72%) of **1d** as a yellow, crystalline solid.

Data for **1d**:

m.p.: 102 °C (decomp.)

^{1}H-NMR: (500 MHz, CD_3OD)

9.04 (d, *J* = 4.5 Hz, 1 H), 8.89 (s, 1 H), 8.77 (d, *J* = 9.0 Hz, 1 H), 8.59 (d, *J* = 5.8 Hz, 1 H), 8.45 (d, *J* = 9.0 Hz, 1 H), 8.30 - 8.17 (m, 3 H), 7.94 (dt, *J* = 12.5, 5.7 Hz, 3 H), 7.85 - 7.71 (m, 2 H), 7.69 - 7.59 (m, 2 H), 6.95 (s, 1 H), 6.41 (ddd, *J* = 15.4, 10.7, 5.3 Hz, 2 H), 5.91 (d, *J* = 14.0 Hz, 1 H), 5.75 - 5.62 (m, 2 H), 5.55 (d, *J* = 10.5 Hz, 1 H), 4.99 (t, *J* = 13.3 Hz, 2 H), 4.60 - 4.36 (m, 4 H), 3.80 (dd, *J* = 7.5, 3.2 Hz, 1 H), 3.24 (t, *J* = 11.6 Hz, 1 H), 2.90 (td, *J* = 11.2, 4.9 Hz, 1 H), 2.54 - 2.35 (m, 2 H), 2.18 (t, *J* = 11.2 Hz, 1 H), 1.97 (d, *J* = 2.5 Hz, 1 H), 1.61 (dd, *J* = 24.9, 12.3 Hz, 2 H).

^{13}C NMR: (126 MHz, CD_3OD)

151.05, 149.35, 142.99, 138.54, 134.81, 134.71, 134.62, 133.92, 133.10, 133.03, 131.53, 131.30, 131.15, 130.60, 129.45, 129.43, 129.25, 127.09, 126.66, 126.56, 125.42, 124.94, 124.45, 121.68, 119.05, 118.91, 117.80, 71.42, 70.04, 63.50, 57.41, 53.65, 39.50, 27.32, 26.26, 23.34.

LRMS: (ESI^+, Q-tof)

191.1 (10), 335.2 (5), 525.3 (100, M-Br^+)

HRMS: $C_{37}H_{37}N_2O^+$ (ESI^+, Q-tof)

Calcd: 525.2906

Found: 525.2906

TLC: R_f 0.32 (CH_2Cl_2/MeOH, 10:1) [silica gel, I_2]

Preparation of *O*-Allyl-*N*-(*2*-Naphthylmethyl)cinchonidinium Bromide (2d)

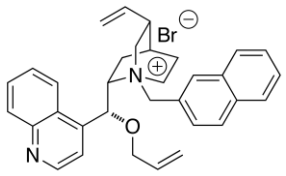

2d

Following General Procedure I, a solution of *O*-allyl-cinchonidine (201 mg, 0.598 mmol) in MeCN (6.00 mL, 0.1 M) was combined with 2-bromomethylnaphthalene (146 mg, 0.660 mmol, 1.10 equiv) in a 10-mL, single-neck, round-bottomed flask fitted with an argon inlet and the mixture was stirred overnight. The solvent was removed on a rotavap (20 mm Hg, 25 °C) and the solid residue was triturated with Et_2O (10 mL) and then filtered. The filter cake was purified by silica gel flash chromatography (20 g SiO_2, ∅ = 20, 100:0 to 10:1, CH_2Cl_2/MeOH, gradient elution) to afford 215 mg (64%) of **2d** as an off-white, crystalline solid.

Data for **2d**:

m.p.: 133 °C (decomp.)

^{1}H-NMR: (500 MHz, CD_3OD)

8.99 (d, *J* = 4.4 Hz, 1 H), 8.31 (d, *J* = 6.4 Hz, 2 H), 8.17 (d, *J* = 8.4 Hz, 1 H), 8.07 (dd, *J* = 18.2, 8.2 Hz, 2 H), 7.99 (d, *J* = 7.6 Hz, 1 H), 7.94 - 7.80 (m, 3 H), 7.77 (d, *J* = 8.4 Hz, 1 H), 7.68 - 7.59 (m, 2 H), 6.53 (s, 1 H), 6.28 (dq, *J* = 10.5, 5.8 Hz, 1 H), 5.71 (ddd, *J* = 17.3, 10.4, 7.0 Hz, 1 H), 5.52 (d, *J* = 17.2 Hz, 1 H), 5.41 (d, *J* = 10.4 Hz, 1 H), 5.28 (d, *J* = 12.4 Hz, 1 H), 5.14 (d, *J* = 14.7 Hz, 2 H), 5.01 (d, *J* = 10.5 Hz, 1 H), 4.41 - 4.19 (m, 3 H), 4.06 (t, *J* = 8.6 Hz, 1 H), 3.77 - 3.65 (m, 1 H), 3.63 - 3.45 (m, 2 H), 2.69 (s, 1 H), 2.51 - 2.37 (m, 1 H), 2.28 (t, *J* = 11.6 Hz, 1 H), 2.10 (d, *J* = 2.1 Hz, 1 H), 1.90 (t, *J* = 10.1 Hz, 1 H), 1.58 (dd, *J* = 13.1, 10.9 Hz, 1 H).

^{13}C-NMR: (126 MHz, CD_3OD)

151.04, 149.22, 143.33, 138.54, 135.49, 135.42, 134.76, 134.56, 131.43, 130.75, 130.58, 130.17, 129.54, 129.41, 129.00, 128.86, 128.22, 126.87, 125.79, 124.10, 121.39, 119.40, 117.69, 73.98, 71.34, 69.77, 66.05, 62.13, 53.10, 39.02, 28.08, 25.95, 22.80.

LRMS: (ESI^+, Q-tof)

475.3 (100, M-Br^+)

HRMS: $C_{33}H_{35}N_2O^+$ (ESI^+, Q-tof)

Calcd: 475.2749

Found: 475.2758

TLC: R_f 0.33 (CH_2Cl_2/MeOH, 10:1) [silica gel, I_2]

Preparation of *O*-Allyl-*N*-(1-Naphthylmethyl)cinchonidinium Bromide (3d)

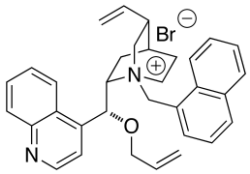

3d

Following General Procedure I, a solution of *O*-allyl-cinchonidine (201 mg, 0.598 mmol) in MeCN (6.00 mL, 0.1 M) was combined with 1-bromomethylnaphthalene (146 mg, 0.660 mmol, 1.10 equiv) in a 10-mL, single-neck, round-bottomed flask fitted with an argon inlet and the mixture was stirred overnight. The solvent was removed on a rotavap (20 mm Hg, 25 °C) and the solid residue was triturated with Et_2O (10 mL) then filtered. The filter cake was purified by silica gel flash chromatography (20 g SiO_2, ∅ = 20, 100:0 to 10:1, CH_2Cl_2/MeOH, gradient elution) to afford 280 mg (84%) of **3d** as a white, crystalline solid.

Data for **3d**:

m.p.: 119 °C (decomp.)

^{1}H-NMR: (500 MHz, CD_3OD)

9.01 (d, J = 4.5 Hz, 1 H), 8.42 (d, J = 8.1 Hz, 1 H), 8.30 (d, J = 8.5 Hz, 1 H), 8.18 (t, J = 7.3 Hz, 2 H), 8.06 (dd, J = 15.2, 7.6 Hz, 2 H), 7.95 - 7.83 (m, 3 H), 7.72 (dd, J = 15.4, 8.0 Hz, 2 H), 7.65 (t, J = 7.5 Hz, 1 H), 6.69 (s, 1 H), 6.35 (ddd, J =

22.2, 10.9, 5.6 Hz, 1 H), 5.71 (ddd, *J* = 17.3, 15.9, 10.1 Hz, 2 H), 5.60 (dd, *J* = 17.2, 1.2 Hz, 1 H), 5.49 (d, *J* = 10.5 Hz, 1 H), 5.38 (d, *J* = 13.0 Hz, 1 H), 5.12 (d, *J* = 17.2 Hz, 1 H), 4.99 (d, *J* = 10.5 Hz, 1 H), 4.38 (ddd, *J* = 17.4, 12.3, 5.6 Hz, 3 H), 4.23 (t, *J* = 9.1 Hz, 1 H), 3.90 - 3.75 (m, 1 H), 3.55 (t, *J* = 11.7 Hz, 1 H), 3.24 (td, *J* = 11.4, 4.5 Hz, 1 H), 2.65 (s, 1 H), 2.44 (dd, *J* = 13.2, 8.3 Hz, 1 H), 2.23 (dd, *J* = 19.5, 7.7 Hz, 1 H), 2.07 (d, *J* = 2.4 Hz, 1 H), 1.79 (t, *J* = 9.3 Hz, 1 H), 1.55 (dd, *J* = 13.1, 10.6 Hz, 1 H).

^{13}C-NMR: (126 MHz, CD_3OD)

151.04, 149.27, 143.04, 138.51, 135.76, 134.72, 134.67, 133.21, 131.45, 130.71, 130.60, 129.42, 128.92, 127.64, 126.91, 126.47, 124.45, 124.32, 124.17, 121.43, 119.28, 117.69, 71.40, 69.73, 62.60, 61.86, 53.49, 39.19, 27.67, 26.04, 23.07.

LRMS: (ESI^+, Q-tof)

335.2 (5), 475.3 (100, M-Br^+)

HRMS: $C_{33}H_{35}N_2O^+$ (ESI^+, Q-tof)

Calcd: 475.2749

Found: 475.2758

TLC: R_f 0.28 (CH_2Cl_2/MeOH, 10:1) [silica gel, I_2]

Preparation of *O*-Allyl-*N*-(Benzyl)cinchonidinium Bromide (4d)

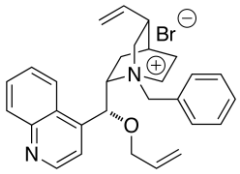

4d

Following General Procedure I, a solution of *O*-allyl-cinchonidine (201 mg, 0.598 mmol) in MeCN (6.00 mL, 0.1 M) was combined with benzyl bromide (78.5 µL, 0.660 mmol, 1.10 equiv) in a 10-mL, single-neck, round bottom flask fitted with an argon inlet and the mixture was stirred overnight. The solvent was removed on a rotavap (20 mm Hg, 25 °C) and the solid residue was triturated with hexane then filtered. The filter cake was purified by silica gel flash chromatography (20 g SiO_2, ∅ = 20, 100:0 to 10:1, CH_2Cl_2/MeOH, gradient elution) to afford 222 mg (73%) of of **4d** as a white, crystalline solid.

Data for **4d**:

m.p.: 123 °C (decomp.)

^{1}H-NMR: (500 MHz, CD_3OD)

8.98 (d, *J* = 4.5 Hz, 1 H), 8.28 (d, *J* = 8.3 Hz, 1 H), 8.16 (d, *J* = 8.4 Hz, 1 H), 7.94 - 7.80 (m, 3 H), 7.73 (dd, *J* = 6.3, 2.7 Hz, 2 H), 7.65 - 7.55 (m, 3 H), 6.47 (s, 1 H), 6.24 (ddd, *J* = 22.9, 11.0, 5.8 Hz, 1 H), 5.69 (ddd, *J* = 17.3, 10.5, 6.9 Hz, 1 H), 5.49 (dd, *J* = 17.2, 1.3 Hz, 1 H), 5.38 (d, *J* = 10.4 Hz, 1 H), 5.12 (t, *J* = 14.9 Hz, 2 H), 4.99 (dd, *J* = 18.8, 11.4 Hz, 2 H), 4.26 (ddd, *J* = 17.5, 12.3, 5.7 Hz, 3 H), 4.01 (t, *J* = 9.0 Hz, 1 H), 3.63 (ddd, *J* = 12.6, 5.1, 3.1 Hz, 1 H), 3.56 - 3.38 (m, 2 H), 2.72 (s, 1 H), 2.42 (dd, *J* = 13.1, 7.9 Hz, 1 H), 2.32 - 2.19 (m, 1 H), 2.10 (d, *J* = 2.8 Hz, 1 H), 1.92 (t, *J* = 9.5 Hz, 1 H), 1.61 - 1.48 (m, 1 H).

^{13}C-NMR: (126 MHz, CD_3OD)

151.02, 149.22, 143.25, 138.52, 134.91, 134.69, 131.87, 131.40, 130.59, 130.47, 129.39, 128.51, 126.84, 124.07, 121.37, 119.43, 117.68, 73.99, 71.33, 69.76, 65.86, 62.02, 52.94, 38.98, 28.08, 25.92, 22.80.

LRMS: (ESI^+, Q-tof)

425.3 (100, $M\text{-}Br^+$)

HRMS: $C_{29}H_{33}N_2O^+$ (ESI^+, Q-tof)

Calcd: 425.2593

Found: 425.2603

TLC: R_f 0.28 (CH_2Cl_2/MeOH, 10:1) [silica gel, I_2]

Preparation of *O*-Allyl-*N*-(3,5-Bistrifluoromethylbenzyl)cinchonidinium Bromide (5d)

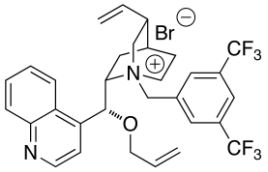

5d

Following General Procedure I, a solution of *O*-allyl-cinchonidine (201 mg, 0.598 mmol) in MeCN (6.00 mL, 0.1 M) was combined with bis-(3,5-trifluoromethyl)benzyl bromide (121 μL, 0.660 mmol, 1.10 equiv) in a 10-mL, single-neck, round-bottomed flask fitted with an argon inlet and the mixture was stirred overnight. The solvent was removed on a rotavap (20 mm Hg, 25 °C) and the solid residue was triturated with hexane then filtered. The filter cake was purified by silica gel flash chromatography (20 g SiO_2, ∅ = 20, 100:0 to 10:1, CH_2Cl_2/MeOH, gradient elution) to afford 307 mg (85%) of **5d** as a white, crystalline solid.

Data for **5d:**

m.p.: 140 °C (decomp.)

^{1}H-NMR: (500 MHz, CD_3OD)

8.98 (d, *J* = 4.6 Hz, 1 H), 8.46 (s, 2 H), 8.31 (d, *J* = 8.2 Hz, 1 H), 8.26 (s, 1 H), 8.20 - 8.13 (m, 1 H), 7.94 - 7.81 (m, 3 H), 6.45 (s, 1 H), 6.24 (ddd, *J* = 22.9, 10.9, 5.7 Hz, 1 H), 5.70 (ddd, *J* = 17.3, 10.5, 7.0 Hz, 1 H), 5.49 (dd, *J* = 17.2, 1.5 Hz, 1 H), 5.36 (dd, *J* = 10.5, 1.2 Hz, 1 H), 5.27 (dd, *J* = 36.6, 12.6 Hz, 2 H), 5.15 (d, *J* = 17.2 Hz, 1 H), 5.02 (d, *J* = 10.5 Hz, 1 H), 4.37 (td, *J* = 11.8, 4.7 Hz, 2 H), 4.19 (dd, *J* = 12.2, 5.5 Hz, 1 H), 4.10 - 3.98 (m, 1 H), 3.71 (ddd, *J* = 12.3, 5.0, 3.1 Hz, 1 H), 3.54 - 3.40 (m, 2 H), 2.74 (s, 1 H), 2.48 (dd, *J* = 13.1, 7.8 Hz, 1 H), 2.35 - 2.23 (m, 1 H), 2.13 (d, *J* = 2.9 Hz, 1 H), 1.95 (t, *J* = 9.5 Hz, 1 H), 1.59 (td, *J* = 10.5, 3.1 Hz, 1 H).

^{13}C-NMR: (126 MHz, CD_3OD)

151.02, 149.25, 143.04, 138.29, 135.50, 134.81, 133.74 (q, $J_{C\text{-}F}$ = 33.9 Hz), 131.81, 131.43, 130.62, 129.48, 126.79, 125.77, 125.58, 124.08, 123.41, 121.35, 119.05, 117.89, 73.95, 71.30, 70.58, 64.18, 61.95, 53.27, 39.00, 27.97, 25.87, 22.76.

LRMS: (ESI^+, Q-tof)

561.2 (100, M-Br^+)

HRMS: $C_{31}H_{31}N_2OF_6^+$ (ESI^+, Q-tof)

Calcd: 561.2341

Found: 561.2344

TLC: R_f 0.32 (CH_2Cl_2/MeOH, 10:1) [silica gel, I_2]

Preparation of Cinchonidinium Salts in Series E

Preparation of *O*-Methyl-*N*-(9-Anthracenylmethyl)cinchonidinium Bromide (1e)

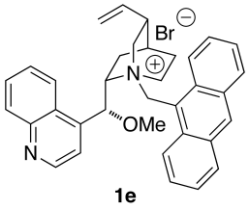

1e

Following General Procedure I, *O*-methyl-cinchonidine (100 mg, 0.324 mmol), MeCN (3.2 mL, 0.1 M), and 9-bromomethylanthracene (97.0 mg, 0.360 mmol, 1.10 equiv) were combined in a 10-mL, single-neck, round-bottomed flask fitted with an argon inlet, wrapped in aluminum foil and the mixture was stirred overnight. Care was taken to avoid light exposure. The solvent was removed on a rotavap (20 mm Hg, 25 °C) and the yellow solid residue was then purified by silica gel flash chromatography (15 g SiO_2, ∅ = 20, 100:0 to 10:1, CH_2Cl_2/MeOH, gradient elution) to afford 141 mg (75%) of **1e** as a light-yellow, crystalline solid.

Data for **1e**:

m.p.: 120 °C (decomp.)

^{1}H-NMR: (500 MHz, CD_3OD)

9.05 (d, *J* = 4.5 Hz, 1 H), 8.89 (s, 1 H), 8.75 (d, *J* = 9.0 Hz, 1 H), 8.57 (d, *J* = 8.7 Hz, 1 H), 8.52 (d, *J* = 9.0 Hz, 1 H), 8.23 (ddd, *J* = 9.2, 7.7, 4.6 Hz, 3 H), 7.98 - 7.89 (m, 3 H), 7.85 (ddd, *J* = 8.9, 6.6, 1.2 Hz, 1 H), 7.80 (ddd, *J* = 8.9, 6.5, 1.2 Hz, 1 H), 7.65 (ddd, *J* = 11.6, 8.3, 6.8 Hz, 2 H), 6.82 (s, 1 H), 6.42 (d, *J* = 14.0 Hz, 1 H), 5.90 (d, *J* = 14.0 Hz, 1 H), 5.69 (ddd, *J* = 17.4, 10.4, 7.3 Hz, 1 H), 5.04 - 4.93 (m, 2 H), 4.55 - 4.40 (m, 2 H), 3.85 (s, 3 H), 3.78 (ddd, *J* = 12.5, 5.4, 3.1 Hz, 1 H), 3.24 (dd, *J* = 12.4, 10.9 Hz, 1 H), 2.95 - 2.85 (m, 1 H), 2.42 (dd, *J* = 15.6, 5.0 Hz, 2 H), 2.20 - 2.08 (m, 1 H), 1.95 (d, *J* = 2.8 Hz, 1 H), 1.58 (ddd, *J* = 13.8, 13.4, 8.4 Hz, 2 H).

^{13}C-NMR: (126 MHz, CD_3OD)

151.06, 149.35, 142.98, 138.54, 134.79, 134.66, 133.90, 133.09, 133.05, 131.50, 131.28, 131.17, 130.59, 129.43, 129.41, 129.36, 127.23, 126.65, 126.61, 125.37, 124.81, 124.44, 121.67, 119.00, 117.77, 70.22, 63.45, 57.51, 57.48, 53.77, 39.53, 27.31, 26.22, 23.13.

LRMS: (ESI$^+$, Q-tof)

191.1 (15), 499.3 (100, M-Br$^+$)

HRMS: $C_{35}H_{35}N_2O^+$ (ESI$^+$, Q-tof)

Calcd: 499.2749

Found: 499.2739

TLC: R_f 0.34 (CH_2Cl_2/MeOH, 10:1) [silica gel, I_2]

Preparation of *O*-Methyl-*N*-(2-Naphthylmethyl)cinchonidinium Bromide (2e)

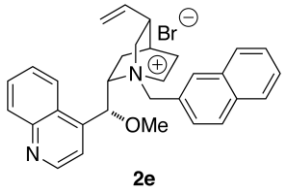

2e

Following General Procedure I, *O*-methyl-cinchonidine (185 mg, 0.600 mmol), MeCN (6.0 mL, 0.1 M), and 2-bromomethylnaphthalene (146 mg, 0.660 mmol, 1.10 equiv) were combined in a 10-mL, single-neck, round-bottomed flask fitted with an argon inlet and the mixture was stirred overnight. The solvent was removed on a rotavap (20 mm Hg, 25 °C) and the solid residue was then purified by silica gel flash chromatography (15 g SiO_2, ∅ = 20, 100:0 to 10:1, CH_2Cl_2/MeOH, gradient elution) to afford 265 mg (83%) of **2e** as an off-white, crystalline solid.

Data for **2e**:

m.p.: 144 °C (decomp.)

^{1}H-NMR: (500 MHz, CD_3OD)

9.00 (d, *J* = 4.5 Hz, 1 H), 8.39 - 8.28 (m, 2 H), 8.17 (d, *J* = 8.4 Hz, 1 H), 8.07 (dd, *J* = 16.9, 7.8 Hz, 2 H), 8.00 (d, *J* = 8.3 Hz, 1 H), 7.93 - 7.87 (m, 1 H), 7.87 - 7.77 (m, 3 H), 7.68 - 7.59 (m, 2 H), 6.39 (s, 1 H), 5.70 (ddd, *J* = 17.3, 10.4, 6.9 Hz, 1 H), 5.27 (d, *J* = 12.4 Hz, 1 H), 5.14 (dd, *J* = 15.1, 4.8 Hz, 2 H), 5.01 (d, *J* = 10.5 Hz, 1 H), 4.33 (t, *J* = 10.8 Hz, 1 H), 4.04 (t, *J* = 9.0 Hz, 1 H), 3.78 - 3.69 (m, 1 H), 3.65 (s, 3 H), 3.54 (dd, *J* = 22.1, 9.9 Hz, 2 H), 2.69 (s, 1 H), 2.39 (dd, *J* = 13.1, 8.1 Hz, 1 H), 2.25 (t, *J* = 11.6 Hz, 1 H), 2.08 (d, *J* = 2.5 Hz, 1 H), 1.88 (t, *J* = 9.4 Hz, 1 H), 1.54 (dd, *J* = 13.3, 10.6 Hz, 1 H).

^{13}C-NMR: (126 MHz, CD_3OD)

151.04, 149.23, 143.10, 138.58, 135.54, 135.42, 134.57, 131.39, 130.81, 130.55, 130.10, 129.53, 129.36, 128.97, 128.86, 128.19, 127.01, 125.88, 124.15, 121.34, 117.65, 76.06, 69.81, 66.04, 62.04, 57.42, 53.03, 39.03, 28.05, 25.90, 22.74.

LRMS: (ESI^+, Q-tof)

449.2 (100, M-Br^+)

HRMS: $C_{31}H_{33}N_2O^+$ (ESI^+, Q-tof)

Calcd: 449.2593

Found: 449.2594

TLC: R_f 0.38 (CH_2Cl_2:MeOH, 10:1) [silica gel, I_2]

Preparation of *O*-Methyl-N-(1-Naphthylmethyl)cinchonidinium Bromide (3e)

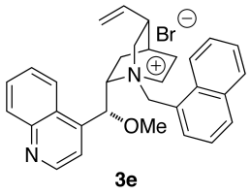

3e

Following General Procedure I, *O*-methyl-cinchonidine (185 mg, 0.600 mmol), MeCN (6.0 mL, 0.1 M), and 1-bromomethylnaphthalene (146 mg, 0.660 mmol, 1.10 equiv) were combined in a 10-mL, single-neck, round-bottomed flask fitted with an argon inlet and the mixture was stirred overnight. The solvent was removed on a rotavap (20 mm Hg, 25 °C) and the solid residue was triturated with Et_2O then filtered. The filter cake was purified by silica gel flash chromatography (15 g SiO_2, ∅ = 20, 100:0 to 10:1, CH_2Cl_2/MeOH, gradient elution) to afford 287 mg (90%) of **3e** as a white, crystalline solid.

Data for **3e**:

m.p.: 132 °C (decomp.)

^{1}H-NMR: (500 MHz, CD_3OD)

9.02 (d, *J* = 4.5 Hz, 1 H), 8.40 (d, *J* = 8.2 Hz, 1 H), 8.34 (d, *J* = 8.6 Hz, 1 H), 8.21 - 8.14 (m, 2 H), 8.06 (dd, *J* = 11.3, 7.7 Hz, 2 H), 7.94 - 7.83 (m, 3 H), 7.79 (dd, *J* = 11.3, 4.1 Hz, 1 H), 7.75 - 7.69 (m, 1 H), 7.66 (t, *J* = 7.5 Hz, 1 H), 6.55 (s, 1 H), 5.70 (ddd, *J* = 17.3, 16.5, 10.0 Hz, 2 H), 5.37 (d, *J* = 13.1 Hz, 1 H), 5.10 (d, *J* =

17.2 Hz, 1 H), 4.99 (d, *J* = 10.5 Hz, 1 H), 4.39 (ddd, *J* = 11.7, 8.0, 4.6 Hz, 1 H), 4.21 (t, *J* = 9.0 Hz, 1 H), 3.78 (ddd, *J* = 12.7, 5.0, 3.2 Hz, 1 H), 3.74 (s, 3 H), 3.56 - 3.45 (m, 1 H), 3.30 - 3.21 (m, 1 H), 2.63 (s, 1 H), 2.40 (dd, *J* = 13.3, 8.0 Hz, 1 H), 2.21 (dd, *J* = 19.5, 8.4 Hz, 1 H), 2.05 (d, *J* = 2.9 Hz, 1 H), 1.86 - 1.71 (m, 1 H), 1.54 (td, *J* = 10.5, 3.1 Hz, 1 H).

^{13}C-NMR: (126 MHz, CD_3OD)

151.05, 149.30, 143.00, 138.51, 135.82, 135.77, 134.71, 133.22, 131.42, 130.71, 130.60, 129.37, 129.07, 127.65, 127.07, 126.45, 124.39, 124.37, 124.18, 121.42, 117.69, 76.30, 69.98, 62.55, 62.03, 57.43, 53.53, 39.24, 27.70, 26.03, 22.87.

LRMS: (ESI^+, Q-tof)

449.2 (100, M-Br^+)

HRMS: $C_{31}H_{33}N_2O^+$ (ESI^+, Q-tof)

Calcd: 449.2593

Found: 449.2574

TLC: R_f 0.38 (CH_2Cl_2/MeOH, 10:1) [silica gel, I_2]

Preparation of *O*-Methyl-*N*-(Benzyl)cinchonidinium Bromide (4e)

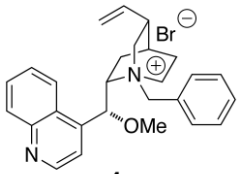

4e

Following General Procedure I, *O*-methyl-cinchonidine (185 mg, 0.60 mmol), MeCN (6.0 mL, 0.1 M), and benzyl bromide (78.0 μL, 0.660 mmol, 1.10 equiv) were combined in a 10-mL, single-neck, round-bottomed flask fitted with an argon inlet and the mixture was stirred for 41 h. The solvent was removed on a rotavap (20 mm Hg, 25 °C) and the solid residue was triturated with hexanes then filtered. The filter cake was purified by silica gel flash chromatography (15 g SiO_2, ∅ = 20, 100:0 to 10:1, CH_2Cl_2/MeOH, gradient elution) to afford 211 mg (73%) of **4e** as a white, crystalline solid.

Data **4e**:

m.p.: 140 °C (decomp.)

^{1}H-NMR: (500 MHz, CD_3OD)

8.98 (d, *J* = 4.5 Hz, 1 H), 8.28 (d, *J* = 8.3 Hz, 1 H), 8.19 - 8.12 (m, 1 H), 7.93 - 7.86 (m, 1 H), 7.84 (dd, *J* = 11.4, 3.1 Hz, 2 H), 7.76 (dd, *J* = 6.6, 2.9 Hz, 2 H), 7.60 (dd, *J* = 4.0, 1.8 Hz, 3 H), 6.33 (s, 1 H), 5.68 (ddd, *J* = 17.3, 10.5, 6.9 Hz, 1 H), 5.18 - 5.06 (m, 2 H), 4.98 (dd, *J* = 16.9, 11.4 Hz, 2 H), 4.28 - 4.16 (m, 1 H), 3.98 (t, *J* = 9.1 Hz, 1 H), 3.69 - 3.56 (m, 4 H), 3.53 - 3.38 (m, 2 H), 2.71 (s, 1 H), 2.42 - 2.31 (m, 1 H), 2.23 (tdd, *J* = 10.9, 6.9, 4.3 Hz, 1 H), 2.08 (d, *J* = 2.9 Hz, 1 H), 1.96 - 1.83 (m, 1 H), 1.58 - 1.45 (m, 1 H).

^{13}C-NMR: (126 MHz, CD_3OD)

151.02, 149.24, 143.03, 138.56, 134.95, 131.83, 131.36, 130.56, 130.43, 129.33, 128.59, 126.98, 124.10, 121.32, 117.64, 76.03, 69.85, 65.90, 61.95, 57.36, 52.90, 39.00, 28.05, 25.88, 22.72.

LRMS: (ESI^+, Q-tof)

399.2 (100, M-Br^+)

HRMS: $C_{27}H_{31}N_2O^+$ (ESI^+, Q-tof)

Calcd: 399.2436

Found: 399.2420

TLC: R_f 0.38 (CH_2Cl_2:MeOH, 10:1) [silica gel, I_2]

Preparation of *O*-Methyl-*N*-(3,5-Bistrifluoromethylbenzyl)cinchonidinium Bromide (5e)

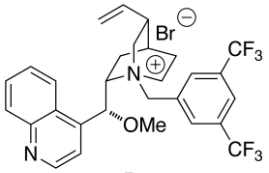

5e

Following General Procedure I, *O*-methyl-cinchonidine (185 mg, 0.600 mmol), MeCN (6.0 mL, 0.1 M), and bis-(3,5-trifluoromethyl)benzyl bromide (121 μL, 0.660 mmol, 1.10 equiv) were combined in a 10-mL, single-neck, round-bottomed flask fitted with an argon inlet and the mixture was stirred for 41 h. The solvent was removed on a rotavap (20 mm Hg, 25 °C) and the solid residue was triturated with hexane then filtered. The filter cake was purified by silica gel flash chromatography (15 g SiO_2, ∅ = 20, 100:0 to 10:1, CH_2Cl_2/MeOH, gradient elution) to afford 249 mg (67%) of **5e** as a white, crystalline solid.

Data for **5e**:

m.p.: 154 °C (decomp.)

^{1}H-NMR: (500 MHz, CD_3OD)

8.99 (d, *J* = 4.5 Hz, 1 H), 8.51 (s, 2 H), 8.32 (d, *J* = 8.3 Hz, 1 H), 8.26 (s, 1 H), 8.16 (d, *J* = 8.4 Hz, 1 H), 7.94 - 7.78 (m, 3 H), 6.30 (s, 1 H), 5.68 (ddd, *J* = 17.3, 10.5, 6.9 Hz, 1 H), 5.25 (q, *J* = 12.6 Hz, 2 H), 5.15 (d, *J* = 17.2 Hz, 1 H), 5.01 (d, *J* = 10.5 Hz, 1 H), 4.39 (t, *J* = 11.2 Hz, 1 H), 4.01 (t, *J* = 9.1 Hz, 1 H), 3.76 - 3.68 (m, 1 H), 3.62 (s, 3 H), 3.45 (t, *J* = 11.5 Hz, 2 H), 2.73 (s, 1 H), 2.40 (dd, *J* = 12.3, 9.1 Hz, 1 H), 2.24 (dd, *J* = 19.5, 8.4 Hz, 1 H), 2.11 (s, 1 H), 1.93 (t, *J* = 11.7 Hz, 1 H), 1.54 (t, *J* = 11.8 Hz, 1 H).

^{13}C NMR: (126 MHz, CD_3OD)

151.03, 149.27, 142.72, 138.36, 135.55, 133.72 (q, $J_{C\text{-}F}$ = 33.9 Hz). 131.90, 131.40, 130.62, 129.43, 126.94, 125.69, 125.61, 124.08, 123.44, 121.35, 117.83, 76.01, 70.52, 64.05, 61.90, 57.49, 53.21, 39.01, 27.92, 25.81, 22.79

LRMS: (ESI^+, Q-tof)

535.2 (100, M-Br^+)

HRMS: $C_{29}H_{29}N_2OF_6^+$ (ESI^+, Q-tof)

Calcd: 535.2184

Found: 535.2187

TLC: R_f 0.34 (CH_2Cl_2/MeOH, 10:1) [silica gel, I_2]

Preparation of Cinchonidinium Salts in Series F

Preparation of *O*-Methyl-*N*-(9-Anthracenylmethyl)-*epi*-cinchonidinium Bromide (1f)

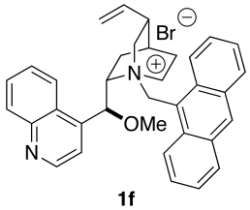

1f

Following General Procedure I, *O*-methyl-*epi*-cinchonidine (81 mg, 0.26 mmol), MeCN (2.6 mL, 0.1 M), and 9-bromomethylanthracene (78 mg, 0.29 mmol, 1.1 equiv) were combined in a 10-mL, single-neck, round-bottomed flask fitted with an argon inlet, wrapped in aluminum foil and the mixture was stirred overnight. Care was taken to avoid light exposure. The reaction mixture was diluted with CH_2Cl_2 (~5 mL) and then was loaded directly on a silica gel column (15 g SiO_2, ∅ = 20, 100:0 to 2.5:1, TBME/MeOH, gradient elution) to afford 136 mg (90%) of **1f** as a light-yellow, crystalline solid.

Data for **1f**:

m.p.: 143 °C (decomp.)

^{1}H-NMR: (500 MHz, CD_3OD)

9.04 (d, *J* = 4.5 Hz, 1 H), 8.89 (s, 1 H), 8.76 (d, *J* = 9.0 Hz, 1 H), 8.58 (d, *J* = 7.4 Hz, 1 H), 8.51 (d, *J* = 9.0 Hz, 1 H), 8.22 (ddd, *J* = 9.5, 7.5, 4.6 Hz, 3 H), 7.98 - 7.89 (m, 3 H), 7.88 - 7.76 (m, 2 H), 7.65 (ddd, *J* = 11.8, 8.3, 6.7 Hz, 2 H), 6.82 (s, 1 H), 6.42 (d, *J* = 14.0 Hz, 1 H), 5.91 (d, *J* = 14.0 Hz, 1 H), 5.69 (ddd, *J* = 17.4, 10.4, 7.3 Hz, 1 H), 4.99 (m, 2 H), 4.53 - 4.40 (m, 2 H), 3.85 (s, 3 H), 3.79 (ddd, *J* = 12.5, 5.4, 3.0 Hz, 1 H), 3.23 (dd, *J* = 12.4, 10.9 Hz, 1 H), 2.90 (td, *J* = 11.0, 4.7 Hz, 1 H), 2.41 (dd, *J* = 15.4, 4.6 Hz, 2 H), 2.20 - 2.08 (m, 1 H), 1.95 (d, *J* = 3.0 Hz, 1 H), 1.66 - 1.49 (m, 2 H)

^{13}C-NMR: (126 MHz, CD_3OD)

151.05, 149.37, 142.95, 138.54, 134.79, 134.66, 133.89, 133.09, 133.05, 131.48, 131.27, 131.16, 130.61, 129.43, 129.41, 129.36, 127.23, 126.64, 126.60, 125.39, 124.80, 124.45, 121.67, 118.99, 117.76, 76.83, 70.24, 63.48, 61.55, 57.53, 53.79, 39.52, 27.31, 26.23, 23.15

LRMS: (ESI^+, Q-tof)

191.1 (10), 499.3 (100, M-Br^+)

HRMS: $C_{35}H_{35}N_2O^+$ (ESI^+, Q-tof)

Calcd: 499.2749

Found: 499.2741

TLC: R_f 0.36 (CH_2Cl_2/MeOH, 10:1) [silica gel, I_2]

Preparation of *O*-Methyl-*N*-(2-Naphthylmethyl)-*epi*-cinchonidinium Bromide (2f)

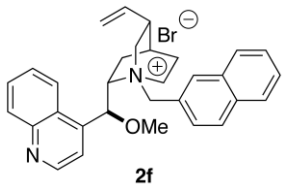

2f

Following General Procedure I, *O*-methyl-*epi*-cinchonidine (90 mg, 0.29 mmol), MeCN (2.9 mL, 0.1 M), and 2-bromomethylnaphthalene (71 mg, 0.32 mmol, 1.1 equiv) were combined in a 10-mL, single-neck, round-bottomed flask fitted with an argon inlet and the mixture was stirred overnight. The reaction mixture was diluted with CH_2Cl_2 (~5 mL) and then was loaded directly on a silica gel column (15 g SiO_2, ∅ = 20, 100:0 to 10:1, CH_2Cl_2/MeOH, gradient elution) to afford 170 mg of **2f** as an off-white, crystalline solid. The entire product was further purified by trituration in Et_2O (~10 mL) then filtered to afford 115 mg (74%) of **2f** as an off-white crystalline solid.

Data for **2f**:

m.p.: 163 °C (decomp.)

^{1}H-NMR: (500 MHz, CD_3OD)

9.00 (d, *J* = 4.4 Hz, 1 H), 8.38 - 8.26 (m, 2 H), 8.17 (d, *J* = 8.3 Hz, 1 H), 8.12 - 8.02 (m, 2 H), 7.99 (d, *J* = 6.9 Hz, 1 H), 7.93 - 7.76 (m, 4 H), 7.70 - 7.58 (m, 2 H), 6.38 (s, 1 H), 5.70 (ddd, *J* = 17.3, 10.5, 6.9 Hz, 1 H), 5.27 (d, *J* = 12.4 Hz, 1 H), 5.19 - 5.08 (m, 2 H), 5.01 (d, *J* = 10.4 Hz, 1 H), 4.33 (t, *J* = 10.4 Hz, 1 H), 4.04 (t, *J* = 8.7 Hz, 1 H), 3.77 - 3.68 (m, 1 H), 3.65 (s, 3 H), 3.61 - 3.45 (m, 3 H), 2.68 (s, 1 H), 2.46 - 2.33 (m, 1 H), 2.24 (dd, *J* = 18.6, 8.0 Hz, 1 H), 2.08 (s, 1 H), 1.88 (t, *J* = 11.6 Hz, 1 H), 1.54 (t, *J* = 10.5 Hz, 1 H).

^{13}C-NMR: (126 MHz, CD_3OD)

151.04, 149.25, 143.07, 138.57, 135.52, 135.42, 134.57, 131.37, 130.79, 130.58, 130.11, 129.53, 129.35, 128.97, 128.85, 128.19, 127.01, 125.86, 124.12, 121.34, 117.65, 76.08, 69.84, 66.07, 62.10, 57.42, 53.05, 39.03, 28.05, 25.91, 22.75.

LRMS: (ESI^+, Q-tof)

142.0 (10), 449.2 (100, $M\text{-}Br^+$)

HRMS: $C_{31}H_{33}N_2O^+$ (ESI^+, Q-tof)

Calcd: 449.2593

Found: 449.2576

TLC: R_f 0.36 (CH_2Cl_2/MeOH, 10:1) [silica gel, I_2]

Preparation of *O*-Methyl-*N*-(1-Naphthylmethyl)-*epi*-cinchonidinium bromide (3f)

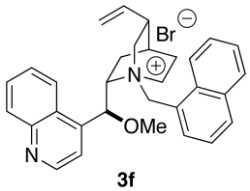

3f

Following General Procedure I, *O*-methyl-*epi*-cinchonidine (90 mg, 0.29 mmol), MeCN (2.9 mL, 0.1 M), and 1-bromomethylnaphthalene (71 mg, 0.32 mmol, 1.1 equiv) were combined in a 10-mL, single-neck, round-bottomed flask fitted with an argon inlet and the mixture was stirred overnight. The reaction mixture was diluted with CH_2Cl_2 (~5 mL) then loaded directly on a silica gel column (15 g SiO_2, ∅ = 20, 100:0 to 10:1, CH_2Cl_2/MeOH, gradient elution) to afford 176 mg of **3f** as an off-white, crystalline solid. The entire product was further purified by trituration in Et_2O (~10 mL) the filtered to afford 111 mg (72%) of **3f** as an off-white, crystalline solid.

Data for **3f**:

m.p.: 158 °C (decomp.)

^{1}H-NMR: (500 MHz, CD_3OD)

9.01 (d, *J* = 4.5 Hz, 1 H), 8.40 (d, *J* = 8.2 Hz, 1 H), 8.34 (d, *J* = 8.5 Hz, 1 H), 8.22 - 8.14 (m, 2 H), 8.06 (t, *J* = 8.4 Hz, 2 H), 7.95 - 7.83 (m, 3 H), 7.78 (ddd, *J* = 8.4, 6.9, 1.2 Hz, 1 H), 7.72 (dd, *J* = 8.1, 7.3 Hz, 1 H), 7.66 (t, *J* = 7.2 Hz, 1 H), 6.55 (s, 1 H), 5.80 - 5.62 (m, 2 H), 5.38 (d, *J* = 13.1 Hz, 1 H), 5.10 (d, *J* = 17.2 Hz, 1 H),

4.99 (d, J = 10.5 Hz, 1 H), 4.45 - 4.34 (m, 1 H), 4.21 (t, J = 9.0 Hz, 1 H), 3.83 - 3.69 (m, 4 H), 3.56 - 3.47 (m, 1 H), 3.29 - 3.21 (m, 1 H), 2.63 (s, 1 H), 2.46 - 2.34 (m, 1 H), 2.21 (ddd, J = 10.8, 8.7, 4.8 Hz, 1 H), 2.05 (d, J = 2.9 Hz, 1 H), 1.85 - 1.73 (m, 1 H), 1.54 (td, J = 10.3, 3.0 Hz, 1 H).

^{13}C-NMR: (126 MHz, CD_3OD)

151.05, 149.26, 143.03, 138.52, 135.79, 134.71, 133.20, 131.43, 130.70, 130.56, 129.38, 129.07, 127.64, 127.07, 126.45, 124.40, 124.39, 124.22, 121.42, 117.69, 76.26, 69.93, 62.48, 61.99, 57.42, 53.51, 39.25, 27.70, 26.02, 22.86.

LRMS: (ESI^+, Q-tof)

449.2 m/z (100, M-Br^+)

HRMS: $C_{31}H_{33}N_2O^+$ (ESI^+, Q-tof)

Calcd: 449.2593

Found: 449.2580

TLC: R_f 0.33 (CH_2Cl_2/MeOH, 10:1) [silica gel, I_2]

Preparation of *O*-Methyl-*N*-(Benzyl)-*epi*-cinchonidinium Bromide (4f)

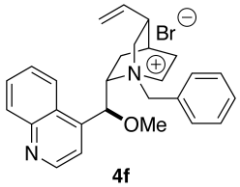

4f

Following General Procedure I, *O*-methyl-*epi*-cinchonidine (90 mg, 0.29 mmol), MeCN (2.9 mL, 0.1 M), and beznyl bromide (38 μL, 0.32 mmol, 1.1 equiv) were combined in a 10-mL, single-neck, round-bottomed flask fitted with an argon inlet and the mixture was stirred overnight. The reaction mixture was diluted with CH_2Cl_2 (~5 mL) and then was loaded directly on a silica gel column (15 g SiO_2, ∅ = 20, 100:0 to 10:1, CH_2Cl_2/MeOH, gradient elution) to afford 156 mg of **4f** as a light-yellow, crystalline solid. The entire product was further purified by trituration in Et_2O (~10 mL) and then filtered to afford 136 mg (97%) of **4f** as an off-white, crystalline solid.

Data for **4f**:

m.p.: 176 – 180 °C (decomp.)

^{1}H-NMR: (500 MHz, $CDCl_3$)

8.98 (d, *J* = 4.5 Hz, 1 H), 8.93 (d, *J* = 8.6 Hz, 1H), 8.15 (d, *J* = 8.4 Hz, 1H), 8.02 - 7.93 (m, 3 H), 7.82 (t, *J* = 7.2 Hz, 1 H), 7.54 - 7.50 (m, 3 H), 6.74 (d, *J* = 11.8 Hz, 1 H), 6.06 (d, *J* = 3.2 Hz, 1 H), 5.74 (ddd, *J* = 17.0, 10.5, 6.3 Hz, 1 H), 5.41 (dd, *J* = 17.2, 1.3 Hz, 1 H), 5.05 (dd, *J* = 10.6, 1.3 Hz, 2 H), 4.79 (s, 1 H), 4.51 (d, *J* = 11.8 Hz, 1 H), 4.33 - 4.23 (m, 1 H), 3.54 (s, 3 H), 3.51 - 3.39 (m, 1 H), 3.19 (dd, *J* = 12.9, 10.8 Hz, 1 H), 2.59 (s, 1 H), 2.10 (ddd, *J* = 31.5, 20.0, 9.3 Hz, 3 H), 1.78 (dd, *J* = 19.3, 11.5 Hz, 1 H), 1.40 (t, *J* = 14.3 Hz, 1 H).

^{13}C-NMR: (126 MHz, CD_3OD)

LRMS: (ESI^+, Q-tof)

142.0 (20), 178.9 (10), 309.2 (5), 329.9 (10), 399.2 (100, M-Br^+), 449.3 (5)

HRMS: $C_{27}H_{31}N_2O^+$ (ESI^+, Q-tof)

Calcd: 399.2436

Found: 399.2421

Preparation of *O*-Methyl-*N*-(3,5-Bistrifluoromethylbenzyl)-*epi*-cinchonidinium Bromide (5f)

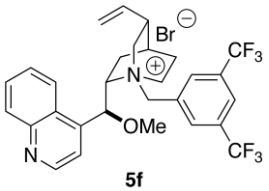

5f

Following General Procedure I, *O*-methyl-*epi*-cinchonidine (90 mg, 0.29 mmol), MeCN (2.9 mL, 0.1 M), and bis-(3,5-trifluoromethyl)benzyl bromide (59 μL, 0.32 mmol, 1.1 equiv) were combined in a 10-mL, single-neck, round-bottomed flask fitted with an argon inlet and the mixture was stirred overnight. The reaction mixture was diluted with CH_2Cl_2 (~5 mL) and then was loaded directly on a silica gel column (15 g SiO_2, ∅ = 20, 100:0 to 10:1, CH_2Cl_2/MeOH, gradient elution) to afford 168 mg (93%) of **5f** as a white, crystalline solid.

Data for **5f**:

m.p.: 165 °C (decomp.)

^{1}H-NMR: (500 MHz, CD_3OD)

8.99 (d, *J* = 4.5 Hz, 1 H), 8.51 (s, 2 H), 8.32 (d, *J* = 8.1 Hz, 1 H), 8.25 (s, 1 H), 8.16 (dd, *J* = 8.4, 1.0 Hz, 1 H), 7.92 - 7.80 (m, 3 H), 6.30 (s, 1 H), 5.68 (ddd, *J* = 17.3, 10.5, 6.9 Hz, 1 H), 5.30 - 5.20 (m, 2 H), 5.15 (d, *J* = 17.2 Hz, 1 H), 5.00 (d, *J* = 10.5 Hz, 1 H), 4.44 - 4.33 (m, 1 H), 4.01 (dd, *J* = 9.8, 8.5 Hz, 1 H), 3.73 (ddd, *J* = 12.4, 4.8, 3.2 Hz, 1 H), 3.63 (s, 3 H), 3.45 (dd, *J* = 14.9, 8.2 Hz, 2 H), 2.73 (d, *J* = 1.5 Hz, 1 H), 2.46 - 2.34 (m, 1 H), 2.31 - 2.19 (m, 1 H), 2.11 (d, *J* = 2.8 Hz, 1 H), 1.93 (ddd, *J* = 15.2, 5.0, 2.4 Hz, 1 H), 1.59 - 1.47 (m, 1 H).

^{13}C NMR: (126 MHz, CD_3OD)

151.03, 149.27, 142.73, 138.36, 135.56, 133.72 (q, $J_{C\text{-}F}$ = 33.8 Hz), 131.91, 131.40, 130.61, 129.43, 126.94, 125.61, 124.10, 123.44, 121.35, 117.83, 76.02, 70.51, 64.05, 61.90, 57.49, 53.21, 39.01, 27.92, 25.81, 22.80.

LRMS: (ESI^+, Q-tof)

535.2 (100, M-Br^+)

HRMS: $C_{29}H_{29}N_2OF_6^+$ (ESI^+, Q-tof)

Calcd: 535.2184

Found: 535.2179

TLC: R_f 0.34 (CH_2Cl_2/MeOH, 10:1) [silica gel, I_2]

Preparation of Cinchonidinium Salts in Series G

Preparation of *N*-(9-Anthracenylmethyl)deoxyfluorocinchonidinium Bromide (1g)

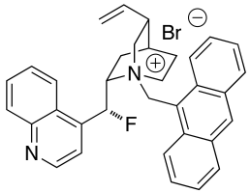

1g

Following General Procedure I, deoxyfluorocinchonidine (50 mg, 0.17 mmol), MeCN (1.7 mL, 0.1 M), and 9-bromomethylanthracene (48 mg, 0.18 mmol, 1.05 equiv) were combined in a 5-mL, single-neck, round-bottomed flask fitted with an argon inlet, wrapped in aluminum and the mixture was stirred for 2 days. Care was taken to avoid light exposure. The reaction mixture was cooled to 0 °C (external) in an ice bath and the product was then precipitated with ice-cold Et_2O (3-4 mL). The reaction mixture was filtered and the filter cake was washed several times with cold Et_2O (5-10 mL) to afford 84 mg (88%) of **1g** as a yellow, crystalline solid. The entire product was further purified by recrystallization from a concentrated CH_2Cl_2 solution (2-4 mL), layering Et_2O (6-12 mL), and then cooling overnight at -20 °C.

Data for **1g**:

m.p.: 183 – 186 °C (decomp.)

^{1}H-NMR: (500 MHz, $CDCl_3$)

9.68 (d, *J* = 9.0 Hz, 1 H), 9.03 (d, *J* = 4.4 Hz, 1 H), 8.93 (d, *J* = 8.4 Hz, 1 H), 8.67 (s, 1 H), 8.35 (d, *J* = 9.0 Hz, 1 H), 8.18 (dd, *J* = 8.4, 0.9 Hz, 1 H), 8.12 (d, *J* = 8.3 Hz, 1 H), 8.07 (d, *J* = 8.4 Hz, 1 H), 7.96 - 7.90 (m, 2 H), 7.88 (ddd, *J* = 8.9, 6.5, 1.2 Hz, 1 H), 7.83 (ddd, *J* = 8.2, 6.9, 1.1 Hz, 1 H), 7.73 (dd, *J* = 49.6, 1.9 Hz, 1 H), 7.72 (ddd, *J* = 8.9, 6.5, 1.2 Hz, 1 H), 7.57 (ddd, *J* = 13.3, 8.2, 6.6 Hz, 2 H), 7.25 (d, *J* = 13.5 Hz, 1 H), 6.26 - 6.09 (m, 2 H), 5.99 (ddd, *J* = 17.3, 10.5, 7.1 Hz, 1 H), 5.33 - 5.20 (m, 2 H), 5.14 (d, *J* = 9.9 Hz, 1 H), 4.14 (t, *J* = 11.7 Hz, 1 H), 3.23 (dd, *J* = 12.8, 10.7 Hz, 1 H), 2.67 (td, *J* = 12.4, 4.9 Hz, 1 H), 2.39 (s, 1 H), 2.08 - 1.90 (m, 3 H), 1.84 (td, *J* = 10.6, 3.2 Hz, 1 H), 1.54 (s, 3H), 1.25 (s, 1 H).

^{13}C-NMR: (126 MHz, CD_3OD)

151.06, 149.06, 141.87 (d, $^2J_{C\text{-}F}$ = 20.0 Hz), 137.94, 134.86, 134.62, 134.12, 133.13, 133.05, 131.68, 131.22 (d, $^3J_{C\text{-}F}$ = 6.3 Hz), 130.75, 129.59, 129.51, 126.66

(d, J = 3.4 Hz), 125.15, 124.95, 124.32, 120.43 (d, $^3J_{C\text{-}F}$ = 12.5 Hz), 118.68, 118.10, 87.83 (d, $^1J_{C\text{-}F}$ = 182.0 Hz), 70.41 (d, $^2J_{C\text{-}F}$ = 20.3 Hz), 62.68, 58.47, 54.15 (d, $^3J_{C\text{-}F}$ = 7.4 Hz), 39.49, 27.30, 25.95, 22.17.

^{19}F-NMR: (376 MHz, $CDCl_3$)

198.65 (dd, J = 48.8, 33.7 Hz).

LRMS: (ESI^+, Q-tof)

150 (20), 191.1 (70), 487.2 (100, M-Br^+)

HRMS: $C_{34}H_{32}N_2F^+$ (ESI^+, Q-tof)

Calcd: 487.2550

Found: 487.2551

TLC: R_f 0.60 (CH_2Cl_2/MeOH, 5:1) [silica gel, I_2]

Preparation of *N*-(2-Naphthylmethyl)deoxyfluorocinchonidinium Bromide (2g)

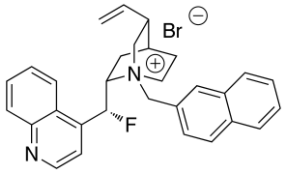

2g

Following General Procedure I, deoxyfluorocinchonidine (100 mg, 0.337 mmol), MeCN (3.4 mL, 0.1 M), and 1-bromomethylnaphthalene (82.0 mg, 0.371 mmol, 1.10 equiv) were combined in a 10-mL, single-neck, round-bottomed flask fitted with an argon inlet and the mixture was stirred for 2 days. The reaction mixture was diluted with CH_2Cl_2 (~5 mL) and MeOH (<1 mL) and then was loaded directly on a silica gel column (20 g SiO_2, ∅ = 20, 100:0 to 5:1, CH_2Cl_2/MeOH, gradient elution) to afford 126 mg (72%) of **2g** as a light-orange, crystalline solid.

The entire product was further purified by recrystallization from a CH_2Cl_2 solution (2-4 mL), layered with Et_2O (6-12 mL), and then was allowed to cool overnight in a freezer to afford **2g** as an off-white, crystalline solid.

Data for **2g**:

m.p.: 210-213 °C (decomp.)

^{1}H-NMR: (500 MHz, CD_3OD)

9.01 (d, J = 4.6 Hz, 1 H), 8.27 (s, 1 H), 8.18 (dd, J = 12.9, 8.3 Hz, 2 H), 8.08 (d, J = 8.5 Hz, 1 H), 8.00 (d, J = 8.1 Hz, 2 H), 7.95 - 7.89 (m, 1 H), 7.87 - 7.79 (m, 2 H), 7.73 (d, $J_{H\text{-}F}$ = 48.0 Hz, 1 H), 7.76 (m, 1 H), 7.64 (pd, J = 7.0, 1.4 Hz, 2 H), 5.79 (ddd, J = 17.4, 10.4, 7.2 Hz, 1 H), 5.54 (d, J = 12.5 Hz, 1 H), 5.22 - 5.05 (m, 3 H), 4.35 (ddd, J = 30.6, 10.9, 6.3 Hz, 1 H), 4.17 - 4.07 (m, 1 H), 3.78 - 3.54 (m, 3 H), 2.75 (dd, J = 15.9, 7.6 Hz, 1 H), 2.42 - 2.21 (m, 2 H), 2.15 (d, J = 2.7 Hz, 1 H), 1.99 (t, J = 11.4 Hz, 1 H), 1.86 (dd, J = 13.7, 11.1 Hz, 1 H)

^{13}C-NMR: (126 MHz, CD_3OD)

151.05, 148.97, 141.69 (d, $^{2}J_{C\text{-}F}$ = 19.7 Hz), 138.09, 135.47, 134.56, 131.63, 130.73, 130.56, 130.29, 129.56, 129.50, 129.09, 128.89, 128.29, 125.55, 125.24 (d, $^{3}J_{C\text{-}F}$ = 5.2 Hz), 124.04, 121.34, 120.24 (d, $^{3}J_{C\text{-}F}$ = 12.5 Hz), 118.08, 87.26 (d, $^{1}J_{C\text{-}F}$ = 182.3 Hz), 69.28 (d, $^{2}J_{C\text{-}F}$ = 20.4 Hz), 66.22, 61.84, 53.18, 39.15, 28.10, 25.68, 21.87

^{19}F-NMR: (376 MHz, CD_3OD)

-199.46 (dd, J = 48.0, 30.8 Hz)

LRMS: (ESI^+, Q-tof)

150 (8), 437.2 (100, M-Br^+)

HRMS: $C_{30}H_{30}N_2F^+$ (ESI^+, Q-tof)

Calcd: 437.2393

Found: 437.2400

TLC: R_f 0.60 (CH_2Cl_2/MeOH, 5:1) [silica gel, I_2]

Preparation of *N*-(1-Naphthylmethyl)deoxyfluorocinchonidinium Bromide (3g)

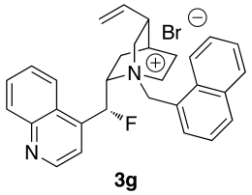

3g

Following General Procedure I, deoxyfluorocinchonidine (100 mg, 0.337 mmol), MeCN (3.4 mL, 0.1 M), and 1-bromomethylnaphthalene (82.0 mg, 0.371 mmol, 1.10 equiv) were combined in a 10-mL, single-neck, round-bottomed flask fitted with an argon inlet and the mixture was stirred for 2 days. The reaction mixture was diluted with CH_2Cl_2 (~5 mL) and then was loaded directly on a silica gel column (15 g SiO_2, ∅ = 20, 100:0 to 10:1, CH_2Cl_2/MeOH, gradient elution) to afford 90 mg (52%) of **3g** as a light-orange, crystalline solid.

The entire product was further purified by recrystallization from a CH_2Cl_2 solution (2-4 mL), layered with Et_2O (6-12 mL), and then was allowed to cool overnight in a freezer to afford **3g** as an light-amber, crystalline solid.

Data for **3g**:

m.p.: 150 – 155 °C (decomp.)

^{1}H-NMR: (500 MHz, CD_3OD)

9.03 (d, *J* = 4.5 Hz, 1 H), 8.40 (d, *J* = 8.6 Hz, 1 H), 8.27 - 8.16 (m, 3 H), 8.07 (d, *J* = 8.2 Hz, 1 H), 7.99 (d, *J* = 6.8 Hz, 1 H), 7.96 - 7.79 (m, 4 H), 7.77 - 7.68 (m, 2 H), 7.65 (t, *J* = 7.3 Hz, 1 H), 5.94 (d, *J* = 13.1 Hz, 1 H), 5.77 (ddd, *J* = 17.4, 10.4, 7.2 Hz, 1 H), 5.38 (d, *J* = 13.0 Hz, 1 H), 5.08 (dd, *J* = 18.8, 13.8 Hz, 2 H), 4.57 (ddd, *J* = 30.7, 10.6, 6.0 Hz, 1 H), 4.17 (dd, *J* = 16.0, 7.5 Hz, 1 H), 3.71 (ddd, *J* = 12.5, 6.7, 3.0 Hz, 1 H), 3.60 - 3.41 (m, 2 H), 2.65 (d, *J* = 8.3 Hz, 1 H), 2.38 (d, *J* = 13.7 Hz, 1 H), 2.32 - 2.20 (m, 1 H), 2.11 (d, *J* = 2.6 Hz, 1 H), 1.90 (dd, *J* = 27.2, 13.6 Hz, 2 H)

^{13}C-NMR: (126 MHz, CD_3OD)

151.05, 148.99, 141.79 (d, $^2J_{C\text{-}F}$ = 19.8 Hz), 137.97, 135.85, 135.73, 134.67, 133.40, 131.65, 130.71 (d, $^3J_{C\text{-}F}$ = 4.1 Hz), 129.59, 129.10, 127.72, 126.44, 125.30, 125.26, 124.52, 124.19, 124.10, 120.32 (d, $^3J_{C\text{-}F}$ = 12.4 Hz), 118.10, 87.40

(d, $^{1}J_{C\text{-}F}$ = 182.2 Hz), 69.95 (d, $^{2}J_{C\text{-}F}$ = 20.1 Hz), 62.62, 62.12, 53.50, 39.29, 27.75, 25.78, 21.94

^{19}F-NMR: (376 MHz, CD_3OD)

-199.38 (dd, *J* = 48.0, 31.0 Hz)

LRMS: (ESI^+, Q-tof)

437.2 (100, M-Br^+)

HRMS: $C_{30}H_{30}N_2F^+$ (ESI^+, Q-tof)

Calcd: 437.2393

Found: 437.2400

TLC: R_f 0.60 (CH_2Cl_2/MeOH, 5:1) [silica gel, I_2]

Preparation of *N*-(Benzyl)deoxyfluorocinchonidinium Bromide (4g)

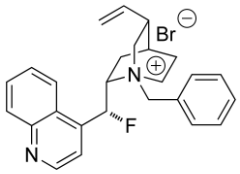

4g

Following General Procedure I, deoxyfluorocinchonidine (50.0 mg, 0.170 mmol), MeCN (1.70 mL, 0.10 M), and benzyl bromide (21.0 μL, 0.180 mmol, 1.05 equiv) were combined in a 5-mL, single-neck, round-bottomed flask fitted with an argon inlet and the mixture was stirred for 2 days. The reaction mixture was cooled to 0 °C (external) in an ice bath and then the product was precipitated with ice-cold Et_2O (3-4 mL). The suspension was filtered and then washed several times with cold Et_2O (~5 mL) to afford 65 mg (82%) of **4g** as a light-yellow, crystalline solid. The entire product was further purified by recrystallization from a concentrated CH_2Cl_2 solution (2-4 mL), layered with Et_2O (6-12 mL), and was then allowed to cool in a freezer overnight.

Data for **4g**:

m.p.: 150-155 °C (decomp.)

^{1}H-NMR: (500 MHz, $CDCl_3$)

8.98 (d, *J* = 4.5 Hz, 1 H), 8.77 (d, *J* = 8.4 Hz, 1 H), 8.15 (d, *J* = 8.4 Hz, 1 H), 7.94 (dt, *J* = 5.4, 3.2 Hz, 3 H), 7.82 (t, *J* = 7.2 Hz, 1 H), 7.64 (d, *J* = 4.4 Hz, 1 H), 7.56

- 7.46 (m, 4 H), 7.32 (d, J = 49.8 Hz, 2 H), 6.73 (d, J = 11.8 Hz, 1 H), 5.82 (ddd, J = 17.1, 10.6, 6.5 Hz, 1 H), 5.43 (dd, J = 17.2, 1.2 Hz, 1 H), 5.28 (dt, J = 20.2, 9.8 Hz, 1 H), 5.21 - 5.15 (m, 1 H), 5.13 (dd, J = 10.6, 1.2 Hz, 1 H), 4.78 (d, J = 11.8 Hz, 1 H), 3.97 (t, J = 11.4 Hz, 1 H), 3.54 - 3.47 (m, 1 H), 3.32 (dd, J = 13.0, 10.7 Hz, 1 H), 2.65 (s, 1H), 2.22 - 2.13 (m, 1 H), 2.11 (d, J = 2.3 Hz, 1 H), 1.99 (dd, J = 13.6, 8.8 Hz, 1 H), 1.88 (t, J = 14.2 Hz, 1 H), 1.68 (td, J = 10.3, 3.1 Hz, 1 H)

^{13}C-NMR: (126 MHz, CD_3OD)

151.04, 148.98, 141.63 (d, $^2J_{C\text{-}F}$ = 20.3 Hz), 138.08, 134.82, 132.02, 131.61, 130.74, 130.56, 129.54, 128.29, 125.21 (d, $^3J_{C\text{-}F}$ = 5.3 Hz), 123.99, 120.21 (d, $^3J_{C\text{-}F}$ = 12.5 Hz), 118.06, 87.20 (d, $^1J_{C\text{-}F}$ = 182.3 Hz), 69.37 (d, $^2J_{C\text{-}F}$ = 20.3 Hz), 66.04, 61.68, 52.99 (d, $^3J_{C\text{-}F}$ = 7.2 Hz), 39.10, 28.10, 25.64, 21.84 (d, $^4J_{C\text{-}F}$ = 3.9 Hz)

^{19}F-NMR: (376 MHz, $CDCl_3$)

-201.07 (dd, J = 48.9, 32.7 Hz)

LRMS: (ESI^+, Q-tof)

367.2 (5), 387.2 (100, M-Br^+)

HRMS: $C_{26}H_{28}N_2F^+$ (ESI^+, Q-tof)

Calcd: 387.2237

Found: 387.2246

TLC: R_f 0.49 (CH_2Cl_2/MeOH, 5:1) [silica gel, I_2]

Preparation of *N*-(9-Anthracenylmethyl)deoxyfluorocinchonidinium Bromide (5g)

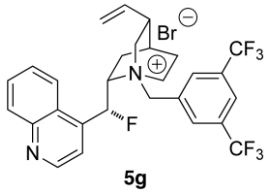

5g

Following General Procedure I, deoxyfluorocinchonidine (44 mg, 0.15 mmol), MeCN (1.5 mL), and bis-(3,5-trifluoromethyl)benzyl bromide (28 μL, 0.16 mmol, 1.05 equiv) were combined in a 5-mL, single-neck, round-bottomed flask fitted with an argon inlet and the mixture was stirred for 4 days. The reaction mixture was cooled to 0 °C (external) in an ice bath and then the product was precipitated with ice-cold Et_2O (3-4 mL) then filtered. The filter cake was washed several times with ice-cold Et_2O (~5 mL) to afford 68 mg (76%) of **5g** as a light-orange, crystalline solid.

The entire product was further purified by recrystallization from a CH_2Cl_2 solution (2-4 mL), layered with Et_2O (6-12 mL), and then was allowed to cool overnight in a freezer.

Data for **5g**:

m.p.: 150-155 °C (decomp.)

^{1}H-NMR: (500 MHz, $CDCl_3$)

8.98 (d, J = 4.5 Hz, 1 H), 8.80 (d, J = 8.4 Hz, 1 H), 8.56 (s, 2 H), 8.14 (d, J = 8.3 Hz, 1 H), 8.06 (s, 1 H), 7.92 (t, J = 7.7 Hz, 1 H), 7.81 (t, J = 7.6 Hz, 1 H), 7.63 (d, J = 4.4 Hz, 1 H), 7.33 (dd, J = 30.5, 23.3 Hz, 2 H), 5.81 (ddd, J = 17.1, 10.6, 6.4 Hz, 1 H), 5.54 - 5.30 (m, 4 H), 5.16 (d, J = 10.5 Hz, 1 H), 4.92 (d, J = 12.1 Hz, 1 H), 4.10 (s, 1 H), 3.36 (td, J = 11.8, 4.3 Hz, 1 H), 3.14 (dd, J = 12.5, 10.8 Hz, 1 H), 2.71 (s, 1 H), 2.23 (dd, J = 19.2, 8.6 Hz, 1 H), 2.17 (s, 1 H), 2.08 - 1.99 (m, 1 H), 1.94 (t, J = 15.2 Hz, 1 H), 1.69 (dd, J = 13.1, 10.1 Hz, 1 H)

^{13}C-NMR: (126 MHz, CD_3OD)

151.06, 149.00, 141.32 (d, $^2J_{C\text{-}F}$ = 20.7 Hz), 137.87, 135.35, 133.72 (dd, $J_{C\text{-}F}$ = 36.5, 31.1 Hz), 131.66, 131.53, 130.80, 129.65, 125.92, 125.54, 125.14 (d, $^3J_{C\text{-}F}$ = 5.3 Hz), 123.91, 120.21 (d, $^3J_{C\text{-}F}$ = 12.5 Hz), 118.27, 87.10 (d, $^1J_{C\text{-}F}$ = 182.9 Hz), 70.00 (d, $^2J_{C\text{-}F}$ = 20.4 Hz), 64.14, 61.75, 53.16, 39.11, 27.95, 25.56, 21.87

^{19}F-NMR: (376 MHz, $CDCl_3$)

-63.03 (s, 6 F), -200.89 (dd, J = 48.1, 32.3 Hz, 1 F)

LRMS: (ESI$^+$, Q-tof)

503.2 (5), 523.2 (100, M-Br$^+$)

HRMS: $C_{28}H_{26}N_2F_7^+$ (ESI$^+$, Q-tof)

Calcd: 523.1984

Found: 523.1984

TLC: R_f 0.49 (CH_2Cl_2/MeOH, 5:1) [silica gel, I_2]

Preparation of Cinchonidinium Salts in Series H

Preparation of *N*-(9-Anthracenylmethyl)deoxycinchonidinium Bromide (1h)

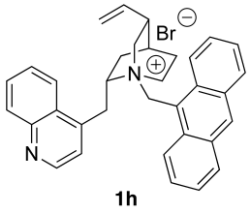

1h

Following General Procedure I, deoxycinchonidine (100 mg, 0.359 mmol), MeCN (3.6 mL), and 9-bromomethylanthracene (107 mg, 0.390 mmol, 1.10 equiv) were combined in a 10-mL, single-neck, round-bottomed flask fitted with an argon inlet, wrapped in aluminum foil and the mixture was stirred for 4 h. Care was taken to avoid light exposure. The solvent was removed on a rotavap (20 mm Hg, 25 °C) and the yellow, solid residue was sonicated in Et_2O (10 mL) in an ultrasonic bath then filtered.

The entire product was purified by recrystallization from a concentrated CH_2Cl_2 solution by a slow diffusion of Et_2O in a chamber stored in a freezer. The first crop of recrystallized product afforded 29.0 mg (15%) of **1h** as a light-yellow, crystalline solid.

Data for **1h**:

m.p.: 132 °C (decomp.)

^{1}H-NMR: (500 MHz, $CDCl_3$)

9.16 (d, *J* = 9.0 Hz, 1 H), 8.80 (d, *J* = 8.9 Hz, 1 H), 8.45 (d, *J* = 8.2 Hz, 1 H), 8.40 (s, 1 H), 8.04 (s, 2 H), 7.98 (d, *J* = 8.2 Hz, 1 H), 7.81 (d, *J* = 8.2 Hz, 1 H), 7.77 - 7.68 (m, 2 H), 7.55 - 7.38 (m, 4 H), 7.33 - 7.27 (m, 1 H), 6.74 (d, *J* = 14.2 Hz, 1 H), 6.04 (d, *J* = 14.2 Hz, 1 H), 5.60 (ddd, *J* = 17.2, 10.5, 6.8 Hz, 1 H), 5.45 - 5.32 (m, 1 H), 4.98 (dd, *J* = 32.1, 13.8 Hz, 2 H), 4.75 (dd, *J* = 13.4, 4.7 Hz, 1 H), 4.55 (t, *J* = 11.5 Hz, 1 H), 4.43 (t, *J* = 12.5 Hz, 1 H), 3.75 (dd, *J* = 11.7, 5.0 Hz, 1 H), 2.94 (td, *J* = 11.9, 6.1 Hz, 1 H), 2.84 (dd, *J* = 13.0, 10.7 Hz, 1 H), 2.13 (d, *J* = 7.3 Hz, 1 H), 1.99 - 1.87 (m, 1 H), 1.81 (dd, *J* = 13.6, 10.7 Hz, 1 H), 1.66 (d, *J* = 2.5 Hz, 1 H), 1.52 (t, *J* = 10.0 Hz, 1 H), 1.21 (dd, *J* = 18.2, 11.2 Hz, 1 H).

LRMS: (ESI^+, Q-tof)

191.1 (80), 279.2 (35), 469.3 (100, M-Br^+)

HRMS: $C_{34}H_{33}N_2^+$ (ESI^+, Q-tof)

Calcd: 469.2644

Found: 469.2639

Preparation of *N*-(*2*-Naphthylmethyl)deoxycinchonidinium Bromide (2h)

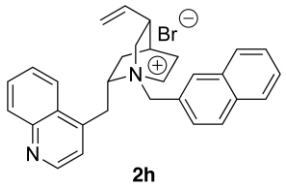

2h

Following General Procedure I, deoxycinchonidine (100 mg, 0.359 mmol), MeCN (3.60 mL, 0.1 M), and 2-bromomethylnaphthalene (87.0 mg, 0.390 mmol, 1.10 equiv) were combined in a 10-mL, single-neck, round-bottomed flask fitted with an argon inlet and the mixture was stirred for 3 h. The solvent was removed on a rotavap (20 mm Hg, 25 °C) and the solid residue was triturated with Et_2O (10 mL) then filtered. The filter cake was then sonicated in TBME (10 mL) in an ultrasonic bath and then filtered to afford 156 mg (87%) of **2h** as an off-white, crystalline solid.

Data for **2h**:

m.p.: 165 °C (decomp.)

^{1}H-NMR: (500 MHz, $CDCl_3$)

8.61 (d, *J* = 4.4 Hz, 1 H), 8.44 - 8.37 (m, 1 H), 8.09 (s, 1 H), 8.02 - 7.95 (m, 1 H), 7.72 - 7.57 (m, 5 H), 7.52 (d, *J* = 8.4 Hz, 1 H), 7.48 - 7.43 (m, 1 H), 7.43 - 7.36 (m, 2 H), 5.88 (d, *J* = 12.8 Hz, 1 H), 5.65 (ddd, *J* = 17.2, 14.4, 9.9 Hz, 2 H), 5.12 (dd, *J* = 13.7, 9.2 Hz, 2 H), 4.52 (dt, *J* = 13.9, 8.4 Hz, 2 H), 4.37 (dd, *J* = 14.5, 3.7 Hz, 1 H), 3.97 - 3.79 (m, 3 H), 3.50 - 3.39 (m, 1 H), 2.65 (dd, *J* = 16.6, 7.5 Hz, 1 H), 2.08 (dd, *J* = 18.4, 11.5 Hz, 1 H), 1.96 - 1.77 (m, 3 H), 1.61 (s (br), 1 H), 1.36 (d, *J* = 13.2 Hz, 1 H).

^{13}C-NMR: (126 MHz, CD_3OD)

150.90, 148.95, 143.86, 137.88, 135.41, 134.96, 134.54, 131.36, 130.26, 130.24, 129.42, 129.07, 128.95, 128.93, 128.85, 128.22, 125.91, 125.05, 123.30, 118.11, 66.03, 65.89, 61.41, 50.93, 39.22, 33.22, 28.38, 27.62, 25.54.

LRMS: (ESI^+, Q-tof)

419.2 (100, M-Br^+)

HRMS: $C_{30}H_{31}N_2^+$ (ESI^+, Q-tof)

Calcd: 419.2487

Found: 419.2491

TLC: R_f 0.55 (CH_2Cl_2/MeOH, 10:1) [silica gel, I_2]

Preparation of *N*-(*1*-Naphthylmethyl)deoxycinchonidinium Bromide (3h)

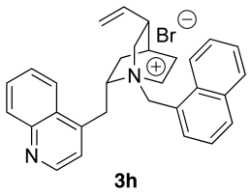

3h

Following General Procedure I, deoxycinchonidine (100 mg, 0.359 mmol), MeCN (3.60 mL, 0.1 M), and 2-bromomethylnaphthalene (87.0 mg, 0.390 mmol, 1.10 equiv) were combined in a 10-mL, single-neck, round-bottomed flask fitted with an argon inlet and the mixture was stirred for 2 days. The solvent was removed on a rotavap (20 mm Hg, 25 °C) and the solid residue was triturated with Et_2O (10 mL) then filtered. The filter cake was then sonicated in TBME (10 mL) in an ultrasonic bath and then filtered to afford 156 mg (87%) of **2h** as an off-white, crystalline solid.

Data for **3h**

m.p.: 165 °C (decomp.)

^{1}H-NMR: (500 MHz, $CDCl_3$)

8.64 (d, *J* = 8.6 Hz, 1 H), 8.30 (dd, *J* = 10.2, 6.4 Hz, 2 H), 8.02 (d, *J* = 7.0 Hz, 1 H), 7.90 (dd, *J* = 8.3, 1.1 Hz, 1 H), 7.69 - 7.53 (m, 5 H), 7.48 - 7.38 (m, 2 H), 6.96 - 6.88 (m, 1 H), 6.42 (d, *J* = 13.1 Hz, 1 H), 5.86 (d, *J* = 13.2 Hz, 1 H), 5.59 (ddd, *J* = 17.3, 10.5, 7.0 Hz, 1 H), 5.01 (dd, *J* = 27.1, 13.8 Hz, 2 H), 4.92 (dt, *J* = 15.7, 5.3 Hz, 1 H), 4.64 (t, *J* = 12.0 Hz, 1 H), 4.42 (dd, *J* = 13.8, 4.8 Hz, 1 H), 4.09 - 4.00 (m, 1 H), 3.53 - 3.35 (m, 2 H), 3.10 (dd, *J* = 13.0, 10.6 Hz, 1 H), 2.33 (d, *J* = 9.2 Hz, 1 H), 1.99 (dd, *J* = 17.1, 10.8 Hz, 1 H), 1.80 - 1.62 (m, 3 H), 1.19 (d, *J* = 10.3 Hz, 1 H)

^{13}C-NMR: (126 MHz, $CDCl_3$)

153.60, 141.23, 136.86, 136.67, 135.52, 134.41, 133.33, 132.72, 131.70, 130.65,

129.51, 128.25, 128.10, 126.94, 125.67, 124.88, 124.44, 122.84, 122.35, 121.78, 118.61, 66.25, 60.83, 59.68, 48.67, 37.76, 33.26, 27.16, 25.98, 24.94

LRMS: (ESI^+, Q-tof)

110.1 (20), 141.1 (80), 170.1 (8), 279.2 (100), 419.2 (50, $M\text{-}Br^+$)

HRMS: $C_{30}H_{31}N_2^+$ (ESI^+, Q-tof)

Calcd: 419.2487

Found: 419.2490

Preparation of *N*-(Benzyl)deoxycinchonidinium Bromide (4h)

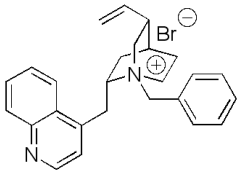

4h

Following General Procedure I, deoxycinchonidine (101 mg, 0.362 mmol), MeCN (3.60 mL, 0.1 M), and benzyl bromide (47.0 μL, 0.400 mmol, 1.10 equiv) were combined in a 10-mL, single-neck, round-bottomed flask fitted with an argon inlet and the mixture was stirred for 3 h. The solvent removed was removed on a rotavap (20 mm Hg, 25 °C) and the solid residue was then triturated with hexane and filtered. The filter cake sonicated twice with Et_2O (2 x 10 mL) in an ultrasonic bath and then filtered to afford 136 mg (84%) of **4h** as a pale-green, crystalline solid.

Data for **4h**:

m.p.: 113 °C (decomp)

^{1}H-NMR: (500 MHz, $CDCl_3$)

8.73 (d, *J* = 4.5 Hz, 1 H), 8.50 - 8.44 (m, 1 H), 8.06 (dd, *J* = 8.2, 1.2 Hz, 1 H), 7.75 - 7.62 (m, 4 H), 7.44 (d, *J* = 4.5 Hz, 1 H), 7.31 - 7.25 (m, 1 H), 7.22 (t, *J* = 7.3 Hz, 2 H), 5.75 - 5.59 (m, 2 H), 5.45 (d, *J* = 12.7 Hz, 1 H), 5.16 (dd, *J* = 17.8, 14.0 Hz, 2 H), 4.62 - 4.46 (m, 2 H), 4.27 (dd, *J* = 14.5, 3.6 Hz, 1 H), 3.86 (dd, *J* = 25.2, 12.8 Hz, 2 H), 3.79 - 3.69 (m, 1 H), 3.54 - 3.44 (m, 1 H), 2.69 (dd, *J* = 16.0, 7.6 Hz, 1 H), 2.15 - 2.03 (m, 1 H), 1.97 - 1.83 (m, 3 H), 1.44 - 1.34 (m, 1 H).

LRMS: (ESI^+, Q-tof)

91.1 (10), 110.1 (10), 279.2 (40), 369.2 (100, M-Br^+)

HRMS: $C_{26}H_{29}N_2^+$ (ESI^+, Q-tof)

Calcd: 369.2331

Found: 369.2337

TLC: R_f 0.54 (CH_2Cl_2/MeOH, 10:1) [silica gel, I_2]

5.2.2. PTC Alkylation Kinetics

General Procedure II. PTC Alkylation of *N*-(Diphenylmethylene)glycine *tert*-Butyl Ester (1)

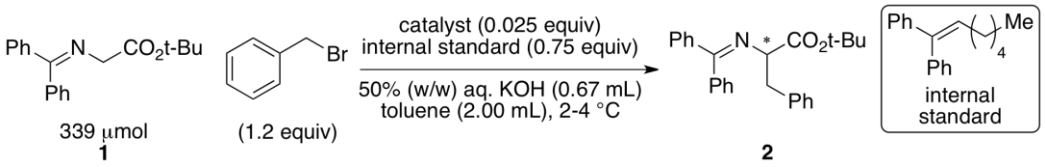

A 2 mL scintillation vial was fitted with a Teflon lined rubber septum and *tert*-butyl 2-(diphenylmethyleneamino)acetate (100 mg, 0.34 mmol), and the phase transfer catalyst (8.48 μmol, 0.025 equiv) were added. The liquid reagents, benzyl bromide (800 μL, 0.51 M in toluene, 1.2 equiv), internal standard (790 μL, 0.32 M in tolune, 0.75 equiv), and toluene (410 μL) were added via syringe. Then, a 1.5 cm egg-shaped magnetic stir bar was placed in the vial and the contents were briefly agitated in an ultrasonic bath (10-20 s). Reaction vials were then transferred to a cold room maintained at 2-4 ^{o}C and were allowed to equilibrate for at least 1 h with stirring while immersed in a water bath to control temperature fluctuations. Lastly, 50% aq. (w/w) KOH solution (670 μL, 11.9 mmol, 17.8 M, 35.0 equiv) was added to the rapidly stirred (1600 rpm) organic phase. Aliquots were taken at the indicated times and analyzed as follows.

The internal standard employed in these reactions was 1,1-diphenyl-1-heptene.

General Procedure III. Performing Kinetics and Enantioselectivity Measurements on PTC Alkylations

Three seconds prior to the indicated time interval, the stirrer was turned off. At the indicated time interval a 10-μL aliquot of the organic layer was removed and then was injected into MeCN (2.0 mL) containing glacial acetic acid (several drops). This clear solution was filtered through a small plug of silica gel (0.5 x 1 cm) and the filtrate was analyzed by Reverse Phase-HPLC Method 1.

For the PTC alkylations that reached near to full completion (70-85% conversion to product), a 10-μL aliquot was taken from the organic phase and injected into *i*-PrOH (2 mL). This aliquot was filtered through a small plug of silica gel (0.5 x 1 cm) and the filtrate was analyzed by CSP-HPLC Method 2

For the PTC alkylations that did not reach full completion (<70% conversion to product), the organic phase was first separated from the aqueous base *via* pipette. The alkylation product was obtained by preparative thin-layer chromatography (8 x 10 cm plate) using 0.5 - 1.0 mL of the organic phase directly. The product was eluted with 5:95 TBME/hexane. The product band was removed, suspended in *i*-PrOH (4 mL), and the silica gel was removed by filtration. The solvent was removed on a rotavap (20 mm Hg, 35-40 °C). The product was then dissolved in an appropriate amount of *i*-PrOH (1 mg/mL) and then analyzed by CSP-HPLC Method 2.

Kinetic Analyzses of Catalysts in Series A

Catalyst **1a**: Run 1

Time (min)	Standard (µmol)	Standard Area	Product Area	Product (µmol)	% Product
0	254.0	1.00	0.00	0.00	0.0
4	254.0	6315.24	68.36	3.27	1.0
8	254.0	6655.10	462.93	21.03	6.2
12	254.0	6107.59	1115.00	55.20	16.3
16	254.0	5897.88	2466.57	126.45	37.3
20	254.0	6424.48	3549.97	167.08	49.3
24	254.0	7382.42	4765.74	195.19	57.6
28	254.0	6173.24	4297.34	210.48	62.1
32	254.0	6503.01	4885.58	227.16	67.0
36	254.0	7039.97	5559.75	238.79	70.4
40	254.0	6655.06	5052.67	229.56	67.7

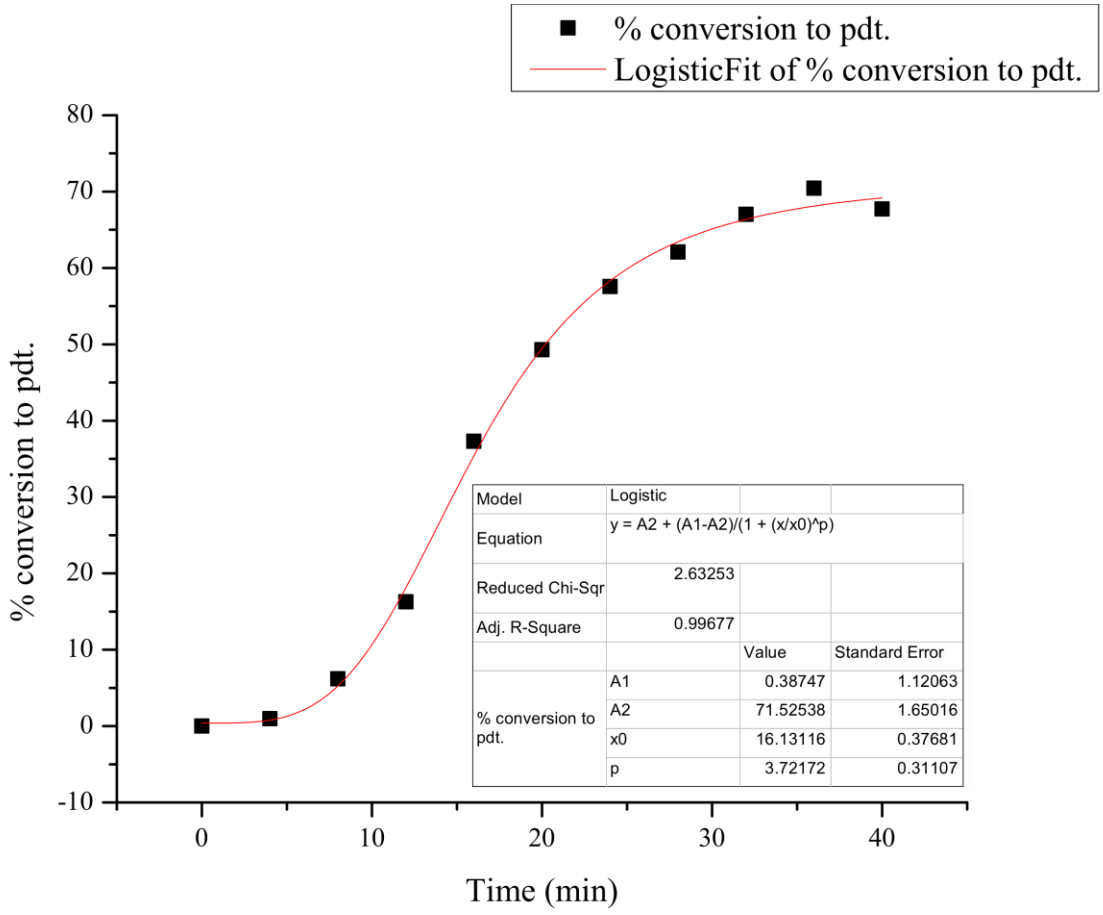

Half-Life = 20 min

Catalyst **1a**: Run 2

Time (min)	Standard (µmol)	Standard Area	Product Area	Product (µmol)	% Product
0	254.0	1.00	0.00	0.0	0.0
4	254.0	6525.65	70.70	3.3	1.0
8	254.0	6077.37	336.71	16.8	4.9
12	254.0	6667.15	879.72	39.9	11.8
16	254.0	6060.03	1905.65	95.1	28.0
20	254.0	6189.47	3102.61	151.6	44.7
24	254.0	6697.23	4101.86	185.2	54.6
28	254.0	7045.90	4652.70	199.7	58.9
32	254.0	6297.25	4608.70	221.3	65.3
36	254.0	8091.08	6307.97	235.7	69.5
40	254.0	7020.25	5777.23	248.8	73.4

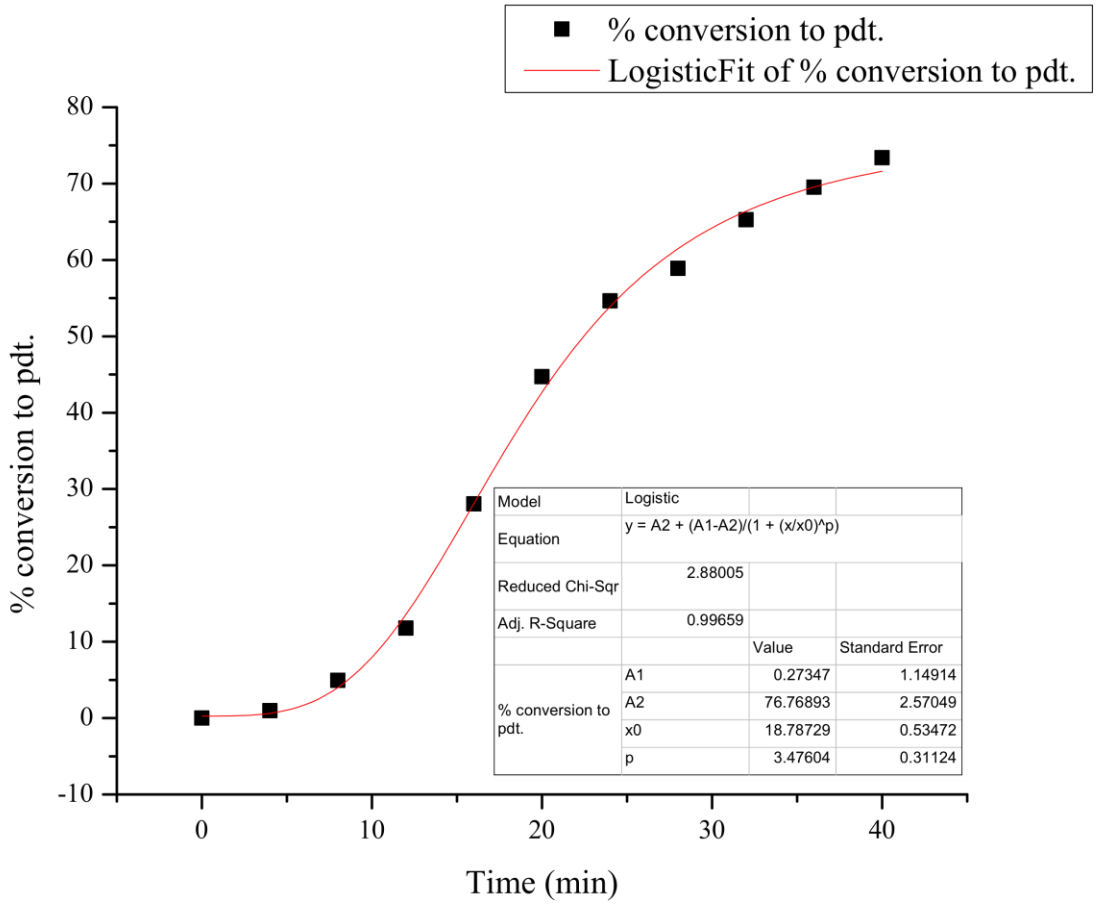

Half-Life = 22 min

Average Half-Life = 21 min

Catalyst **2a**: Run 1

Time (min)	Standard (umol)	Standard Area	Product Area	Product (umol)	% Product
0	254.4	1.00	0.00	0.0	0.0
30	254.4	6090.60	113.01	5.6	1.7
61	254.4	6386.44	362.39	17.2	5.1
120	254.4	7553.15	1097.38	44.0	13.0
180	254.4	7437.62	1885.13	76.8	22.6
244	254.4	7170.76	2708.80	114.4	33.7
300	254.4	7017.54	3317.81	143.2	42.2
360	254.4	7163.19	3952.86	167.1	49.3
420	254.4	7223.67	4427.49	185.6	54.8
480	254.4	7401.25	4928.23	201.6	59.5
540	254.4	7653.35	5427.32	214.8	63.3
600	254.4	7117.47	5262.02	223.9	66.0
1320	254.4	7197.75	5979.38	251.6	74.2
1860	254.4	7042.44	5868.89	252.4	74.4
2760	254.4	7217.98	6162.11	258.5	76.3

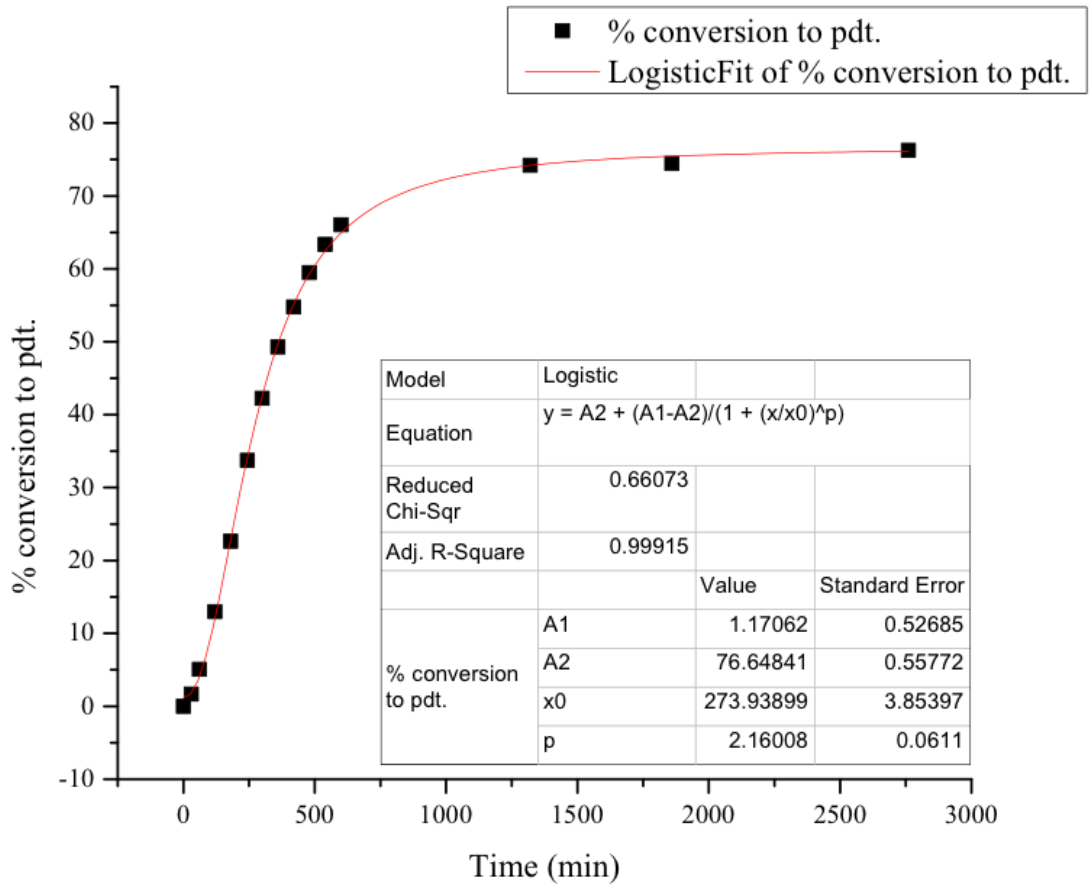

Half-Life = 363 min

Catalyst **2a**: Run 2

Time (min)	Standard (µmol)	Standard Area	Product Area	Product (µmol)	% Product
0	254.4	1.00	0.00	0.0	0.0
60	254.4	7764.86	557.63	21.7	6.4
120	254.4	7135.54	1641.45	69.7	20.5
180	254.4	7211.92	2565.60	107.7	31.8
240	254.4	7838.86	3141.89	121.4	35.8
300	254.4	7704.01	4191.80	164.8	48.6
360	254.4	7821.57	4611.86	178.6	52.7
420	254.4	7893.62	5272.90	202.3	59.7
1103	254.4	6816.47	5738.17	254.9	75.2
1468	254.4	7103.48	5878.89	250.6	73.9
2550	254.4	7509.56	6426.51	259.2	76.4

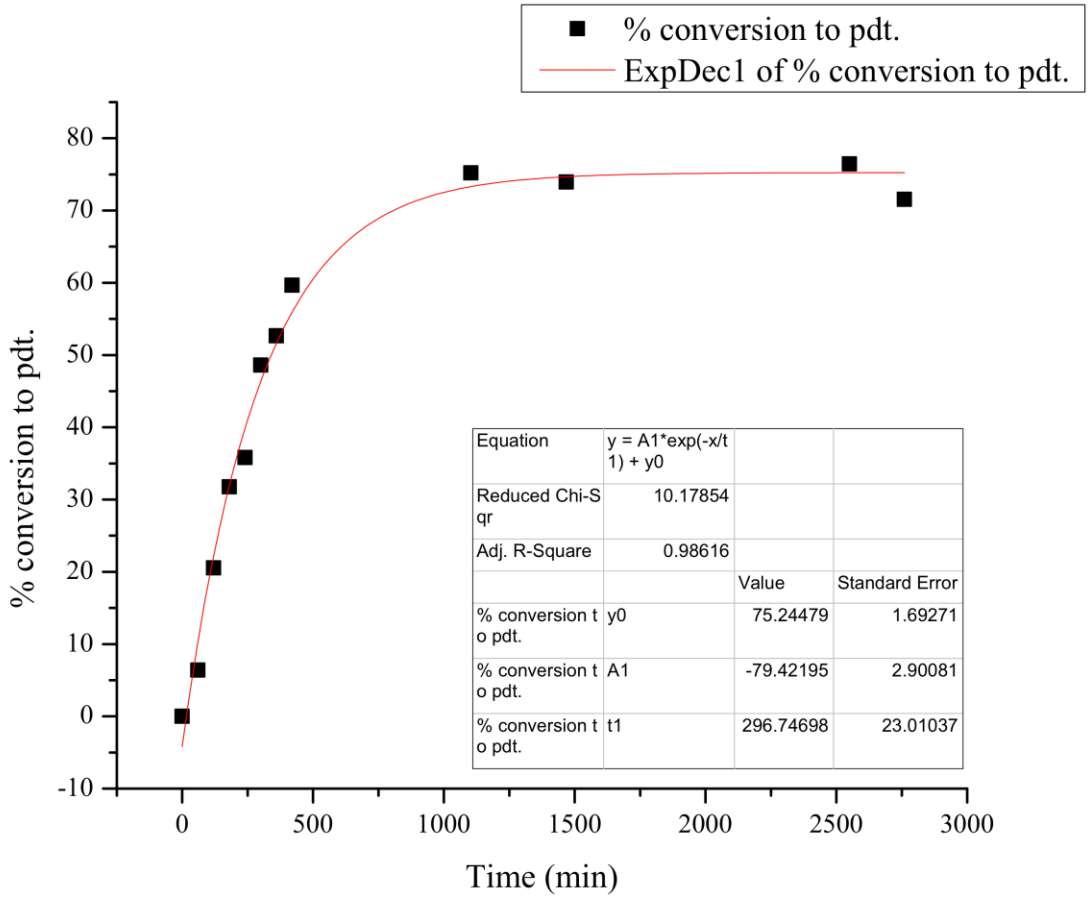

Half-Life = 340 min

Average Half-Life = 351 min

Catalyst **3a**: Run 1

Time (min)	Standard (µmol)	Standard Area	Product Area	Product (µmol)	% Product
0	254.0	1.00	0.00	0.0	0.0
3	254.0	5724.09	20.61	1.1	0.3
9	254.0	5899.33	112.17	5.7	1.7
18	254.0	6511.32	404.84	18.8	5.5
30	254.0	6584.82	961.62	44.2	13.0
45	254.0	7436.89	2004.76	81.5	24.0
63	254.0	6987.36	2794.91	120.9	35.7
84	254.0	7502.23	4116.53	165.9	48.9
108	254.0	6968.71	4740.95	205.7	60.7
135	254.0	7027.91	5503.32	236.8	69.8
165	254.0	7938.40	6373.96	242.8	71.6

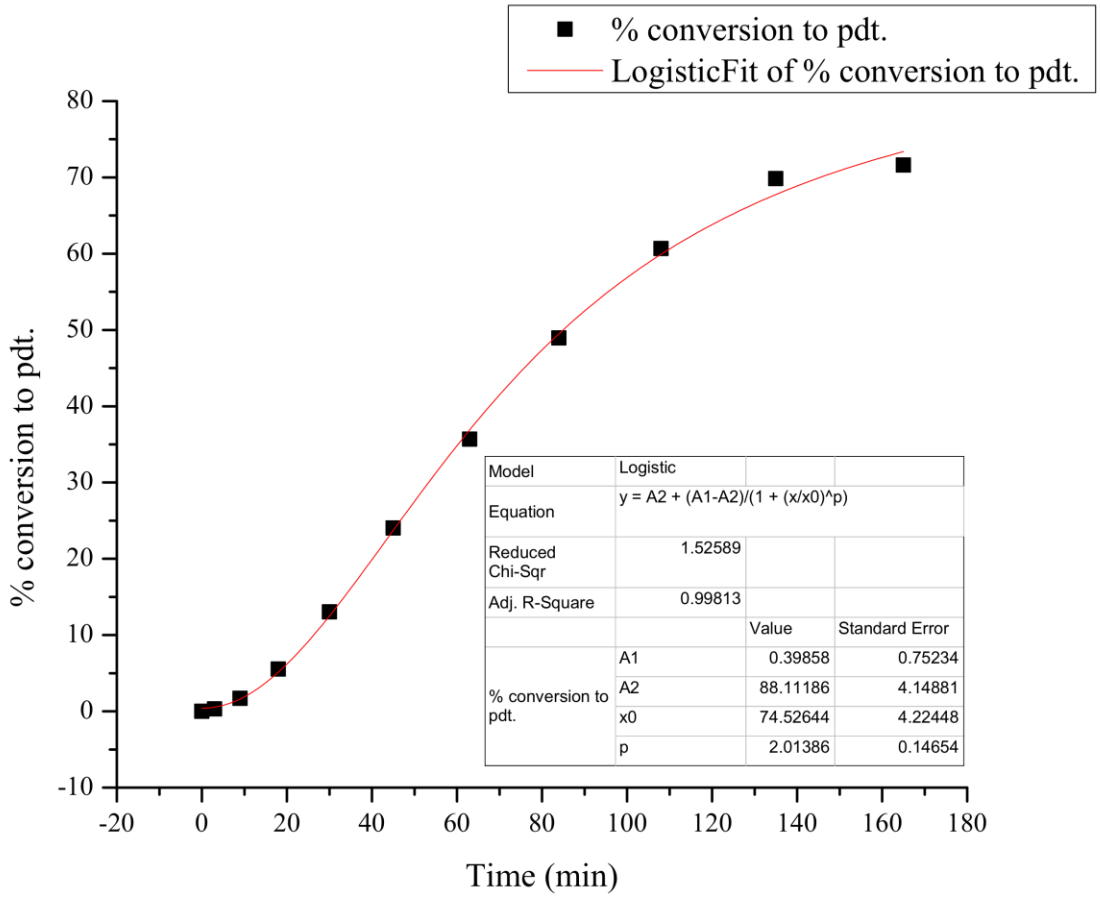

Half-Life = 85 min

Catalyst **3a**: Run 2

Time (min)	Standard (µmol)	Standard Area	Product Area	Product (µmol)	% Product
0	254.0	1.00	0.00	0.0	0.0
5	254.0	7109.33	115.26	4.9	1.4
10	254.0	8054.54	347.28	13.0	3.8
20	254.0	7641.84	831.24	32.9	9.7
30	254.0	7735.89	1426.57	55.8	16.4
45	254.0	7214.04	2169.73	90.9	26.8
60	254.0	7402.72	3129.77	127.8	37.7
90	254.0	7277.34	4554.41	189.2	55.8
120	254.0	7206.75	5415.82	227.2	67.0
180	254.0	7633.05	6456.10	255.7	75.4
240	254.0	7413.94	6464.79	263.7	77.8
300	254.0	7155.78	6019.47	254.3	75.0
1020	254.0	8491.11	7208.87	256.7	75.7

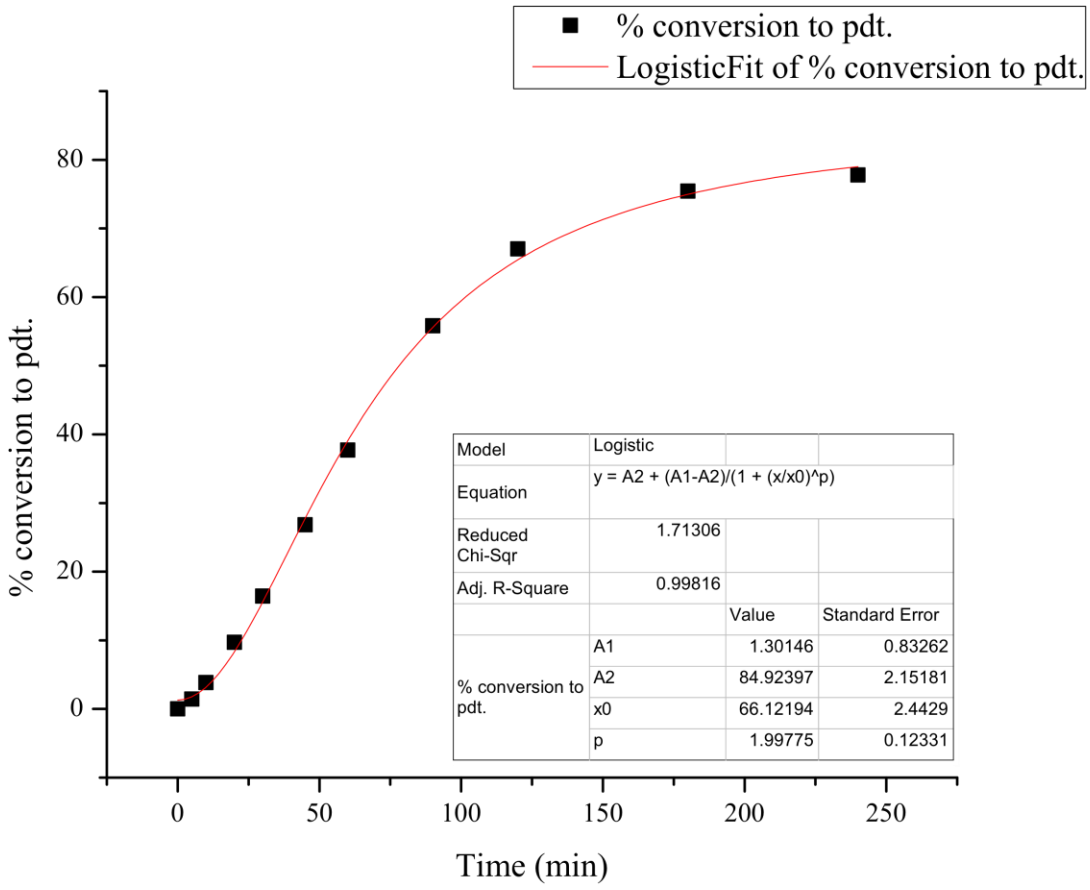

Half-Life = 78 min

Average Half-Life = 82 min

Catalyst **4a**: Run 1

Time (min)	Standard (µmol)	Standard Area	Product Area	Product (µmol)	% Product
0	254.0	1.00	0.00	0.0	0.0
7	254.0	8099.77	491.92	18.4	5.4
14	254.0	6473.20	988.06	46.2	13.6
21	254.0	6481.47	1618.83	75.5	22.3
28	254.0	6848.23	2427.94	107.2	31.6
30	254.0	7449.53	3034.09	123.1	36.3
35	254.0	6195.73	2686.33	131.1	38.7
42	254.0	6774.26	3486.69	155.6	45.9
49	254.0	6132.76	3660.82	180.5	53.2
56	254.0	6327.44	4259.80	203.6	60.0
60	254.0	6343.97	4323.58	206.1	60.8
63	254.0	7591.06	5350.65	213.1	62.9
70	254.0	6811.49	5282.45	234.5	69.2
90	254.0	6360.96	5518.83	262.3	77.4
120	254.0	4711.11	4270.64	274.1	80.9
150	254.0	7115.57	6684.37	284.0	83.8
182	254.0	5451.71	5158.49	286.1	84.4

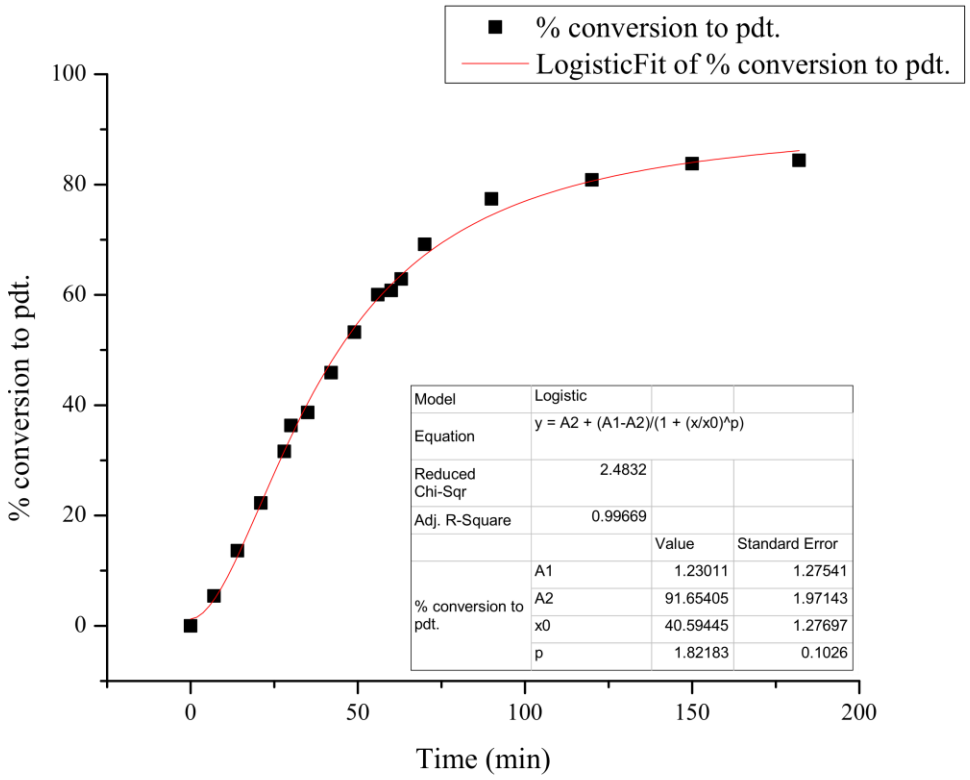

Half-Life = 44 min

Catalyst **4a**: Run 2

Time (min)	Standard (µmol)	Standard Area	Product Area	Product (µmol)	% Product
0	254.0	1.00	0.00	0.0	0.0
5	254.0	6956.27	246.78	10.7	3.2
10	254.0	6983.71	671.26	29.1	8.6
20	254.0	7170.84	1646.42	69.4	20.5
30	254.0	7011.34	2755.72	118.8	35.1
45	254.0	6993.50	3834.21	165.8	48.9
60	254.0	6879.12	4722.85	207.6	61.2
90	254.0	6727.30	5568.84	250.3	73.8
120	254.0	7350.99	6770.02	278.5	82.1
180	254.0	7308.84	6618.29	273.8	80.8
240	254.0	7265.55	6626.65	275.8	81.3

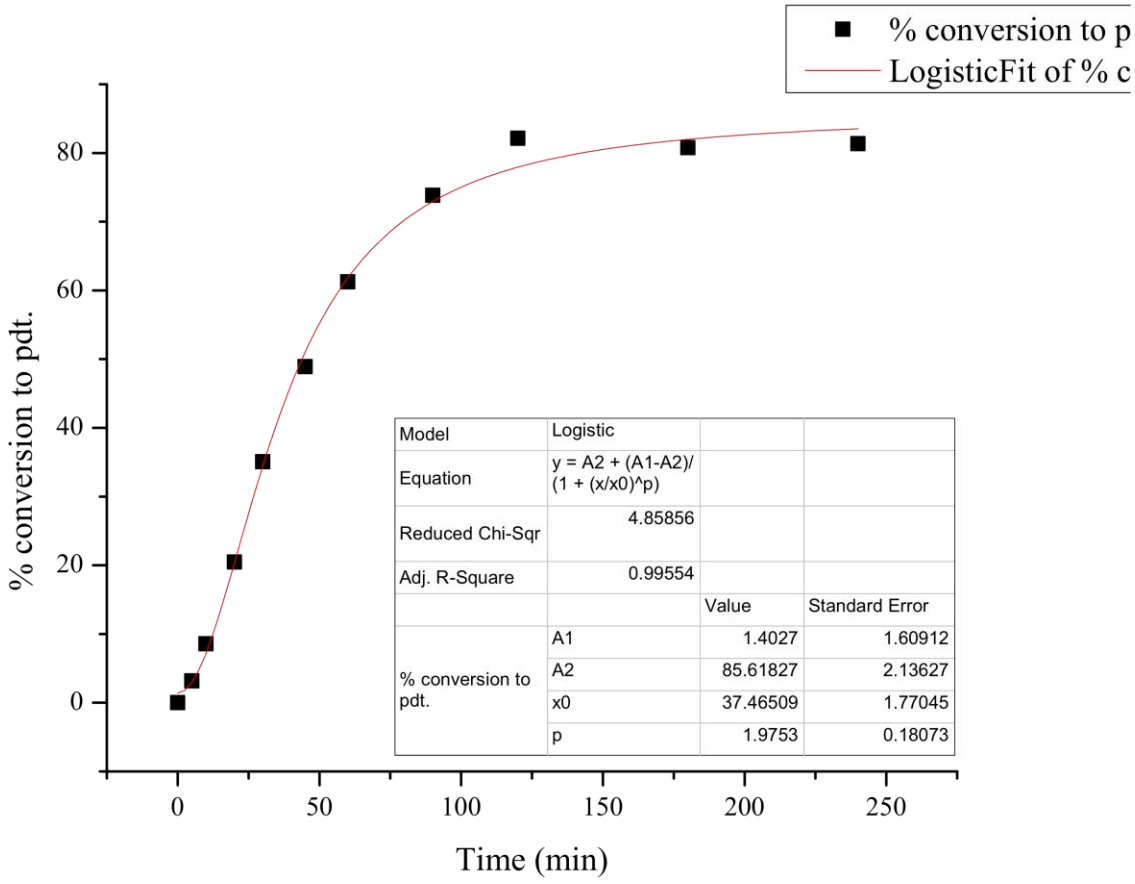

Half-Life = 44 min

Average Half-Life = 44 min

Catalyst **5a**: Run 1

Time (min)	Standard (µmol)	Standard Area	Product Area	Product (µmol)	% Product
0	254.0	1.00	0.00	0.00	0.00
60	254.0	6551.96	646.15	29.82	8.80
120	254.0	6880.21	1634.19	71.82	21.19
180	254.0	6970.26	2422.03	105.06	30.99
240	254.0	6266.68	2842.73	137.16	40.46
300	254.0	6886.98	3625.36	159.17	46.95
360	254.0	7310.40	4273.93	176.77	52.15
420	254.0	7259.71	4668.02	194.42	57.35
480	254.0	7312.95	4913.18	203.14	59.92
540	254.0	7515.24	5182.03	208.49	61.50
600	254.0	6708.92	4674.66	210.68	62.15
1440.00	254.00	6427.62	4976.42	234.10	69.05

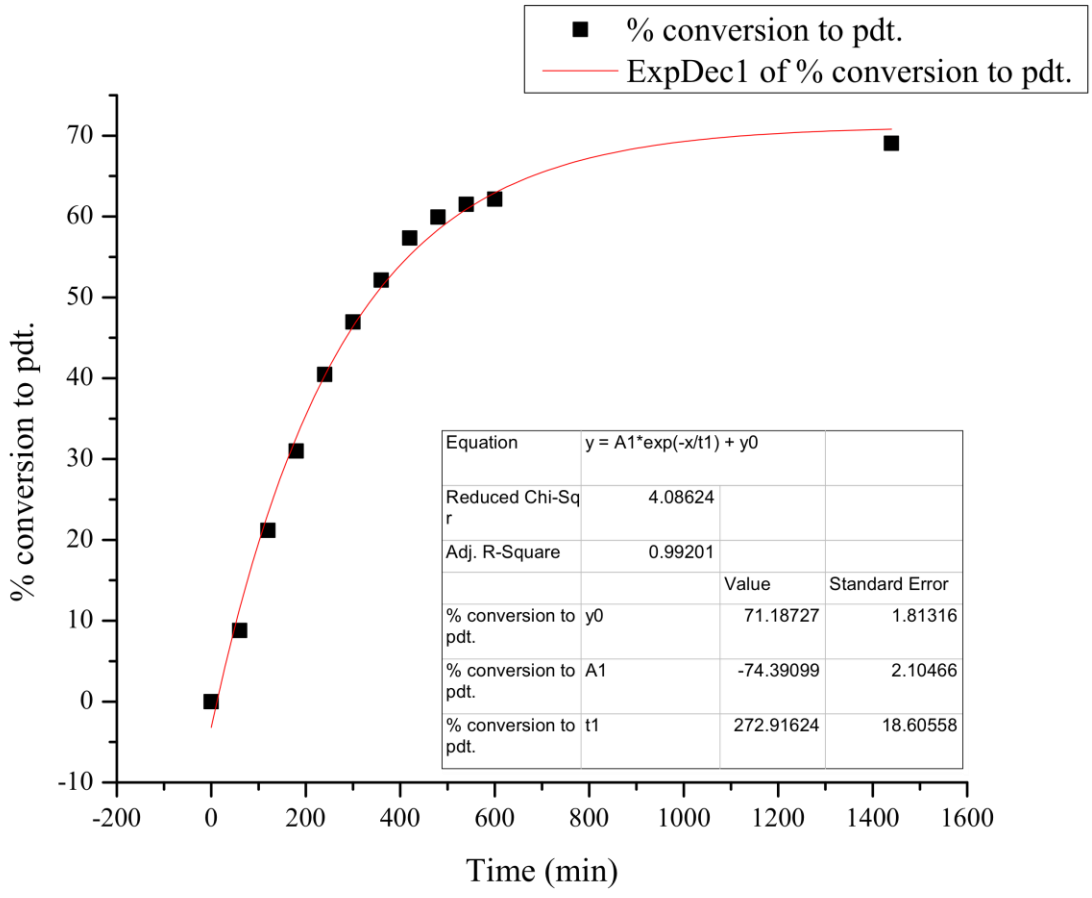

Half-Life = 343 min

Catalyst **5a**: Run 2

Time (min)	Standard (µmol)	Standard Area	Product Area	Product (µmol)	% Product
0	254.4	1.00	0.00	0.0	0.0
30	254.4	6588.01	481.52	22.1	6.5
60	254.4	6964.99	963.41	41.9	12.4
90	254.4	6707.41	1436.32	64.8	19.1
120	254.4	6766.07	1799.51	80.5	23.8
180	254.4	6944.72	2876.93	125.5	37.0
240	254.4	6749.27	3543.57	159.0	46.9
300	254.4	7027.41	4341.94	187.1	55.2
360	254.4	6643.04	4358.22	198.7	58.6
420	254.4	6885.22	4763.41	209.5	61.8
1153	254.4	6768.02	6137.83	274.6	81.0
1478	254.4	6887.19	6364.26	279.8	82.5

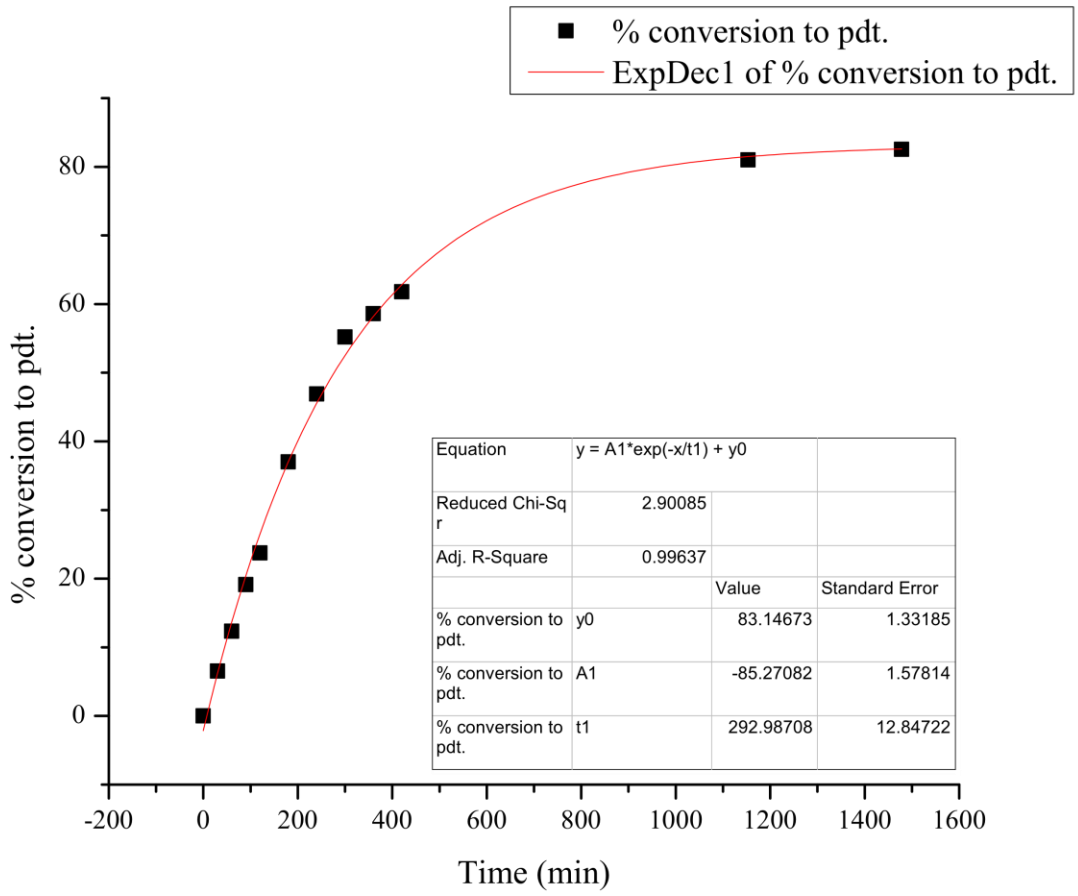

Half-Life = 277 min

Average Half-Life = 310 min

Kinetic Analyzses of Catalysts in Series B

Catalyst **1b**: Run 1

Time (min)	Standard (µmol)	Standard Area	Product Area	Product (µmol)	% Product
0	254.0	1.00	0.00	0.0	0.0
6	254.0	7748.79	985.04	38.4	11.3
12	254.0	6567.97	1942.93	89.4	26.4
20	254.0	6318.09	3202.96	153.3	45.2
30	254.0	6684.17	4851.38	219.5	64.7
42	254.0	7460.54	6563.10	266.0	78.5
56	254.0	7489.41	7423.38	299.7	88.4
72	254.0	6878.57	6611.26	290.6	85.7
90	254.0	7598.74	7197.71	286.4	84.5
110	254.0	7548.24	7130.15	285.6	84.3
300	254.0	6857.69	6376.37	281.1	82.9

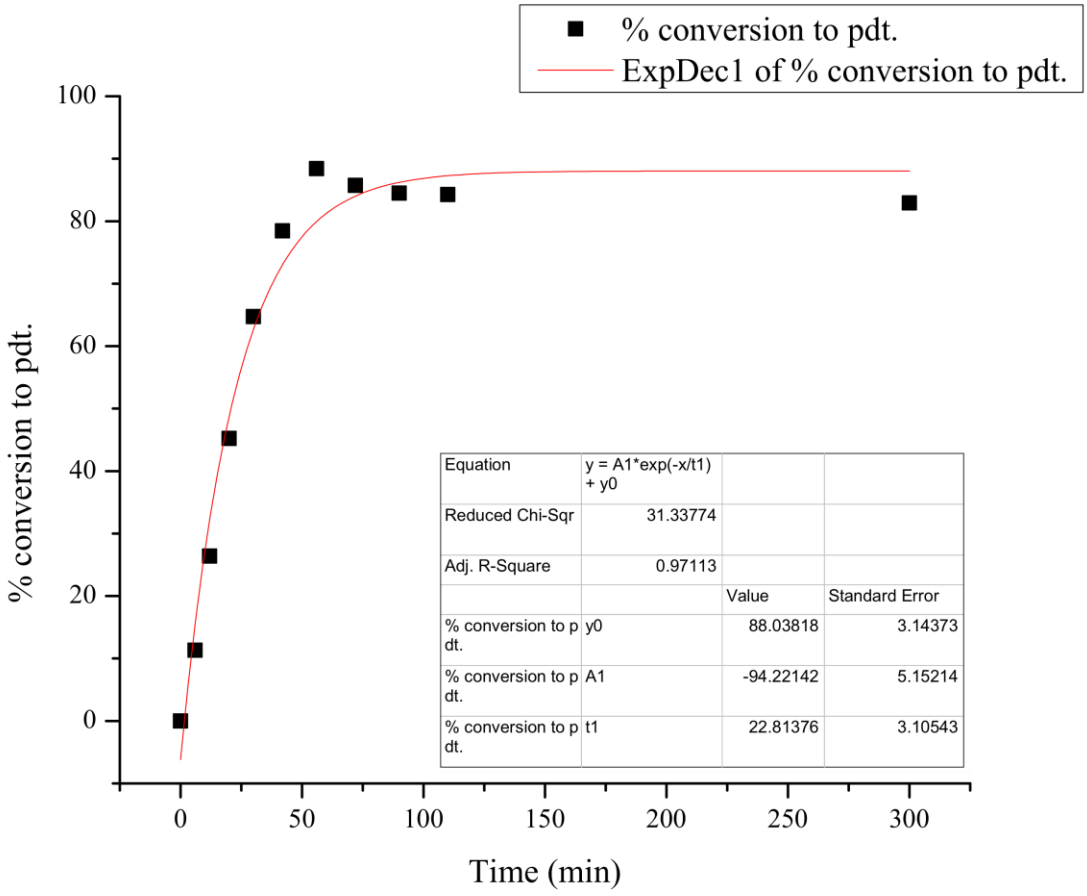

Half-Life = 21 min

Catalyst **1b**: Run 2

Time (min)	Standard (µmol)	Standard Area	Product Area	Product (µmol)	% Product
0	254.0	1.00	0.00	0.00	0.0
2	254.0	6518.76	184.72	8.57	2.5
6	254.0	7542.25	970.35	38.90	11.5
12	254.0	6598.10	2082.50	95.43	28.2
20	254.0	6865.16	3758.28	165.53	48.8
30	254.0	6773.70	4987.07	222.61	65.7
42	254.0	7644.02	6455.82	255.36	75.3
56	254.0	6410.66	5388.35	254.14	75.0
72	254.0	7777.18	6948.31	270.14	79.7
90	254.0	7805.40	7196.24	278.76	82.2
110	254.0	6747.65	5967.86	267.42	78.9
300	254.0	6757.47	6230.80	278.80	82.2

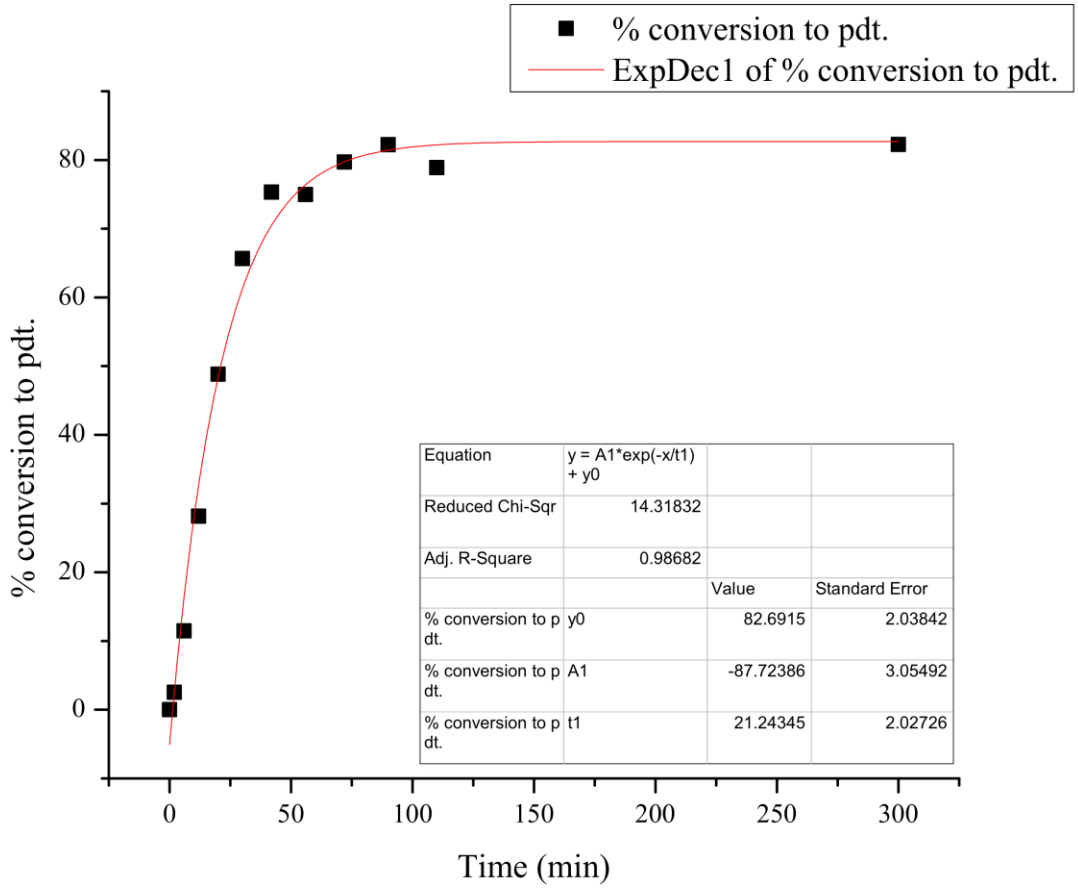

Half-Life = 21 min

Average Half-Life = 21 min

Catalyst **2b**: Run 1

Time (min)	Standard (µmol)	Standard Area	Product Area	Product (µmol)	% Product
0	254.0	1.00	0.00	0.0	0.0
5	254.0	7879.88	0.00	0.0	0.0
30	254.0	7671.50	40.44	1.6	0.5
60	254.0	7635.95	456.30	18.1	5.3
120	254.0	7556.02	2331.50	93.3	27.5
180	254.0	7112.89	3454.01	146.8	43.3
240	254.0	7590.22	4029.87	160.5	47.4
300	254.0	7260.17	4909.52	204.5	60.3
1341	254.0	7782.06	6790.97	263.9	77.8
1837	254.0	8306.82	7412.94	269.8	79.6

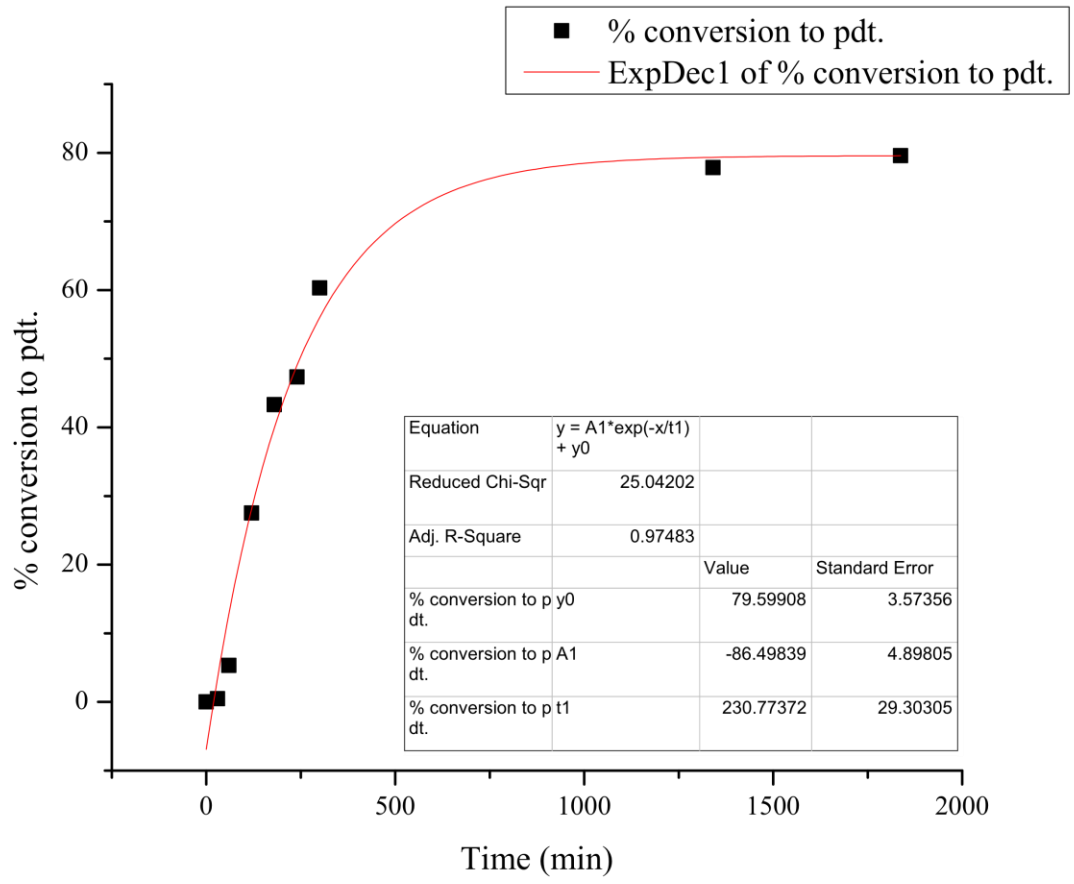

Half-Life = 247 min

Catalyst **2b**: Run 2

Time (min)	Standard (umol)	Standard Area	Product Area	Product (µmol)	% Product
0	254.0	1.00	0.00	0.0	0.0
5	254.0	7841.88	0.00	0.0	0.0
30	254.0	6461.39	107.85	5.0	1.5
60	254.0	6917.40	978.41	42.8	12.6
120	254.0	7423.29	2971.22	121.0	35.7
180	254.0	6886.53	3387.69	148.7	43.9
240	254.0	7504.17	3946.61	159.0	46.9
300	254.0	7686.25	4676.79	184.0	54.3
1341	254.0	7581.39	6448.81	257.2	75.9
1837	254.0	7969.25	6801.76	258.1	76.1

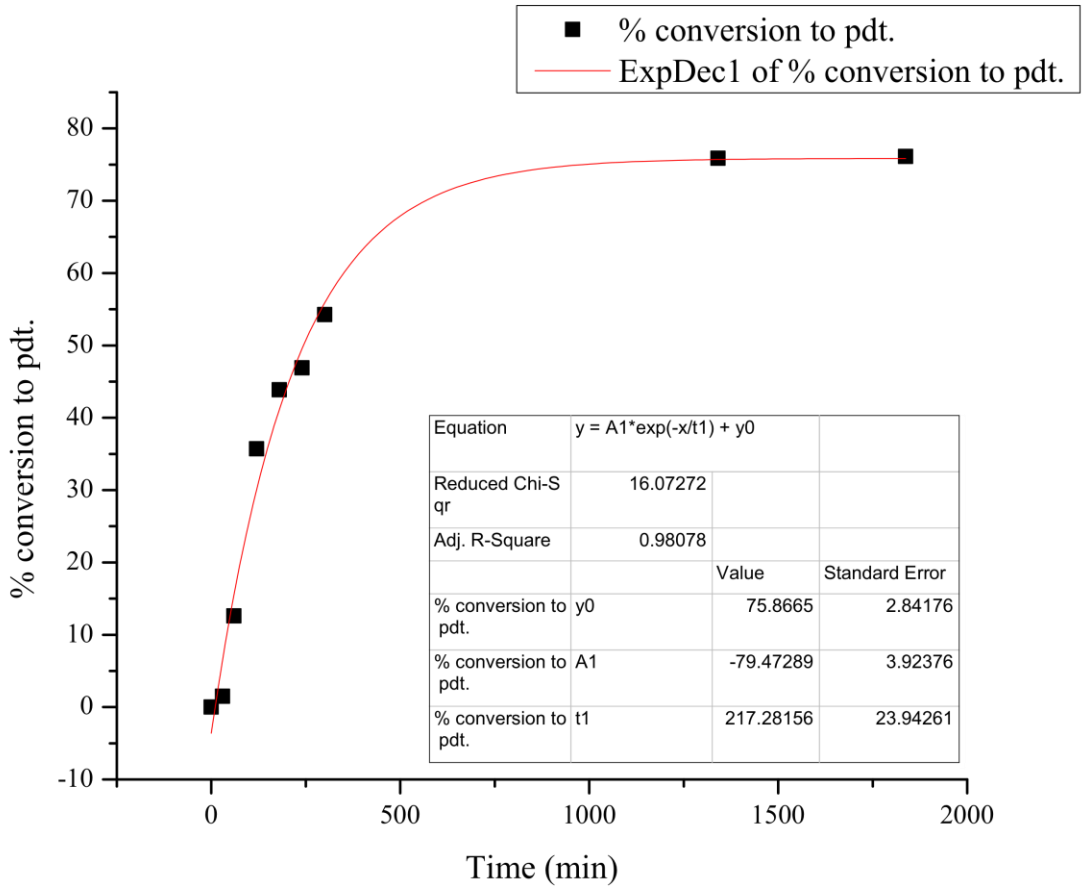

Half-Life = 244 min

Average Half-Life = 246 min

Catalyst **3b**: Run 1

Time (min)	Standard (µmol)	Standard Area	Product Area	Product (µmol)	% Product
0	254.0	1.00	0.00	0.0	0.0
5	254.0	7116.94	0.00	0.0	0.0
15	254.0	7529.49	78.86	3.2	0.9
30	254.0	6689.77	486.96	22.0	6.5
45	254.0	8134.10	1481.62	55.1	16.2
60	254.0	6632.84	1941.55	88.5	26.1
90	254.0	7293.13	3324.44	137.8	40.7
120	254.0	7563.81	4471.39	178.7	52.7
180	254.0	6919.37	5506.73	240.6	71.0
240	254.0	6872.94	5607.03	246.7	72.8
300	254.0	7407.61	6136.27	250.5	73.9
1042	254.0	6839.24	5655.01	250.0	73.7

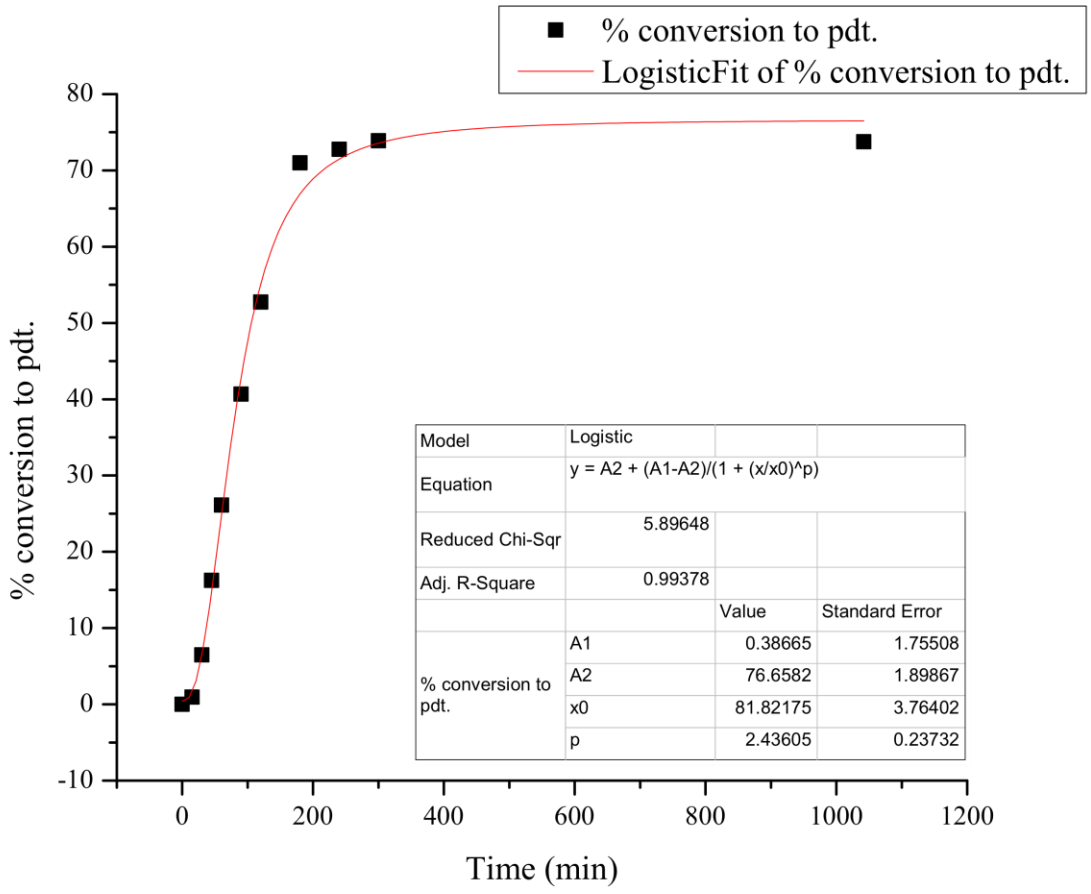

Half-Life = 106 min

Catalyst **3b**: Run 2

Time (min)	Standard (µmol)	Product Area	Standard Area	Product (µmol)	% Product
0	254.0	0.00	1.00	0.0	0.0
5	254.0	0.00	7250.08	0.0	0.0
15	254.0	90.06	7390.36	3.7	1.1
30	254.0	579.70	7280.64	24.1	7.1
45	254.0	1385.53	6780.43	61.8	18.2
60	254.0	2690.50	7804.84	104.2	30.7
90	254.0	4150.43	7281.74	172.3	50.8
120	254.0	5310.07	7363.24	218.1	64.3
180	254.0	6169.84	6990.93	266.8	78.7
240	254.0	5813.56	6602.04	266.3	78.5
300	254.0	6631.58	7357.89	272.5	80.4
1042	254.0	6154.85	7266.25	256.1	75.5

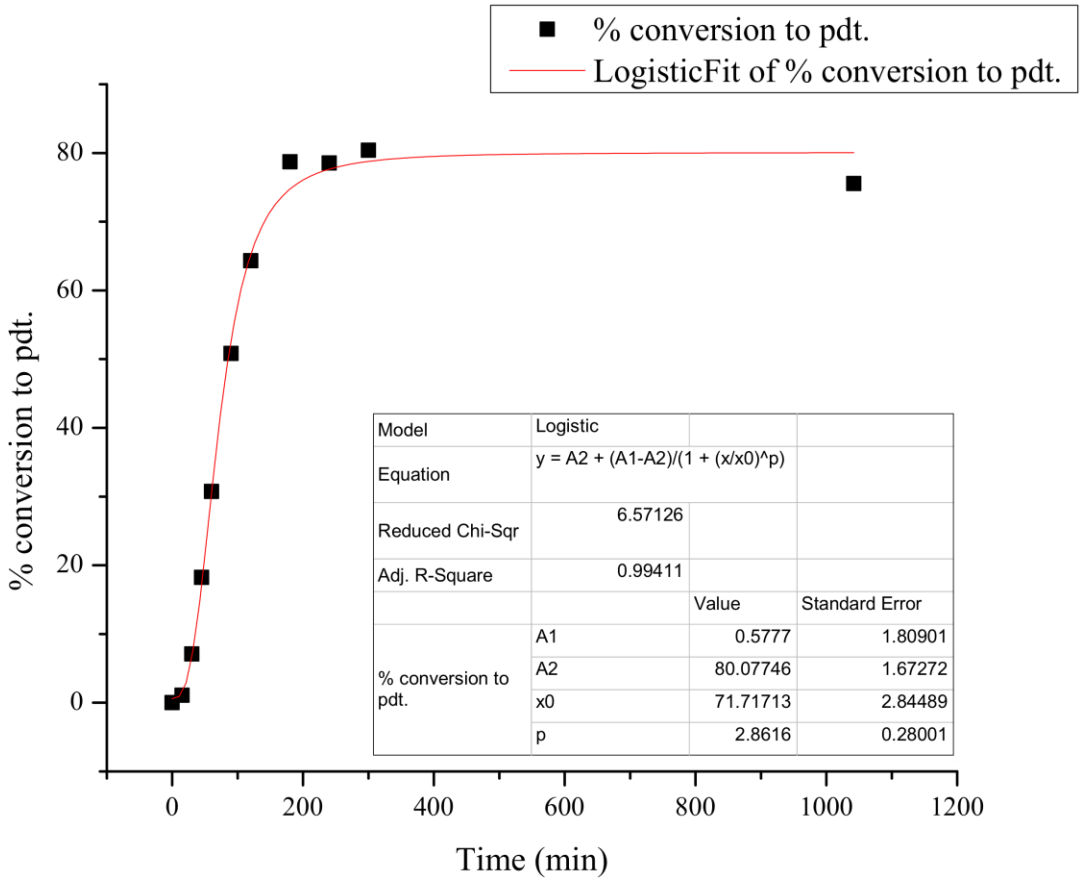

Half-Life = 85 min

Average Half-Life = 95 min

Catalyst **4b**: Run 1

Time (min)	Standard (µmol)	Standard Area	Product Area	Product (µmol)	% Product
0	254.0	1.00	0.00	0.0	0.0
5	254.0	6915.34	783.53	34.3	10.1
15	254.0	6980.95	2308.70	100.0	29.5
30	254.0	6784.76	3985.27	177.6	52.4
45	254.0	7278.12	5281.28	219.4	64.7
60	254.0	7019.90	6137.38	264.3	78.0
90	254.0	7091.19	5962.76	254.2	75.0
120	254.0	6239.32	5139.75	249.1	73.5
180	254.0	7578.16	6326.69	252.4	74.5
240	254.0	6972.50	5818.39	252.3	74.4
300	254.0	7026.35	5921.27	254.8	75.2
1039	254.0	6420.38	5643.17	265.8	78.4

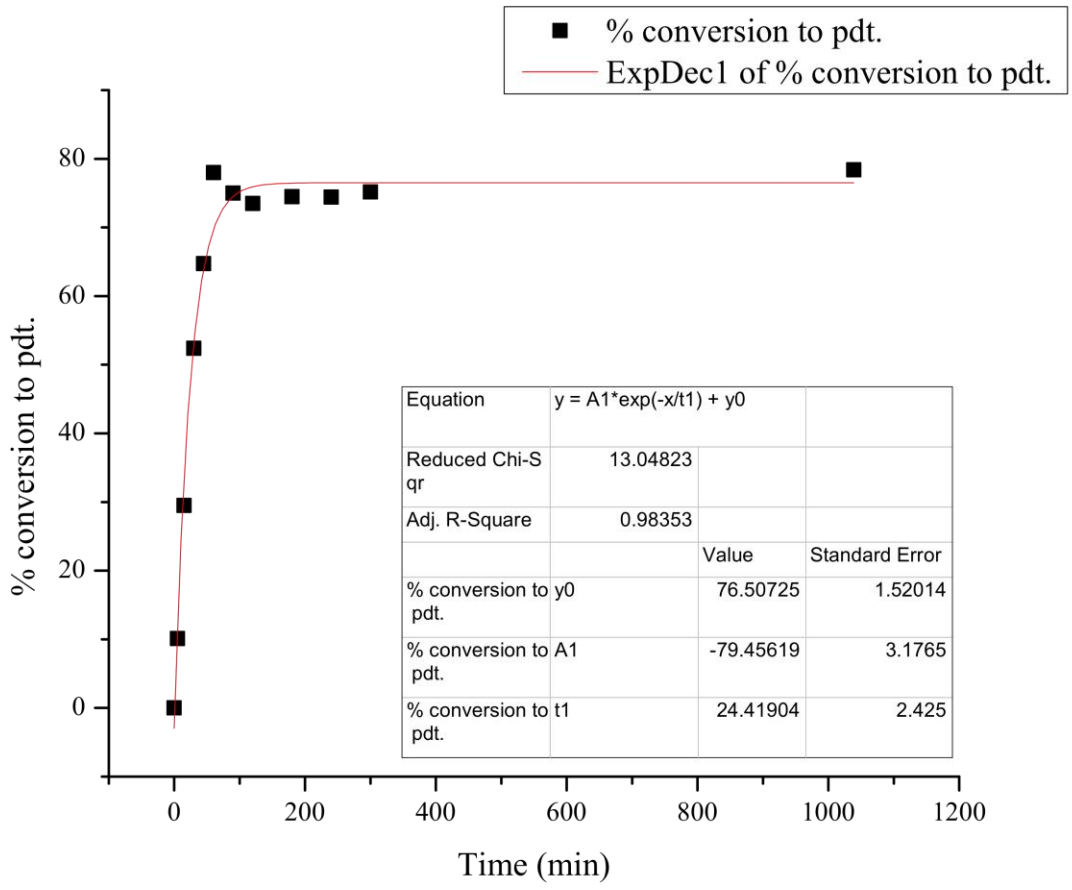

Half-Life = 27 min

Catalyst **4b**: Run 2

Time (min)	Standard (µmol)	Standard Area	Product Area	Product (µmol)	% Product
0	254.0	1.00	0.00	0.0	0.0
5	254.0	8268.86	752.64	27.5	8.1
15	254.0	7168.00	2337.65	98.6	29.1
30	254.0	6913.03	3949.39	172.7	51.0
45	254.0	8533.48	6104.96	216.3	63.8
60	254.0	7106.51	5246.87	223.2	65.9
90	254.0	6864.22	5574.94	245.6	72.4
120	254.0	6501.38	5222.00	242.9	71.6
180	254.0	7052.11	5870.49	251.7	74.2
240	254.0	7260.77	5750.17	239.5	70.6
300	254.0	7612.69	6545.06	260.0	76.7
1039	254.0	6977.30	6410.19	277.8	81.9

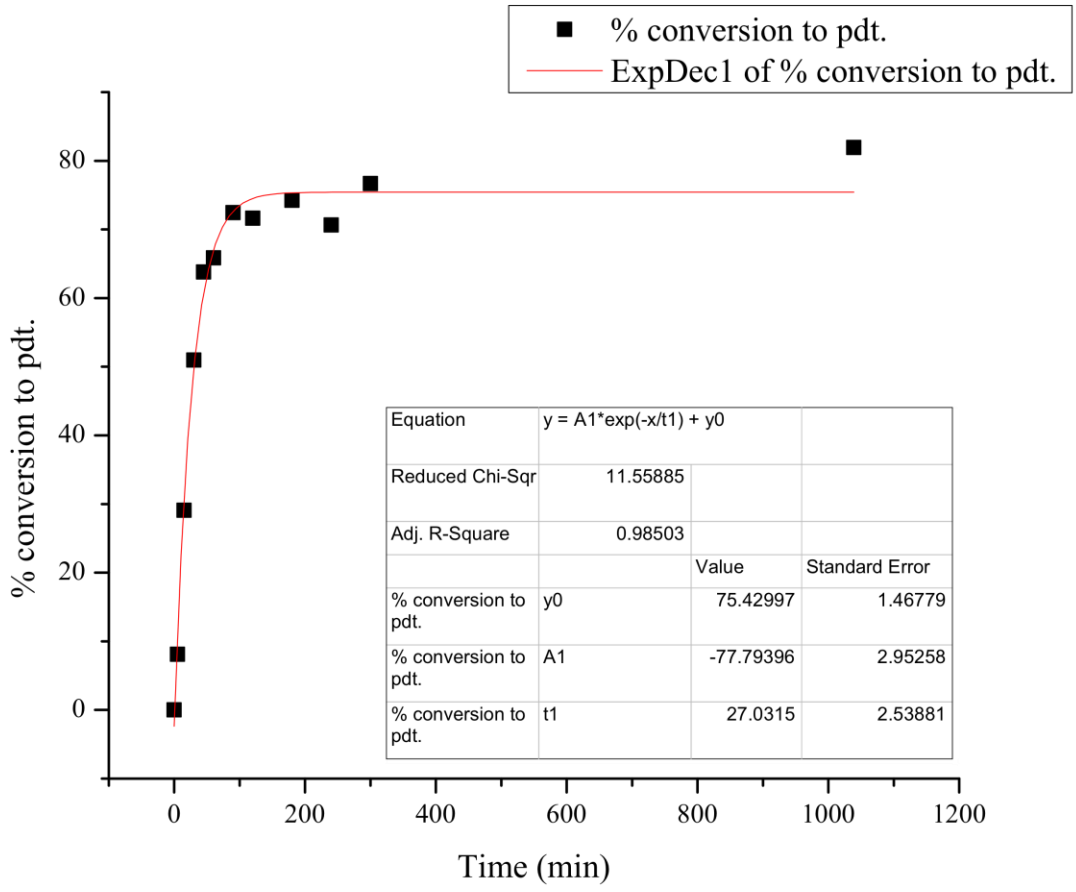

Half-Life = 30 min

Average Half-Life = 29 min

Catalyst **5b**: Run 1

Time (min)	Standard (µmol)	Standard Area	Product Area	Product (µmol)	% Prodcut
0	254.0	1.00	0.00	0	0.0
60	254.0	7515.93	648.02	26.06956273	7.7
120	254.0	7213.64	1646.44	69.01101463	20.4
180	254.0	7913.31	2972.46	113.5755569	33.5
240	254.0	6753.74	3360.49	150.4474812	44.4
300	254.0	8002.67	4513.40	170.5276886	50.3
360	254.0	7199.20	4499.93	188.9939234	55.8
420	254.0	7478.48	4977.12	201.229079	59.4
480	254.0	7621.79	5265.14	208.8716046	61.6
1260	254.0	7331.66	6477.10	267.1191093	78.8
4320	254.0	5576.05	4908.26	266.1507443	78.5

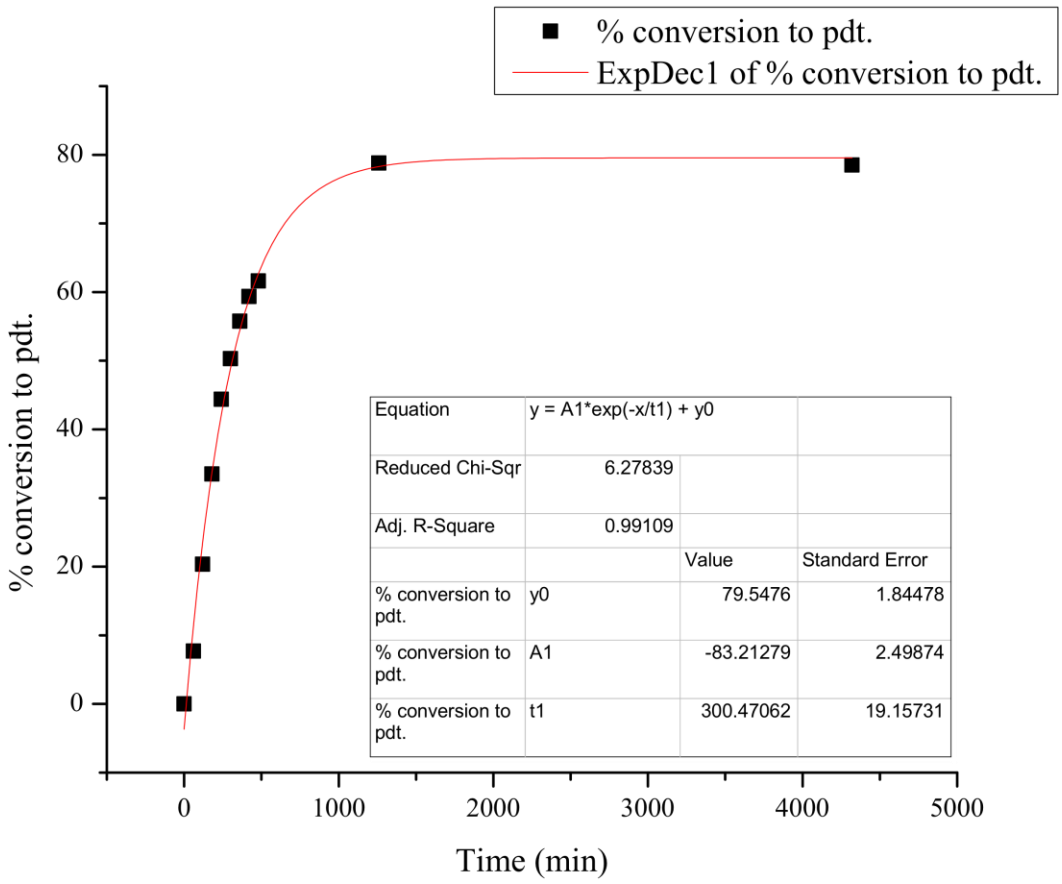

Half-Life = 311 min

Catalyst **5b**: Run 2

Time (min)	Standard (µmol)	Standard Area	Product Area	Product (µmol)	% Product
0	254.0	1.00	0.00	0.0	0.0
60	254.0	7351.52	670.73	27.6	8.1
120	254.0	7540.39	1830.13	73.4	21.6
180	254.0	7364.30	2762.87	113.4	33.5
240	254.0	8103.71	3953.71	147.5	43.5
300	254.0	7115.94	4055.55	172.3	50.8
360	254.0	7554.33	4646.77	186.0	54.9
420	254.0	8041.56	5237.67	196.9	58.1
480	254.0	7699.79	5380.62	211.3	62.3
1260	254.0	8157.51	6690.44	248.0	73.2
4320	254.0	7505.50	6188.76	249.3	73.5

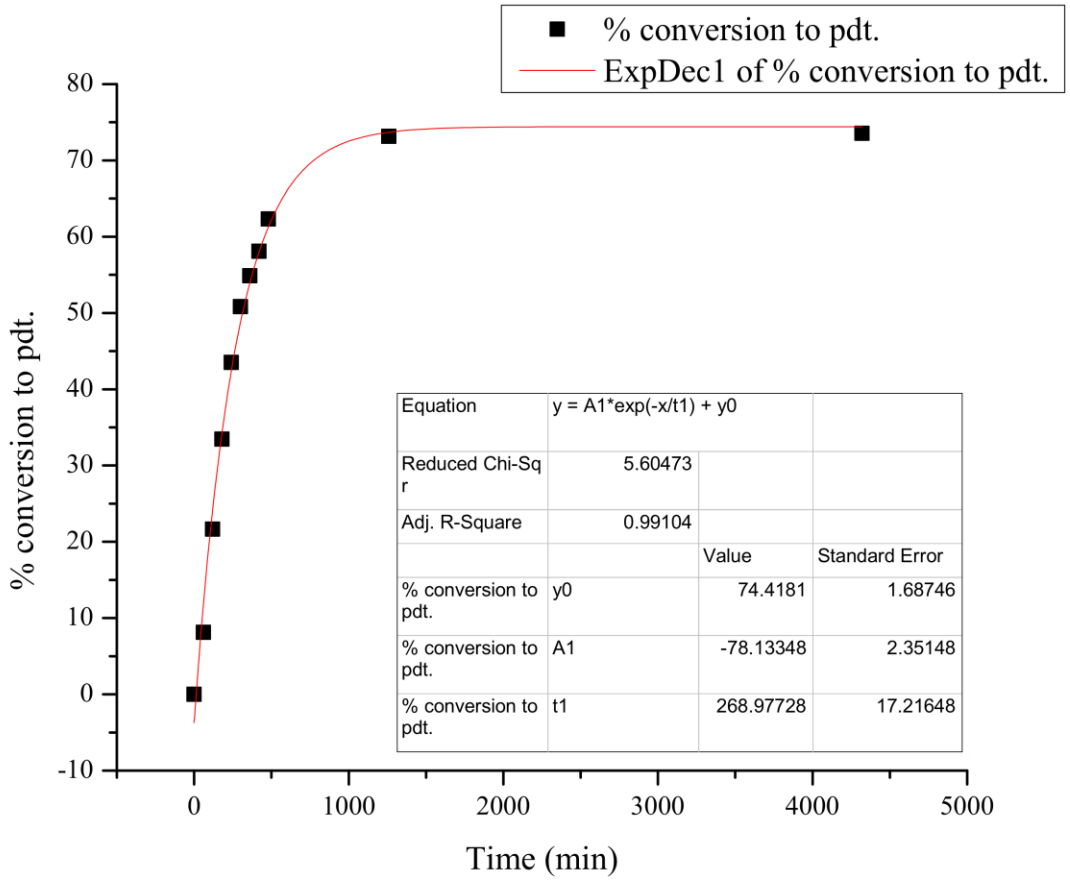

Half-Life = 313 min

Average Half-Life = 312 min

Kinetic Analyzses of Catalysts in Series C

Catalyst **1c**: Run 1

Time (min)	Standard (µmol)	Standard Area	Product Area	Product (µmol)	% Product
0	254.0	1.00	0.00	0.0	0.0
5	254.0	7229.86	157.52	6.6	1.9
15	254.0	7227.43	715.20	29.9	8.8
30	254.0	6995.94	1360.21	58.8	17.3
45	254.0	6953.89	1844.50	80.2	23.7
60	254.0	5980.81	2065.91	104.4	30.8
90	254.0	6568.27	2955.29	136.0	40.1
120	254.0	7866.16	4215.99	162.1	47.8
180	254.0	6561.58	4296.26	198.0	58.4
240	254.0	5995.08	4624.01	233.2	68.8
300	254.0	6436.51	5480.08	257.4	75.9
1044	254.0	6175.21	5432.38	266.0	78.5

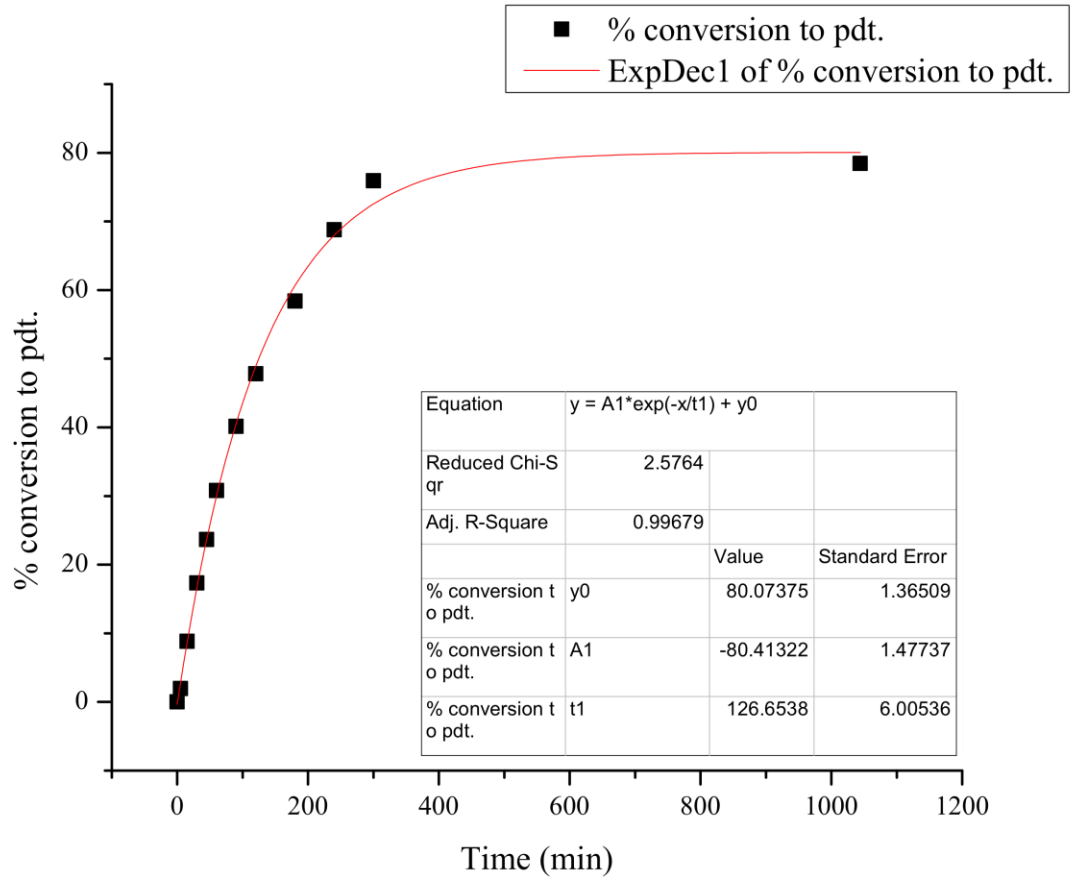

Half-Life = 125 min

Catalyst **1c**: Run 2

Time (min)	Standard (µmol)	Standard Area	Product Area	Product (µmol)	% Product
0	254.4	1.00	0.00	0.0	0.0
5	254.4	7566.30	462.68	18.5	5.5
10	254.4	6850.47	952.01	42.1	12.4
20	254.4	7288.12	2061.08	85.6	25.3
30	254.4	6502.60	2648.20	123.3	36.4
45	254.4	6975.58	3500.42	152.0	44.8
60	254.4	7321.79	4625.62	191.3	56.4
90	254.4	6842.20	5492.58	243.1	71.7
120	254.4	7374.77	5984.07	245.7	72.5
180	254.4	7073.91	5517.55	236.2	69.7
240	254.4	6882.90	6210.53	273.3	80.6
300	254.4	7013.31	5829.00	251.7	74.2
1020	254.4	7014.34	6614.44	285.6	84.2

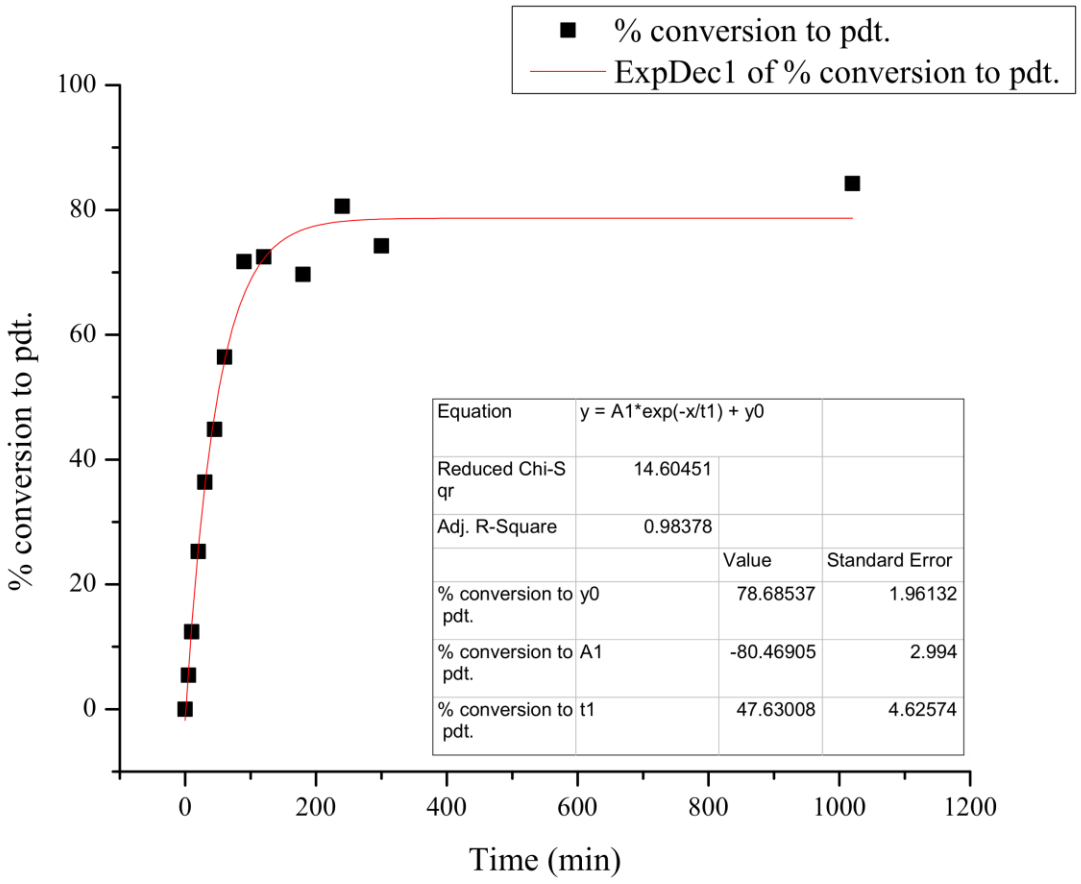

Half-Life = 49 min

Average Half = 87 min

Catalyst **2c**: Run 1

Time (min)	Standard (µmol)	Standard Area	Product Area	Product (µmol)	% Product
0	254.0	1.00	0.00	0.0	0.0
5	254.0	6948.18	1947.79	84.8	25.0
10	254.0	6930.96	2691.80	117.4	34.6
15	254.0	6307.47	3143.71	150.7	44.5
30	254.0	7164.98	4270.94	180.2	53.2
45	254.0	7140.67	5408.34	229.0	67.6
60	254.0	6757.77	5358.52	239.8	70.7
90	254.0	7322.81	5914.76	244.2	72.0
120	254.0	8230.17	6404.85	235.3	69.4
240	254.0	5617.81	4482.36	241.2	71.2
390	254.0	6697.65	5419.45	244.7	72.2

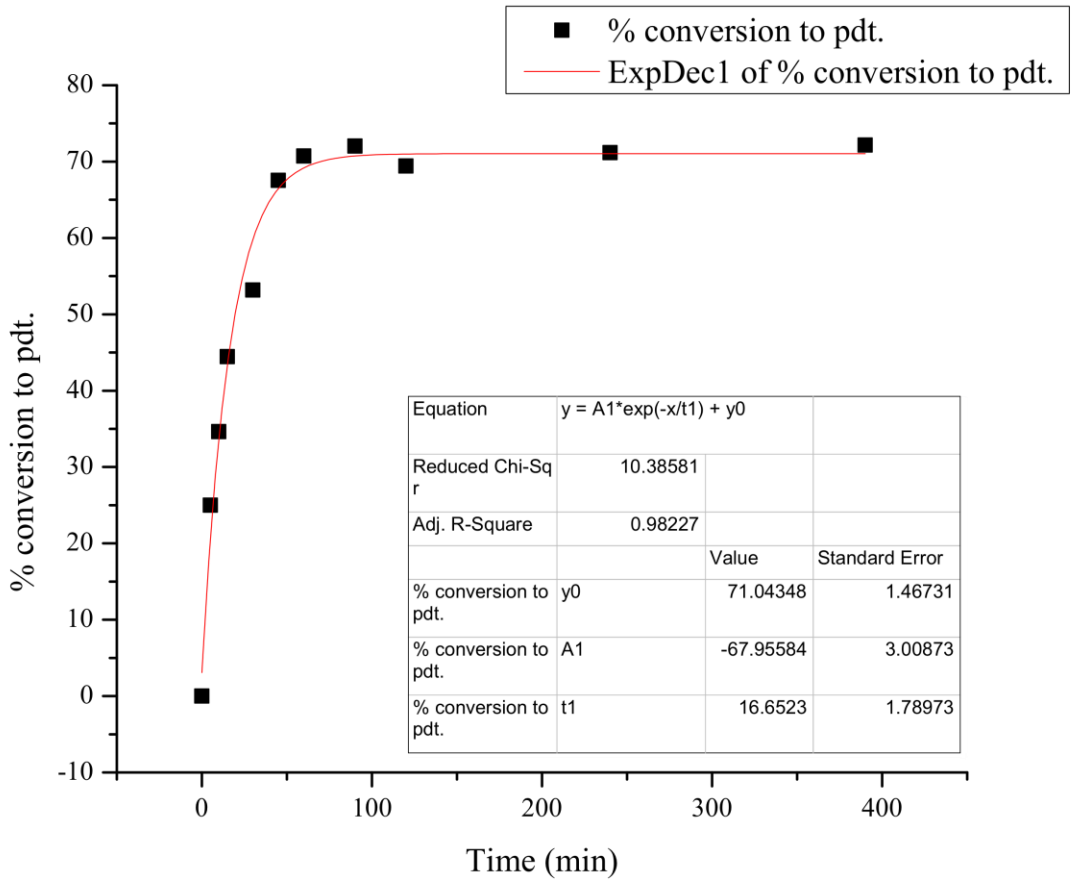

Half-Life = 20 min

Catalyst **2c**: Run 2

Time (min)	Standard (µmol)	Standard Area	Prodcut Area	Product (µmol)	% Product
0	254.0	1.00	0.00	0.0	0.0
5	254.0	6953.20	1845.14	80.2	23.7
10	254.0	6970.82	2801.66	121.5	35.8
15	254.0	6513.41	3364.79	156.2	46.1
30	254.0	5798.28	3899.58	203.4	60.0
45	254.0	6796.95	5018.23	223.2	65.9
60	254.0	7426.89	5575.46	227.0	67.0
90	254.0	6143.65	5050.34	248.6	73.3
120	254.0	7148.17	5951.79	251.8	74.3
180	254.0	7203.04	5868.43	246.3	72.7
240	254.0	6860.76	5555.94	244.9	72.2
390	254.0	6819.18	5583.45	247.6	73.0

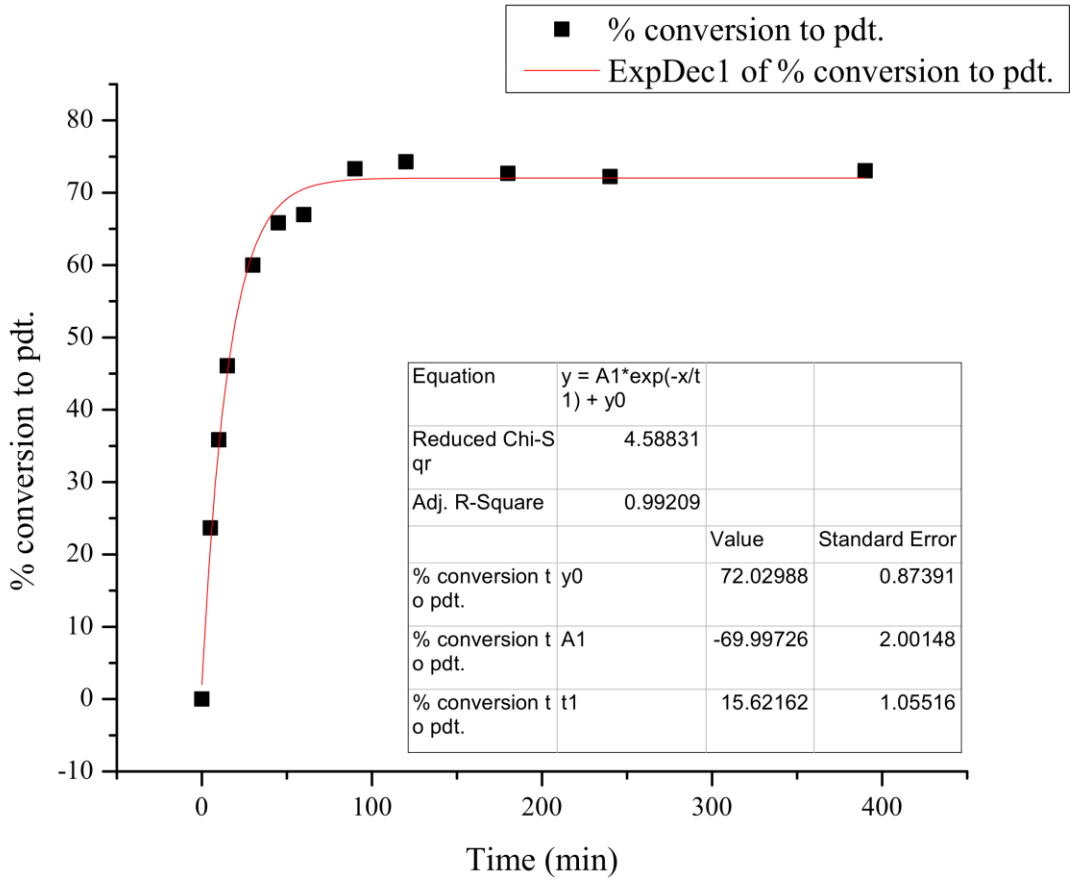

Half-Life = 18 min

Average Half-Life = 19 min

Catalyst **3c**: Run 1

Time (min)	Standard (µmol)	Standard Area	Product Area	Product (µmol)	% Product
0	254.0	1.00	0.00	0.0	0.0
5	254.0	6366.78	1987.10	94.4	27.8
10	254.0	7271.42	3898.83	162.1	47.8
15	254.0	6256.49	4213.33	203.6	60.1
30	254.0	7361.20	6309.61	259.2	76.5
45	254.0	6798.22	5649.22	251.3	74.1
60	254.0	6758.95	5936.93	265.6	78.3
90	254.0	6501.51	5679.15	264.1	77.9
120	254.0	7536.02	6606.41	265.1	78.2
180	254.0	6462.61	5706.41	267.0	78.8
240	254.0	7300.15	6235.80	258.3	76.2
390	254.0	6181.25	5085.59	248.8	73.4

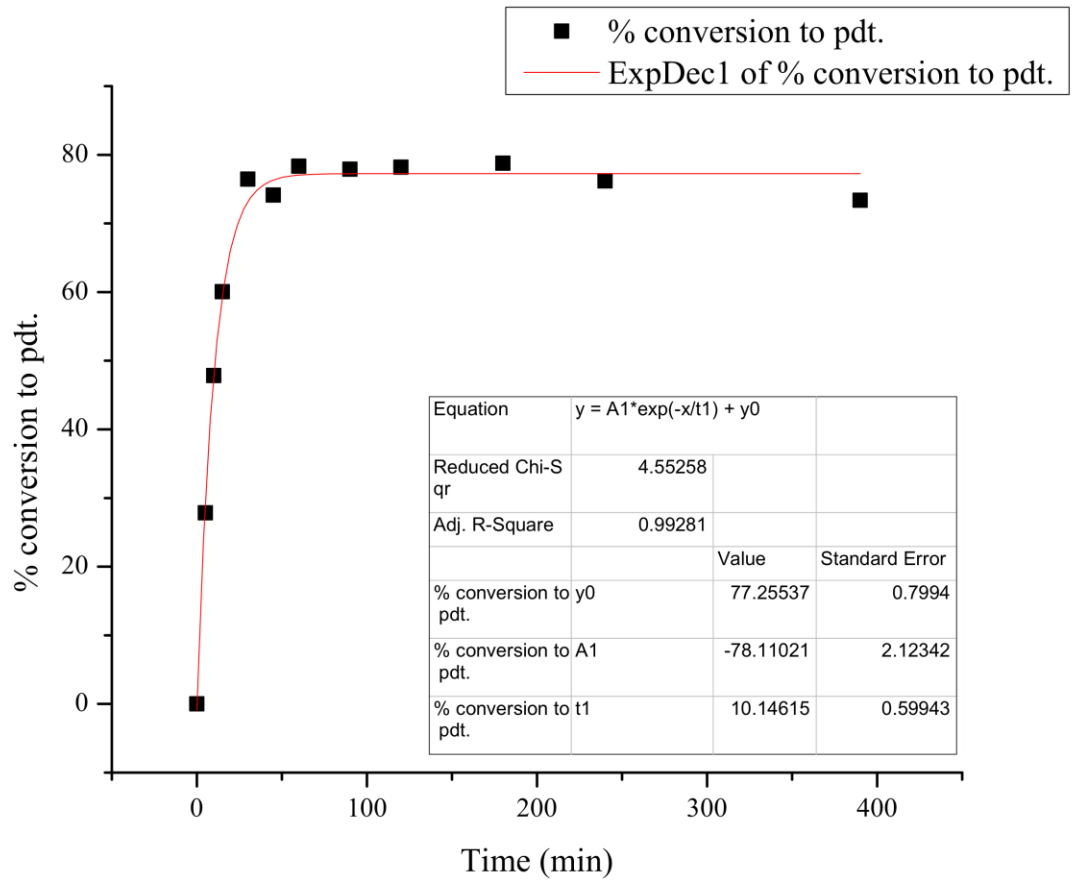

Half-Life = 11 min

Catalyst **3c**: Run 2

Time (min)	Standard (µmol)	Standard Area	Product Area	Product (µmol)	% Product
0	254.0	1.00	0.00	0.0	0.0
5	254.0	6497.60	2556.45	119.0	35.1
10	254.0	6409.23	3971.14	187.3	55.3
15	254.0	6714.73	5077.76	228.6	67.4
30	254.0	6316.60	5565.02	266.4	78.6
45	254.0	7164.22	6347.19	267.9	79.0
60	254.0	7023.72	6111.76	263.1	77.6
90	254.0	6812.49	6027.83	267.5	78.9
120	254.0	6956.38	6147.80	267.2	78.8
180	254.0	7296.56	6422.69	266.1	78.5
240	254.0	6965.82	6136.37	266.4	78.6
390	254.0	6369.80	5385.45	255.6	75.4

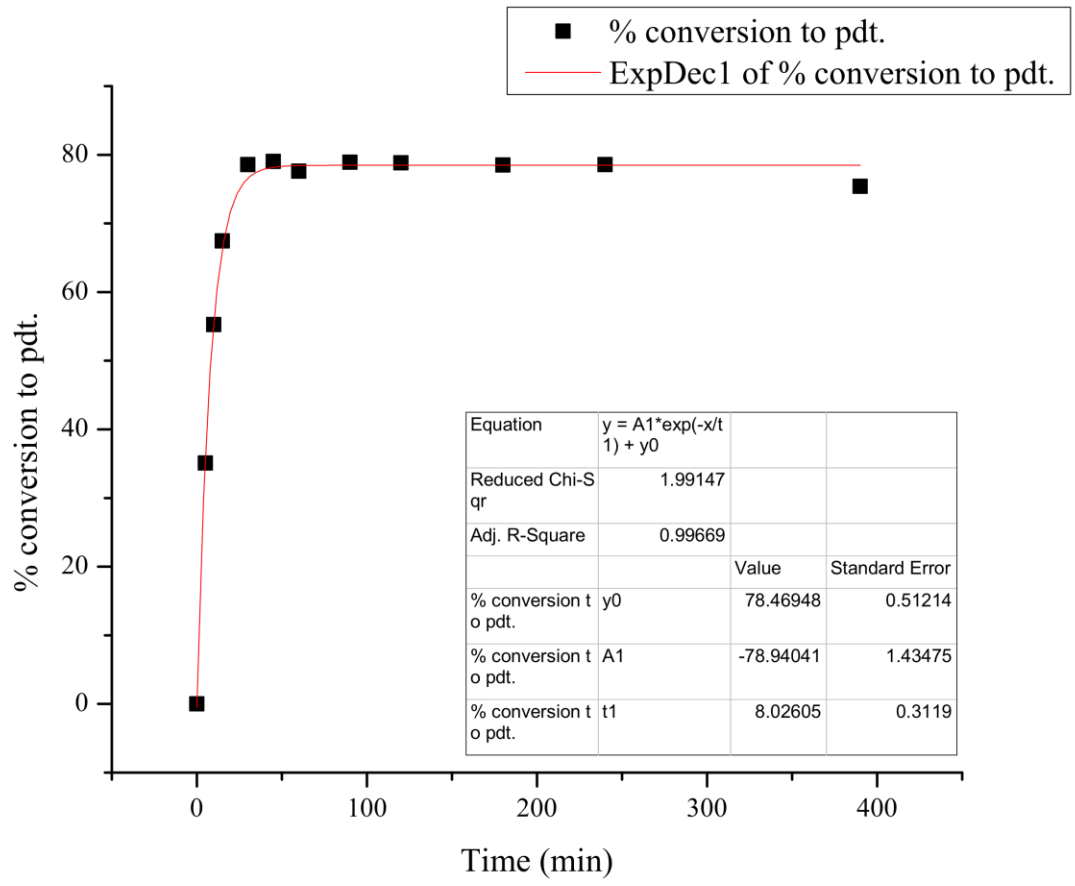

Half-Life = 8 min

Average Half-Life = 9 min

Catalyst **4c**: Run 1

Time (min)	Standard (µmol)	Standard Area	Product Area	Product (µmol)	% Product
0	254.4	1.00	0.00	0.0	0.0
30	254.4	7863.59	474.71	18.3	5.4
60	254.4	7367.71	840.71	34.6	10.2
120	254.4	7404.97	1189.20	48.6	14.3
180	254.4	7649.45	1421.59	56.3	16.6
240	254.4	6730.51	1595.53	71.8	21.2
300	254.4	7201.13	1955.34	82.2	24.3
360	254.4	8112.84	2425.10	90.5	26.7
420	254.4	7489.21	2506.72	101.4	29.9
1096	254.4	7413.32	4588.50	187.4	55.3
1463	254.4	6053.13	4300.86	215.2	63.5
2546	254.4	6367.19	5077.05	241.5	71.2

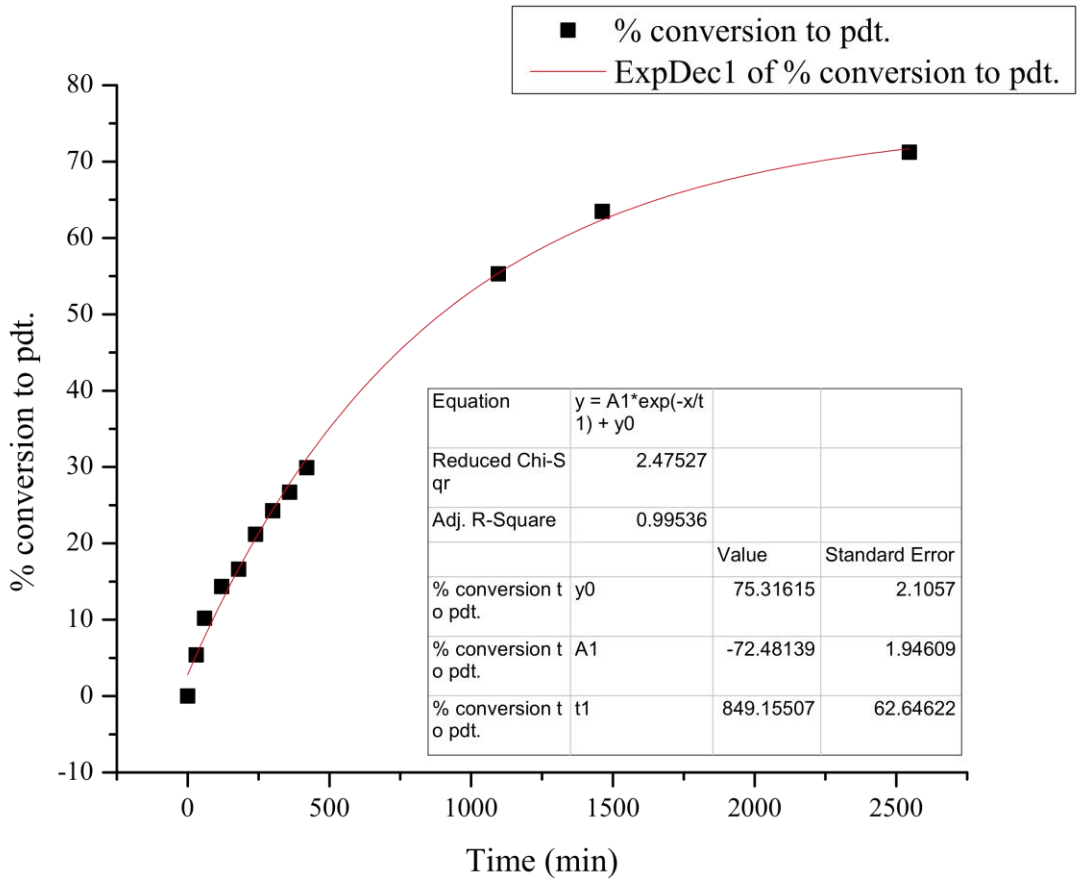

Half-Life = 893 min

Catalyst **4c**: Run 2

Time (min)	Standard (umol)	Standard Area	Product Area	Product (umol)	% Product
0	254.4	1.00	0.00	0.0	0.0
30	254.4	10788.78	814.29	22.9	6.7
61	254.4	7527.68	843.86	33.9	10.0
120	254.4	7031.33	1206.67	52.0	15.3
180	254.4	8256.95	1782.66	65.4	19.3
240	254.4	7013.87	1877.42	81.1	23.9
300	254.4	8866.15	2744.85	93.8	27.7
360	254.4	7546.60	2610.97	104.8	30.9
420	254.4	7389.24	2834.78	116.2	34.3
480	254.4	7238.21	2989.89	125.1	36.9
540	254.4	7519.02	3385.00	136.3	40.2
600	254.4	8010.17	3787.29	143.2	42.2
1320	254.4	7710.55	5073.11	199.3	58.8
1860	254.4	7707.93	5663.60	222.5	65.6
2760	254.4	7732.30	6165.50	241.5	71.2

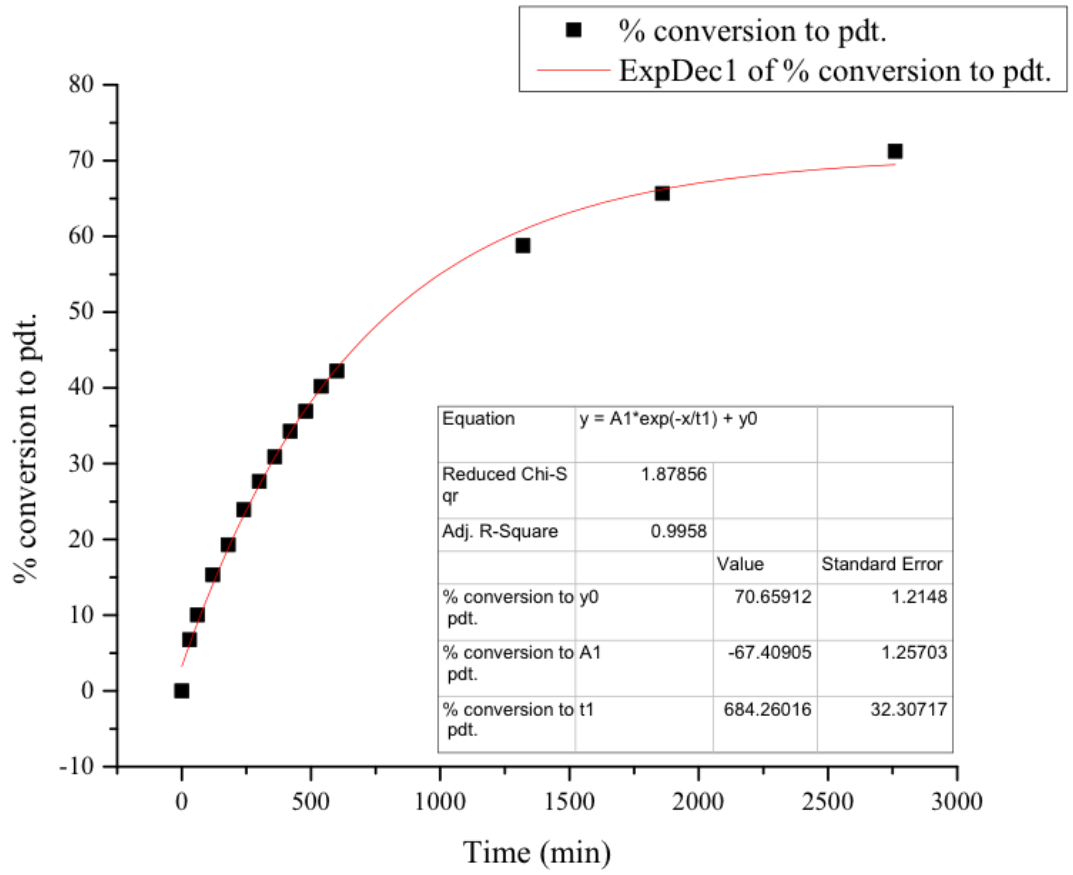

Half-Life = 809 min

Average Half-Life = 851 min

Catalyst **5c**: Run 1

Time (min)	Standard (µmol)	Standard Area	Product Area	Product (µmol)	% Product
0	254.0	1.00	0.00	0.0	0.0
60	254.0	6368.39	629.97	29.9	8.8
120	254.0	8045.95	1132.05	42.5	12.5
180	254.0	8135.70	1627.98	60.5	17.8
240	254.0	7363.66	2208.14	90.7	26.7
300	254.0	8024.54	3125.56	117.8	34.7
360	254.0	7958.76	3637.38	138.2	40.8
420	254.0	7431.97	3903.86	158.8	46.9
480	254.0	7875.20	4543.85	174.5	51.5
1260	254.0	8115.78	5868.77	218.6	64.5
4320	254.0	7319.30	4992.20	206.2	60.8

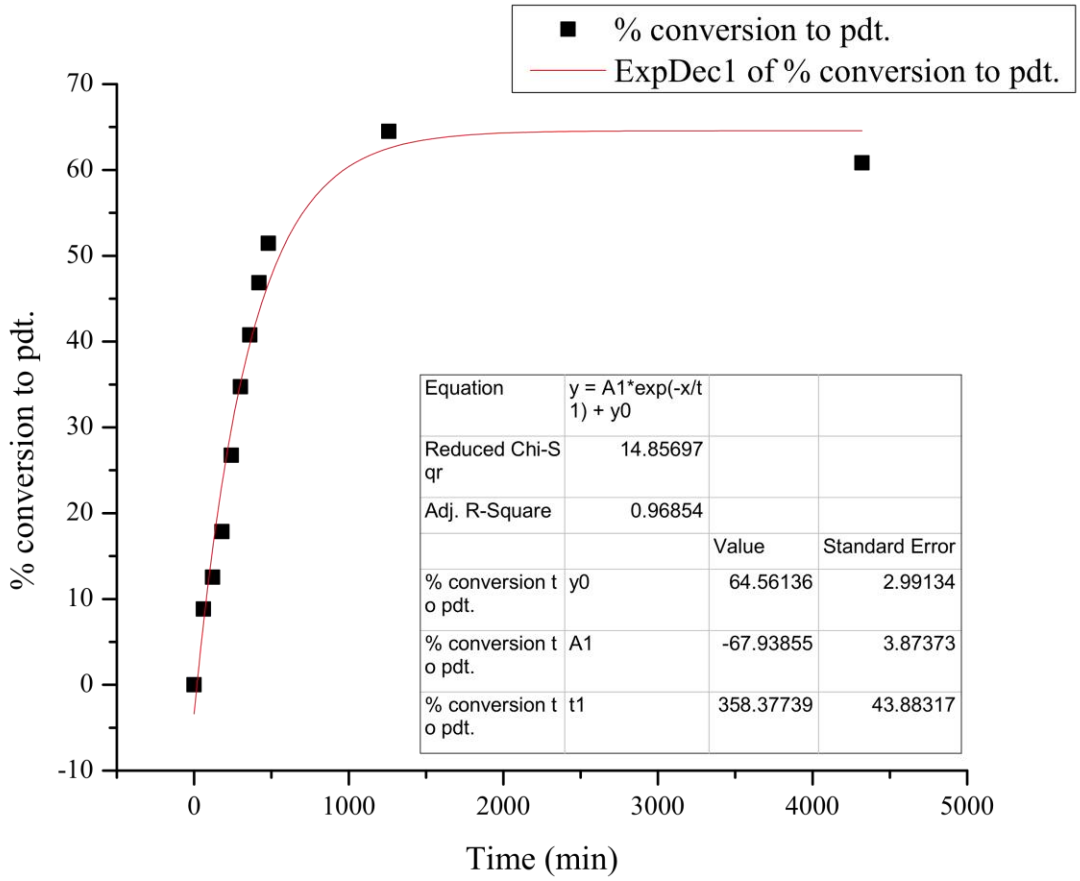

Half-Life = 552 min

Catalyst **5c**: Run 2

Time (min)	Standard (µmol)	Standard Area	Product Area	Product (µmol)	% Product
0	254.4	1.00	0.00	0.0	0.0
30	254.4	7941.61	824.43	31.4	9.3
60	254.4	7515.06	1058.79	42.7	12.6
90	254.4	7593.52	1051.55	41.9	12.4
120	254.4	7550.88	1271.89	51.0	15.0
180	254.4	7588.20	1711.40	68.3	20.1
240	254.4	7637.43	2287.61	90.7	26.8
300	254.4	7619.27	2586.18	102.8	30.3
360	254.4	8407.72	3149.90	113.5	33.5
420	254.4	7873.94	3838.21	147.6	43.5
480	254.4	8463.36	4825.66	172.7	50.9
1153	254.4	8061.29	5340.12	200.6	59.2
1478	254.4	7598.65	5239.92	208.8	61.6

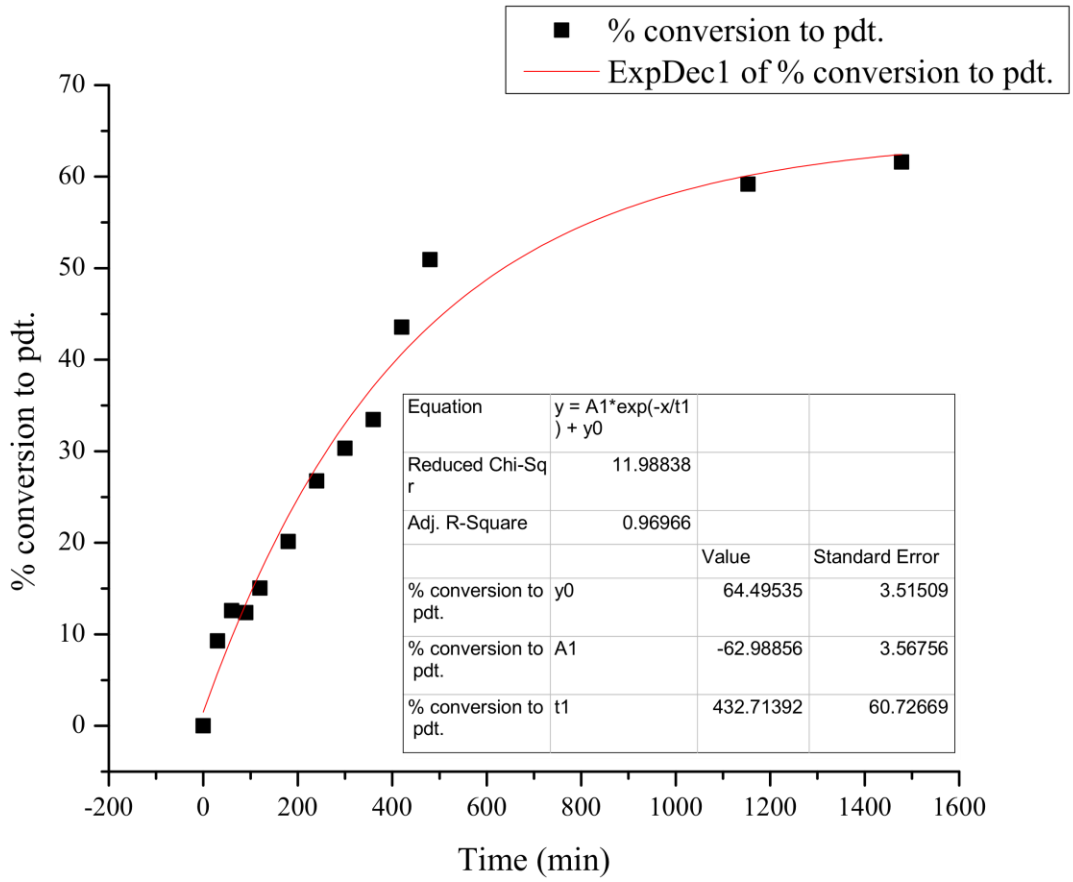

Half-Life = 636 min

Average Half-Life = 594 min

Kinetic Analyzses of Catalysts in Series D

Catalyst **1d**: Run 1

Time (min)	Standard (µmol)	Standard Area	Product Area	Product (µmol)	% Product
0	254.0	1.00	0.00	0.0	0.0
30	254.0	5406.24	1359.20	76.0	22.4
60	254.0	5597.67	2322.44	125.4	37.0
90	254.0	6022.80	3061.08	153.7	45.3
120	254.0	5849.00	3388.52	175.2	51.7
150	254.0	6356.35	4236.60	201.5	59.4
180	254.0	6318.85	4449.16	212.9	62.8
210	254.0	7329.06	5406.82	223.1	65.8
240	254.0	7373.65	5588.14	229.1	67.6
270	254.0	6735.73	5379.98	241.5	71.2
300	254.0	7544.71	6096.67	244.3	72.1

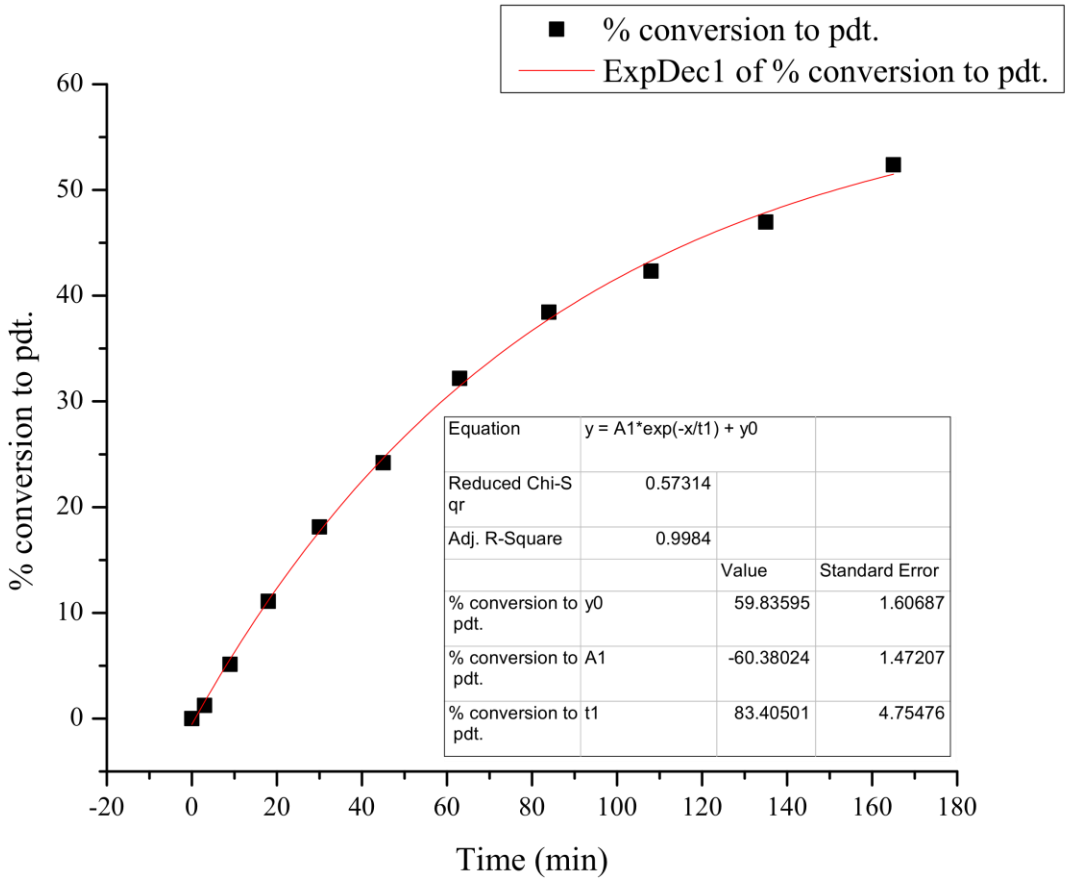

Half-Life = 151 min

Catalyst **1d**: Run 2

Time (min)	Standard (µmol)	Standard Area	Product Area	Product (µmol)	% Product
0	254.0	1.00	0.00	0.0	0.0
3	254.0	7510.25	152.92	6.2	1.8
9	254.0	7171.84	633.84	26.7	7.9
18	254.0	6894.65	1217.50	53.4	15.8
30	254.0	7108.05	1922.28	81.8	24.1
45	254.0	6914.86	2451.89	107.2	31.6
63	254.0	6219.46	2806.25	136.4	40.2
84	254.0	7238.37	3738.36	156.2	46.1
108	254.0	7818.04	4546.39	175.8	51.9
135	254.0	7537.11	4559.36	182.9	54.0
165	254.0	6789.20	4447.95	198.1	58.4

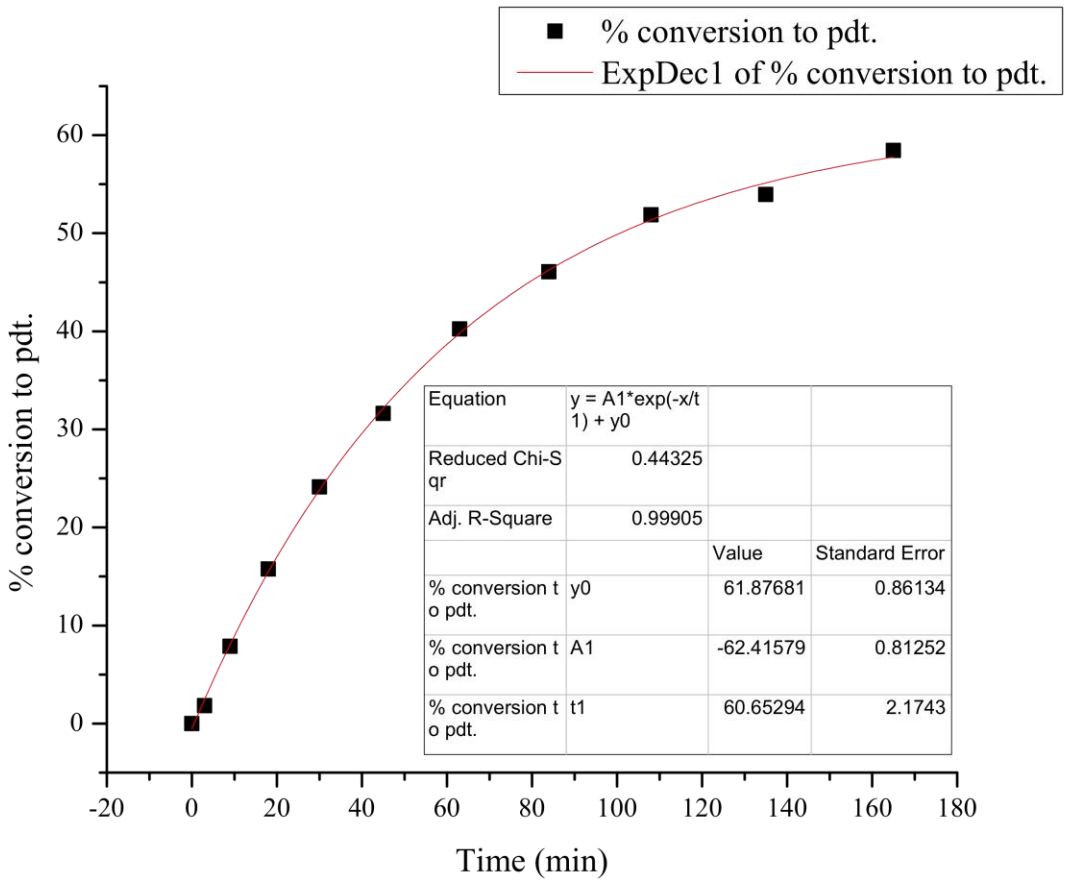

Half-Life = 101 min

Average Half-Life = 126 min

Catalyst **2d**: Run 1

Time (min)	Standard (µmol)	Standard Area	Product Area	Product (µmol)	% Product
0	254.0	1.00	0.00	0.00	0.00
3	254.0	7452.19	1874.83	76.07	22.44
6	254.0	6532.27	2598.15	120.26	35.48
9	254.0	7411.18	3663.17	149.45	44.09
12	254.0	6859.63	4003.37	176.46	52.05
15	254.0	7120.64	4338.85	184.24	54.35
18	254.0	7146.26	4860.47	205.65	60.66
21	254.0	6564.03	4590.67	211.46	62.38
24	254.0	6910.47	5137.96	224.81	66.31
27	254.0	6548.18	5147.46	237.68	70.11
30	254.0	6246.98	5100.82	246.89	72.83
60	254.0	6088.17	5485.47	272.43	80.36
90	254.0	6532.30	5906.09	273.38	80.64

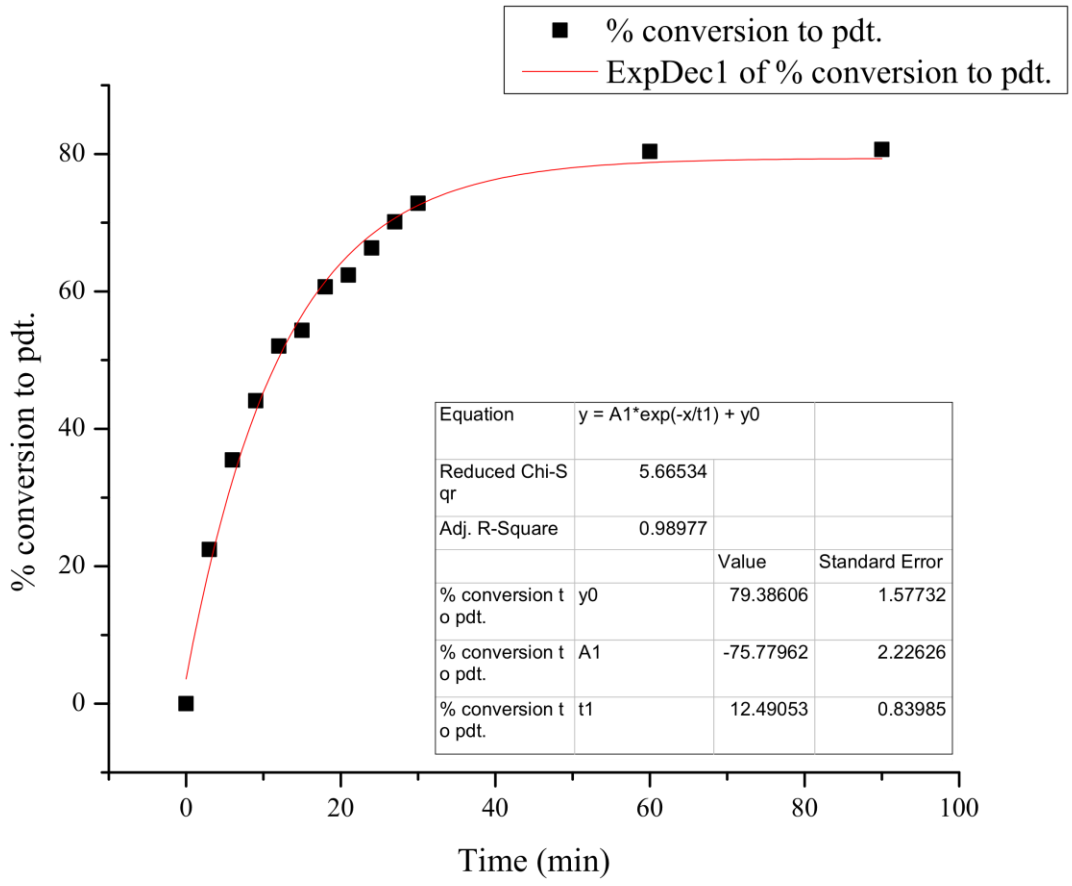

Half-Life = 12 min

Catalyst **2d**: Run 2

Time (min)	Standard (µmol)	Standard Area	Product Area	Product (µmol)	% Product
0	254.0	1.00	0.00	0.0	0.0
2	254.0	6657.24	1299.59	59.0	14.8
4	254.0	6625.67	1886.22	86.1	21.6
6	254.0	6654.65	2261.85	102.8	25.8
8	254.0	5937.63	2420.91	123.3	30.9
10	254.0	5945.19	2667.42	135.7	34.0
15	254.0	7215.81	4097.74	171.7	43.0
30	254.0	6335.24	4894.49	233.6	58.5
45	254.0	6563.80	5590.47	257.5	64.5
60	254.0	6914.90	6391.83	279.5	70.0
90	254.0	6598.44	6016.79	275.7	69.1

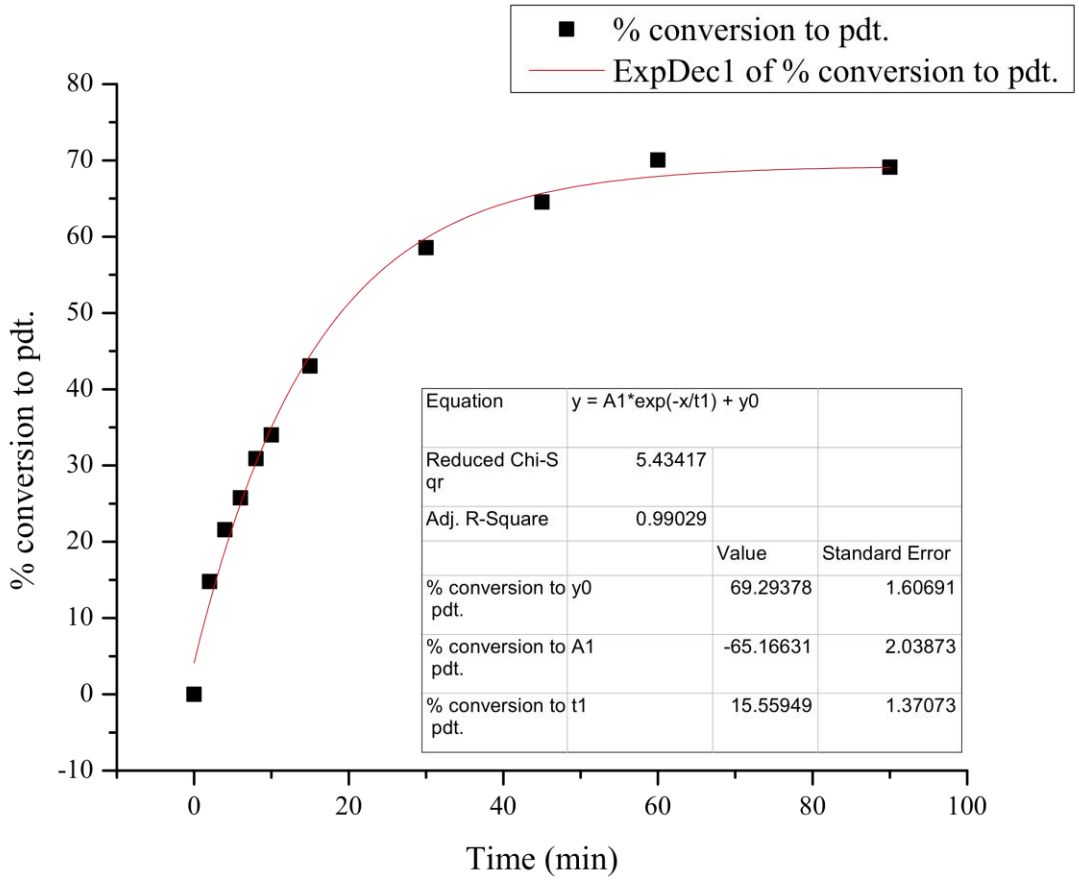

Half-Life = 19 min

Average Half-Life = 15 min

Catalyst **3d**: Run 1

Time (min)	Standard (µmol)	Standard Area	Product Area	Product (µmol)	% Product
0	254.0	1.00	0.00	0.0	0.0
6	254.0	6734.66	2362.89	106.1	31.3
12	254.0	6056.31	2956.87	147.6	43.5
18	254.0	6426.49	4178.60	196.6	58.0
24	254.0	6750.96	4853.43	217.4	64.1
30	254.0	6287.08	5133.21	246.9	72.8
36	254.0	6644.98	5394.88	245.5	72.4
42	254.0	7858.06	6203.65	238.7	70.4
48	254.0	6605.05	5815.88	266.2	78.5
54	254.0	6342.74	5657.64	269.7	79.6
60	254.0	6043.27	5389.82	269.7	79.5

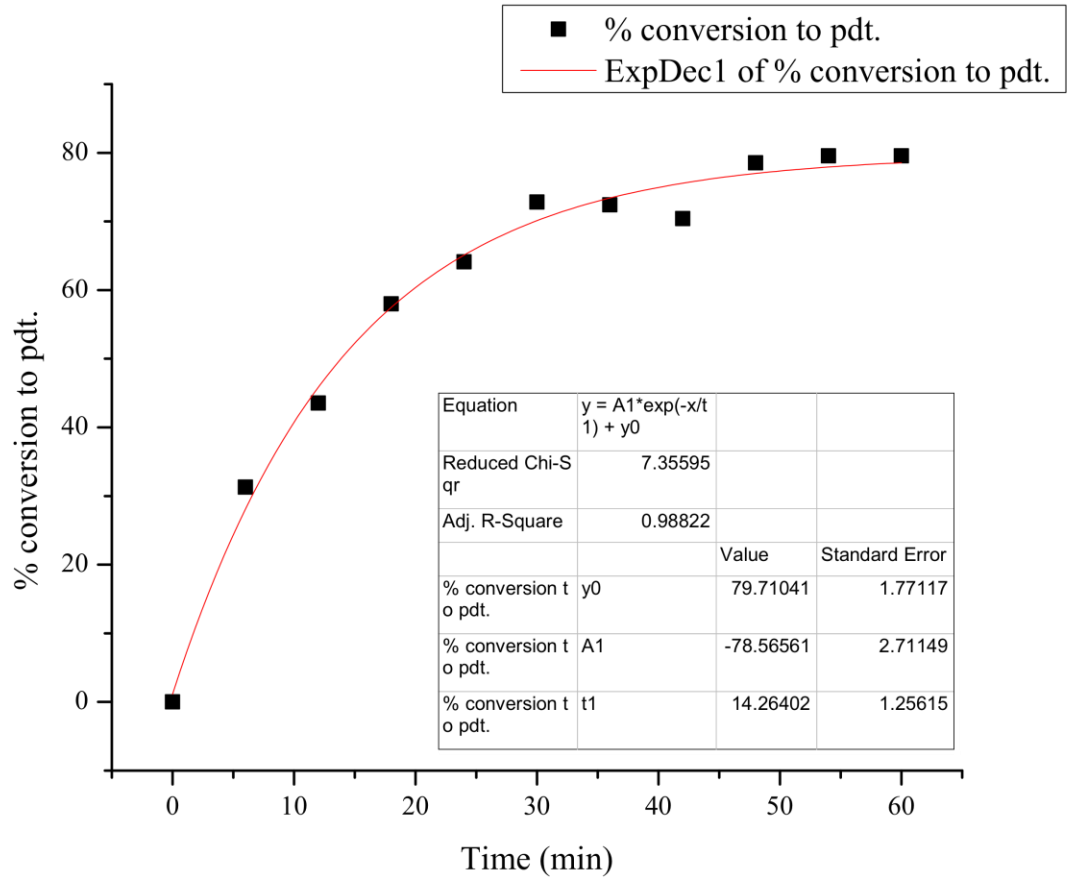

Half-Life = 14 min

Catalyst **3d**: Run 2

Time (min)	Standard (µmol)	Standard Area	Product Area	Product (µmol)	% Product
0	254.0	1.00	0.00	0.0	0.0
3	254.0	6489.00	1653.27	77.0	22.7
9	254.0	5305.57	3070.89	175.0	51.6
18	254.0	6664.46	5076.20	230.3	67.9
30	254.0	6245.48	4917.91	238.1	70.2
45	254.0	6719.35	5513.31	248.1	73.2
63	254.0	6735.43	5660.49	254.1	75.0
84	254.0	7491.39	5979.50	241.3	71.2
108	254.0	6943.75	5782.35	251.8	74.3
135	254.0	7099.50	5840.60	248.7	73.4
165	254.0	7991.96	6587.32	249.2	73.5

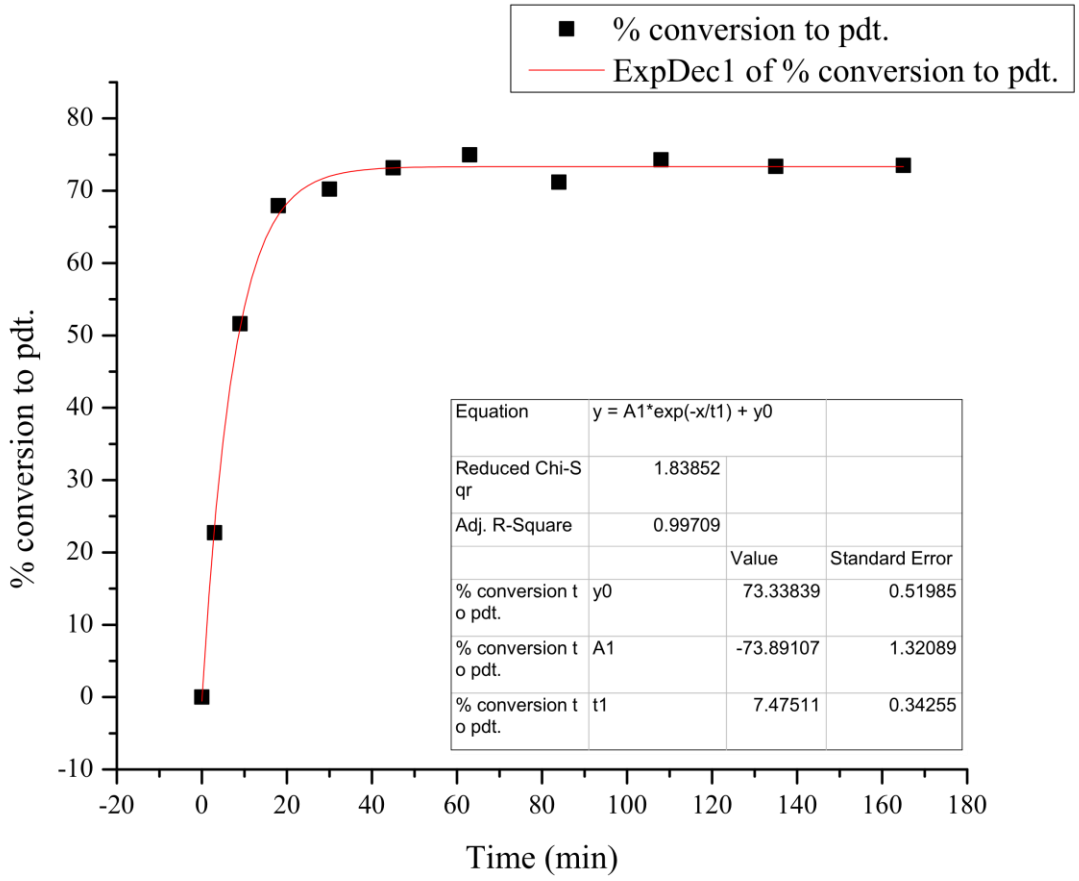

Half-Life = 9 min

Average Half-Life = 11 min

Catalyst **4d**: Run 1

Time (min)	Standard (µmol)	Standard Area	Product Area	Product (µmol)	% Product
0	254.0	1.00	0.00	0.0	0.0
60	254.0	6546.90	774.40	35.8	10.6
120	254.0	7212.06	1150.39	48.2	14.2
180	254.0	7857.01	1744.91	67.1	19.8
240	254.0	7190.91	2047.66	86.1	25.4
300	254.0	8232.91	2921.40	107.3	31.6
360	254.0	7411.91	3252.86	132.7	39.1
420	254.0	7772.49	3857.10	150.0	44.3
480	254.0	7283.47	4225.35	175.4	51.7
540	254.0	7539.71	4745.14	190.3	56.1
600	254.0	7667.28	5138.08	202.6	59.8
1440	254.0	6692.90	5291.19	239.0	70.5

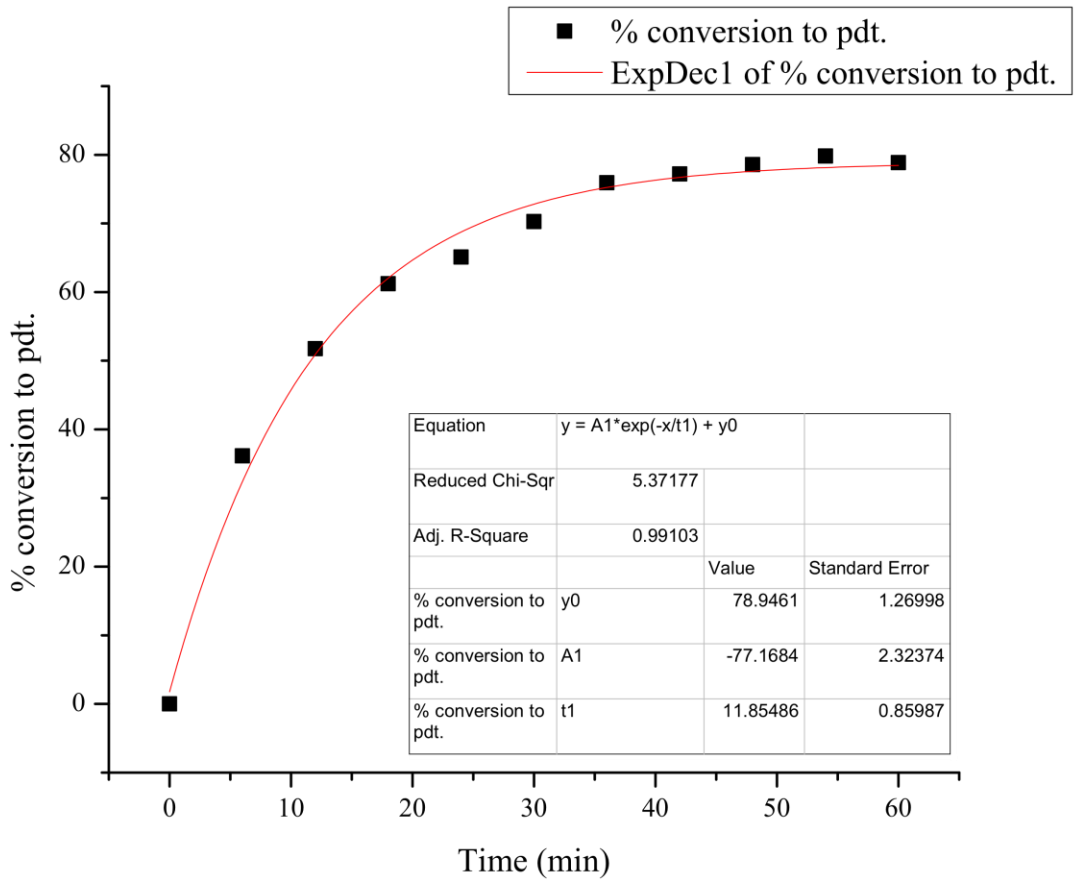

Half-Life = 12 min

Catalyst **4d**: Run 2

Time (min)	Standard (µmol)	Standard Area	Product Area	Product (µmol)	% Product
0	254.4	1.00	0.00	0.0	0.0
30	254.4	7838.54	638.49	24.7	7.3
60	254.4	7546.78	975.79	39.2	11.6
90	254.4	7084.29	1143.68	48.9	14.4
120	254.4	7580.74	1380.32	55.1	16.3
180	254.4	7560.03	1557.28	62.4	18.4
240	254.4	8045.52	2350.86	88.5	26.1
300	254.4	7200.37	2371.19	99.7	29.4
480	254.4	8617.36	4650.85	163.4	48.2
1153	254.4	5196.10	4010.78	233.8	69.0
1478	254.4	7756.88	6064.77	236.8	69.8

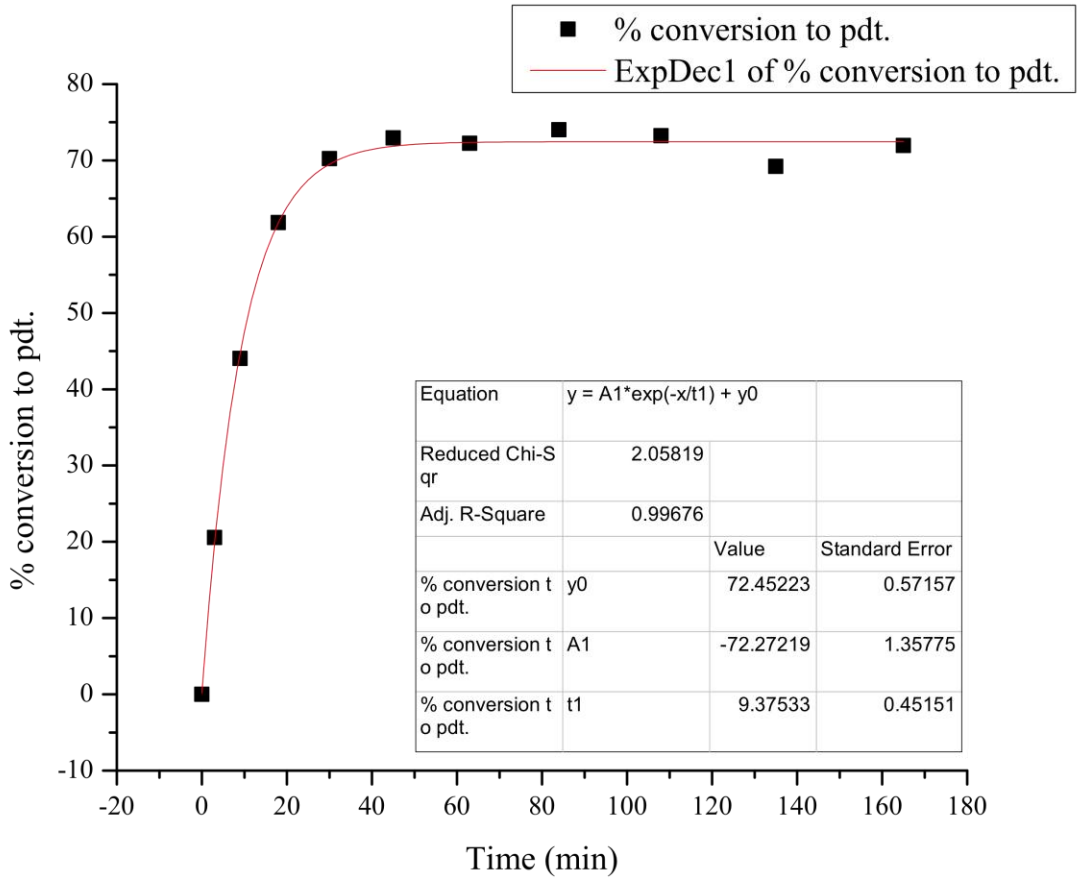

Half-Life = 11 min

Average Half-Life = 11 min

Catalyst **5d**: Run 1

Time (min)	Standard (µmol)	Standard Area	Product Area	Product (µmol)	% Product
0	254.0	1.00	0.00	0.0	0.0
60	254.0	6546.90	774.40	35.8	10.6
120	254.0	7212.06	1150.39	48.2	14.2
180	254.0	7857.01	1744.91	67.1	19.8
240	254.0	7190.91	2047.66	86.1	25.4
300	254.0	8232.91	2921.40	107.3	31.6
360	254.0	7411.91	3252.86	132.7	39.1
420	254.0	7772.49	3857.10	150.0	44.3
480	254.0	7283.47	4225.35	175.4	51.7
540	254.0	7539.71	4745.14	190.3	56.1
600	254.0	7667.28	5138.08	202.6	59.8
1440	254.0	6692.90	5291.19	239.0	70.5

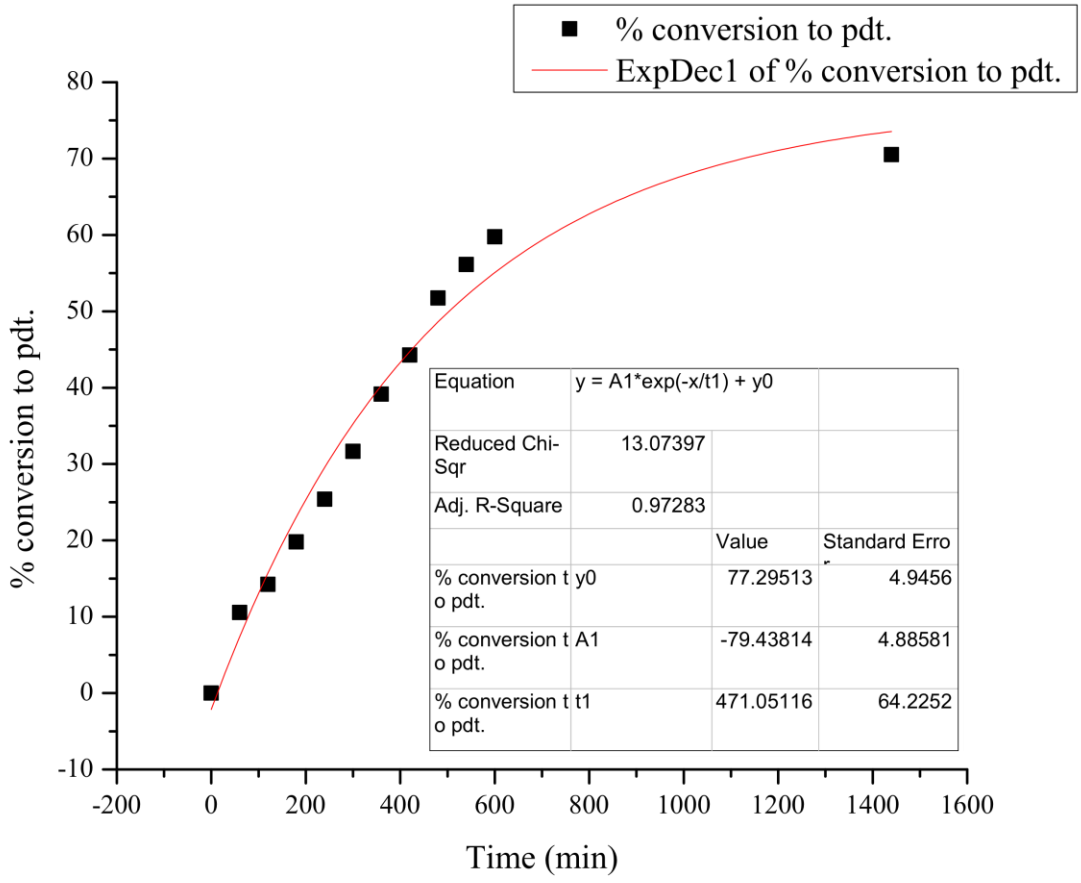

Half-Life = 503 min

Catalyst **5d**: Run 2

Time (min)	Standard (µmol)	Standard Area	Product Area	Product (µmol)	% Product
0	254.4	1.00	0.00	0.0	0.0
30	254.4	7838.54	638.49	24.7	7.3
60	254.4	7546.78	975.79	39.2	11.6
90	254.4	7084.29	1143.68	48.9	14.4
120	254.4	7580.74	1380.32	55.1	16.3
180	254.4	7560.03	1557.28	62.4	18.4
240	254.4	8045.52	2350.86	88.5	26.1
300	254.4	7200.37	2371.19	99.7	29.4
480	254.4	8617.36	4650.85	163.4	48.2
1153	254.4	5196.10	4010.78	233.8	69.0
1478	254.4	7756.88	6064.77	236.8	69.8

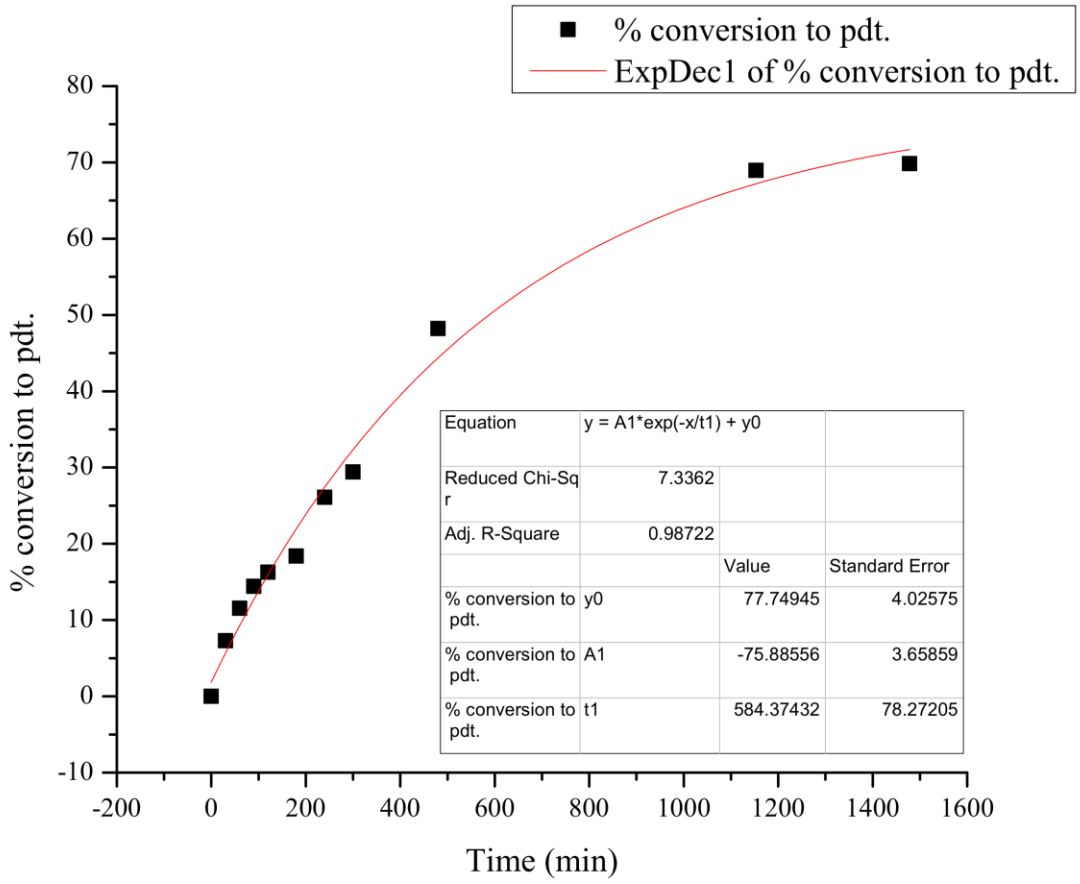

Half-Life = 588 min

Average Half-Life = 546 min

Kinetic Analyzses of Catalysts in Series E

Catalyst **1e**: Run 1

Time (min)	Standard (µmol)	Standard Area	Product Area	Product (µmol)	% Product
0	254.0	1.00	0.00	0.0	0.0
3	254.0	6882.99	828.49	36.4	10.7
9	254.0	8570.29	2953.49	104.2	30.7
18	254.0	5777.19	2847.38	149.0	44.0
30	254.0	7714.14	4008.40	157.1	46.3
45	254.0	6368.22	4712.73	223.8	66.0
63	254.0	6953.42	5236.57	227.7	67.2
84	254.0	7315.55	6023.74	249.0	73.4
108	254.0	6751.74	5595.77	250.6	73.9
135	254.0	6672.18	5583.20	253.0	74.6
165	254.0	6291.08	5132.58	246.7	72.8

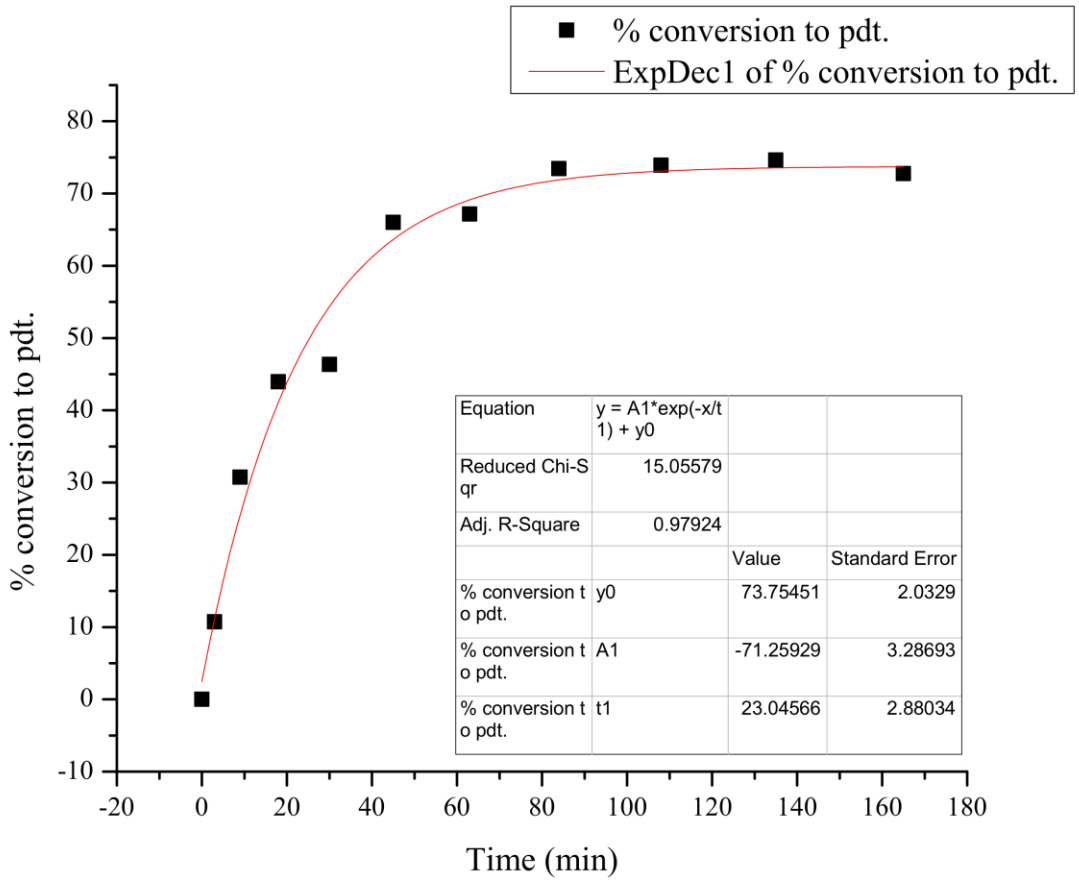

Half-Life = 25 min

Catalyst **1e**: Run 2

Time (min)	Standard (µmol)	Standard Area	Product Area	Product (µmol)	% Product
0	254.0	1.00	0.00	0.0	0.0
3	254.0	7234.79	1084.52	45.3	13.4
9	254.0	6823.99	3065.34	135.8	40.1
18	254.0	6804.85	4217.07	187.4	55.3
30	254.0	6794.97	5397.66	240.2	70.9
45	254.0	7175.81	5900.93	248.6	73.3
63	254.0	7830.53	6754.11	260.8	76.9
84	254.0	7106.46	5837.28	248.4	73.3
108	254.0	7390.44	6250.08	255.7	75.4
135	254.0	7153.57	5922.00	250.3	73.8
165	254.0	7339.00	6055.46	249.5	73.6

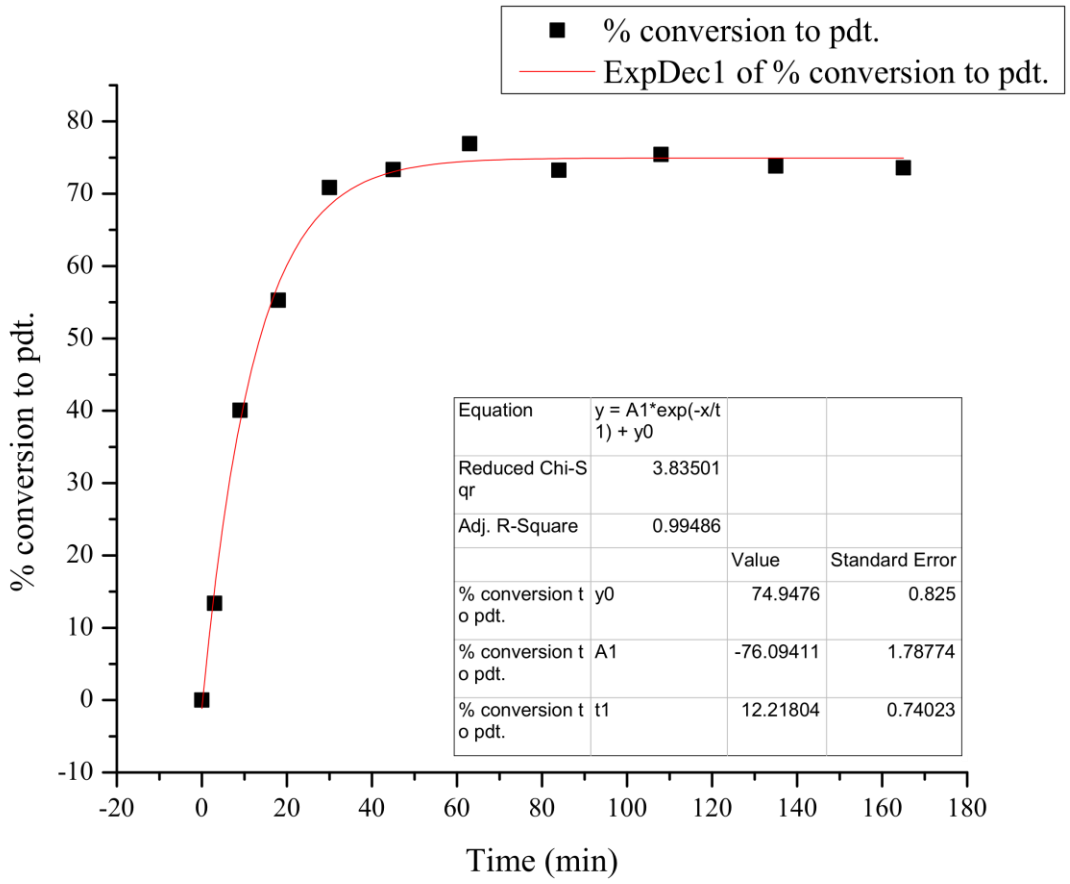

Half-Life = 14 min

Average Half-Life = 19 min

Catalyst **2e**: Run 1

Time (min)	Standard (µmol)	Standard Area	Product Area	Product (µmol)	% Product
0	254.0	1.00	0.00	0.0	0.0
3	254.0	6239.34	1004.37	48.7	14.4
9	254.0	5956.21	1963.61	99.7	29.4
18	254.0	6389.58	3242.29	153.4	45.3
30	254.0	6714.18	4574.33	206.0	60.8
45	254.0	6706.44	5554.85	250.4	73.9
63	254.0	7280.79	6275.59	260.6	76.9
84	254.0	6529.20	5428.99	251.4	74.2
108	254.0	7678.27	6514.85	256.5	75.7
135	254.0	7619.53	6361.20	252.4	74.5
165	254.0	7499.82	6115.74	246.6	72.7

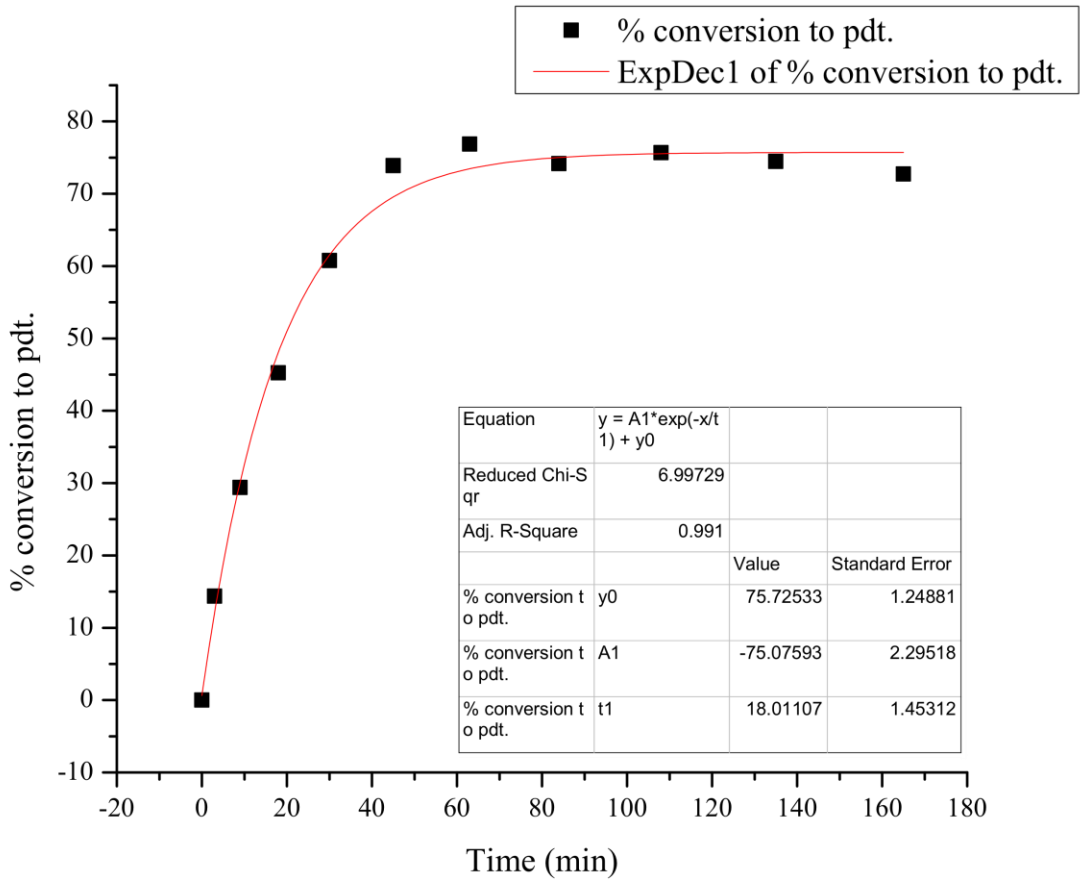

Half-Life = 19 min

Catalyst **2e**: Run 2

Time (min)	Standard (µmol)	Standard Area	Product Area	Product (µmol)	% Product
0	254.0	1.00	0.00	0.0	0.0
3	254.0	7412.62	1650.78	67.3	19.9
9	254.0	6779.88	2923.76	130.4	38.5
18	254.0	7300.21	4759.80	197.1	58.2
30	254.0	7593.24	5761.56	229.4	67.7
45	254.0	7793.95	6227.00	241.6	71.3
63	254.0	8408.63	6764.48	243.2	71.8
84	254.0	8153.02	6578.51	244.0	72.0
108	254.0	7526.92	6135.04	246.4	72.7
135	254.0	7776.50	6397.54	248.7	73.4
165	254.0	8493.77	6966.35	248.0	73.2

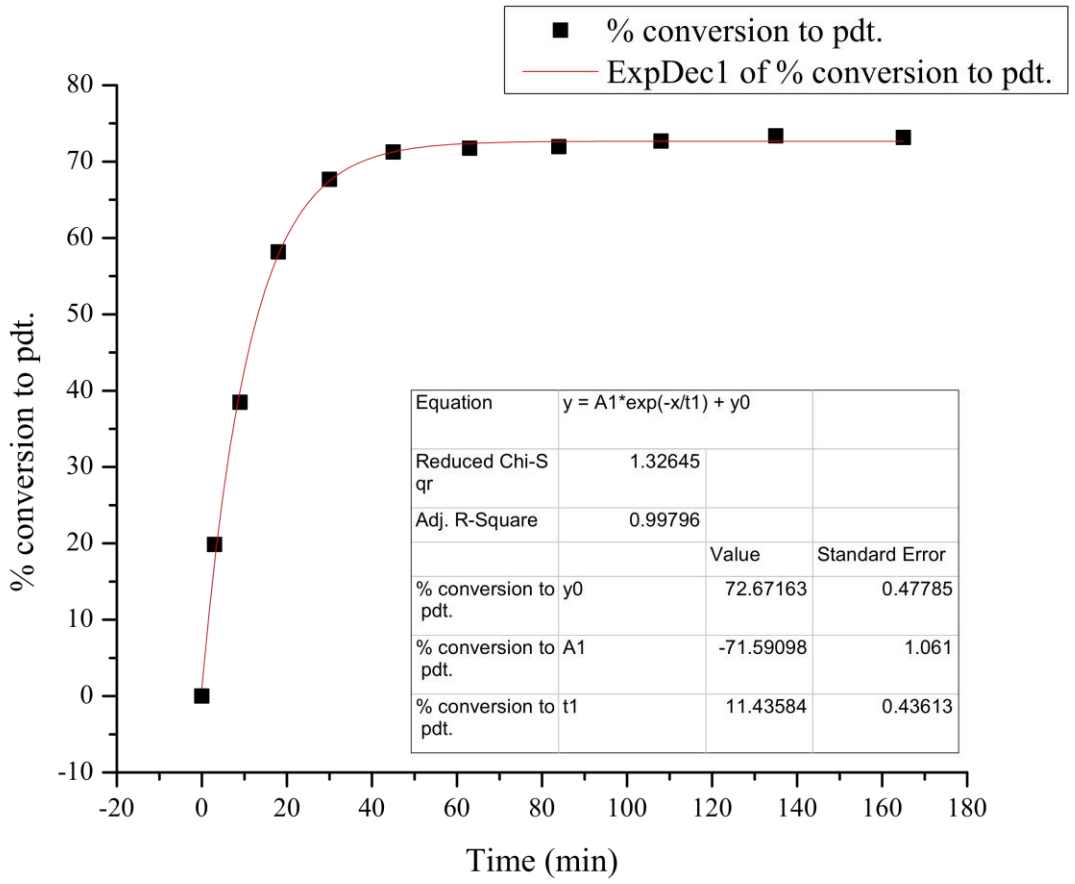

Half-Life = 13 min

Average Half-Life = 16 min

Catalyst **3e**: Run 1

Time (min)	Standard (µmol)	Standard Area	Product Area	Product (µmol)	% Product
0	254.0	1.00	0.00	0.0	0.0
3	254.0	6120.53	404.98	20.0	5.9
9	254.0	6216.99	1002.48	48.8	14.4
18	254.0	6722.38	1963.40	88.3	26.1
30	254.0	6362.14	2626.00	124.8	36.8
45	254.0	6585.24	3349.33	153.8	45.4
63	254.0	6746.52	4015.37	180.0	53.1
84	254.0	6693.50	4643.27	209.7	61.9
108	254.0	6446.70	4914.72	230.5	68.0
135	254.0	6889.46	5521.58	242.3	71.5
165	254.0	7153.94	5798.73	245.1	72.3

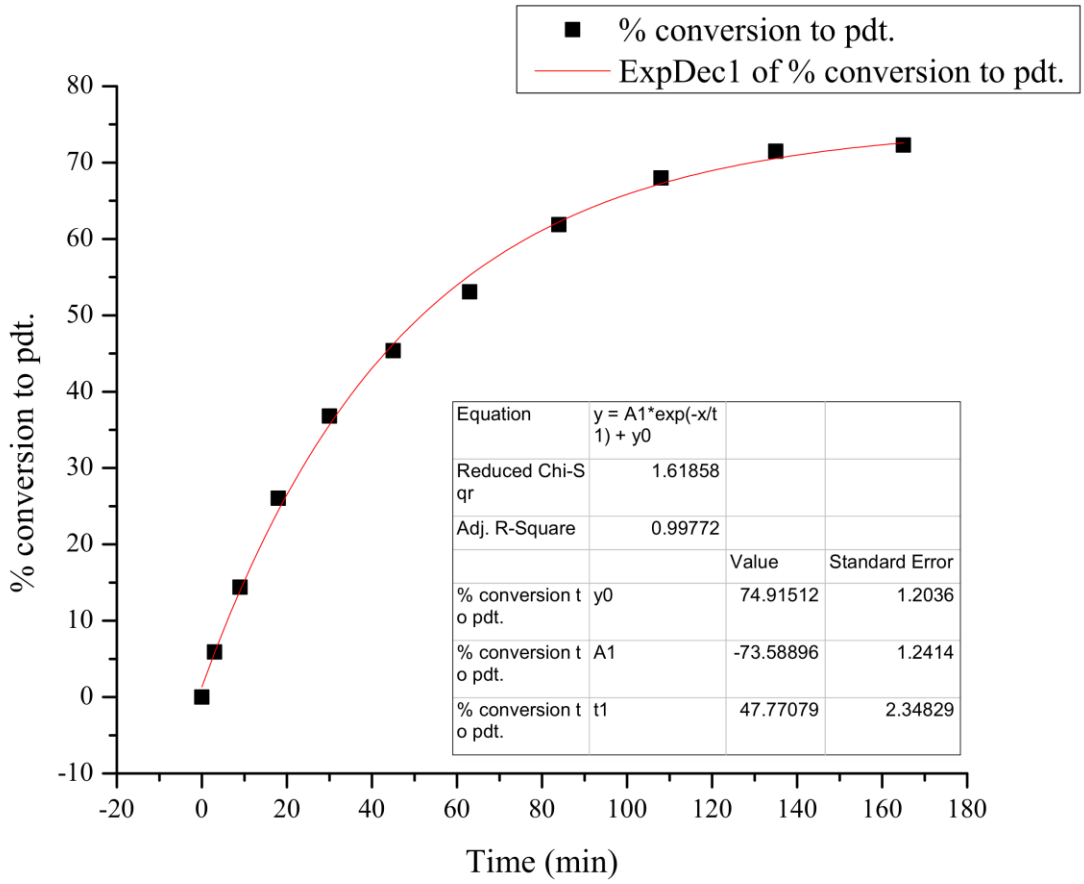

Half-Life = 52 min

Catalyst **3e**: Run 2

Time (min)	Standard (µmol)	Standard Area	Product Area	Product (µmol)	% Product
0	254.0	1.00	0.00	0.0	0.0
3	254.0	6604.29	547.47	25.1	7.4
9	254.0	6912.08	1403.08	61.4	18.1
18	254.0	6703.31	2373.20	107.0	31.6
30	254.0	7172.43	3515.76	148.2	43.7
45	254.0	6816.97	4103.24	182.0	53.7
63	254.0	6987.07	4896.22	211.9	62.5
84	254.0	7132.50	5304.48	224.9	66.3
108	254.0	7104.38	5790.27	246.4	72.7
135	254.0	7345.73	5933.77	244.2	72.0
165	254.0	8554.62	6688.04	236.4	69.7

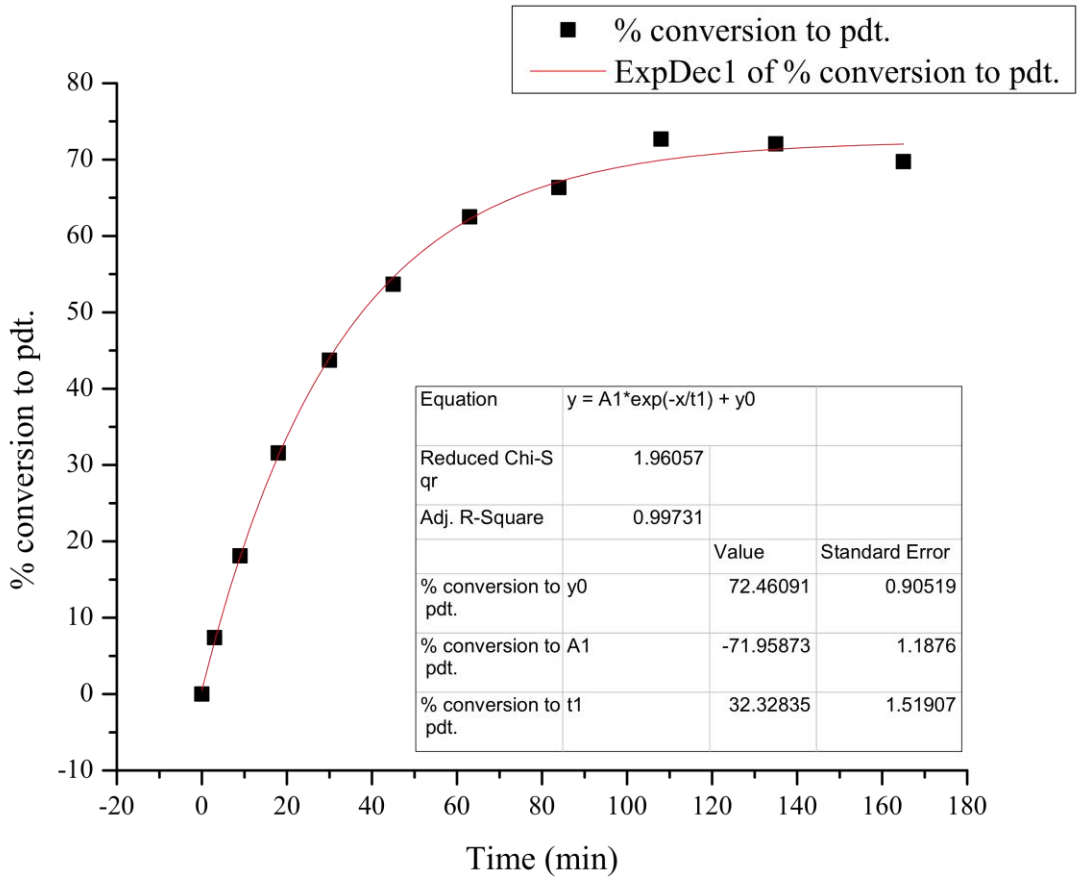

Half-Life = 38 min

Average Half-Life = 45 min

Catalyst **4e**: Run 1

Time (min)	Standard (µmol)	Standard Area	Product Area	Product (µmol)	% Product
0	254.0	1.00	0.00	0.0	0.0
3	254.0	6034.20	1681.63	84.3	24.9
9	254.0	5815.10	3265.33	169.8	50.1
18	254.0	7693.56	5776.40	227.0	67.0
30	254.0	7152.44	5979.27	252.8	74.6
45	254.0	7464.03	6305.21	255.4	75.3
63	254.0	6860.98	5798.58	255.5	75.4
84	254.0	6520.74	5640.82	261.6	77.2
108	254.0	6816.84	5923.90	262.8	77.5
135	254.0	7308.24	6179.92	255.7	75.4
165	254.0	6008.21	5063.76	254.8	75.2

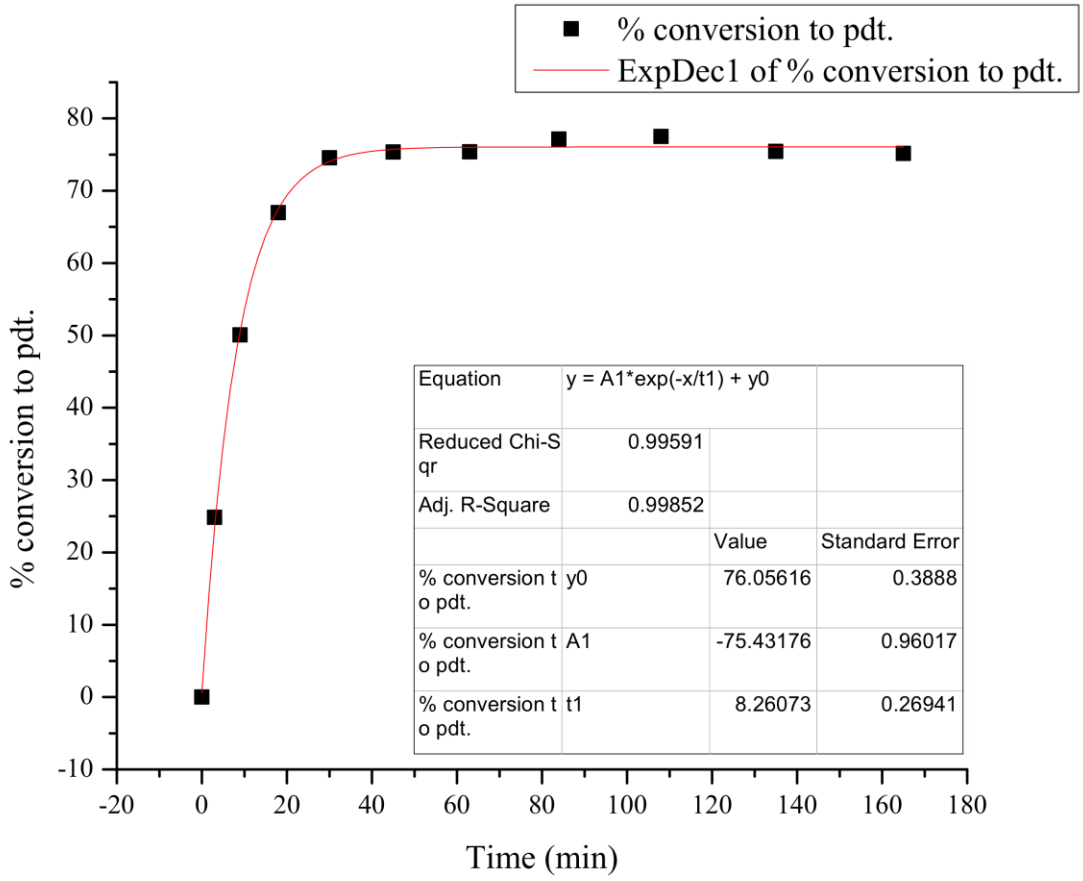

Half-Life = 9 min

Catalyst **4e**: Run 2

Time (min)	Standard (µmol)	Standard Area	Product Area	Product (µmol)	% Product
0	254.0	1.00	0.00	0.0	0.0
6	254.0	7408.90	3181.06	129.8	38.3
12	254.0	6486.04	4100.11	191.1	56.4
18	254.0	9219.50	6773.80	222.2	65.5
24	254.0	6842.62	5428.10	239.9	70.8
36	254.0	14846.30	13414.10	273.2	80.6
42	254.0	6787.48	5690.50	253.5	74.8
48	254.0	6829.84	5728.66	253.6	74.8
54	254.0	6693.96	5558.16	251.1	74.1
60	254.0	6649.07	5620.00	255.6	75.4

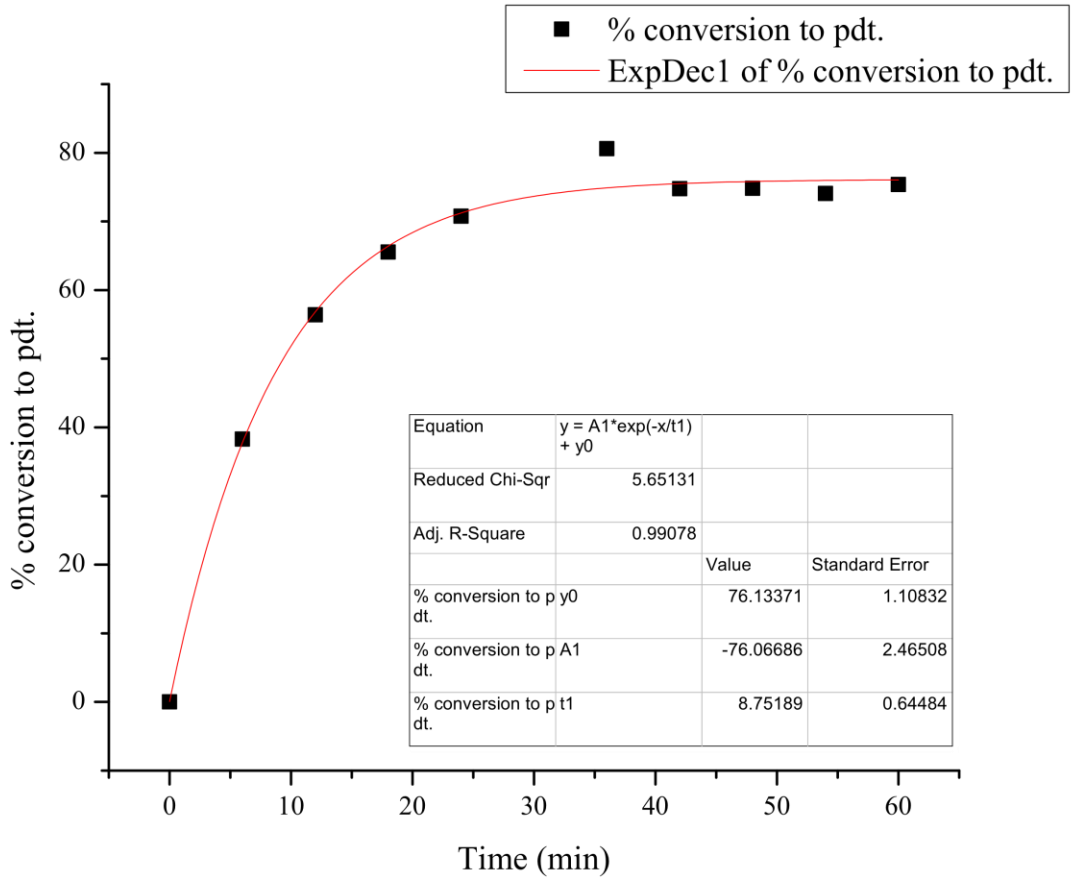

Half-Life = 9 min

Average Half-Life = 9 min

Catalyst **5e**: Run 1

Time (min)	Standard (µmol)	Standard Area	Product Area	Product (µmol)	% Product
0	254.0	1.00	0.00	0.0	0.0
60	254.0	7802.71	1114.30	43.2	12.7
120	254.0	8225.37	1433.34	52.7	15.5
180	254.0	6856.91	1591.42	70.2	20.7
240	254.0	7626.93	2416.44	95.8	28.3
300	254.0	8083.26	3058.24	114.4	33.7
360	254.0	7515.24	3412.32	137.3	40.5
420	254.0	4895.07	2307.47	142.5	42.0
480	254.0	8446.94	4589.99	164.3	48.5
1440	254.0	8084.39	6235.59	233.2	68.8

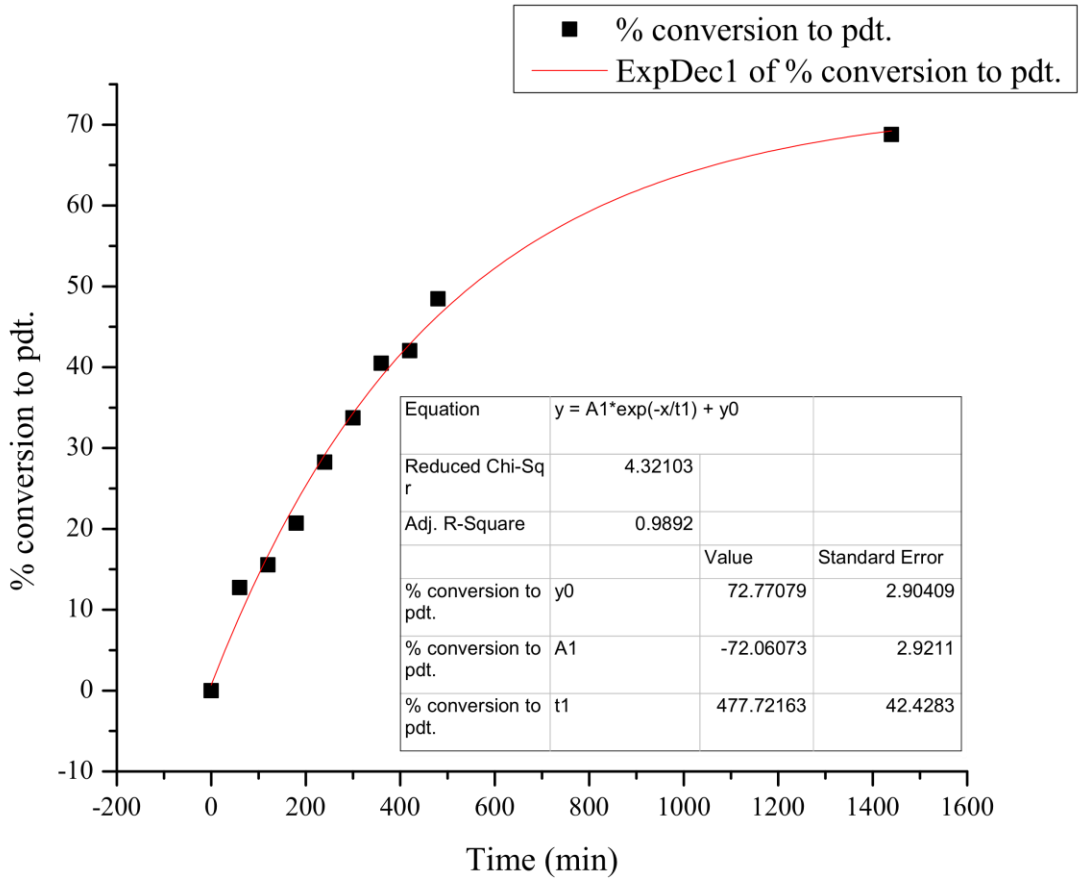

Half-Life = 550 min

Catalyst **5e**: Run 2

Time (min)	Standard (µmol)	Standard Area	Product Area	Product (µmol)	% Product
0	254.0	1.00	0.00	0.0	0.0
60	254.0	5736.16	776.53	40.9	12.1
120	254.0	2850.93	449.61	47.7	14.1
180	254.0	4661.94	1013.96	65.8	19.4
240	254.0	6389.07	1775.61	84.0	24.8
300	254.0	9501.85	3374.84	107.4	31.7
360	254.0	5738.45	2442.08	128.7	38.0
420	254.0	5254.53	2615.95	150.5	44.4
480	254.0	3907.70	2226.49	172.3	50.8
540	254.0	5259.69	3173.95	182.5	53.8
600	254.0	4111.57	2688.67	197.7	58.3
1440	254.0	6744.83	5156.23	231.1	68.2

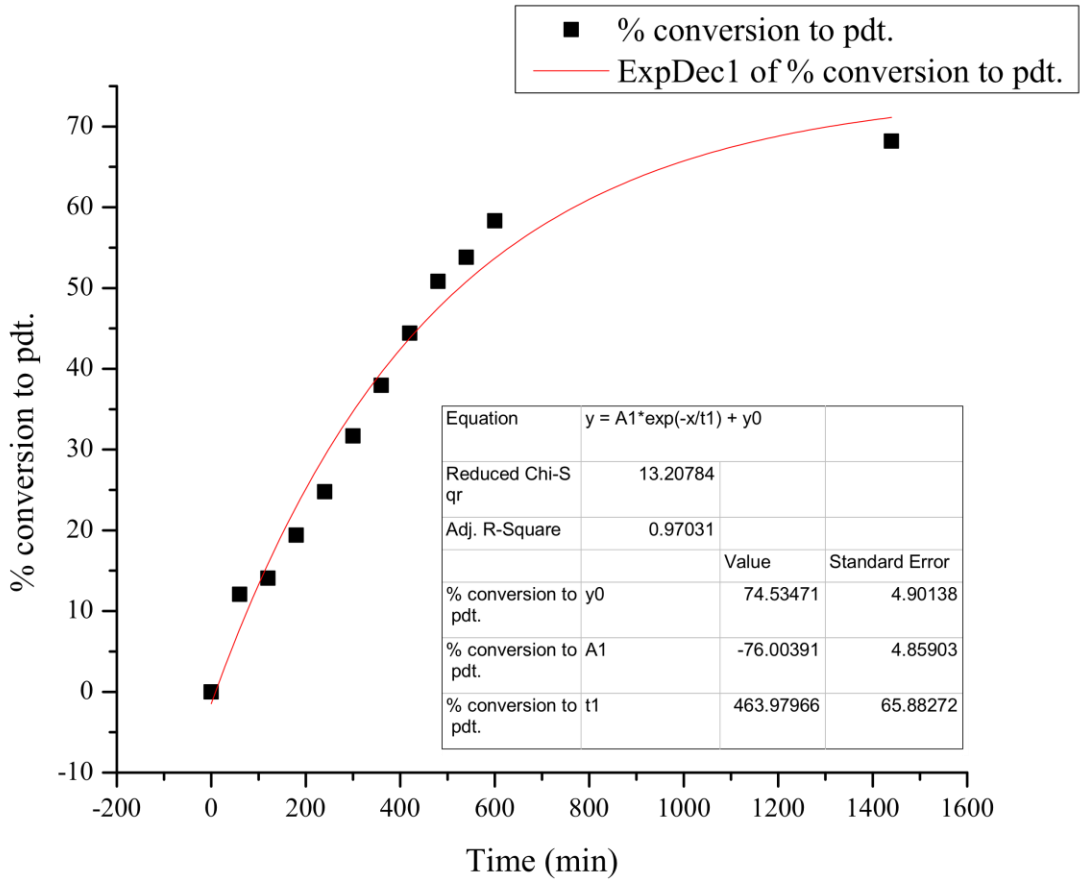

Half-Life = 525 min

Average Half-Life = 537 min

Kinetic Analyzses of Catalysts in Series F

Catalyst **1f**: Run 1

Time (min)	Standard (µmol)	Standard Area	Product Area	Product (µmol)	% Product
0	254.0	1.00	0.00	0.0	0.0
2	254.0	6746.20	689.73	30.9	9.1
6	254.0	6197.64	1415.62	69.1	20.4
12	254.0	6219.61	2211.64	107.5	31.7
20	254.0	6887.98	3290.58	144.4	42.6
30	254.0	6410.00	3887.26	183.4	54.1
42	254.0	6988.92	5046.74	218.3	64.4
56	254.0	7510.71	6032.30	242.8	71.6
72	254.0	7749.14	6671.50	260.3	76.8
90	254.0	6479.14	5612.92	261.9	77.3
110	254.0	7366.58	6070.10	249.1	73.5
300	254.0	7157.27	6408.50	270.7	79.9

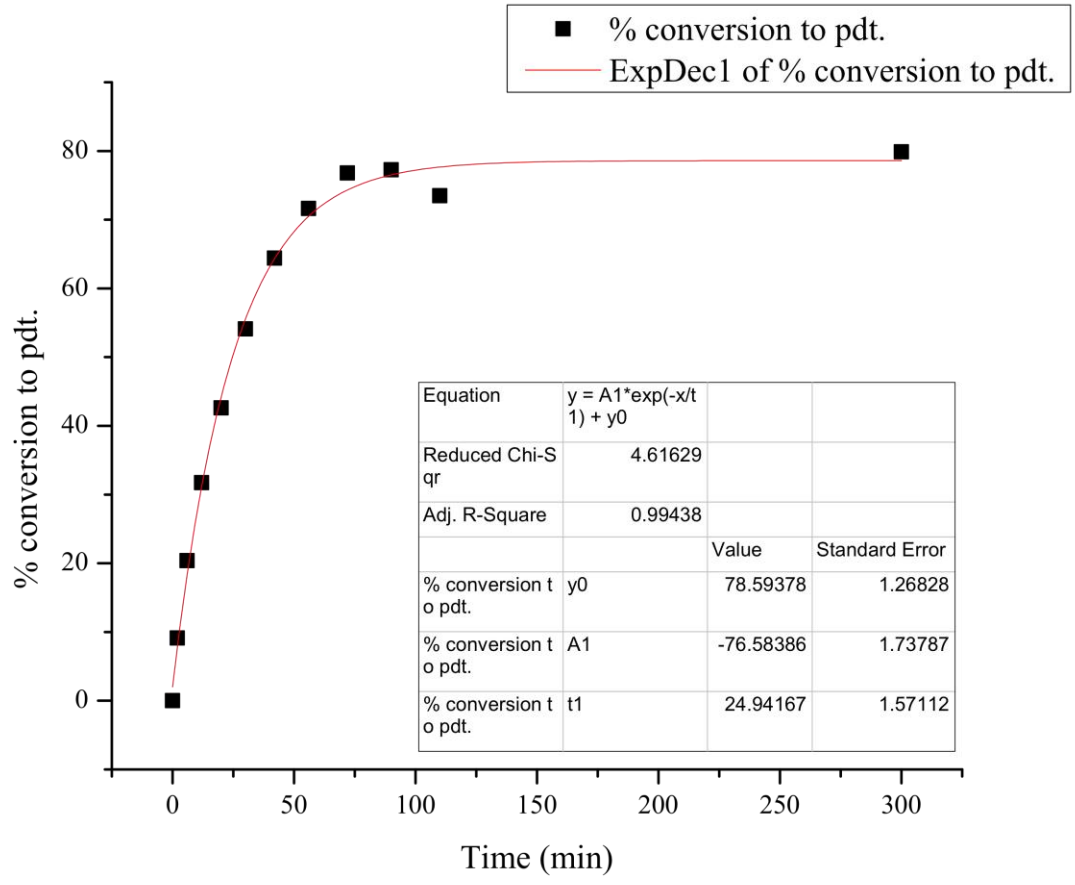

Half-Life = 25 min

Catalyst **1f**: Run 2

Time (min)	Standard (µmol)	Standard Area	Product Area	Product (µmol)	% Product
0	254.0	1.00	0.00	0.0	0.0
2	254.0	5080.48	644.75	38.4	11.3
6	254.0	5237.71	1632.97	94.3	27.8
12	254.0	6424.64	3309.58	155.8	45.9
20	254.0	6994.52	4578.36	197.9	58.4
30	254.0	7068.22	5386.00	230.4	68.0
42	254.0	6840.88	5606.84	247.8	73.1
56	254.0	6560.04	5537.58	255.2	75.3
72	254.0	6075.60	5238.96	260.7	76.9
90	254.0	7615.96	6618.52	262.8	77.5
110	254.0	6549.97	5671.33	261.8	77.2
300	254.0	7417.62	6411.60	261.4	77.1

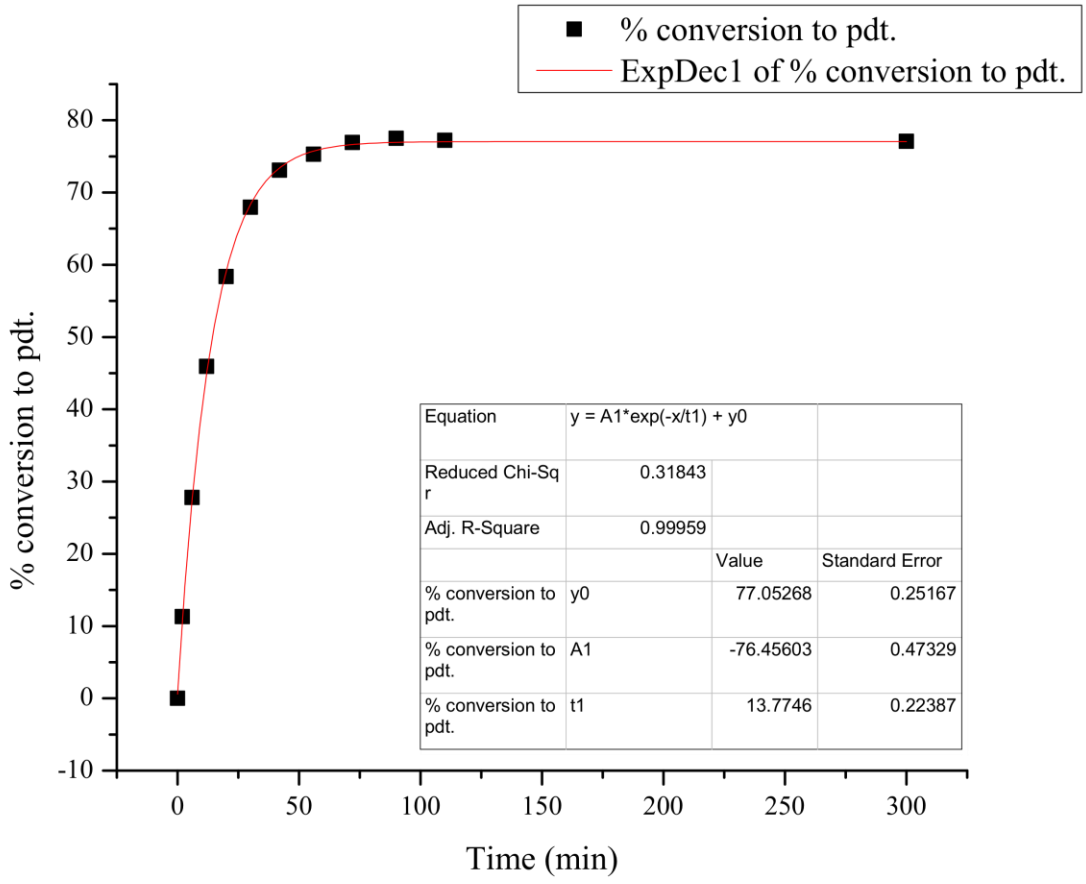

Half-Life = 14 min
Average Half-Life = 19 min

Catalyst **2f**: Run 1

Time (min)	Standard (µmol)	Standard Area	Product Area	Product (µmol)	% Product
0	254.0	1.00	0.00	0.0	0.0
12	254.0	6324.66	1567.39	74.9	22.1
24	254.0	5366.03	2291.07	129.1	38.1
36	254.0	6418.06	3533.47	166.5	49.1
48	254.0	6675.58	4220.13	191.1	56.4
60	254.0	6671.54	4712.91	213.6	63.0
120	254.0	7093.22	6534.59	278.5	82.2
180	254.0	6775.49	6791.46	303.1	89.4
240	254.0	6865.26	7235.56	318.7	94.0
300	254.0	6482.36	6879.45	320.9	94.7
360	254.0	7270.22	7736.72	321.8	94.9

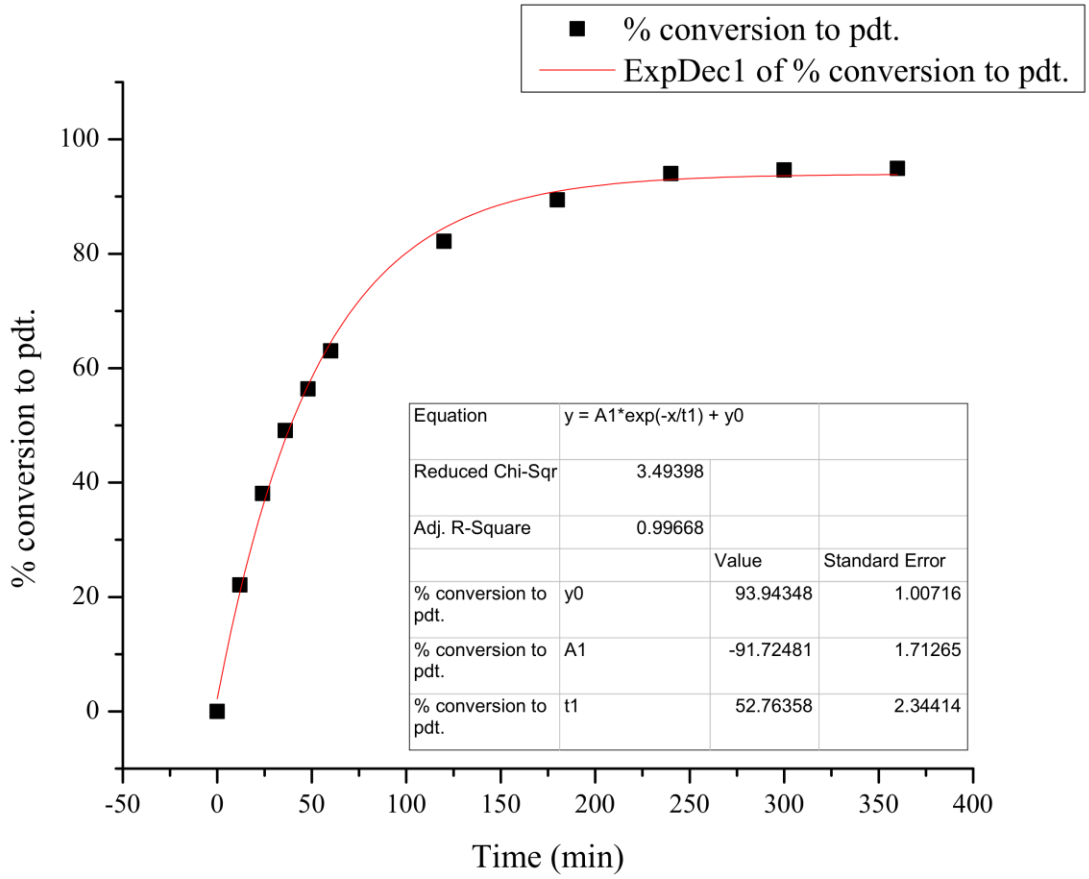

Half-Life = 39 min

Catalyst **2f**: Run 2

Time (min)	Standard (µmol)	Standard Area	Product Area	Product (µmol)	% Product
0	254.0	1.00	0.00	0.0	0.0
12	254.0	6927.88	1612.46	70.4	20.8
24	254.0	7272.62	2798.99	116.4	34.3
36	254.0	6758.99	3329.83	149.0	43.9
48	254.0	6662.96	3724.54	169.0	49.9
60	254.0	7018.41	4168.07	179.6	53.0
120	254.0	7401.03	5717.94	233.6	68.9
180	254.0	7034.90	6083.71	261.5	77.1
240	254.0	6652.70	5988.91	272.2	80.3
300	254.0	7370.92	6729.16	276.0	81.4
360	254.0	7207.37	6541.66	274.4	81.0

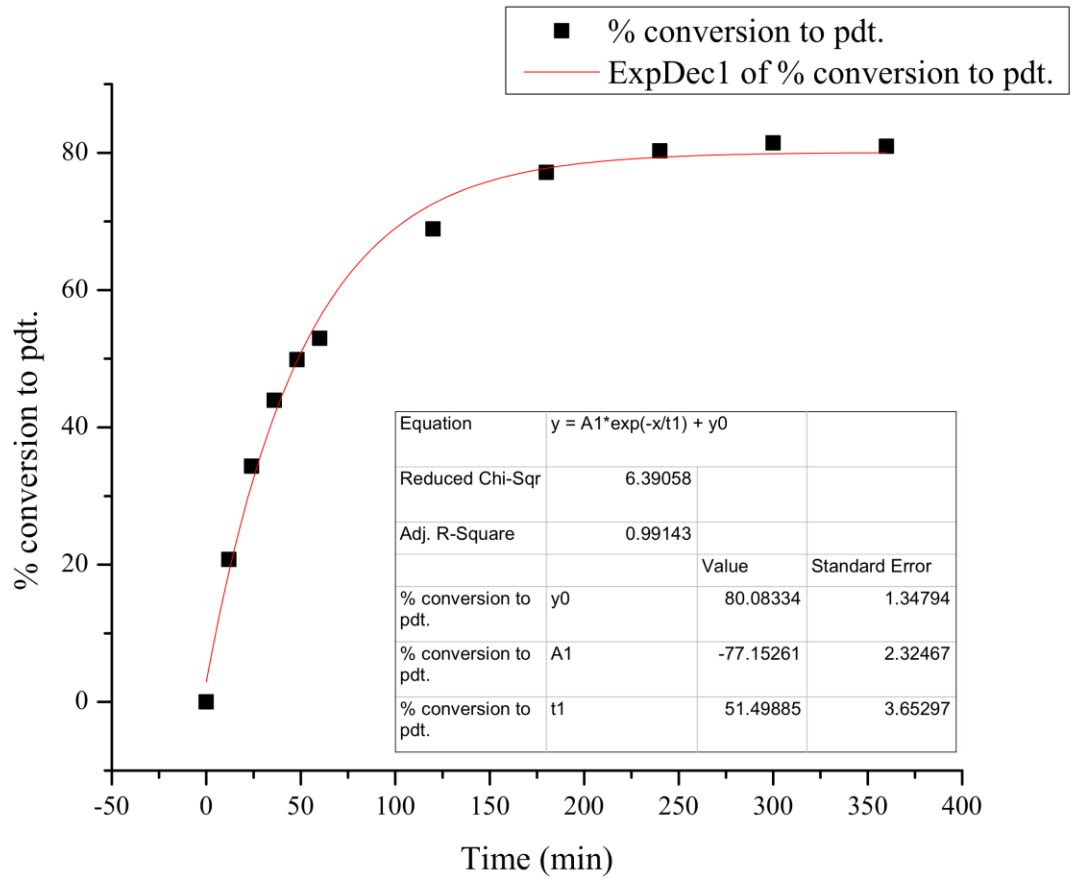

Half-Life = 49 min

Average Half-Life = 44 min

Catalyst **3f**: Run 1

Time (min)	Standard (µmol)	Standard Area	Product Area	Product (µmol)	% Product
0	254.0	1.00	0.00	0.0	0.0
12	254.0	6696.54	1815.67	82.0	24.2
24	254.0	5904.32	2640.73	135.2	39.9
36	254.0	6676.11	3768.43	170.7	50.3
48	254.0	6494.00	4199.48	195.5	57.7
60	254.0	6996.87	4941.47	213.5	63.0
120	254.0	6669.55	6049.20	274.2	80.9
180	254.0	6278.46	6013.98	289.6	85.4
240	254.0	6974.64	6792.46	294.5	86.9
300	254.0	6438.08	6240.71	293.1	86.5
360	254.0	7661.69	7422.68	292.9	86.4

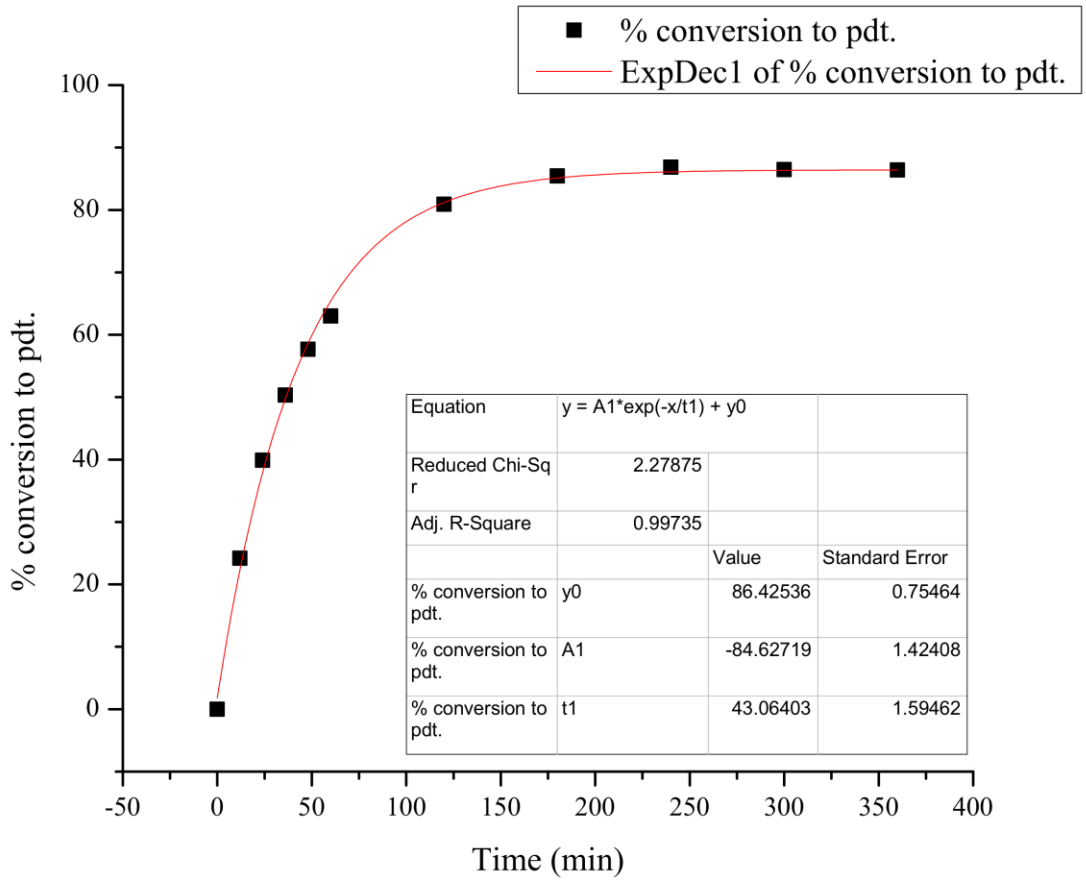

Half-Life = 36 min

Catalyst **3f**: Run 2

Time (min)	Standard (µmol)	Standard Area	Product Area	Product (µmol)	% Product
0	254.0	1.00	0.00	0.0	0.0
12	254.0	7204.22	2552.93	107.1	31.6
24	254.0	5943.56	3083.08	156.8	46.3
36	254.0	6007.45	3816.28	192.1	56.7
48	254.0	6786.74	4810.62	214.3	63.2
60	254.0	7396.10	5661.89	231.5	68.3
120	254.0	6214.94	5820.62	283.2	83.5
180	254.0	6575.49	6480.29	298.0	87.9
240	254.0	6611.76	6435.94	294.3	86.8
300	254.0	6406.46	6114.86	288.6	85.1
360	254.0	6888.95	6344.32	278.5	82.1

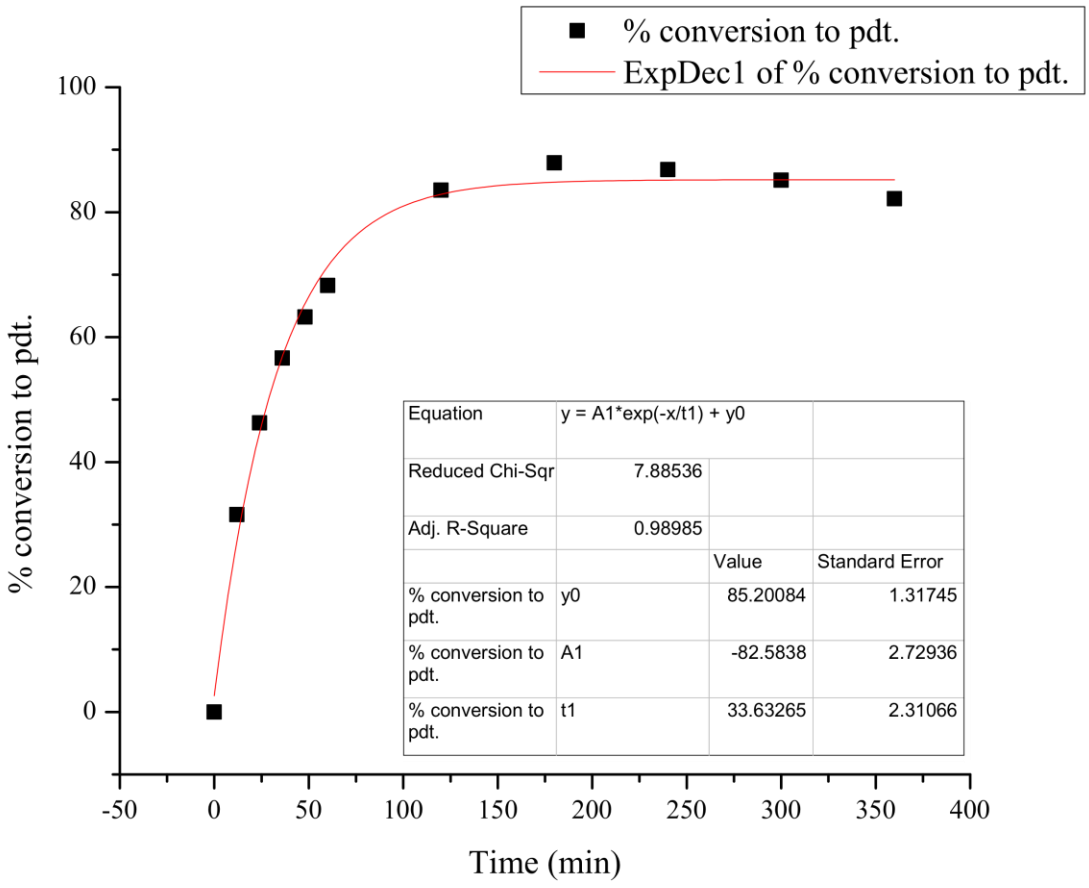

Half-Life = 29 min

Average Half-Life = 32 min

Catalyst **4f**: Run 1

Time (min)	Standard (µmol)	Standard Area	Product Area	Product (µmol)	% Product
0	254.0	1.00	0.00	0.0	0.0
2	254.0	8302.52	505.63	18.4	5.4
6	254.0	8506.73	1537.43	54.6	16.1
12	254.0	7923.75	2583.53	98.6	29.1
20	254.0	7614.71	3222.40	128.0	37.7
30	254.0	8226.42	4489.79	165.0	48.7
42	254.0	8094.67	5048.39	188.6	55.6
56	254.0	8570.60	6196.11	218.6	64.5
72	254.0	8062.57	6122.82	229.6	67.7
90	254.0	8202.17	6581.54	242.6	71.6
110	254.0	9014.30	7392.26	248.0	73.1
450	254.0	8553.64	7156.44	253.0	74.6

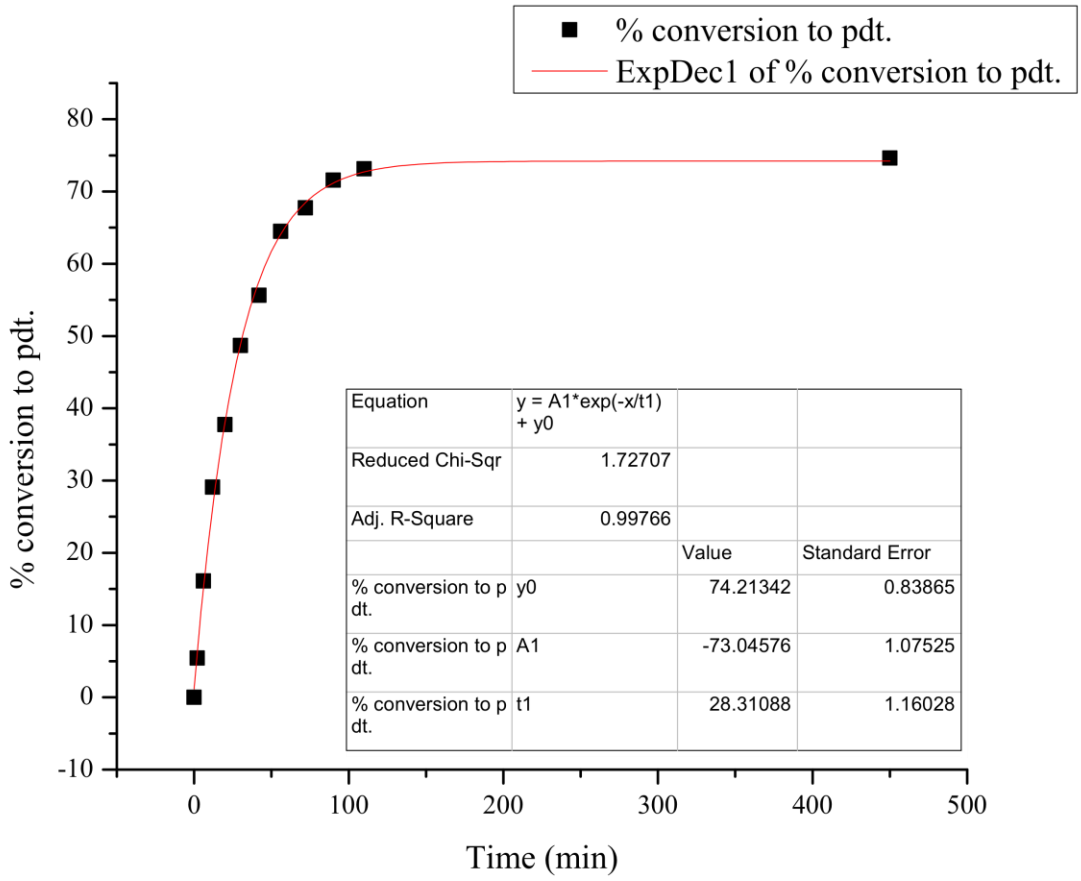

Half-Life = 31 min

Catalyst **4f**: Run 2

Time (min)	Standard (µmol)	Standard Area	Product Area	Product (µmol)	% Product
0	254.0	1.00	0.00	0.0	0.0
2	254.0	8189.52	514.56	19.0	5.6
6	254.0	6596.58	1266.05	58.0	17.1
12	254.0	6805.55	2231.29	99.1	29.2
20	254.0	8318.14	3846.29	139.8	41.2
30	254.0	6211.89	3626.47	176.5	52.1
42	254.0	7508.75	4711.72	189.7	56.0
56	254.0	6662.03	4899.97	222.4	65.6
72	254.0	6309.02	4707.80	225.6	66.6
90	254.0	6673.20	5217.23	236.4	69.7
110	254.0	7273.48	5498.61	228.6	67.4
450	254.0	6265.72	4932.82	238.0	70.2

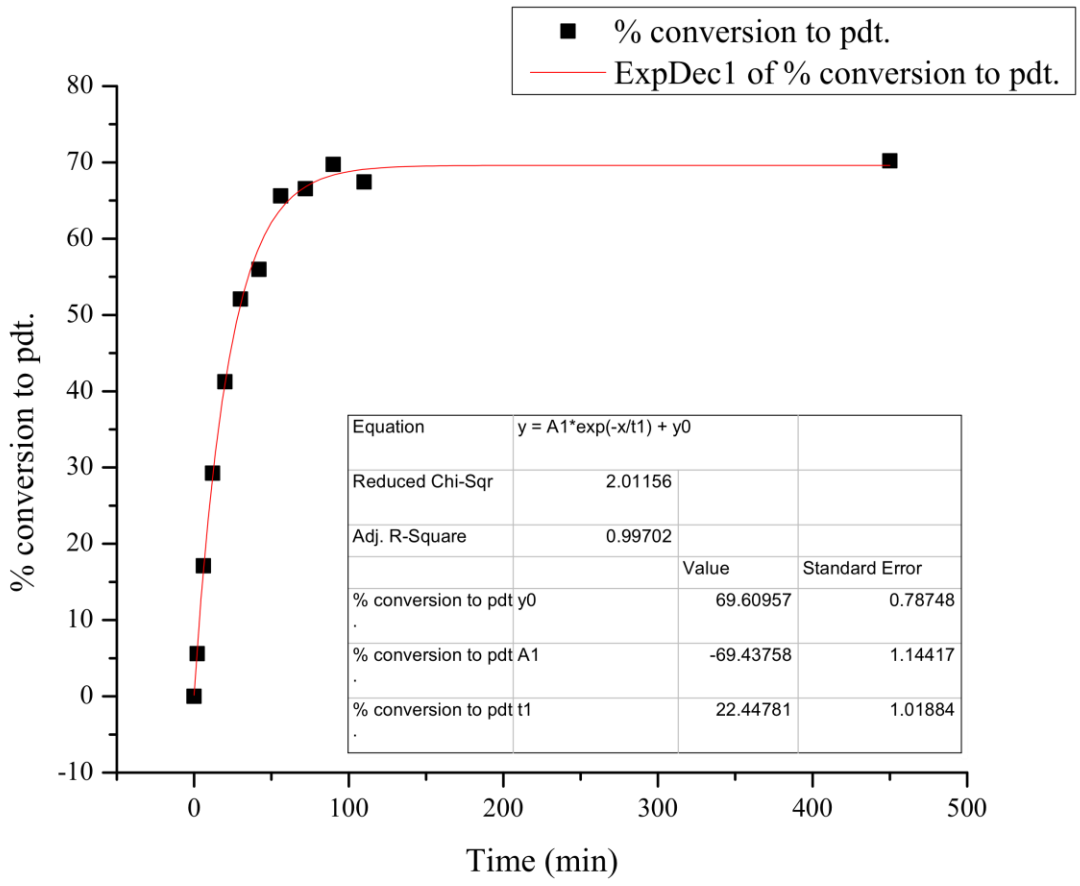

Half-Life = 28 min

Average Half-Life = 30 min

Catalyst **5f**: Run 1

Time (min)	Standard (µmol)	Standard Area	Product Area	Product (µmol)	% Product
0	254.0	1.00	0.00	0.0	0.0
60	254.0	6608.52	893.80	40.9	12.1
120	254.0	6852.95	1218.56	53.8	15.9
180	254.0	7020.18	1806.02	77.8	22.9
240	254.0	6545.57	2252.42	104.0	30.7
300	254.0	6793.92	2850.32	126.9	37.4
360	254.0	6628.84	3477.13	158.6	46.8
1011	254.0	7481.96	6413.33	259.2	76.5
1440	254.0	7024.42	6051.69	260.5	76.8

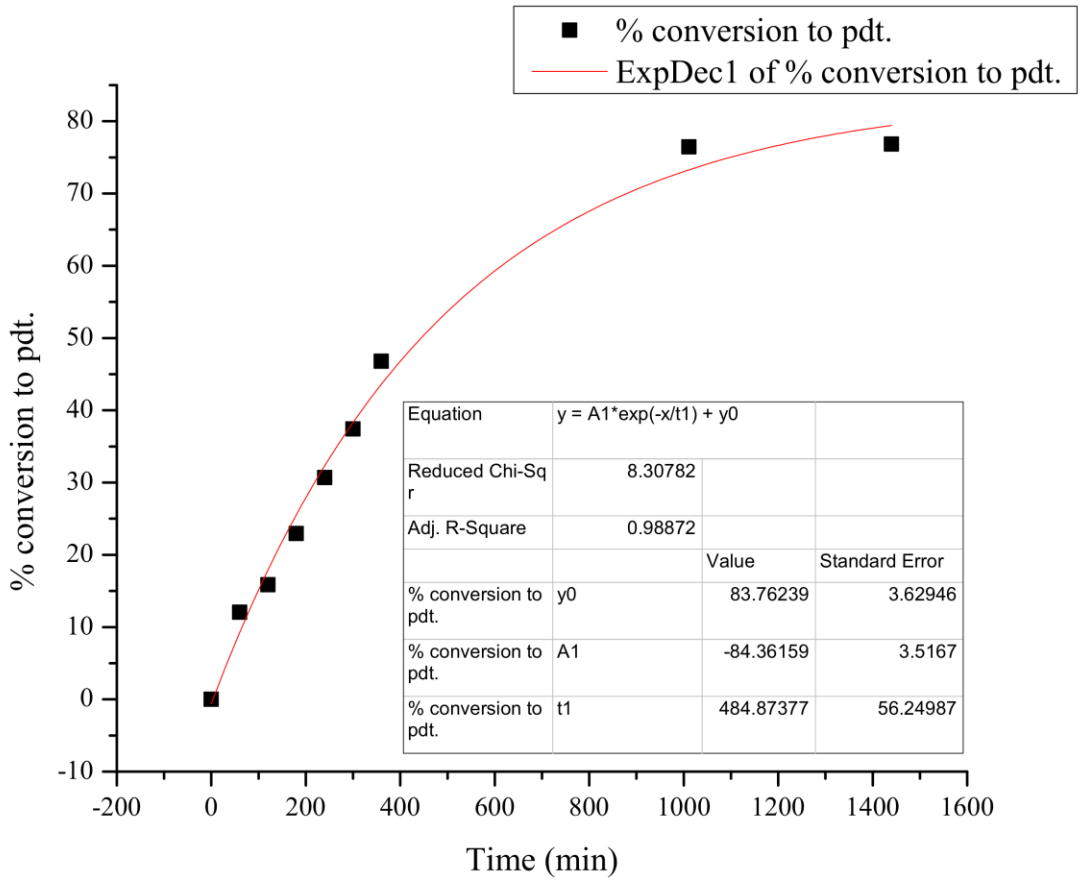

Half-Life = 444 min

Catalyst **5f**: Run 2

Time (min)	Standard (µmol)	Standard Area	Product Area	Product (µmol)	% Product
0	254.0	1.00	0.00	0.0	0.0
60	254.0	6451.04	808.15	37.9	11.2
120	254.0	6972.20	1199.07	52.0	15.3
180	254.0	6673.80	1702.65	77.1	22.8
240	254.0	7158.30	2469.27	104.3	30.8
300	254.0	6765.32	2842.87	127.1	37.5
360	254.0	6806.36	3370.52	149.7	44.2
1011	254.0	7313.61	6734.09	278.4	82.1
1440	254.0	6722.68	6236.44	280.5	82.7

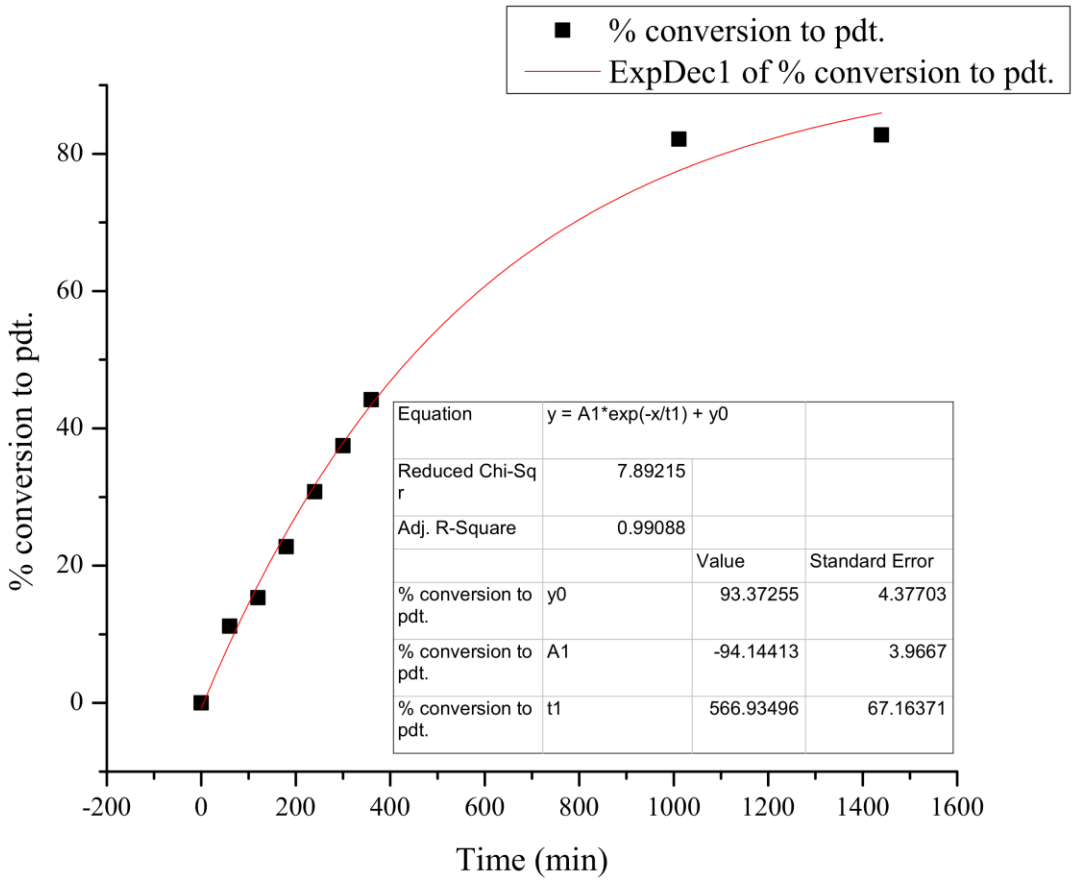

Half-Life = 439 min

Average Half-Life = 442 min

Kinetic Analyzses of Catalysts in Series G

Catalyst **1g**: Run 1

Time (min)	Standard (µmol)	Standard Area	Product Area	Product (µmol)	% Product
0	254.0	1.00	0.00	0.0	0.0
5	254.0	4785.40	0.00	0.0	0.0
10	254.0	6481.61	0.00	0.0	0.0
15	254.0	6278.11	0.00	0.0	0.0
30	254.0	6196.21	0.00	0.0	0.0
45	254.0	7055.98	29.33	1.3	0.4
60	254.0	7036.21	43.22	1.9	0.5
90	254.0	7040.81	70.43	3.0	0.9
120	254.0	6788.59	99.73	4.4	1.3
180	254.0	6166.88	155.59	7.6	2.3
240	254.0	7618.04	281.53	11.2	3.3
1407	254.0	3124.85	977.35	94.6	27.9
1705	254.0	7065.51	2760.89	118.1	34.9
2544	254.0	5809.74	3190.58	166.1	49.0
3993	254.0	6635.87	4481.06	204.2	60.2
5460	254.0	8019.76	5833.45	219.9	64.9

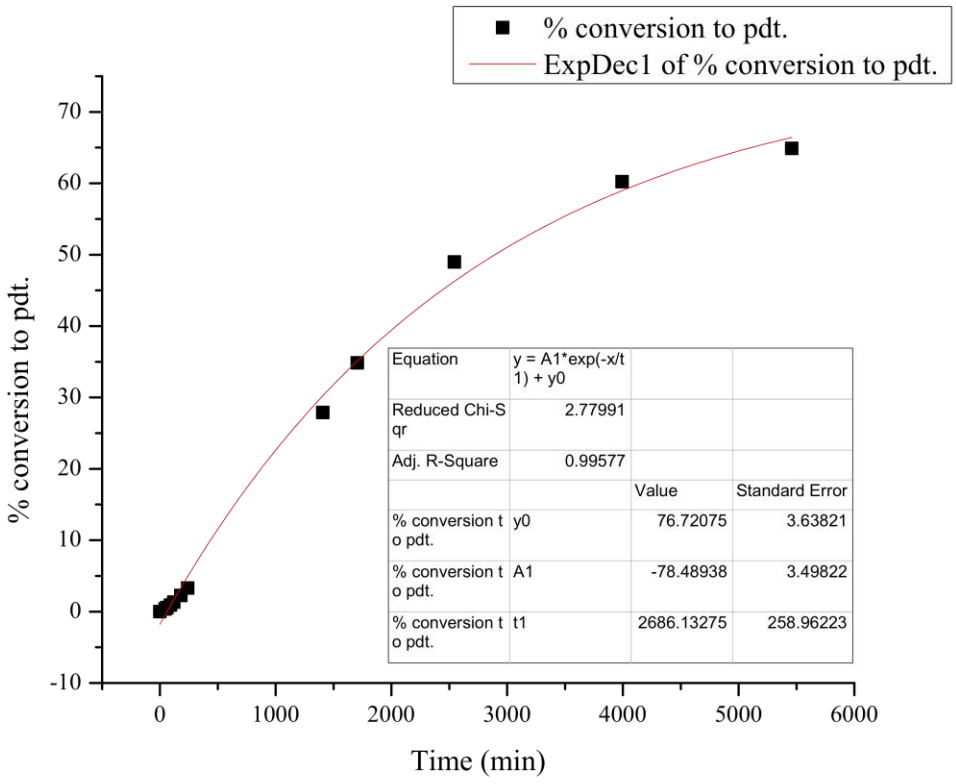

Half-Life = 2894 min

Catalyst **1g**: Run 2

Time (min)	Standard (µmol)	Standard Area	Product Area	Product (µmol)	% Product
0	254.0	1.00	0.00	0.0	0.0
60	254.0	6226.14	44.30	2.2	0.6
120	254.0	6555.16	96.03	4.4	1.3
180	254.0	6917.37	158.11	6.9	2.0
240	254.0	6946.54	225.34	9.8	2.9
300	254.0	7093.78	286.27	12.2	3.6
360	254.0	7195.26	351.78	14.8	4.4
1224	254.0	6945.15	1515.48	66.0	19.5
1620	254.0	7602.57	2194.78	87.3	25.7
2640	254.0	6005.86	2518.23	126.8	37.4
4026	254.0	7049.26	3888.84	166.8	49.2
5673	254.0	7061.82	4263.06	182.5	53.8

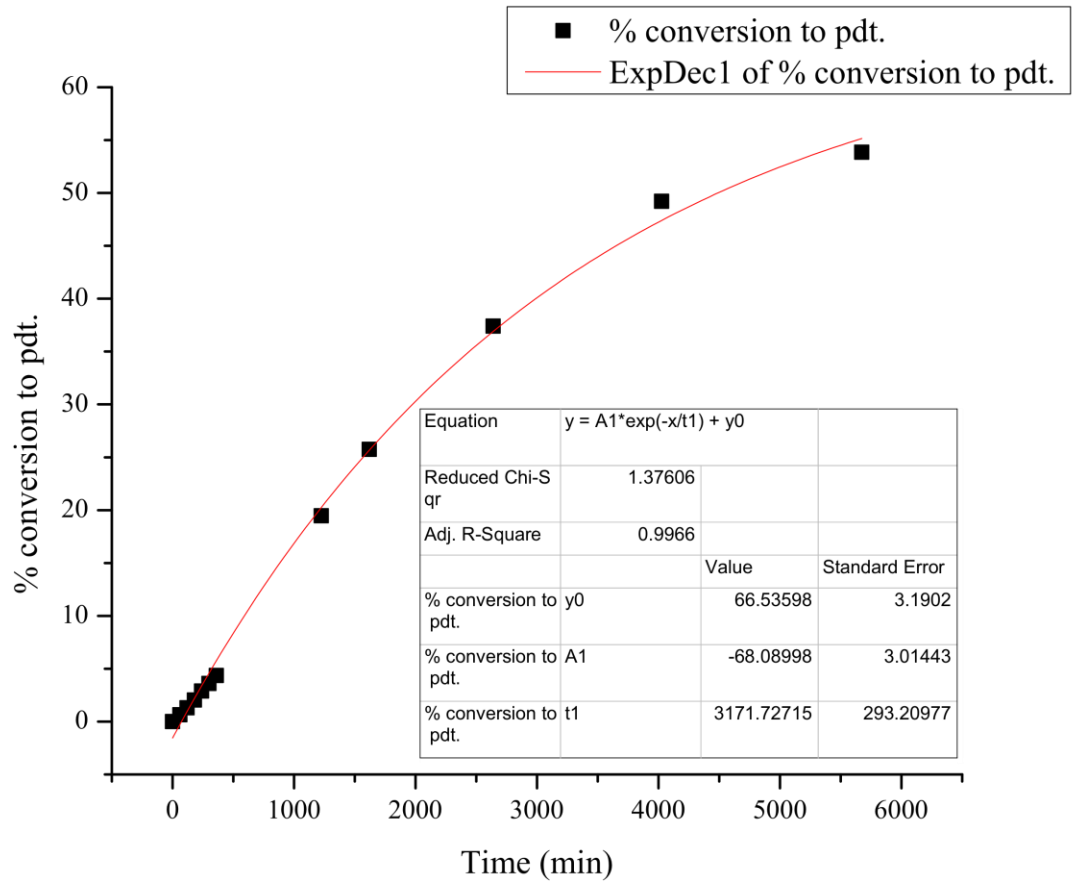

Half-Life = 4489 min

Average Half-Life = 3692 min

Catalyst **2g**: Run 1

Time (min)	Standard (µmol)	Standard Area	Product Area	Product (µmol)	% Product
0	254.4	1.00	0.00	0.0	0.0
30	254.4	6787.93	609.88	27.2	8.0
60	254.4	7257.10	1481.89	61.8	18.2
120	254.4	7551.69	3204.37	128.5	37.9
187	254.4	7887.53	4220.36	162.0	47.8
240	254.4	7380.23	4514.83	185.3	54.6
300	254.4	8035.92	5323.30	200.6	59.2
360	254.4	8171.71	5955.57	220.7	65.1
420	254.4	7824.91	5666.78	219.3	64.7
1147	254.4	8168.60	7071.88	262.2	77.3
1560	254.4	7224.20	6097.69	255.6	75.4

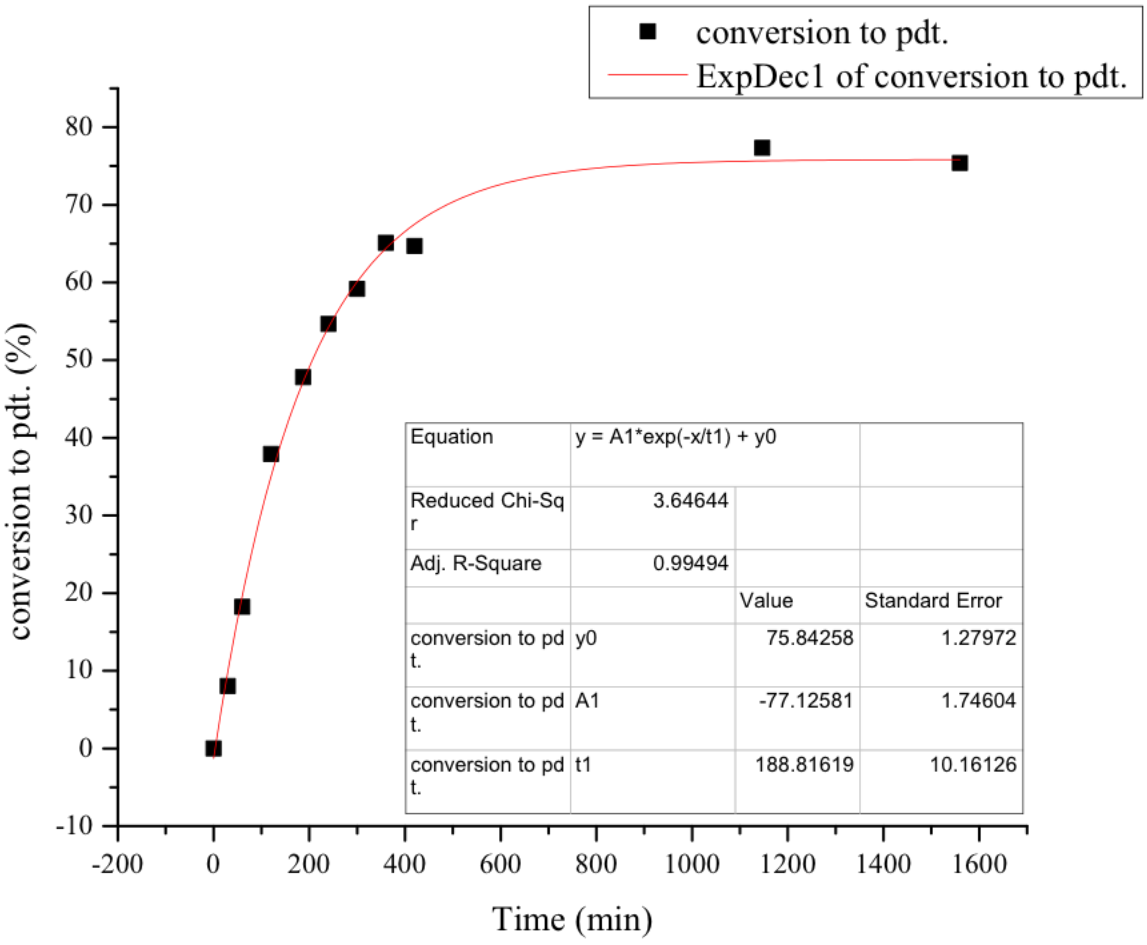

Half-Life = 206 min

Catalyst **2g**: Run 2

Time (min)	Standard (µmol)	Standard Area	Product Area	Product (µmol)	% Product
0	254.4	1.00	0.00	0.0	0.0
30	254.4	7879.70	974.28	37.4	11.0
60	254.4	7632.34	2021.67	80.2	23.7
120	254.4	7338.45	3373.79	139.2	41.1
187	254.4	7725.06	4531.65	177.6	52.4
240	254.4	7509.69	4875.33	196.6	58.0
300	254.4	7493.59	5189.88	209.7	61.9
360	254.4	8120.01	5647.67	210.6	62.1
420	254.4	7942.36	5629.66	214.7	63.3
1147	254.4	8318.25	7305.35	266.0	78.5
1560	254.4	7807.39	6619.81	256.8	75.7

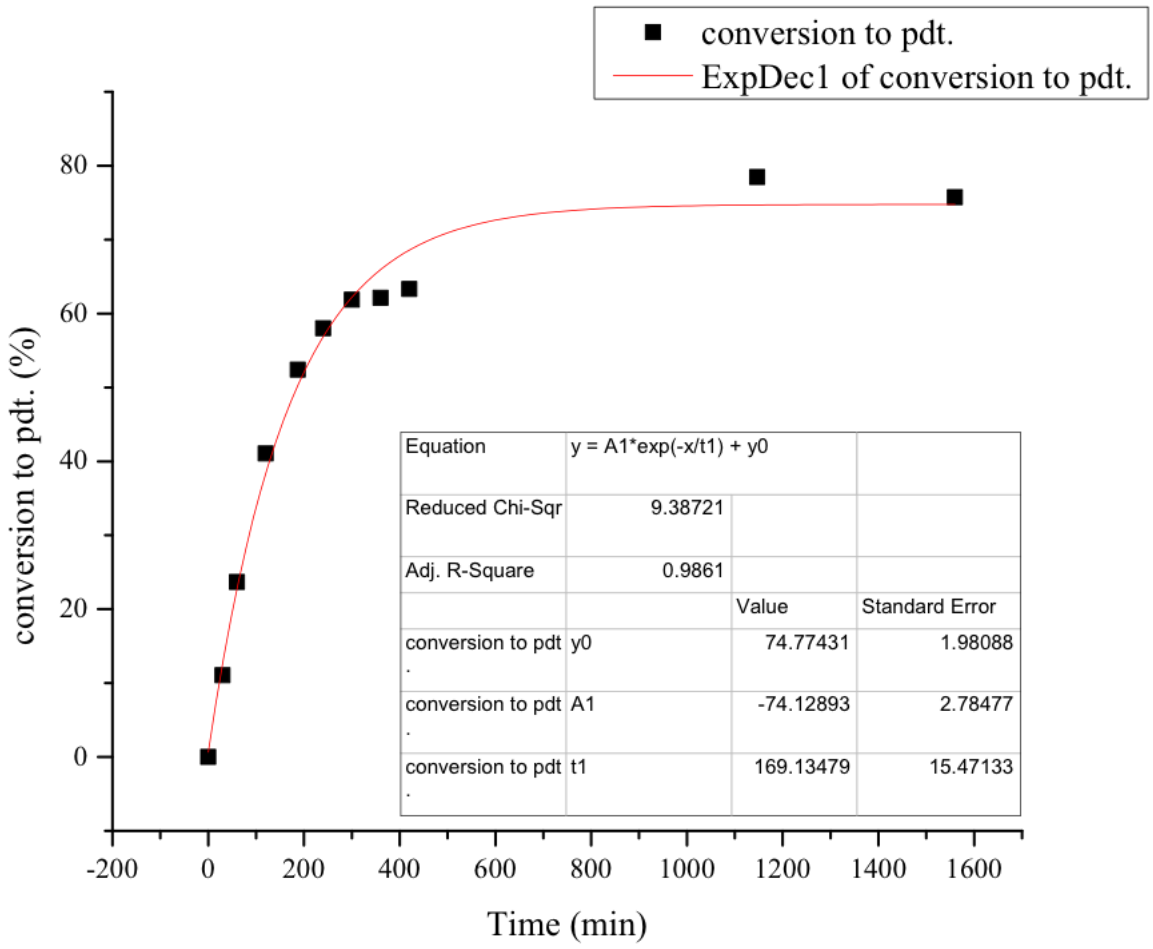

Half-Life = 185 min

Average Half-Life = 196 min

Catalyst **3g**: Run 1

Time (min)	Standard (µmol)	Standard Area	Product Area	Product (µmol)	% Product
0	254.4	1.00	0.00	0.0	0.0
5	254.4	7555.78	137.60	5.5	1.6
15	254.4	7675.03	269.49	10.6	3.1
30	254.4	7437.46	467.38	19.0	5.6
60	254.4	8236.57	1348.06	49.6	14.6
90	254.4	7395.39	2152.72	88.2	26.0
120	254.4	7192.46	2890.21	121.7	35.9
180	254.4	8134.50	4423.51	164.7	48.6
240	254.4	7371.72	4797.26	197.1	58.1
300	254.4	7601.25	5521.92	220.0	64.9
360	254.4	8066.03	6149.84	230.9	68.1
1145	254.4	7824.90	7006.29	271.2	80.0
1560	254.4	7618.68	6837.57	271.8	80.2

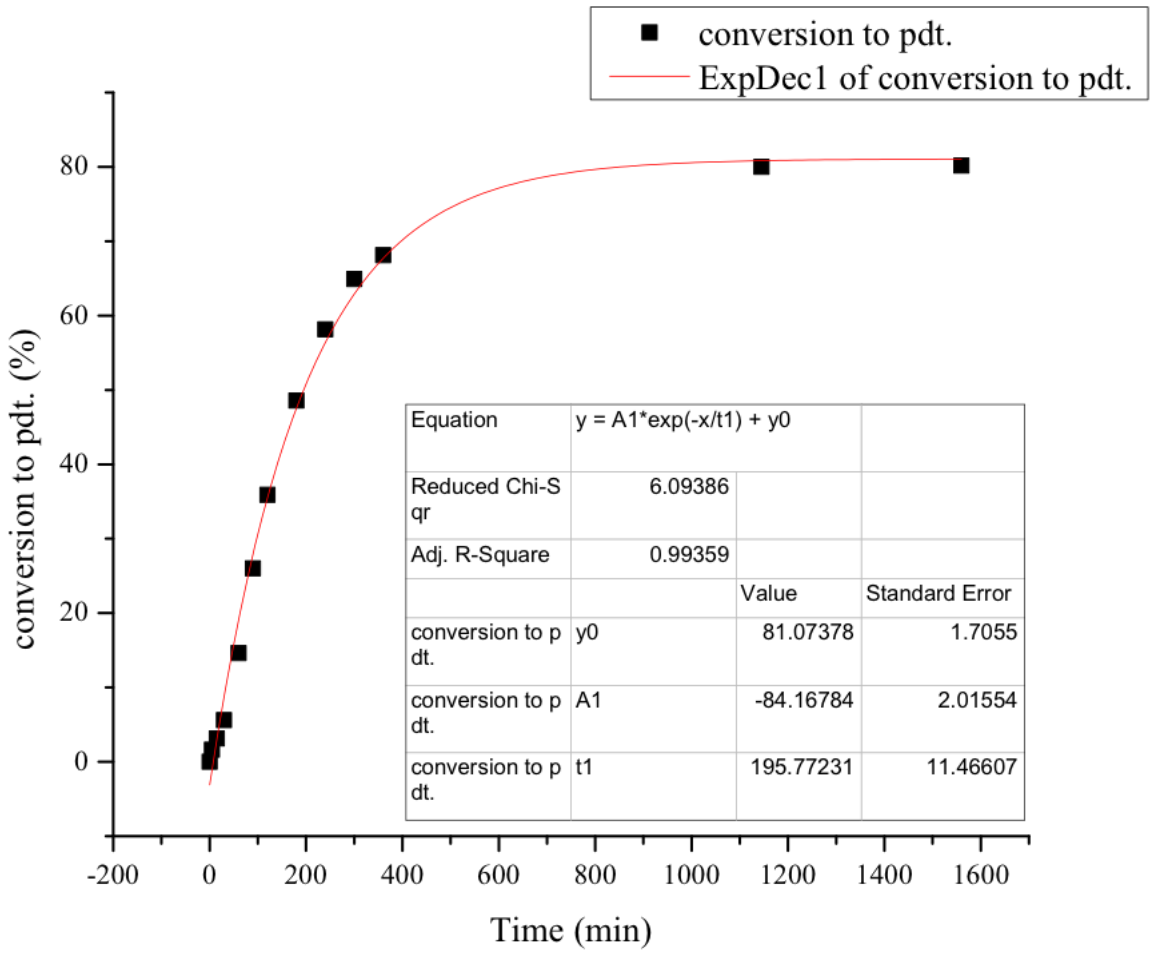

Half-Life = 195 min

Catalyst **3g**: Run 2

Time (min)	Standard (µmol)	Standard Area	Product Area	Product (µmol)	% Product
0	254.4	1.00	0.00	0.0	0.0
5	254.4	7015.07	161.58	7.0	2.1
15	254.4	8256.07	306.73	11.3	3.3
30	254.4	7499.40	535.31	21.6	6.4
60	254.4	7462.14	1404.07	57.0	16.8
90	254.4	7326.29	2214.59	91.5	27.0
120	254.4	7777.68	3203.36	124.7	36.8
180	254.4	8064.22	4403.38	165.4	48.8
240	254.4	7774.00	4752.02	185.1	54.6
300	254.4	7759.49	5227.26	204.0	60.2
1145	254.4	8132.78	6851.19	255.1	75.3
1560	254.4	7680.57	6628.07	261.3	77.1

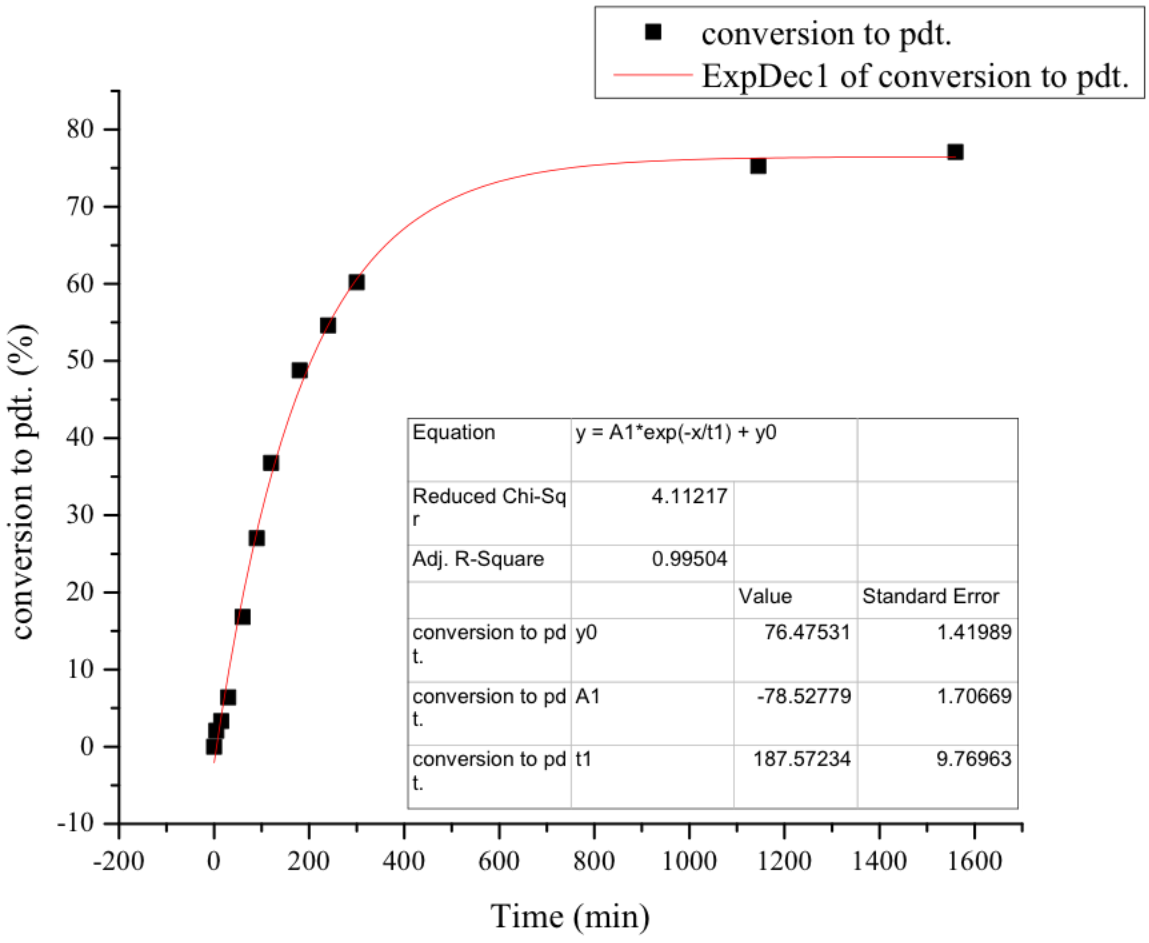

Half-Life = 204 min

Average Half-Life = 200 min

Catalyst **4g**: Run 1

Time (min)	Standard (µmol)	Standard Area	Product Area	Product (µmol)	% Product
0	254.0	1.00	0.00	0.0	0.0
5	254.0	6852.17	110.72	4.9	1.4
10	254.0	6817.03	158.95	7.0	2.1
15	254.0	7699.92	215.54	8.5	2.5
30	254.0	6630.67	281.05	12.8	3.8
45	254.0	7347.50	441.68	18.2	5.4
60	254.0	7795.26	662.70	25.7	7.6
90	254.0	6685.08	986.00	44.6	13.2
120	254.0	3378.30	604.63	54.1	16.0
180	254.0	7588.50	2102.34	83.8	24.7
240	254.0	7529.30	2813.65	113.0	33.3
420	254.0	8020.55	3789.02	142.8	42.1
1402	254.0	7165.58	4748.75	200.4	59.1
1700	254.0	7360.62	4932.70	202.6	59.8
2540	254.0	7336.59	5072.65	209.1	61.7
3988	254.0	7775.68	5465.47	212.5	62.7
5455	254.0	7686.08	5322.10	209.4	61.8

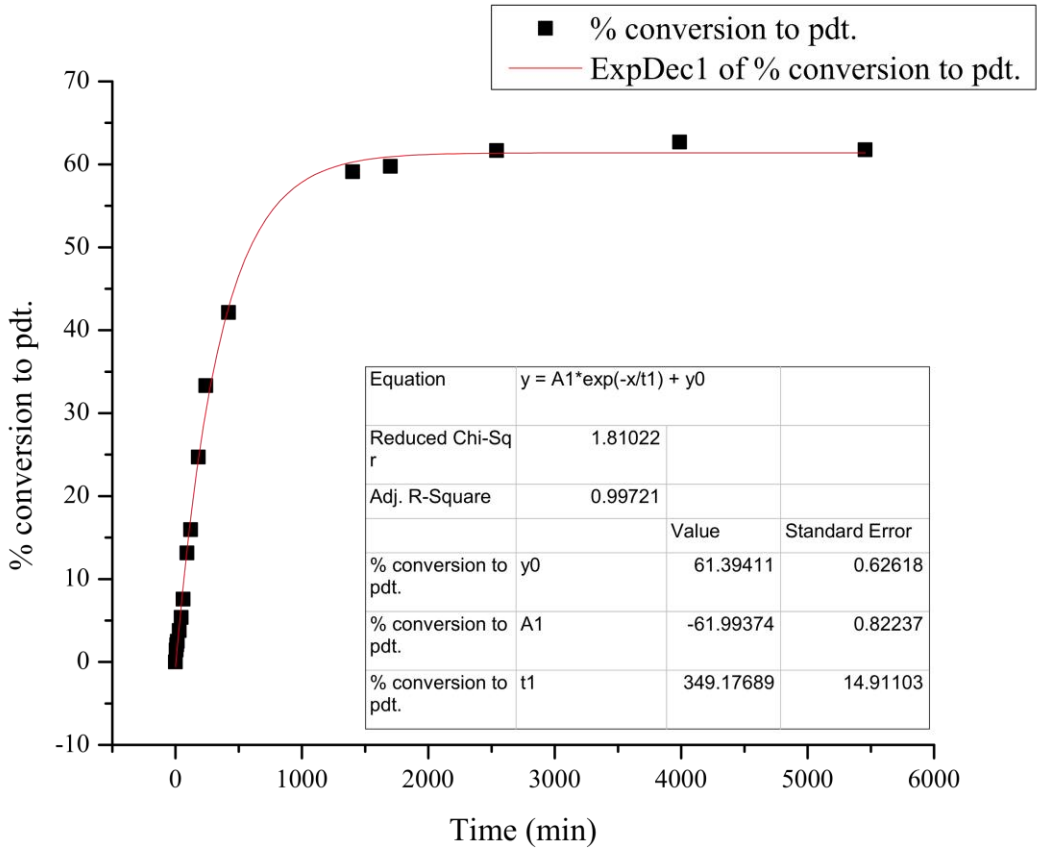

Half-Life = 591 min

Catalyst **4g**: Run 2

Time (min)	Standard (µmol)	Standard Area	Product Area	Product (µmol)	% Product
0	254.0	1.00	0.00	0.0	0.0
60	254.0	6065.59	515.52	25.7	7.6
120	254.0	6510.57	1245.10	57.8	17.1
180	254.0	6607.95	1771.45	81.1	23.9
240	254.0	6189.82	2115.38	103.3	30.5
300	254.0	6698.55	2625.93	118.5	35.0
360	254.0	7265.78	3099.91	129.0	38.1
420	254.0	7283.71	3425.02	142.2	41.9
595	254.0	8157.31	4603.36	170.6	50.3
1224	254.0	7028.87	5247.63	225.7	66.6
1620	254.0	7270.08	5561.25	231.3	68.2
2640	254.0	5815.63	4528.96	235.5	69.5
4026	254.0	6589.75	5139.52	235.8	69.6
5673	254.0	7112.28	5681.54	241.5	71.2

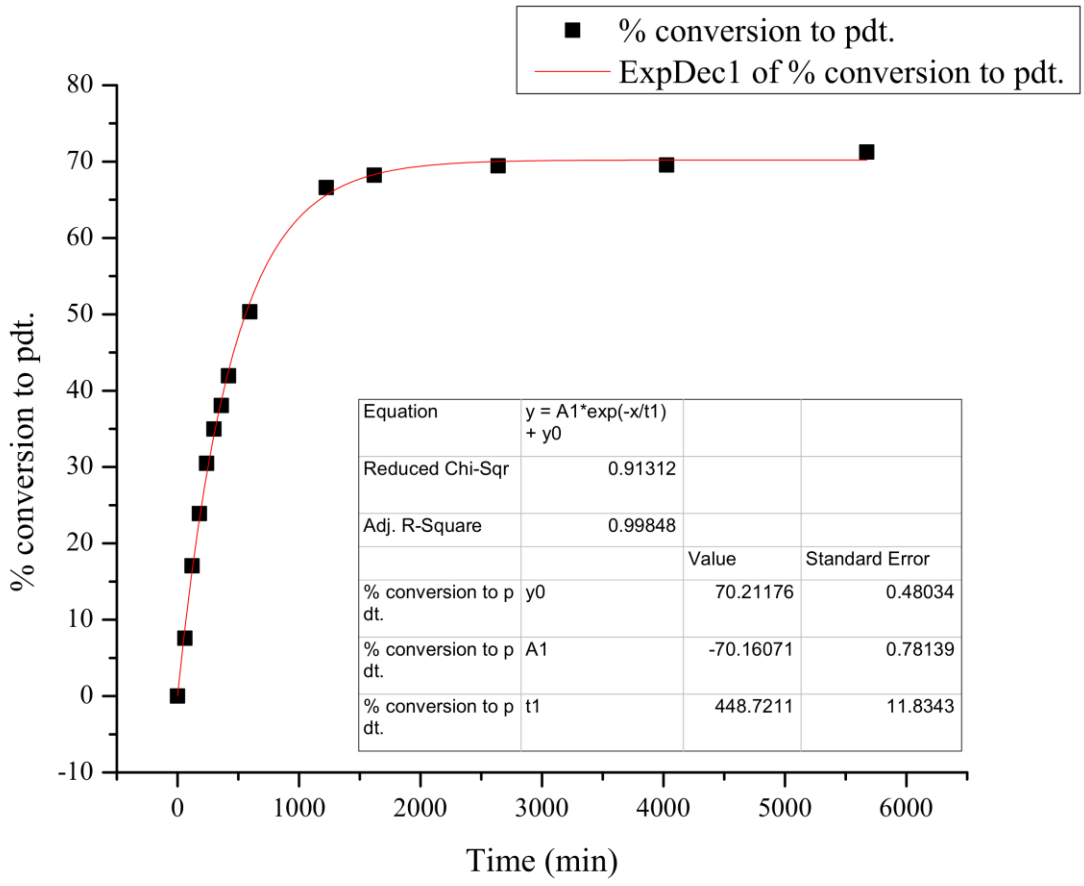

Half-Life = 558 min

Average Half-Life = 575 min

Catalyst **5g**: Run 1

Time (min)	Standard (µmol)	Standard Area	Product Area	Product (µmol)	% Product
0	254.0	1.00	0.00	0.0	0.0
20	254.0	6704.03	24.82	1.1	0.3
40	254.0	7061.44	29.39	1.3	0.4
60	254.0	6941.09	29.71	1.3	0.4
120	254.0	6517.55	37.89	1.8	0.5
180	254.0	7593.26	58.47	2.3	0.7
240	254.0	7134.07	73.46	3.1	0.9
1397	254.0	7796.78	1482.19	57.5	17.0
1695	254.0	7398.42	1949.06	79.7	23.5
2535	254.0	7565.42	3368.12	134.6	39.7
3983	254.0	7863.07	5236.10	201.3	59.4
5450	254.0	7261.97	5102.63	212.5	62.7
5982	254.0	6722.67	4899.27	220.4	65.0

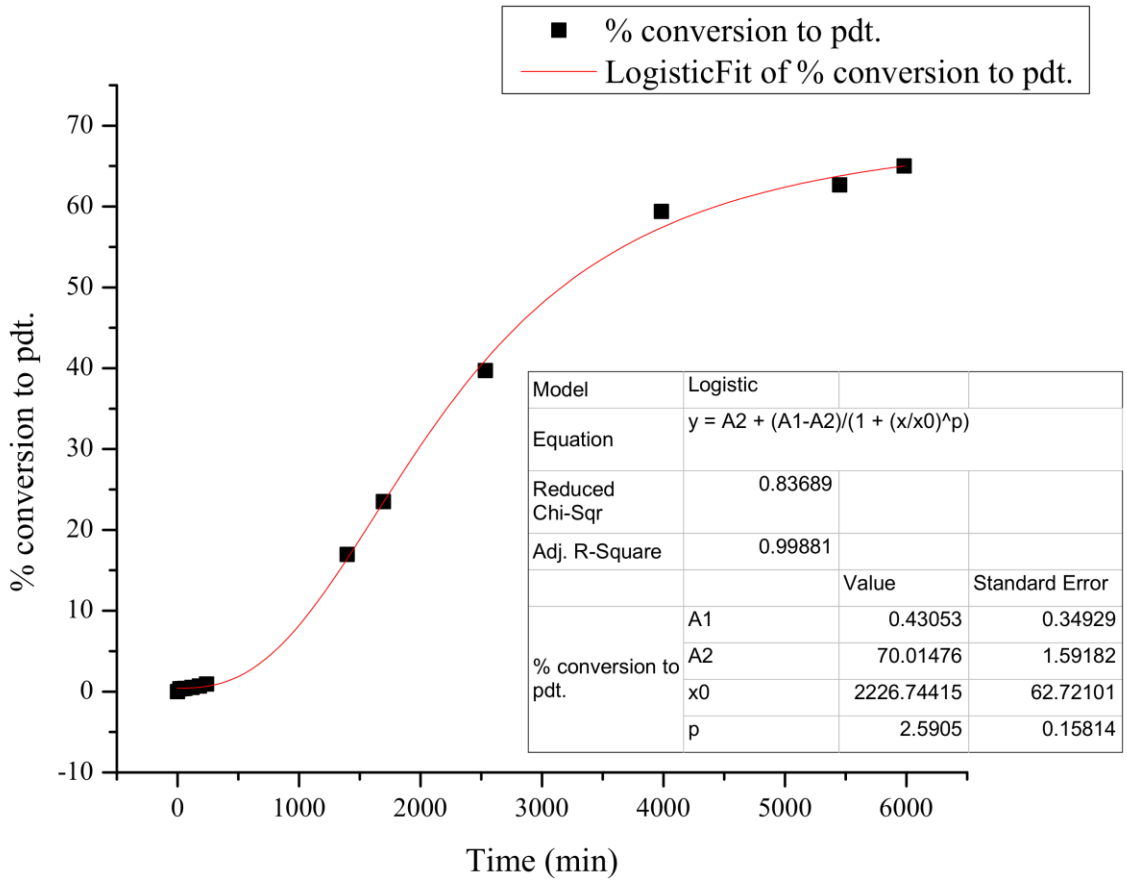

Half-Life = 3160 min

Catalyst **5g**: Run 2

Time (min)	Standard (µmol)	Standard Area	Product Area	Product (µmol)	% Product
0	254.0	1.00	0.00	0.0	0.0
20	254.0	6810.74	22.83	1.0	0.3
40	254.0	7555.66	31.60	1.3	0.4
60	254.0	7428.10	26.43	1.1	0.3
120	254.0	6894.61	34.74	1.5	0.4
180	254.0	7584.21	47.24	1.9	0.6
240	254.0	6978.06	54.40	2.4	0.7
420	254.0	7301.12	127.65	5.3	1.6
1397	254.0	7504.53	1322.42	53.3	15.7
1695	254.0	7643.58	1916.64	75.8	22.4
2535	254.0	7144.83	3052.49	129.2	38.1
3983	254.0	7119.85	4665.06	198.1	58.4
5450	254.0	7699.37	5449.40	214.0	63.1
5982	254.0	6928.39	5159.28	225.2	66.4

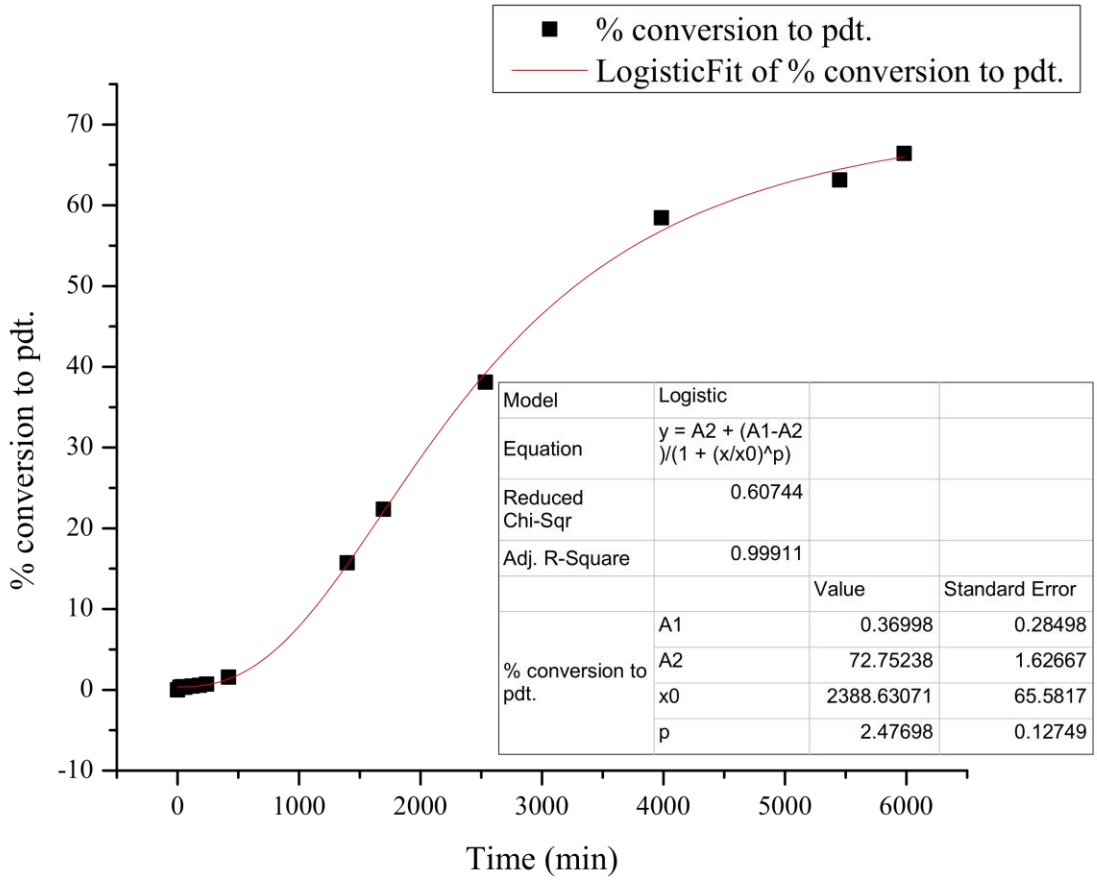

Half-Life = 3273 min

Average Half-Life = 3216 min

Kinetic Analyzses of Catalysts in Series H

Catalyst **1h**: Run 1

Time (min)	Standard (µmol)	Standard Area	Product Area	Product (µmol)	% Product
0	254.0	1.00	0.00	0.0	0.0
1276	254.0	5044.18	1520.27	91.1	26.9
2888	254.0	6706.97	3865.74	174.3	51.4
3852	254.0	5659.38	3583.60	191.5	56.5
4543	254.0	7840.04	5115.84	197.3	58.2
5702	254.0	6757.42	4455.41	199.4	58.8

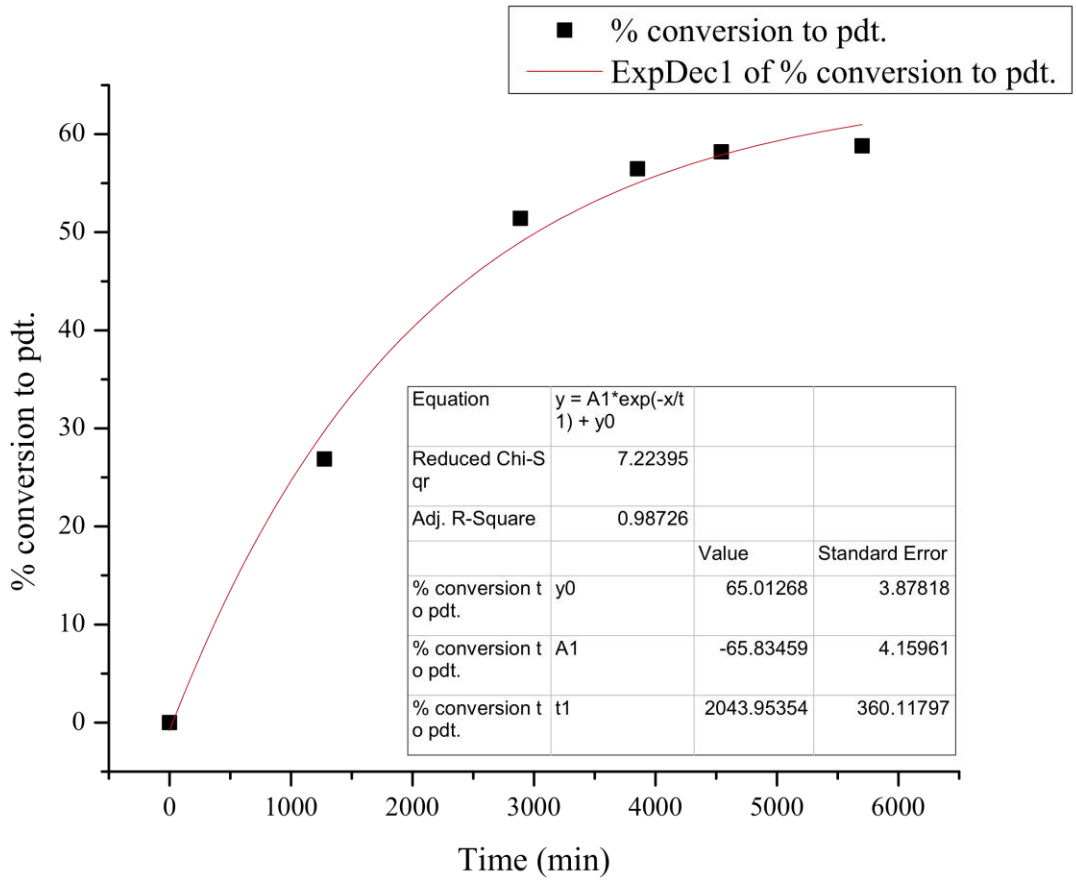

Half-Life = 3021 min

Catalyst **1h**: Run 2

Time (min)	Standard (µmol)	Standard Area	Product Area	Product (µmol)	% Product
0	254.0	1.00	0.00	0.0	0.0
1276	254.0	5857.86	2095.20	108.1	31.9
2888	254.0	6751.11	3896.04	174.5	51.5
3852	254.0	7596.78	5098.87	202.9	59.9
4543	254.0	7845.55	5377.01	207.2	61.1
5702	254.0	7161.18	5379.07	227.1	67.0

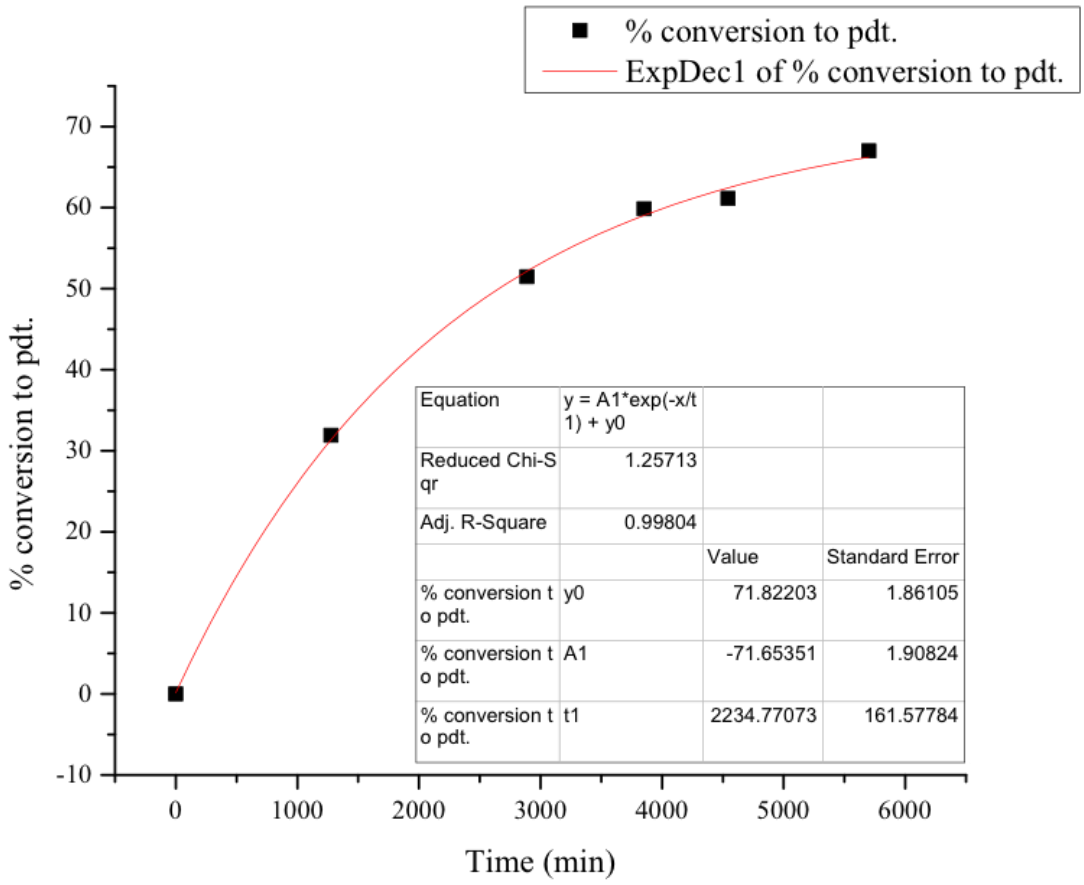

Half-Life = 2657 min

Average Half-Life = 2839 min

Catalyst **2h**: Run 1

Time (min)	Standard (µmol)	Standard Area	Product Area	Product (µmol)	% Product
0	254.0	1.00	0.00	0.0	0.0
1276	254.0	6692.21	2912.20	131.6	38.8
2888	254.0	6891.21	4552.77	199.8	58.9
3852	254.0	6510.76	4440.45	206.2	60.8
4543	254.0	6905.02	4875.40	213.5	63.0
5702	254.0	6350.41	4321.55	205.8	60.7

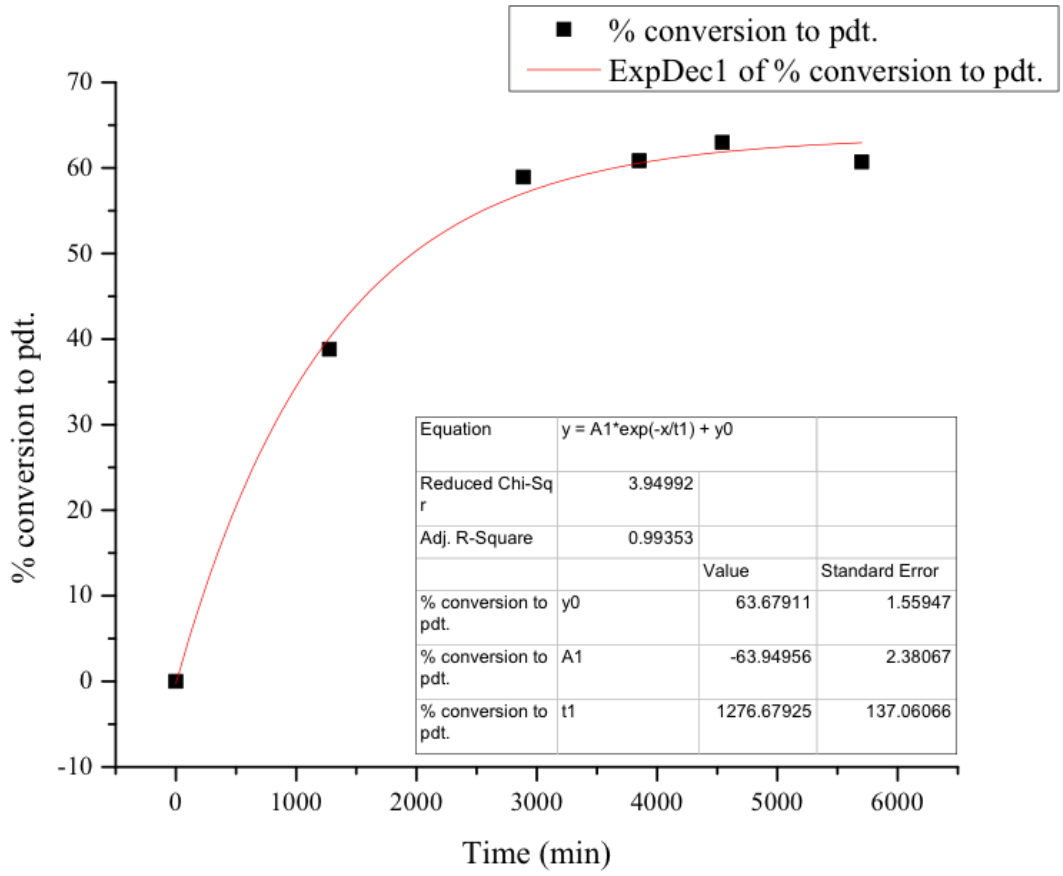

Half-Life = 1969 min

Catalyst **2h**: Run 2

Time (min)	Standard (µmol)	Standard Area	Product Area	Product (µmol)	% Product
0	254.4	1.00	0.00	0.0	0.0
60	254.4	7952.52	47.53	1.8	0.5
423	254.4	7724.03	510.09	20.0	5.9
1102	254.4	7640.90	2267.59	89.9	26.5
1468	254.4	7368.77	2733.70	112.3	33.1
2550	254.4	7712.36	3827.83	150.3	44.3
4042	254.4	9474.91	5588.37	178.6	52.7
5620	254.4	7859.00	4951.41	190.8	56.3

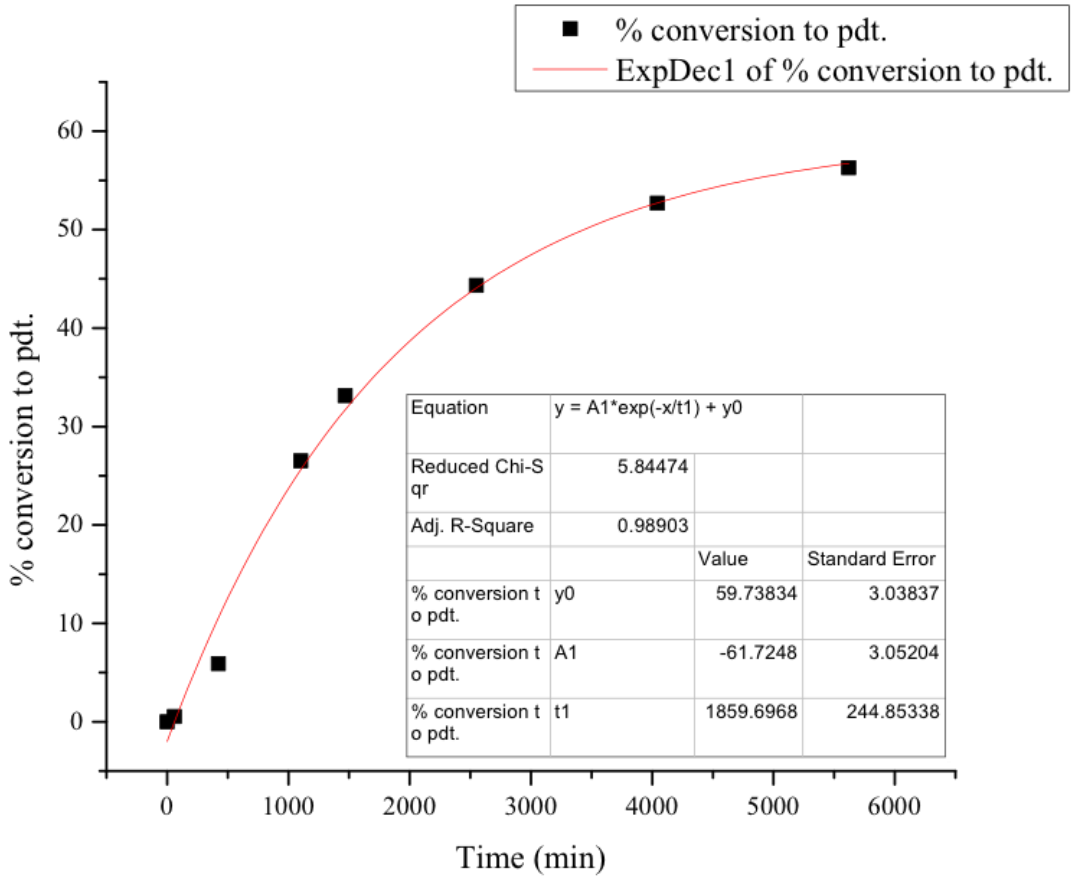

Half-Life = 3434 min

Average Half-Life = 2702 min

Catalyst **3h**: Run 1

Time (min)	Standard (µmol)	Standard Area	Product Area	Product (µmol)	% Product
0	254.0	1.00	0.00	0.0	0.0
60	254.0	5737.46	26.01	1.4	0.4
414	254.0	6992.29	711.57	30.8	9.1
1187	254.0	6390.86	2281.63	107.9	32.1
1649	254.0	7496.73	3125.42	126.1	37.5
3188	254.0	5325.90	2687.77	152.6	45.4
4516	254.0	7979.26	4269.13	161.8	48.1
5912	254.0	7060.27	3903.97	167.2	49.7

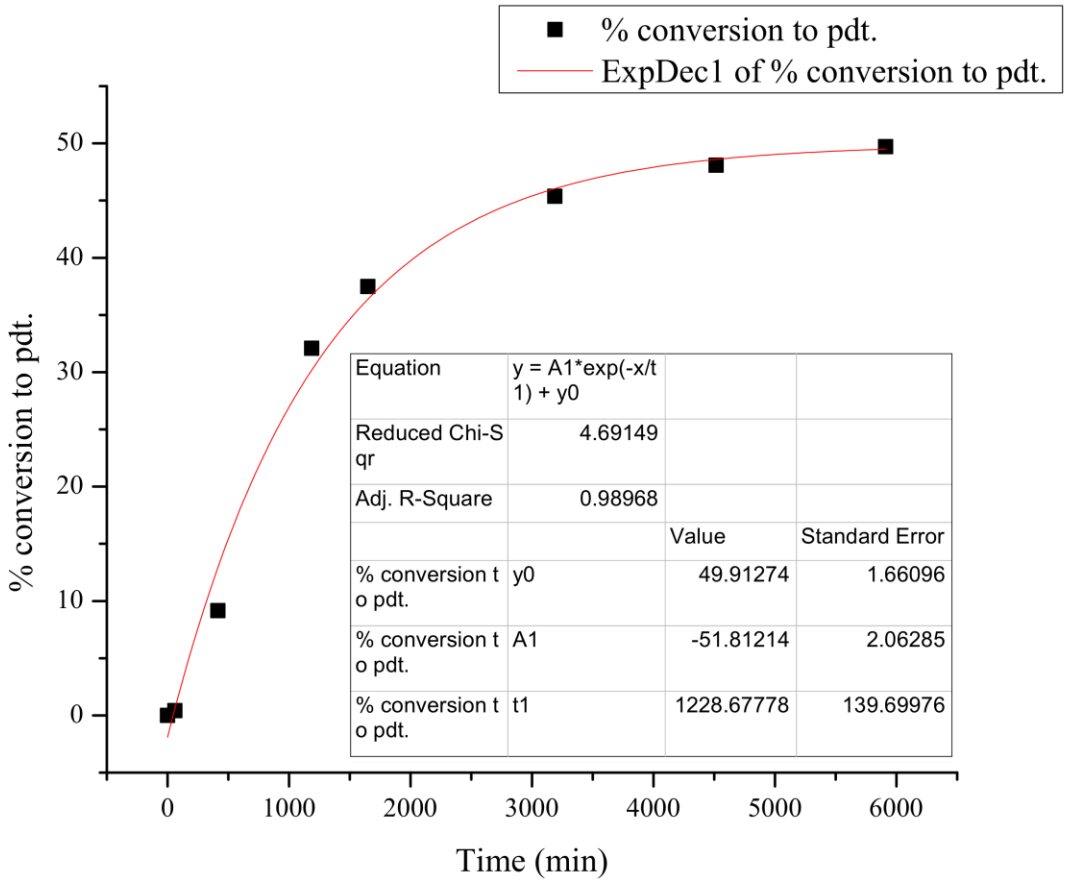

Half-Life = 5912 min

Catalyst **3h**: Run 2

Time (min)	Standard (µmol)	Standard Area	Product Area	Product (µmol)	% Product
0	254.0	1.00	0.00	0.0	0.0
60	254.0	6080.03	35.79	1.8	0.5
414	254.0	6877.12	590.05	25.9	7.7
1187	254.0	6898.09	2455.45	107.6	32.0
1649	254.0	6284.74	2781.60	133.8	39.8
3188	254.0	6769.44	3985.13	178.0	52.9
4516	254.0	6445.00	4194.09	196.8	58.5
5912	254.0	6846.86	4804.95	212.2	63.1

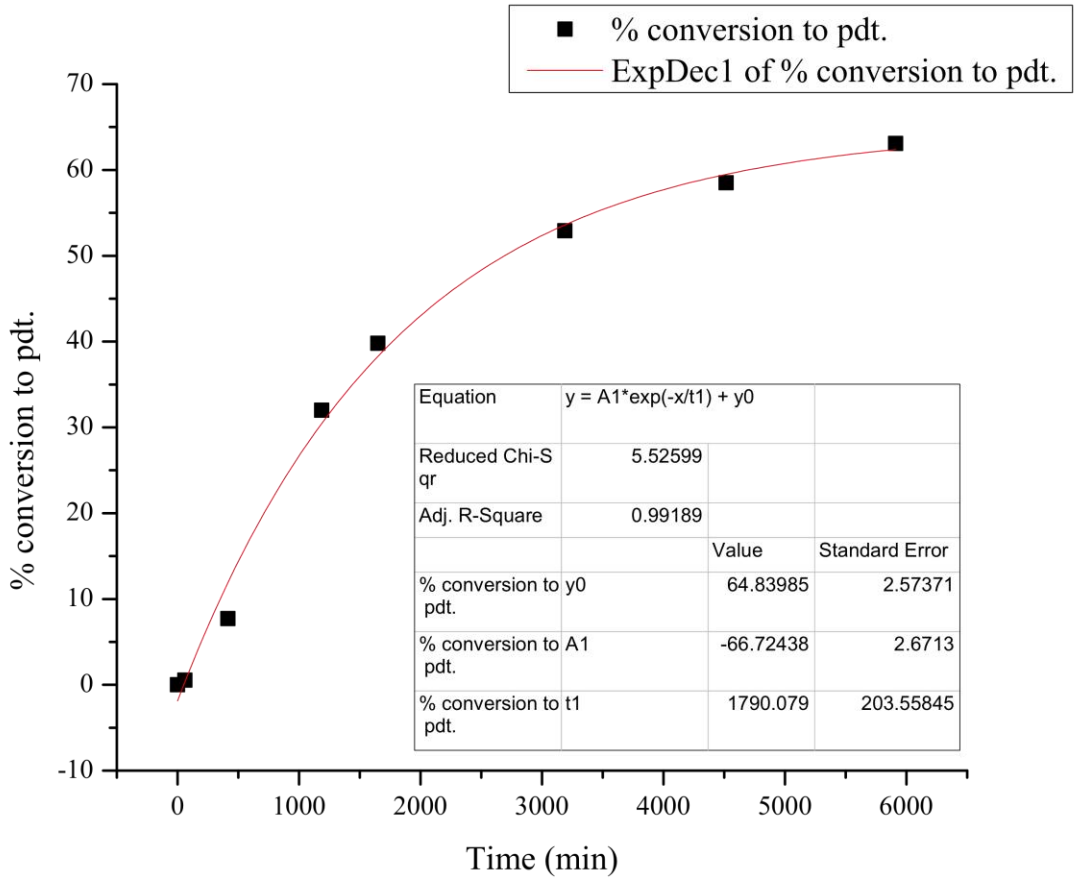

Half-Life = 2691 min

Average Half-Life = 4301

Catalyst **4h**: Run 1

Time (min)	Standard (µmol)	Standard Area	Product Area	Product (µmol)	% Product
0	254.0	1.00	0.00	0.0	0.0
60	254.0	6670.25	59.28	2.7	0.8
414	254.0	7258.66	790.51	32.9	9.7
1187	254.0	7639.41	2535.21	100.3	29.6
1649	254.0	6456.36	2853.02	133.6	39.4
3188	254.0	7128.59	4175.76	177.1	52.2
4516	254.0	6641.67	4380.18	199.4	58.8
5912	254.0	6893.22	4624.21	202.8	59.8

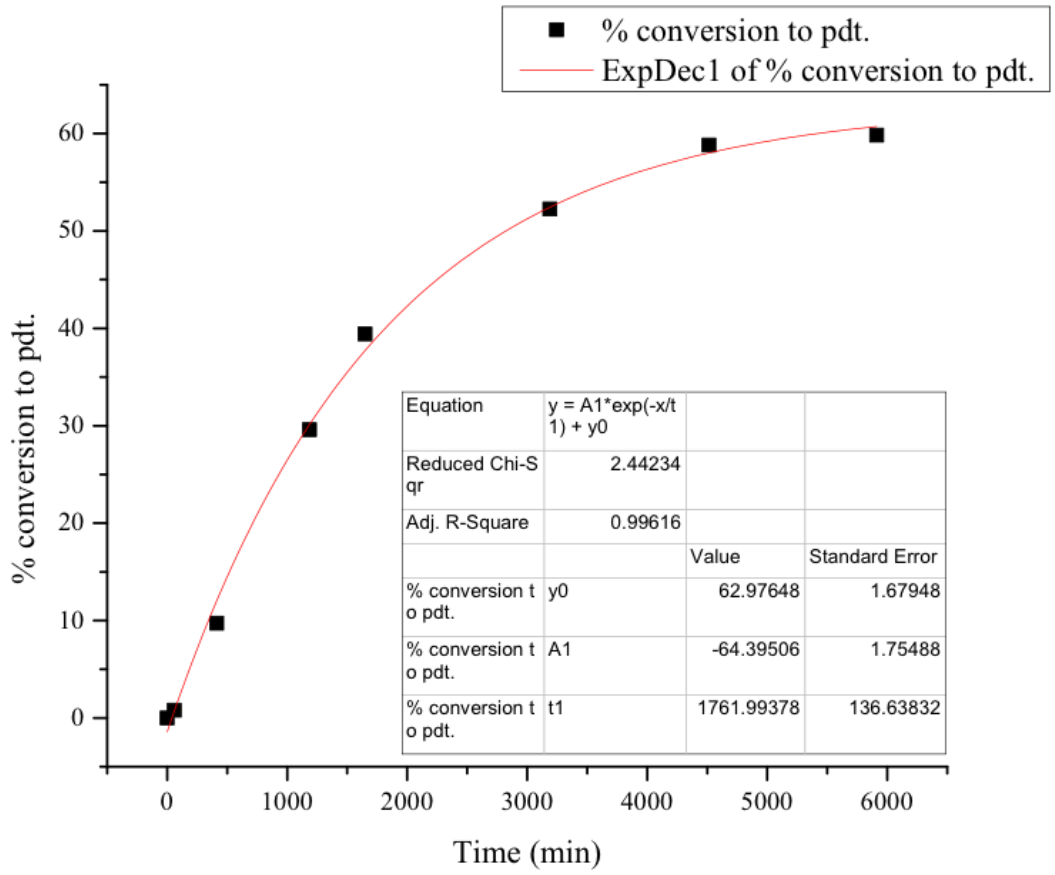

Half-Life = 2823 min

Catalyst **4h**: Run 2

Time (min)	Standard (µmol)	Standard Area	Product Area	Product (µmol)	% Product
0	254.4	1.00	0.00	0.0	0.0
60	254.4	7350.67	32.88	1.4	0.4
423	254.4	7464.41	725.62	29.4	8.7
1102	254.4	7208.55	2300.29	96.6	28.5
1468	254.4	7326.11	2862.31	118.3	34.9
2550	254.4	7321.29	3977.12	164.5	48.5
4042	254.4	9678.18	6186.04	193.6	57.1
5620	254.4	7968.50	5485.01	208.5	61.5

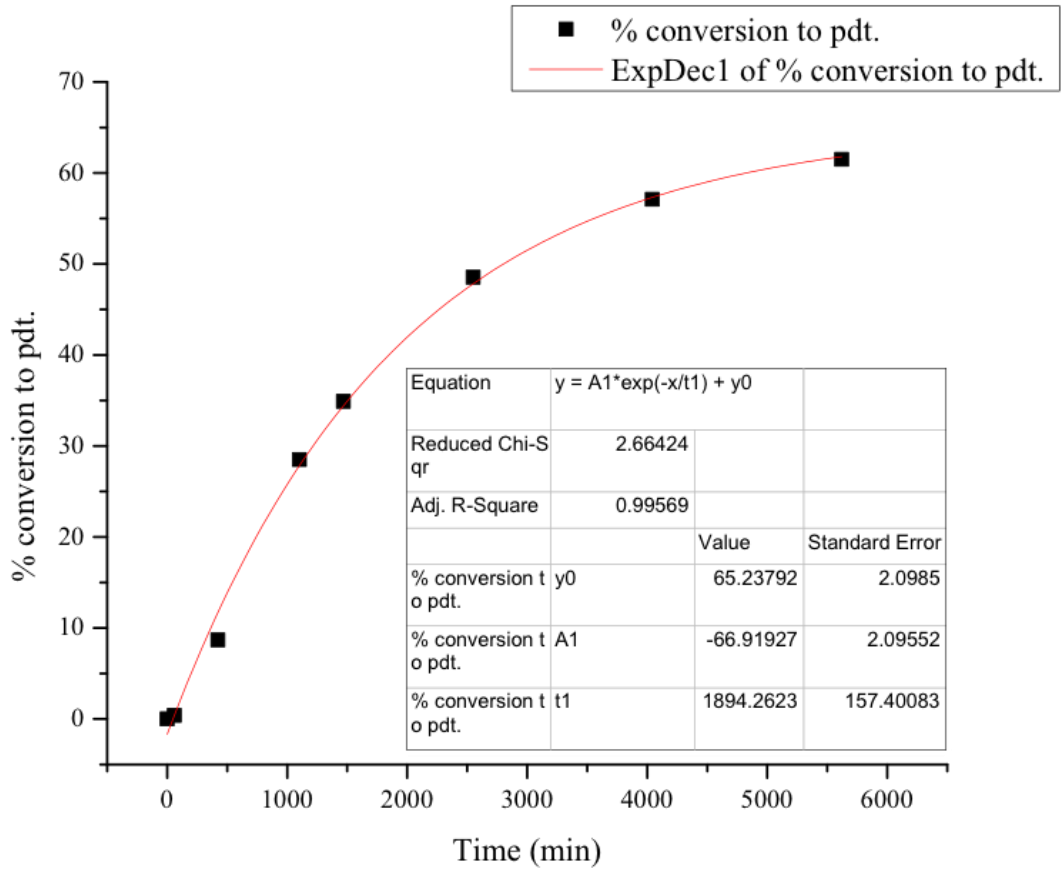

Half-Life = 2803 min

Average Half-Life = 2813 min

Tabular Summary of Kinetics Data

Catalyst	Run #	Exponential Fit Equation	y0	A1	t1		R^2	Half-Life, $t_{1/2}$ (min.)	mean half life, $t_{1/2}$ (min.)	Std. Dev. Half Life, $t_{1/2}$ (min.)	% Std. Dev./Mean
2a	1	See Logistic Fit Table						363	351	15.9	4.5
2a	2	y = A1*exp(-x/t1) + y0	75.24479	-79.422	296.747		0.9862	340			
5a	1	y = A1*exp(-x/t1) + y0	71.18727	-74.391	272.916		0.9920	343	310	46.6	15.0
5a	2	y = A1*exp(-x/t1) + y0	83.14673	-85.271	292.987		0.9964	277			
1b	1	y = A1*exp(-x/t1) + y0	88.03818	-94.221	22.814		0.9711	21	21	0.2	0.9
1b	2	y = A1*exp(-x/t1) + y0	82.6915	-87.724	21.243		0.9868	21			
2b	1	y = A1*exp(-x/t1) + y0	79.59908	-86.498	230.774		0.9748	247	246	2.5	1.0
2b	2	y = A1*exp(-x/t1) + y0	75.8665	-79.473	217.282		0.9808	244			
4b	1	y = A1*exp(-x/t1) + y0	76.50725	-79.456	24.419		0.9835	27	29	2.4	8.5
4b	2	y = A1*exp(-x/t1) + y0	75.42997	-77.794	27.032		0.9850	30			
5b	1	y = A1*exp(-x/t1) + y0	79.5476	-83.213	300.471		0.9911	311	312	1.2	0.4
5b	2	y = A1*exp(-x/t1) + y0	74.4181	-78.133	268.977		0.9910	313			
1c	1	y = A1*exp(-x/t1) + y0	80.07375	-80.413	126.654		0.9968	125	87	53.3	61.4
1c	2	y = A1*exp(-x/t1) + y0	78.68537	-80.469	47.630		0.9838	49			
2c	1	y = A1*exp(-x/t1) + y0	71.04348	-67.956	16.652		0.9823	20	19	1.0	5.5
2c	2	y = A1*exp(-x/t1) + y0	72.02988	-69.997	15.622		0.9921	18			
3c	1	y = A1*exp(-x/t1) + y0	77.25537	-78.110	10.146		0.9928	11	9	1.8	18.7
3c	2	y = A1*exp(-x/t1) + y0	78.46948	-78.940	8.026		0.9967	8			
4c	1	y = A1*exp(-x/t1) + y0	75.31615	-72.481	849.155		0.9954	893	851	59.4	7.0
4c	2	y = A1*exp(-x/t1) + y0	70.65912	-67.409	684.260		0.9958	809			
5c	1	y = A1*exp(-x/t1) + y0	64.56136	-67.939	358.377		0.9685	552	594	59.2	10.0
5c	2	y = A1*exp(-x/t1) + y0	64.49535	-62.989	432.714		0.9697	636			
1d	1	y = A1*exp(-x/t1) + y0	59.83595	-60.380	83.405		0.9984	151	126	35.9	28.5
1d	2	y = A1*exp(-x/t1) + y0	61.87681	-62.416	60.653		0.9991	101			
2d	1	y = A1*exp(-x/t1) + y0	79.38606	-75.780	12.491		0.9898	12	15	5.0	32.7
2d	2	y = A1*exp(-x/t1) + y0	69.29378	-65.166	15.559		0.9903	19			
3d	1	y = A1*exp(-x/t1) + y0	79.71041	-78.566	14.264		0.9882	14	11	3.7	33.1
3d	2	y = A1*exp(-x/t1) + y0	73.33839	-73.891	7.475		0.9971	9			
4d	1	y = A1*exp(-x/t1) + y0	78.9461	-77.168	11.855		0.9910	12	11	0.5	4.2
4d	2	y = A1*exp(-x/t1) + y0	72.45223	-72.272	9.375		0.9968	11			

Tabular Summary of Kinetics Data, cont.

5d	1	y = A1*exp(-x/t1) + y0	77.29513	-79.438	471.051		0.9728	503	546	59.9	11.0
5d	2	y = A1*exp(-x/t1) + y0	77.74945	-75.886	584.374		0.9872	588			
1e	1	y = A1*exp(-x/t1) + y0	73.75451	-71.259	23.046		0.9792	25	19	8.3	42.5
1e	2	y = A1*exp(-x/t1) + y0	74.9476	-76.094	12.218		0.9949	14			
2e	1	y = A1*exp(-x/t1) + y0	75.72533	-75.076	18.011		0.9910	19	16	4.3	26.8
2e	2	y = A1*exp(-x/t1) + y0	72.67163	-71.591	11.436		0.9980	13			
3e	1	y = A1*exp(-x/t1) + y0	74.91512	-73.589	47.771		0.9977	52	45	10.0	22.3
3e	2	y = A1*exp(-x/t1) + y0	72.46091	-71.959	32.328		0.9973	38			
4e	1	y = A1*exp(-x/t1) + y0	76.05616	-75.432	8.261		0.9985	9	9	0.4	4.4
4e	2	y = A1*exp(-x/t1) + y0	76.13371	-76.067	8.752		0.9908	9			
5e	1	y = A1*exp(-x/t1) + y0	72.77079	-72.061	477.722		0.9892	550	537	18.2	3.4
5e	2	y = A1*exp(-x/t1) + y0	74.53471	-76.004	463.980		0.9703	525			
1f	1	y = A1*exp(-x/t1) + y0	78.59378	-76.584	24.942		0.9944	25	19	7.3	37.3
1f	2	y = A1*exp(-x/t1) + y0	77.05268	-76.456	13.775		0.9996	14			
2f	1	y = A1*exp(-x/t1) + y0	93.94348	-91.725	52.764		0.9967	39	44	6.8	15.7
2f	2	y = A1*exp(-x/t1) + y0	80.08334	-77.153	51.499		0.9914	49			
3f	1	y = A1*exp(-x/t1) + y0	86.42536	-84.627	43.064		0.9974	36	32	5.4	16.6
3f	2	y = A1*exp(-x/t1) + y0	85.20084	-82.584	33.633		0.9899	29			
4f	1	y = A1*exp(-x/t1) + y0	74.21342	-73.046	28.311		0.9977	31	30	2.0	6.8
4f	2	y = A1*exp(-x/t1) + y0	69.60957	-69.438	22.448		0.9970	28			
5f	1	y = A1*exp(-x/t1) + y0	83.76239	-84.362	484.874		0.9887	444	442	3.3	0.7
5f	2	y = A1*exp(-x/t1) + y0	93.37255	-94.144	566.935		0.9909	439			
1g	1	y = A1*exp(-x/t1) + y0	76.72075	-78.489	2686.133		0.9958	2894	3692	1127.5	30.5
1g	2	y = A1*exp(-x/t1) + y0	66.53598	-68.090	3171.727		0.9966	4489			
2g	1	y = A1*exp(-x/t1) + y0	75.84258	-77.126	188.816		0.9949	206	196	14.9	7.6
2g	2	y = A1*exp(-x/t1) + y0	74.77431	-74.129	169.135		0.9861	185			
3g	1	y = A1*exp(-x/t1) + y0	81.07378	-84.168	195.772		0.9936	195	200	6.3	3.1
3g	2	y = A1*exp(-x/t1) + y0	76.47531	-78.528	187.572		0.9950	204			
4g	1	y = A1*exp(-x/t1) + y0	61.39411	-61.994	349.177		0.9972	591	575	23.4	4.1
4g	2	y = A1*exp(-x/t1) + y0	70.21176	-70.161	448.721		0.9985	558			
1h	1	y = A1*exp(-x/t1) + y0	65.01268	-65.835	2043.954		0.9873	3021	2839	257.7	9.1
1h	2	y = A1*exp(-x/t1) + y0	71.82203	-71.654	2234.771		0.9980	2657			
2h	1	y = A1*exp(-x/t1) + y0	63.67911	-63.950	1276.679		0.9935	1969	2702	1036.1	38.4
2h	2	y = A1*exp(-x/t1) + y0	59.73834	-61.725	1859.697		0.9890	3434			

Tabular Summary of Kinetics Data, cont.

3h	1	y = A1*exp(-x/t1) + y0	49.91274	-51.812	1228.678		0.9897	5912	4301	2277.6	53.0
3h	2	y = A1*exp(-x/t1) + y0	64.83985	-66.724	1790.079		0.9919	2691			
4h	1	y = A1*exp(-x/t1) + y0	62.97648	-64.395	1761.994		0.9962	2823	2813	13.9	0.5
4h	2	y = A1*exp(-x/t1) + y0	65.23792	-66.919	1894.262		0.9957	2803			

Catalyst	Run #	Logistic Fit Equation	A1	A2	x0	p	R_2	Half-Life, $t_{1/2}$ (min.)	Mean Half-Life, $t_{1/2}$ (min.)	Std. Dev. Half Life, $t_{1/2}$ (min.)	% Std. Dev./Mean
1a	1	y = A2 + (A1-A2)/(1+(x/x0)^p)	0.3875	71.5254	16.131	3.7217	0.9968	20	21	1.6	7.5
1a	2	y = A2 + (A1-A2)/(1+(x/x0)^p)	0.2735	76.7689	18.787	3.4760	0.9966	22			
2a	1	y = A2 + (A1-A2)/(1+(x/x0)^p)	1.1706	76.6484	273.939	2.1601	0.9992	363	351	15.9	4.5
2a	2	See Exponential Fit						340			
3a	1	y = A2 + (A1-A2)/(1+(x/x0)^p)	0.3986	88.1119	74.526	2.0139	0.9981	85	82	4.8	5.9
3a	2	y = A2 + (A1-A2)/(1+(x/x0)^p)	1.3015	84.9240	66.122	1.9978	0.9982	78			
4a	1	y = A2 + (A1-A2)/(1+(x/x0)^p)	1.2301	91.6541	40.594	1.8218	0.9967	44	44	0.3	0.7
4a	2	y = A2 + (A1-A2)/(1+(x/x0)^p)	1.4027	85.6183	37.465	1.9753	0.9955	44			
3b	1	y = A2 + (A1-A2)/(1+(x/x0)^p)	0.3867	76.6582	81.822	2.4361	0.9938	106	95	14.3	15.0
3b	2	y = A2 + (A1-A2)/(1+(x/x0)^p)	0.5777	80.0775	71.717	2.8616	0.9941	85			
5g	1	y = A2 + (A1-A2)/(1+(x/x0)^p)	0.4305	70.0148	2226.744	2.5905	0.9988	3160	3216	79.5	2.5
5g	2	y = A2 + (A1-A2)/(1+(x/x0)^p)	0.3700	72.7524	2388.631	2.4770	0.9991	3273			

5.2.3. Variable Stirring Speed Kinetics

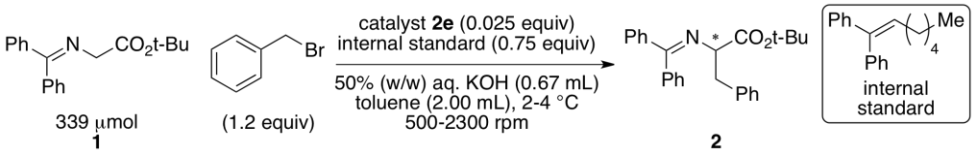

A 2 mL scintillation vial was fitted with a Teflon lined rubber septum and *tert*-butyl 2-(diphenylmethyleneamino)acetate (100 mg, 0.34 mmol), and catalyst **2e** (4.5 mg, 8.48 μmol, 0.025 equiv) were added. The liquid reagents, benzyl bromide (800 μL, 0.51 M in toluene, 1.2 equiv), internal standard (790 μL, 0.32 M in tolune, 0.75 equiv), and toluene (410 μL) were added via syringe. Then, a 1.5 cm egg-shaped magnetic stir bar was placed in the vial and the contents were briefly agitated in an ultrasonic bath (10-20 s). Reaction vials were then transferred to a cold room maintained at 2-4 ^{o}C and were allowed to equilibrate for at least 1 h.

The stirring was conducted with the aid of an adjustable electric motor, which had been calibrated for 500, 1000, 1500, 2000, and 2300 rpm. Lastly, 50% aq. (w/w) KOH solution (670 μL, 11.9 mmol, 17.8 M, 35.0 equiv) was added to the rapidly stirred organic phase. Aliquots were taken at the indicated times and analyzed as follows.

The internal standard employed in these reactions was 1,1-diphenyl-1-heptene.

500 rpm, run #1:

Time (min)	Standard (µmol)	Standard Area	Product Area	Product (µmol)	% Product
0	254.4	1.00	0.00	0.0	0.0
2	254.4	6437.92	132.45	6.2	1.8
4	254.4	6637.03	281.99	12.9	3.8
6	254.4	7181.21	433.58	18.3	5.4
8	254.4	7047.37	587.57	25.2	7.4
10	254.4	7057.40	758.58	32.6	9.6
20	254.4	7078.95	1597.66	68.3	20.2
30	254.4	6943.09	1967.14	85.8	25.3
45	254.4	7163.60	2650.90	112.1	33.1
60	254.4	7258.78	3303.17	137.8	40.7
120	254.4	7982.79	4586.44	174.0	51.3

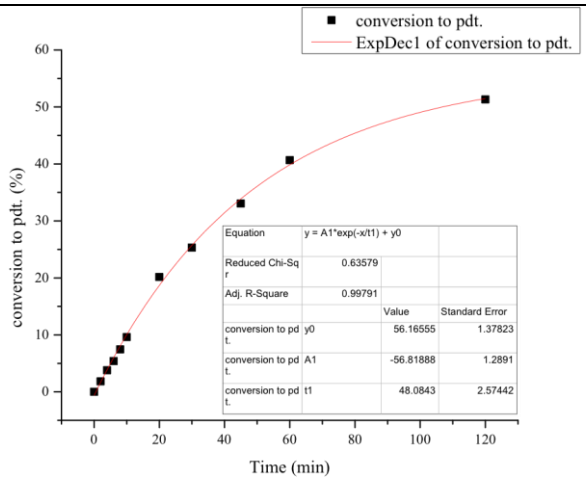

Half Life = 106.8 min

500 rpm, run #2:

Time (min)	Standard (µmol)	Standard Area	Product Area	Product (µmol)	% Product
0	254.4	1.00	0.00	0.0	0.0
2	254.4	7631.87	115.88	4.6	1.4
4	254.4	7120.02	248.01	10.5	3.1
6	254.4	7015.93	375.41	16.2	4.8
8	254.4	8023.84	555.25	21.0	6.2
10	254.4	6709.50	615.91	27.8	8.2
20	254.4	7292.47	1727.03	71.7	21.2
30	254.4	7631.40	2453.57	97.4	28.7
45	254.4	7739.22	3125.34	122.3	36.1
60	254.4	7620.41	3433.52	136.4	40.3
120	254.4	7005.24	3274.78	141.6	41.8

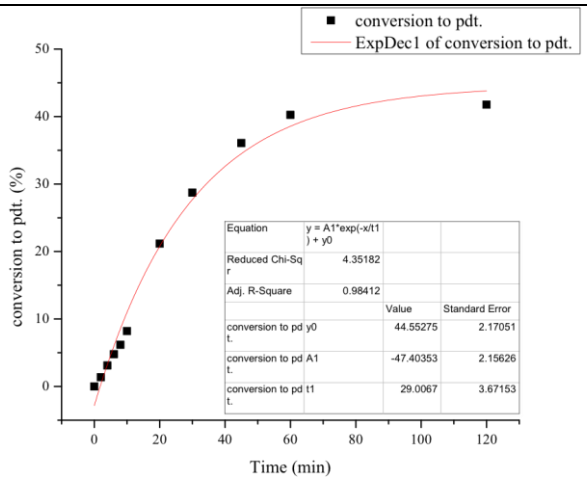

Half-Life = N/A

Mean Half-Life = 106.8 min

Std. Dev. Half-Life = N/A

1000 rpm, run #1:

Time (min)	Standard (µmol)	Standard Area	Product Area	Product (µmol)	% Product
0	254.4	1.00	0.00	0.0	0.0
2	254.4	6907.60	666.70	29.2	8.6
4	254.4	7569.94	969.85	38.8	11.4
6	254.4	7271.96	1284.57	53.5	15.8
8	254.4	7109.72	1969.87	83.9	24.8
10	254.4	6975.17	2564.42	111.3	32.8
20	254.4	7507.12	4052.65	163.5	48.2
30	254.4	7625.62	5216.00	207.1	61.1
60	254.4	7040.61	5230.99	225.0	66.4
90	254.4	7544.90	5847.38	234.7	69.2
120	254.4	7749.85	6435.76	251.5	74.2

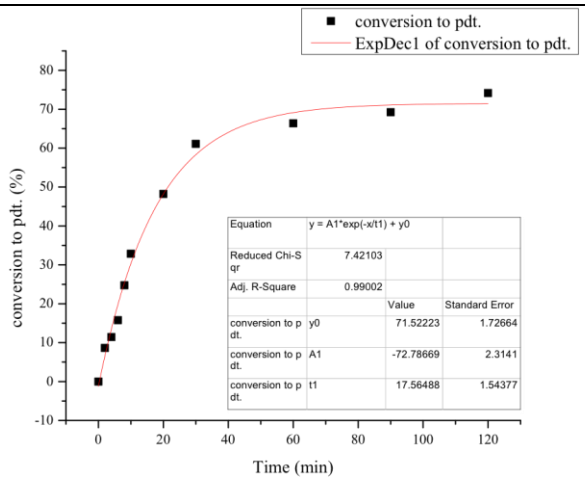

Half-Life = 21.4 min

1000 rpm, run #2:

Time (min)	Standard (µmol)	Standard Area	Product Area	Product (µmol)	% Product
0	254.4	1.00	0.00	0.0	0.0
2	254.4	7742.97	635.95	24.9	7.3
4	254.4	7798.82	1196.63	46.5	13.7
6	254.4	8498.09	1876.61	66.9	19.7
8	254.4	7154.80	1967.00	83.3	24.6
10	254.4	7919.97	2668.84	102.0	30.1
20	254.4	8827.49	4574.43	156.9	46.3
30	254.4	7102.79	4089.52	174.4	51.4
60	254.4	8225.70	5931.56	218.4	64.4
90	254.4	7150.95	6123.30	259.3	76.5
120	254.4	8223.83	7148.37	263.2	77.7

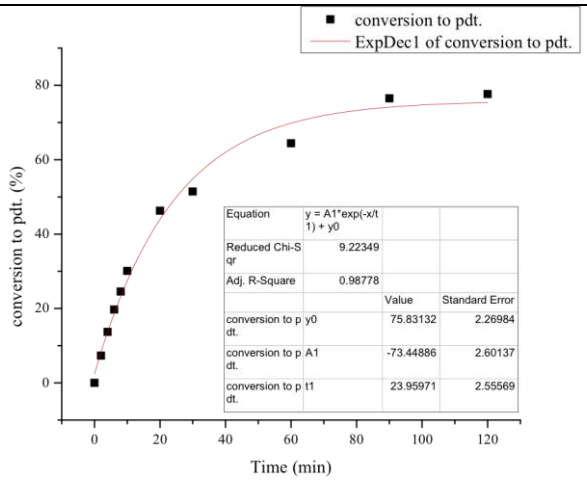

Half-Life = 25.0 min

1000 rpm, run #3:

Time (min)	Standard (µmol)	Standard Area	Product Area	Product (µmol)	% Product
0	253.0	1.00	0.00	0.0	0.0
2	253.0	7406.06	317.85	12.9	3.8
4	253.0	7134.87	808.99	34.1	10.1
6	253.0	7720.24	1284.24	50.1	14.8
8	253.0	7612.40	1655.88	65.5	19.3
10	253.0	7429.29	1966.75	79.7	23.5
20	253.0	7685.22	3678.26	144.1	42.5
30	253.0	7854.41	4155.35	159.3	47.0
60	253.0	7835.35	4663.45	179.3	52.9
90	253.0	7600.92	5056.73	200.4	59.1
120	253.0	6996.34	5046.64	217.2	64.1

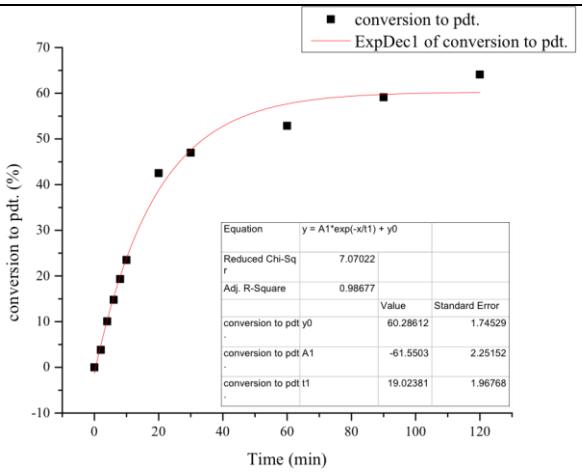

Half-Life = 34.0 min

Mean Half-Life = 26.8 min

Std. Dev. Half-Life = 6.5 min

1500 rpm, run #1:

Time (min)	Standard (µmol)	Standard Area	Product Area	Product (µmol)	% Product
0	254.4	1.00	0.00	0.0	0.0
1	254.4	8377.79	483.31	17.5	5.2
2	254.4	7465.36	892.07	36.2	10.7
4	254.4	8402.12	1942.10	70.0	20.6
6	254.4	8015.91	2563.79	96.9	28.6
10	254.4	8232.21	3887.93	143.0	42.2
20	254.4	7482.32	5155.25	208.7	61.5
30	254.4	7483.57	5752.44	232.8	68.7
60	254.4	8196.79	7093.93	262.1	77.3
90	254.4	7735.65	6733.55	263.6	77.8
120	254.4	7617.29	6565.23	261.0	77.0

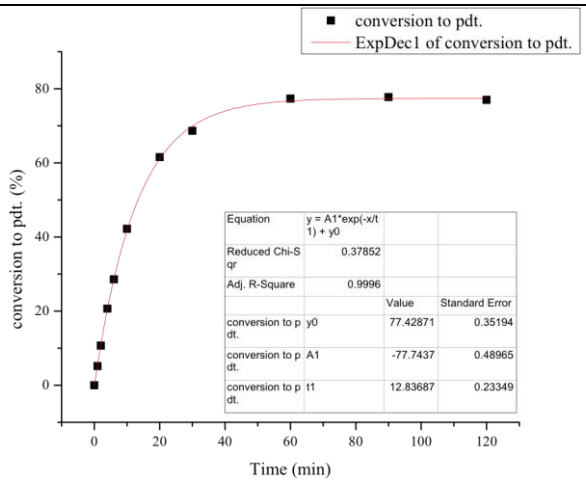

Half-Life = 13.4 min

1500 rpm, run #2:

Time (min)	Standard (µmol)	Standard Area	Product Area	Product (µmol)	% Product
0	253.0	1.00	0.00	0.0	0.0
1	253.0	7286.60	326.66	13.5	4.0
2	253.0	7145.05	740.24	31.2	9.2
4	253.0	7855.38	1663.44	63.8	18.8
6	253.0	7608.65	2315.22	91.6	27.0
10	253.0	7688.90	3650.55	143.0	42.2
20	253.0	7114.52	4766.10	201.8	59.5
30	253.0	7877.26	5626.12	215.1	63.5
60	253.0	8438.24	6217.95	221.9	65.5
90	253.0	7514.21	5876.77	235.5	69.5
120	253.0	8105.07	6396.96	237.7	70.1

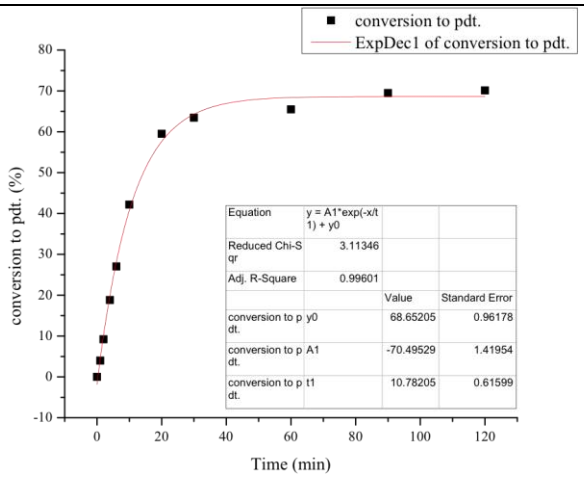

Half-Life = 14.3 min

1500 rpm, run #3:

Time (min)	Standard (µmol)	Standard Area	Product Area	Product (µmol)	% Product
0	253.0	1.00	0.00	0.0	0.0
1	253.0	7446.05	263.12	10.6	3.1
2	253.0	7699.97	765.31	29.9	8.8
4	253.0	7544.21	1860.18	74.3	21.9
6	253.0	7780.83	2657.92	102.9	30.3
10	253.0	7364.03	3856.57	157.7	46.5
20	253.0	7656.47	5103.86	200.8	59.2
30	253.0	7959.16	5425.05	205.3	60.6
60	253.0	7714.38	5716.63	223.2	65.8
90	253.0	7695.83	5613.79	219.7	64.8
120	253.0	7360.48	6018.39	246.3	72.6

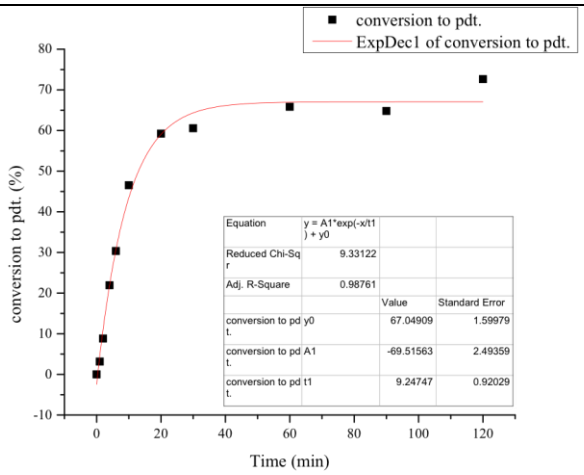

Half-Life = 13.0 min

Mean Half-Life = 13.6 min

Std. Dev. Half-Life = 0.7 min

2000 rpm, run #1:

Time (min)	Standard (umol)	Standard Area	Product Area	Product (umol)	% Product
0	254.4	1.00	0.00	0.0	0.0
2	254.4	5653.04	1134.85	60.8	17.9
5	254.4	7351.38	3232.63	133.2	39.3
10	254.4	6749.59	4171.90	187.2	55.2
15	254.4	7169.98	4982.19	210.4	62.1
20	254.4	6653.72	4997.43	227.5	67.1
30	254.4	7133.76	5366.90	227.8	67.2
40	254.4	8019.39	6269.67	236.8	69.8
50	254.4	6773.78	5336.10	238.6	70.4
60	254.4	7433.37	5996.49	244.3	72.1
90	254.4	7119.14	5754.32	244.8	72.2

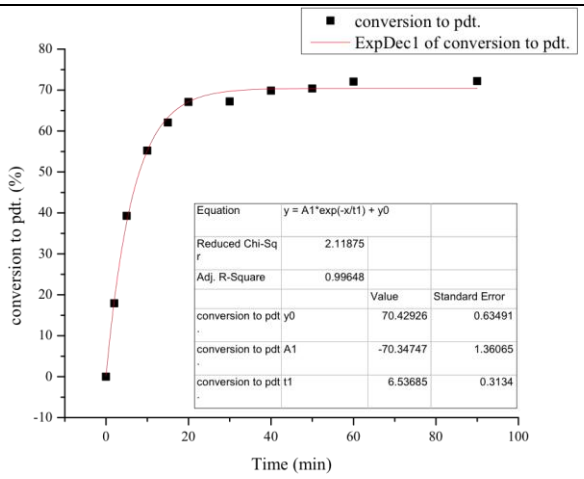

Half-Life = 8.1 min

2000 rpm, run #2:

Time (min)	Standard (umol)	Standard Area	Product Area	Product (umol)	% Product
0	254.4	1.00	0.00	0.0	0.0
2	254.4	6972.05	1263.41	54.9	16.2
5	254.4	8026.83	3445.32	130.0	38.3
10	254.4	7548.45	4507.19	180.8	53.3
15	254.4	7328.14	4933.91	203.9	60.1
20	254.4	7583.32	5659.04	226.0	66.7
30	254.4	7173.76	5472.64	231.0	68.1
40	254.4	7765.54	6102.93	238.0	70.2
50	254.4	7295.28	5803.40	240.9	71.1
60	254.4	7464.10	5882.34	238.7	70.4
90	254.4	7117.35	5730.68	243.8	71.9

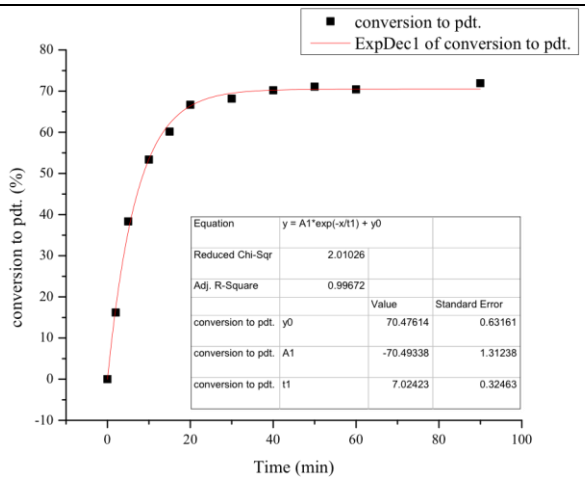

Half-Life = 8.7 min

2000 rpm, run #3:

Time (min)	Standard (µmol)	Standard Area	Product Area	Product (µmol)	% Product
0	253.0	1.00	0.00	0.0	0.0
1	253.0	8359.90	342.30	12.3	3.6
2	253.0	7725.21	992.16	38.7	11.4
3	253.0	7871.34	1843.81	70.5	20.8
5	253.0	7393.20	2735.44	111.4	32.9
7	253.0	8030.21	3581.43	134.3	39.6
10	253.0	7451.54	3717.45	150.2	44.3
20	253.0	8663.43	4770.92	165.9	48.9
30	253.0	8727.97	5143.40	177.5	52.4
60	253.0	7918.46	5055.23	192.3	56.7
90	253.0	8354.42	5974.50	215.4	63.5

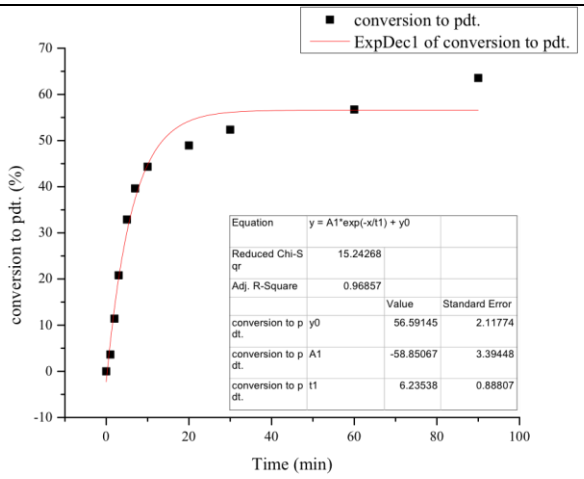

Half-Life = 13.7 min

Mean Half-Life = 10.1 min

Std. Dev. Half-Life = 3.1 min

2300 rpm, run #1:

Time (min)	Standard (µmol)	Standard Area	Product Area	Product (µmol)	% Product
0	254.4	1.00	0.00	0.0	0.0
1	254.4	7123.56	691.73	29.4	8.7
2	254.4	7518.77	1671.71	67.3	19.9
4	254.4	7708.58	3240.43	127.3	37.6
6	254.4	7249.74	3911.00	163.4	48.2
10	254.4	7621.18	4585.20	182.2	53.7
15	254.4	7236.83	4712.44	197.2	58.2
20	254.4	7652.51	5565.63	220.3	65.0
30	254.4	8012.57	5100.21	192.8	56.9
40	254.4	7004.13	5104.24	220.7	65.1
60	254.4	7242.69	4969.38	207.8	61.3

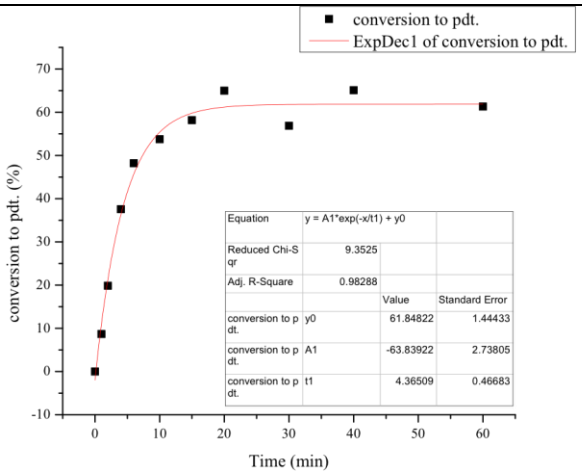

Half-Life = 7.4 min

2300 rpm, run #2:

Time (min)	Standard (µmol)	Standard Area	Product Area	Product (µmol)	% Product
0	254.4	1.00	0.00	0.0	0.0
1	254.4	7443.34	701.80	28.6	8.4
2	254.4	7405.37	1322.74	54.1	16.0
3	254.4	7318.67	1891.89	78.3	23.1
4	254.4	7543.53	2976.50	119.5	35.2
5	254.4	7593.28	3091.76	123.3	36.4
10	254.4	7811.98	5341.21	207.1	61.1
20	254.4	7430.44	4758.20	193.9	57.2
30	254.4	7198.15	5663.44	238.3	70.3
40	254.4	6969.31	5006.45	217.5	64.2
60	254.4	7267.40	5196.27	216.5	63.9

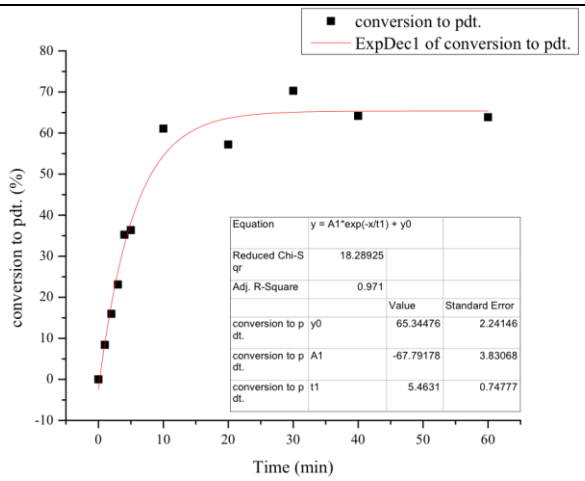

Half-Life = 8.1 min

2300 rpm, run #3:

Time (min)	Standard (µmol)	Standard Area	Product Area	Product (µmol)	% Product
0	253.0	1.00	0.00	0.0	0.0
1	253.0	8272.83	385.47	14.0	4.1
2	253.0	8024.14	1128.75	42.4	12.5
3	253.0	8157.81	1896.86	70.0	20.7
5	253.0	7896.12	2925.50	111.6	32.9
7	253.0	8263.07	3861.98	140.8	41.5
10	253.0	7400.10	4131.48	168.1	49.6
20	253.0	7708.77	5651.04	220.8	65.1
30	253.0	7564.32	5843.62	232.7	68.6
45	253.0	7984.10	6480.25	244.4	72.1
60	253.0	7823.20	6333.40	243.8	71.9

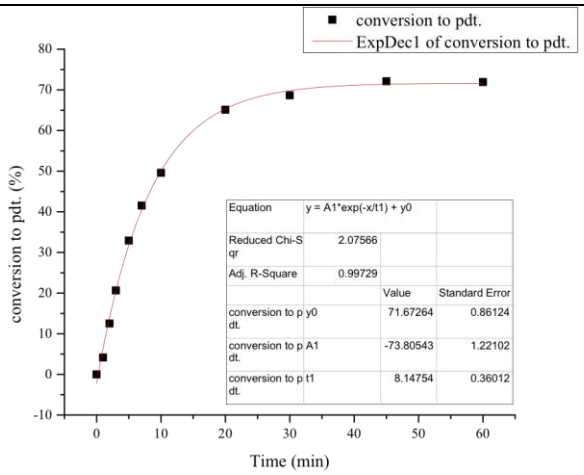

Half-Life = 10 min

Mean Half-Life = 8.5 min

Std. Dev. Half-Life = 1.4 min

Variable Stirring Speed Tabular Summary

Catalyst	Run #	Stirring Speed	Origin Fit Parameters					Half-Life, $t_{1/2}$ (min)	Mean Half-Life, $t_{1/2}$ (min)	Std. Dev. Half-Life, $t_{1/2}$ (min)
			Equation	y0	A1	t1	R^2			
2e	1	500	y = A1*exp(-x/t1) + y0	56.16555	-56.81888	48.0843	0.99791	106.8	106.8	N/A
2e	2	500	y = A1*exp(-x/t1) + y0	44.55275	-47.40353	29.0067	0.98412	N/A		
2e	1	1000	y = A1*exp(-x/t1) + y0	71.52223	-72.78669	17.56488	0.99002	21.4		
2e	2	1000	y = A1*exp(-x/t1) + y0	75.83132	-73.44886	23.95971	0.98778	25.0	26.8	6.5
2e	3	1000	y = A1*exp(-x/t1) + y0	60.28612	-61.5503	19.02381	0.98677	34.0		
2e	1	1500	y = A1*exp(-x/t1) + y0	77.42871	-77.7437	12.83687	0.9996	13.4		
2e	2	1500	y = A1*exp(-x/t1) + y0	68.65205	-70.49529	10.78205	0.99601	14.3	13.6	0.7
2e	3	1500	y = A1*exp(-x/t1) + y0	67.04909	-69.51563	9.24747	0.98761	13.0		
2e	1	2000	y = A1*exp(-x/t1) + y0	70.42926	-70.34747	6.53685	0.99648	8.1		
2e	2	2000	y = A1*exp(-x/t1) + y0	70.47614	-70.49338	7.02423	0.99672	8.7	10.1	3.1
2e	3	2000	y = A1*exp(-x/t1) + y0	56.59145	-58.85067	6.23538	0.96857	13.7		
2e	1	2300	y = A1*exp(-x/t1) + y0	61.84822	-63.83922	4.36509	0.98288	7.4		
2e	2	2300	y = A1*exp(-x/t1) + y0	65.34476	-67.79178	5.4631	0.971	8.1	8.5	1.4
2e	3	2300	y = A1*exp(-x/t1) + y0	71.67264	-73.80543	8.14754	0.99729	10.0		

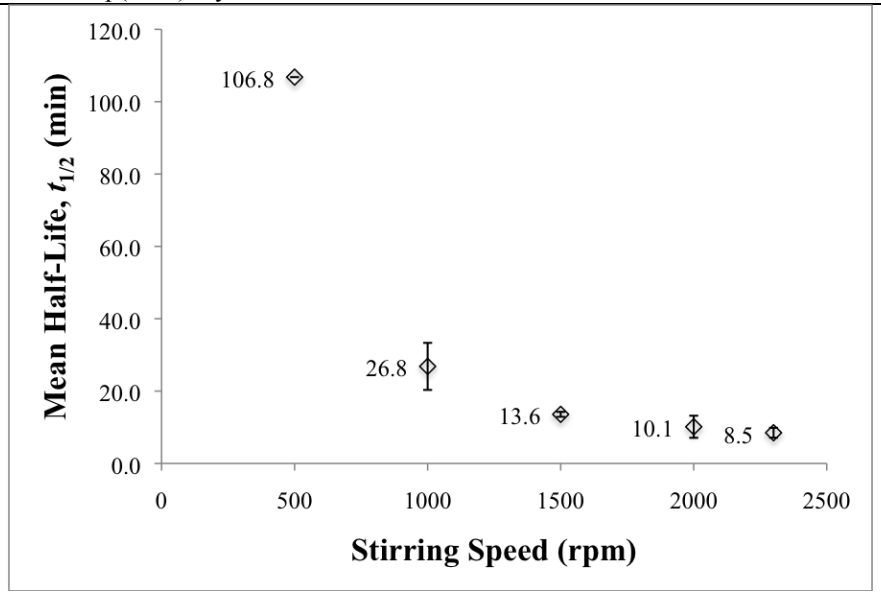

5.3 Chapter 3

5.3.1. Substrate Synthesis

Preparation of benzeneacetonitrile, α-(2-propen-1-yloxy)- (12)[200]

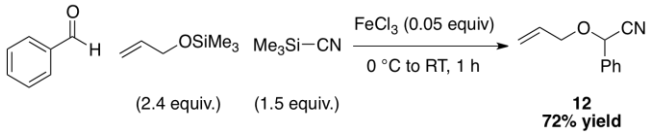

To a 5.0 mL round-bottom flask fitted with an argon inlet and magnetic stir-bar, was added ferric (III) chloride (43 mg, 246 μmol, 0.054 equiv.), benzaldehyde (0.50 mL, 4.92 mmol), and then trimethylsilyl allyl ether (2.1 mL, 11.8 mmol, 2.4 equiv.). The reaction mixture was then cooled to 0 °C on an ice-bath for 2 h. Trimethylsilyl cyanide (0.98 mL, 7.38 mmol, 1.5 equiv.) was then added dropwise via syringe under argon. After addition was complete, the reaction mixture was allowed to warm to room temperature over 1 h.

The reaction mixture was then diluted with $CHCl_3$ (10 mL) and then poured into a 50 mL separatory funnel containing a 50 mM solution of KH_2PO_4 pH 7 buffer (10 mL). Phases were separated and the aqueous phase was extracted with additional $CHCl_3$ (3 x 10 mL). The organic phases were combined and washed with more pH 7 buffer (10 mL), followed by brine (10 mL). The organic phase was dried over Na_2SO_4 and the solvent was removed on a rotary evaporator. The oily residue was then further dried on high-vacuum (<1 mm Hg) overnight. No additional purification was found to be necessary.

Data for **12**:

^{1}H-NMR: (500 MHz, $CDCl_3$)
7.53-7.47 (m, 2H), 7.47-7.39 (m, 3H), 6.00-5.88 (dddd, *J* = 17.2, 10.4, 6.4, 5.4 Hz, 1H), 5.45-5.37 (dd, *J* = 17.2, 1.5 Hz, 1H), 5.36-5.30 (d, *J* = 10.4 Hz, 1H), 5.30 (s, 1H), 4.34-4.27 (dd, *J* = 12.3, 5.4 Hz, 1H), 4.21-4.13 (dd, *J* = 12.3, 6.5 Hz, 2H)

^{13}C-NMR: (126 MHz, $CDCl_3$)
133.44, 132.47, 129.79, 129.02, 127.32, 119.58, 117.22, 70.68, 69.54

Preparation of benzeneacetonitrile, α-((*E*)-2-buten-1-yloxy)- (13)

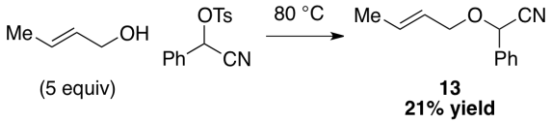

To a 5.0 mL one-piece, round-bottom flask/condenser, fitted with an argon inlet, was added alpha-tosyl-phenylacetonitrile (1.000 g, 3.13 mmol) followed by (*E*)-2-buten-4-ol (1.32 mL, 15.7 mmol, 5 equiv.). The reaction mixture was heated to 80 °C on an oil bath and heated overnight.

The reaction mixture was diluted with EtOAc (10 mL) and poured into a 60 mL separatory funnel containing a 50 mM KH_2HO_4 pH 7 buffer (10 mL). The phases were separated and the organic phase was dried over Na_2SO_4. The solvent was then removed on a rotatory evaporator to afford a dark brown oil.

This oil was purified by silica gel flash chromatography (4□ g SiO_2, ∅□=□2□□□5% to 10% MTBE /hexane) to afford 123 mg (21%) of **13** as a clear, yellow oil.

Data for **13**:

^{1}H-NMR: (500 MHz, $CDCl_3$)

7.52-7.46 (dd, *J* = 7.4, 2.0 Hz, 2H), 7.46-7.39 (dd, *J* = 4.9, 2.2 Hz, 3H), 5.92-5.80 (m, 1H), 5.65-5.56 (m, 1H), 5.27 (s, 1H), 4.29-4.21 (ddt, *J* = 11.6, 5.9, 1.2 Hz, 1H), 4.14-4.08 (dd, *J* = 11.5, 7.3 Hz, 1H), 1.79-1.74 (d, *J* = 6.5 Hz, 3H)

Preparation of silane, trimethyl[(3-methyl-2-buten-1-yl)oxy]- (18)

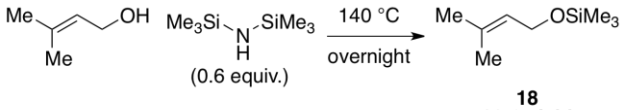

18
93% yield

To a 50 mL, single-neck, round-bottom flask, fitted with a condenser and an argon inlet, was added 3-methyl-2-buten-1-ol (10.0 mL, 98.5 mmol) followed by hexamethyldisilazane (12.5 mL, 59.1 mmol, 0.6 equiv.). This solution was then placed in a 140 °C oil bath and was allowed to stir overnight (> 14 h) under argon.

The reaction was then removed from the heating bath and allowed to cool to room temperature. The condenser was removed and a 10 cm fractional distillation column (glass helices) was attached. The reaction was then placed back into the heating bath set to 180 °C and the product was collected by distillation under argon at 145-146 °C. The distillation afforded 14.51 g (93%) of **18** as a clear, colorless liquid.

Data for **18**:

^{1}H-NMR: (500 MHz, $CDCl_3$)

5.36-5.29 (m, 1H), 4.15-4.09 (d, J = 6.8 Hz, 2H), 1.72 (s, 3H), 1.65 (s, 3H), 0.13 (s, 9H)

^{13}C-NMR: (126 MHz, CDCl3)

134.61, 123.92, 59.36, 25.79, 17.83, -0.36

Preparation of benzene, [bis[(3-methyl-2-buten-1-yl)oxy]methyl]- (16)

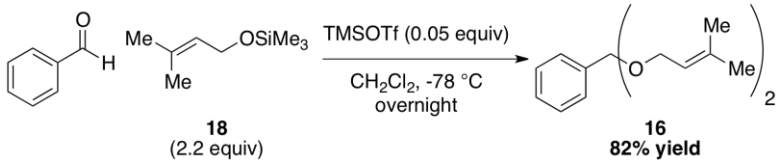

To a 25 mL, single-neck, round-bottom flask, fitted with a argon inlet/septum, was added **18** (1.711 g, 10.8 mmol, 2.2 equiv.), benzaldehyde (0.50 mL, 4.92 mmol), and CH_2Cl_2 (10 mL, 0.49 M). The reaction mixture was cooled to -75 °C (external) with a refrigerator unit in a 2-propanol bath. To this mixture trimethylsilyl-trifluoromethylsulfonate (50 µL, 250 µmol, 0.05 equiv.) was added dropwise via syringe while cold. The reaction mixture turned homogeneous after the addition was complete. The reaction was stirred overnight at -75 °C.

The reaction mixture was quenched with dry pyridine (2.0 mL) at -75 °C and then warmed to room temperature. The quenched reaction was then poured into a 60 mL separatory funnel containing a 50 mM KH_2PO_4 pH 7 buffer solution (15 mL) and diluted with CH_2Cl_2 (30 mL). The phases were separated and the organic phase was washed with H_2O (2 x 15 mL) and then brine (15 mL). The organic phase was dried over Na_2SO_4 and the solvent removed on a rotatory evaporator to afford a crude **16** as a light amber oil.

The crude **16** was purified by silica gel flash chromatography (50 g SiO_2, ∅ = 30, 5% MTBE in hexane) to afford 1.051 g (82%) of **16** as a colorless liquid after drying several hours under high-vacuum (<1 mm Hg).

Data for **16**:

^{1}H-NMR: (500 MHz, $CDCl_3$)

7.53-7.46 (m, 2H), 7.40-7.32 (m, 2H), 7.34-7.27 (m, 1H), 5.58 (s, 1H), 5.43-5.34 (dddt, *J* = 7.0, 5.6, 2.7, 1.3 Hz, 2H), 4.11-3.99 (m, 4H), 1.75 (s, 6H), 1.65 (s, 6H)

^{13}C-NMR: (126 MHz, $CDCl_3$)

139.17, 136.70, 128.20, 128.11, 126.84, 121.10, 100.50, 61.93, 25.71, 17.97

Preparation of benzeneacetonitrile, α-(3-methyl-2-buten-1-yloxy)- (14)

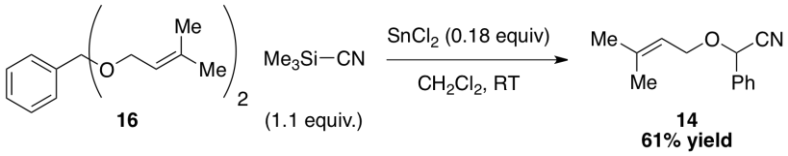

To a 2.0 mL react-vial, fitted with a septum cap, was charged with stannous (II) chloride (40 mg, 173 μmol, 0.18 equiv.) in an argon glove box. The vial was sealed and removed from the box and then a solution of **16** (299 mg, 1.15 mmol) in CH_2Cl_2 (0.5 mL, 2.3 M) was added via syringe under argon. The reaction mixture was stirred for several minutes at room temperature and then trimethylsilyl cyanide (170 μL, 1.27 mmol, 1.1 equiv.) was added via syringe under argon. The reaction mixture became gradually darker over the course of one hour to an amber/honey color.

After 3.5 h the reaction mixture was diluted with Et_2O (~1 mL) and poured into a test tube containing a solution of saturated aqueous $NaHCO_3$ (5-6 mL). The phases were separated and the aqueous phase was extracted with additional Et_2O (3 x 5 mL). The organic phases were combined, dried over Na_2SO_4, and then the solvent was removed on a rotatory evaporator to afford crude **14** as yellow oil.

This oil was purified by silica gel flash chromatography (30 g SiO_2, ∅ = 20, 10% MTBE in hexane) to afford 140 mg (61%) of **14** as a light yellow oil.

Data for **14**:

^{1}H-NMR: (500 MHz, CDCl3)

7.53 -7.46 (dd, *J* = 7.6, 2.0 Hz, 2H), 7.45-7.38 (dq, *J* = 8.8, 3.1, 2.4 Hz, 3H), 5.41-5.34 (tdd, *J* = 8.0, 2.6, 1.3 Hz, 1H), 5.28 (s, 1H), 4.30-4.17 (m, 2H), 1.79 (s, 3H), 1.73 (s, 3H)

^{13}C-NMR: (100 MHz, $CDCl_3$)

140.43, 133.76, 129.66, 128.96, 127.35, 118.82, 117.50, 69.25, 66.18, 25.87, 18.17

Preparation of 2-butenoic, 3-phenyl-, ethyl ester, (2*E*)- (20) and 2-butenoic, 3-phenyl-, ethyl ester, (2*Z*)- (21)[201]

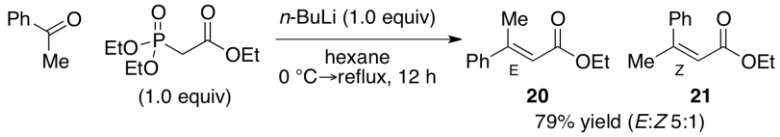

To a 250 mL, three-neck, round-bottom flask, fitted with a condenser, argon inlet, septum, and thermometer, was added triethylphosphonoacetate (10.1 mL, 50 mmol), hexane (50 mL, 1 M). This solution was then cooled to 0 °C (internal) on an ice-bath. To this solution 2.5 M *n*-BuLi in hexane (20.0 mL, 50 mmol, 1.0 equiv.) was added dropwise via gas-tight syringe over 2 h, keeping the internal temperature between 3-5 °C. The addition of base afforded a white suspension.

Acetophenone (5.9 mL, 50.0 mmol, 1.0 equiv.) was then added dropwise via syringe, keeping the internal temperature between 2-10 °C. The reaction was then removed from the ice bath and the septum and thermometer replaced with glass stoppers. The reaction was then placed in a 70 C oil bath and heated to reflux overnight (>12 h).

The reaction mixture was removed from the oil bath and cooled to room temperature. This mixture was then poured into a 500 mL separatory funnel containing a saturated aqueous solution of Na_2CO_3 (100 mL). The phases were separated and the aqueous phase was extracted with Et_2O (5 x 100 mL). The organic extracts were combined and washed with H_2O (3 x 50 mL) and then dried over $MgSO_4$. The solvent was then removed on a rotatory evaporator to afford crude **20**/**21** as an amber/orange oil. ^{1}H-NMR spectroscopic analysis indicated this crude product mixture was a 5:1 ratio of *E* to *Z* isomers with a trace amount of acetophenone.[202]

The crude **20**/**21** oil was purified by successive (>3) silica gel flash columns (300 g, ∅ = 60, 5% EtOAc in hexane) to afford 6.155 g (65%) of **20** as a light yellow oil and 1.402 g (15%) of **21** as a light yellow oil.

Data for **20**:

^{1}H-NMR: (500 MHz, $CDCl_3$)

7.51-7.45 (m, 2H), 7.41-7.34 (m, 3H), 6.16-6.11 (q, J = 1.3 Hz, 1H), 4.27-4.15 (q, J = 7.1 Hz, 2H), 2.61-2.54 (d, J = 1.3 Hz, 3H), 1.36-1.28 (t, J = 7.1 Hz, 3H)

Data for **21**:

^{1}H-NMR: (500 MHz, CDCl3)

7.38-7.27 (m, 3H), 7.23-7.17 (m, 2H), 5.93-5.89 (q, J = 1.4 Hz, 1H), 4.04-3.96 (q, J = 7.1 Hz, 2H), 2.20-2.16 (d, J = 1.5 Hz, 3H), 1.11-1.05 (t, J = 7.1 Hz, 3H)

Preparation of (*E*)-3-phenyl-2-buten-1-ol (22)

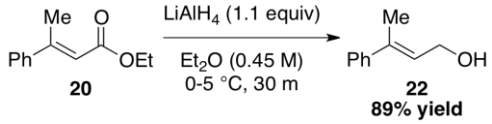

To a 250 mL, three-neck, round-bottom flask, fitted with a thermometer, 50 mL pressure-equilibrate addition funnel, and an argon inlet/septum, was added lithium aluminum hydride (2.470 g, 61.7 mmol, 1.1 equiv.) and then Et_2O (75 mL). This suspension was then cooled to 0 °C (internal) on an ice-bath. The addition funnel was then charged with a solution of **20** (10.679 g, 56.1 mmol) in Et_2O (50 mL, 1.12 M) and this was added dropwise to the hydride suspension over 2-3 h, keeping the temperature under 5 °C (internal).

After the addition was complete, the reaction mixture was then stirred for 30 min at 0 °C (internal). The septum was removed and under a steady stream of argon the reaction was carefully quenched, first H_2O (2.5 mL), second 15% (w/w) aq. NaOH (2.5 mL), and third H_2O (7.5 mL). A small amount of $MgSO_4$ (<1 g) was added the reaction mixture was allowed to warm to room temperature over 1-2 h. The off-white precipitate that formed was removed by filtration through a Buchner funnel. The filter cake was washed with boiling Et_2O (~100 mL) and the resulting filtrate was concentrated on a rotatory evaporator to afford crude **22** as a colorless oil.

The crude **22** was purified by silica gel flash chromatography (300 g SiO2 , 0 = 60, 40% EtOAc in hexane) to afford 7.440 g (89%) of **22** as a clear, colorless oil.

Data for **22**:

^{1}H-NMR: (500 MHz, $CDCl_3$)

7.44-7.39 (m, 2H), 7.36-7.30 (m, 2H), 7.30-7.24 (m, 1H), 6.03-5.94 (td, *J* = 6.7, 1.3 Hz, 1H), 4.43-4.31 (d, *J* = 3.9 Hz, 2H), 2.13-2.06 (d, *J* = 0.6 Hz, 3H), 1.39 (br s, 1H)

Preparation of silane, trimethyl[(3-phenyl-2-butenyl)oxy] (19)

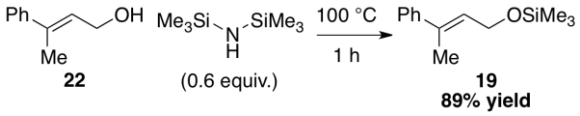

To a 25 mL, single-neck, round-bottom flask, fitted with a condenser and an argon inlet, was added **22** (2.414 g, 16.29 mmol) followed by freshly distilled hexamethyldisilazane (2.00 mL, 9.77 mmol, 0.59 equiv.). This solution was then heated to 100 °C on an oil-bath and stirred for 1 h. The reaction mixture became a clear yellow solution while heating. After 1 h, the reaction was cooled to room temperature.

The product was isolated by Kugelrohr distillation (160-170 °C, 0.45-0.55 mmHg) to afford 3.552 g (99%) of a semi-pure **19**. This compound was further purified by short-path distillation (75-78 °C, 0.57 mmHg) to afford 3.192 g (89%) of **19** as a clear, colorless oil.

Data for **19**:

^{1}H-NMR: (500 MHz, $CDCl_3$)

7.44-7.38 (m, 2H), 7.35-7.29 (m, 2H), 7.26-7.22 (m, 1H), 5.94-5.87 (td, J = 6.3, 1.4 Hz, 1H), 4.41-4.31 (d, J = 7.1 Hz, 2H), 2.08-2.02 (d, J = 1.1 Hz, 3H), 0.17 (s, 9H)

^{13}C-NMR: (126 MHz, $CDCl_3$)

143.04, 135.96, 128.18, 127.35, 127.01, 125.73, 60.11, 16.00, -0.29

Preparation of benzene, [bis[(3-phenyl-(*E*)-2-buten-1-yl)oxy]methyl]- (17)

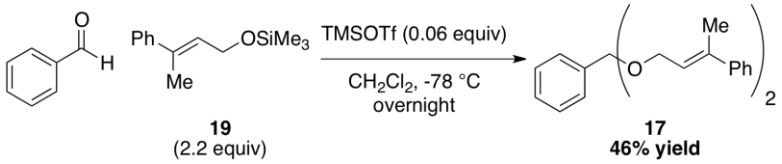

19 (2.2 equiv) **17** **46% yield**

To a 25 mL, single-neck, round-bottom flask, fitted with a argon inlet/septum, was added **19** (2.082 g, 9.45 mmol, 2.2 equiv), benzaldehyde (440 µL, 4.33 mmol), and CH_2Cl_2 (10 mL, 0.43 M). The reaction mixture was cooled to -77 °C (external) with the aid of refrigerator unit on a 2-propanol bath and then stirred for 30 m. Trimethylsilyl-trifluoromethlysulfonate (50 µL, 256 µmol, 0.06 equiv.) was added via syringe. This mixture was stirred overnight (> 16 h) at -77 °C (external).

The reaction mixture was quenched with dry pyridine (0.2 mL, 2.48 mmol) at -80 °C (external) and was then warmed to room temperature. This mixture was then poured into a 60 mL separatory funnel containing a saturated aqueous solution of $NaHCO_3$ (20 mL). The phases were separated and the aqueous phase was then extracted with Et_2O (2 x 10 mL). The organic phases were combined and then washed with a 50 mM KH_2PO_4 pH 7 buffer solution (10 mL) followed by brine (10 mL). The organic phase was then dried over Na_2SO_4 and the solvent removed on a rotatory evaporator to afford crude **17** as an amber oil.

The crude **17** was purified by two consecutive silica gel flash columns (#1: 100 g SiO_2, ∅ = 40, 5% MTBE in hexane, #2: 140 g SiO_2, ∅ = 40, 2% Et_3N, 5% MTBE in hexane) to afford 773 mg (46%) of **17** as a colorless/very pale yellow oil.

Data for **17**:

^{1}H-NMR: (500 MHz, $CDCl_3$)
7.60-7.53 (dd, *J* = 8.0, 1.4 Hz, 2H), 7.44-7.38 (m, 6H), 7.38-7.29 (m, 5H), 7.29-7.22 (m, 2H), 6.04-5.96 (td, *J* = 6.6, 1.3 Hz, 2H), 5.74 (s, 1H), 4.39-4.25 (qd, *J* = 12.5, 6.6 Hz, 4H), 2.06 (s, 6H)

^{13}C-NMR: (126 MHz, $CDCl_3$)
142.86, 138.57, 138.30, 128.45, 128.25, 128.19, 127.17, 126.80, 125.75, 124.01, 100.63, 62.40, 16.18

Preparation of benzeneacetonitrile, α-(3-phenyl-(*E*)-2-buten-1-yloxy)- (15)

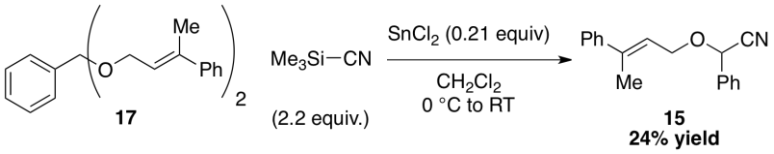

To a 10.0 mL, single-neck, round-bottom flask, fitted with an argon inlet and a septum, was added stannous (II) chloride (40 mg, 197 μmol, 0.11 equiv.) in an argon glove box. The flask was removed from the box and then a solution of **17** (758 mg, 1.97 mmol) in CH_2Cl_2 (2.5 mL, 0.79 M) was added via syringe under argon. The reaction mixture was then cooled to 0 °C on an ice-bath for 45 m. Trimethylsilyl cyanide (290 μL, 2.17 mmol, 1.1 equiv) was then added via syringe under argon at 0 °C and stirred for 10 m. The reaction mixture was then warmed to room temperature.

After 4 h, more stannous (II) chloride (38 mg, 0.10 equiv.) was added, and at 5 h additional trimethylsilyl cyanide (290 μL, 1.1 equiv.) was added. After 8 h, the reaction mixture was diluted with Et_2O (25 mL) and then poured in a 60 mL separatory funnel containing a saturated aqueous solution of $NaHCO_3$ (25 mL). The phases were separated and the aqueous phase was extracted with Et_2O (3 x 25 mL). The organic phases were combined and dried over Na_2SO_4. The solvent was then removed on a rotatory evaporatory to afford crude **15** as a dark amber oil.

This crude oil was purified by two consecutive silica gel flash chromatography columns (#1: 60 g SiO_2, ∅ = 30, 5% to 10% MTBE in hexane, #2: 10 g SiO_2, ∅ = 10, 5% EtOAc in hexane) to afford 125 mg (24% of 15 as a light amber oil.

Data for **15**:

^{1}H-NMR: (500 MHz, $CDCl_3$)

7.56-7.49 (m, 2H), 7.48-7.39 (m, 5H), 7.39-7.31 (t, *J* = 7.6 Hz, 2H), 7.31-7.27 (d, *J* = 7.3 Hz, 1H), 5.97-5.91 (m, 1H), 5.35 (s, 1H), 4.52-4.39 (m, 2H), 2.13 (s, 3H)

5.3.2. PTC [2,3]-Wittig Rearrangements

PTC [2,3]-rearrangement of benzeneacetonitrile, α-(2-propen-1-yloxy)- (12)

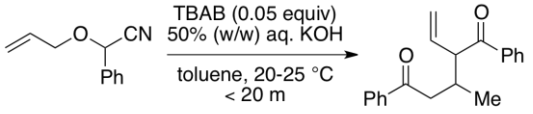

12 **23** **51% yield**

To a 4.0 mL dram vial was added 12 (101 mg, 583 μmol), toluene (2.0 mL, 0.29 M), and tetra(*n*-butyl)ammonium bromide (9.5 mg, 29.2 μmol, 0.05 equiv.). A solution of 50% (w/w) aq. KOH (670 μL) was then added at room temperature and the reaction mixture was vigorously stirred for 20 m.

The phases were then allowed to separate, the organic phase was saved and the aqueous phase was extracted with additional toluene (2 x 1 mL). The organic phases were combined and washed with a saturated aqueous solution of NH_4Cl (2-3 mL) followed by brine (1-2 mL). The organic phase was dried over Na_2SO_4 and the solvent was then removed on a rotatory evaporator to afford 73 mg (86%) of crude **23** as a dark orange oil

The crude **23** was purified by silica gel flash chromatography (7 g SiO_2, ∅ = 10, 5% to 10% MTBE in hexane) to afford 43 mg (51%) of **23** as a pale yellow oil.

Data for **23**:

^{1}H-NMR: (500 MHz, $CDCl_3$)

8.05-7.99 (dd, *J* = 8.3, 1.1 Hz, 2H), 7.81-7.76 (dd, *J* = 8.3, 1.2 Hz, 2H), 7.61-7.35 (m, 16H), 5.95-5.84 (m, 2H), 5.79-5.69 (m, 2H), 5.35-5.28 (dd, *J* = 17.2, 1.7 Hz, 2H), 5.22-5.19 (m, 1H), 5.19-5.07 (dddd, *J* = 44.1, 10.5, 2.9, 1.4 Hz, 3H), 4.12-3.96 (ddd, *J* = 38.0, 12.1, 5.3 Hz, 4H), 3.80-3.64 (m, 5H), 3.04-2.86 (m, 6H), 2.84-2.75 (d, *J* = 13.9 Hz, 2H), 1.28-1.22 (d, *J* = 6.1 Hz, 3H), 0.86-0.83 (d, *J* = 6.6 Hz, 3H).

^{13}C-NMR: (126 MHz, $CDCl_3$)

198.48, 197.51, 137.04, 136.66, 135.97, 135.65, 133.16, 133.09, 132.88, 129.49, 129.44, 128.91, 128.87, 128.57, 128.53, 128.15, 127.96, 126.58, 126.41, 117.62, 117.28, 117.21, 117.10, 85.44, 85.03, 67.83, 67.82, 41.16, 40.96, 40.84, 40.58, 15.70, 15.45

LRMS: (CI^+, 70 VSE(A))

105.0 (100), 147.1 (11.0), 175.0 (12.5), 262.1 (97.5), 293.1 ($M+H^+$, 63.7)

PTC [2,3]-Wittig rearrangement of benzeneacetonitrile, α-((*E*)-2-buten-1-yloxy)- (13)

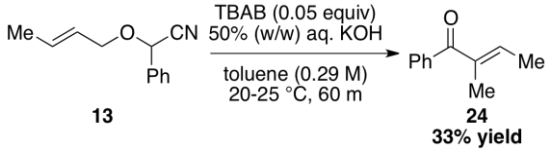

13 **24**

33% yield

To a 4.0 mL dram vial, fitted with a septum cap, was charged **13** (107 mg, 571 μmol), toluene (2.0 mL, 0.29 M), and tetra(*n*-butyl)ammonium bromide (9.5 mg, 29.5 μmol, 0.05 equiv.). To this reaction mixture was added a solution of 50% (w/w) aq. KOH (670 μL) and the mixture was vigorously stirred for 1 h at room temperature (20-25 °C).

The stirring was then ceased and the phases were allowed to separate. The organic phase was set aside and the aqueous phase extracted with additional toluene (2 x 1 mL). The organic phases were then combined and washed with a saturated aqueous solution of NH_4Cl (2-3 mL), followed by brine (1-2 mL), and then dried over Na_2SO_4. The solvent was then removed on a rotatory evaporator to afford 74 mg (81%) of crude **24**.

The crude **24** was then purified by silica gel flash chromatography (7-8 g SiO_2, ∅ = 10, 5% to 10% MTBE in hexane) to afford 30 mg (33%) of **24** as a yellow oil.

Data for **24**:

^{1}H-NMR: (500 MHz, $CDCl_3$)

7.67-7.57 (dd, *J* = 8.2, 1.4 Hz, 2H), 7.53-7.44 (m, 1H), 7.43-7.33 (m, 2H), 6.46-6.34 (dddd, *J* = 8.3, 6.9, 5.5, 1.4 Hz, 1H), 2.00-1.93 (m, 3H), 1.91-1.85 (dd, *J* = 6.9, 1.1 Hz, 3H)

^{13}C-NMR: (126 MHz, $CDCl_3$)

198.85, 141.45, 138.80, 137.62, 131.17, 129.14, 127.95, 14.73, 12.11

PTC [2,3]-Wittig rearrangement of benzeneacetonitrile, α-(3-methyl-2-buten-1-yloxy)- (14)

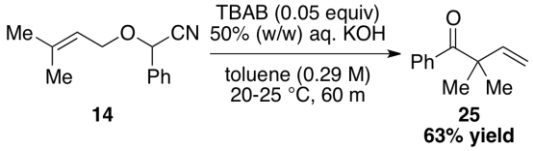

To a 4.0 mL dram vial was added 14 (59 mg, 293 umol), toluene (1.00 mL, 0.29 M), and tetra(*n*-butyl)ammonium bromide (4.8 mg, 15 umol, 0.05 equiv.). To this a solution of 50% (w/w) aq. KOH (330 µL) was added at room temperature. The reaction mixture was vigorously stirred for 60 m at room temperature.

The stirring was ceased and the phases allowed to separate. The aqueous phase was extracted with EtOAc (2 x 1 mL). The organic phases were combined and washed with a saturated aqueous solution of NH4Cl (3-4 mL). The organic phase was then dried over Na2SO4 and the solvent was removed on a rotatory evaporator to afford 44 mg (86%) of crude **25**.

The crude **25** was purified by silica gel flash chromatography (5 g SiO_2, ∅ = 10, 5% MTBE in hexane) to afford 32 mg (63%) of **25** as a colorless oil.

Data for **25**:

^{1}H-NMR: (500 MHz, $CDCl_3$)

7.92-7.82 (dd, *J* = 8.5, 1.4 Hz, 2H), 7.50-7.42 (m, 1H), 7.41-7.32 (m, 2H), 6.24-6.13 (dd, *J* = 17.6, 10.6 Hz, 1H), 5.29-5.17 (m, 2H), 1.40 (s, 6H)

^{13}C-NMR: (126 MHz, $CDCl_3$)

204.61, 143.86, 137.11, 131.60, 129.24, 127.91, 114.03, 50.15, 26.04

PTC [2,3]-Wittig rearrangement of benzeneacetonitrile, α-(3-phenyl-(*E*)-2-buten-1-yloxy)- (15)

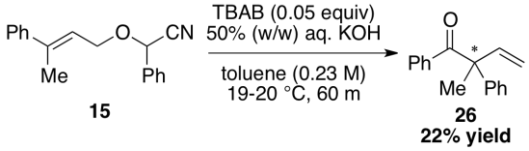

To a 1.0 mL glass conical vial was charged with **15** (30 mg, 114 μmol), toluene (0.50 mL, 0.23 M), and tetra(*n*-butyl)ammonium bromide (1.8 mg, 5.7 μmol, 0.05 equiv.). The reaction mixture was stirred for several minutes at room temperature and then a solution 50% (w/w) aq. KOH (150 μL) was added. This mixture was vigorously stirred for 60 m and then diluted with additional Et_2O (~5 mL).

The stirring was ceased and the phases were allowed to separate. The organic phase was removed and then washed with a saturated aqueous solution of NH_4Cl (~2 mL). The organic phase was then concentrated on a rotatory evaporator to afford 29 mg of crude **26** as a yellow oil.

The product was purified by preparative thin-layer chromatography on an analytical silica gel plate (20 x 20 cm, 5% MTBE in hexane) to afford 6 mg (22%) of **26** as a colorless oil.

Data for **26**:

^{1}H-NMR: (500 MHz, $CDCl_3$)
7.57-7.51 (m, 2H), 7.41-7.31 (m, 3H), 7.31-7.20 (m, 5H), 6.67-6.56 (dd, *J* = 17.4, 10.8 Hz, 1H), 5.34-5.27 (dd, *J* = 10.7, 0.8 Hz, 1H), 5.20-5.12 (dd, *J* = 17.4, 0.8 Hz, 1H), 1.67 (s, 3H)

TLC: R_f 0.31 (5% MTBE in hexane) [Silica gel, UV]

CSP-SFC: (Chiralcel OJ, SFC Method 1)
3.2 m (50%), 4.4 m (50%), α= 1.5

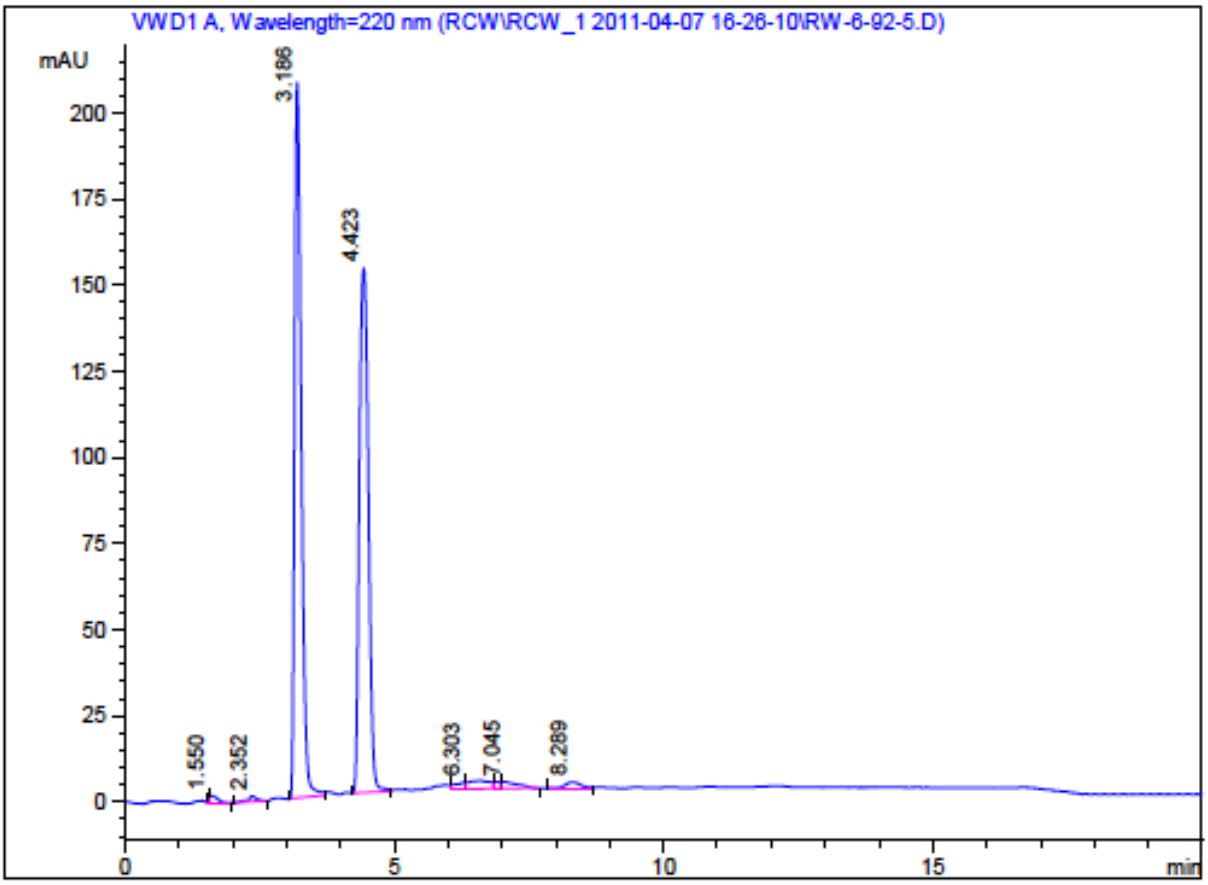

#	Time	Height	Area	Area %
1	1.550	2.286	5.439	0.142
2	1.583	2.282	22.150	0.578
3	2.352	1.730	22.169	0.578
4	3.186	207.905	1797.276	46.890
5	4.423	152.273	1793.223	46.784
6	6.303	1.948	28.893	0.754
7	6.579	2.455	65.864	1.718
8	6.902	2.034	17.070	0.445
9	7.045	1.975	44.094	1.150
10	8.289	1.793	36.818	0.961

APTC [2,3]-Wittig rearrangement of benzeneacetonitrile, α-(3-phenyl-(*E*)-2-buten-1-yloxy)- (15)

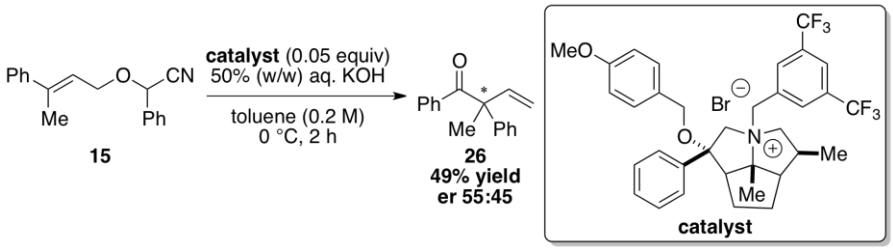

To a 2.0 mL conical, glass vial, fitted with a septum cap, was charged **15** (52 mg, 197 μmol), toluene (1.0 mL, 0.2 M), and **catalyst** (6.7 mg, 9.85 μmol, 0.05 equiv.). The reaction mixture was then cooled to 0 °C (external) on an ice-bath for 1 h. A solution of 50% (w/w) aq. KOH (300 μL) was then added and the mixture was vigorously stirred for 2 h.

The stirred was ceased and the reaction was poured into a test tube containing a solution of saturated aqueous NH_4Cl (2-3 mL) and Et_2O (2-3 mL). The phases were separated and the aqueous phase was extracted with additional Et_2O (2 x 1-2 mL). The organic phases were combined, passed through a pipette silica gel plug (0.5 x 1.0 cm), and then concentrated on a rotatory evaporator to afford crude **26** as a yellow oil.

The crude **26** was purified by silica gel flash chromatography (6 g SiO_2, ∅ = 10, 5% MTBE in hexane) to afford 23 mg (49%) of **26** as a very pale amber oil.

Data for **26**:

CSP-SFC: (Chiralcel, SFC Method 1)

3.1 m (major, 55%), 4.3 m (minor, 45%)

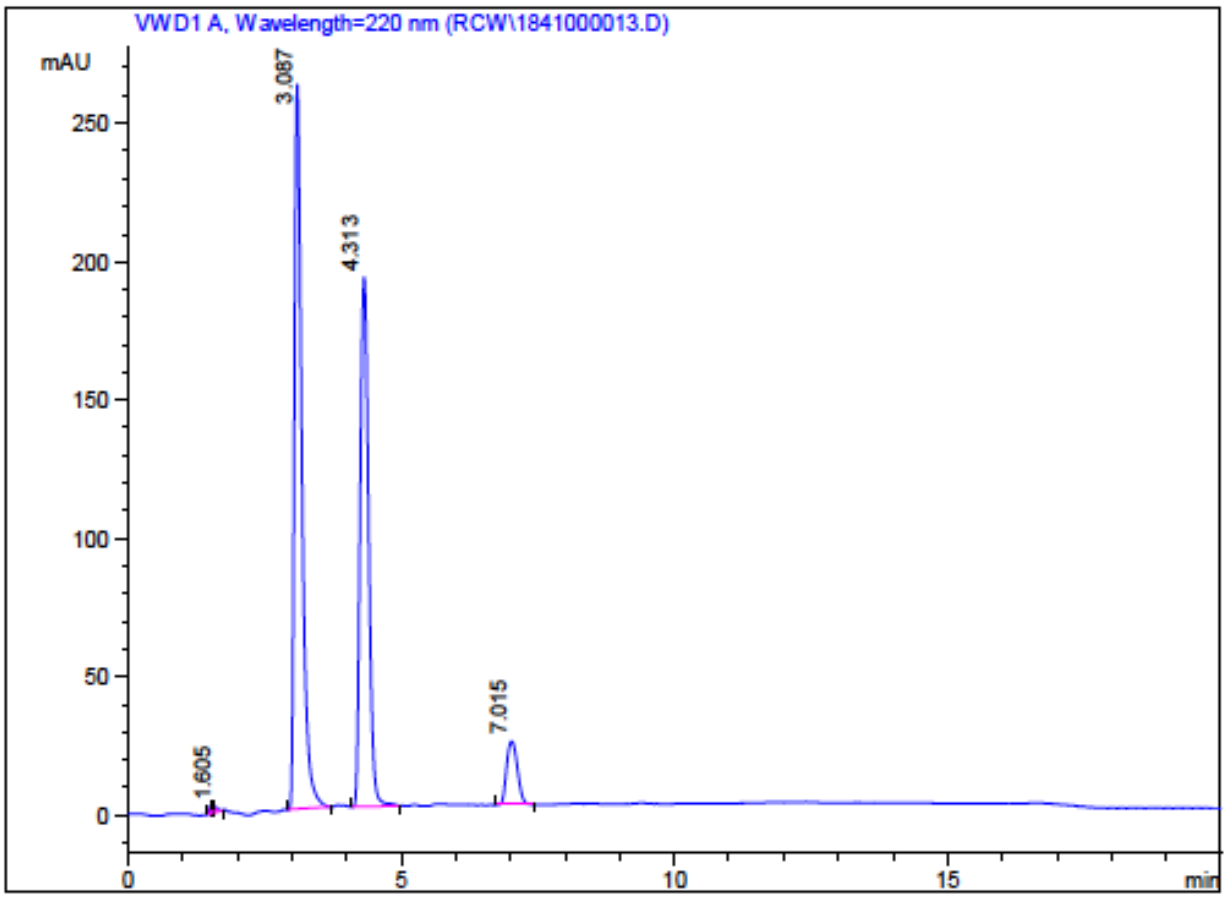

#	Time	Height	Area	Area %
1	1.489	2.669	5.100	0.104
2	1.567	2.244	10.501	0.214
3	1.605	1.952	7.226	0.147
4	3.087	261.966	2508.690	51.043
5	4.313	191.178	2063.687	41.988
6	7.015	22.982	319.700	6.505

5.4 Chapter 4

5.4.1 Preparation of Quaternary Ammonium Hydroxides

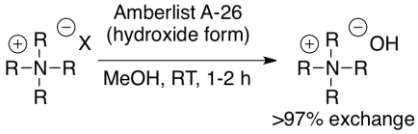

An amberlist A-26 hydroxide form resin was utilized to generate the quaternary ammonium hydroxide solutions from the bromides or iodides, The protocol of Harlow, Noble and Wild was followed closely with the exception that anhydrous methanol was utilized rather than isopropanol. In a typical exchange ~10 mmols of quaternary ammonium bromide was brought up in minimal amount of methanol (~20 mL) and added to the top of the amberlyst resin, which was pre-packed in a standard 30 mm column with anhydrous methanol. The resultant suspension was allowed to sit undisturbed for 3-6 h, then eluted slowly (~2 h) total. The resin was rinsed with another 100 mL of methanol overnight (~12 h). Between each pass over the resin the hydroxide form was regenerated, following the same procedure, eluting with 1 M NaOH in methanol (3 times) followed anhydrous methanol (~1 L) until the eluent was neutral. Typically this process was repeated six times. The final solution was concentrated to ~0.5 molar and tritrated to a phenolphthalein endpoint in a solution of methanol and water (1:1) as well as titrated for bromide (weight %) of the solution.

compound number	ammonium cation	OH conc, [M][a]	st. dev.	Br, weight %[b]	Br, mmol %[d]
31	methyl$_4$N$^+$	0.127	0.0095	0.16	1.56
32	ethyl$_4$N$^+$	0.668	0.0014	0.33	0.61
33	*n*-propyl$_4$N$^+$	0.229	0.0050	0.34	1.82
34	*n*-butyl$_4$N$^+$	0.588	0.0054	<0.1[c]	<0.10
35	*n*-hexyl$_4$N$^+$	0.685	0.0096	0.31	0.56
36	*n*-octyl$_4$N$^+$	0.426	0.0013	0.41	1.19

[a.] Total base titrations are an average of 3-6 determinations to a phenolphthalein endpoint. [b.] Bromide weight percentage is an average of 2-3 determinations by ion selective electrode. [c.] Prepared from the quaternary ammonium iodide and no residual iodide could be detected. [d.] The total mmols of anions is taken as the mmols of hydroxide plus the mmols of bromide.

Preparation of N,N,N-trimethyl-Methanaminium, hydroxide

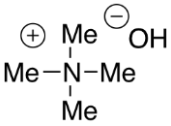

	acid, mL	acid, [M]	acid, mmol	base, mmol	base, mL	base, [M]
	1.338	0.100	0.1338	0.1338	0.200	0.6690
	1.365	0.100	0.1365	0.1365	0.200	0.6825
	1.306	0.100	0.1306	0.1306	0.200	0.6530
avg	1.3363	0.100	0.1336	0.1336	0.000	0.668
dev	0.0295	0.000	0.0030	0.0030	0.000	0.014

Residual Halide: 0.16 weight %

Preparation of Ethanaminium, N,N,N-triethyl-, hydroxide

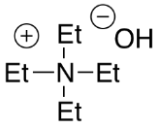

	acid, mL	**acid, [M]**	**acid, mmol**	**base, mmol**	**base, mL**	**base, [M]**
	1.1500	0.1000	0.1150	0.1150	0.9000	0.1278
	1.1400	0.1000	0.1140	0.1140	0.9000	0.1267
	1.1500	0.1000	0.1150	0.1150	0.9000	0.1278
	1.1200	0.1000	0.1120	0.1120	0.9000	0.1244
	1.1520	0.1000	0.1152	0.1152	0.9000	0.1280
	1.1300	0.1000	0.1130	0.1130	0.9000	0.1256
avg.	1.1403	0.1000	0.1140	0.1140	0.9000	0.1267
dev.	0.0130	0.0000	0.0013	0.0013	0.0000	0.0014

Residual Halide: 0.33 weight %

Preparation of Propanaminium, N,N,N-tripropyl-, hydroxide

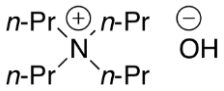

	acid, mL	acid, [M]	acid, mmol	base, mmol	base, mL	base, [M]
	0.4570	0.1000	0.0457	0.0457	0.2000	0.2285
	0.4490	0.1000	0.0449	0.0449	0.2000	0.2245
	0.4690	0.1000	0.0469	0.0469	0.2000	0.2345
avg	0.4583	0.1000	0.0458	0.0458	0.2000	0.2292
dev	0.0101	0.0000	0.0010	0.0010	0.0000	0.0050

Residual Halide: 0.34 weight %

Preparation of Butanaminium, N,N,N-tributyl-, hydroxide

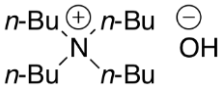

	acid, mL	acid, [M]	acid, mmol	base, mmol	base, mL	base, [M]
	1.0400	0.1000	0.1040	0.1040	0.1750	0.5943
	1.0220	0.1000	0.1022	0.1022	0.1750	0.5840
	1.0260	0.1000	0.1026	0.1026	0.1750	0.5863
avg	1.0293	0.1000	0.1029	0.1029	0.1750	0.5882
dev	0.0095	0.0000	0.0009	0.0009	0.0000	0.0054

Residual Halide: <0.01 weight %

Preparation of Hexanaminium, N,N,N-trihexyl-, hydroxide

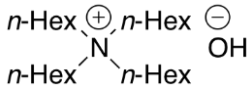

	acid, mL	acid [M]	acid, mmol	base, mmol	base, mL	base, [M]
	1.1800	0.1000	0.1180	0.1180	0.1750	0.6743
	1.2080	0.1000	0.1208	0.1208	0.1750	0.6903
	1.2100	0.1000	0.1210	0.1210	0.1750	0.6914
avg	1.1993	0.1000	0.1199	0.1199	0.1750	0.6853
dev	0.0168	0.0000	0.0017	0.0017	0.0000	0.0096

Residual Halide: 0.31 weight %

Preparation of Octanaminium, N,N,N-trioctyl-, hydroxide

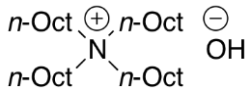

	acid, mL	acid [M]	acid, mmol	base, mmol	base, mL	base, [M]
	0.7580	0.1000	0.0758	0.0758	0.1750	0.4331
	0.7580	0.1000	0.0758	0.0758	0.1750	0.4331
	0.7200	0.1000	0.0720	0.0720	0.1750	0.4114
	0.7200	0.1000	0.0720	0.0720	0.1750	0.4114
avg	0.7390	0.1000	0.0745	0.0745	0.1750	0.4259
dev	0.0219	0.0000	0.0022	0.0022	0.0000	0.0125

Residual Halide: 0.41 weight %

5.4.2 Preparation of Quaternary Ammonium Phenoxides

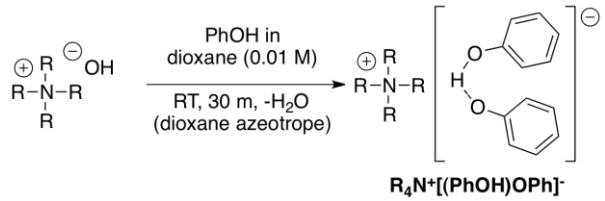

To a 250-mL, one-necked, round-bottomed flask fitted a septa, magnetic stir bar, and nitrogen inlet adaptor was added phenol (62.7 mg, 0.2 mmol) followed by dioxane (100 mL). To the clear solution was added the appropriate quaternary ammonium hydroxide (0.1 mmol). The resulting solution was stirred for 30 min, then concentrated by rotary evaporation. Another 100 mL of dioxane was added and the solution was again concentrated by rotary evaporation. This process was repeated three times, then again three times with hexanes (100 mL portions). The resulting solid quaternary ammonium phenolate complexes were used within 1 hour.

The stoichiometry of the ammonium phenoxide complexes prepared in this way was checked by quenching a small sample into an acetonitrile solution containing a large excess of benzyl bromide and a standard. After being stirred overnight, the relative amounts of phenol and benzyl phenyl ether were determined by gas chromatography. The stoichiometry was found to be 1:1 (+/- 0.04) in all cases.

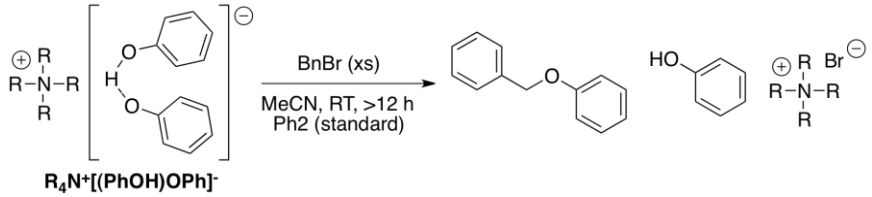

R	PhOH/PhOBn, mol/mol
methyl	1.04
ethyl	0.98
n-propyl	1.02
n-butyl	1.00
n-hexyl	0.94
n-octyl	0.98

Preparation of Tetramethylammonium phenol-phenolate (A)

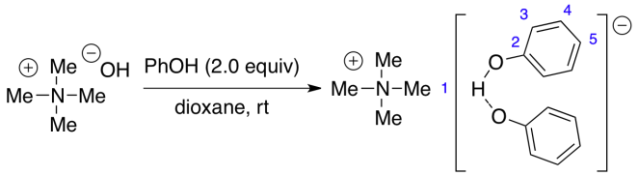

Data for **A**:

^{1}H-NMR: (500 MHz, CD_3CN)

6.99 (t, *J* = 8.7, 4 H, HC(3)), 6.63 (dd, *J* = 8.6, 1.2, 4 H HC(4)), 6.42 (t, J = 7.2, HC(5)), 6.13 (s, 1 H, HO), 3.03 (s, 12 H, HC(1))

^{13}C-NMR: (126 MHz, CD_3CN)

165.6 (C(2)), 129.7 (C(4)), 118.0 (C(5)), 114.4 (C(3)), 55.8 (C(1))

Preparation of Tetraethylammonium phenol-phenolate (B)

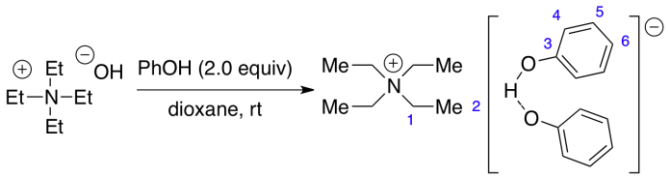

Data for **B**:

^{1}H-NMR: (500 MHz, CD_3CN)

9.09 (s, 1 HO)), 6.96 (t, *J* = 7.5, 4 H, HC(x)), 6.57 (d, 4 H, *J* = 7.8), 6.35 (t, 2H, *J* = 7.2), 3.12 (q, 8 H, *J* = 7.4), 1.16 (m, 12 H, HC(x))

^{13}C-NMR: (126 MHz, CD_3CN)

166.7 (C(5)), 129.6 (C(6)), 118.0 (C(4)), 113.4 (C(3)), 52.8 (C(1)), 7.4 (C(2)),

Preparation of Tetrapropylammonium phenol-phenolate (C)

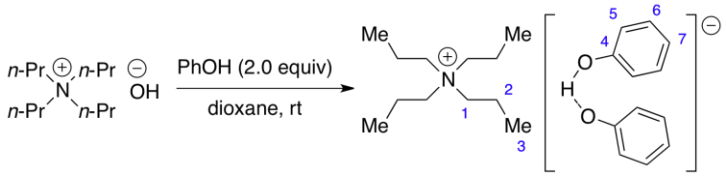

Data for **C**:

^{1}H-NMR: (500 MHz, CD_3CN)

11.5-13 (broad s, 1 H HO), 6.98 (t, *J* = 8.0, 4 H, HC(x)), 6.61 (d, *J* = 8.4, 4 H HC(x)), 6.39 (t, *J* = 7.2, 2 H, HC(x)), 3.02 (ddd, J = 8.6, 4.9, 3.7, 8 H, HC(x)) 1.61 (m, 8 H, HC(x)), 0.92 (t, *J* = 7.3, 12 H, HC(x))

^{13}C-NMR: (126 MHz, CD_3CN)

165.95 (C(6)), 129.63 (C(7)), 118.00 (C(5)), 114.00 (C(4)), 60.73 (C(1)), 15.77 (C(2)), 10.55 (C(3))

Preparation of Tetrabutylammonium phenol-phenolate (D)

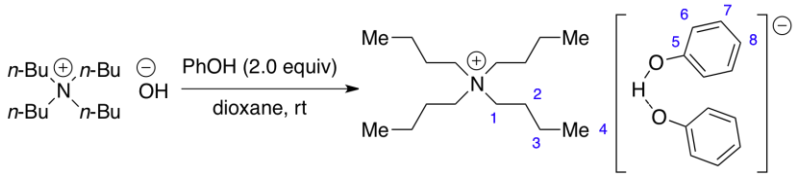

Data for **D**:

^{1}H-NMR: (500 MHz, CD_3CN)

7.05 (t, *J* = 7.8, 4 H, HC(6)), 6.73 (d, J = 7.5, 4 H, HC(7)) 6.49 (t, *J* = 7.2 2 H, HC(8)) 3.05 (m, 8 H, HC(1)), 1.55 (t, *J* = 11.6, 8 H, HC(2)) 1.35 (qd, *J* = 7.2, 14.3, 8 H, HC(3)) 0.98 (t, *J* = 7.3, 12 H, HC(4))

^{13}C-NMR: (126 MHz, $CDCl_3$)

165.07 C(7), 129.76 C(6), 117.84 C(5), 114.89 C(8), 59.01 C(1), 24.17 C(2), 20.12 C(3), 13.73 C(4)

Preparation of Tetrahextylammonium phenol-phenolate (E)

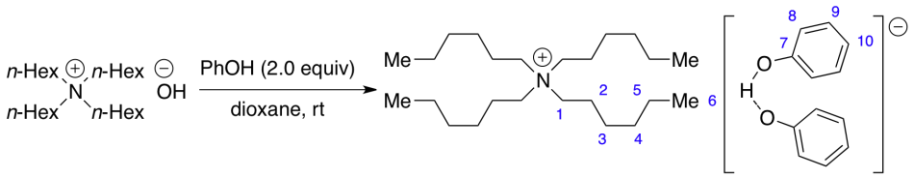

Data for **E**:

[1]H-NMR: (500 MHz, CD_3CN)

7.04 (t, *J* = 7.7, 4 H, HC(8)) 6.72 (d, *J* = 7.8, 4 H, HC(9)) 6.47 (t, *J* = 7.2, 2 H, HC(10)) 3.04 (m, 8 H, HC(1)) 0.96 (t, *J* = 6.6, 8 H, HC(2)) 1.57 (m, 24 H, HC(3) HC(4) HC(5)) 1.35 (m, 12 H, HC(6))

[13]C-NMR: (126 MHz, CD_3CN)

265.54 HC(9), 129.86 HC(8), 118.22 HC(7), 114.63 HC(10), 59.35 HC(1), 31.78 HC(2), 26.48 HC(3), 23.14 HC(4), 22.95 HC(5), 14.24 HC(6)

Preparation of Tetraoctylammonium phenol-phenolate (F)

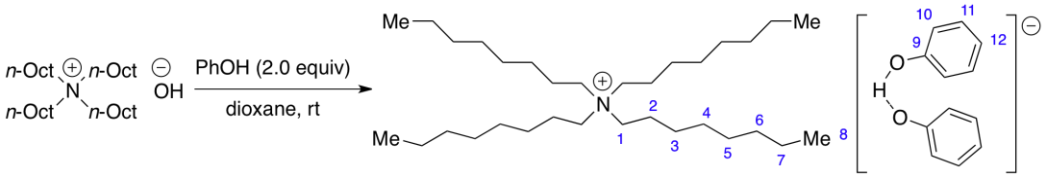

Data for **F**:

[1]H-NMR: (500 MHz, CD_3CN)

7.05 (t, *J* = 7.8, 1H, HC(10)) 6.77 (d, J = 7.6, 4 H, HC(1)) 6.52 (t, J = 7.2, 2H, HC(12)) 3.01 (m, 8 H, HC(1)) ppm 1.44 (m, 48 H, HC(2-7)) 0.92 (m, 12H, HC(8))

[13]C-NMR: (126 MHz, CD_3CN)

164.68 C(11), 129.91 HC(10), 117.99 HC(9), 115.53 HC(12), 59.25 HC(1), 35.40 HC(2), 32.49 HC(3), 29.73 HC(4), 26.88 HC(5), 23.41 HC(6), 22.39 HC(7), 14.49 HC(8),

5.4.3 Kinetic Analysis Procedure

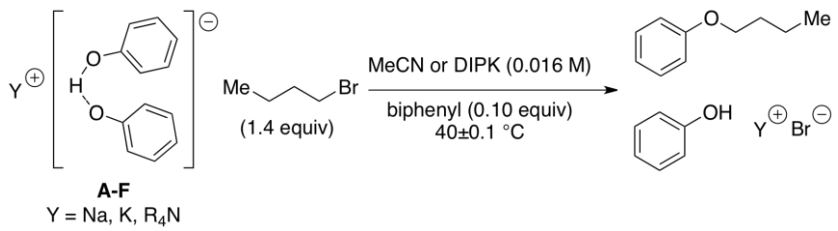

A-F
Y = Na, K, R_4N

In a drybox, a stock solution of biphenyl (, 21.0 μmol) was made up in the appropriate solvent (CH_3CN or DIPK, 18.75 mL). The solution was then added to the appropriate quaternaryammonium phenol-phenolate complex at room temperature. The resulting solution was transferred removed from the drybox and transferred to three one-neck, 10-mL round-bottom flasks with magnetic stir bars fitted with reflux condensers, and nitrogen inlet adaptors. Each of the flasks were placed in a 40 ^{0}C oil bath for 20 minutes prior to initiation of a kinetic run. Reaction progress was monitored by GC analysis. Sampling of the reaction was performed by removing 300 μL aliquots of the mixture by syringe and quenching the aliquots at regular intervals. The quench was performed as follows: the withdrawn aliquot of the reaction mixture was injected into 200 μL of a biphase of NH_4Cl (aq, 50 μL) and MTBE (150 μL). The organic solution was filtered through a 0.5 x 1.0 cm plug of silica gel rinsing with ~200 μL of EtOAc. The resulting sample was subjected to GC analysis, Method 1. Response factors were obtained by Eqn 6.1 and are shown below:

Response Factors

Phenol (2.087 minutes, Ph_2, 6.085 minutes, GC Method 1)

entry	PhOH, mg	Ph_2, mg	PhOH, mmol	Ph_2, mmol	PhOH, area	Ph_2 area	R_f
1	2.3	5.51	0.024439	0.035731	22.134	77.866	2.406186
2	2.3	5.51	0.024439	0.035731	22.099	77.901	2.41108
3	2.3	5.51	0.024439	0.035731	22.021	77.979	2.422043
4	10.2	4.1	0.108382	0.026588	59.214	39.682	2.73181
5	10.2	4.1	0.108382	0.026588	59.71	40.015	2.731852
6	10.2	4.1	0.108382	0.026588	59.829	40.171	2.737047
7	6.4	5.64	0.068005	0.036574	43.124	56.876	2.452313
8	6.4	5.64	0.068005	0.036574	42.224	57.776	2.544216
9	6.4	5.64	0.068005	0.036574	41.732	58.268	2.596132
10	3.0	6.14	0.031877	0.039816	26.494	73.506	2.221228
11	3.0	6.14	0.031877	0.039816	25.284	74.716	2.365842
12	3.0	6.14	0.031877	0.039816	24.721	75.279	2.437955
						average	**2.504809**
						st. dev	**0.16493**

PhO*n*-Bu (4.950 minutes, Ph_2, 6.085 minutes, GC Method 1)

entry	PhO*n*-Bu, mg	Ph_2, mg	PhO*n*-Bu, mmol	Ph_2, mmol	PhO*n*-Bu, area	Ph_2 area	R_f
1	7.07	2.7	0.047065	0.017509	63.952	36.048	1.515194
2	7.07	2.7	0.047065	0.017509	64.015	35.958	1.509924
3	8.68	4.56	0.057783	0.02957	57.285	42.715	1.457068
4	8.68	4.56	0.057783	0.02957	57.019	42.981	1.472982
5	6.54	6.06	0.043537	0.039298	44.144	55.856	1.401809
6	6.54	6.06	0.043537	0.039298	43.439	56.561	1.44254
7	2.96	7.9	0.019705	0.05123	23.175	76.825	1.275067
8	2.96	7.9	0.019705	0.05123	21.705	78.295	1.387472
9	5.65	9.3	0.037612	0.060308	29.339	70.661	1.502054
10	5.65	9.3	0.037612	0.060308	29.463	70.537	1.493107
						average	**1.445722**
						st. dev	**0.074307**

PhOBn (8.242 minutes, Ph_2, 6.085 minutes, GC Method 1)

entry	PhOBn, mg	Ph_2, mg	PhOBn, mmol	Ph_2, mmol	PhOBn, area	Ph_2 area	R_f
1	4.76	7.5	0.025837	0.048636	36.409	63.591	0.927833
2	4.76	7.5	0.025837	0.048636	36.569	63.431	0.921449
3	4.76	7.5	0.025837	0.048636	36.723	63.277	0.915357
4	2.86	10.81	0.015524	0.0701	20.689	79.311	0.848929
5	2.86	10.81	0.015524	0.0701	19.949	80.051	0.888634
6	2.86	10.81	0.015524	0.0701	19.649	80.351	0.905583
7	6.93	9.81	0.037615	0.063615	37.792	62.208	0.973302
8	6.93	9.81	0.037615	0.063615	38.257	61.743	0.954285
9	6.93	9.81	0.037615	0.063615	38.562	61.438	0.94206
						average	**0.919715**
						st. dev	**0.036794**

Kinetic Alkylation of Phenol-Phenolates in Acetonitrile

Na^+, MeCN, run 1:

time, seconds	standard, µmol	standard, area	product, area	product, µmol	product, [M]x1000	product, %
0	0.000	7.000	0.000	0.000	0.000	0.000
360	6.673	7.341	0.475	0.625	0.104	0.625
540	6.673	7.297	0.678	0.896	0.149	0.896
720	6.673	7.314	0.938	1.237	0.206	1.237
900	6.673	7.299	1.188	1.570	0.262	1.570
1080	6.673	7.312	1.474	1.945	0.324	1.945
1260	6.673	7.276	1.713	2.271	0.378	2.271
1440	6.673	7.323	1.954	2.574	0.429	2.574
1620	6.673	7.278	2.226	2.951	0.492	2.951
1800	6.673	7.324	2.501	3.295	0.549	3.295
2700	6.673	7.315	3.734	4.924	0.821	4.924

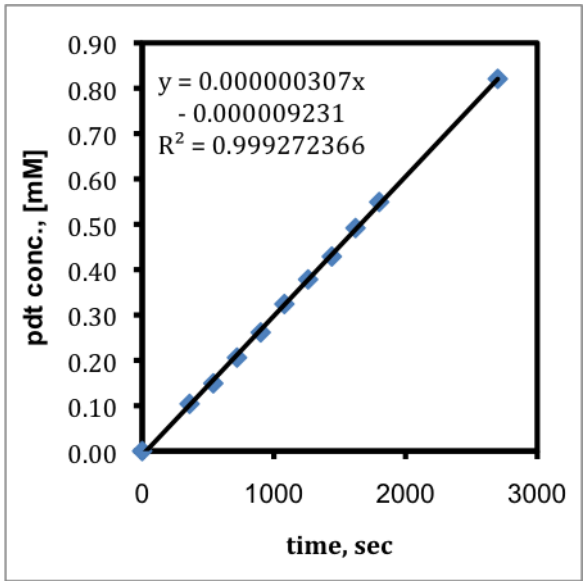

Na^+, MeCN, run 2:

time, seconds	standard, µmol	standard, area	product, area	product, µmol	product, [M]x1000	product, %
0	0.000	0.000	0.000	0.000	0.000	0.000
360	6.673	7.339	0.518	0.680	0.113	0.001
540	6.673	7.320	0.824	1.086	0.181	0.001
720	6.673	7.305	1.156	1.527	0.254	0.002
900	6.673	7.290	1.444	1.911	0.318	0.002
1080	6.673	7.277	1.792	2.376	0.395	0.002
1260	6.673	7.308	2.047	2.702	0.450	0.003
1440	6.673	7.283	2.334	3.092	0.515	0.003
1620	6.673	7.259	2.645	3.515	0.585	0.004
1800	6.673	7.277	3.004	3.982	0.663	0.004
2700	6.673	7.262	4.420	5.872	0.978	0.006

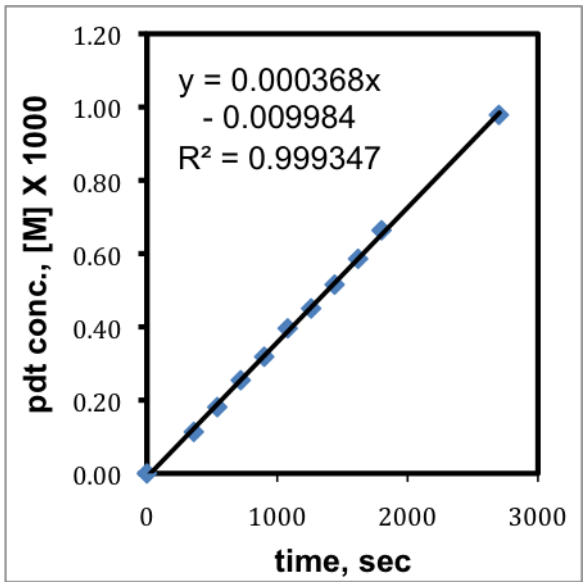

Na^+, MeCN, run 3:

time, seconds	standard, µmol	standard, area	product, area	product, µmol	product, [M]x1000	product, %
0	6.673	7.000	0.000	0.000	0	0.00
360	6.673	7.338	0.597	0.785	0.1308	0.78
540	6.673	7.283	0.886	1.173	0.1955	1.17
720	6.673	7.364	1.185	1.553	0.2588	1.55
900	6.673	7.321	1.495	1.970	0.3283	1.97
1080	6.673	7.423	1.768	2.298	0.3830	2.30
1260	6.673	7.320	2.033	2.679	0.4466	2.68
1440	6.673	7.259	2.359	3.135	0.5225	3.13
1620	6.673	7.358	2.649	3.473	0.5788	3.47
1800	6.673	7.310	2.965	3.913	0.6521	3.91
2700	6.673	7.264	4.331	5.751	0.9585	5.75

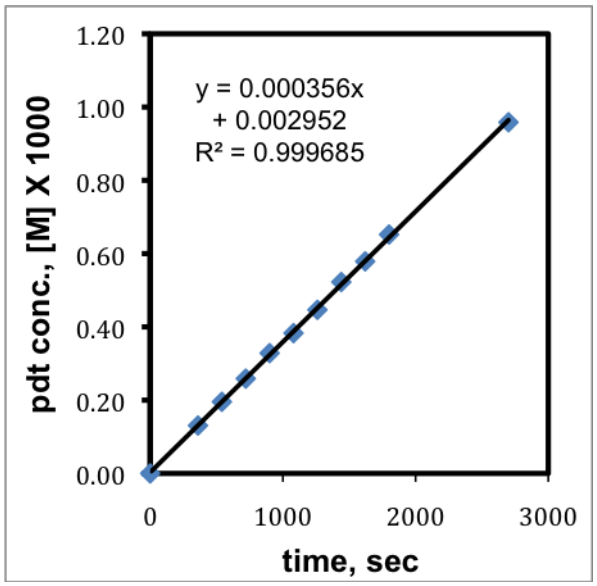

K^+, MeCN, run 1:

time, seconds	standard, µmol	standard, area	product, area	product, µmol	product, [M]x1000	product, %
0	6.67	7.000	0.000	0.000	0.0000	0.00
60	6.67	7.444	1.079	1.398	0.2331	1.40
120	6.67	7.497	2.166	2.788	0.4646	2.79
180	6.67	7.358	3.115	4.084	0.6807	4.08
240	6.67	7.288	4.026	5.329	0.8882	5.33
360	6.67	7.622	5.848	7.402	1.2336	7.40
480	6.67	7.390	7.162	9.357	1.5595	9.36
600	6.67	7.137	8.497	11.486	1.9143	11.49

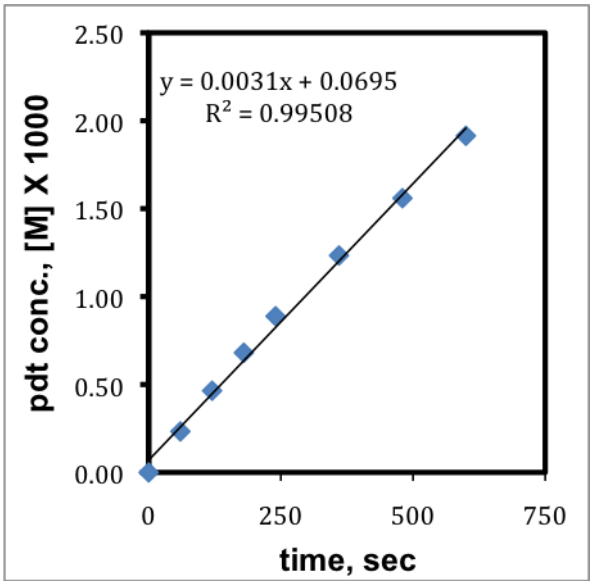

K^+, MeCN, run 2:

time, seconds	standard, µmol	standard, area	product, area	product, µmol	product, [M]x1000	product, %
0	6.67	7.000	0.000	0.000	0.0000	0.00
60	6.67	7.421	1.268	1.648	0.2746	1.65
120	6.67	7.454	2.163	2.800	0.4666	2.80
180	6.67	7.384	3.160	4.128	0.6880	4.13
240	6.67	7.528	4.154	5.328	0.8881	5.33
360	6.67	7.318	5.859	7.724	1.2873	7.72
480	6.67	7.227	7.557	10.088	1.6813	10.09
600	6.67	7.273	9.180	12.176	2.0294	12.18

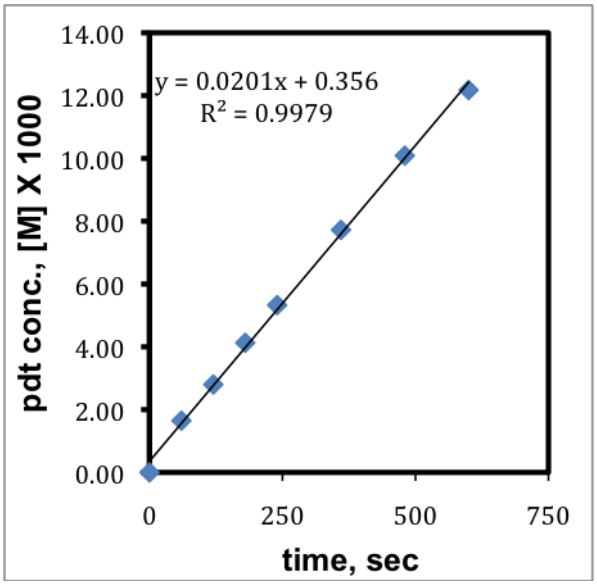

K^+, MeCN, run 3:

time, seconds	standard, µmol	standard, area	product, area	product, µmol	product, [M]x1000	product, %
0	6.67	7.000	0.000	0.000	0.0000	0.00
60	6.67	7.143	1.054	1.423	0.2372	1.42
120	6.67	7.080	1.936	2.638	0.4397	2.64
180	6.67	7.130	2.834	3.834	0.6390	3.83
240	6.67	7.056	3.694	5.051	0.8418	5.05
300	6.67	7.074	4.530	6.177	1.0296	6.18
360	6.67	7.060	5.325	7.277	1.2128	7.28
480	6.67	7.066	6.595	9.004	1.5007	9.00

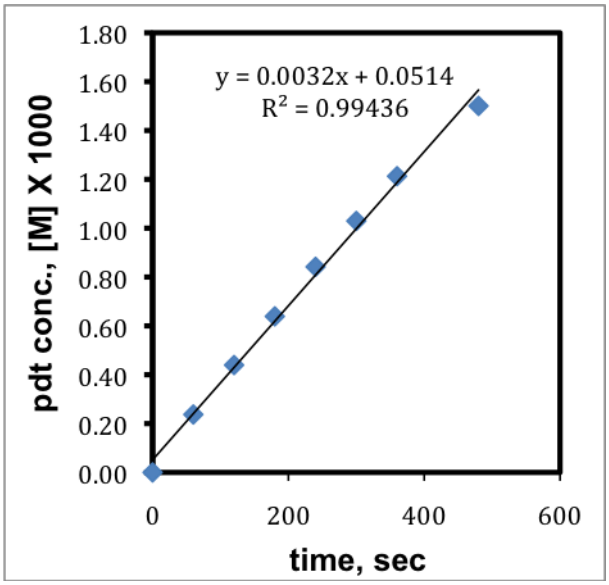

Me_4N^+, MeCN, run 1:

time, seconds	standard, μmol	standard, area	product, area	product, μmol	product, [M]x1000	product, %
0	6.67	7.000	0.000	0.000	0.0000	0.00
60	6.67	7.027	0.928	1.275	0.2125	1.28
120	6.67	7.086	1.806	2.461	0.4101	2.46
180	6.67	6.918	2.647	3.691	0.6152	3.69
240	6.67	6.912	3.531	4.928	0.8214	4.93
300	6.67	6.887	4.347	6.090	1.0149	6.09
360	6.67	6.918	5.007	6.982	1.1636	6.98
480	6.67	6.939	6.315	8.779	1.4631	8.78

Me_4N^+, MeCN, run 2:

time, seconds	standard, µmol	standard, area	product, area	product, µmol	product, [M]x1000	product, %
0	6.67	7.000	0.000	0.000	0.0000	0.00
60	6.67	7.269	0.949	1.260	0.2099	1.26
120	6.67	7.213	1.841	2.462	0.4104	2.46
180	6.67	7.172	2.737	3.681	0.6136	3.68
240	6.67	7.245	3.646	4.855	0.8092	4.86
300	6.67	7.189	4.368	5.861	0.9769	5.86
360	6.67	7.165	5.116	6.888	1.1481	6.89
480	6.67	7.092	6.372	8.668	1.4446	8.67

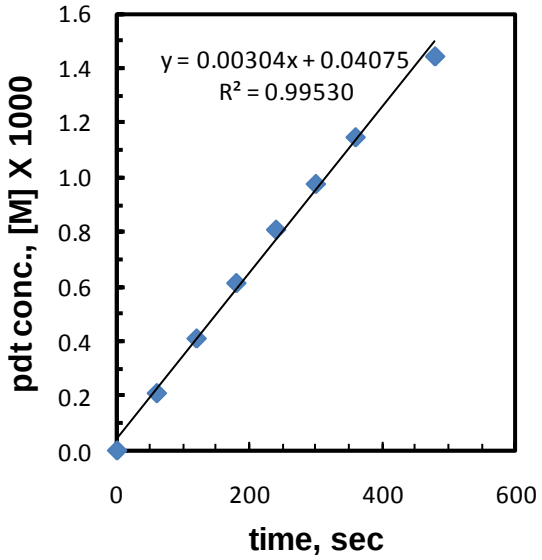

Me_4N^+, MeCN, run 3:

time, seconds	standard, µmol	standard, area	product, area	product, µmol	product, [M]x1000	product, %
0	6.67	7.000	0.000	0.000	0.0000	0.00
60	6.67	7.612	1.958	2.492	0.4153	2.49
120	6.67	7.298	3.495	4.621	0.7701	4.62
180	6.67	7.151	5.151	6.950	1.1583	6.95
240	6.67	7.223	6.439	8.600	1.4333	8.60
300	6.67	7.119	7.640	10.354	1.7256	10.35
360	6.67	7.110	8.770	11.899	1.9832	11.90

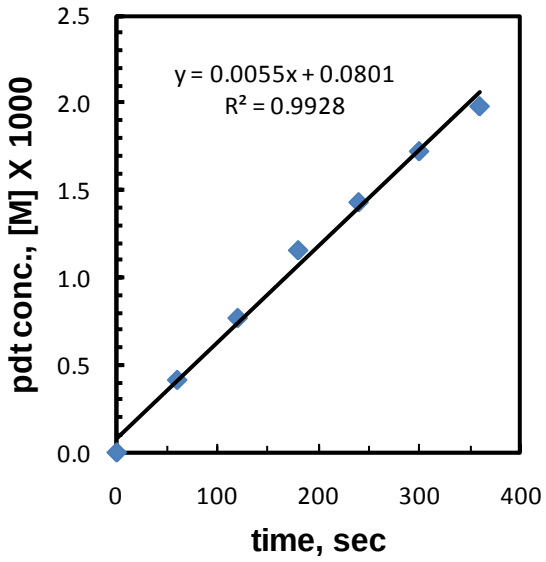

Me_4N^+, MeCN, run 4:

time, seconds	standard, µmol	standard, area	product, area	product, µmol	product, [M]x1000	product, %
0	6.67	7.000	0.000	0.000	0.0000	0.00
60	6.67	7.271	0.689	0.914	0.1524	0.91
90	6.67	7.301	1.062	1.403	0.2338	1.40
120	6.67	7.229	1.371	1.830	0.3050	1.83
180	6.67	7.334	2.036	2.678	0.4463	2.68
240	6.67	7.274	2.687	3.564	0.5940	3.56
300	6.67	7.231	3.381	4.511	0.7519	4.51
360	6.67	7.259	3.884	5.162	0.8604	5.16
420	6.67	7.214	4.328	5.788	0.9646	5.79

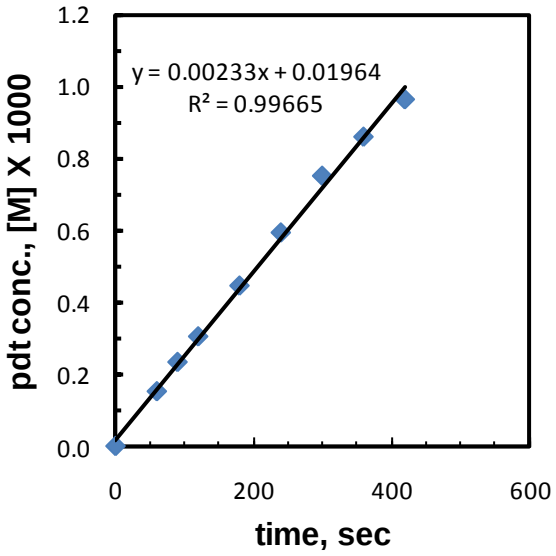

Me_4N^+, MeCN, run 5:

time, seconds	standard, µmol	standard, area	product, area	product, µmol	product, [M]x1000	product, %
0	6.67	7.000	0.000	0.000	0.0000	0.00
60	6.67	7.323	0.648	0.854	0.1424	0.85
90	6.67	7.349	0.928	1.218	0.2030	1.22
120	6.67	7.405	1.282	1.671	0.2785	1.67
150	6.67	7.411	1.584	2.062	0.3436	2.06
180	6.67	7.412	1.917	2.496	0.4159	2.50
240	6.67	7.357	2.589	3.395	0.5658	3.39
300	6.67	7.386	3.287	4.294	0.7156	4.29
360	6.67	7.388	4.016	5.244	0.8739	5.24

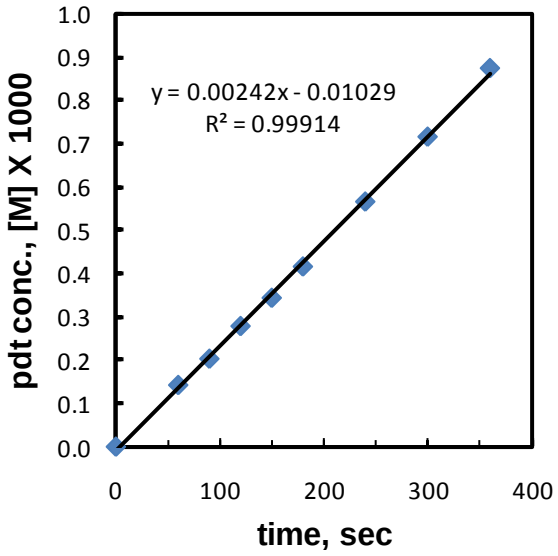

Me_4N^+, MeCN, run 6:

time, seconds	standard, µmol	standard, area	product, area	product, µmol	product, [M]x1000	product, %
0	6.67	7.000	0.000	0.000	0.0000	0.00
60	6.67	7.465	0.855	1.105	0.1841	1.10
90	6.67	7.500	1.265	1.627	0.2711	1.63
120	6.67	7.445	1.657	2.148	0.3579	2.15
150	6.67	7.499	2.060	2.650	0.4416	2.65
180	6.67	7.409	2.374	3.091	0.5152	3.09
240	6.67	7.405	3.052	3.977	0.6628	3.98
300	6.67	7.395	3.694	4.819	0.8031	4.82
360	6.67	7.390	4.296	5.609	0.9348	5.61

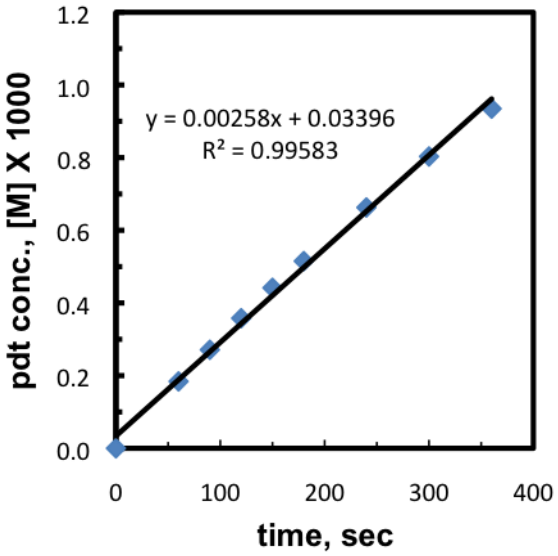

Et_4N^+, MeCN, run 1:

time, seconds	standard, µmol	standard, area	product, area	product, µmol	product, [M]x1000	product, %
0	6.67	7.000	0.000	0.000	0.0000	0.000
30	6.67	7.016	0.675	0.928	0.1547	0.928
60	6.67	7.044	1.300	1.780	0.2967	1.780
90	6.67	7.000	1.995	2.743	0.4571	2.743
120	6.67	7.000	2.629	3.623	0.6038	3.623
180	6.67	6.955	3.910	5.423	0.9038	5.423
240	6.67	6.896	5.007	6.974	1.1624	6.974
300	6.67	6.877	6.180	8.593	1.4322	8.593
360	6.67	6.877	6.869	9.636	1.6060	9.636

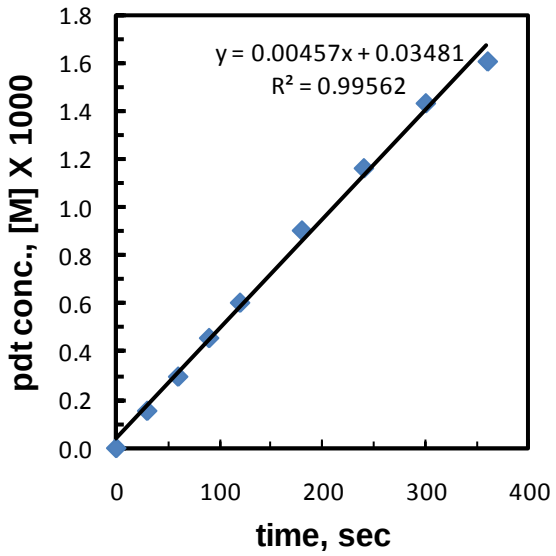

Et_4N^+, MeCN, run 2:

time, seconds	standard, µmol	standard, area	product, area	product, µmol	product, [M]x1000	product, %
0	6.67	7.000	0.000	0.000	0.0000	0.00
30	6.67	7.138	0.690	0.933	0.1554	0.93
60	6.67	7.112	1.335	1.810	0.3017	1.81
90	6.67	7.110	1.941	2.634	0.4390	2.63
120	6.67	7.103	2.557	3.473	0.5788	3.47
180	6.67	7.043	3.614	4.949	0.8249	4.95
240	6.67	7.030	4.628	6.351	1.0585	6.35
300	6.67	6.989	5.512	7.609	1.2682	7.61
360	6.67	6.965	6.319	8.753	1.4588	8.75

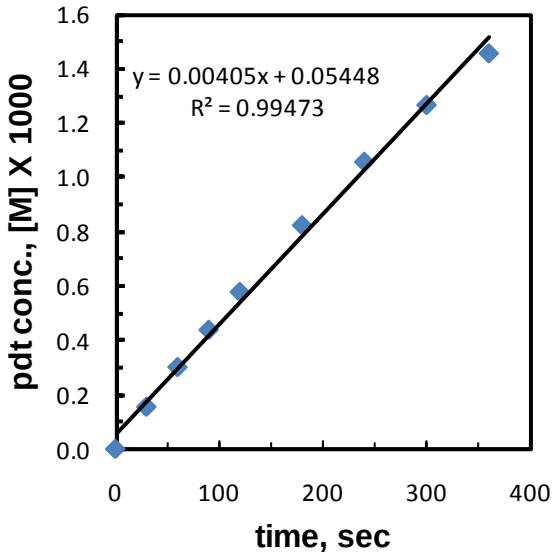

Et_4N^+, MeCN, run 3:

time, seconds	standard, µmol	standard, area	product, area	product, µmol	product, [M]x1000	product, %
0	6.67	7.000	0.000	0.000	0.0000	0.00
30	6.67	7.231	0.603	0.804	0.1340	0.80
60	6.67	7.108	1.157	1.570	0.2617	1.57
90	6.67	7.144	1.814	2.449	0.4082	2.45
120	6.67	7.102	2.340	3.179	0.5298	3.18
180	6.67	7.114	3.460	4.692	0.7820	4.69
240	6.67	7.034	4.541	6.228	1.0380	6.23
300	6.67	7.048	5.621	7.694	1.2824	7.69
360	6.67	6.918	7.178	10.017	1.6695	10.02

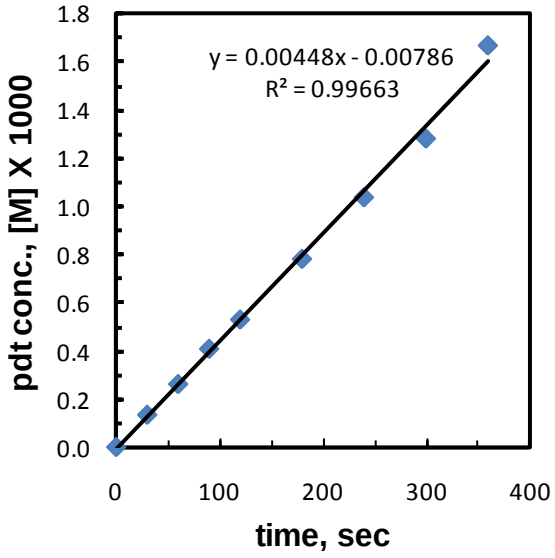

Et_4N^+, MeCN, run 4:

time, seconds	standard, µmol	standard, area	product, area	product, µmol	product, [M]x1000	product, %
0	9.34	7.000	0.000	0.000	0.0000	0.00
30	9.34	10.122	1.225	1.634	0.2723	1.63
60	9.34	10.090	2.205	2.950	0.4916	2.95
90	9.34	9.993	3.115	4.208	0.7013	4.21
120	9.34	9.843	3.818	5.236	0.8727	5.24
150	9.34	9.866	4.510	6.171	1.0284	6.17
180	9.34	9.792	5.114	7.051	1.1751	7.05
240	9.34	9.779	6.122	8.452	1.4087	8.45
300	9.34	9.729	7.064	9.803	1.6338	9.80

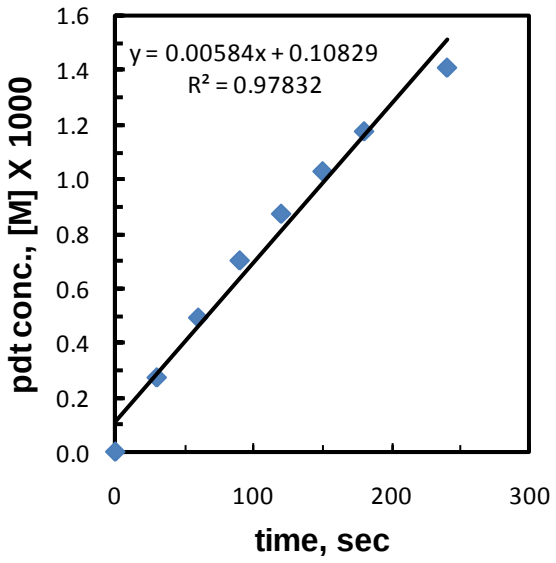

Et_4N^+, MeCN, run 5:

time, seconds	standard, µmol	standard, area	product, area	product, µmol	product, [M]x1000	product, %
0	9.338	7.000	0.000	0.000	0.0000	0.00
30	9.338	10.078	1.116	1.494	0.2490	1.49
60	9.338	9.858	2.137	2.926	0.4877	2.93
90	9.338	9.817	2.972	4.087	0.6811	4.09
120	9.338	9.807	3.690	5.079	0.8465	5.08
150	9.338	9.798	4.349	5.993	0.9988	5.99
180	9.338	10.055	5.077	6.817	1.1361	6.82
240	9.338	9.707	5.882	8.181	1.3635	8.18
300	9.338	9.579	6.787	9.565	1.5942	9.57

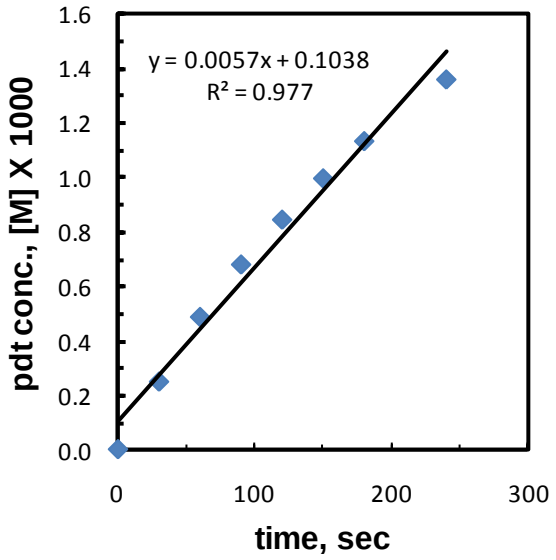

Pr_4N^+, MeCN, run 1:

time, seconds	standard, µmol	standard, area	product, area	product, µmol	product, [M]x1000	product, %
0	6.673	7.000	0.000	0.000	0.0000	0.00
30	6.673	7.068	0.645	0.881	0.1468	0.88
60	6.673	7.104	1.355	1.840	0.3067	1.84
90	6.673	7.113	2.151	2.918	0.4863	2.92
120	6.673	7.036	3.015	4.135	0.6891	4.13
180	6.673	6.936	4.655	6.474	1.0790	6.47
240	6.673	7.005	6.334	8.723	1.4538	8.72
300	6.673	6.940	7.793	10.833	1.8055	10.83
360	6.673	6.863	9.154	12.868	2.1447	12.87

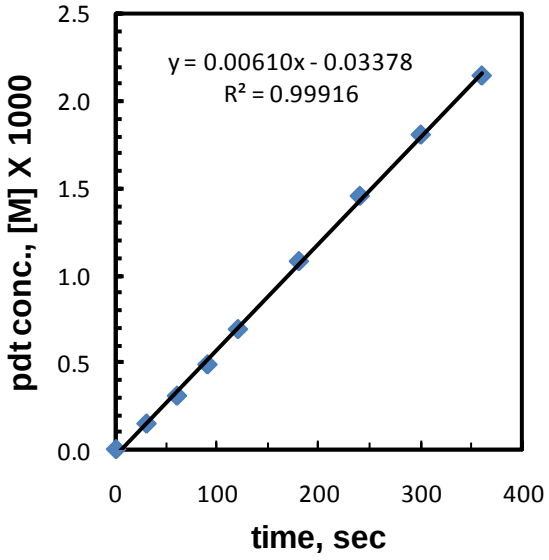

Pr_4N^+, MeCN, run 2:

time, seconds	standard, µmol	standard, area	product, area	product, µmol	product, [M]x1000	product, %
0	6.673	7.000	0.000	0.000	0.0000	0.00
30	6.673	7.168	1.303	1.753	0.2922	1.75
60	6.673	7.067	2.367	3.231	0.5385	3.23
90	6.673	7.077	3.169	4.318	0.7197	4.32
120	6.673	7.011	4.506	6.200	1.0333	6.20
180	6.673	7.051	6.428	8.795	1.4658	8.80
240	6.673	6.931	7.980	11.109	1.8514	11.11
300	6.673	6.953	9.363	12.991	2.1652	12.99
360	6.673	6.886	10.555	14.789	2.4648	14.79

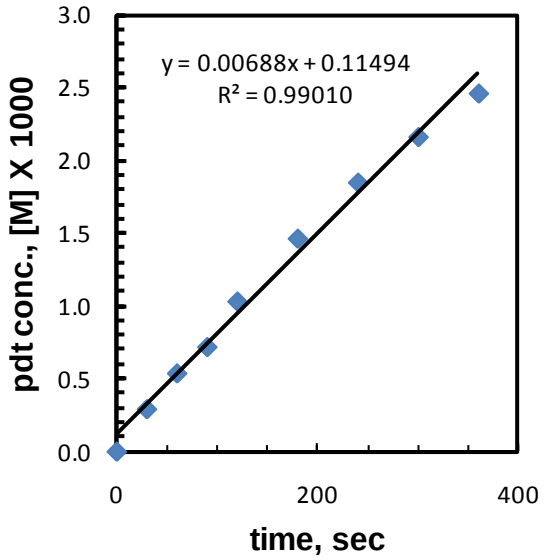

Bu_4N^+, MeCN, run 1:

time, seconds	standard, µmol	standard, area	product, area	product, µmol	product, [M]x1000	product, %
0	6.466	7.000	0.000	0.000	0.0000	0.00
30	6.466	7.396	0.941	1.189	0.1982	1.19
45	6.466	7.400	1.487	1.878	0.3130	1.88
60	6.466	7.444	1.962	2.464	0.4107	2.46
90	6.466	7.408	2.799	3.532	0.5887	3.53
120	6.466	7.347	3.417	4.345	0.7242	4.35
150	6.466	7.328	4.500	5.741	0.9568	5.74
180	6.466	7.290	4.890	6.270	1.0450	6.27
210	6.466	7.272	6.007	7.723	1.2871	7.72
240	6.466	7.268	6.846	8.806	1.4677	8.81
300	6.466	7.293	8.099	10.382	1.7303	10.38

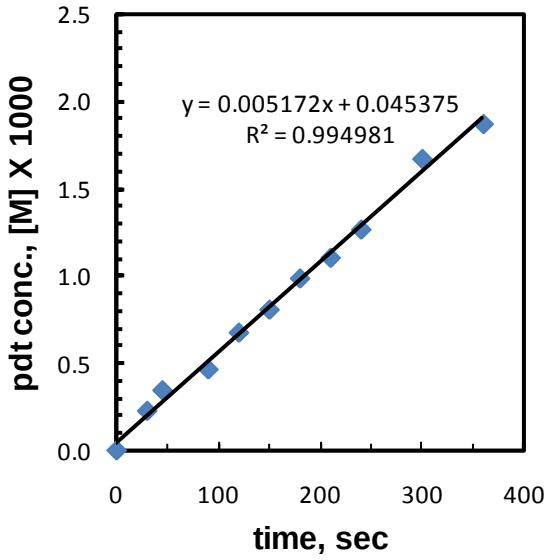

Bu_4N^+, MeCN, run 2:

time, seconds	standard, µmol	standard, area	product, area	product, µmol	product, [M]x1000	product, %
0	6.673	7.000	0.000	0.000	0.0000	0.00
30	0.000	7.910	1.242	1.515	0.2525	1.51
60	0.000	7.942	2.521	3.062	0.5104	3.06
90	6.673	7.841	3.773	4.642	0.7737	4.64
300	0.000	7.656	9.895	12.468	2.0781	12.47

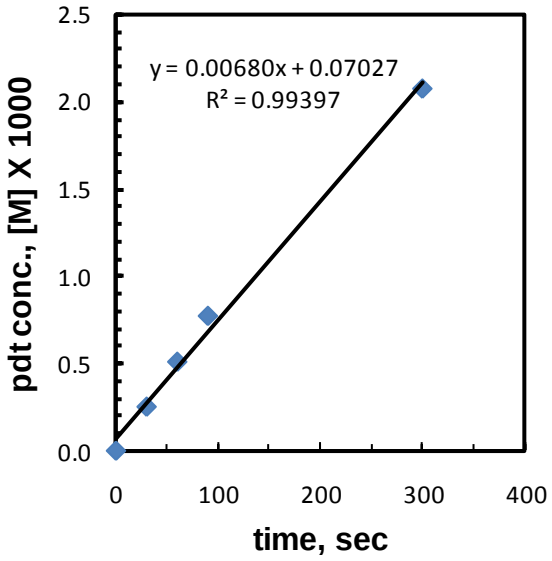

Bu_4N^+, MeCN, run 3:

time, seconds	standard, µmol	standard, area	product, area	product, µmol	product, [M]x1000	product, %
0	6.466	7.000	0.000	0.000	0.0000	0.00
30	6.466	7.459	1.085	1.359	0.2266	1.36
45	6.466	7.502	1.660	2.069	0.3448	2.07
90	6.466	7.475	2.229	2.788	0.4646	2.79
120	6.466	7.425	3.219	4.053	0.6755	4.05
150	6.466	7.367	3.817	4.844	0.8073	4.84
180	6.466	7.299	4.621	5.918	0.9864	5.92
210	6.466	7.312	5.184	6.628	1.1047	6.63
240	6.466	7.241	5.888	7.601	1.2669	7.60
300	6.466	7.193	7.720	10.033	1.6722	10.03
360	6.466	7.467	8.974	11.235	1.8725	11.23

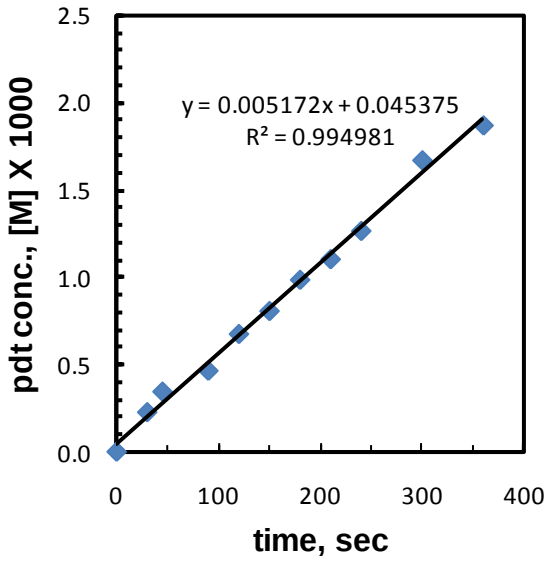

Bu_4N^+, MeCN, run 4:

time, seconds	standard, µmol	standard, area	product, area	product, µmol	product, [M]x1000	product, %
0	5.910	7.000	0.000	0.000	0.0000	0.00
30	5.910	7.400	1.158	1.337	0.2228	1.34
45	5.910	7.396	1.761	2.034	0.3391	2.03
60	5.910	7.410	2.279	2.628	0.4380	2.63
90	5.910	7.403	3.328	3.841	0.6402	3.84
120	5.910	7.341	4.269	4.969	0.8282	4.97
150	5.910	7.439	5.154	5.921	0.9868	5.92
180	5.910	7.330	5.980	6.972	1.1619	6.97
210	5.910	7.403	6.806	7.857	1.3095	7.86
240	5.910	7.251	7.426	8.751	1.4584	8.75
300	5.910	7.252	8.728	10.284	1.7140	10.28

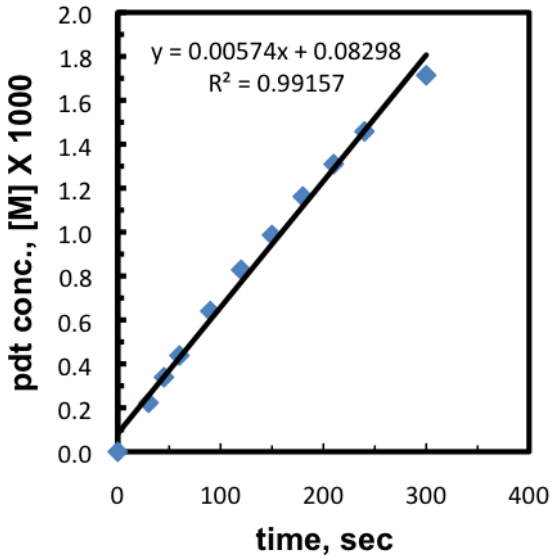

Hexyl$_4$N$^+$, MeCN, run 1:

time, seconds	standard, µmol	standard, area	product, area	product, µmol	product, [M]x1000	product, %
0	6.673	7.000	0.000	0.000	0.0000	0.00
30	6.673	7.652	1.022	1.288	0.2147	1.29
60	6.673	7.719	1.879	2.348	0.3914	2.35
90	6.673	7.627	2.909	3.679	0.6132	3.68
300	6.673	7.446	8.290	10.741	1.7901	10.74

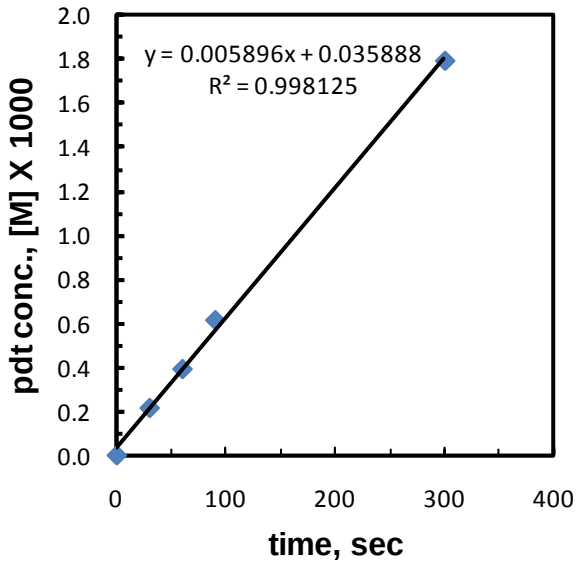

Hexyl$_4$N$^+$, MeCN, run 2:

time, seconds	standard, µmol	standard, area	product, area	product, µmol	product, [M]x1000	product, %
0	5.910	7.000	0.000	0.000	0.0000	0.00
45	5.910	7.242	0.426	0.503	0.0838	0.50
75	5.910	7.245	0.692	0.816	0.1360	0.82
90	5.910	7.445	0.883	1.013	0.1689	1.01
120	5.910	7.498	1.176	1.340	0.2234	1.34
180	5.910	7.494	1.836	2.093	0.3489	2.09
270	5.910	7.291	2.516	2.949	0.4914	2.95
300	5.910	7.358	2.944	3.419	0.5698	3.42

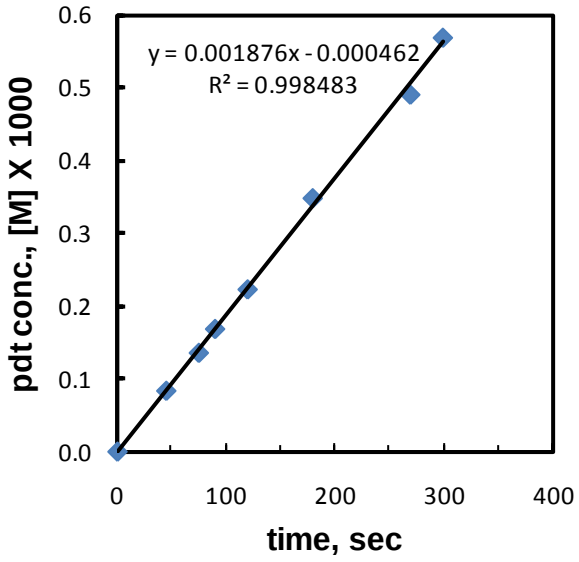

$Hexyl_4N^+$, MeCN, run 3:

time, seconds	standard, µmol	standard, area	product, area	product, µmol	product, [M]x1000	product, %
0	0.000	7.000	0.000	0.000	0.0000	0.00
30	0.000	7.369	1.107	1.284	0.2139	1.28
60	0.000	7.185	1.886	2.243	0.3738	2.24
90	0.000	7.226	2.847	3.367	0.5611	3.37
120	0.000	7.201	3.707	4.399	0.7331	4.40
150	0.000	7.244	4.474	5.277	0.8796	5.28
180	0.000	7.260	5.329	6.272	1.0453	6.27
240	0.000	7.266	6.346	7.463	1.2438	7.46
360	0.000	7.118	8.326	9.995	1.6658	9.99

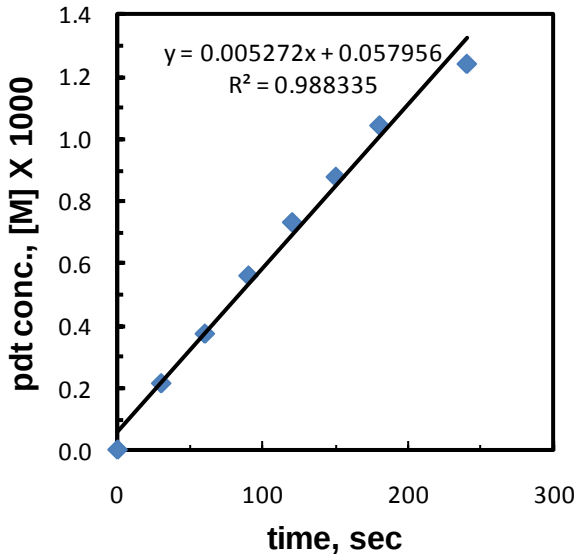

Hexyl$_4$N$^+$, MeCN, run 4:

time, seconds	standard, µmol	standard, area	product, area	product, µmol	product, [M]x1000	product, %
0	5.910	7.000	0.000	0.000	0.0000	0.00
60	5.910	7.291	1.220	1.430	0.2383	1.43
90	5.910	7.303	1.929	2.257	0.3762	2.26
120	5.910	7.266	2.615	3.075	0.5125	3.08
210	5.910	7.271	4.553	5.351	0.8918	5.35
240	5.910	7.316	5.104	5.961	0.9935	5.96
300	5.910	7.077	5.996	7.240	1.2066	7.24
360	5.910	7.228	7.214	8.528	1.4214	8.53

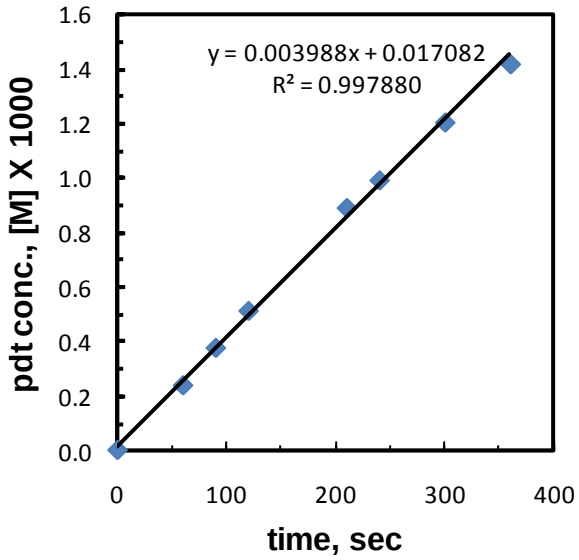

Octyl$_4$N$^+$, MeCN, run 1:

time, seconds	standard, µmol	standard, area	product, area	product, µmol	product, [M]x1000	product, %
0	6.206	7.000	0.000	0.000	0.0000	0.00
30	6.206	7.192	0.654	0.816	0.1360	0.82
60	6.206	7.183	1.181	1.475	0.2459	1.48
90	6.206	7.057	1.910	2.429	0.4048	2.43
105	6.206	7.211	2.201	2.739	0.4565	2.74
120	6.206	6.995	2.507	3.216	0.5360	3.22
150	6.206	7.093	3.075	3.889	0.6482	3.89
165	6.206	6.829	3.305	4.342	0.7237	4.34
180	6.206	6.566	3.389	4.630	0.7717	4.63
210	6.206	6.625	3.861	5.228	0.8714	5.23
240	6.206	6.857	4.429	5.795	0.9658	5.80

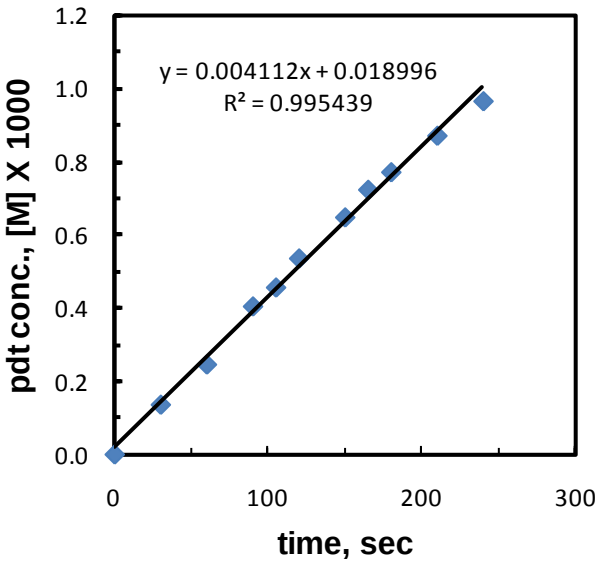

Octyl$_4$N$^+$, MeCN, run 2:

time, seconds	standard, µmol	standard, area	product, area	product, µmol	product, [M]x1000	product, %
0	6.906	7.000	0.000	0.000	0.0000	0.00
30	6.906	7.045	0.591	0.837	0.1395	0.84
45	6.906	6.935	0.944	1.358	0.2264	1.36
60	6.906	6.831	1.196	1.748	0.2913	1.75
75	6.906	5.546	1.174	2.113	0.3521	2.11
90	6.906	6.296	1.425	2.258	0.3763	2.26
120	6.906	7.073	2.358	3.328	0.5547	3.33

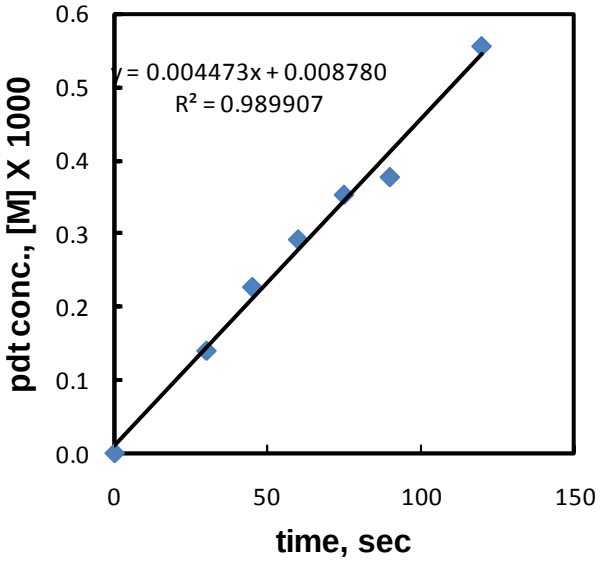

Octyl$_4$N$^+$, MeCN, run 3:

time, seconds	standard, µmol	standard, area	product, area	product, µmol	product, [M]x1000	product, %
0	6.906	7.000	0.000	0.000	0.0000	0.00
60	6.906	7.312	0.660	0.901	0.1502	0.90
75	6.906	7.342	0.842	1.144	0.1906	1.14
90	6.906	7.354	0.977	1.326	0.2210	1.33
120	6.906	7.322	1.257	1.714	0.2856	1.71
180	6.906	7.307	1.808	2.469	0.4116	2.47
240	6.906	6.220	1.993	3.199	0.5332	3.20
300	6.906	6.827	2.659	3.889	0.6482	3.89
360	6.906	7.199	3.288	4.560	0.7599	4.56

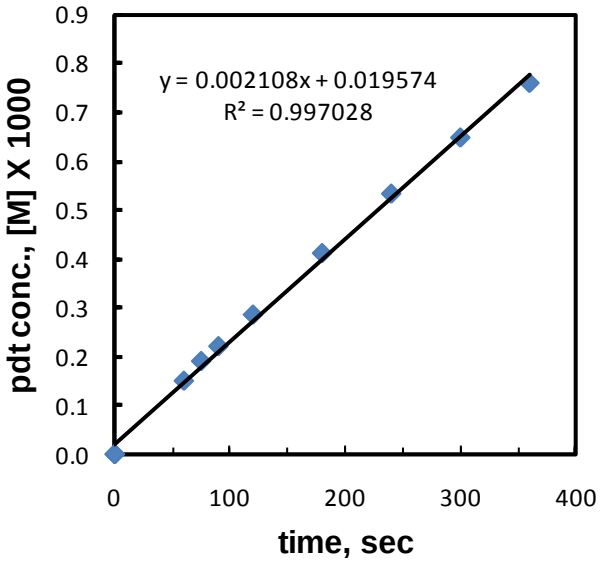

Kinetic Alkylation of Phenol-Phenolates in Diisopropyl Ketone (DIPK)

Na^+, DIPK, run 1:

time, seconds	standard, µmol	standard, area	product, area	product, µmol	product, [M] x 1000	product, %
0	19.454	17.000	0.000	0.000	0.0000	0.00
900	19.454	17.611	0.000	0.000	0.0000	0.00
1800	19.454	18.795	0.000	0.000	0.0000	0.00
3600	19.454	17.995	0.000	0.000	0.0000	0.00
7200	19.454	18.012	0.364	0.568	0.0947	0.57
10800	19.454	17.754	0.536	0.849	0.1415	0.85
21600	19.454	18.069	1.150	1.790	0.2983	1.79
28800	19.454	18.206	1.548	2.391	0.3986	2.39
68400	19.454	17.763	3.649	5.778	0.9630	5.78
79200	19.454	17.738	4.165	6.604	1.1007	6.60

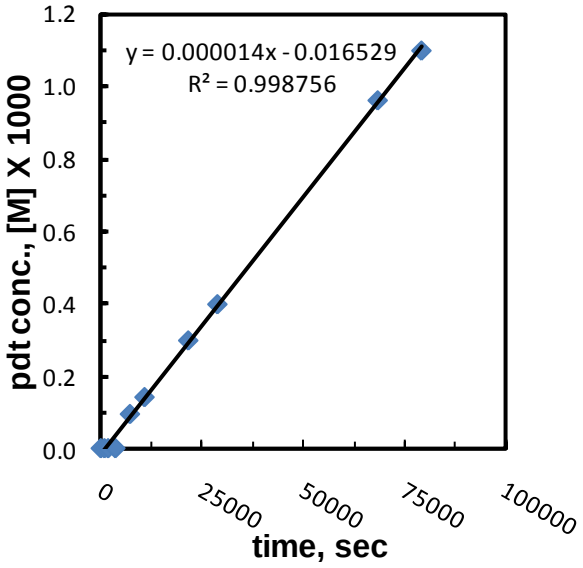

Na^+, DIPK, run 2:

time, seconds	standard, µmol	standard, area	product, area	product, µmol	product, [M] x 1000	product, %
0	49.933	15.000	0.000	0.000	0.0000	0.00
9000	49.933	15.335	0.528	2.486	0.4143	2.49
14400	49.933	15.237	0.795	3.766	0.6277	3.77
16200	49.933	15.545	0.929	4.314	0.7190	4.31
28800	49.933	15.134	1.722	8.214	1.3690	8.21
30600	49.933	15.404	1.857	8.703	1.4504	8.70

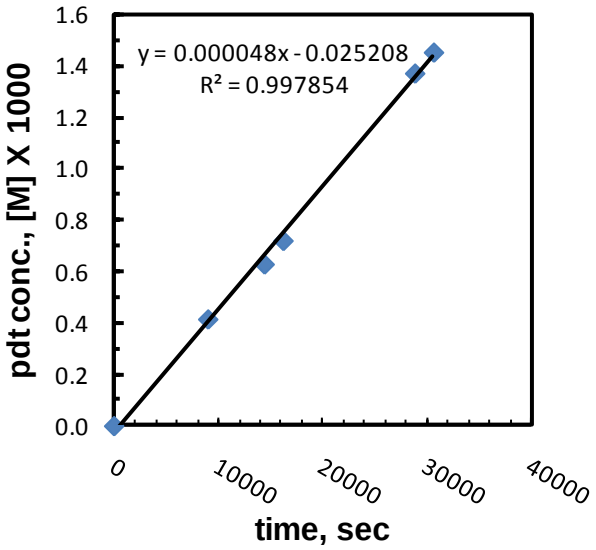

Na^+, DIPK, run 3:

time, seconds	standard, µmol	standard, area	product, area	product, µmol	product, [M]x1000	product, %
0	49.933	15.000	0.000	0.000	0.0000	0.00
9000	49.933	15.893	0.509	2.312	0.3853	2.31
14400	49.933	16.021	0.818	3.686	0.6143	3.69
16200	49.933	16.284	0.915	4.056	0.6760	4.06
28800	49.933	15.240	1.712	8.109	1.3516	8.11
30600	49.933	16.144	1.956	8.746	1.4577	8.75

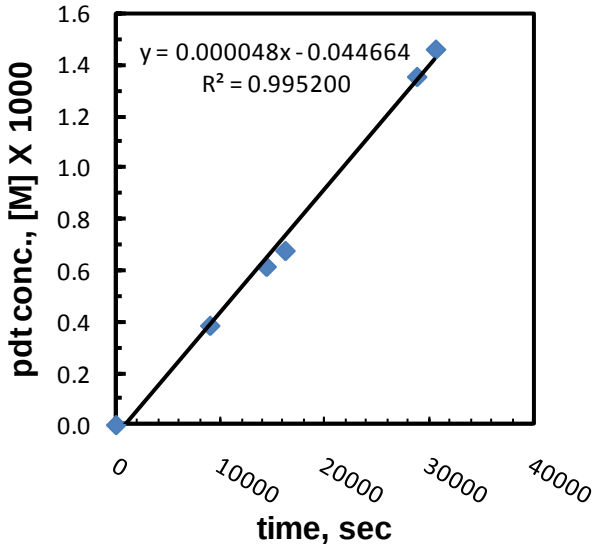

Na^+, DIPK, run 4:

time, seconds	standard, µmol	standard, area	product, area	product, µmol	product, [M]x1000	product, %
0	49.933	15.000	0.000	0.000	0.0000	0.00
9000	49.933	15.943	0.554	2.508	0.4181	2.51
14400	49.933	15.445	0.841	3.931	0.6551	3.93
16200	49.933	16.104	1.100	4.931	0.8218	4.93
28800	49.933	15.280	1.866	8.816	1.4693	8.82
30600	49.933	15.380	1.976	9.275	1.5458	9.27

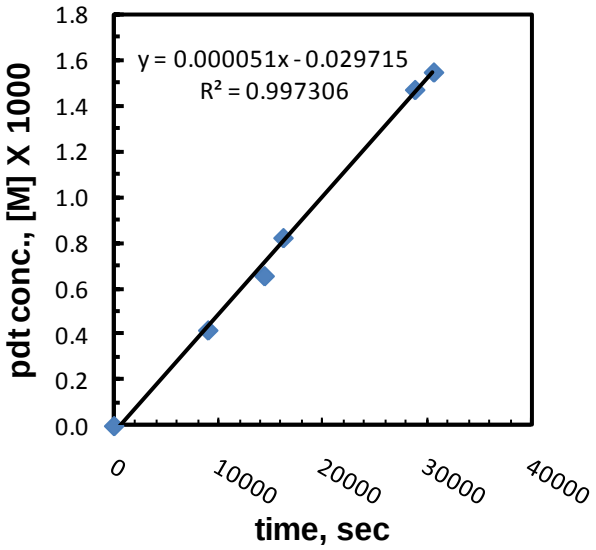

K^+, DIPK, run 1:

time, seconds	standard, µmol	standard, area	product, area	product, µmol	product, [M] x 1000	product, %
0	15.563	7.000	0.000	0.000	0.0000	0.00
900	15.563	20.722	0.933	1.013	0.1688	1.01
1800	15.563	19.845	1.787	2.026	0.3377	2.03
3600	15.563	19.518	3.571	4.117	0.6861	4.12
7200	15.563	19.561	7.169	8.246	1.3744	8.25
10800	15.563	19.953	10.977	12.378	2.0631	12.38
20700	15.563	17.775	18.666	23.628	3.9380	23.63
27900	15.563	18.030	24.128	30.110	5.0184	30.11

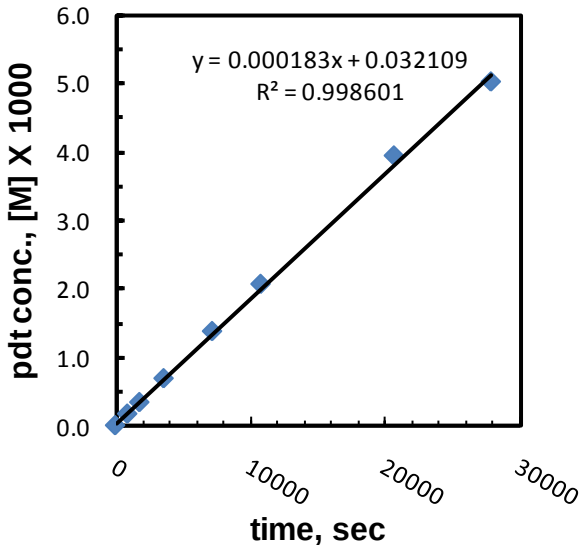

K^+, DIPK, run 2:

time, seconds	standard, µmol	standard, area	product, area	product, µmol	product, [M]x1000	product, %
0	6.906	7.000	0.000	0.000	0.0000	0.00
900	6.906	6.983	0.398	0.570	0.0949	0.57
1600	6.906	6.947	0.711	1.022	0.1704	1.02
1900	6.906	7.028	0.886	1.259	0.2099	1.26
2200	6.906	7.037	1.025	1.455	0.2426	1.46
2600	6.906	7.025	1.267	1.803	0.3005	1.80
3200	6.906	6.897	1.552	2.247	0.3745	2.25
4200	6.906	6.946	2.067	2.958	0.4930	2.96
6600	6.906	6.967	3.345	4.808	0.8013	4.81
9000	6.906	6.785	4.580	6.741	1.1235	6.74

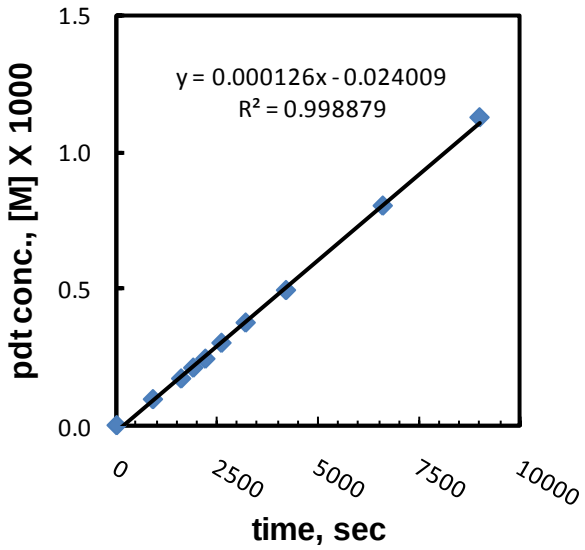

K^+, DIPK, run 3:

time, seconds	standard, µmol	standard, area	product, area	product, µmol	product, [M] x 1000	product, %
0	6.906	7.000	0.000	0.000	0.0000	0.00
1500	6.906	6.968	0.732	1.049	0.1748	1.05
1800	6.906	7.014	0.912	1.298	0.2163	1.30
2100	6.906	6.950	1.052	1.511	0.2518	1.51
2400	6.906	6.966	1.234	1.769	0.2949	1.77
3000	6.906	7.069	1.548	2.186	0.3644	2.19
3600	6.906	6.924	1.925	2.776	0.4626	2.78
5400	6.906	7.067	2.796	3.950	0.6583	3.95
9000	6.906	6.805	4.525	6.640	1.1067	6.64

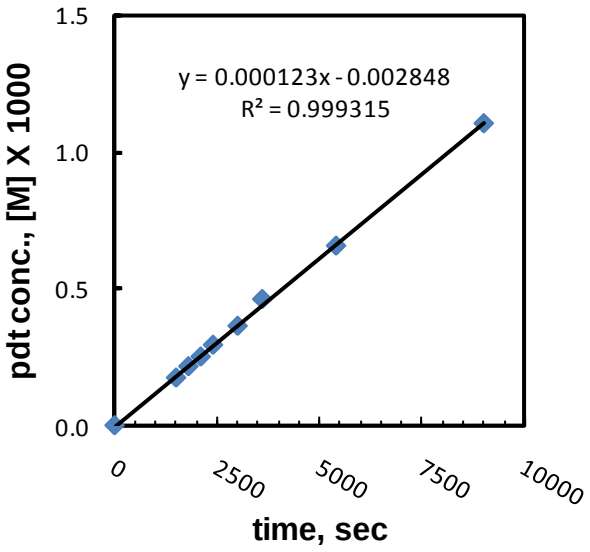

K^+, DIPK, run 4:

time, seconds	standard, µmol	standard, area	product, area	product, µmol	product, [M]x1000	product, %
0	6.906	7.000	0.000	0.000	0.0000	0.00
1500	6.906	7.195	0.685	0.950	0.1584	0.95
1800	6.906	7.118	0.808	1.133	0.1889	1.13
2100	6.906	7.168	0.941	1.311	0.2185	1.31
2400	6.906	7.360	1.112	1.511	0.2518	1.51
3000	6.906	7.097	1.387	1.953	0.3255	1.95
3600	6.906	7.261	1.583	2.178	0.3631	2.18
5400	6.906	7.048	2.375	3.365	0.5608	3.36
9000	6.906	6.938	4.189	6.029	1.0048	6.03

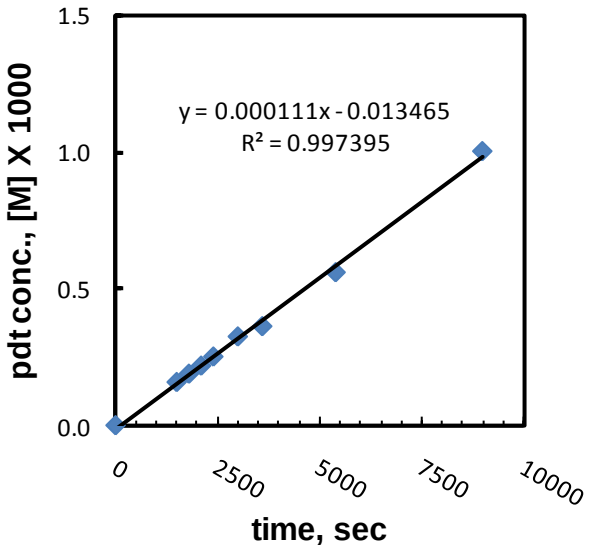

Me_4N^+, DIPK, run 1:

time, seconds	standard, µmol	standard, area	product, area	product, µmol	product, [M]x1000	product, %
0	6.91	7.000	0.000	0.000	0.0000	0.00
180	6.91	7.164	0.353	0.491	0.0819	0.49
240	6.91	7.143	0.458	0.640	0.1066	0.64
300	6.91	7.154	0.692	0.778	0.1296	0.78
360	6.91	7.154	0.692	0.966	0.1610	0.97
420	6.91	7.143	0.833	1.169	0.1948	1.16

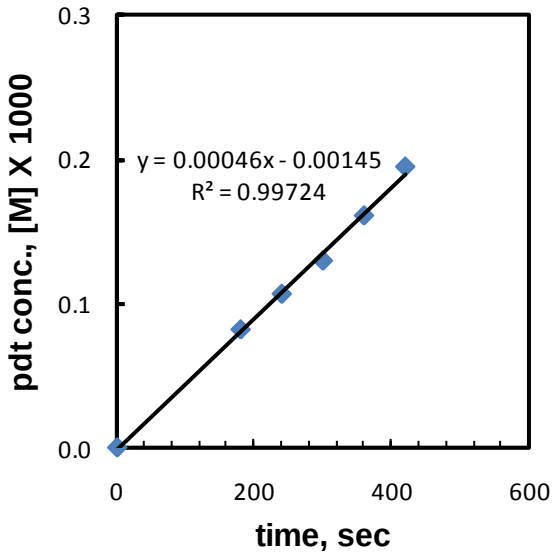

Me_4N^+, DIPK, run 2:

time, seconds	standard, □mol	standard, area	product, area	product, µmol	product, [M] x 1000	product, %
0	6.906	7.000	0.000	0.000	0.0000	0.00
180	6.906	7.097	0.380	0.534	0.0890	0.53
240	6.906	7.131	0.507	0.710	0.1183	0.71
300	6.906	7.180	0.646	0.898	0.1497	0.90
360	6.906	7.296	0.791	1.082	0.1804	1.08
420	6.906	7.240	0.922	1.272	0.2119	1.27

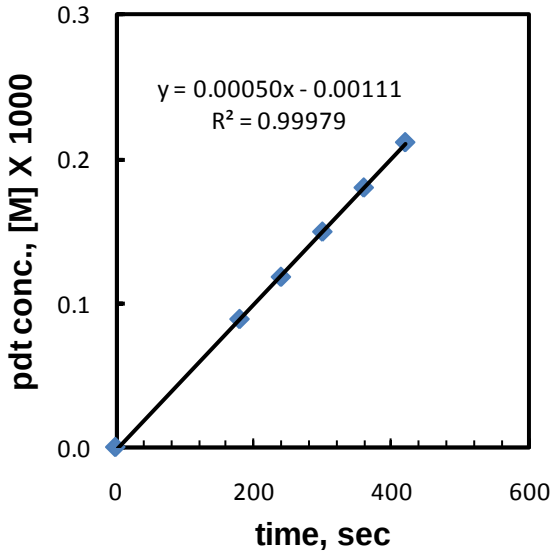

Me_4N^+, DIPK, run 3:

time, seconds	standard, □mol	standard, area	product, area	product, µmol	product, [M] x 1000	product, %
0	6.906	7.000	0.000	0.000	0.0000	0.00
180	6.906	7.173	0.372	0.518	0.0863	0.52
240	6.906	7.153	0.518	0.723	0.1205	0.72
300	6.906	7.035	0.644	0.913	0.1522	0.91
360	6.906	7.163	0.774	1.079	0.1798	1.08
420	6.906	7.240	0.922	1.272	0.2119	1.27

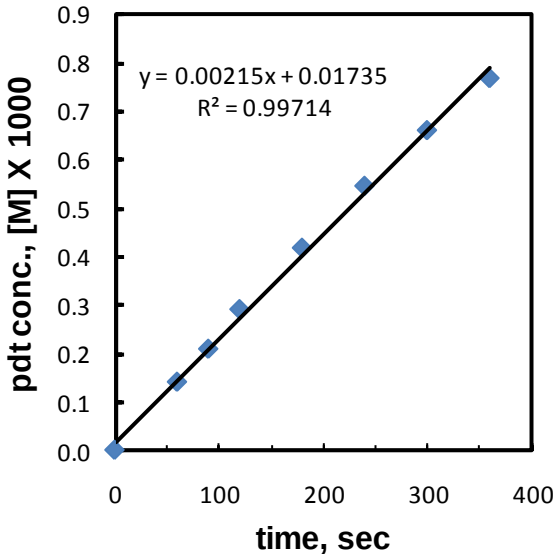

Et_4N^+, DIPK, run 1:

time, seconds	standard, µmol	standard, area	product, area	product, µmol	product, [M]x1000	product, %
0	6.91	7.000	0.000	0.000	0.0000	0.00
60	6.91	7.284	0.627	0.847	0.1412	0.85
90	6.91	7.243	0.913	1.258	0.2097	1.24
120	6.91	7.133	1.235	1.751	0.2919	1.70
180	6.91	7.117	1.769	2.516	0.4193	2.45
240	6.91	7.109	2.309	3.287	0.5478	3.20
300	6.91	7.105	2.794	3.980	0.6633	3.87
360	6.91	7.083	3.239	4.628	0.7714	4.50

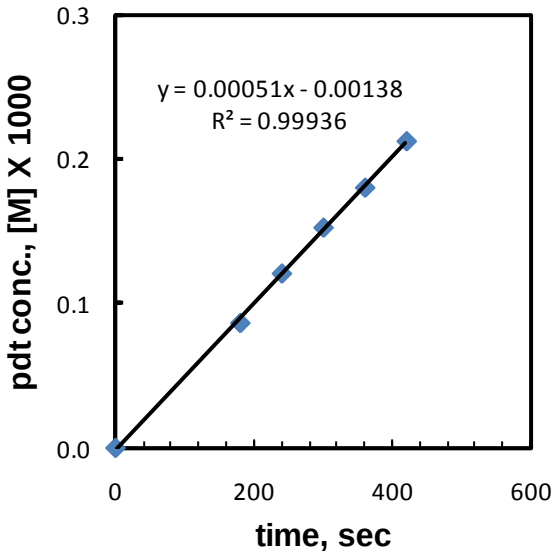

Et_4N^+, DIPK, run 2:

time, seconds	standard, µmol	standard, area	product, area	product, µmol	product, [M]x1000	product, %
0	6.81	7.000	0.000	0.000	0.0000	0.00
60	6.81	7.139	0.586	0.808	0.1347	0.81
90	6.81	7.276	0.877	1.186	0.1976	1.19
120	6.81	7.171	1.156	1.587	0.2645	1.59
180	6.81	7.129	1.690	2.334	0.3889	2.33
240	6.81	7.180	2.195	3.009	0.5014	3.01
300	6.81	7.091	2.657	3.689	0.6148	3.69
360	6.81	7.058	3.114	4.159	0.6931	4.34

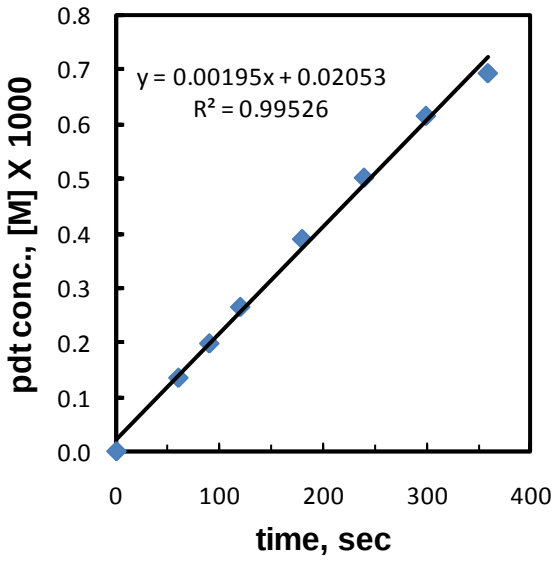

Et_4N^+, DIPK, run 3:

time, seconds	standard, µmol	standard, area	product, area	product, µmol	product, [M]x1000	product, %
0	6.91	7.000	0.000	0.000	0.0000	0.00
60	6.91	7.220	0.669	0.925	0.1542	0.93
90	0.00	7.150	1.126	1.572	0.2621	1.57
120	6.91	7.076	1.271	1.794	0.2989	1.79
180	6.91	7.156	1.818	2.536	0.4227	2.54
240	0.00	7.096	2.326	3.273	0.5455	3.27
300	6.91	7.112	2.834	3.979	0.6631	3.98
360	0.00	6.945	3.315	4.766	0.7943	4.77

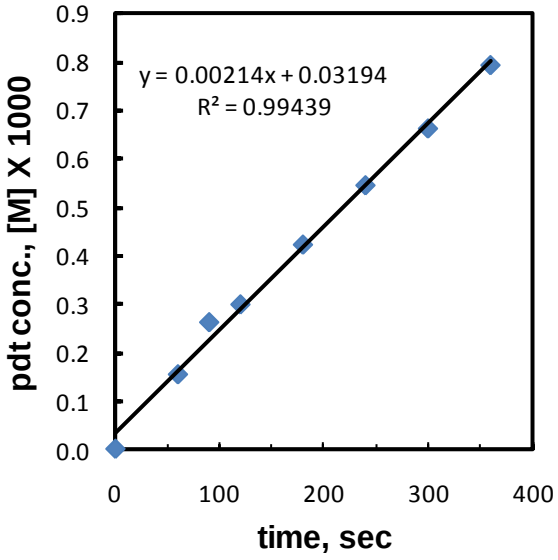

Pr_4N^+, DIPK, run 1:

time, seconds	standard, µmol	standard, area	product, area	product, µmol	product, [M]x1000	product, %
0	6.906	7.000	0.000	0.000	0.0000	0.00
45	6.906	7.221	0.838	1.159	0.1932	1.16
60	6.906	7.094	1.082	1.523	0.2538	1.52
90	6.906	7.050	1.539	2.179	0.3632	2.18
120	6.906	7.120	1.995	2.798	0.4663	2.80
180	6.906	7.116	2.865	4.021	0.6701	4.02
240	6.906	7.096	3.644	5.127	0.8546	5.13
300	6.906	6.988	4.298	6.141	1.0235	6.14
360	6.906	6.948	4.944	7.105	1.1842	7.11

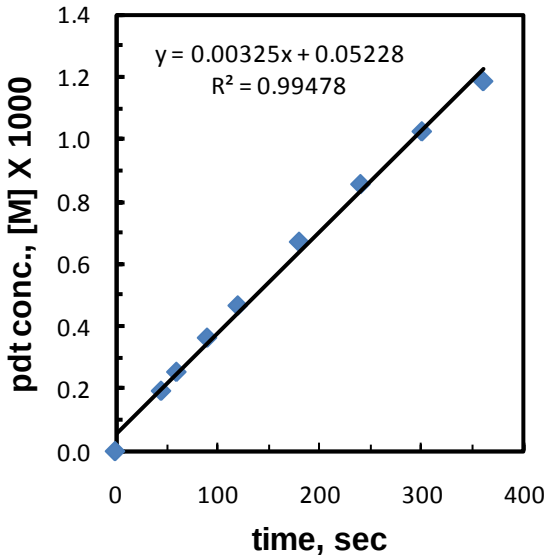

Pr_4N^+, DIPK, run 2:

time, seconds	standard, µmol	standard, area	product, area	product, µmol	product, [M]x1000	product, %
0	6.906	7.000	0.000	0.000	0.0000	0.00
45	6.906	7.301	0.809	1.106	0.1843	1.11
60	6.906	7.311	1.042	1.423	0.2372	1.42
90	6.906	7.161	1.466	2.044	0.3407	2.04
120	6.906	7.100	1.900	2.672	0.4453	2.67
180	6.906	7.134	2.739	3.833	0.6388	3.83
240	6.906	7.082	3.425	4.828	0.8047	4.83
300	6.906	7.027	4.087	5.806	0.9677	5.81
360	6.906	6.974	4.812	6.889	1.1482	6.89

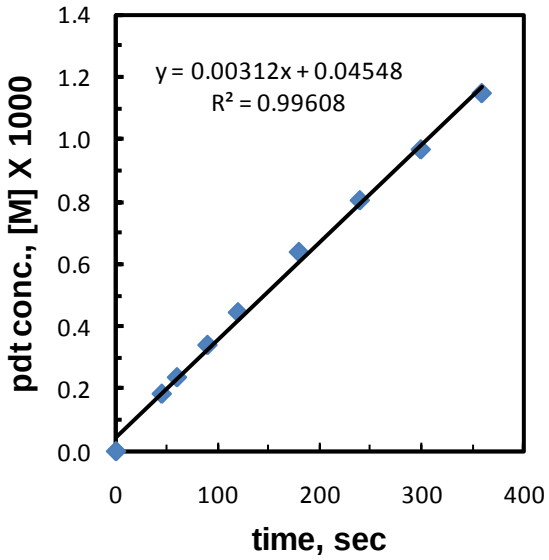

Pr_4N^+, DIPK, run 3:

time, seconds	standard, µmol	standard, area	product, area	product, µmol	product, [M]x1000	product, %
0	6.906	7.000	0.000	0.000	0.0000	0.00
45	6.906	7.270	0.752	1.033	0.1721	1.03
60	6.906	7.291	1.002	1.372	0.2286	1.37
90	6.906	7.224	1.405	1.942	0.3236	1.94
120	6.906	7.136	1.877	2.626	0.4377	2.63
180	6.906	7.032	2.647	3.759	0.6265	3.76
240	6.906	7.154	3.392	4.734	0.7890	4.73
300	6.906	7.036	4.147	5.885	0.9808	5.88
360	6.906	6.962	4.639	6.652	1.1087	6.65

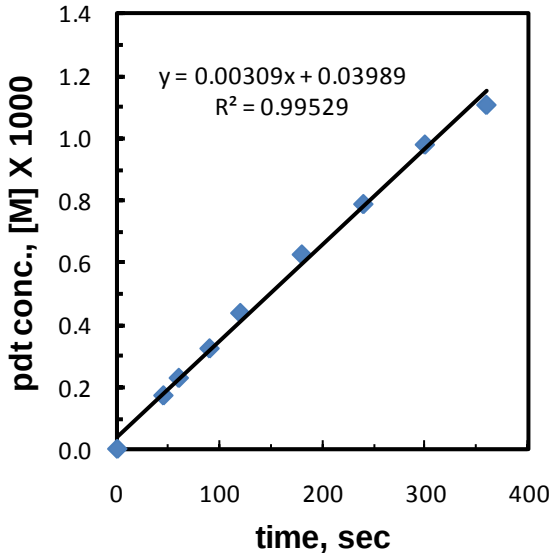

Bu_4N^+, DIPK, run 1:

time, seconds	standard, µmol	standard, area	product, area	product, µmol	product, [M]x1000	product, %
0	9.338	7.000	0.000	0.000	0.0000	0.00
45	9.338	9.751	0.809	1.120	0.1867	1.12
60	9.338	9.557	0.982	1.387	0.2311	1.39
75	9.338	9.594	1.241	1.746	0.2910	1.75
90	9.338	9.574	1.464	2.065	0.3441	2.06
120	9.338	9.466	1.856	2.647	0.4412	2.65
180	9.338	9.621	2.710	3.804	0.6340	3.80
240	9.338	9.343	3.423	4.946	0.8243	4.95
300	9.338	9.341	4.064	5.873	0.9789	5.87

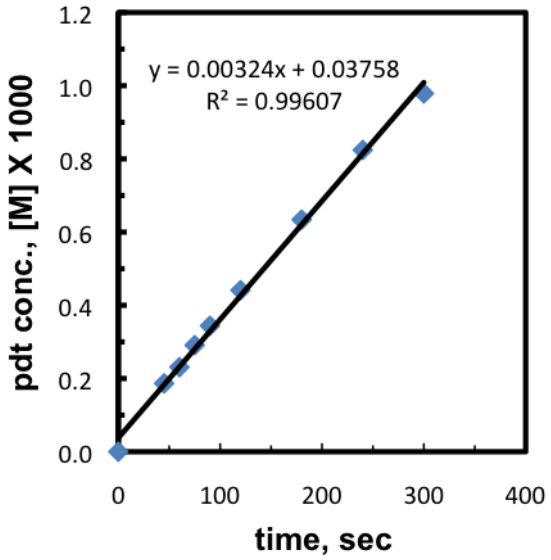

Bu_4N^+, DIPK, run 2:

time, seconds	standard, µmol	standard, area	product, area	product, µmol	product, [M]x1000	product, %
0	9.338	7.000	0.000	0.000	0.0000	0.00
30	9.338	9.639	0.648	0.907	0.1512	0.91
45	0.000	9.539	0.969	1.371	0.2286	1.37
60	9.338	9.431	1.305	1.868	0.3113	1.87
75	9.338	9.481	1.666	2.372	0.3953	2.37
90	0.000	9.384	1.985	2.856	0.4760	2.86
120	9.338	9.466	2.382	3.397	0.5662	3.40
180	9.338	9.506	3.331	4.730	0.7883	4.73
240	0.000	9.365	4.099	5.910	0.9849	5.91
300	9.338	9.333	4.639	6.710	1.1184	6.71

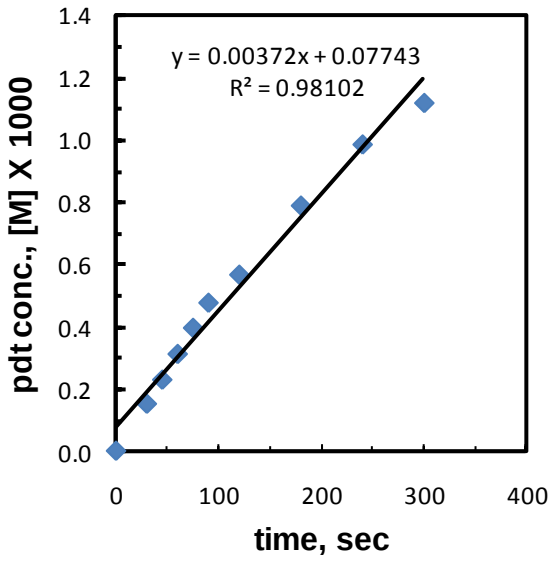

Bu_4N^+, DIPK, run 3:

time, seconds	standard, µmol	standard, area	product, area	product, µmol	product, [M]x1000	product, %
0	9.338	7.000	0.000	0.000	0.0000	0.00
30	9.338	9.581	0.582	0.819	0.1366	0.82
45	0.000	9.568	0.854	1.205	0.2008	1.20
60	9.338	9.592	1.127	1.586	0.2644	1.59
75	9.338	9.514	1.450	2.058	0.3429	2.06
90	0.000	9.514	1.630	2.313	0.3855	2.31
120	9.338	9.527	2.068	2.930	0.4883	2.93
180	9.338	9.449	2.929	4.184	0.6973	4.18
240	0.000	9.382	3.848	5.537	0.9228	5.54
300	9.338	9.317	4.471	6.478	1.0796	6.48

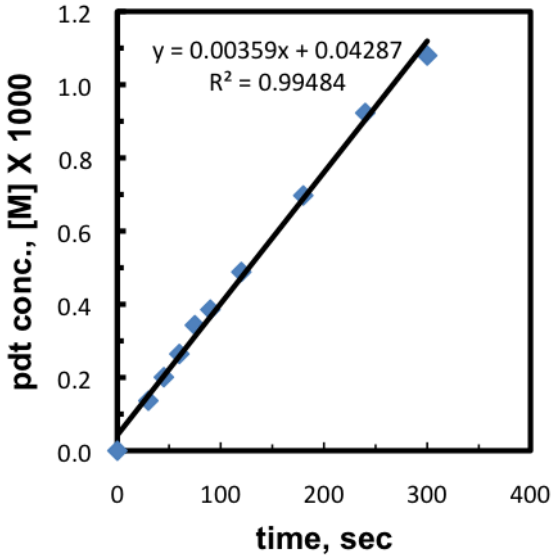

Hexyl$_4$N$^+$, DIPK, run 1:

time, seconds	standard, µmol	standard, area	product, area	product, µmol	product, [M]x1000	product, %
0	6.906	7.000	0.000	0.000	0.0000	0.00
90	6.906	7.386	0.856	1.159	0.1931	1.16
120	6.906	7.533	1.122	1.487	0.2478	1.49
180	6.906	7.276	1.652	2.268	0.3779	2.27
240	6.906	7.273	2.155	2.958	0.4929	2.96
300	6.906	7.236	2.739	3.780	0.6299	3.78
360	6.906	7.360	3.209	4.353	0.7255	4.35
420	6.906	7.264	3.744	5.146	0.8577	5.15

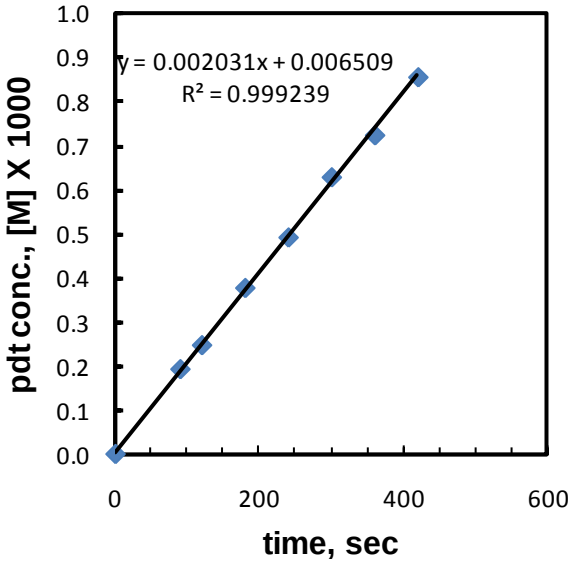

Hexyl$_4$N$^+$, DIPK, run 2:

time, seconds	standard, µmol	standard, area	product, area	product, µmol	product, [M]x1000	product, %
0	6.906	7.000	0.000	0.000	0.0000	0.00
60	6.906	7.419	0.682	0.917	0.1529	0.92
75	6.906	7.426	0.825	1.109	0.1848	1.11
90	6.906	7.354	1.002	1.360	0.2267	1.36
120	6.906	7.435	1.284	1.724	0.2874	1.72
180	6.906	7.354	1.913	2.597	0.4328	2.60
240	6.906	7.448	2.576	3.453	0.5755	3.45
300	6.906	7.323	3.180	4.336	0.7227	4.34
360	6.906	7.179	3.617	5.031	0.8384	5.03
420	6.906	7.367	4.186	5.674	0.9457	5.67

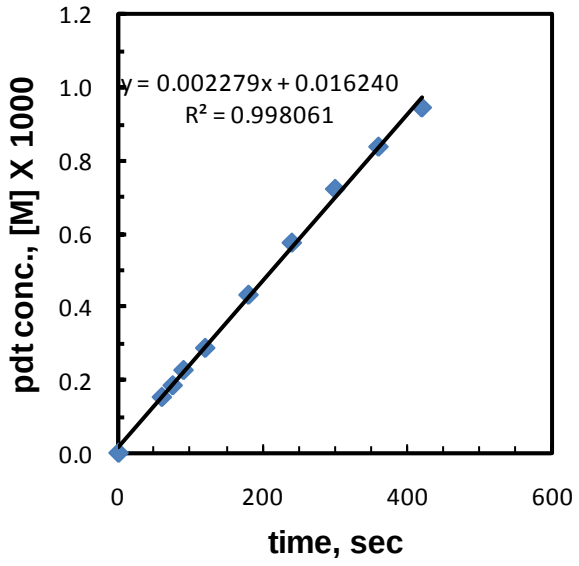

Hexyl$_4$N$^+$, DIPK, run 3:

time, seconds	standard, µmol	standard, area	product, area	product, µmol	product, [M]x1000	product, %
0	6.906	7.000	0.000	0.000	0.0000	0.00
60	6.906	7.230	0.744	1.029	0.1715	1.03
75	6.906	7.106	0.965	1.355	0.2259	1.36
90	6.906	7.239	1.152	1.588	0.2647	1.59
120	6.906	7.116	1.436	2.015	0.3358	2.01
180	6.906	7.451	2.164	2.899	0.4831	2.90
240	6.906	7.295	2.905	3.976	0.6627	3.98
300	6.906	7.309	3.416	4.668	0.7781	4.67
360	6.906	7.221	4.020	5.556	0.9260	5.56
420	6.906	7.102	4.433	6.232	1.0387	6.23

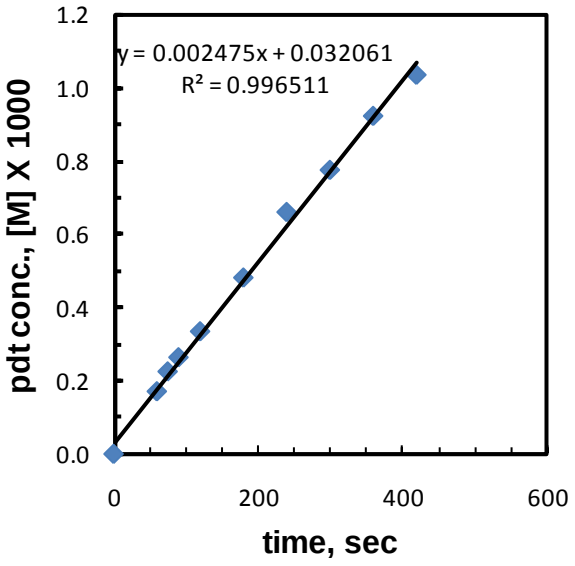

Octyl$_4$N$^+$, DIPK, run 1:

time, seconds	standard, µmol	standard, area	product, area	product, µmol	product, [M]x1000	product, %
0	6.906	7.000	0.000	0.000	0.0000	0.00
60	6.906	7.297	0.595	0.813	0.1356	0.81
75	6.906	7.157	0.790	1.102	0.1836	1.10
90	6.906	7.010	0.945	1.346	0.2243	1.35
120	6.906	7.146	1.175	1.642	0.2736	1.64
150	6.906	7.053	1.487	2.112	0.3520	2.11
210	6.906	7.049	1.980	2.802	0.4670	2.80
270	6.906	7.144	2.706	3.784	0.6306	3.78
330	6.906	7.173	3.246	4.517	0.7529	4.52
360	6.906	7.099	3.401	4.783	0.7972	4.78

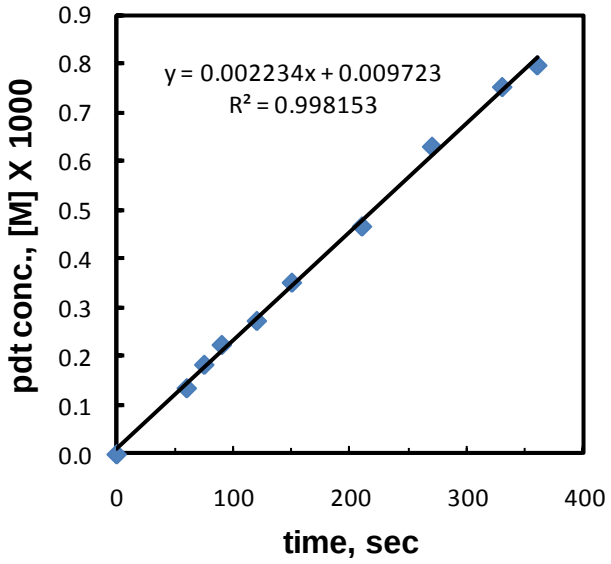

Octyl$_4$N$^+$, DIPK, run 2:

time, seconds	standard, µmol	standard, area	product, area	product, µmol	product, [M]x1000	product, %
0	7.198	7.000	0.000	0.000	0.0000	0.00
90	7.198	7.254	0.816	1.172	0.1953	1.17
120	7.198	7.356	1.050	1.486	0.2476	1.49
180	7.198	7.269	1.521	2.178	0.3629	2.18
240	7.198	7.169	2.053	2.982	0.4969	2.98
300	7.198	7.060	2.481	3.657	0.6095	3.66
360	7.198	7.284	3.074	4.391	0.7318	4.39

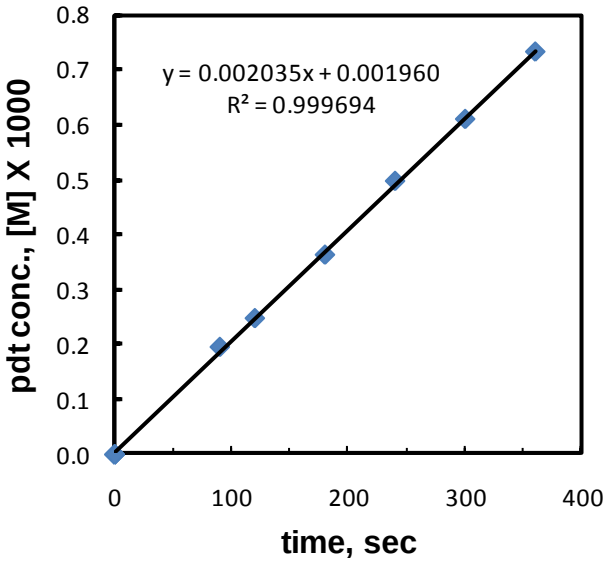

Octyl$_4$N$^+$, DIPK, run 3:

time, seconds	standard, µmol	standard, area	product, area	product, µmol	product, [M]x1000	product, %
0	6.906	7.000	0.000	0.000	0.0000	0.00
60	6.906	7.312	0.660	0.901	0.1502	0.90
75	6.906	7.342	0.842	1.144	0.1906	1.14
90	6.906	7.354	0.977	1.326	0.2210	1.33
120	6.906	7.322	1.257	1.714	0.2856	1.71
180	6.906	7.307	1.808	2.469	0.4116	2.47
240	6.906	6.220	1.993	3.199	0.5332	3.20
300	6.906	6.827	2.659	3.889	0.6482	3.89
360	6.906	7.199	3.288	4.560	0.7599	4.56

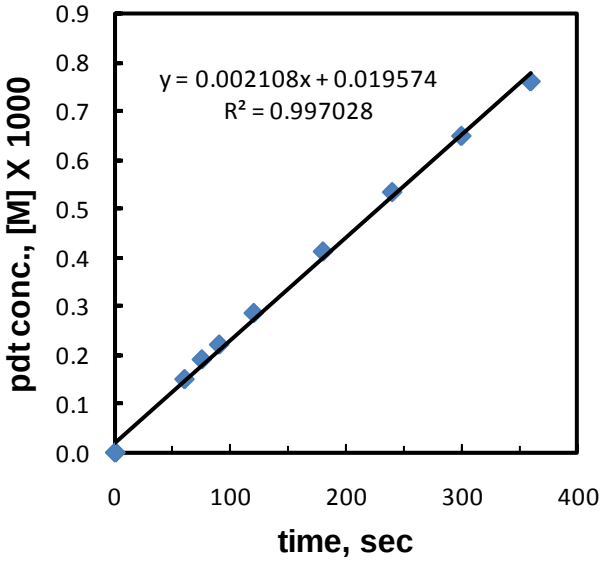

Summary Table for Ammonium Phenoxide Alkylation Under Homogeneous Conditions

compound number	cation, Y^+	R	solvent	k_i, s^{-1} x 10,000	$\log(k_i/k_{Na\text{-}DIPK})$	$\log(k_i/k_{Na\text{-}CH3CN)}$	$\log(k_i/k_{Na\text{-}DIPK})$
43	Na^+	-	DIPK	0.03±0.001	0		0.00±0.02
44	K^+	-	DIPK	0.09±0.021	0.46		0.46±0.02
37	R_4N^+	methyl	DIPK	0.24±0.096	0.9		0.90±0.10
38	R_4N^+	ethyl	DIPK	1.91±0.10	1.81		1.81±0.02
39	R_4N^+	*n*-propyl	DIPK	1.97±0.05	1.81		1.81±0.01
40	R_4N^+	*n*-butyl	DIPK	2.20±0.10	1.86		1.86±0.03
41	R_4N^+	*n*-hexyl	DIPK	1.41±0.10	1.66		1.66±0.04
42	R_4N^+	*n*-octyl	DIPK	1.36±0.06	1.64		1.64±0.02
43	Na^+	-	CH_3CN	0.215±0.02		0	0.85±0.04
44	K^+	-	CH_3CN	1.98±0.1		0.96	1.81±0.03
37	R_4N^+	methyl	CH_3CN	1.9±0.1		0.91	1.76±0.06
38	R_4N^+	ethyl	CH_3CN	2.77±0.07		1.11	1.96±0.03
39	R_4N^+	*n*-propyl	CH_3CN	3.16±0.06		1.16	2.01±0.08
40	R_4N^+	*n*-butyl	CH_3CN	3.37±0.05		1.19	2.04±0.02
41	R_4N^+	*n*-hexyl	CH_3CN	3.14±0.09		1.16	2.01±0.09
42	R_4N^+	*n*-octyl	CH_3CN	2.23±0.09		0.99	1.84±0.17

5.4.4 Catalyst Survey Kinetics

To a 4 mL dram vial, the respective quaternary ammonium bromide (4.1 to 29.6 mg, 26.6 to 53.1 μmol) was added followed by a solution of phenol (50 mg, 531 μmol) and biphenyl (20.4 to 20.7 mg, 132 to 134 μmol) in 2,4-dimethyl-3-pentanone (2.0 mL). A 5 M aqueous KOH solution (0.70 mL) was then added followed by the addition of a 1.5 cm egg-shaped magnetic stir-bar. A septa screw-cap was then installed on the vial.

This vial was placed on a silicone oil bath kept at 40-42 °C on a hotplate/stirrer and was allowed to come to temperature with moderate stirring for at least 30 minutes. To start the reaction, *n*-butyl bromide (68 μL, 637 μmol, 1.2 equiv) was added via syringe and the stirring speed was set to maximum (~2000 rpm).

Reaction aliquots were withdrawn directly from the organic phase (15-20 μL) approximately 2 seconds after the reaction had stopped stirring. Aliquots were quenched in a biphasic mixture of ethyl acetate (1-2 mL) and a saturated aqueous ammonium chloride solution (1-2 mL). After a quick mixing via pipette the organic phase was passed through a silica gel plug (1-2 cm x 0.5 cm) into a vial and used directly for GC analysis (GC Method 1).

Background Reaction, Run #1:

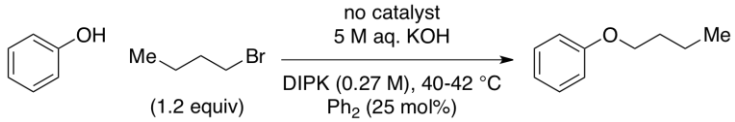

Time (m)	Time (s)	Ph_2 (µmol)	Ph_2 Area	(*n*-Bu)OPh Area	(*n*-Bu)OPh (µmol)	(*n*-Bu)OPh (mol)	(*n*-Bu)OPh (mol/L)	% conversion
0	0	134	1.000	0.000	0.0	0.00E+00	0.00E+00	0.0
1380	82800	134	18000.668	532.301	5.7	5.73E-06	2.86E-03	1.1
2760	165600	134	21154.184	1059.274	9.7	9.70E-06	4.85E-03	1.8
4260	255600	134	19539.275	1471.788	14.6	1.46E-05	7.30E-03	2.7
5640	338400	134	20528.344	2147.449	20.3	2.03E-05	1.01E-02	3.8
7140	428400	134	20009.566	2721.034	26.3	2.63E-05	1.32E-02	5.0
					0.0036	6.00E-11	3.00E-08	
					Rate (µmol/min)	**Rate (mol/s)**	**Rate (mol/L*s)**	

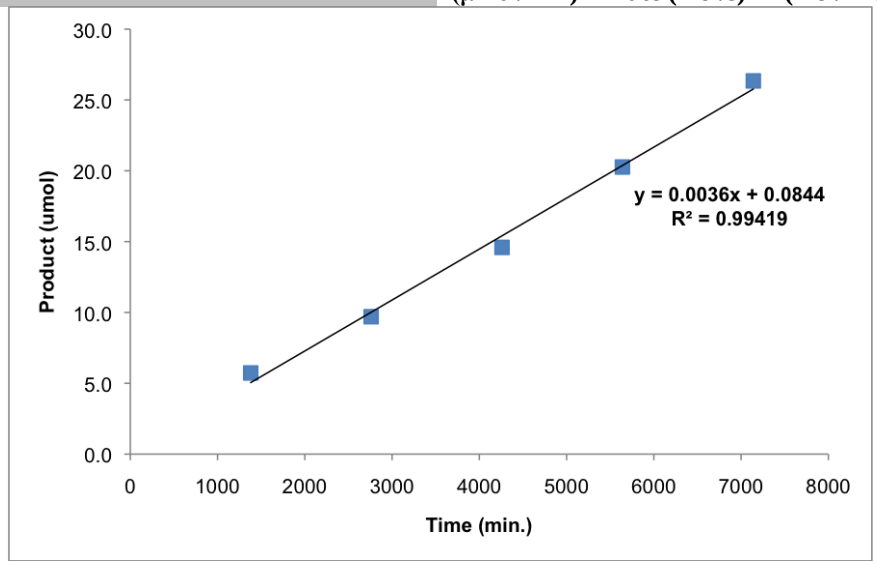

Background Reaction, Run #2:

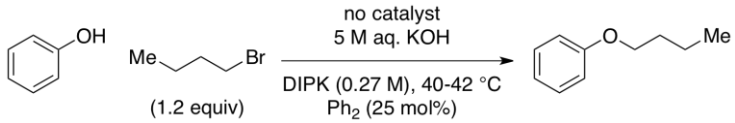

Time (m)	Time (s)	Ph_2 (µmol)	Ph_2 Area	(*n*-Bu)OPh Area	(*n*-Bu)OPh (µmol)	(*n*-Bu)OPh (mol)	(*n*-Bu)OPh (mol/L)	% conversion
0	0	134	1.000	0.000	0.0	0.00E+00	0.00E+00	0.0
1380	82800	134	21059.742	563.531	5.2	5.18E-06	2.59E-03	1.0
2760	165600	134	21483.316	953.002	8.6	8.59E-06	4.30E-03	1.6
4260	255600	134	23499.623	1855.842	15.3	1.53E-05	7.65E-03	2.9
5640	338400	134	24459.049	2567.105	20.3	2.03E-05	1.02E-02	3.8
7140	428400	134	23474.443	3027.089	25.0	2.50E-05	1.25E-02	4.7
					3.57E-03	5.94E-11	2.97E-08	
					Rate (µmol/min)	**Rate (mol/s)**	**Rate (mol/L*s)**	

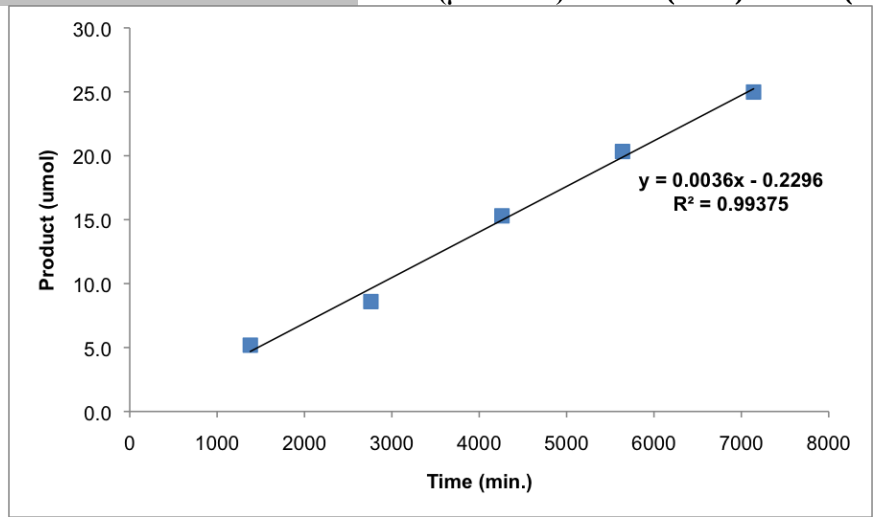

Mean alkylation rate = $2.99*10^{-8}$ ($mol*L^{-1}*s^{-1}$)

Std. Dev. alkylation rate = $1.86*10^{-10}$ ($mol*L^{-1}*s^{-1}$)

Tetramethylammonium Bromide (0.05 equivalents), Run #1:

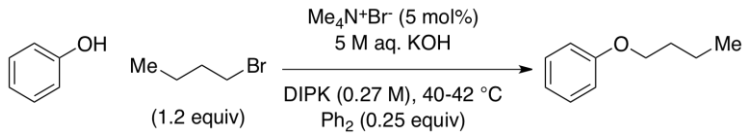

Time (h)	Time (m)	Time (s)	Ph_2 (µmol)	Ph_2 Area	(*n*-Bu)OPh Area	(*n*-Bu)OPh (µmol)	(*n*-Bu)OPh (mol)	(*n*-Bu)OPh (mol/L)	% conversion
0	0	0	134	1.000	0.000	0.0	0.0000E+00	0.0000E+00	0.0
21	1260	75600	134	20060.613	0.000	0.0	0.0000E+00	0.0000E+00	0.0
44	2640	158400	134	20029.234	1133.176	11.0	1.0960E-05	5.4801E-03	2.1
53	3180	190800	134	21138.584	1377.045	12.6	1.2620E-05	6.3099E-03	2.4
75	4500	270000	134	21437.701	1842.787	16.7	1.6653E-05	8.3263E-03	3.1
92	5520	331200	134	20137.510	2140.704	20.6	2.0594E-05	1.0297E-02	3.9
116	6960	417600	134	21719.225	2822.385	25.2	2.5174E-05	1.2587E-02	4.7
140	8400	504000	134	23890.166	3690.465	29.9	2.9926E-05	1.4963E-02	5.6
164	9850	591000	134	24804.859	4607.494	36.0	3.5984E-05	1.7992E-02	6.8
						3.4310E-03	5.7183E-11	2.8591E-08	
						Rate (µmol/min)	**Rate (mol/s)**	**Rate (mol*L^{-1}*s^{-1})**	

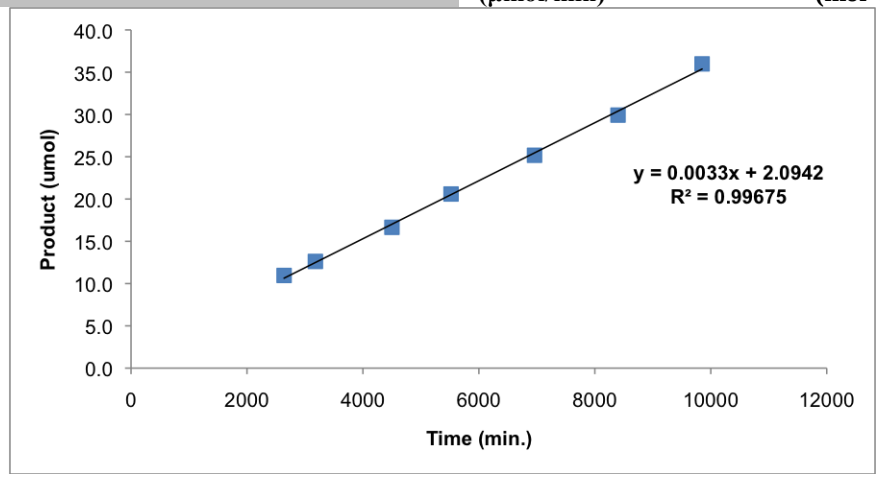

Tetramethylammonium Bromide (0.05 equivalents), Run #2:

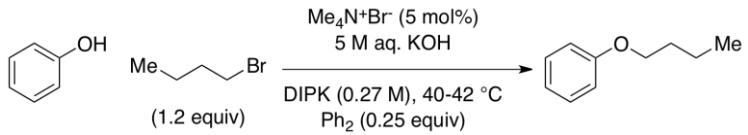

Time (h)	Time (m)	Time (s)	Ph_2 (µmol)	Ph_2 Area	(*n*-Bu)OPh Area	(*n*-Bu)OPh (µmol)	(*n*-Bu)OPh (mol)	(*n*-Bu)OPh (mol/L)	% conversion
0	0	0	134	1.000	0.000	0.0	0.0000E+00	0.0000E+00	0.0
21	1260	75600	134	19966.896	0.000	0.0	0.0000E+00	0.0000E+00	0.0
44	2640	158400	134	21664.426	1121.914	10.0	1.0032E-05	5.0161E-03	1.9
53	3180	190800	134	22068.523	1440.381	12.6	1.2644E-05	6.3220E-03	2.4
75	4500	270000	134	20048.412	1735.472	16.8	1.6770E-05	8.3848E-03	3.2
92	5520	331200	134	22057.816	2255.092	19.8	1.9805E-05	9.9027E-03	3.7
116	6960	417600	134	23611.295	2932.789	24.1	2.4063E-05	1.2031E-02	4.5
140	8400	504000	134	23097.730	3484.897	29.2	2.9228E-05	1.4614E-02	5.5
164	9850	591000	134	23780.686	4049.721	33.0	3.2990E-05	1.6495E-02	6.2
						3.1553E-03	5.2588E-11	2.6294E-08	
						Rate (µmol/min)	**Rate (mol/s)**	**Rate (mol*L^{-1}*s^{-1})**	

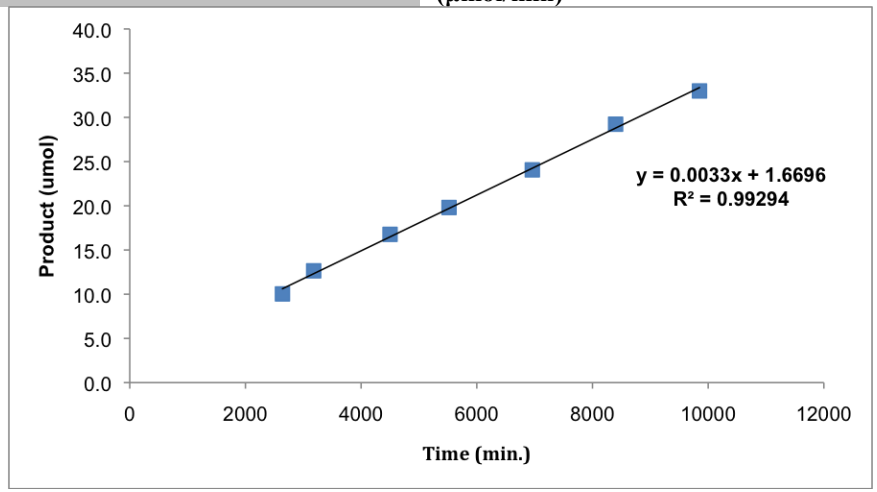

Mean alkylation rate = $2.74*10^{-8}$ (mol*L^{-1}*s^{-1})

Std. Dev. alkylation rate = $1.62*10^{-9}$ (mol*L^{-1}*s^{-1})

Tetraethylammonium Bromide (0.05 equivalents), Run #1:

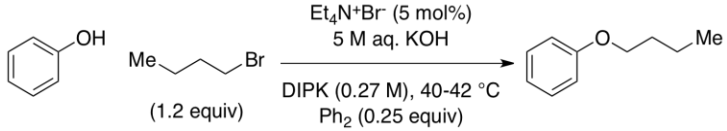

Time (h)	Time (m)	Time (s)	Ph_2 (µmol)	Ph_2 Area	(*n*-Bu)OPh Area	(*n*-Bu)OPh (µmol)	(*n*-Bu)OPh (mol)	(*n*-Bu)OPh (mol/L)	% conversion
0	0	0	132	1.000	0.000	0.0	0.0000E+00	0.0000E+00	0.0
19	1140	68400	132	17414.016	1625.749	17.8	1.7816E-05	8.9079E-03	3.4
24	1440	86400	132	18371.736	2364.149	24.6	2.4557E-05	1.2279E-02	4.6
28	1680	100800	132	13959.378	2219.996	30.3	3.0349E-05	1.5174E-02	5.7
43	2580	154800	132	17251.484	3777.865	41.8	4.1790E-05	2.0895E-02	7.9
48	2880	172800	132	17583.271	4442.323	48.2	4.8213E-05	2.4106E-02	9.1
55	3300	198000	132	17524.023	4876.349	53.1	5.3102E-05	2.6551E-02	10.0
67	4020	241200	132	16557.992	5854.275	67.5	6.7471E-05	3.3736E-02	12.7
75	4500	270000	132	16183.960	6259.519	73.8	7.3809E-05	3.6904E-02	13.9
						1.6309E-02	2.7181E-10	1.3591E-07	
						Rate (µmol/min)	**Rate (mol/s)**	**Rate (mol*L^{-1}*s^{-1})**	

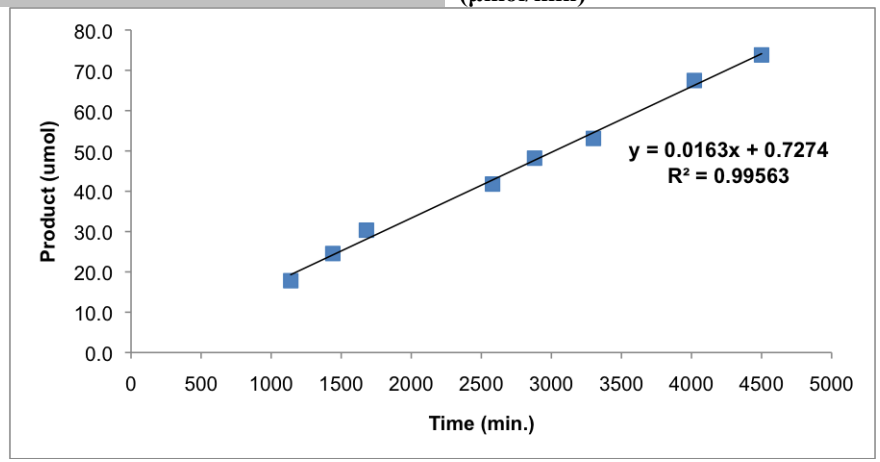

Tetraethylammonium Bromide (0.05 equivalents), Run #2:

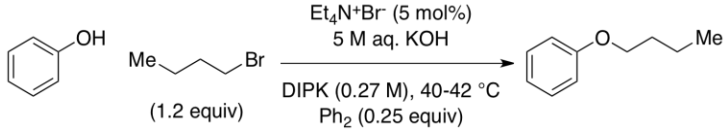

Time (h)	Time (m)	Time (s)	Ph_2 (µmol)	Ph_2 Area	(*n*-Bu)OPh Area	(*n*-Bu)OPh (µmol)	(*n*-Bu)OPh (mol)	(*n*-Bu)OPh (mol/L)	% conversion
0	0	0	132	1.000	0.000	0.0	0.0000E+00	0.0000E+00	0.0
19	1140	68400	132	18497.441	1859.863	19.2	1.9188E-05	9.5938E-03	3.6
24	1440	86400	132	16267.138	2120.483	24.9	2.4876E-05	1.2438E-02	4.7
28	1680	100800	132	13267.677	1982.330	28.5	2.8512E-05	1.4256E-02	5.4
43	2580	154800	132	16960.045	3994.921	45.0	4.4950E-05	2.2475E-02	8.5
48	2880	172800	132	17910.084	4705.736	50.1	5.0140E-05	2.5070E-02	9.4
55	3300	198000	132	17149.270	5223.124	58.1	5.8121E-05	2.9061E-02	10.9
67	4020	241200	132	17440.840	6306.243	69.0	6.9001E-05	3.4501E-02	13.0
75	4500	270000	132	18916.951	7931.071	80.0	8.0008E-05	4.0004E-02	15.1
						1.7803E-02	2.9672E-10	1.4836E-07	
						Rate (µmol/min)	**Rate (mol/s)**	**Rate (mol*L^{-1}*s^{-1})**	

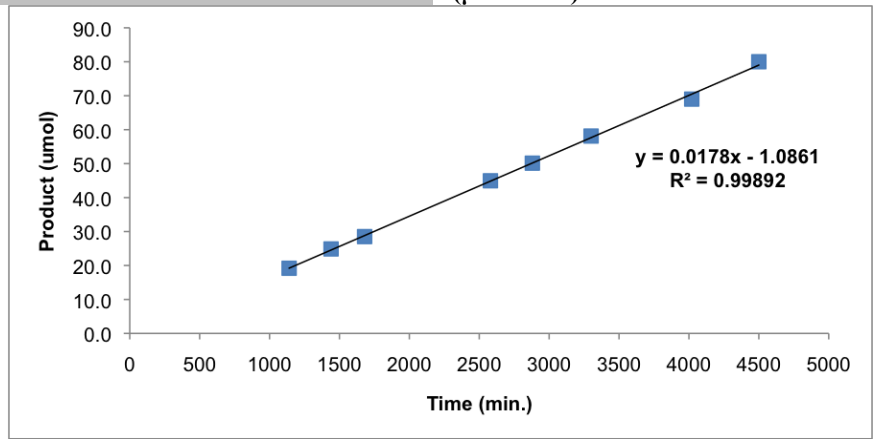

Tetraethylammonium Bromide (0.05 equivalents), Run #3:

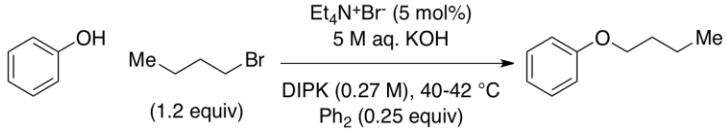

Time (h)	Time (m)	Time (s)	Ph_2 (µmol)	Ph_2 Area	(*n*-Bu)OPh Area	(*n*-Bu)OPh (µmol)	(*n*-Bu)OPh (mol)	(*n*-Bu)OPh (mol/L)	% conversion
0	0	0	133	1.000	0.000	0.0	0.0000E+00	0.0000E+00	0.0
16	960	57600	133	13775.634	1164.866	16.3	1.6259E-05	8.1295E-03	3.1
27	1620	97200	133	18171.801	2637.678	27.9	2.7910E-05	1.3955E-02	5.2
45	2700	162000	133	15997.878	3974.793	47.8	4.7773E-05	2.3886E-02	9.0
68	4080	244800	133	15771.731	5845.070	71.3	7.1259E-05	3.5630E-02	13.4
88	5280	316800	133	16996.545	7545.832	85.4	8.5364E-05	4.2682E-02	16.0
						1.6284E-02	2.7141E-10	1.3570E-07	
						Rate (µmol/min)	**Rate (mol/s)**	**Rate (mol*L^{-1}*s^{-1})**	

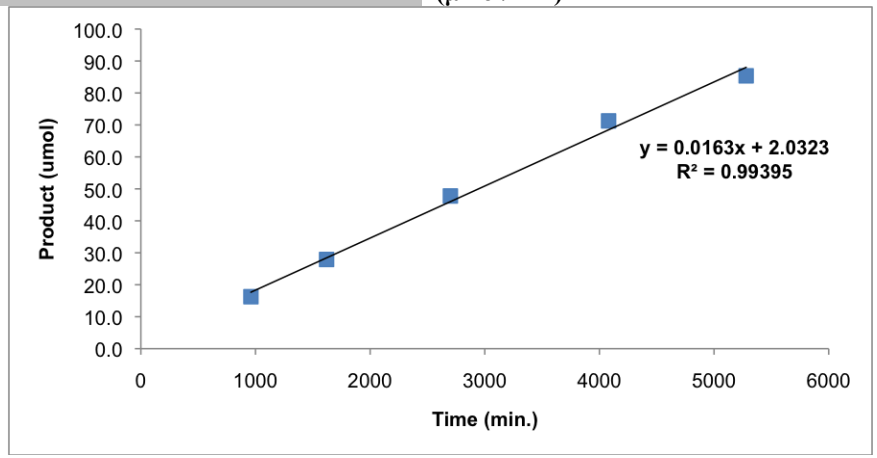

Tetraethylammonium Bromide (0.05 equivalents), Run #4:

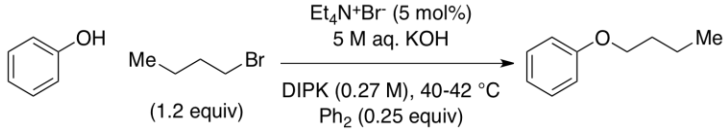

Time (h)	Time (m)	Time (s)	Ph_2 (µmol)	Ph_2 Area	(*n*-Bu)OPh Area	(*n*-Bu)OPh (µmol)	(*n*-Bu)OPh (mol)	(*n*-Bu)OPh (mol/L)	% conversion
0	0	0	133	1.000	0.000	0.0	0.0000E+00	0.0000E+00	0.0
16	960	57600	133	15902.801	1292.565	15.6	1.5628E-05	7.8141E-03	2.9
27	1620	97200	133	16994.441	2350.526	26.6	2.6594E-05	1.3297E-02	5.0
45	2700	162000	133	16510.598	3820.847	44.5	4.4497E-05	2.2248E-02	8.4
68	4080	244800	133	18948.859	6179.663	62.7	6.2706E-05	3.1353E-02	11.8
88	5280	316800	133	17013.270	7131.009	80.6	8.0592E-05	4.0296E-02	15.1
						1.4894E-02	2.4824E-10	1.2412E-07	
						Rate (µmol/min)	**Rate (mol/s)**	**Rate (mol*L^{-1}*s^{-1})**	

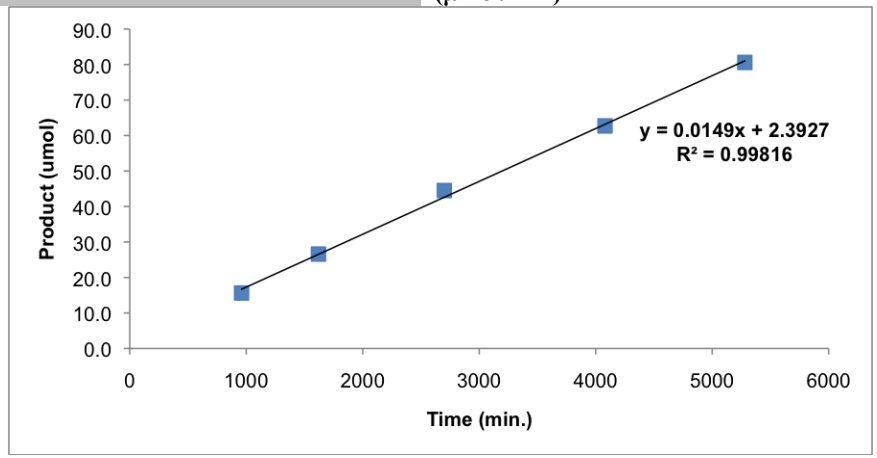

Mean alkylation rate = $1.36*10^{-7}$ (mol*L^{-1}*s^{-1})

Std. Dev. alkylation rate = $9.90*10^{-9}$ (mol*L^{-1}*s^{-1})

Tetra(*n*-propyl)ammonium Bromide (0.05 equivalents), Run #1:

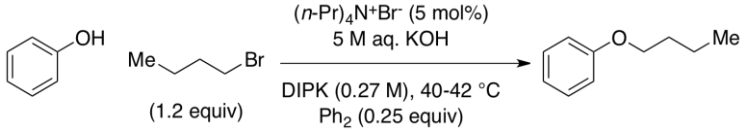

Time (m)	Time (s)	Ph_2 (µmol)	Ph_2 Area	(*n*-Bu)OPh Area	(*n*-Bu)OPh (µmol)	(*n*-Bu)OPh (mol)	(*n*-Bu)OPh (mol/L)	% conversion
0	0	132	1.000	0.000	0.0	0.0000E+00	0.0000E+00	0.0
15	900	132	18822.996	608.495	6.2	6.1691E-06	3.0845E-03	1.2
30	1800	132	19753.721	1303.879	12.6	1.2596E-05	6.2981E-03	2.4
45	2700	132	19617.428	1892.916	18.4	1.8414E-05	9.2069E-03	3.5
60	3600	132	19687.752	2703.854	26.2	2.6208E-05	1.3104E-02	4.9
90	5400	132	21077.332	4272.436	38.7	3.8682E-05	1.9341E-02	7.3
120	7200	132	20215.801	5527.928	52.2	5.2182E-05	2.6091E-02	9.8
187	11220	132	22014.656	9312.616	80.7	8.0726E-05	4.0363E-02	15.2
					4.3533E-01	7.2555E-09	3.6278E-06	
					Rate (µmol/min)	**Rate (mol/s)**	**Rate (mol*L^{-1}*s^{-1})**	

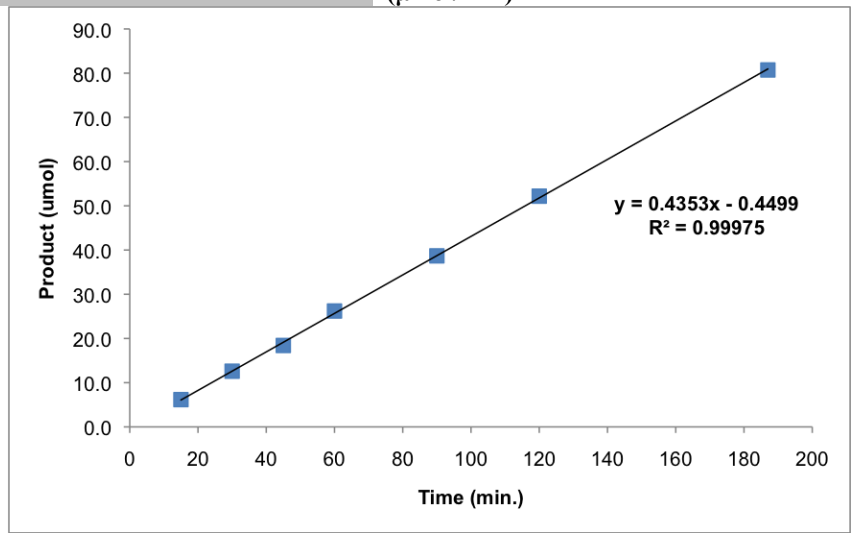

Tetra(*n*-propyl)ammonium Bromide (0.05 equivalents), Run #2:

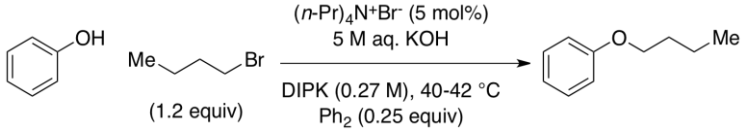

Time (m)	Time (s)	Ph_2 (µmol)	Ph_2 Area	(*n*-Bu)OPh Area	(*n*-Bu)OPh (µmol)	(*n*-Bu)OPh (mol)	(*n*-Bu)OPh (mol/L)	% conversion
0	0	132	1.000	0.000	0.0	0.0000E+00	0.0000E+00	0.0
12	720	132	20379.836	737.315	6.9	6.9041E-06	3.4520E-03	1.3
24	1440	132	18766.324	813.123	8.3	8.2685E-06	4.1343E-03	1.6
36	2160	132	21809.865	1660.214	14.5	1.4527E-05	7.2633E-03	2.7
48	2880	132	19263.789	1947.858	19.3	1.9296E-05	9.6480E-03	3.6
60	3600	132	19488.670	2584.348	25.3	2.5306E-05	1.2653E-02	4.8
72	4320	132	19766.701	3154.050	30.4	3.0450E-05	1.5225E-02	5.7
84	5040	132	23830.998	4639.583	37.2	3.7153E-05	1.8576E-02	7.0
96	5760	132	18739.170	4151.652	42.3	4.2279E-05	2.1139E-02	8.0
108	6480	132	19802.281	5000.891	48.2	4.8193E-05	2.4097E-02	9.1
120	7200	132	19638.748	5506.706	53.5	5.3509E-05	2.6755E-02	10.1
					4.5272E-01	7.5454E-09	3.7727E-06	
					Rate (µmol/min)	**Rate (mol/s)**	**Rate (mol*L^{-1}*s^{-1})**	

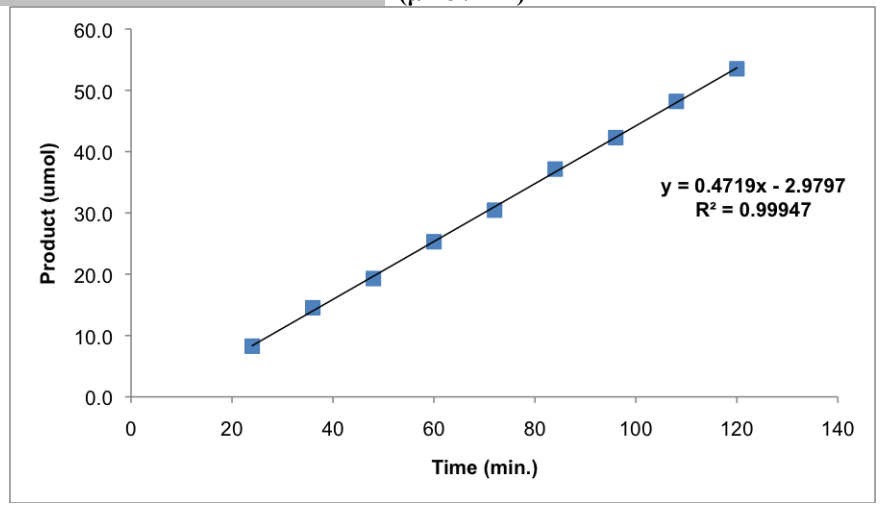

Tetra(*n*-propyl)ammonium Bromide (0.05 equivalents), Run #3:

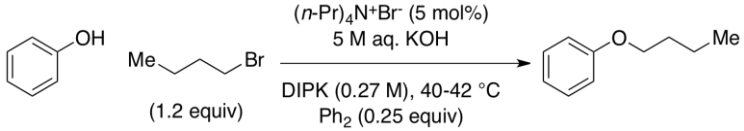

Time (m)	Time (s)	Ph_2 (µmol)	Ph_2 Area	(*n*-Bu)OPh Area	(*n*-Bu)OPh (µmol)	(*n*-Bu)OPh (mol)	(*n*-Bu)OPh (mol/L)	% conversion
0	0	132	1.000	0.000	0.0	0.0000E+00	0.0000E+00	0.0
12	720	132	22757.387	664.239	5.6	5.5700E-06	2.7850E-03	1.0
24	1440	132	18992.676	940.222	9.4	9.4471E-06	4.7235E-03	1.8
36	2160	132	18804.895	1393.647	14.1	1.4143E-05	7.0714E-03	2.7
48	2880	132	20526.416	2029.130	18.9	1.8865E-05	9.4323E-03	3.6
60	3600	132	18308.018	2199.208	22.9	2.2923E-05	1.1462E-02	4.3
72	4320	132	20383.789	2967.208	27.8	2.7779E-05	1.3889E-02	5.2
84	5040	132	19019.729	3210.219	32.2	3.2209E-05	1.6105E-02	6.1
96	5760	132	19091.594	3706.319	37.0	3.7047E-05	1.8523E-02	7.0
108	6480	132	19577.986	4303.996	42.0	4.1952E-05	2.0976E-02	7.9
120	7200	132	18042.338	4533.514	48.0	4.7951E-05	2.3975E-02	9.0
					3.8807E-01	6.4678E-09	3.2339E-06	
					Rate (µmol/min)	**Rate (mol/s)**	**Rate (mol*L^{-1}*s^{-1})**	

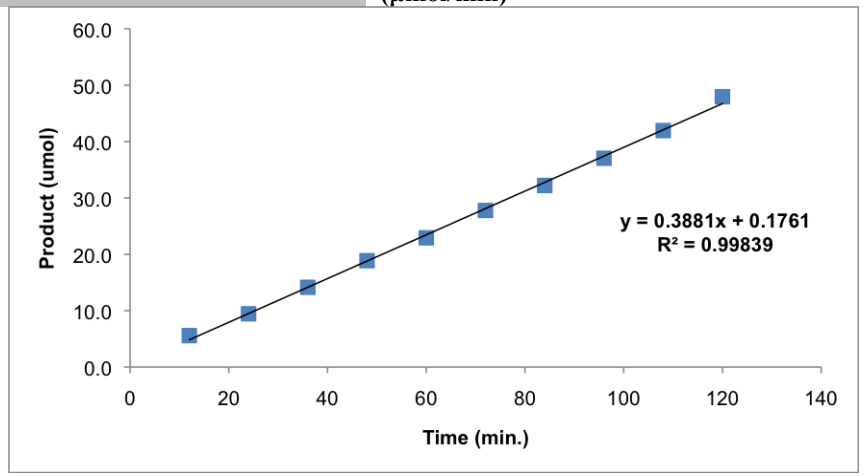

Tetra(*n*-propyl)ammonium Bromide (0.05 equivalents), Run #4:

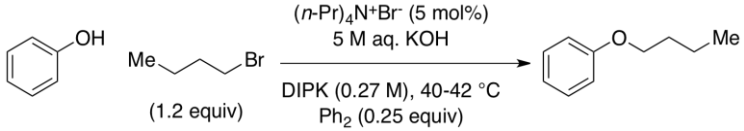

Time (m)	Time (s)	Ph_2 (µmol)	Ph_2 Area	(*n*-Bu)OPh Area	(*n*-Bu)OPh (µmol)	(*n*-Bu)OPh (mol)	(*n*-Bu)OPh (mol/L)	% conversion
0	0	134	1.000	0.000	0.0	0.0000E+00	0.0000E+00	0.0
12	720	134	18210.188	0.000	0.0	0.0000E+00	0.0000E+00	0.0
24	1440	134	18531.648	869.086	9.1	9.0851E-06	4.5426E-03	1.7
36	2160	134	17067.246	1283.855	14.6	1.4573E-05	7.2863E-03	2.7
48	2880	134	17912.191	1850.186	20.0	2.0010E-05	1.0005E-02	3.8
60	3600	134	16681.412	2156.954	25.0	2.5049E-05	1.2525E-02	4.7
72	4320	134	18994.670	2935.339	29.9	2.9937E-05	1.4969E-02	5.6
84	5040	134	18774.553	3337.103	34.4	3.4434E-05	1.7217E-02	6.5
96	5760	134	16841.502	3475.806	40.0	3.9981E-05	1.9991E-02	7.5
108	6480	134	17945.006	4191.219	45.2	4.5246E-05	2.2623E-02	8.5
120	7200	134	19587.809	5155.014	51.0	5.0983E-05	2.5492E-02	9.6
					4.2908E-01	7.1514E-09	3.5757E-06	
					Rate (µmol/min)	**Rate (mol/s)**	**Rate (mol*L^{-1}*s^{-1})**	

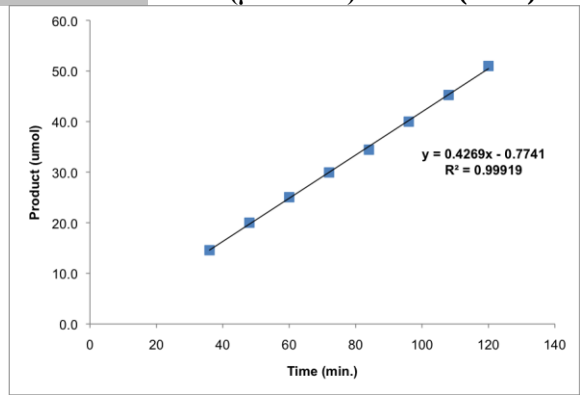

Mean alkylation rate = $3.55*10^{-6}$ (mol*L^{-1}*s^{-1})

Std. Dev. alkylation rate = $2.28*10^{-7}$ (mol*L^{-1}*s^{-1})

Tetra(*n*-butyl)ammonium Bromide (0.05 equivalents), Run #1:

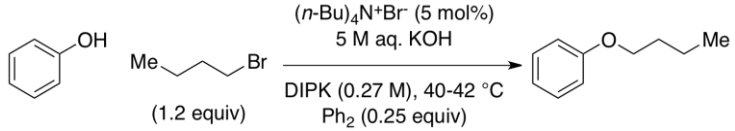

Time (m)	Time (s)	Ph_2 (µmol)	Ph_2 Area	(*n*-Bu)OPh Area	(*n*-Bu)OPh (µmol)	(*n*-Bu)OPh (mol)	(*n*-Bu)OPh (mol/L)	% conversion
0	0	132.0	1.000	0.000	0.0	0.0000E+00	0.0000E+00	0.0
2	120	132.0	15621.172	0.000	0.0	0.0000E+00	0.0000E+00	0.0
4	240	132.0	15957.985	756.020	9.0	9.0408E-06	4.5204E-03	1.7
6	360	132.0	15363.379	1174.770	14.6	1.4592E-05	7.2961E-03	2.7
8	480	132.0	16118.517	1609.172	19.1	1.9052E-05	9.5258E-03	3.6
10	600	132.0	14945.260	1789.216	22.8	2.2846E-05	1.1423E-02	4.3
12	720	132.0	15437.999	2224.325	27.5	2.7495E-05	1.3748E-02	5.2
14	840	132.0	14088.265	2438.603	33.0	3.3032E-05	1.6516E-02	6.2
16	960	132.0	15432.511	3069.000	38.0	3.7950E-05	1.8975E-02	7.1
18	1080	132.0	14637.714	3319.178	43.3	4.3272E-05	2.1636E-02	8.1
20	1200	132.0	16727.932	4320.749	49.3	4.9291E-05	2.4646E-02	9.3
					2.4585E+00	4.0976E-08	2.0488E-05	
					Rate (µmol/min)	**Rate (mol/s)**	**Rate (mol*L^{-1}*s^{-1})**	

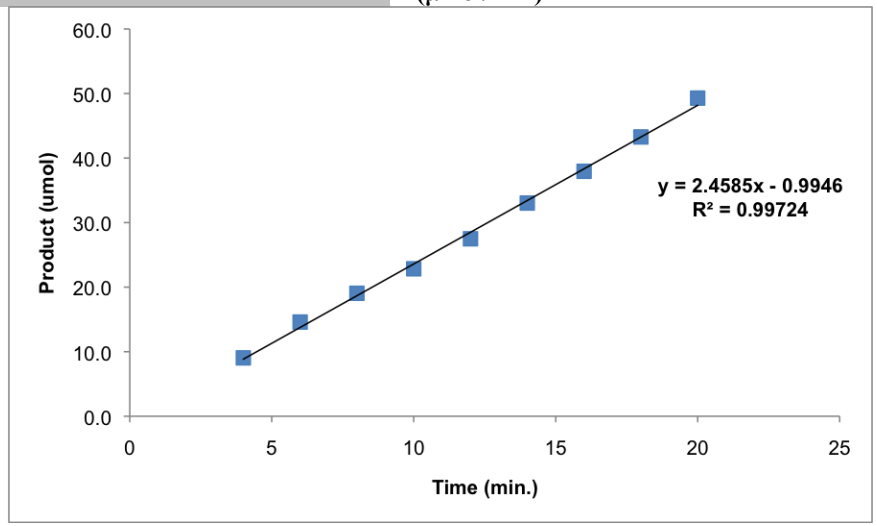

Tetra(*n*-butyl)ammonium Bromide (0.05 equivalents), Run #2:

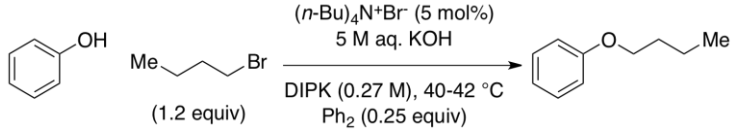

Time (m)	Time (s)	Ph_2 (µmol)	Ph_2 Area	(*n*-Bu)OPh Area	(*n*-Bu)OPh (µmol)	(*n*-Bu)OPh (mol)	(*n*-Bu)OPh (mol/L)	% conversion
0	0	132.0	1.000	0.000	0.0	0.0000E+00	0.0000E+00	0.0
2	120	132.0	16591.078	640.342	7.4	7.3653E-06	3.6826E-03	1.4
4	240	132.0	20913.287	1319.675	12.0	1.2042E-05	6.0210E-03	2.3
6	360	132.0	16104.247	1509.696	17.9	1.7890E-05	8.9448E-03	3.4
8	480	132.0	16265.122	1930.510	22.6	2.2650E-05	1.1325E-02	4.3
10	600	132.0	16589.773	2433.773	28.0	2.7996E-05	1.3998E-02	5.3
12	720	132.0	16976.654	3029.749	34.1	3.4057E-05	1.7029E-02	6.4
14	840	132.0	15814.946	3214.189	38.8	3.8784E-05	1.9392E-02	7.3
16	960	132.0	17102.354	4040.927	45.1	4.5090E-05	2.2545E-02	8.5
18	1080	132.0	17426.592	4628.763	50.7	5.0688E-05	2.5344E-02	9.5
20	1200	132.0	17858.295	5400.289	57.7	5.7707E-05	2.8854E-02	10.9
					2.7699E+00	4.6165E-08	2.3082E-05	
					Rate (µmol/min)	**Rate (mol/s)**	**Rate (mol*L^{-1}*s^{-1})**	

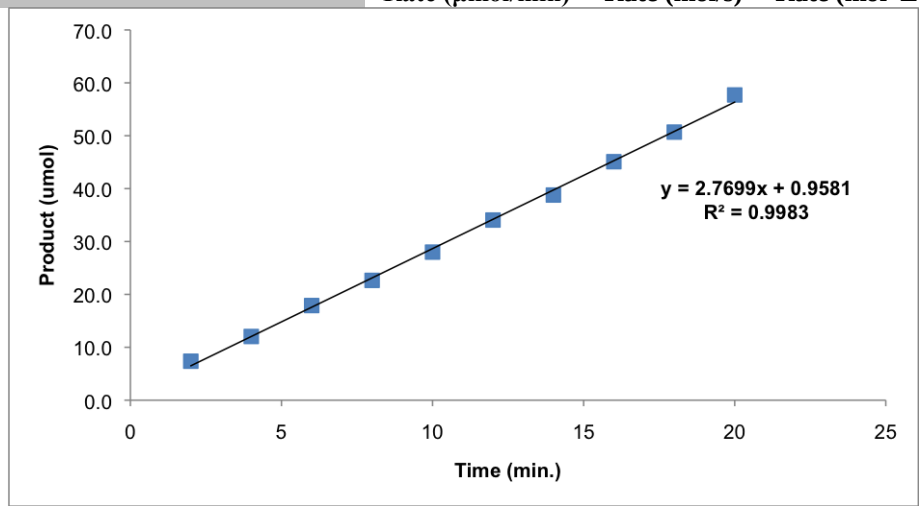

Tetra(*n*-butyl)ammonium Bromide (0.05 equivalents), Run #3:

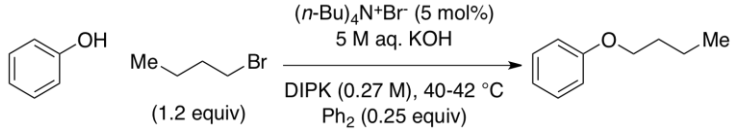

Time (m)	Time (s)	Ph_2 (µmol)	Ph_2 Area	(*n*-Bu)OPh Area	(*n*-Bu)OPh (µmol)	(*n*-Bu)OPh (mol)	(*n*-Bu)OPh (mol/L)	% conversion
0	0	132	1.000	0.000	0.0	0.0000E+00	0.0000E+00	0.0
2	120	132	24062.645	546.988	4.3	4.3380E-06	2.1690E-03	0.8
4	240	132	19211.037	967.760	9.6	9.6132E-06	4.8066E-03	1.8
6	360	132	20913.420	1508.631	13.8	1.3766E-05	6.8830E-03	2.6
8	480	132	20446.957	1890.851	17.6	1.7647E-05	8.8237E-03	3.3
10	600	132	20848.557	2371.605	21.7	2.1708E-05	1.0854E-02	4.1
12	720	132	19769.068	2659.623	25.7	2.5674E-05	1.2837E-02	4.8
14	840	132	19474.953	3013.777	29.5	2.9532E-05	1.4766E-02	5.6
16	960	132	21764.037	3929.550	34.5	3.4455E-05	1.7228E-02	6.5
18	1080	132	21847.590	4511.358	39.4	3.9405E-05	1.9703E-02	7.4
20	1200	132	21726.320	5063.462	44.5	4.4475E-05	2.2237E-02	8.4
					2.1601E+00	3.6002E-08	1.8001E-05	
					Rate (µmol/min)	**Rate (mol/s)**	**Rate (mol*L^{-1}*s^{-1})**	

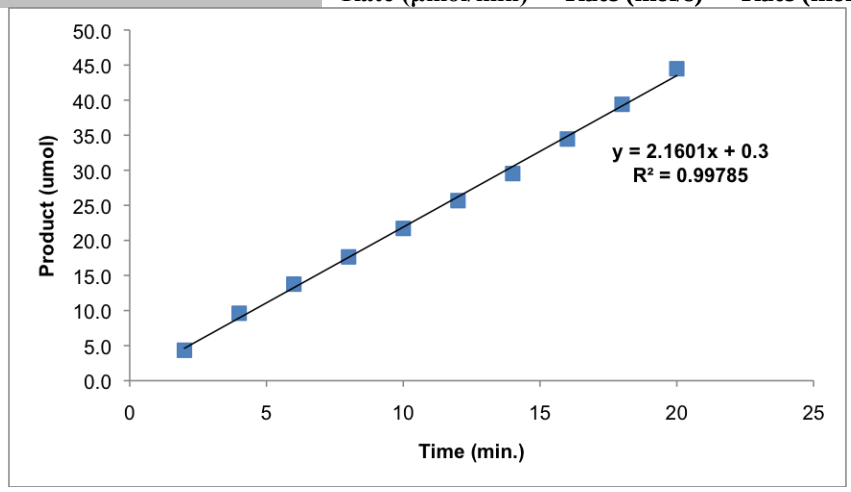

Tetra(*n*-butyl)ammonium Bromide (0.05 equivalents), Run #4:

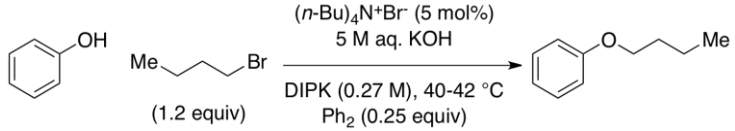

Time (m)	Time (s)	Ph_2 (µmol)	Ph_2 Area	(*n*-Bu)OPh Area	(*n*-Bu)OPh (µmol)	(*n*-Bu)OPh (mol)	(*n*-Bu)OPh (mol/L)	% conversion
0	0	132	1.000	0.000	0.0	0.0000E+00	0.0000E+00	0.0
4	240	132	22249.770	1092.949	9.4	9.3740E-06	4.6870E-03	1.8
6	360	132	20966.783	1548.639	14.1	1.4095E-05	7.0476E-03	2.7
8	480	132	20990.369	1910.011	17.4	1.7365E-05	8.6824E-03	3.3
10	600	132	20985.277	2321.097	21.1	2.1107E-05	1.0554E-02	4.0
12	720	132	20912.549	2833.490	25.9	2.5856E-05	1.2928E-02	4.9
14	840	132	20521.619	3257.438	30.3	3.0291E-05	1.5146E-02	5.7
16	960	132	21514.344	3919.235	34.8	3.4764E-05	1.7382E-02	6.5
18	1080	132	21670.379	4431.456	39.0	3.9024E-05	1.9512E-02	7.3
20	1200	132	20554.740	4631.587	43.0	4.3000E-05	2.1500E-02	8.1
					2.1106E+00	3.5177E-08	1.7588E-05	
					Rate (µmol/min)	**Rate (mol/s)**	**Rate (mol*L^{-1}*s^{-1})**	

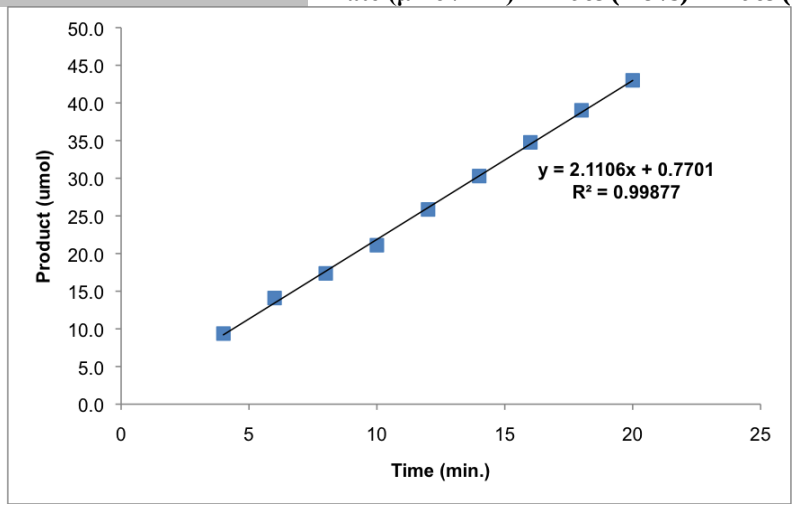

Mean alkylation rate = 1.98 x 10^{-5} (mol*L^{-1}*s^{-1})

Std. Dev. alkylation rate = 2.54 x 10^{-6} (mol*L^{-1}*s^{-1})

Tetra(*n*-hexyl)ammonium Bromide (0.05 equivalents), Run #1:

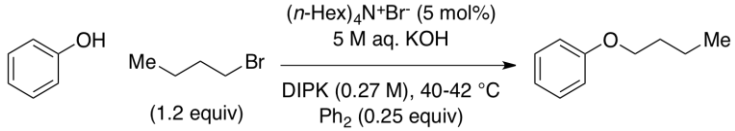

Time (m)	Time (s)	Ph_2 (µmol)	Ph_2 Area	(*n*-Bu)OPh Area	(*n*-Bu)OPh (µmol)	(*n*-Bu)OPh (mol)	(*n*-Bu)OPh (mol/L)	% conversion
0	0	132	1.000	0.000	0.0	0.0000E+00	0.0000E+00	0.0
3	180	132	17780.926	562.245	6.0	6.0343E-06	3.0171E-03	1.1
6	360	132	17775.883	1077.838	11.6	1.1571E-05	5.7855E-03	2.2
9	540	132	18549.613	1755.370	18.1	1.8059E-05	9.0293E-03	3.4
12	720	132	17165.291	2136.299	23.7	2.3750E-05	1.1875E-02	4.5
15	900	132	20682.494	3460.648	31.9	3.1931E-05	1.5965E-02	6.0
18	1080	132	18365.193	3589.561	37.3	3.7299E-05	1.8650E-02	7.0
21	1260	132	19137.742	4302.681	42.9	4.2904E-05	2.1452E-02	8.1
24	1440	132	19944.793	5252.229	50.3	5.0253E-05	2.5127E-02	9.5
27	1620	132	19583.066	5856.311	57.1	5.7068E-05	2.8534E-02	10.7
30	1800	132	22480.775	7623.636	64.7	6.4715E-05	3.2357E-02	12.2
					2.1624E+00	3.6041E-08	1.8020E-05	
					Rate (µmol/min)	**Rate (mol/s)**	**Rate (mol*L^{-1}*s^{-1})**	

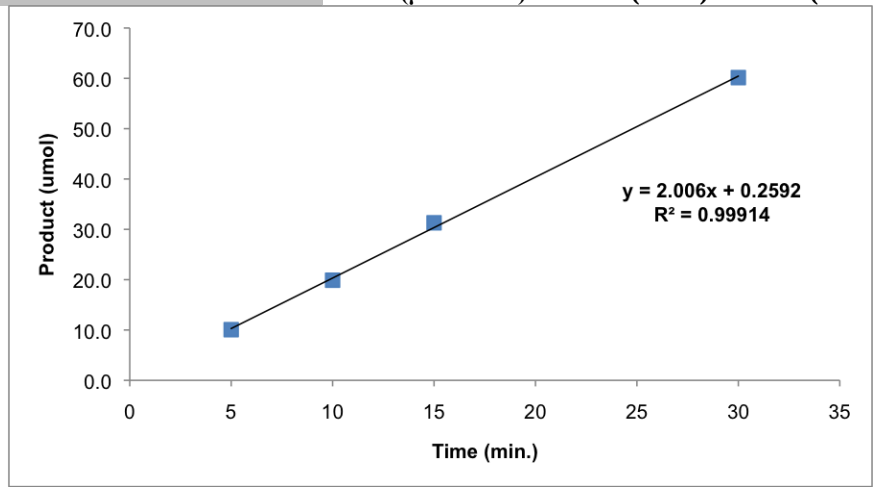

Tetra(*n*-hexyl)ammonium Bromide (0.05 equivalents), Run #2:

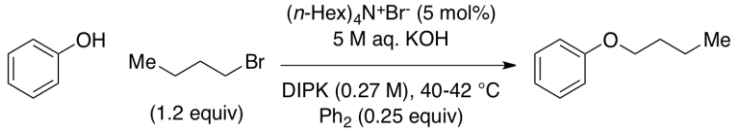

Time (m)	Time (s)	Ph_2 (µmol)	Ph_2 Area	(*n*-Bu)OPh Area	(*n*-Bu)OPh (µmol)	(*n*-Bu)OPh (mol)	(*n*-Bu)OPh (mol/L)	% conversion
0	0	132	1.000	0.000	0.0	0.0000E+00	0.0000E+00	0.0
3	180	132	18885.441	841.258	8.5	8.5007E-06	4.2503E-03	1.6
6	360	132	19229.857	1237.680	12.3	1.2282E-05	6.1412E-03	2.3
9	540	132	19255.857	1893.360	18.8	1.8764E-05	9.3819E-03	3.5
12	720	132	18878.090	2390.944	24.2	2.4169E-05	1.2085E-02	4.6
15	900	132	20511.934	3417.555	31.8	3.1795E-05	1.5898E-02	6.0
18	1080	132	20971.201	4103.237	37.3	3.7338E-05	1.8669E-02	7.0
21	1260	132	19565.414	4488.589	43.8	4.3780E-05	2.1890E-02	8.2
24	1440	132	18694.328	4964.882	50.7	5.0682E-05	2.5341E-02	9.5
27	1620	132	21175.969	6478.634	58.4	5.8384E-05	2.9192E-02	11.0
30	1800	132	19731.643	6662.090	64.4	6.4432E-05	3.2216E-02	12.1
					2.1213E+00	3.5355E-08	1.7678E-05	
					Rate (µmol/min)	**Rate (mol/s)**	**Rate (mol*L^{-1}*s^{-1})**	

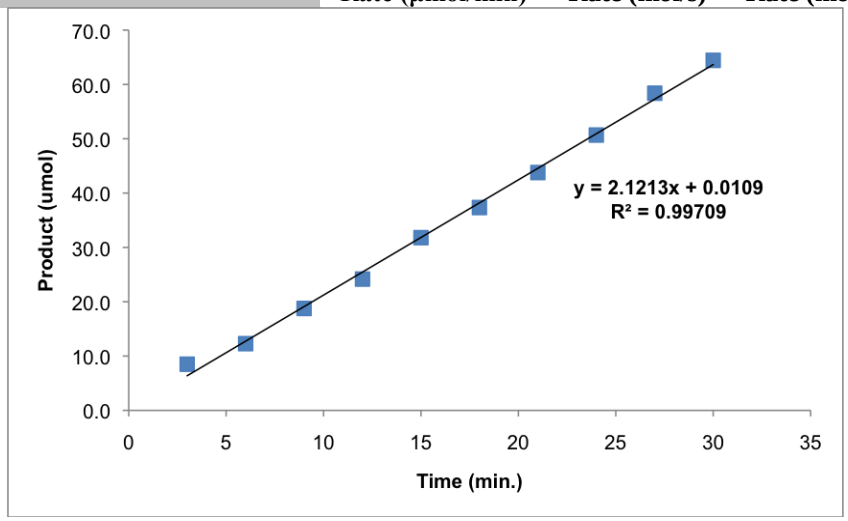

Tetra(*n*-hexyl)ammonium Bromide (0.05 equivalents), Run #3:

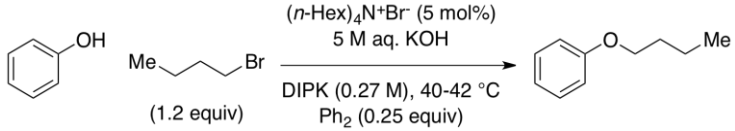

Time (m)	Time (s)	Ph_2 (µmol)	Ph_2 Area	(*n*-Bu)OPh Area	(*n*-Bu)OPh (µmol)	(*n*-Bu)OPh (mol)	(*n*-Bu)OPh (mol/L)	% conversion
0	0	132	1.000	0.000	0.0	0.0000E+00	0.0000E+00	0.0
3	180	132	16910.492	608.387	6.9	6.8656E-06	3.4328E-03	1.3
6	360	132	18094.947	1212.190	12.8	1.2784E-05	6.3920E-03	2.4
9	540	132	18019.420	1687.266	17.9	1.7869E-05	8.9344E-03	3.4
12	720	132	17973.168	2253.632	23.9	2.3928E-05	1.1964E-02	4.5
15	900	132	18338.520	2856.433	29.7	2.9724E-05	1.4862E-02	5.6
18	1080	132	17691.598	3336.920	36.0	3.5994E-05	1.7997E-02	6.8
21	1260	132	17828.934	3974.319	42.5	4.2539E-05	2.1270E-02	8.0
24	1440	132	18024.189	4570.026	48.4	4.8385E-05	2.4193E-02	9.1
27	1620	132	17297.961	4915.972	54.2	5.4233E-05	2.7117E-02	10.2
30	1800	132	17376.840	5425.734	59.6	5.9585E-05	2.9793E-02	11.2
					1.9784E+00	3.2973E-08	1.6487E-05	
					Rate (µmol/min)	**Rate (mol/s)**	**Rate (mol*L^{-1}*s^{-1})**	

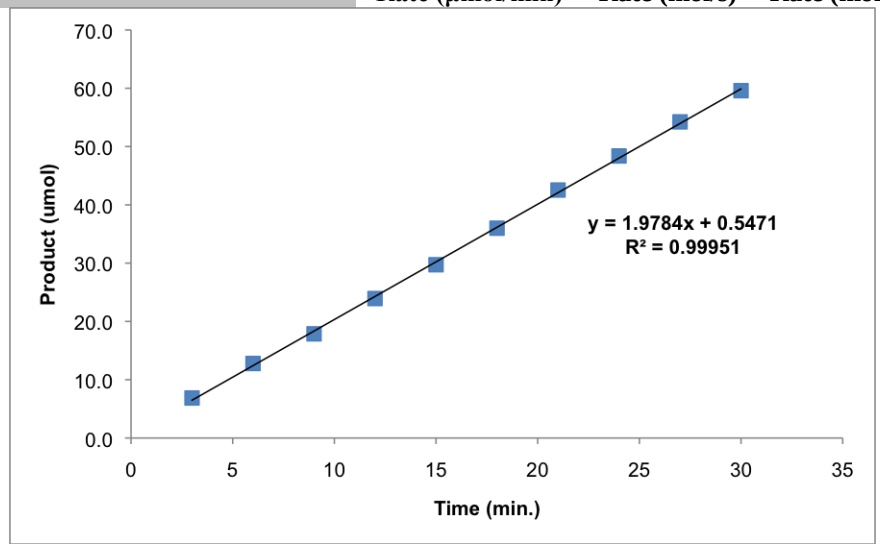

Tetra(*n*-hexyl)ammonium Bromide (0.05 equivalents), Run #4:

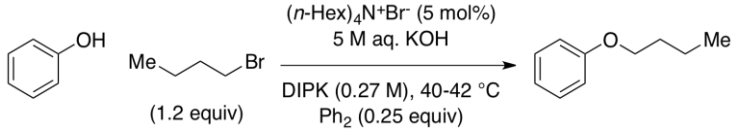

Time (m)	Time (s)	Ph_2 (µmol)	Ph_2 Area	(*n*-Bu)OPh Area	(*n*-Bu)OPh (µmol)	(*n*-Bu)OPh (mol)	(*n*-Bu)OPh (mol/L)	% conversion
0	0	132	1.000	0.000	0.0	0.0000E+00	0.0000E+00	0.0
3	180	132	17941.457	613.306	6.5	6.5234E-06	3.2617E-03	1.2
6	360	132	18011.992	1114.191	11.8	1.1805E-05	5.9023E-03	2.2
9	540	132	18316.498	1686.764	17.6	1.7574E-05	8.7869E-03	3.3
12	720	132	18952.941	2208.558	22.2	2.2237E-05	1.1119E-02	4.2
15	900	132	18859.777	2925.014	29.6	2.9597E-05	1.4798E-02	5.6
18	1080	132	19396.598	3530.699	34.7	3.4737E-05	1.7368E-02	6.5
21	1260	132	18153.938	4048.538	42.6	4.2558E-05	2.1279E-02	8.0
24	1440	132	18385.504	4602.769	47.8	4.7774E-05	2.3887E-02	9.0
27	1620	132	17753.719	4931.075	53.0	5.3003E-05	2.6502E-02	10.0
30	1800	132	18245.191	5675.559	59.4	5.9363E-05	2.9681E-02	11.2
					1.9819E+00	3.3032E-08	1.6516E-05	
					Rate (µmol/min)	**Rate (mol/s)**	**Rate (mol*L^{-1}*s^{-1})**	

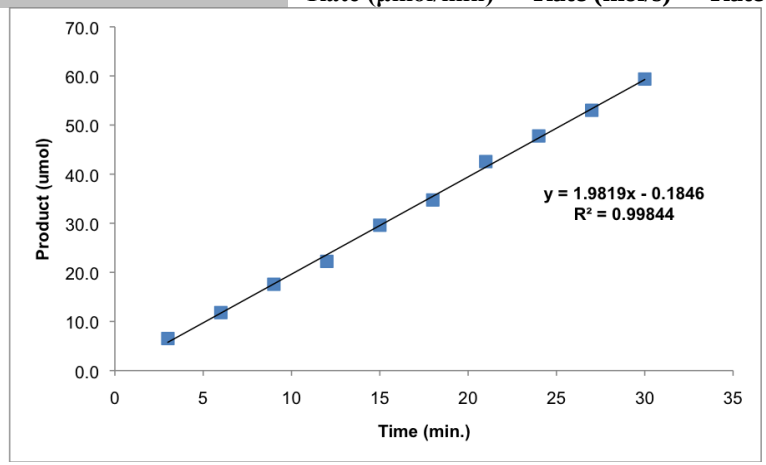

Mean alkylation rate = $1.72*10^{-5}$ (mol*L^{-1}*s^{-1})

Std. Dev. alkylation rate = $7.91*10^{-7}$ (mol*L^{-1}*s^{-1})

Tetra(*n*-octyl)ammonium Bromide (0.05 equivalents), Run #1:

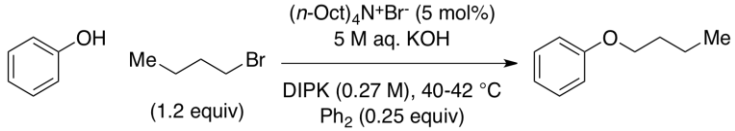

Time (m)	Time (s)	Ph_2 (µmol)	Ph_2 Area	(*n*-Bu)OPh Area	(*n*-Bu)OPh (µmol)	(*n*-Bu)OPh (mol)	(*n*-Bu)OPh (mol/L)	% conversion
0	0	132.0	1.000	0.000	0.0	0.0000E+00	0.0000E+00	0.0
3	180	132.0	18326.430	748.054	7.8	7.7895E-06	3.8947E-03	1.5
6	360	132.0	18523.816	1569.206	16.2	1.6166E-05	8.0830E-03	3.0
9	540	132.0	18666.947	2384.030	24.4	2.4372E-05	1.2186E-02	4.6
12	720	132.0	18970.623	3101.016	31.2	3.1194E-05	1.5597E-02	5.9
15	900	132.0	18743.129	3805.236	38.7	3.8743E-05	1.9371E-02	7.3
18	1080	132.0	18143.180	4280.708	45.0	4.5025E-05	2.2513E-02	8.5
21	1260	132.0	17908.512	4984.355	53.1	5.3113E-05	2.6557E-02	10.0
24	1440	132.0	19779.768	6075.881	58.6	5.8619E-05	2.9310E-02	11.0
27	1620	132.0	18690.652	6353.627	64.9	6.4871E-05	3.2435E-02	12.2
30	1800	132.0	18629.602	7069.021	72.4	7.2412E-05	3.6206E-02	13.6
					2.3552	3.9253E-08	1.9626E-05	
					Rate (µmol/min)	**Rate (mol/s)**	**Rate (mol*L^{-1}*s^{-1})**	

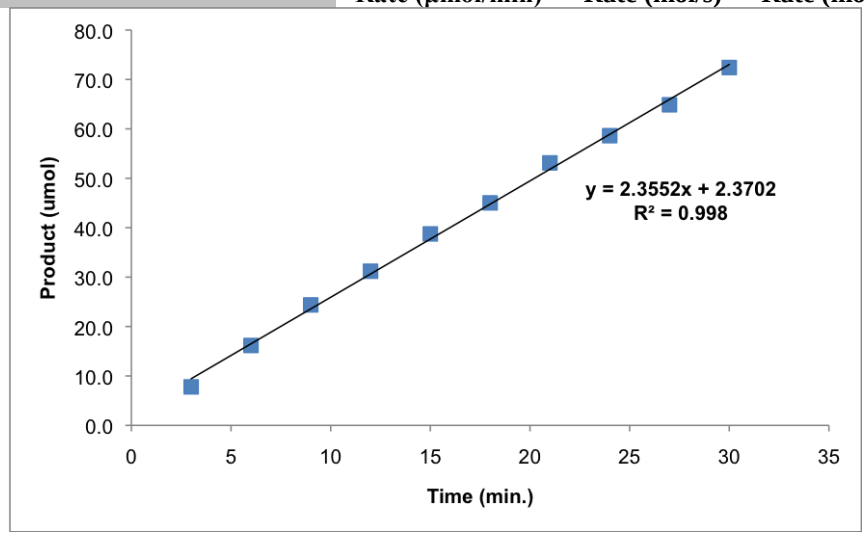

Tetra(*n*-octyl)ammonium Bromide (0.05 equivalents), Run #2:

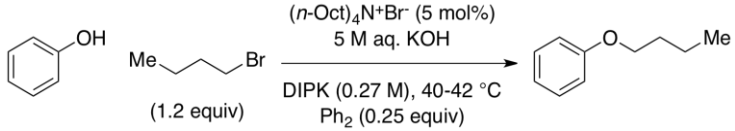

Time (m)	Time (s)	Ph_2 (µmol)	Ph_2 Area	(*n*-Bu)OPh Area	(*n*-Bu)OPh (µmol)	(*n*-Bu)OPh (mol)	(*n*-Bu)OPh (mol/L)	% conversion
0	0	132.0	1.000	0.000	0.0	0.0000E+00	0.0000E+00	0.0
3	180	132.0	19269.652	700.652	6.9	6.9387E-06	3.4694E-03	1.3
6	360	132.0	19649.195	1509.247	14.7	1.4658E-05	7.3289E-03	2.8
9	540	132.0	20258.846	2314.564	21.8	2.1803E-05	1.0901E-02	4.1
12	720	132.0	19426.961	2904.022	28.5	2.8526E-05	1.4263E-02	5.4
15	900	132.0	19096.477	3581.094	35.8	3.5786E-05	1.7893E-02	6.7
18	1080	132.0	20357.695	4519.990	42.4	4.2370E-05	2.1185E-02	8.0
21	1260	132.0	19987.555	5078.420	48.5	4.8487E-05	2.4243E-02	9.1
24	1440	132.0	20373.727	5782.203	54.2	5.4160E-05	2.7080E-02	10.2
27	1620	132.0	20251.730	6632.335	62.5	6.2497E-05	3.1248E-02	11.8
30	1800	132.0	19183.154	6779.519	67.4	6.7442E-05	3.3721E-02	12.7
					2.2377E+00	3.7295E-08	1.8647E-05	
					Rate (µmol/min)	**Rate (mol/s)**	**Rate (mol*L^{-1}*s^{-1})**	

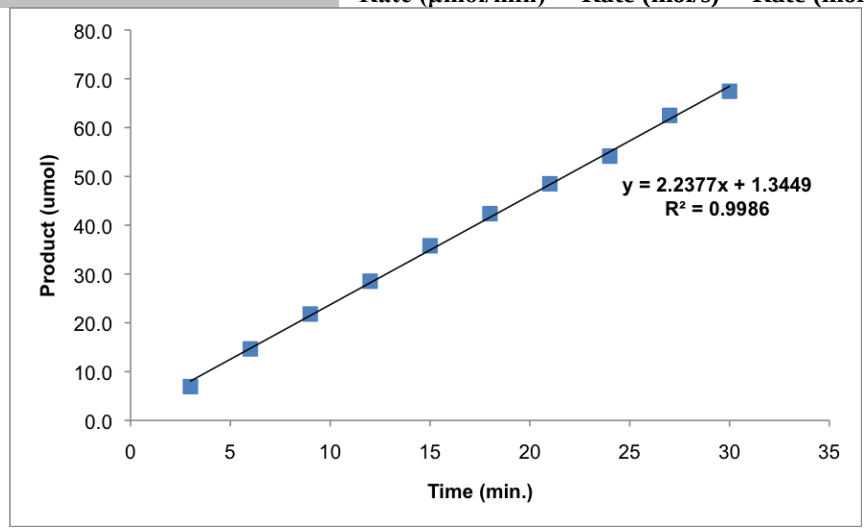

Tetra(*n*-octyl)ammonium Bromide (0.05 equivalents), Run #3:

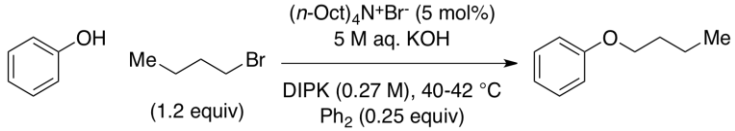

Time (m)	Time (s)	Ph_2 (µmol)	Ph_2 Area	(*n*-Bu)OPh Area	(*n*-Bu)OPh (µmol)	(*n*-Bu)OPh (mol)	(*n*-Bu)OPh (mol/L)	% conversion
0	0	132	1.000	0.000	0.0	0.0000E+00	0.0000E+00	0.0
3	180	132	18317.436	580.605	6.0	6.0488E-06	3.0244E-03	1.1
6	360	132	18806.389	1206.228	12.2	1.2240E-05	6.1199E-03	2.3
9	540	132	19164.662	1888.988	18.8	1.8810E-05	9.4048E-03	3.5
12	720	132	20264.848	2497.524	23.5	2.3519E-05	1.1759E-02	4.4
15	900	132	19576.225	3047.416	29.7	2.9707E-05	1.4853E-02	5.6
18	1080	132	19448.631	3739.889	36.7	3.6696E-05	1.8348E-02	6.9
21	1260	132	18219.752	4160.171	43.6	4.3573E-05	2.1787E-02	8.2
24	1440	132	17836.674	4643.236	49.7	4.9677E-05	2.4839E-02	9.4
27	1620	132	19029.469	5586.287	56.0	5.6021E-05	2.8010E-02	10.6
30	1800	132	18115.148	5880.961	62.0	6.1952E-05	3.0976E-02	11.7
					2.1	3.4717E-08	1.7358E-05	
					Rate (µmol/min)	**Rate (mol/s)**	**Rate (mol*L^{-1}*s^{-1})**	

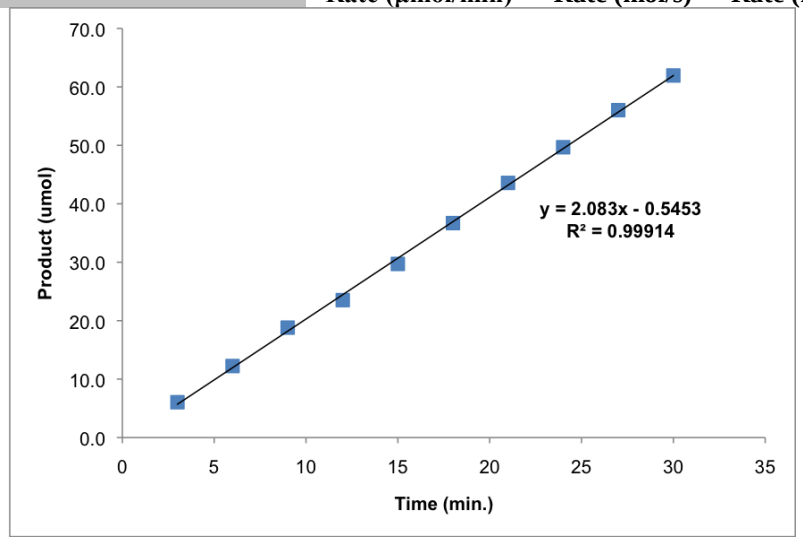

Tetra(*n*-octyl)ammonium Bromide (0.05 equivalents), Run #4:

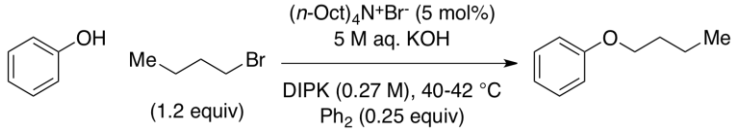

Time (m)	Time (s)	Ph_2 (µmol)	Ph_2 Area	(*n*-Bu)OPh Area	(*n*-Bu)OPh (µmol)	(*n*-Bu)OPh (mol)	(*n*-Bu)OPh (mol/L)	% conversion
0	0	132	1.000	0.000	0.0	0.0000E+00	0.0000E+00	0.0
3	180	132	19202.187	666.477	6.6	6.6235E-06	3.3117E-03	1.2
6	360	132	18307.521	1143.449	11.9	1.1919E-05	5.9595E-03	2.2
9	540	132	19446.437	1785.877	17.5	1.7525E-05	8.7626E-03	3.3
12	720	132	18387.725	2260.998	23.5	2.3465E-05	1.1733E-02	4.4
15	900	132	19146.879	2863.752	28.5	2.8542E-05	1.4271E-02	5.4
18	1080	132	20514.203	3670.185	34.1	3.4142E-05	1.7071E-02	6.4
21	1260	132	18363.830	3958.304	41.1	4.1134E-05	2.0567E-02	7.7
24	1440	132	19427.721	4772.564	46.9	4.6879E-05	2.3440E-02	8.8
27	1620	132	18628.213	5168.787	53.0	5.2950E-05	2.6475E-02	10.0
30	1800	132	20172.975	6154.693	58.2	5.8222E-05	2.9111E-02	11.0
					1.9333E+00	3.2222E-08	1.6111E-05	
					Rate (µmol/min)	**Rate (mol/s)**	**Rate (mol*L^{-1}*s^{-1})**	

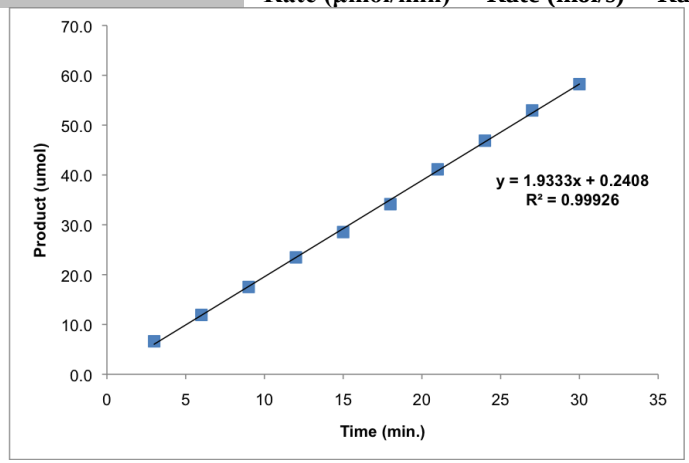

Mean alkylation rate = 1.79 x 10^{-5} (mol*L^{-1}*s^{-1})

Std. Dev. alkylation rate = 1.53 x 10^{-6} (mol*L^{-1}*s^{-1})

Tetra(*n*-propyl)ammonium Bromide (0.10 equivalents), Run #1:

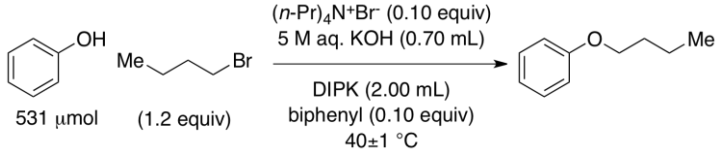

Time (m)	Time (s)	BuOPh Area	Ph_2 Area	Ph_2 (μmol)	BuOPh (μmol)	BuOPh (mol)	BuOPh (mol/L)	% BuOPh
0	0	0.00000E+00	1.00000E+00	53.1	0.00	0.0000E+00	0.0000E+00	0.0
8	480	0.00000E+00	7.80588E+03	53.1	0.00	0.0000E+00	0.0000E+00	0.0
16	960	7.11030E+02	8.11791E+03	53.1	6.72	6.7238E-06	3.3619E-03	1.3
24	1440	1.48136E+03	8.23338E+03	53.1	13.81	1.3812E-05	6.9060E-03	2.6
32	1920	2.37177E+03	9.56143E+03	53.1	19.04	1.9042E-05	9.5212E-03	3.6
40	2400	3.37955E+03	9.01435E+03	53.1	28.78	2.8780E-05	1.4390E-02	5.4
48	2880	3.35195E+03	8.13227E+03	53.1	31.64	3.1642E-05	1.5821E-02	6.0
56	3360	4.99929E+03	8.84425E+03	53.1	43.39	4.3393E-05	2.1697E-02	8.2
64	3840	6.14175E+03	9.66288E+03	53.1	48.79	4.8793E-05	2.4397E-02	9.2
72	4320	6.65866E+03	9.30460E+03	53.1	54.94	5.4937E-05	2.7468E-02	10.3
80	4800	7.26408E+03	9.05144E+03	53.1	61.61	6.1608E-05	3.0804E-02	11.6
					8.6880E-01	1.4480E-08	7.2400E-06	
					Rate (μmol/min)	**Rate (mol/s)**	**Rate (mol*L^{-1}*s^{-1})**	

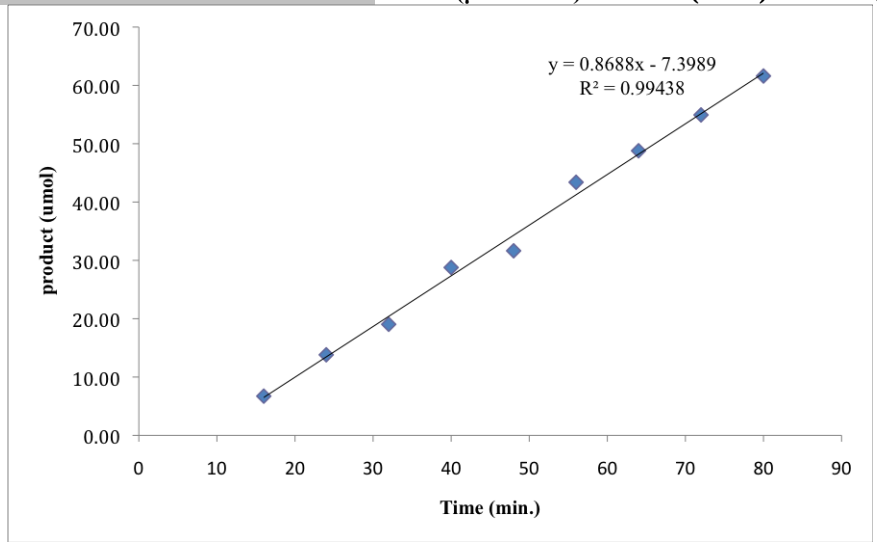

Tetra(*n*-propyl)ammonium Bromide (0.10 equivalents), Run #2:

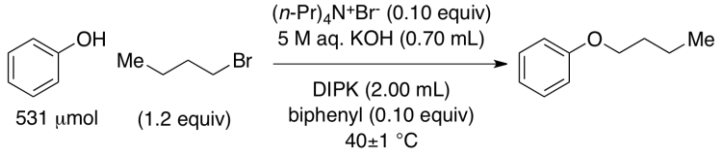

Time (m)	Time (s)	BuOPh Area	Ph_2 Area	Ph_2 (μmol)	BuOPh (μmol)	BuOPh (mol)	BuOPh (mol/L)	% BuOPh
0	0	0.00000E+00	1.00000E+00	53.1	0.00	0.0000E+00	0.0000E+00	0.0
8	480	6.99895E+02	9.90766E+03	53.1	5.42	5.4229E-06	2.7115E-03	1.0
16	960	1.28801E+03	9.88497E+03	53.1	10.00	1.0003E-05	5.0013E-03	1.9
24	1440	2.05058E+03	1.01701E+04	53.1	15.48	1.5478E-05	7.7392E-03	2.9
32	1920	2.23957E+03	8.58246E+03	53.1	20.03	2.0032E-05	1.0016E-02	3.8
40	2400	3.16078E+03	8.93171E+03	53.1	27.17	2.7166E-05	1.3583E-02	5.1
48	2880	4.16467E+03	9.22703E+03	53.1	34.65	3.4649E-05	1.7325E-02	6.5
56	3360	4.87753E+03	8.79651E+03	53.1	42.57	4.2566E-05	2.1283E-02	8.0
64	3840	5.99856E+03	9.44050E+03	53.1	48.78	4.8778E-05	2.4389E-02	9.2
72	4320	6.37354E+03	8.69722E+03	53.1	56.26	5.6257E-05	2.8128E-02	10.6
80	4800	7.91624E+03	9.31255E+03	53.1	65.26	6.5256E-05	3.2628E-02	12.3
					8.3626E-01	1.3938E-08	6.9688E-06	
					Rate (μmol/min)	**Rate (mol/s)**	**Rate (mol*L^{-1}*s^{-1})**	

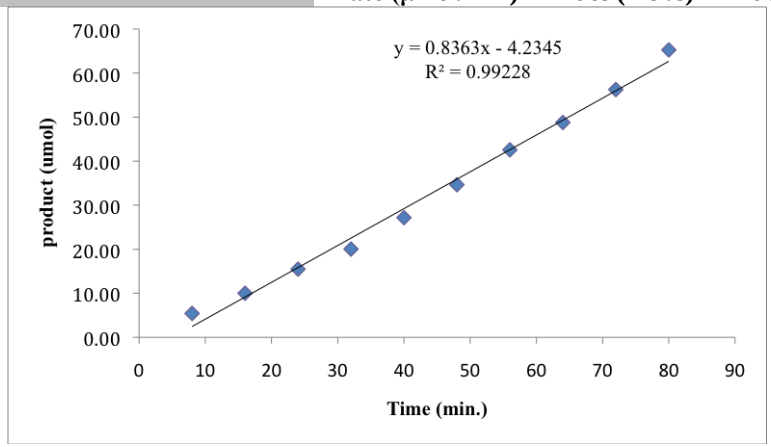

Tetra(*n*-propyl)ammonium Bromide (0.10 equivalents), Run #3:

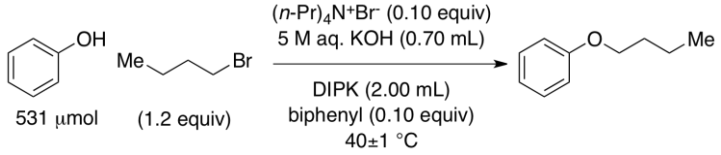

Time (m)	Time (s)	BuOPh Area	Ph_2 Area	Ph_2 (μmol)	BuOPh (μmol)	BuOPh (mol)	BuOPh (mol/L)	% BuOPh
0	0	0.00000E+00	1.00000E+00	53.1	0.00	0.0000E+00	0.0000E+00	0.0
8	480	0.00000E+00	9.25049E+03	53.1	0.00	0.0000E+00	0.0000E+00	0.0
16	960	0.00000E+00	6.42325E+03	53.1	0.00	0.0000E+00	0.0000E+00	0.0
24	1440	1.53851E+03	8.93887E+03	53.1	13.21	1.3213E-05	6.6063E-03	2.5
32	1920	2.23293E+03	8.66409E+03	53.1	19.78	1.9784E-05	9.8922E-03	3.7
40	2400	2.89299E+03	8.69515E+03	53.1	25.54	2.5541E-05	1.2771E-02	4.8
48	2880	3.83745E+03	8.78137E+03	53.1	33.55	3.3547E-05	1.6773E-02	6.3
56	3360	4.74619E+03	8.92585E+03	53.1	40.82	4.0820E-05	2.0410E-02	7.7
64	3840	5.41873E+03	9.03231E+03	53.1	46.05	4.6054E-05	2.3027E-02	8.7
72	4320	6.49239E+03	9.31183E+03	53.1	53.52	5.3523E-05	2.6762E-02	10.1
80	4800	7.05517E+03	9.04687E+03	53.1	59.87	5.9866E-05	2.9933E-02	11.3
					8.3941E-01	1.3990E-08	6.9950E-06	
					Rate (μmol/min)	**Rate (mol/s)**	**Rate (mol*L^{-1}*s^{-1})**	

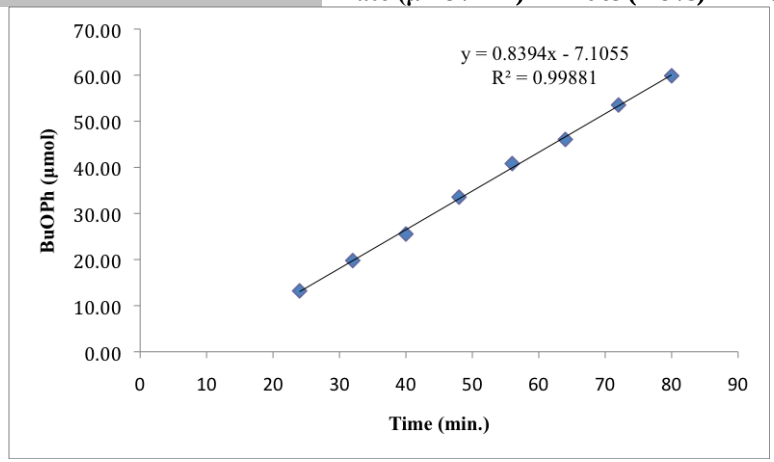

Mean alkylation rate = 7.07*10^{-6} (mol*L^{-1}*s^{-1})

Std. Dev. alkylation rate = 1.50 x 10^{-7} (mol*L^{-1}*s^{-1})

Tetra(*n*-butyl)ammonium Bromide (0.10 equivalents), Run #1:

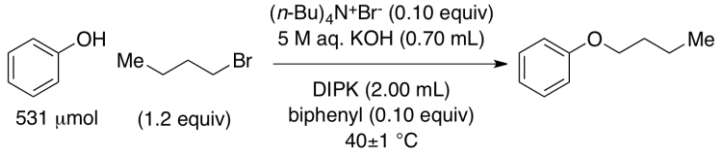

Time (m)	Time (s)	BuOPh Area	Ph_2 Area	Ph_2 (μmol)	BuOPh (μmol)	BuOPh (mol)	BuOPh (mol/L)	% BuOPh
0	0	0.00000E+00	1.00000E+00	53.1	0.0	0.0000E+00	0.0000E+00	0.0
2	120	0.00000E+00	8.35043E+03	53.1	0.0	0.0000E+00	0.0000E+00	0.0
4	240	1.86600E+03	9.13133E+03	53.1	15.7	1.5694E-05	7.8470E-03	3.0
6	360	3.25994E+03	8.71325E+03	53.1	28.7	2.8733E-05	1.4367E-02	5.4
8	480	4.88684E+03	9.15984E+03	53.1	41.0	4.0973E-05	2.0486E-02	7.7
10	600	5.45489E+03	7.62418E+03	53.1	54.9	5.4948E-05	2.7474E-02	10.3
12	720	7.51201E+03	8.58504E+03	53.1	67.2	6.7200E-05	3.3600E-02	12.7
14	840	8.92237E+03	8.59003E+03	53.1	79.8	7.9770E-05	3.9885E-02	15.0
16	960	1.01872E+04	8.42147E+03	53.1	92.9	9.2901E-05	4.6451E-02	17.5
18	1080	1.22909E+04	9.12937E+03	53.1	103.4	1.0339E-04	5.1697E-02	19.5
20	1200	1.43553E+04	1.00484E+04	53.1	109.7	1.0972E-04	5.4858E-02	20.7
					6.0729E+00	1.0122E-07	5.0608E-05	
					Rate (μmol/min)	**Rate (mol/s)**	**Rate (mol*L^{-1}*s^{-1})**	

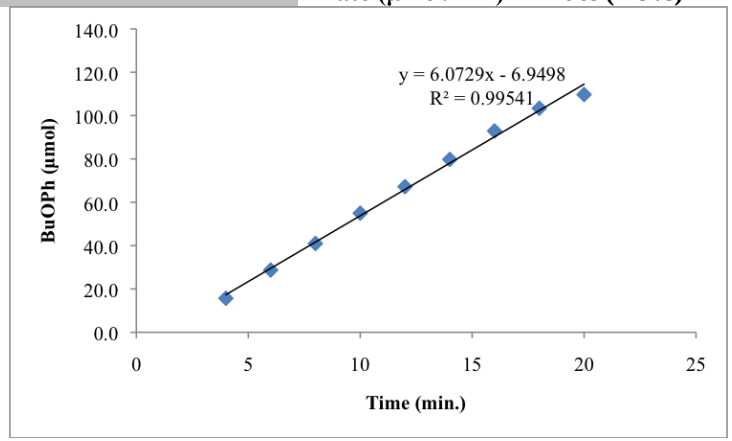

Tetra(*n*-butyl)ammonium Bromide (0.10 equivalents), Run #2:

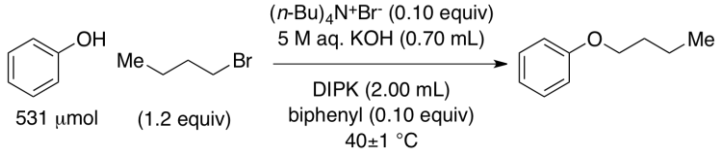

Time (m)	Time (s)	BuOPh Area	Ph_2 Area	Ph_2 (μmol)	BuOPh (μmol)	BuOPh (mol)	BuOPh (mol/L)	% BuOPh
0	0	0.00000E+00	1.00000E+00	53.1	0.0	0.0000E+00	0.0000E+00	0.0
2	120	0.00000E+00	8.44260E+03	53.1	0.0	0.0000E+00	0.0000E+00	0.0
4	240	2.10866E+03	8.98792E+03	53.1	18.0	1.8018E-05	9.0089E-03	3.4
6	360	3.85356E+03	8.87515E+03	53.1	33.3	3.3346E-05	1.6673E-02	6.3
8	480	5.26495E+03	8.69945E+03	53.1	46.5	4.6479E-05	2.3240E-02	8.8
10	600	6.26426E+03	8.39049E+03	53.1	57.3	5.7337E-05	2.8669E-02	10.8
12	720	8.29656E+03	8.70735E+03	53.1	73.2	7.3176E-05	3.6588E-02	13.8
14	840	9.89915E+03	8.91692E+03	53.1	85.3	8.5259E-05	4.2629E-02	16.1
16	960	1.20210E+04	9.60396E+03	53.1	96.1	9.6127E-05	4.8064E-02	18.1
18	1080	1.31338E+04	9.37198E+03	53.1	107.6	1.0763E-04	5.3813E-02	20.3
20	1200	1.40261E+04	8.97624E+03	53.1	120.0	1.2000E-04	6.0002E-02	22.6
					6.3167E+00	1.0528E-07	5.2639E-05	
					Rate (μmol/min)	**Rate (mol/s)**	**Rate (mol*L^{-1}*s^{-1})**	

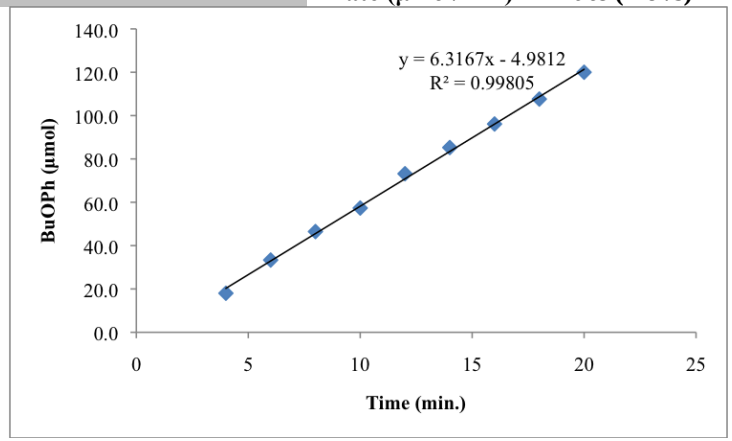

Tetra(*n*-butyl)ammonium Bromide (0.10 equivalents), Run #3:

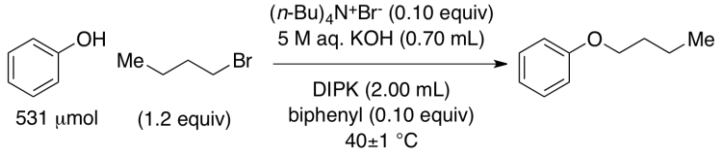

Time (m)	Time (s)	BuOPh Area	Ph_2 Area	Ph_2 (μmol)	BuOPh (μmol)	BuOPh (mol)	BuOPh (mol/L)	% BuOPh
0	0	0.00000E+00	1.00000E+00	53.1	0.0	0.0000E+00	0.0000E+00	0.0
2	120	0.00000E+00	7.30323E+03	53.1	0.0	0.0000E+00	0.0000E+00	0.0
4	240	1.57561E+03	7.61365E+03	53.1	15.9	1.5893E-05	7.9466E-03	3.0
6	360	3.65063E+03	9.12454E+03	53.1	30.7	3.0726E-05	1.5363E-02	5.8
8	480	4.25427E+03	7.91684E+03	53.1	41.3	4.1269E-05	2.0635E-02	7.8
10	600	5.76382E+03	8.22108E+03	53.1	53.8	5.3844E-05	2.6922E-02	10.1
12	720	7.54351E+03	8.62583E+03	53.1	67.2	6.7163E-05	3.3581E-02	12.6
14	840	8.91804E+03	8.81438E+03	53.1	77.7	7.7702E-05	3.8851E-02	14.6
16	960	8.69114E+03	7.15663E+03	53.1	93.3	9.3266E-05	4.6633E-02	17.6
18	1080	1.06282E+04	8.07687E+03	53.1	101.1	1.0106E-04	5.0529E-02	19.0
20	1200	1.22385E+04	8.39941E+03	53.1	111.9	1.1190E-04	5.5951E-02	21.1
					6.0240E+00	1.0040E-07	5.0200E-05	
					Rate (μmol/min)	**Rate (mol/s)**	**Rate (mol*L^{-1}*s^{-1})**	

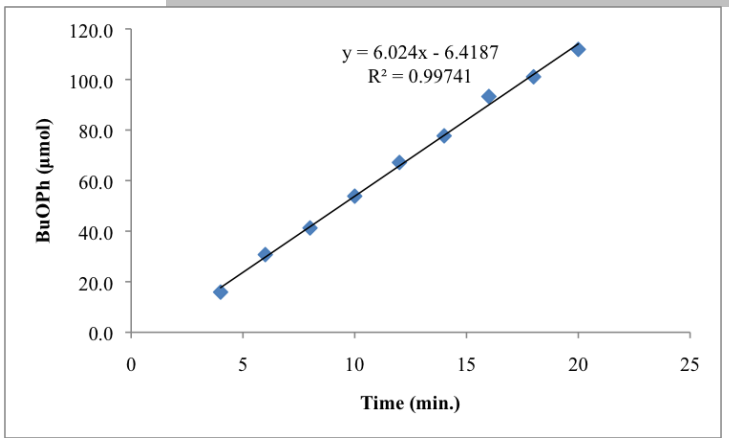

Mean alkylation rate = 3.68 x 10^{-4} (mol/s)

Std. Dev. alkylation rate = 9.41 x 10^{-6} (mol/s)

Tetra(*n*-hexyl)ammonium Bromide (0.10 equivalents), Run #1:

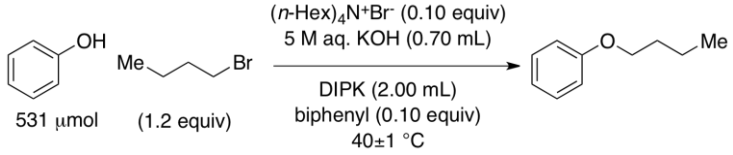

Time (m)	Time (s)	BuOPh Area	Ph_2 Area	Ph_2 (μmol)	BuOPh (μmol)	BuOPh (mol)	BuOPh (mol/L)	% BuOPh
0	0	0.00000E+00	1.00000E+00	53.1	0.0	0.0000E+00	0.0000E+00	0.0
2	120	5.86876E+02	9.37146E+03	53.1	4.8	4.8094E-06	2.4047E-03	0.9
4	240	1.88185E+03	8.96706E+03	53.1	16.1	1.6117E-05	8.0586E-03	3.0
6	360	3.39849E+03	9.18358E+03	53.1	28.4	2.8420E-05	1.4210E-02	5.4
8	480	5.06127E+03	9.00703E+03	53.1	43.2	4.3155E-05	2.1578E-02	8.1
10	600	6.41740E+03	9.09738E+03	53.1	54.2	5.4175E-05	2.7087E-02	10.2
12	720	8.22431E+03	9.42103E+03	53.1	67.0	6.7044E-05	3.3522E-02	12.6
14	840	9.74993E+03	9.40666E+03	53.1	79.6	7.9602E-05	3.9801E-02	15.0
16	960	1.17762E+04	1.02273E+04	53.1	88.4	8.8430E-05	4.4215E-02	16.7
18	1080	1.18292E+04	8.73013E+03	53.1	104.1	1.0406E-04	5.2031E-02	19.6
20	1200	1.41133E+04	9.45045E+03	53.1	114.7	1.1469E-04	5.7346E-02	21.6
					6.1418E+00	1.0236E-07	5.1182E-05	
					Rate (μmol/min)	**Rate (mol/s)**	**Rate (mol*L^{-1}*s^{-1})**	

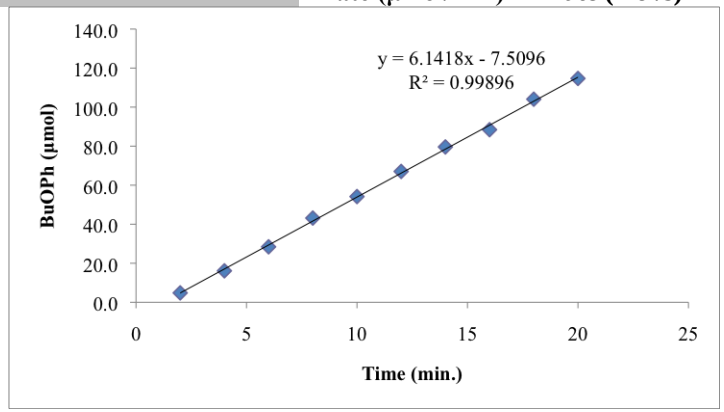

Tetra(*n*-hexyl)ammonium Bromide (0.10 equivalents), Run #2:

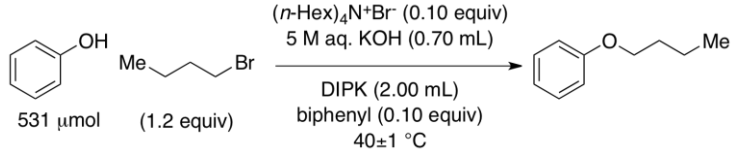

Time (m)	Time (s)	BuOPh Area	Ph_2 Area	Ph_2 (μmol)	BuOPh (μmol)	BuOPh (mol)	BuOPh (mol/L)	% BuOPh
0	0	0.00000E+00	1.00000E+00	53.1	0.0	0.0000E+00	0.0000E+00	0.0
2	120	7.57640E+02	9.11261E+03	53.1	6.4	6.3852E-06	3.1926E-03	1.2
4	240	2.28579E+03	1.00276E+04	53.1	17.5	1.7506E-05	8.7532E-03	3.3
6	360	3.74642E+03	9.48529E+03	53.1	30.3	3.0333E-05	1.5167E-02	5.7
8	480	5.37809E+03	9.60173E+03	53.1	43.0	4.3016E-05	2.1508E-02	8.1
10	600	6.45889E+03	8.85221E+03	53.1	56.0	5.6035E-05	2.8018E-02	10.6
12	720	8.24945E+03	9.29084E+03	53.1	68.2	6.8191E-05	3.4095E-02	12.8
14	840	9.84580E+03	9.71317E+03	53.1	77.8	7.7848E-05	3.8924E-02	14.7
16	960	1.11105E+04	9.22894E+03	53.1	92.5	9.2457E-05	4.6228E-02	17.4
18	1080	1.21504E+04	8.97840E+03	53.1	103.9	1.0393E-04	5.1966E-02	19.6
20	1200	1.45671E+04	9.68352E+03	53.1	115.5	1.1553E-04	5.7765E-02	21.8
					6.1047E+00	1.0174E-07	5.0872E-05	
					Rate (μmol/min)	**Rate (mol/s)**	**Rate (mol*L^{-1}*s^{-1})**	

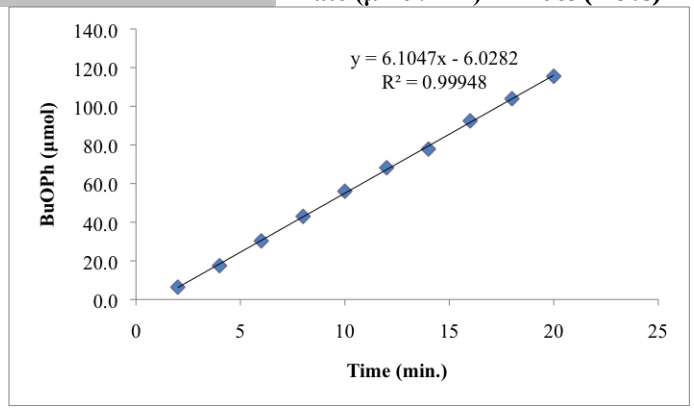

Tetra(*n*-hexyl)ammonium Bromide (0.10 equivalents), Run #3:

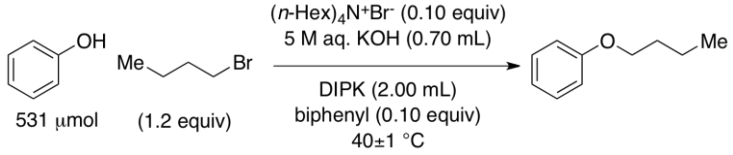

Time (m)	Time (s)	BuOPh Area	Ph_2 Area	Ph_2 (μmol)	BuOPh (μmol)	BuOPh (mol)	BuOPh (mol/L)	% BuOPh
0	0	0.00000E+00	1.00000E+00	53.1	0.0	0.0000E+00	0.0000E+00	0.0
2	120	0.00000E+00	8.37093E+03	53.1	0.0	0.0000E+00	0.0000E+00	0.0
4	240	1.97629E+03	8.95798E+03	53.1	16.9	1.6943E-05	8.4716E-03	3.2
6	360	3.18103E+03	8.44066E+03	53.1	28.9	2.8943E-05	1.4472E-02	5.5
8	480	4.88868E+03	8.51110E+03	53.1	44.1	4.4112E-05	2.2056E-02	8.3
10	600	6.72508E+03	8.95268E+03	53.1	57.7	5.7690E-05	2.8845E-02	10.9
12	720	8.88840E+03	9.51262E+03	53.1	71.8	7.1759E-05	3.5880E-02	13.5
14	840	9.47548E+03	8.77373E+03	53.1	82.9	8.2942E-05	4.1471E-02	15.6
16	960	1.02624E+04	8.32689E+03	53.1	94.7	9.4650E-05	4.7325E-02	17.8
18	1080	1.12789E+04	8.20420E+03	53.1	105.6	1.0558E-04	5.2791E-02	19.9
20	1200	1.34170E+04	8.76092E+03	53.1	117.6	1.1761E-04	5.8807E-02	22.1
					6.3244E+00	1.0541E-07	5.2703E-05	
					Rate (μmol/min)	**Rate (mol/s)**	**Rate (mol*L^{-1}*s^{-1})**	

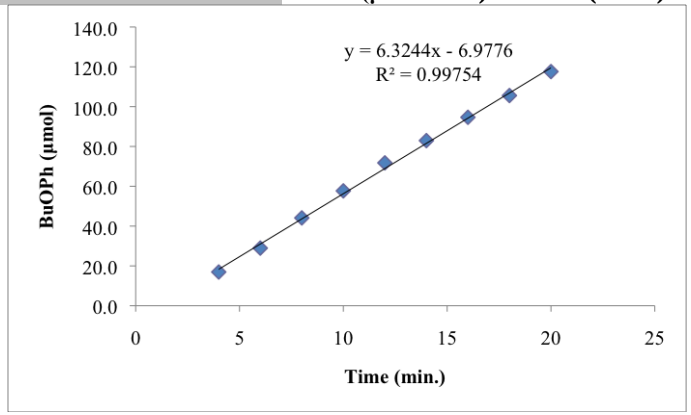

Mean alkylation rate = 5.16*10^{-5} (mol*L^{-1}*s^{-1})

Std. Dev. alkylation rate = 9.80 x 10^{-7} (mol*L^{-1}*s^{-1})

Tetra(*n*-octyl)ammonium Bromide (0.10 equivalents), Run #1:

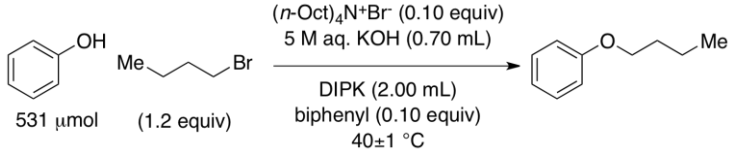

Time (m)	Time (s)	BuOPh Area	Ph_2 Area	Ph_2 (μmol)	BuOPh (μmol)	BuOPh (mol)	BuOPh (mol/L)	% BuOPh
0	0	0.00000E+00	1.00000E+00	53.1	0.0	0.0000E+00	0.0000E+00	0.0
2	120	0.00000E+00	8.13202E+03	53.1	0.0	0.0000E+00	0.0000E+00	0.0
4	240	1.10434E+03	6.17179E+03	53.1	13.7	1.3742E-05	6.8710E-03	2.6
6	360	2.03499E+03	6.31862E+03	53.1	24.7	2.4734E-05	1.2367E-02	4.7
8	480	2.93903E+03	6.26227E+03	53.1	36.0	3.6044E-05	1.8022E-02	6.8
10	600	4.36330E+03	6.49287E+03	53.1	51.6	5.1610E-05	2.5805E-02	9.7
12	720	5.11628E+03	5.86747E+03	53.1	67.0	6.6967E-05	3.3483E-02	12.6
14	840	6.01628E+03	5.97181E+03	53.1	77.4	7.7371E-05	3.8685E-02	14.6
16	960	7.73640E+03	6.54694E+03	53.1	90.8	9.0752E-05	4.5376E-02	17.1
18	1080	8.78446E+03	6.38022E+03	53.1	105.7	1.0574E-04	5.2869E-02	19.9
20	1200	9.57817E+03	6.34676E+03	53.1	115.9	1.1590E-04	5.7950E-02	21.8
					6.5569E+00	1.0928E-07	5.4641E-05	
					Rate (μmol/min)	**Rate (mol/s)**	**Rate (mol*L^{-1}*s^{-1})**	

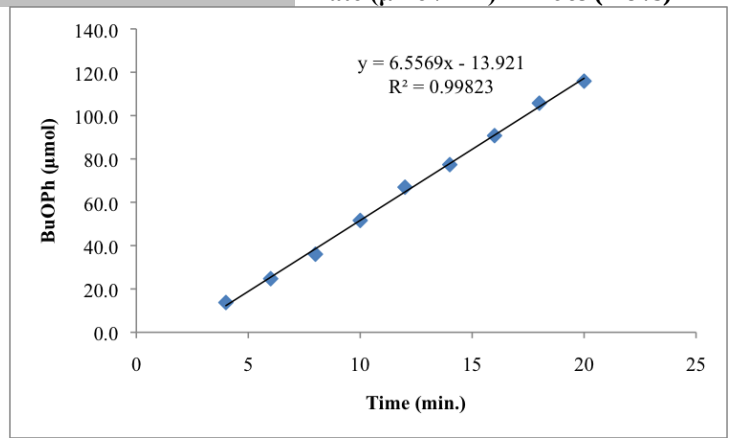

Tetra(*n*-octyl)ammonium Bromide (0.10 equivalents), Run #2:

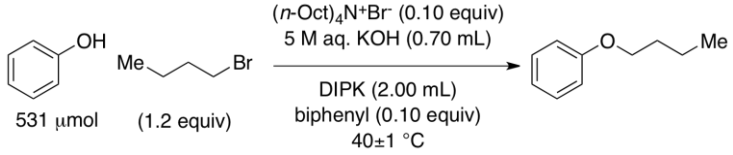

Time (m)	Time (s)	BuOPh Area	Ph_2 Area	Ph_2 (μmol)	BuOPh (μmol)	BuOPh (mol)	BuOPh (mol/L)	% BuOPh
0	0	0.00000E+00	1.00000E+00	53.1	0.0	0.0000E+00	0.0000E+00	0.0
2	120	7.94626E+02	8.35715E+03	53.1	7.3	7.3023E-06	3.6512E-03	1.4
4	240	1.85302E+03	8.17843E+03	53.1	17.4	1.7401E-05	8.7003E-03	3.3
6	360	2.55294E+03	6.83901E+03	53.1	28.7	2.8668E-05	1.4334E-02	5.4
8	480	3.88785E+03	6.90990E+03	53.1	43.2	4.3211E-05	2.1605E-02	8.1
10	600	4.27903E+03	5.70599E+03	53.1	57.6	5.7593E-05	2.8797E-02	10.8
12	720	5.67330E+03	6.41071E+03	53.1	68.0	6.7965E-05	3.3982E-02	12.8
14	840	6.76495E+03	6.58292E+03	53.1	78.9	7.8923E-05	3.9461E-02	14.9
16	960	7.75219E+03	6.28242E+03	53.1	94.8	9.4766E-05	4.7383E-02	17.8
18	1080	9.38949E+03	6.84639E+03	53.1	105.3	1.0533E-04	5.2663E-02	19.8
20	1200	1.07227E+04	6.85605E+03	53.1	120.1	1.2011E-04	6.0056E-02	22.6
					6.2993E+00	1.0499E-07	5.2494E-05	
					Rate (μmol/min)	**Rate (mol/s)**	**Rate (mol*L^{-1}*s^{-1})**	

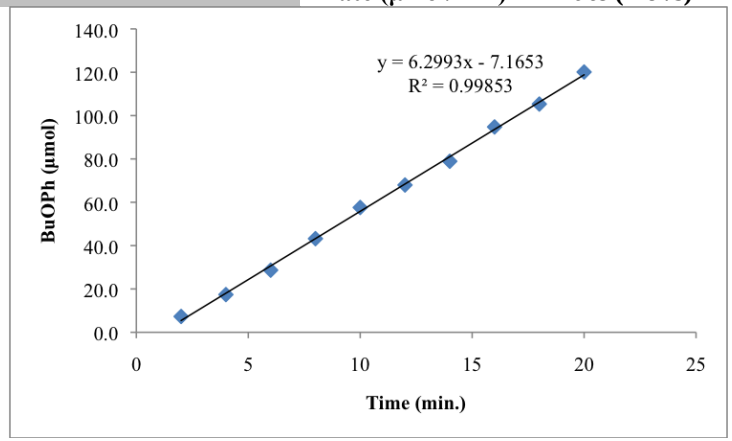

Tetra(*n*-octyl)ammonium Bromide (0.10 equivalents), Run #3:

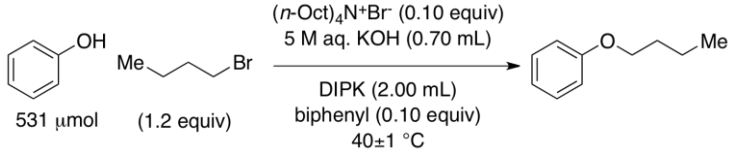

Time (m)	Time (s)	BuOPh Area	Ph_2 Area	Ph_2 (μmol)	BuOPh (μmol)	BuOPh (mol)	BuOPh (mol/L)	% BuOPh
0	0	0.00000E+00	1.00000E+00	53.1	0.0	0.0000E+00	0.0000E+00	0.0
2	120	9.85663E+02	9.64401E+03	53.1	7.8	7.8492E-06	3.9246E-03	1.5
4	240	1.74160E+03	8.58875E+03	53.1	15.6	1.5573E-05	7.7865E-03	2.9
6	360	2.78230E+03	8.51722E+03	53.1	25.1	2.5088E-05	1.2544E-02	4.7
8	480	4.51027E+03	9.17197E+03	53.1	37.8	3.7766E-05	1.8883E-02	7.1
10	600	5.85127E+03	9.27108E+03	53.1	48.5	4.8470E-05	2.4235E-02	9.1
12	720	6.75354E+03	8.75128E+03	53.1	59.3	5.9267E-05	2.9634E-02	11.2
14	840	8.94861E+03	9.46380E+03	53.1	72.6	7.2618E-05	3.6309E-02	13.7
16	960	9.79164E+03	9.14648E+03	53.1	82.2	8.2216E-05	4.1108E-02	15.5
18	1080	1.09697E+04	8.98938E+03	53.1	93.7	9.3717E-05	4.6859E-02	17.6
20	1200	1.23028E+04	8.98669E+03	53.1	105.1	1.0514E-04	5.2569E-02	19.8
					5.5261E+00	9.2101E-08	4.6051E-05	
					Rate (μmol/min)	**Rate (mol/s)**	**Rate (mol*L^{-1}*s^{-1})**	

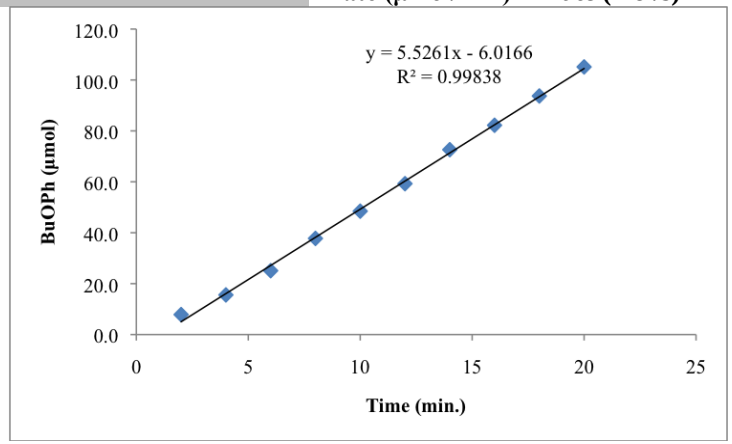

Mean alkylation rate = $5.11*10^{-5}$ (mol*L^{-1}*s^{-1})

Std. Dev. alkylation rate = $4.47*10^{-6}$ (mol*L^{-1}*s^{-1})

5.4.5 Variable Stirring Speed Kinetics

To a 4 mL dram vial, the respective quaternary ammonium bromide (4.1 to 14.5 mg, 26.6 μmol) was added followed by a solution of phenol (50 mg, 531 μmol), biphenyl (20.4 to 20.7 mg, 132 to 134 μmol) in 2,4-dimethyl-3-pentanone (2.0 mL). A 5 M aqueous KOH solution (0.70 mL) was then added followed by the addition of a 1.5 cm egg-shaped magnetic stir-bar. A septa screw-cap was then installed on the vial.

This vial was placed over a variable speed motor calibrated form 250, 500, 1000, 1500, 2000, and 2300 rpm. To start the reaction, *n*-butyl bromide (68 μL, 637 μmol, 1.2 equiv) was added via syringe and the reaction was stirred at the desired speed.

Reaction aliquots were withdrawn directly from the organic phase (15-20 μL) approximately 2 seconds after the reaction had stopped stirring. Aliquots were quenched in a biphasic mixture of ethyl acetate (1-2 mL) and a saturated aqueous ammonium chloride solution (1-2 mL). After a quick mixing via pipette the organic phase was passed through a silica gel plug (1-2 cm x 0.5 cm) into a vial and used directly for GC analysis (GC Method 1).

Variable Stir Speed Kinetics

2000 rpm, Run #1:

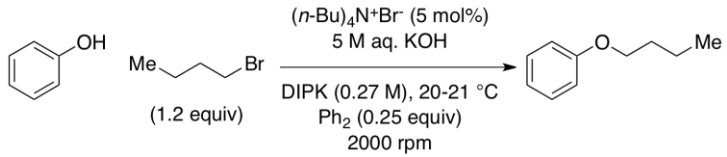

Time (m)	Time (s)	Ph_2 (µmol)	Ph_2 Area	BuOPh Area	BuOPh (µmol)	BuOPh (mol)	BuOPh (mol/L)	% conversion
0	0	132	1.000	0.000	0.0	0.0000E+00	0.0000E+00	0.0
3	180	132	16133.876	0.000	0.0	0.0000E+00	0.0000E+00	0.0
6	360	132	18379.727	0.000	0.0	0.0000E+00	0.0000E+00	0.0
9	540	132	18042.383	0.000	0.0	0.0000E+00	0.0000E+00	0.0
12	720	132	18082.299	610.567	6.4	6.4436E-06	3.2218E-03	1.2
15	900	132	17981.867	761.269	8.1	8.0790E-06	4.0395E-03	1.5
18	1080	132	19027.209	921.490	9.2	9.2420E-06	4.6210E-03	1.7
21	1260	132	18363.957	1058.832	11.0	1.1003E-05	5.5015E-03	2.1
24	1440	132	18793.695	1223.674	12.4	1.2425E-05	6.2126E-03	2.3
27	1620	132	19442.477	1436.560	14.1	1.4100E-05	7.0501E-03	2.7
30	1800	132	19674.676	1618.099	15.7	1.5695E-05	7.8473E-03	3.0
					5.1165E-01	8.5275E-09	4.2637E-06	
					Rate (µmol/min)	**Rate (mol/s)**	**Rate (mol*L^{-1}*s^{-1})**	

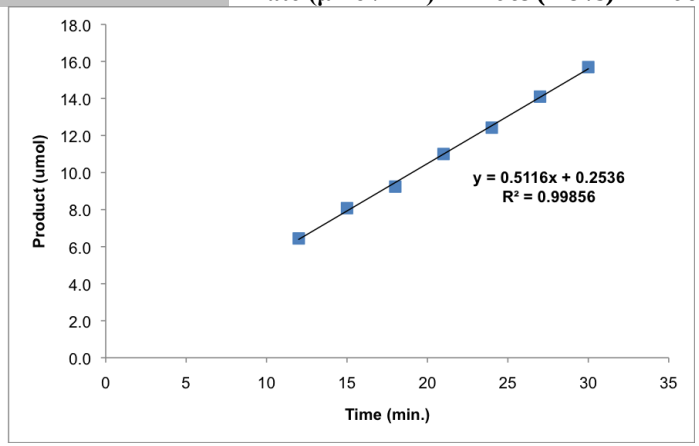

2000 rpm, Run #2:

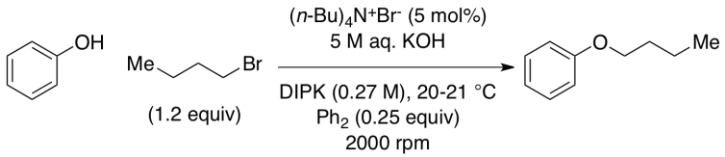

Time (m)	Time (s)	Ph_2 (µmol)	Ph_2 Area	BuOPh Area	BuOPh (µmol)	BuOPh (mol)	BuOPh (mol/L)	% conversion
0	0	132	1.000	0.000	0.0	0.0000E+00	0.0000E+00	0.0
6	360	132	19154.207	0.000	0.0	0.0000E+00	0.0000E+00	0.0
12	720	132	20115.064	611.799	5.8	5.8042E-06	2.9021E-03	1.1
18	1080	132	20737.250	908.483	8.4	8.3602E-06	4.1801E-03	1.6
24	1440	132	21326.658	1225.625	11.0	1.0967E-05	5.4835E-03	2.1
30	1800	132	21562.691	1552.476	13.7	1.3740E-05	6.8698E-03	2.6
36	2160	132	22267.928	1918.987	16.4	1.6445E-05	8.2227E-03	3.1
42	2520	132	23172.057	2313.074	19.0	1.9049E-05	9.5246E-03	3.6
48	2880	132	22271.031	2556.484	21.9	2.1906E-05	1.0953E-02	4.1
54	3240	132	21956.725	2770.256	24.1	2.4077E-05	1.2039E-02	4.5
60	3600	132	21184.178	3078.125	27.7	2.7729E-05	1.3864E-02	5.2
					4.5010E-01	7.5016E-09	3.7508E-06	
					Rate (µmol/min)	**Rate (mol/s)**	**Rate (mol*L^{-1}*s^{-1})**	

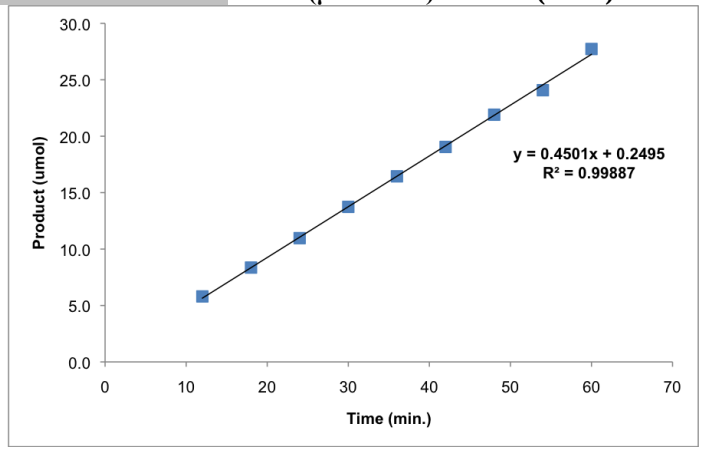

1500 rpm, Run #1:

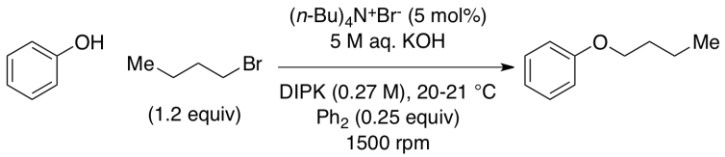

Time (m)	Time (s)	Ph_2 (µmol)	Ph_2 Area	BuOPh Area	BuOPh (µmol)	BuOPh (mol)	BuOPh (mol/L)	% conversion
0	0	132	1.000	0.000	0.0	0.0000E+00	0.0000E+00	0.0
3	180	132	18141.801	0.000	0.0	0.0000E+00	0.0000E+00	0.0
6	360	132	18094.691	0.000	0.0	0.0000E+00	0.0000E+00	0.0
9	540	132	18653.461	0.000	0.0	0.0000E+00	0.0000E+00	0.0
12	720	132	17948.551	623.499	6.6	6.6292E-06	3.3146E-03	1.2
15	900	132	18288.945	775.832	8.1	8.0953E-06	4.0476E-03	1.5
18	1080	132	18366.018	937.435	9.7	9.7404E-06	4.8702E-03	1.8
21	1260	132	18571.088	1092.895	11.2	1.1230E-05	5.6152E-03	2.1
24	1440	132	19109.533	1291.992	12.9	1.2902E-05	6.4511E-03	2.4
27	1620	132	18849.270	1403.524	14.2	1.4209E-05	7.1047E-03	2.7
30	1800	132	17373.400	1484.536	16.3	1.6306E-05	8.1532E-03	3.1
					5.2883E-01	8.8138E-09	4.4069E-06	
					Rate (µmol/min)	**Rate (mol/s)**	**Rate (mol*L^{-1}*s^{-1})**	

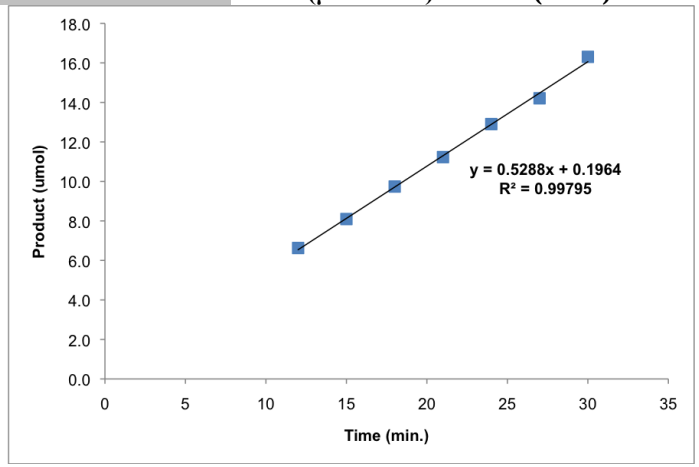

1500 rpm, Run #2:

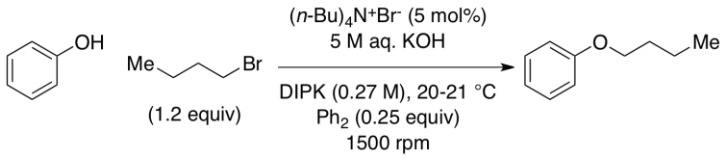

Time (m)	Time (s)	Ph_2 (µmol)	Ph_2 Area	BuOPh Area	BuOPh (µmol)	BuOPh (mol)	BuOPh (mol/L)	% conversion
0	0	132	1.000	0.000	0.0	0.0000E+00	0.0000E+00	0.0
6	360	132	20510.309	0.000	0.0	0.0000E+00	0.0000E+00	0.0
12	720	132	24589.750	780.504	6.1	6.0572E-06	3.0286E-03	1.1
18	1080	132	20270.752	913.762	8.6	8.6023E-06	4.3012E-03	1.6
24	1440	132	20044.488	1185.917	11.3	1.1290E-05	5.6452E-03	2.1
30	1800	132	19895.395	1393.453	13.4	1.3366E-05	6.6829E-03	2.5
36	2160	132	21041.014	1770.095	16.1	1.6054E-05	8.0270E-03	3.0
42	2520	132	20747.127	1967.296	18.1	1.8095E-05	9.0476E-03	3.4
48	2880	132	21329.795	2370.640	21.2	2.1210E-05	1.0605E-02	4.0
54	3240	132	21446.076	2705.987	24.1	2.4079E-05	1.2039E-02	4.5
60	3600	132	21130.963	2960.716	26.7	2.6738E-05	1.3369E-02	5.0
					4.2700E-01	7.1166E-09	3.5583E-06	
					Rate (µmol/min)	**Rate (mol/s)**	**Rate (mol*L^{-1}*s^{-1})**	

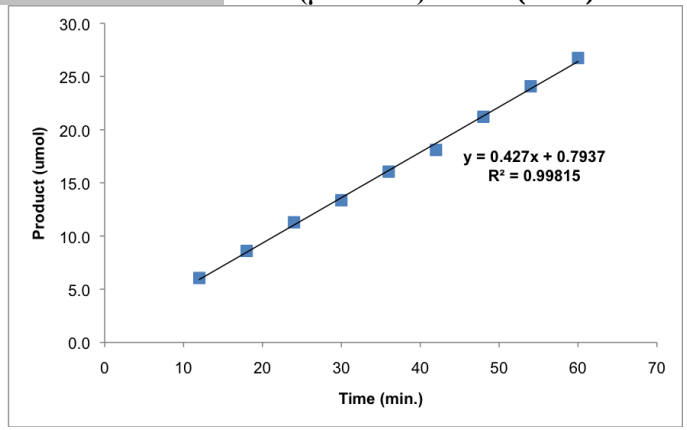

1000 rpm, Run #1:

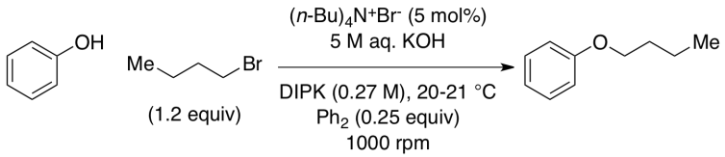

Time (m)	Time (s)	Ph_2 (µmol)	Ph_2 Area	BuOPh Area	BuOPh (µmol)	BuOPh (mol)	BuOPh (mol/L)	% conversion
0	0	132	1.000	0.000	0.0	0.0000E+00	0.0000E+00	0.0
3	180	132	18436.311	0.000	0.0	0.0000E+00	0.0000E+00	0.0
6	360	132	17563.691	0.000	0.0	0.0000E+00	0.0000E+00	0.0
9	540	132	18751.691	0.000	0.0	0.0000E+00	0.0000E+00	0.0
12	720	132	18435.674	657.182	6.8	6.8027E-06	3.4013E-03	1.3
15	900	132	17510.895	759.829	8.3	8.2806E-06	4.1403E-03	1.6
18	1080	132	18984.289	944.427	9.5	9.4935E-06	4.7467E-03	1.8
21	1260	132	17901.709	1058.577	11.3	1.1284E-05	5.6422E-03	2.1
24	1440	132	18326.402	1222.537	12.7	1.2730E-05	6.3651E-03	2.4
27	1620	132	18404.543	1366.709	14.2	1.4171E-05	7.0855E-03	2.7
30	1800	132	18481.400	1524.619	15.7	1.5743E-05	7.8713E-03	3.0
					0.498069743	8.3012E-09	4.1506E-06	
					Rate (µmol/min)	**Rate (mol/s)**	**Rate (mol*L^{-1}*s^{-1})**	

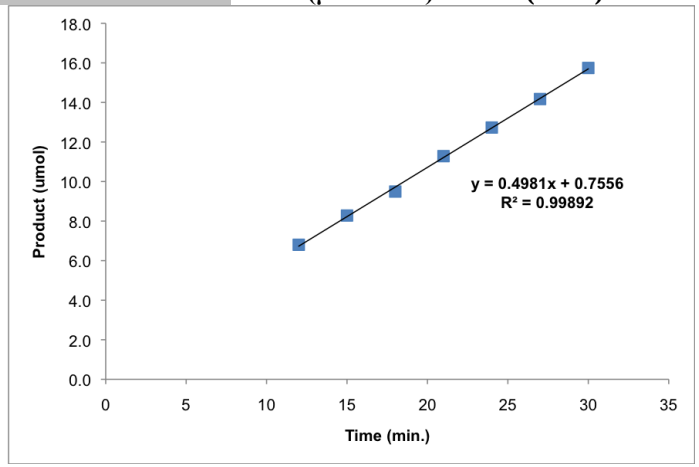

1000 rpm, Run #2:

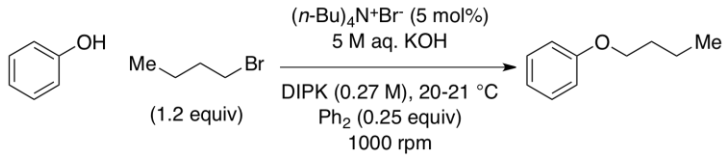

Time (m)	Time (s)	Ph_2 (µmol)	Ph_2 Area	BuOPh Area	BuOPh (µmol)	BuOPh (mol)	BuOPh (mol/L)	% conversion
0	0	134	1.000	0.000	0.0	0.0000E+00	0.0000E+00	0.0
6	360	134	19765.461	0.000	0.0	0.0000E+00	0.0000E+00	0.0
12	720	134	20100.969	537.562	5.2	5.1808E-06	2.5904E-03	1.0
18	1080	134	20877.896	870.900	8.1	8.0810E-06	4.0405E-03	1.5
24	1440	134	19939.379	983.864	9.6	9.5589E-06	4.7794E-03	1.8
30	1800	134	21153.080	1307.975	12.0	1.1979E-05	5.9893E-03	2.3
36	2160	134	20980.887	1569.487	14.5	1.4492E-05	7.2458E-03	2.7
42	2520	134	20770.748	1820.851	17.0	1.6983E-05	8.4913E-03	3.2
48	2880	134	21611.393	2174.031	19.5	1.9488E-05	9.7440E-03	3.7
54	3240	134	21919.750	2506.467	22.2	2.2152E-05	1.1076E-02	4.2
60	3600	134	21745.687	2716.165	24.2	2.4197E-05	1.2099E-02	4.6
					0.397612512	6.6269E-09	3.3134E-06	
					Rate (µmol/min)	**Rate (mol/s)**	**Rate (mol*L^{-1}*s^{-1})**	

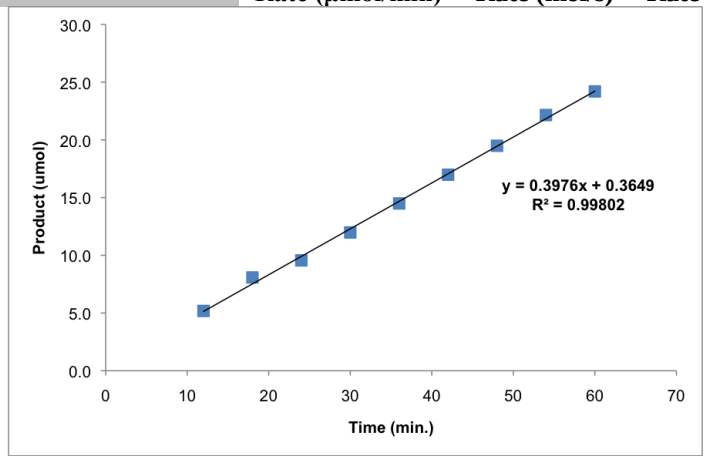

500 rpm, Run #1:

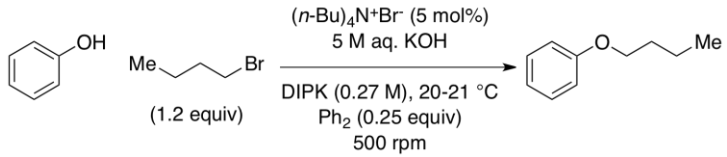

Time (m)	Time (s)	Ph_2 (µmol)	Ph_2 Area	BuOPh Area	BuOPh (µmol)	BuOPh (mol)	BuOPh (mol/L)	% conversion
0	0	132	1.000	0.000	0.0	0.0000E+00	0.0000E+00	0.0
6	360	132	18678.230	0.000	0.0	0.0000E+00	0.0000E+00	0.0
12	720	132	18471.770	588.244	6.1	6.0772E-06	3.0386E-03	1.1
18	1080	132	19371.805	882.908	8.7	8.6976E-06	4.3488E-03	1.6
24	1440	132	19871.393	1185.361	11.4	1.1383E-05	5.6917E-03	2.1
30	1800	132	19891.979	1520.518	14.6	1.4587E-05	7.2935E-03	2.7
36	2160	132	19325.729	1727.349	17.1	1.7057E-05	8.5284E-03	3.2
42	2520	132	18830.988	1980.134	20.1	2.0067E-05	1.0033E-02	3.8
48	2880	132	19981.586	2397.123	22.9	2.2894E-05	1.1447E-02	4.3
54	3240	132	20603.748	2823.536	26.2	2.6152E-05	1.3076E-02	4.9
60	3600	132	19417.041	2962.257	29.1	2.9113E-05	1.4557E-02	5.5
					0.480573955	8.0096E-09	4.0048E-06	
					Rate (µmol/min)	**Rate (mol/s)**	**Rate (mol*L^{-1}*s^{-1})**	

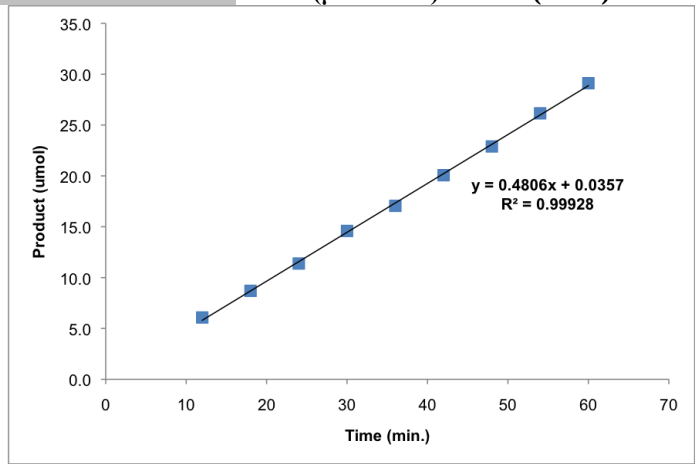

500 rpm, Run #2:

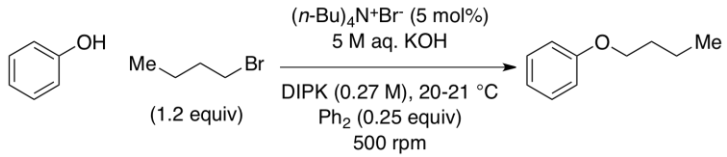

Time (m)	Time (s)	Ph_2 (µmol)	Ph_2 Area	BuOPh Area	BuOPh (µmol)	BuOPh (mol)	BuOPh (mol/L)	% conversion
0	0	134	1.000	0.000	0.0	0.0000E+00	0.0000E+00	0.0
6	360	134	21106.480	0.000	0.0	0.0000E+00	0.0000E+00	0.0
12	720	134	19947.605	578.800	5.6	5.6211E-06	2.8105E-03	1.1
18	1080	134	20303.650	794.731	7.6	7.5828E-06	3.7914E-03	1.4
24	1440	134	22016.443	1119.749	9.9	9.8527E-06	4.9264E-03	1.9
30	1800	134	21540.650	1325.602	11.9	1.1922E-05	5.9608E-03	2.2
36	2160	134	23338.396	1738.896	14.4	1.4434E-05	7.2170E-03	2.7
42	2520	134	21169.238	1891.348	17.3	1.7308E-05	8.6540E-03	3.3
48	2880	134	22386.324	2197.250	19.0	1.9014E-05	9.5071E-03	3.6
54	3240	134	21616.564	2452.141	22.0	2.1976E-05	1.0988E-02	4.1
60	3600	134	20902.004	2681.548	24.9	2.4853E-05	1.2427E-02	4.7
					0.399489245	6.6582E-09	3.3291E-06	
					Rate (µmol/min)	**Rate (mol/s)**	**Rate (mol*L^{-1}*s^{-1})**	

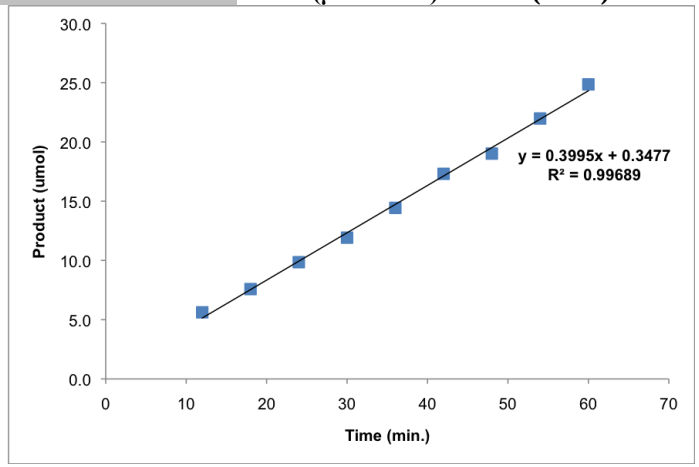

Summary Table for Variable Stirring Speed Study

Run #	Stirring Speed (rpm)	Rate (µmol/min)	Rate (mol/s)	Rate (mol*L^{-1}*s^{-1})	Mean Rate (mol*L^{-1}*s^{-1})	Std. Dev. Rate (mol*L^{-1}*s^{-1})
1	2000	5.1165E-01	8.5275E-09	4.2637E-06	4.01E-06	3.63E-07
2	2000	4.5010E-01	7.5016E-09	3.7508E-06		
1	1500	5.2883E-01	8.8138E-09	4.4069E-06	3.98E-06	6.00E-07
2	1500	4.2700E-01	7.1166E-09	3.5583E-06		
1	1000	4.9807E-01	8.3012E-09	4.1506E-06	3.73E-06	5.92E-07
2	1000	3.9761E-01	6.6269E-09	3.3134E-06		
1	500	4.8057E-01	8.0096E-09	4.0048E-06	3.67E-06	4.78E-07
2	500	3.9949E-01	6.6582E-09	3.3291E-06		

5.4.6 Order in Bromide Kinetics

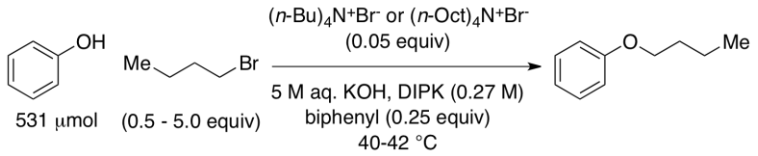

To a 4 mL dram vial, the respective quaternary ammonium bromide (4.1 to 14.5 mg, 26.6 μmol) was added followed by a solution of phenol (50 mg, 531 μmol), biphenyl (20.4 to 20.7 mg, 132 to 134 μmol), and *n*-butyl bromide (28.6 to 286 μL, 0.266 to 2.66 mmol, 0.5 to 5.0 equiv) in 2,4-dimethyl-3-pentanone (2.00 mL). A 1.5 cm egg-shaped magnetic stir-bar and a septa screw-cap were then installed.

This vial was placed on a silicone oil bath kept at 40-42 °C on a hotplate/stirrer and was allowed to come to temperature with moderate stirring for at least 30 minutes. To start the reaction, a 5 M aqueous KOH solution pre-warmed to 40 °C (0.70 mL) was added via syringe and the stirring speed was set to maximum (~2000 rpm).

Reaction aliquots were withdrawn directly from the organic phase (15-20 μL) approximately 2 seconds after the reaction had stopped stirring. Aliquots were quenched in a biphasic mixture of ethyl acetate (1-2 mL) and a saturated aqueous ammonium chloride solution (1-2 mL). After a quick mixing via pipette the organic phase was passed through a silica gel plug (1-2 cm x 0.5 cm) into a vial and used directly for GC analysis.

Tetra(*n*-octyl)ammonium Bromide, 0.5 equiv *n*-BuBr, Run #1:

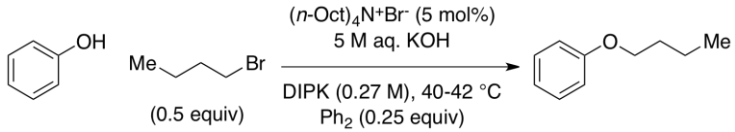

Time (m)	Time (s)	Ph_2 (µmol)	Ph_2 Area	BuOPh Area	BuOPh (µmol)	BuOPh (mol)	BuOPh (mol/L)	% conversion
0	0	134	1.000	0.000	0.0	0.0000E+00	0.0000E+00	0.0
6	360	134	19116.762	0.000	0.0	0.0000E+00	0.0000E+00	0.0
12	720	134	18321.969	926.097	9.8	9.7919E-06	4.8960E-03	1.8
18	1080	134	18412.875	1507.978	15.9	1.5866E-05	7.9328E-03	3.0
24	1440	134	18616.977	2034.148	21.2	2.1167E-05	1.0583E-02	4.0
30	1800	134	17726.965	2453.516	26.8	2.6813E-05	1.3406E-02	5.0
40	2400	134	17644.686	3257.130	35.8	3.5761E-05	1.7880E-02	6.7
50	3000	134	15560.946	3434.936	42.8	4.2763E-05	2.1381E-02	8.1
60	3600	134	19312.191	5121.845	51.4	5.1378E-05	2.5689E-02	9.7
90	5400	134	16342.970	6281.991	74.5	7.4465E-05	3.7232E-02	14.0
120	7200	134	16636.070	7991.484	93.1	9.3059E-05	4.6530E-02	17.5
					7.7440E-01	1.2907E-08	6.4534E-06	
					Rate (µmol/min)	**Rate (mol/s)**	**Rate (mol*L^{-1}*s^{-1})**	

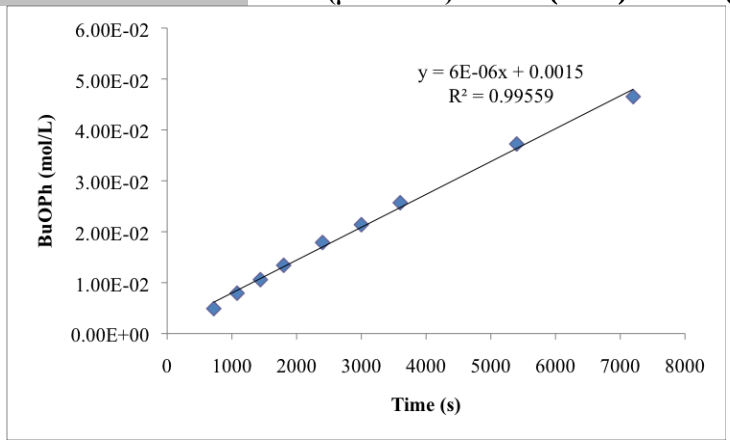

Tetra(*n*-octyl)ammonium Bromide, 0.5 equiv *n*-BuBr, Run #2:

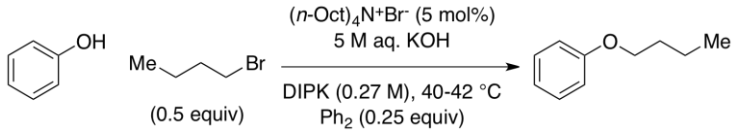

Time (m)	Time (s)	Ph_2 (µmol)	Ph_2 Area	BuOPh Area	BuOPh (µmol)	BuOPh (mol)	BuOPh (mol/L)	% conversion
0	0	134	1.000	0.000	0.0	0.0000E+00	0.0000E+00	0.0
6	360	134	16912.666	0.000	0.0	0.0000E+00	0.0000E+00	0.0
12	720	134	16432.424	888.264	10.5	1.0472E-05	5.2359E-03	2.0
18	1080	134	17465.156	1445.222	16.0	1.6030E-05	8.0152E-03	3.0
24	1440	134	16455.426	1765.310	20.8	2.0782E-05	1.0391E-02	3.9
30	1800	134	17138.990	2222.816	25.1	2.5125E-05	1.2562E-02	4.7
36	2160	134	17290.668	2723.292	30.5	3.0512E-05	1.5256E-02	5.7
42	2520	134	17395.582	3196.808	35.6	3.5601E-05	1.7800E-02	6.7
48	2880	134	17364.268	3629.240	40.5	4.0489E-05	2.0245E-02	7.6
54	3240	134	17443.098	4180.117	46.4	4.6425E-05	2.3212E-02	8.7
60	3600	134	16589.809	4219.333	49.3	4.9270E-05	2.4635E-02	9.3
					8.2296E-01	1.3716E-08	6.8580E-06	
					Rate (µmol/min)	**Rate (mol/s)**	**Rate (mol*L^{-1}*s^{-1})**	

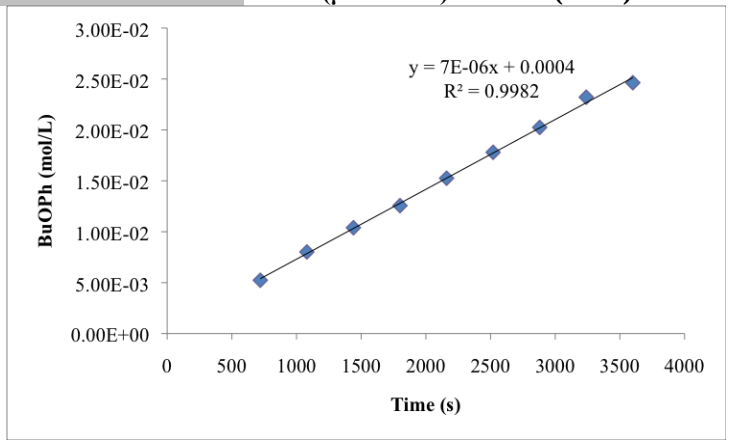

Tetra(*n*-octyl)ammonium Bromide, 0.5 equiv *n*-BuBr, Run #3:

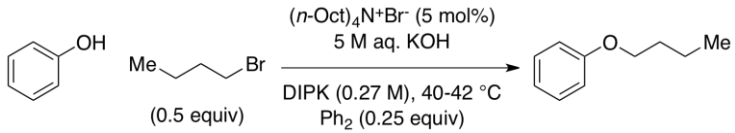

Time (m)	Time (s)	Ph_2 (µmol)	Ph_2 Area	BuOPh Area	BuOPh (µmol)	BuOPh (mol)	BuOPh (mol/L)	% conversion
0	0	134	1.000	0.000	0.0	0.0000E+00	0.0000E+00	0.0
6	360	134	16137.416	0.000	0.0	0.0000E+00	0.0000E+00	0.0
12	720	134	16135.539	945.592	11.4	1.1353E-05	5.6764E-03	2.1
18	1080	134	15899.742	1411.670	17.2	1.7200E-05	8.6000E-03	3.2
24	1440	134	15294.965	1743.929	22.1	2.2088E-05	1.1044E-02	4.2
30	1800	134	17308.473	2395.275	26.8	2.6809E-05	1.3404E-02	5.0
36	2160	134	16147.675	2689.765	32.3	3.2269E-05	1.6135E-02	6.1
42	2520	134	16624.107	3348.275	39.0	3.9018E-05	1.9509E-02	7.3
48	2880	134	16942.193	3833.954	43.8	4.3839E-05	2.1919E-02	8.3
54	3240	134	16540.957	4251.446	49.8	4.9792E-05	2.4896E-02	9.4
60	3600	134	16308.465	4515.718	53.6	5.3641E-05	2.6820E-02	10.1
					8.9622E-01	1.4937E-08	7.4685E-06	
					Rate (µmol/min)	**Rate (mol/s)**	**Rate (mol*L^{-1}*s^{-1})**	

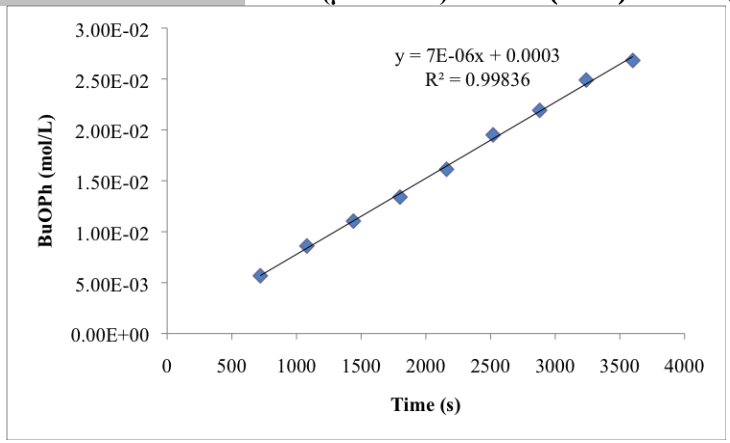

Tetra(*n*-octyl)ammonium Bromide, 0.5 equiv *n*-BuBr, Run #4:

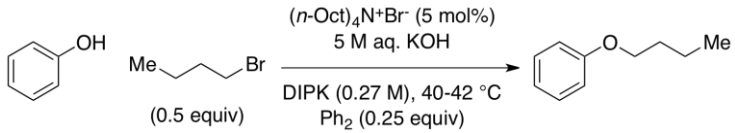

Time (m)	Time (s)	Ph_2 (µmol)	Ph_2 Area	BuOPh Area	BuOPh (µmol)	BuOPh (mol)	BuOPh (mol/L)	% conversion
0	0	134	1.000	0.000	0.0	0.0000E+00	0.0000E+00	0.0
6	360	134	17722.225	593.963	6.5	6.4927E-06	3.2463E-03	1.2
12	720	134	16926.090	1067.862	12.2	1.2222E-05	6.1110E-03	2.3
18	1080	134	17359.869	1624.514	18.1	1.8128E-05	9.0642E-03	3.4
24	1440	134	17543.205	2094.230	23.1	2.3126E-05	1.1563E-02	4.4
30	1800	134	16970.471	2464.934	28.1	2.8138E-05	1.4069E-02	5.3
36	2160	134	17549.732	3079.212	34.0	3.3990E-05	1.6995E-02	6.4
42	2520	134	17323.734	3539.281	39.6	3.9578E-05	1.9789E-02	7.5
48	2880	134	17451.707	4076.067	45.2	4.5247E-05	2.2623E-02	8.5
54	3240	134	17459.871	4586.097	50.9	5.0884E-05	2.5442E-02	9.6
60	3600	134	17268.553	4933.491	55.3	5.5345E-05	2.7673E-02	10.4
					9.1021E-01	1.5170E-08	7.5851E-06	
					Rate (µmol/min)	**Rate (mol/s)**	**Rate (mol*L^{-1}*s^{-1})**	

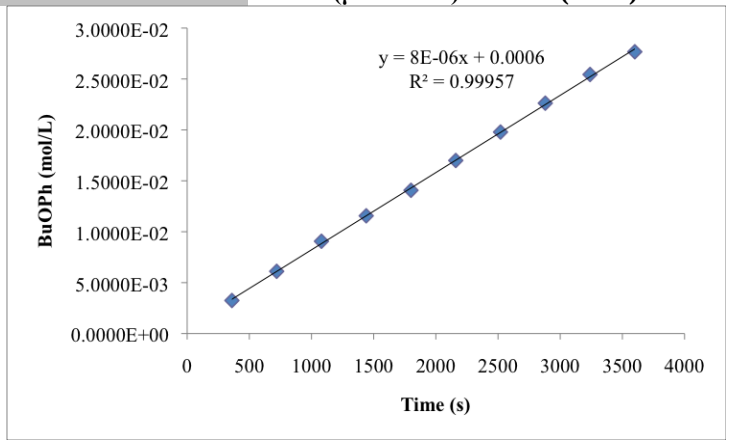

Tetra(*n*-octyl)ammonium Bromide, 1.0 equiv *n*-BuBr, Run #1:

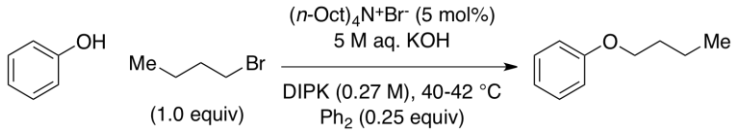

Time (m)	Time (s)	Ph_2 (µmol)	Ph_2 Area	BuOPh Area	BuOPh (µmol)	BuOPh (mol)	BuOPh (mol/L)	% conversion
0	0	134	1.000	0.000	0.0	0.0000E+00	0.0000E+00	0.0
6	360	134	19205.057	1135.245	11.5	1.1451E-05	5.7257E-03	2.2
12	720	134	17851.764	2137.557	23.2	2.3196E-05	1.1598E-02	4.4
18	1080	134	16514.771	2886.055	33.9	3.3854E-05	1.6927E-02	6.4
24	1440	134	18360.842	4453.386	47.0	4.6987E-05	2.3494E-02	8.8
30	1800	134	17567.707	5276.201	58.2	5.8182E-05	2.9091E-02	11.0
40	2400	134	17083.123	6972.653	79.1	7.9070E-05	3.9535E-02	14.9
50	3000	134	19231.742	9664.669	97.4	9.7353E-05	4.8677E-02	18.3
60	3600	134	19222.820	11592.633	116.8	1.1683E-04	5.8414E-02	22.0
90	5400	134	17911.350	15341.968	165.9	1.6593E-04	8.2967E-02	31.2
120	7200	134	18763.369	20401.500	210.6	2.1064E-04	1.0532E-01	39.7
					1.7706E+00	2.9510E-08	1.4755E-05	
					Rate (µmol/min)	**Rate (mol/s)**	**Rate (mol*L^{-1}*s^{-1})**	

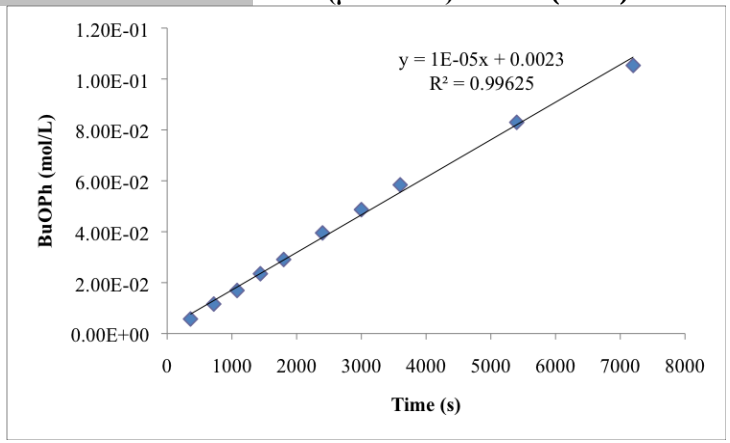

Tetra(*n*-octyl)ammonium Bromide, 1.0 equiv *n*-BuBr, Run #2:

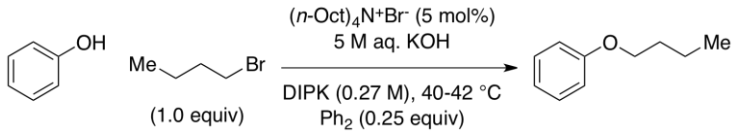

Time (m)	Time (s)	Ph_2 (µmol)	Ph_2 Area	BuOPh Area	BuOPh (µmol)	BuOPh (mol)	BuOPh (mol/L)	% conversion
0	0	134	1.000	0.000	0.0	0.0000E+00	0.0000E+00	0.0
3	180	134	16876.641	0.000	0.0	0.0000E+00	0.0000E+00	0.0
6	360	134	17648.549	953.507	10.5	1.0466E-05	5.2332E-03	2.0
9	540	134	16947.404	1362.769	15.6	1.5578E-05	7.7888E-03	2.9
12	720	134	16672.645	1803.020	20.9	2.0950E-05	1.0475E-02	3.9
15	900	134	15052.370	2025.872	26.1	2.6073E-05	1.3036E-02	4.9
18	1080	134	16311.850	2616.154	31.1	3.1070E-05	1.5535E-02	5.9
21	1260	134	15602.738	2989.149	37.1	3.7113E-05	1.8557E-02	7.0
24	1440	134	15173.535	3466.544	44.3	4.4258E-05	2.2129E-02	8.3
27	1620	134	15059.137	3984.425	51.3	5.1256E-05	2.5628E-02	9.7
30	1800	134	14841.888	4380.361	57.2	5.7175E-05	2.8587E-02	10.8
					1.9529E+00	3.2549E-08	1.6274E-05	
					Rate (µmol/min)	**Rate (mol/s)**	**Rate (mol*L^{-1}*s^{-1})**	

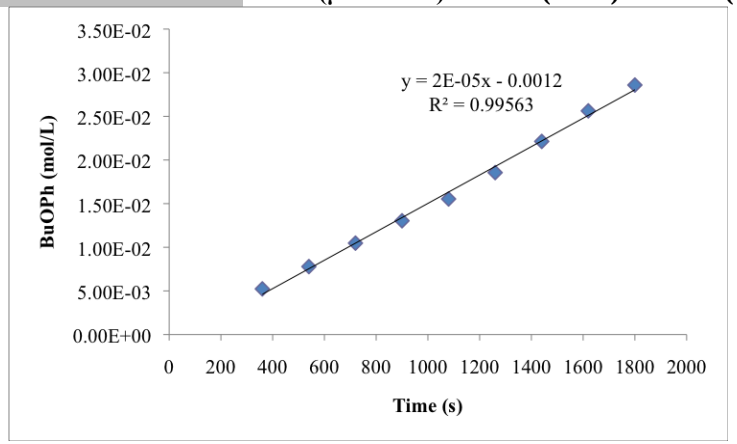

Tetra(*n*-octyl)ammonium Bromide, 1.0 equiv *n*-BuBr, Run #3:

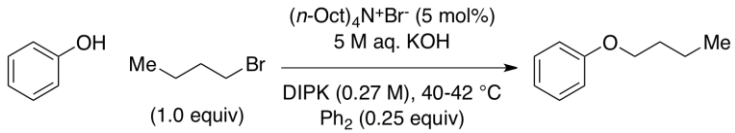

Time (m)	Time (s)	Ph_2 (µmol)	Ph_2 Area	BuOPh Area	BuOPh (µmol)	BuOPh (mol)	BuOPh (mol/L)	% conversion
0	0	134	1.000	0.000	0.0	0.0000E+00	0.0000E+00	0.0
3	180	134	16771.848	0.000	0.0	0.0000E+00	0.0000E+00	0.0
6	360	134	15642.542	854.225	10.6	1.0579E-05	5.2895E-03	2.0
9	540	134	15784.934	1315.799	16.1	1.6148E-05	8.0742E-03	3.0
12	720	134	16208.047	1768.376	21.1	2.1136E-05	1.0568E-02	4.0
15	900	134	17197.801	2378.881	26.8	2.6797E-05	1.3398E-02	5.0
18	1080	134	17167.852	2925.375	33.0	3.3010E-05	1.6505E-02	6.2
21	1260	134	16638.600	3281.548	38.2	3.8207E-05	1.9104E-02	7.2
24	1440	134	17004.162	3975.561	45.3	4.5292E-05	2.2646E-02	8.5
27	1620	134	17108.459	4611.082	52.2	5.2213E-05	2.6106E-02	9.8
30	1800	134	17148.447	5292.197	59.8	5.9785E-05	2.9893E-02	11.3
					2.0263E+00	3.3772E-08	1.6886E-05	
					Rate (µmol/min)	**Rate (mol/s)**	**Rate (mol*L^{-1}*s^{-1})**	

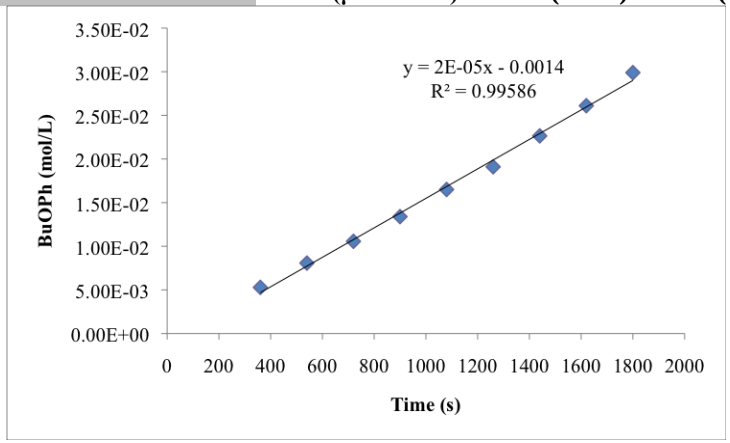

Tetra(*n*-octyl)ammonium Bromide, 1.0 equiv *n*-BuBr, Run #4:

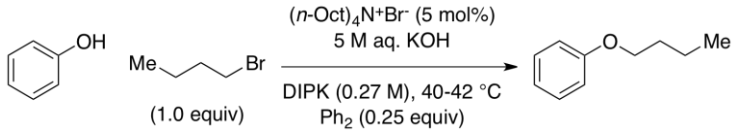

Time (m)	Time (s)	Ph_2 (µmol)	Ph_2 Area	BuOPh Area	BuOPh (µmol)	BuOPh (mol)	BuOPh (mol/L)	% conversion
0	0	134	1.000	0.000	0.0	0.0000E+00	0.0000E+00	0.0
3	180	134	17686.773	552.787	6.1	6.0547E-06	3.0273E-03	1.1
6	360	134	16997.621	953.017	10.9	1.0862E-05	5.4308E-03	2.0
9	540	134	17993.166	1539.975	16.6	1.6580E-05	8.2901E-03	3.1
12	720	134	18225.240	2035.200	21.6	2.1633E-05	1.0817E-02	4.1
15	900	134	18637.783	2617.011	27.2	2.7202E-05	1.3601E-02	5.1
18	1080	134	17680.865	2998.062	32.8	3.2849E-05	1.6424E-02	6.2
21	1260	134	17118.139	3396.530	38.4	3.8438E-05	1.9219E-02	7.2
24	1440	134	17789.273	4248.781	46.3	4.6269E-05	2.3134E-02	8.7
27	1620	134	17952.836	4882.893	52.7	5.2690E-05	2.6345E-02	9.9
30	1800	134	17763.801	5389.050	58.8	5.8770E-05	2.9385E-02	11.1
					1.9631E+00	3.2719E-08	1.6359E-05	
					Rate (µmol/min)	**Rate (mol/s)**	**Rate (mol*L^{-1}*s^{-1})**	

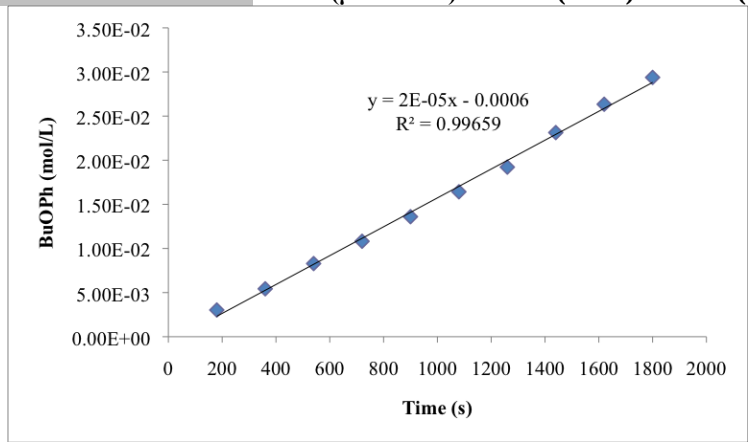

Tetra(*n*-octyl)ammonium Bromide, 2.0 equiv *n*-BuBr, Run #1:

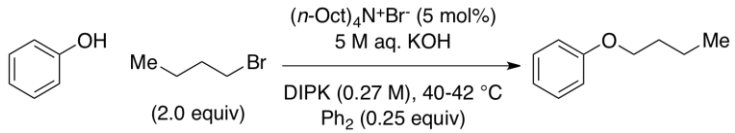

Time (m)	Time (s)	Ph_2 (µmol)	Ph_2 Area	BuOPh Area	BuOPh (µmol)	BuOPh (mol)	BuOPh (mol/L)	% conversion
0	0	134	1.000	0.000	0.0	0.0000E+00	0.0000E+00	0.0
6	360	134	17952.529	1995.944	21.5	2.1538E-05	1.0769E-02	4.1
12	720	134	19525.402	4627.030	45.9	4.5908E-05	2.2954E-02	8.6
18	1080	134	20353.260	7092.437	67.5	6.7506E-05	3.3753E-02	12.7
24	1440	134	20588.752	9416.557	88.6	8.8602E-05	4.4301E-02	16.7
30	1800	134	21019.037	12131.252	111.8	1.1181E-04	5.5904E-02	21.1
40	2400	134	18749.113	14681.182	151.7	1.5169E-04	7.5846E-02	28.6
50	3000	134	18488.639	17471.203	183.1	1.8306E-04	9.1532E-02	34.5
60	3600	134	18905.066	22014.412	225.6	2.2559E-04	1.1279E-01	42.5
90	5400	134	18245.902	30423.691	323.0	3.2302E-04	1.6151E-01	60.8
120	7200	134	18071.594	38418.195	411.8	4.1184E-04	2.0592E-01	77.6
					3.4576E+00	5.7626E-08	2.8813E-05	
					Rate (µmol/min)	**Rate (mol/s)**	**Rate (mol*L^{-1}*s^{-1})**	

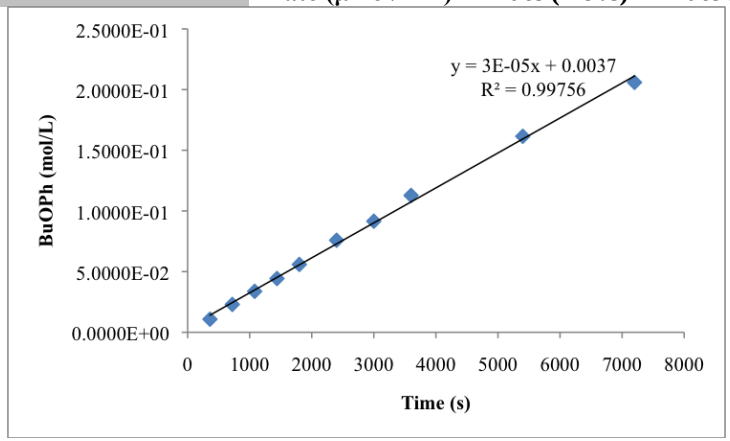

Tetra(*n*-octyl)ammonium Bromide, 2.0 equiv *n*-BuBr, Run #2:

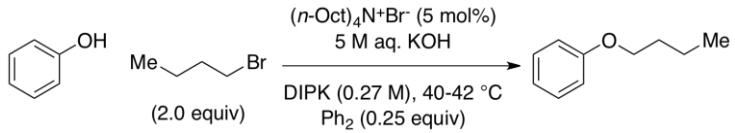

Time (m)	Time (s)	Ph_2 (µmol)	Ph_2 Area	BuOPh Area	BuOPh (µmol)	BuOPh (mol)	BuOPh (mol/L)	% conversion
0	0	134	1.000	0.000	0.0	0.0000E+00	0.0000E+00	0.0
2	120	134	16018.368	538.017	6.5	6.5067E-06	3.2533E-03	1.2
4	240	134	16025.078	1273.523	15.4	1.5395E-05	7.6977E-03	2.9
6	360	134	16056.689	1960.411	23.7	2.3652E-05	1.1826E-02	4.5
8	480	134	16423.863	2791.170	32.9	3.2923E-05	1.6461E-02	6.2
10	600	134	16839.432	3599.622	41.4	4.1411E-05	2.0705E-02	7.8
12	720	134	16633.984	4190.549	48.8	4.8804E-05	2.4402E-02	9.2
14	840	134	17036.426	5080.082	57.8	5.7766E-05	2.8883E-02	10.9
16	960	134	16065.076	5533.494	66.7	6.6727E-05	3.3363E-02	12.6
18	1080	134	15491.553	6214.993	77.7	7.7719E-05	3.8860E-02	14.6
20	1200	134	15408.543	6899.683	86.7	8.6746E-05	4.3373E-02	16.3
					4.4113E+00	7.3521E-08	3.6761E-05	
					Rate (µmol/min)	**Rate (mol/s)**	**Rate (mol*L^{-1}*s^{-1})**	

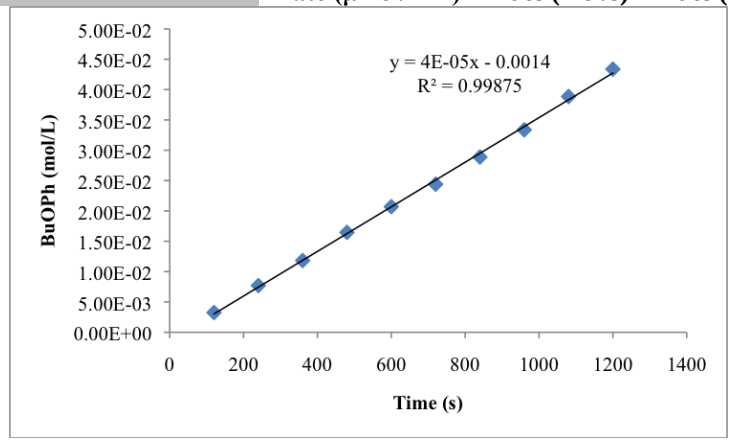

Tetraoctylammonium Bromide, 2.0 equiv *n*-BuBr, Run #3:

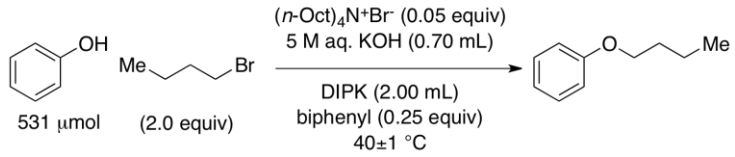

Time (m)	Time (s)	Ph_2 (μmol)	Ph_2 Area	BuOPh Area	BuOPh (μmol)	BuOPh (mol)	BuOPh (mol/L)	% conversion
0	0	134	1.000	0.000	0.0	0.0000E+00	0.0000E+00	0.0
2	120	134	17130.557	545.437	6.2	6.1682E-06	3.0841E-03	1.2
4	240	134	16898.799	1216.992	14.0	1.3951E-05	6.9757E-03	2.6
6	360	134	17377.707	2013.708	22.4	2.2448E-05	1.1224E-02	4.2
8	480	134	16894.469	2732.762	31.3	3.1336E-05	1.5668E-02	5.9
10	600	134	16916.439	3484.008	39.9	3.9898E-05	1.9949E-02	7.5
12	720	134	16232.164	4009.166	47.8	4.7848E-05	2.3924E-02	9.0
14	840	134	15767.396	4521.569	55.6	5.5554E-05	2.7777E-02	10.5
16	960	134	16357.605	5478.212	64.9	6.4879E-05	3.2439E-02	12.2
18	1080	134	16983.475	6559.248	74.8	7.4819E-05	3.7409E-02	14.1
20	1200	134	16729.783	7262.986	84.1	8.4102E-05	4.2051E-02	15.8
					4.3037E+00	7.1729E-08	3.5864E-05	
					Rate (μmol/min)	**Rate (mol/s)**	**Rate (mol*L^{-1}*s^{-1})**	

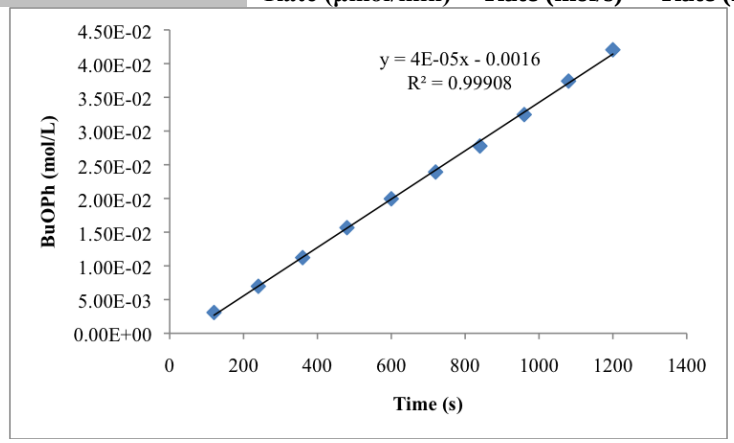

Tetraoctylammonium Bromide, 2.0 equiv *n*-BuBr, Run #4:

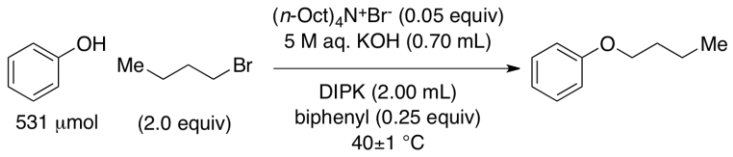

Time (m)	Time (s)	Ph_2 (μmol)	Ph_2 Area	BuOPh Area	BuOPh (μmol)	BuOPh (mol)	BuOPh (mol/L)	% conversion
0	0	134	1.000	0.000	0.0	0.0000E+00	0.0000E+00	0.0
2	120	134	16640.148	686.642	8.0	7.9939E-06	3.9969E-03	1.5
4	240	134	17836.547	1464.321	15.9	1.5904E-05	7.9520E-03	3.0
6	360	134	17108.541	2122.625	24.0	2.4035E-05	1.2017E-02	4.5
8	480	134	18009.631	3004.262	32.3	3.2316E-05	1.6158E-02	6.1
10	600	134	17066.000	3575.138	40.6	4.0583E-05	2.0291E-02	7.6
12	720	134	17069.410	4199.752	47.7	4.7664E-05	2.3832E-02	9.0
14	840	134	17854.418	5014.968	54.4	5.4413E-05	2.7207E-02	10.2
16	960	134	17694.578	5787.599	63.4	6.3364E-05	3.1682E-02	11.9
18	1080	134	17885.973	6664.022	72.2	7.2178E-05	3.6089E-02	13.6
20	1200	134	17215.961	7236.403	81.4	8.1428E-05	4.0714E-02	15.3
					4.0147E+00	6.6911E-08	3.3456E-05	
					Rate (μmol/min)	**Rate (mol/s)**	**Rate (mol*L^{-1}*s^{-1})**	

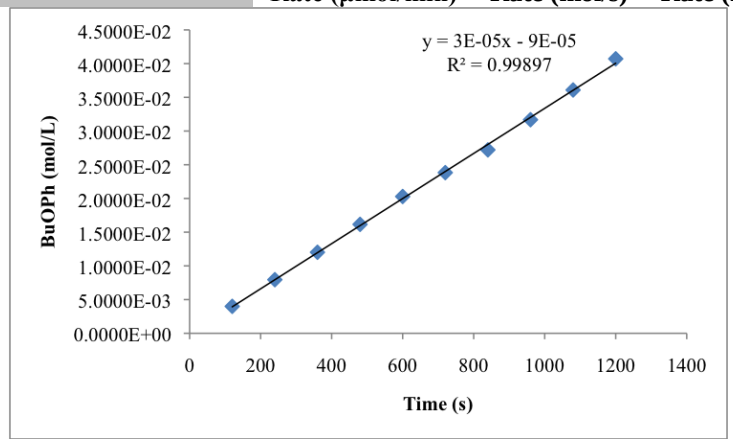

Tetra(*n*-octyl)ammonium Bromide, 5.0 equiv *n*-BuBr, Run #1:

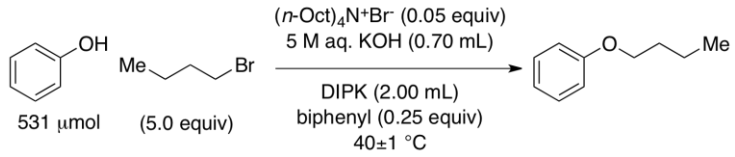

Time (m)	Time (s)	Ph_2 (μmol)	Ph_2 Area	BuOPh Area	BuOPh (μmol)	BuOPh (mol)	BuOPh (mol/L)	% conversion
0	0	134	1.000	0.000	0.0	0.0000E+00	0.0000E+00	0.0
3	180	134	16069.572	1761.991	21.2	2.1241E-05	1.0621E-02	4.0
6	360	134	16861.133	4032.769	46.3	4.6334E-05	2.3167E-02	8.7
9	540	134	17174.434	6524.311	73.6	7.3593E-05	3.6796E-02	13.9
12	720	134	18290.518	9677.358	102.5	1.0250E-04	5.1249E-02	19.3
15	900	134	16849.092	11526.954	132.5	1.3253E-04	6.6266E-02	25.0
18	1080	134	18223.445	14855.421	157.9	1.5792E-04	7.8960E-02	29.7
24	1440	134	17355.617	18942.686	211.4	2.1144E-04	1.0572E-01	39.8
30	1800	134	17294.885	23261.174	260.6	2.6055E-04	1.3028E-01	49.1
45	2700	134	17778.490	35737.348	389.4	3.8941E-04	1.9471E-01	73.3
60	3600	134	18941.723	48688.082	498.0	4.9795E-04	2.4898E-01	93.8
					8.4641E+00	1.4107E-07	7.0534E-05	
					Rate (μmol/min)	**Rate (mol/s)**	**Rate (mol*L^{-1}*s^{-1})**	

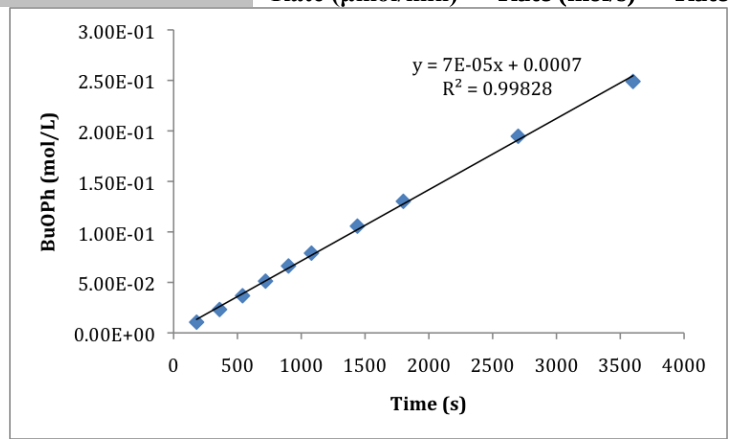

Tetra(*n*-octyl)ammonium Bromide, 5.0 equiv *n*-BuBr, Run #2:

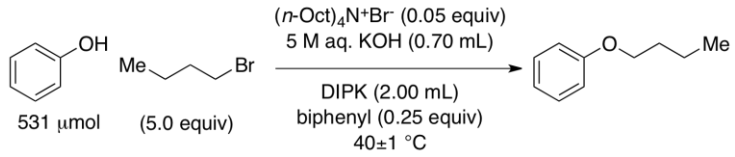

Time (m)	Time (s)	Ph_2 (μmol)	Ph_2 Area	BuOPh Area	BuOPh (μmol)	BuOPh (mol)	BuOPh (mol/L)	% conversion
0	0	134	1.000	0.000	0.0	0.0000E+00	0.0000E+00	0.0
1	60	134	19052.391	0.000	0.0	0.0000E+00	0.0000E+00	0.0
2	120	134	16425.687	1048.422	12.4	1.2365E-05	6.1825E-03	2.3
3	180	134	15873.785	1734.909	21.2	2.1173E-05	1.0586E-02	4.0
4	240	134	15657.118	2694.641	33.3	3.3340E-05	1.6670E-02	6.3
5	300	134	16773.846	3769.521	43.5	4.3535E-05	2.1767E-02	8.2
6	360	134	16375.703	4705.607	55.7	5.5667E-05	2.7834E-02	10.5
7	420	134	17221.859	5972.263	67.2	6.7180E-05	3.3590E-02	12.7
8	480	134	16932.920	6899.025	78.9	7.8929E-05	3.9465E-02	14.9
9	540	134	17127.088	8095.677	91.6	9.1570E-05	4.5785E-02	17.2
10	600	134	16380.119	8568.793	101.3	1.0134E-04	5.0671E-02	19.1
					1.1365E+01	1.8942E-07	9.4711E-05	
					Rate (μmol/min)	**Rate (mol/s)**	**Rate (mol*L^{-1}*s^{-1})**	

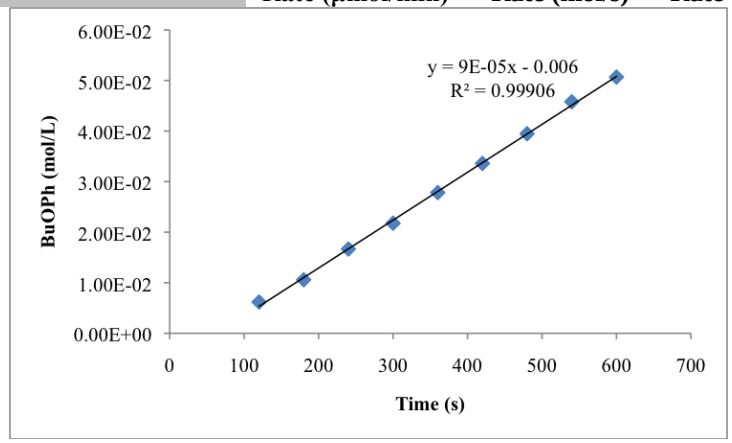

Tetra(*n*-octyl)ammonium Bromide, 5.0 equiv *n*-BuBr, Run #3:

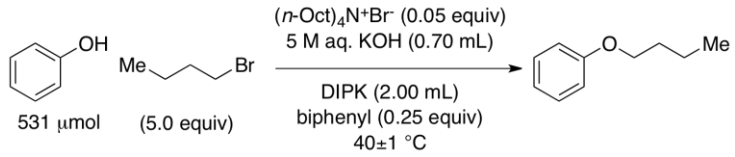

Time (m)	Time (s)	Ph_2 (μmol)	Ph_2 Area	BuOPh Area	BuOPh (μmol)	BuOPh (mol)	BuOPh (mol/L)	% conversion
0	0	134	1.000	0.000	0.0	0.0000E+00	0.0000E+00	0.0
1	60	134	16907.453	0.000	0.0	0.0000E+00	0.0000E+00	0.0
2	120	134	18816.670	1285.343	13.2	1.3233E-05	6.6165E-03	2.5
3	180	134	18771.627	2202.591	22.7	2.2731E-05	1.1365E-02	4.3
4	240	134	19254.100	3303.848	33.2	3.3241E-05	1.6621E-02	6.3
5	300	134	19078.936	4476.478	45.5	4.5453E-05	2.2727E-02	8.6
6	360	134	19456.859	5816.218	57.9	5.7910E-05	2.8955E-02	10.9
7	420	134	19061.941	6968.767	70.8	7.0823E-05	3.5411E-02	13.3
8	480	134	18873.918	8127.806	83.4	8.3425E-05	4.1712E-02	15.7
9	540	134	18926.285	9414.243	96.4	9.6361E-05	4.8181E-02	18.1
10	600	134	19671.955	11117.216	109.5	1.0948E-04	5.4740E-02	20.6
					1.2194E+01	2.0323E-07	1.0161E-04	
					Rate (μmol/min)	**Rate (mol/s)**	**Rate (mol*L^{-1}*s^{-1})**	

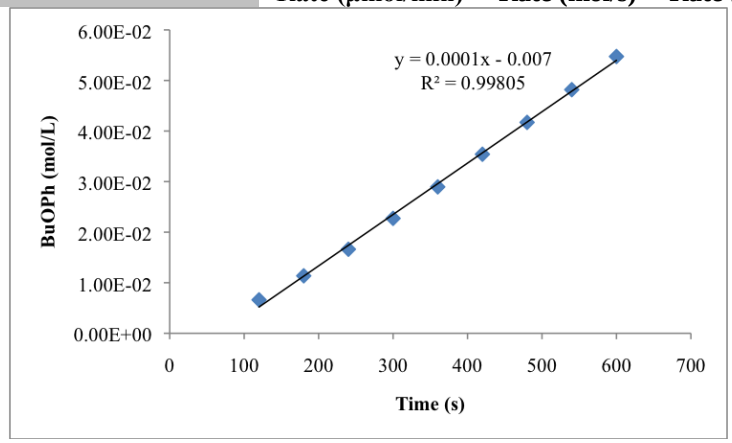

Tetra(*n*-octyl)ammonium Bromide, 5.0 equiv *n*-BuBr, Run #4:

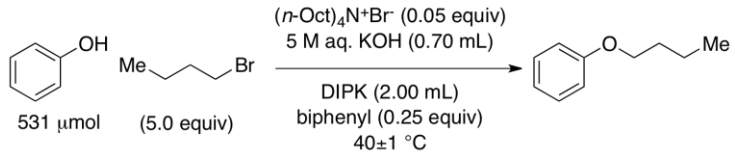

Time (m)	Time (s)	Ph_2 (μmol)	Ph_2 Area	BuOPh Area	BuOPh (μmol)	BuOPh (mol)	BuOPh (mol/L)	% conversion
0	0	134	1.000	0.000	0.0	0.0000E+00	0.0000E+00	0.0
1	60	134	19973.082	833.979	8.1	8.0890E-06	4.0445E-03	1.5
2	120	134	19988.510	1781.591	17.3	1.7267E-05	8.6334E-03	3.3
3	180	134	20049.318	2962.491	28.6	2.8625E-05	1.4312E-02	5.4
4	240	134	20218.346	4252.919	40.7	4.0750E-05	2.0375E-02	7.7
5	300	134	18562.455	5153.062	53.8	5.3779E-05	2.6890E-02	10.1
6	360	134	19844.527	6806.364	66.4	6.6444E-05	3.3222E-02	12.5
7	420	134	19725.836	8177.560	80.3	8.0310E-05	4.0155E-02	15.1
8	480	134	20691.977	9982.395	93.5	9.3458E-05	4.6729E-02	17.6
9	540	134	19931.193	10729.437	104.3	1.0429E-04	5.2143E-02	19.6
10	600	134	19367.439	11566.911	115.7	1.1570E-04	5.7849E-02	21.8
					1.2322E+01	2.0537E-07	1.0268E-04	
					Rate (μmol/min)	**Rate (mol/s)**	**Rate (mol*L^{-1}*s^{-1})**	

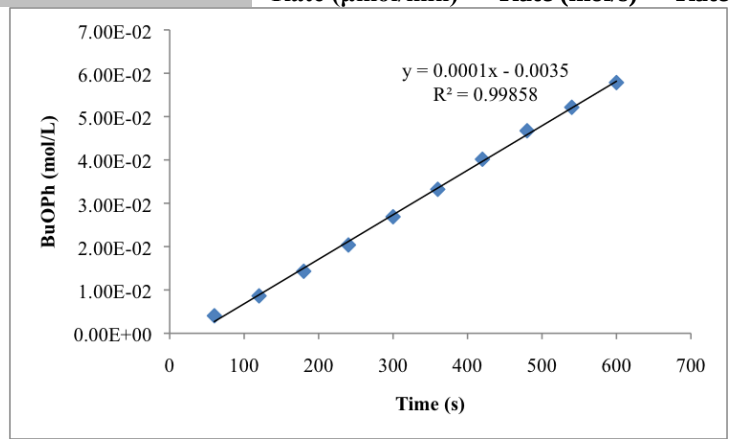

Tetra(*n*-propyl)ammonium Bromide, 0.5 equiv *n*-BuBr, Run #1:

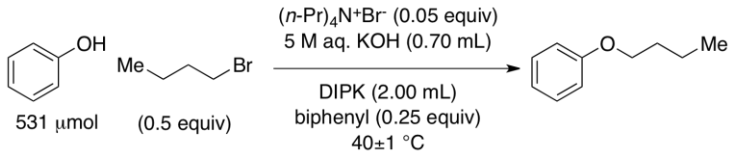

Time (m)	Time (s)	Ph_2 (μmol)	Ph_2 Area	BuOPh Area	BuOPh (μmol)	BuOPh (mol)	BuOPh (mol/L)	% conversion
0	0	134	1.000	0.000	0.0	0.0000E+00	0.0000E+00	0.0
15	900	134	16798.062	733.198	8.5	8.4556E-06	4.2278E-03	1.6
30	1800	134	15475.824	0.000	0.0	0.0000E+00	0.0000E+00	0.0
45	2700	134	14746.916	571.090	7.5	7.5022E-06	3.7511E-03	1.4
60	3600	134	15361.423	830.817	10.5	1.0477E-05	5.2387E-03	2.0
80	4800	134	15842.782	1151.492	14.1	1.4080E-05	7.0402E-03	2.7
100	6000	134	17175.203	1668.922	18.8	1.8824E-05	9.4121E-03	3.5
120	7200	134	16127.535	1857.101	22.3	2.2307E-05	1.1154E-02	4.2
150	9000	134	19236.480	2819.733	28.4	2.8397E-05	1.4198E-02	5.3
180	10800	134	16839.283	3048.878	35.1	3.5075E-05	1.7538E-02	6.6
240	14400	134	18071.572	4520.152	48.5	4.8455E-05	2.4228E-02	9.1
					2.0075E-01	3.3458E-09	1.6729E-06	
					Rate (μmol/min)	**Rate (mol/s)**	**Rate (mol*L^{-1}*s^{-1})**	

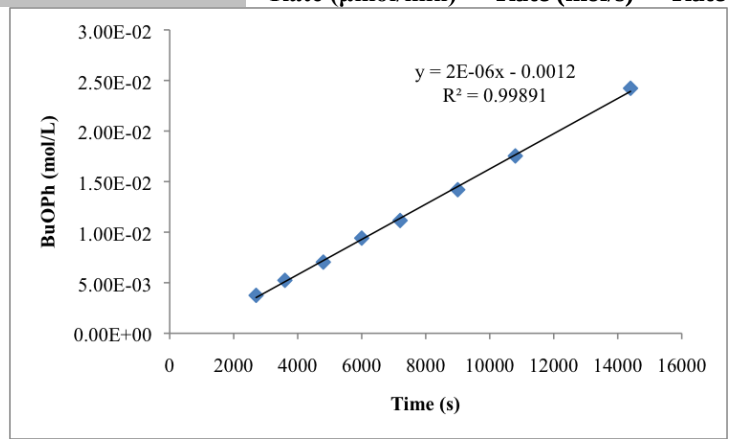

Tetra(*n*-propyl)ammonium Bromide, 0.5 equiv *n*-BuBr, Run #2:

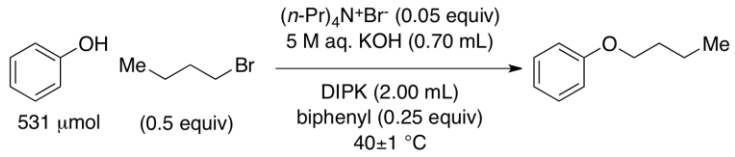

Time (m)	Time (s)	Ph_2 (μmol)	Ph_2 Area	BuOPh Area	BuOPh (μmol)	BuOPh (mol)	BuOPh (mol/L)	% conversion
0	0	134	1.000	0.000	0.0	0.0000E+00	0.0000E+00	0.0
20	1200	134	16500.160	0.000	0.0	0.0000E+00	0.0000E+00	0.0
40	2400	134	17109.801	600.768	6.8	6.8021E-06	3.4011E-03	1.3
60	3600	134	17899.414	1084.273	11.7	1.1735E-05	5.8675E-03	2.2
80	4800	134	19115.289	1655.289	16.8	1.6776E-05	8.3878E-03	3.2
100	6000	134	17257.186	1863.764	20.9	2.0922E-05	1.0461E-02	3.9
120	7200	134	17825.979	2395.327	26.0	2.6031E-05	1.3016E-02	4.9
150	9000	134	18186.732	3019.833	32.2	3.2167E-05	1.6084E-02	6.1
180	10800	134	18705.395	3842.461	39.8	3.9795E-05	1.9897E-02	7.5
210	12600	134	18405.398	4394.477	46.3	4.6254E-05	2.3127E-02	8.7
240	14400	134	18014.529	5034.563	54.1	5.4140E-05	2.7070E-02	10.2
					2.3346E-01	3.8910E-09	1.9455E-06	
					Rate (μmol/min)	**Rate (mol/s)**	**Rate (mol*L^{-1}*s^{-1})**	

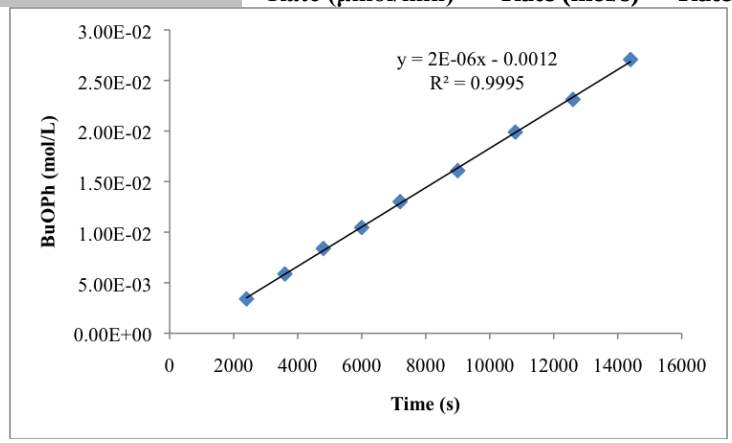

Tetra(*n*-propyl)ammonium Bromide, 0.5 equiv *n*-BuBr, Run #3:

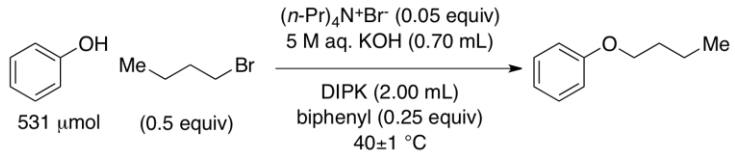

Time (m)	Time (s)	Ph_2 (μmol)	Ph_2 Area	BuOPh Area	BuOPh (μmol)	BuOPh (mol)	BuOPh (mol/L)	% conversion
0	0	134	1.000	0.000	0.0	0.0000E+00	0.0000E+00	0.0
20	1200	134	15754.905	0.000	0.0	0.0000E+00	0.0000E+00	0.0
40	2400	134	16010.921	622.560	7.5	7.5327E-06	3.7663E-03	1.4
60	3600	134	16364.426	956.651	11.3	1.1325E-05	5.6625E-03	2.1
80	4800	134	16565.021	1337.715	15.6	1.5644E-05	7.8221E-03	2.9
100	6000	134	16896.285	1821.663	20.9	2.0886E-05	1.0443E-02	3.9
120	7200	134	19252.555	2384.033	24.0	2.3989E-05	1.1994E-02	4.5
150	9000	134	17808.480	2859.216	31.1	3.1103E-05	1.5552E-02	5.9
180	10800	134	16040.091	3130.693	37.8	3.7811E-05	1.8905E-02	7.1
210	12600	134	17574.354	3971.035	43.8	4.3773E-05	2.1887E-02	8.2
240	14400	134	16406.410	4199.645	49.6	4.9589E-05	2.4794E-02	9.3
					2.1329E-01	3.5548E-09	1.7774E-06	
					Rate (μmol/min)	**Rate (mol/s)**	**Rate (mol*L^{-1}*s^{-1})**	

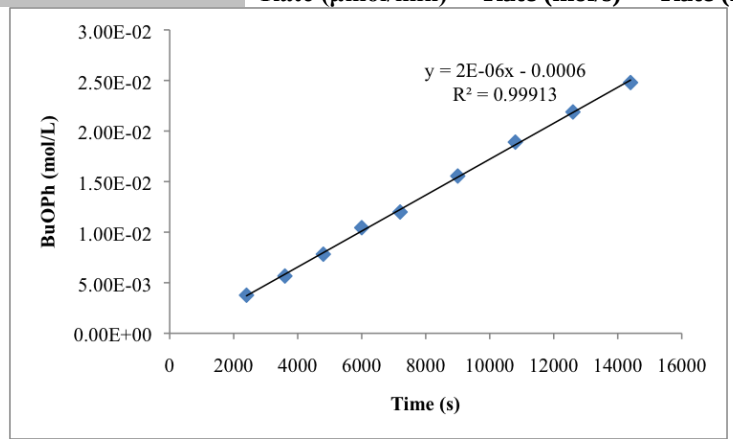

Tetra(*n*-propyl)ammonium Bromide, 0.5 equiv *n*-BuBr, Run #4:

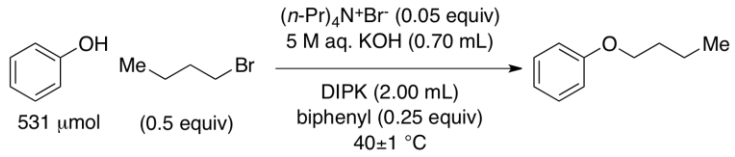

Time (m)	Time (s)	Ph_2 (μmol)	Ph_2 Area	BuOPh Area	BuOPh (μmol)	BuOPh (mol)	BuOPh (mol/L)	% conversion
0	0	134	1.000	0.000	0.0	0.0000E+00	0.0000E+00	0.0
20	1200	134	16950.113	0.000	0.0	0.0000E+00	0.0000E+00	0.0
40	2400	134	16919.953	0.000	0.0	0.0000E+00	0.0000E+00	0.0
60	3600	134	17873.277	835.702	9.1	9.0580E-06	4.5290E-03	1.7
80	4800	134	17961.813	1205.444	13.0	1.3001E-05	6.5005E-03	2.4
100	6000	134	18069.744	1549.028	16.6	1.6607E-05	8.3035E-03	3.1
120	7200	134	18016.549	1865.214	20.1	2.0056E-05	1.0028E-02	3.8
150	9000	134	18083.006	2351.272	25.2	2.5189E-05	1.2595E-02	4.7
180	10800	134	18436.986	3015.612	31.7	3.1686E-05	1.5843E-02	6.0
210	12600	134	18805.910	3601.679	37.1	3.7102E-05	1.8551E-02	7.0
240	14400	134	17250.613	3798.996	42.7	4.2663E-05	2.1331E-02	8.0
					1.8649E-01	3.1081E-09	1.5541E-06	
					Rate (μmol/min)	**Rate (mol/s)**	**Rate (mol*L^{-1}*s^{-1})**	

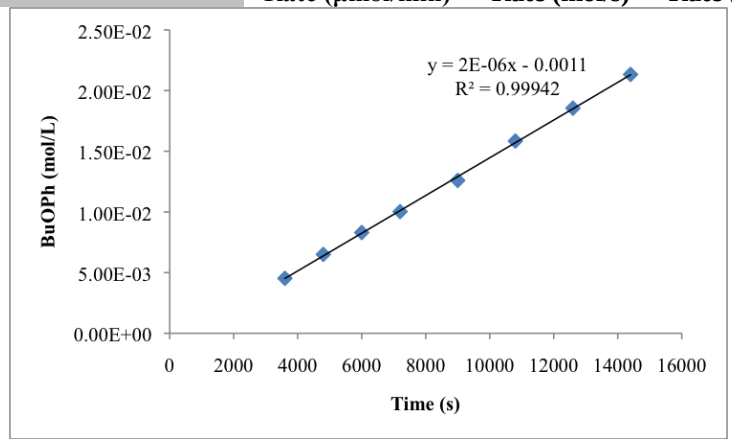

Tetra(*n*-propyl)ammonium Bromide, 1.0 equiv *n*-BuBr, Run #1:

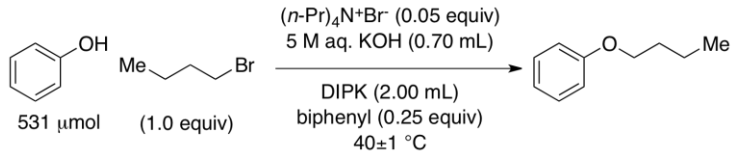

Time (m)	Time (s)	Ph_2 (μmol)	Ph_2 Area	BuOPh Area	BuOPh (μmol)	BuOPh (mol)	BuOPh (mol/L)	% conversion
0	0	134	1.000	0.000	0.0	0.0000E+00	0.0000E+00	0.0
15	900	134	16513.433	0.000	0.0	0.0000E+00	0.0000E+00	0.0
30	1800	134	15948.785	756.941	9.2	9.1943E-06	4.5971E-03	1.7
45	2700	134	16978.656	1275.086	14.5	1.4549E-05	7.2743E-03	2.7
60	3600	134	16223.399	1722.630	20.6	2.0570E-05	1.0285E-02	3.9
80	4800	134	16886.346	2601.729	29.8	2.9848E-05	1.4924E-02	5.6
100	6000	134	18930.512	3570.906	36.5	3.6543E-05	1.8271E-02	6.9
120	7200	134	17302.539	3960.227	44.3	4.4340E-05	2.2170E-02	8.4
150	9000	134	18681.889	5450.530	56.5	5.6520E-05	2.8260E-02	10.6
180	10800	134	16800.131	5850.432	67.5	6.7462E-05	3.3731E-02	12.7
240	14400	134	19824.598	9144.060	89.4	8.9355E-05	4.4677E-02	16.8
					3.8452E-01	6.4087E-09	3.2044E-06	
					Rate (μmol/min)	**Rate (mol/s)**	**Rate (mol*L^{-1}*s^{-1})**	

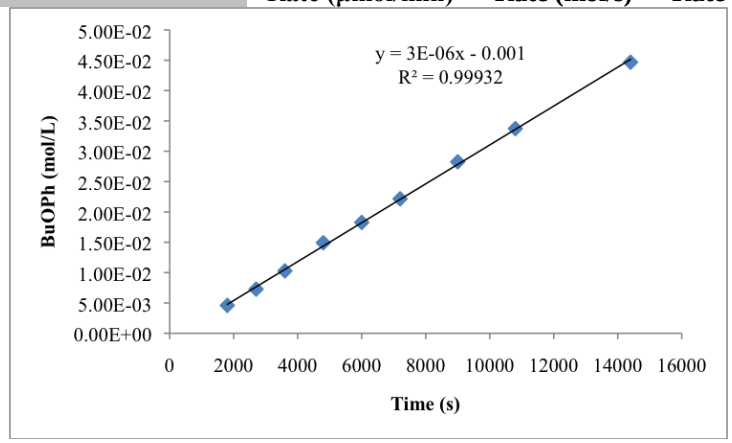

Tetra(*n*-propyl)ammonium Bromide, 1.0 equiv *n*-BuBr, Run #2:

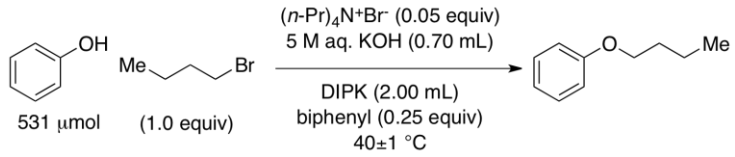

Time (m)	Time (s)	Ph_2 (μmol)	Ph_2 Area	BuOPh Area	BuOPh (μmol)	BuOPh (mol)	BuOPh (mol/L)	% conversion
0	0	134	1.000	0.000	0.0	0.0000E+00	0.0000E+00	0.0
15	900	134	16623.082	0.000	0.0	0.0000E+00	0.0000E+00	0.0
30	1800	134	18253.627	892.452	9.5	9.4715E-06	4.7357E-03	1.8
45	2700	134	17135.385	1291.727	14.6	1.4604E-05	7.3018E-03	2.8
60	3600	134	18144.668	1961.250	20.9	2.0940E-05	1.0470E-02	3.9
75	4500	134	17790.262	2412.805	26.3	2.6274E-05	1.3137E-02	4.9
90	5400	134	18218.141	3094.333	32.9	3.2904E-05	1.6452E-02	6.2
105	6300	134	17159.150	3416.685	38.6	3.8574E-05	1.9287E-02	7.3
120	7200	134	17497.926	4140.083	45.8	4.5836E-05	2.2918E-02	8.6
135	8100	134	17707.867	4727.399	51.7	5.1718E-05	2.5859E-02	9.7
150	9000	134	18706.414	5647.995	58.5	5.8491E-05	2.9245E-02	11.0
					4.1057E-01	6.8428E-09	3.4214E-06	
					Rate (μmol/min)	**Rate (mol/s)**	**Rate (mol*L^{-1}*s^{-1})**	

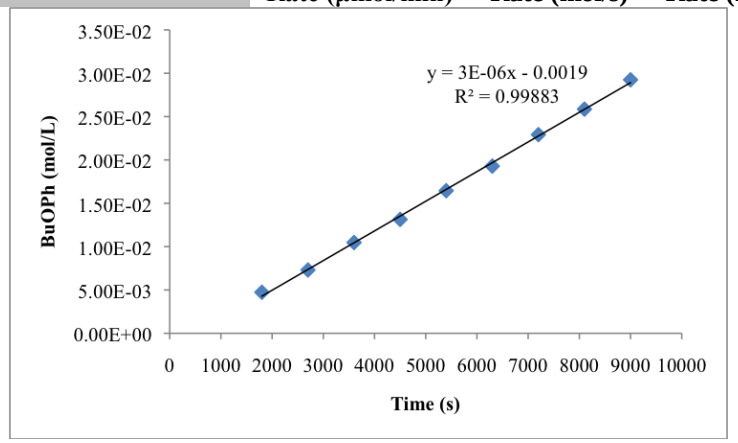

Tetra(*n*-propyl)ammonium Bromide, 1.0 equiv *n*-BuBr, Run #3:

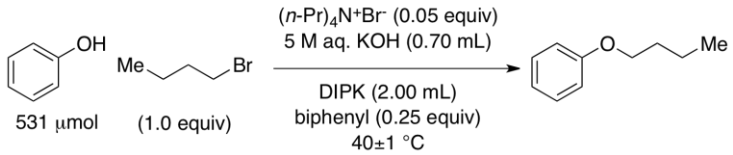

Time (m)	Time (s)	Ph_2 (μmol)	Ph_2 Area	BuOPh Area	BuOPh (μmol)	BuOPh (mol)	BuOPh (mol/L)	% conversion
0	0	134	1.000	0.000	0.0	0.0000E+00	0.0000E+00	0.0
15	900	134	15683.202	0.000	0.0	0.0000E+00	0.0000E+00	0.0
30	1800	134	15954.385	832.368	10.1	1.0107E-05	5.0535E-03	1.9
45	2700	134	16756.893	1385.260	16.0	1.6015E-05	8.0074E-03	3.0
60	3600	134	17117.105	1954.844	22.1	2.2124E-05	1.1062E-02	4.2
75	4500	134	17143.844	2488.902	28.1	2.8124E-05	1.4062E-02	5.3
90	5400	134	18846.715	3328.922	34.2	3.4218E-05	1.7109E-02	6.4
105	6300	134	16086.047	3374.490	40.6	4.0639E-05	2.0319E-02	7.7
120	7200	134	16908.387	4090.666	46.9	4.6868E-05	2.3434E-02	8.8
135	8100	134	16775.576	4558.702	52.6	5.2644E-05	2.6322E-02	9.9
150	9000	134	17872.703	5641.509	61.1	6.1149E-05	3.0574E-02	11.5
					4.1784E-01	6.9640E-09	3.4820E-06	
					Rate (μmol/min)	**Rate (mol/s)**	**Rate (mol*L^{-1}*s^{-1})**	

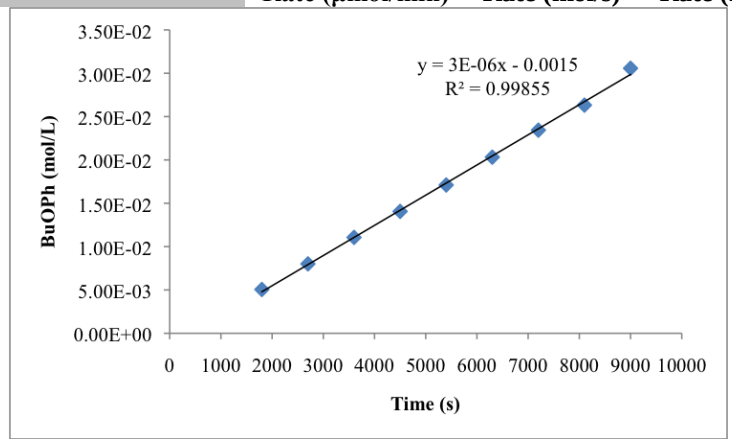

Tetrapropylammonium Bromide, 1.0 equiv *n*-BuBr, Run #4:

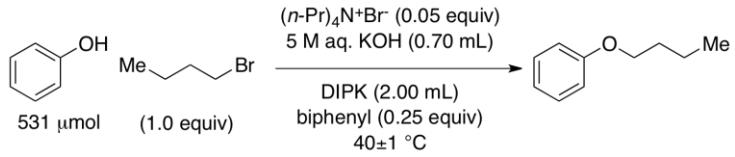

Time (m)	Time (s)	Ph_2 (μmol)	Ph_2 Area	BuOPh Area	BuOPh (μmol)	BuOPh (mol)	BuOPh (mol/L)	% conversion
0	0	134	1.000	0.000	0.0	0.0000E+00	0.0000E+00	0.0
15	900	134	17511.617	0.000	0.0	0.0000E+00	0.0000E+00	0.0
30	1800	134	18703.592	908.722	9.4	9.4122E-06	4.7061E-03	1.8
45	2700	134	18157.174	1447.560	15.4	1.5444E-05	7.7222E-03	2.9
60	3600	134	18538.637	2049.878	21.4	2.1421E-05	1.0710E-02	4.0
75	4500	134	17972.441	2450.591	26.4	2.6415E-05	1.3207E-02	5.0
90	5400	134	17487.186	2989.438	33.1	3.3117E-05	1.6559E-02	6.2
105	6300	134	18711.449	3713.657	38.4	3.8448E-05	1.9224E-02	7.2
120	7200	134	17586.398	4077.940	44.9	4.4921E-05	2.2460E-02	8.5
135	8100	134	18702.449	4917.552	50.9	5.0937E-05	2.5469E-02	9.6
150	9000	134	18473.937	5468.652	57.3	5.7346E-05	2.8673E-02	10.8
					3.9694E-01	6.6157E-09	3.3078E-06	
					Rate (μmol/min)	**Rate (mol/s)**	**Rate (mol*L^{-1}*s^{-1})**	

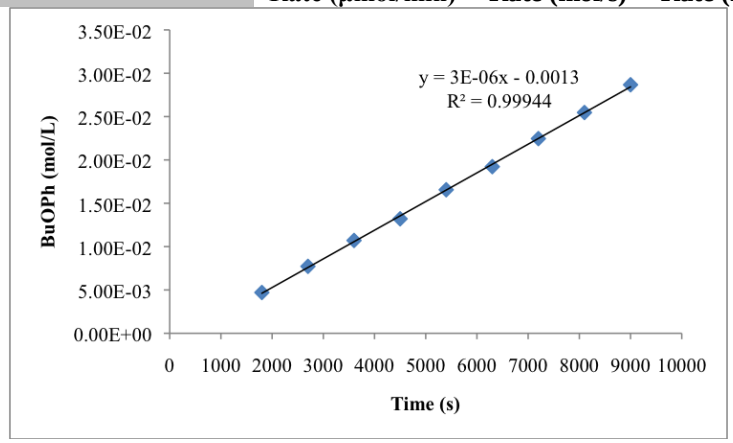

Tetra(*n*-propyl)ammonium Bromide, 2.0 equiv *n*-BuBr, Run #1:

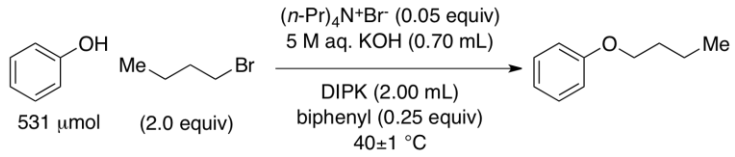

Time (m)	Time (s)	Ph_2 (μmol)	Ph_2 Area	BuOPh Area	BuOPh (μmol)	BuOPh (mol)	BuOPh (mol/L)	% conversion
0	0	134	1.000	0.000	0.0	0.0000E+00	0.0000E+00	0.0
15	900	134	14724.687	0.000	0.0	0.0000E+00	0.0000E+00	0.0
30	1800	134	17326.078	1467.968	16.4	1.6413E-05	8.2067E-03	3.1
45	2700	134	17504.305	2511.926	27.8	2.7800E-05	1.3900E-02	5.2
60	3600	134	17234.621	3286.974	36.9	3.6947E-05	1.8473E-02	7.0
80	4800	134	17708.986	4715.360	51.6	5.1583E-05	2.5791E-02	9.7
100	6000	134	18697.771	6266.645	64.9	6.4927E-05	3.2464E-02	12.2
120	7200	134	17746.354	7270.846	79.4	7.9370E-05	3.9685E-02	14.9
150	9000	134	18229.225	9466.163	100.6	1.0060E-04	5.0299E-02	18.9
180	10800	134	18697.238	11818.046	122.4	1.2245E-04	6.1224E-02	23.1
240	14400	134	18291.600	15789.863	167.2	1.6723E-04	8.3614E-02	31.5
					7.1416E-01	1.1903E-08	5.9663E-06	
					Rate (μmol/min)	**Rate (mol/s)**	**Rate (mol*L^{-1}*s^{-1})**	

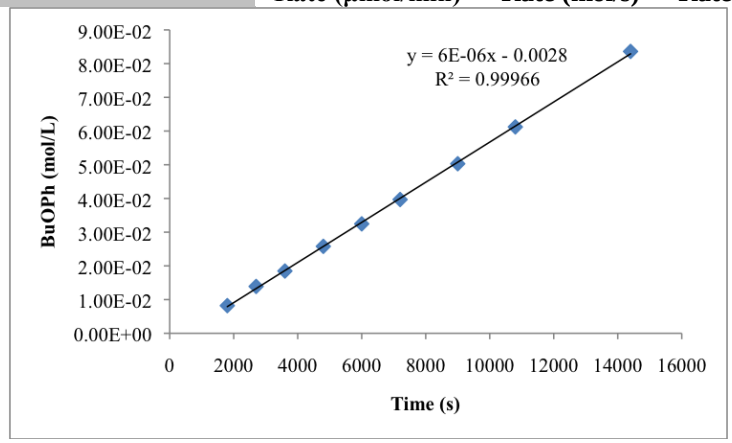

Tetra(*n*-propyl)ammonium Bromide, 2.0 equiv *n*-BuBr, Run #2:

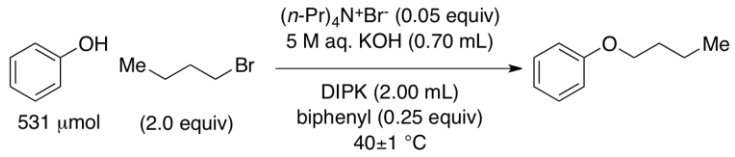

Time (m)	Time (s)	Ph_2 (μmol)	Ph_2 Area	BuOPh Area	BuOPh (μmol)	BuOPh (mol)	BuOPh (mol/L)	% conversion
0	0	134	1.000	0.000	0.0	0.0000E+00	0.0000E+00	0.0
9	540	134	17424.557	0.000	0.0	0.0000E+00	0.0000E+00	0.0
18	1080	134	16655.459	911.100	10.6	1.0597E-05	5.2986E-03	2.0
27	1620	134	17071.463	1507.068	17.1	1.7102E-05	8.5510E-03	3.2
36	2160	134	16165.388	2020.450	24.2	2.4213E-05	1.2106E-02	4.6
45	2700	134	15827.579	2689.815	32.9	3.2922E-05	1.6461E-02	6.2
54	3240	134	16247.039	3246.892	38.7	3.8715E-05	1.9357E-02	7.3
63	3780	134	16360.738	3970.433	47.0	4.7013E-05	2.3506E-02	8.9
72	4320	134	15542.499	4375.651	54.5	5.4539E-05	2.7269E-02	10.3
81	4860	134	16077.034	5135.301	61.9	6.1879E-05	3.0939E-02	11.7
90	5400	134	15409.287	5526.438	69.5	6.9478E-05	3.4739E-02	13.1
					8.2333E-01	1.3722E-08	6.8610E-06	
					Rate (μmol/min)	**Rate (mol/s)**	**Rate (mol*L^{-1}*s^{-1})**	

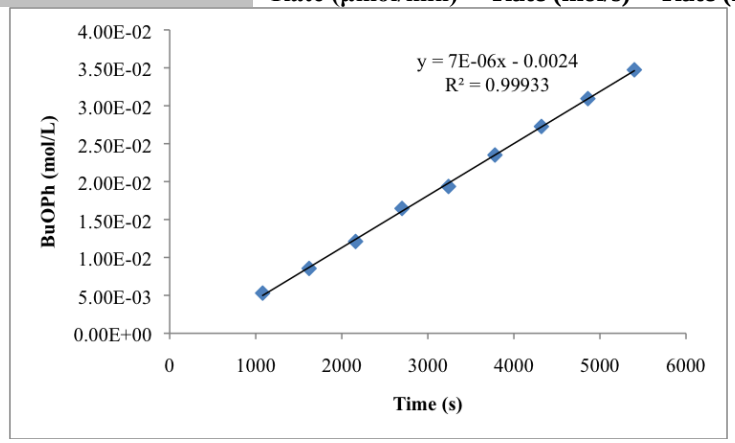

Tetra(*n*-propyl)ammonium Bromide, 2.0 equiv *n*-BuBr, Run #3:

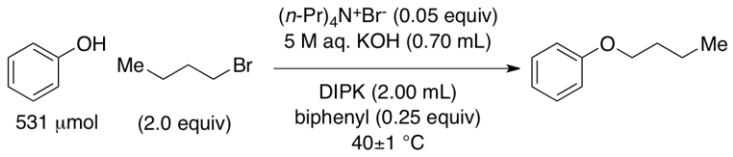

Time (m)	Time (s)	Ph_2 (μmol)	Ph_2 Area	BuOPh Area	BuOPh (μmol)	BuOPh (mol)	BuOPh (mol/L)	% conversion
0	0	134	1.000	0.000	0.0	0.0000E+00	0.0000E+00	0.0
9	540	134	16058.112	0.000	0.0	0.0000E+00	0.0000E+00	0.0
18	1080	134	15504.197	799.676	10.0	9.9919E-06	4.9959E-03	1.9
27	1620	134	16147.185	1427.604	17.1	1.7127E-05	8.5637E-03	3.2
36	2160	134	18026.119	2143.969	23.0	2.3041E-05	1.1520E-02	4.3
45	2700	134	17074.877	2630.333	29.8	2.9843E-05	1.4921E-02	5.6
54	3240	134	17072.818	3088.026	35.0	3.5040E-05	1.7520E-02	6.6
63	3780	134	17386.803	3763.942	41.9	4.1938E-05	2.0969E-02	7.9
72	4320	134	17572.904	4562.116	50.3	5.0293E-05	2.5146E-02	9.5
81	4860	134	18258.828	5299.599	56.2	5.6228E-05	2.8114E-02	10.6
90	5400	134	17120.400	5635.513	63.8	6.3768E-05	3.1884E-02	12.0
					7.3890E-01	1.2315E-08	6.1575E-06	
					Rate (μmol/min)	**Rate (mol/s)**	**Rate (mol*L^{-1}*s^{-1})**	

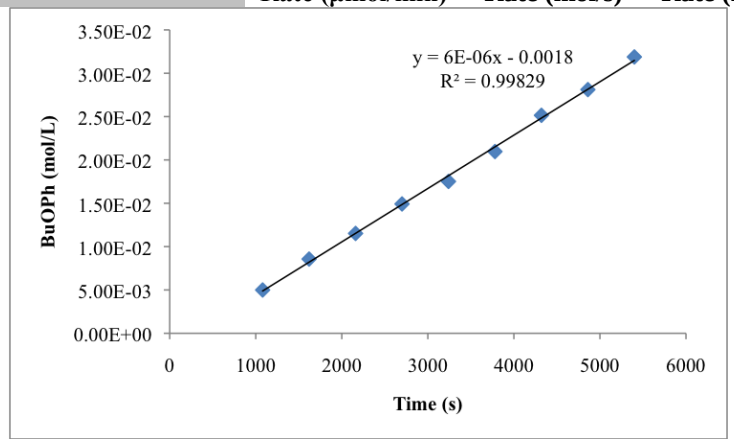

Tetra(*n*-propyl)ammonium Bromide, 2.0 equiv *n*-BuBr, Run #4:

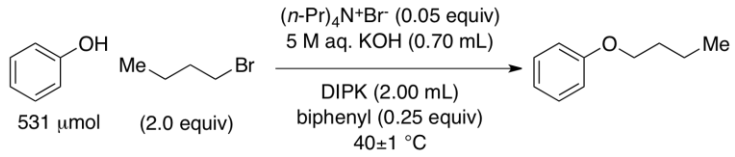

Time (m)	Time (s)	Ph_2 (μmol)	Ph_2 Area	BuOPh Area	BuOPh (μmol)	BuOPh (mol)	BuOPh (mol/L)	% conversion
0	0	134	1.000	0.000	0.0	0.0000E+00	0.0000E+00	0.0
9	540	134	17073.229	0.000	0.0	0.0000E+00	0.0000E+00	0.0
18	1080	134	17758.145	867.811	9.5	9.4670E-06	4.7335E-03	1.8
27	1620	134	16981.619	1372.736	15.7	1.5660E-05	7.8300E-03	2.9
36	2160	134	16950.623	1960.971	22.4	2.2411E-05	1.1206E-02	4.2
45	2700	134	16756.910	2502.348	28.9	2.8929E-05	1.4465E-02	5.4
54	3240	134	17075.320	2994.901	34.0	3.3978E-05	1.6989E-02	6.4
63	3780	134	17581.895	3796.974	41.8	4.1836E-05	2.0918E-02	7.9
72	4320	134	16955.578	4255.677	48.6	4.8623E-05	2.4311E-02	9.2
81	4860	134	16682.818	4654.520	54.0	5.4049E-05	2.7025E-02	10.2
90	5400	134	17084.748	5395.973	61.2	6.1185E-05	3.0592E-02	11.5
					7.1735E-01	1.1956E-08	5.9779E-06	
					Rate (μmol/min)	**Rate (mol/s)**	**Rate (mol*L^{-1}*s^{-1})**	

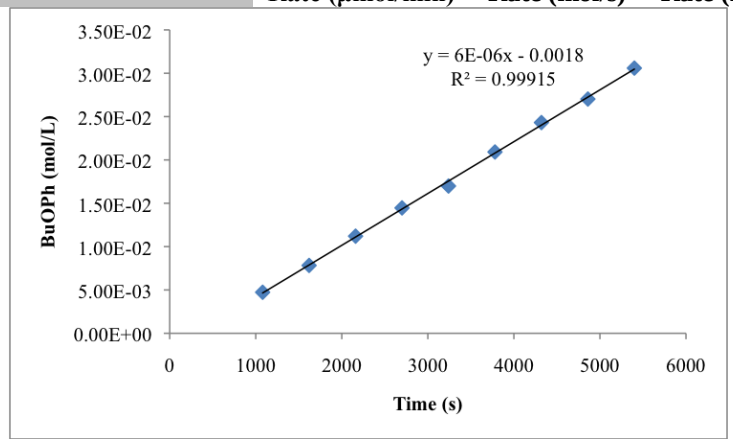

Tetra(*n*-propyl)ammonium Bromide, 5.0 equiv *n*-BuBr, Run #1:

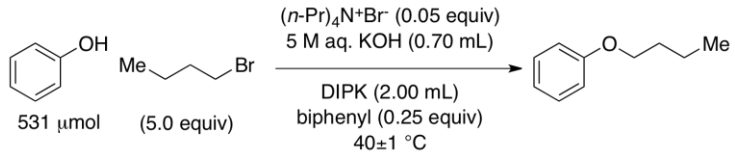

Time (m)	Time (s)	Ph_2 (μmol)	Ph_2 Area	BuOPh Area	BuOPh (μmol)	BuOPh (mol)	BuOPh (mol/L)	% conversion
0	0	134	1.000	0.000	0.0	0.0000E+00	0.0000E+00	0.0
5	300	134	17492.379	0.000	0.0	0.0000E+00	0.0000E+00	0.0
10	600	134	17697.727	549.971	6.0	6.0201E-06	3.0101E-04	1.1
15	900	134	17728.146	1498.214	16.4	1.6372E-05	8.1858E-04	3.1
20	1200	134	17359.793	2333.140	26.0	2.6036E-05	1.3018E-03	4.9
25	1500	134	16907.316	2889.614	33.1	3.3109E-05	1.6555E-03	6.2
30	1800	134	17782.063	4014.719	43.7	4.3738E-05	2.1869E-03	8.2
35	2100	134	17057.668	4780.375	54.3	5.4291E-05	2.7145E-03	10.2
40	2400	134	17839.533	5806.629	63.1	6.3056E-05	3.1528E-03	11.9
45	2700	134	18201.725	6796.105	72.3	7.2332E-05	3.6166E-03	13.6
50	3000	134	19295.496	8118.160	81.5	8.1505E-05	4.0753E-03	15.3
					1.8835E+00	3.1391E-08	1.5696E-06	
					Rate (μmol/min)	**Rate (mol/s)**	**Rate (mol*L^{-1}*s^{-1})**	

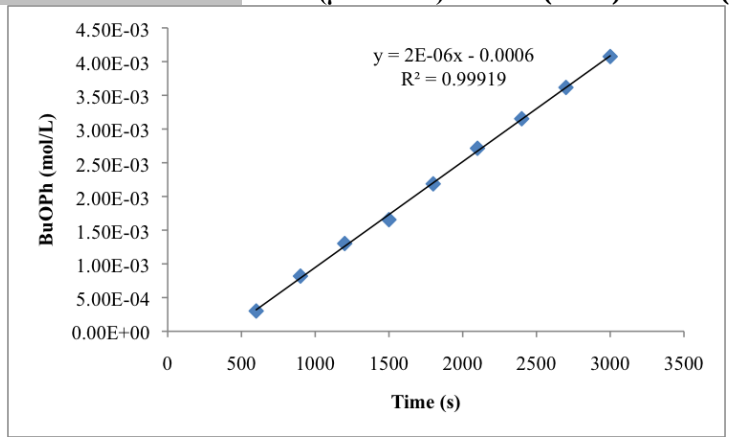

Tetra(*n*-propyl)ammonium Bromide, 5.0 equiv *n*-BuBr, Run #2:

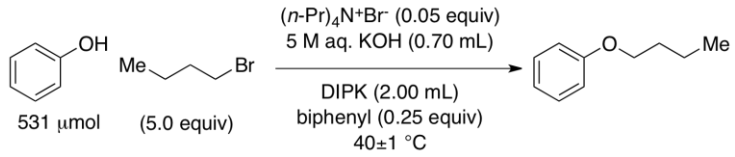

Time (m)	Time (s)	Ph_2 (μmol)	Ph_2 Area	BuOPh Area	BuOPh (μmol)	BuOPh (mol)	BuOPh (mol/L)	% conversion
0	0	134	1.000	0.000	0.0	0.0000E+00	0.0000E+00	0.0
4	240	134	23158.492	0.000	0.0	0.0000E+00	0.0000E+00	0.0
8	480	134	16364.111	803.072	9.5	9.5070E-06	4.7535E-03	1.8
12	720	134	18213.346	1387.367	14.8	1.4757E-05	7.3783E-03	2.8
16	960	134	16715.508	1820.842	21.1	2.1103E-05	1.0551E-02	4.0
20	1200	134	17144.531	2500.375	28.3	2.8253E-05	1.4126E-02	5.3
24	1440	134	16484.236	2941.171	34.6	3.4565E-05	1.7282E-02	6.5
28	1680	134	16734.025	3602.194	41.7	4.1701E-05	2.0851E-02	7.9
32	1920	134	16341.649	4035.906	47.8	4.7844E-05	2.3922E-02	9.0
36	2160	134	15974.229	4508.410	54.7	5.4675E-05	2.7337E-02	10.3
40	2400	134	16409.068	5228.971	61.7	6.1733E-05	3.0866E-02	11.6
					1.6483E+00	2.7471E-08	1.3736E-05	
					Rate (μmol/min)	**Rate (mol/s)**	**Rate (mol*L^{-1}*s^{-1})**	

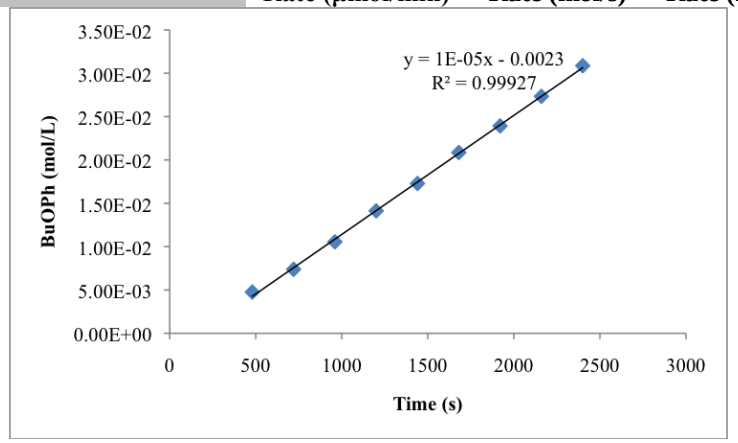

Tetra(*n*-propyl)ammonium Bromide, 5.0 equiv *n*-BuBr, Run #3:

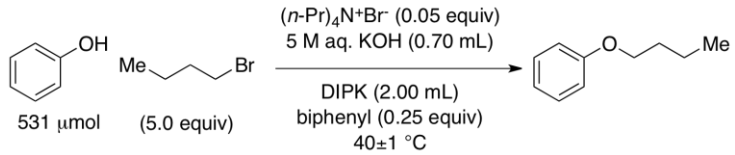

Time (m)	Time (s)	Ph_2 (μmol)	Ph_2 Area	BuOPh Area	BuOPh (μmol)	BuOPh (mol)	BuOPh (mol/L)	% conversion
0	0	134	1.000	0.000	0.0	0.0000E+00	0.0000E+00	0.0
4	240	134	20343.529	0.000	0.0	0.0000E+00	0.0000E+00	0.0
8	480	134	17135.459	704.603	8.0	7.9658E-06	3.9829E-03	1.5
12	720	134	16555.670	1094.000	12.8	1.2801E-05	6.4006E-03	2.4
16	960	134	16503.512	1634.514	19.2	1.9186E-05	9.5932E-03	3.6
20	1200	134	19291.602	2494.398	25.0	2.5048E-05	1.2524E-02	4.7
24	1440	134	18476.527	3121.994	32.7	3.2734E-05	1.6367E-02	6.2
28	1680	134	19005.387	3795.853	38.7	3.8692E-05	1.9346E-02	7.3
32	1920	134	18464.424	4249.274	44.6	4.4582E-05	2.2291E-02	8.4
36	2160	134	18505.396	4935.740	51.7	5.1670E-05	2.5835E-02	9.7
40	2400	134	17094.543	5072.116	57.5	5.7480E-05	2.8740E-02	10.8
					1.5796E+00	2.6326E-08	1.3163E-05	
					Rate (μmol/min)	**Rate (mol/s)**	**Rate (mol*L^{-1}*s^{-1})**	

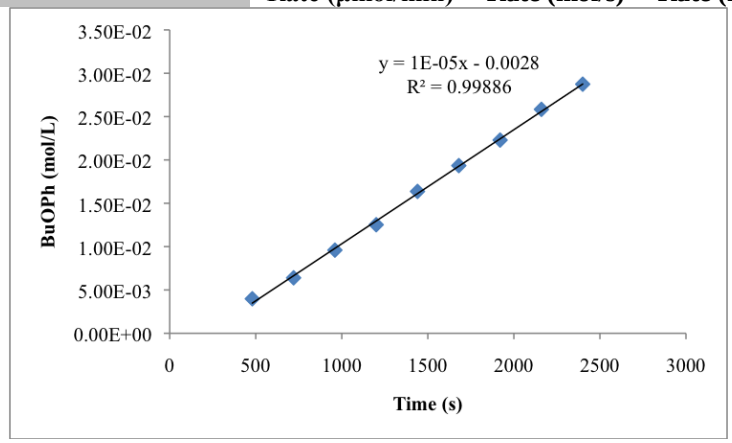

Tetra(*n*-propyl)ammonium Bromide, 5.0 equiv *n*-BuBr, Run #4:

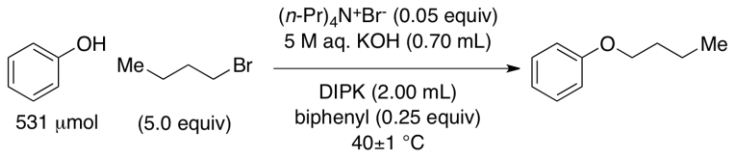

Time (m)	Time (s)	Ph_2 (μmol)	Ph_2 Area	BuOPh Area	BuOPh (μmol)	BuOPh (mol)	BuOPh (mol/L)	% conversion
0	0	134	1.000	0.000	0.0	0.0000E+00	0.0000E+00	0.0
4	240	134	23128.420	541.739	4.5	4.5376E-06	2.2688E-03	0.9
8	480	134	19329.223	957.956	9.6	9.6009E-06	4.8005E-03	1.8
12	720	134	18065.643	1417.589	15.2	1.5201E-05	7.6006E-03	2.9
16	960	134	18757.865	2107.038	21.8	2.1761E-05	1.0880E-02	4.1
20	1200	134	19849.057	2853.130	27.8	2.7846E-05	1.3923E-02	5.2
24	1440	134	19563.494	3585.350	35.5	3.5503E-05	1.7752E-02	6.7
28	1680	134	18421.484	4065.151	42.7	4.2750E-05	2.1375E-02	8.1
32	1920	134	18571.840	4629.634	48.3	4.8292E-05	2.4146E-02	9.1
36	2160	134	18080.941	5139.104	55.1	5.5062E-05	2.7531E-02	10.4
40	2400	134	19159.219	6219.349	62.9	6.2885E-05	3.1443E-02	11.8
					1.6355E+00	2.7258E-08	1.3629E-05	
					Rate (μmol/min)	**Rate (mol/s)**	**Rate (mol*L^{-1}*s^{-1})**	

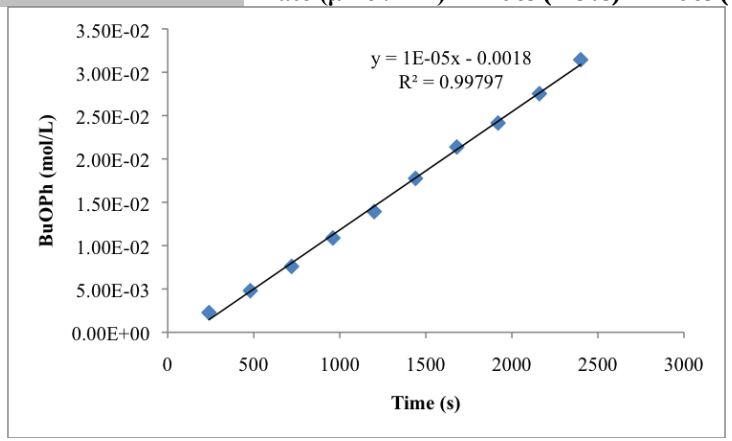

Variable *n*-butyl bromide equivalents summary table

Run #	Catalyst	*n*-BuBr (mol/L)	Rate (µmol/min)	Rate (mol/s)	Rate (mol*L^{-1}*s^{-1})	Mean Rate (mol*L^{-1}*s^{-1})	Std. Dev. Rate (mol*L^{-1}*s^{-1})
1	TPAB	0.13	0.2091	3.4848E-09	1.7424E-06	1.75E-06	1.61E-07
2	TPAB	0.13	0.2335	3.8910E-09	1.9455E-06		
3	TPAB	0.13	0.2133	3.5548E-09	1.7774E-06		
4	TPAB	0.13	0.1865	3.1081E-09	1.5541E-06		
1	TPAB	0.27	0.3845	6.4087E-09	3.2044E-06	3.35E-06	1.23E-07
2	TPAB	0.27	0.4106	6.8428E-09	3.4214E-06		
3	TPAB	0.27	0.4178	6.9640E-09	3.4820E-06		
4	TPAB	0.27	0.3969	6.6157E-09	3.3078E-06		
1	TPAB	0.53	0.7142	1.1903E-08	5.9513E-06	6.24E-06	4.26E-07
2	TPAB	0.53	0.8233	1.3722E-08	6.8610E-06		
3	TPAB	0.53	0.7389	1.2315E-08	6.1575E-06		
4	TPAB	0.53	0.7173	1.1956E-08	5.9779E-06		
1	TPAB	1.33	1.8835	3.1391E-08	1.5696E-05	1.41E-05	1.12E-06
2	TPAB	1.33	1.6483	2.7471E-08	1.3736E-05		
3	TPAB	1.33	1.5796	2.6326E-08	1.3163E-05		
4	TPAB	1.33	1.6355	2.7258E-08	1.3629E-05		
1	TOAB	0.13	0.7744	1.2907E-08	6.4534E-06	7.08E-06	5.23E-07
2	TOAB	0.13	0.8230	1.3716E-08	6.8580E-06		
3	TOAB	0.13	0.8962	1.4937E-08	7.4685E-06		
4	TOAB	0.13	0.9068	1.5113E-08	7.5566E-06		
1	TOAB	0.27	1.7706	2.9510E-08	1.4755E-05	1.61E-05	9.17E-07
2	TOAB	0.27	1.9529	3.2549E-08	1.6274E-05		
3	TOAB	0.27	2.0263	3.3772E-08	1.6886E-05		
4	TOAB	0.27	1.9631	3.2719E-08	1.6359E-05		
1	TOAB	0.53	3.4576	5.7626E-08	2.8813E-05	3.54E-05	1.71E-06
2	TOAB	0.53	4.4113	7.3521E-08	3.6761E-05		
3	TOAB	0.53	4.3037	7.1729E-08	3.5864E-05		
4	TOAB	0.53	4.0147	6.6911E-08	3.3456E-05		
1	TOAB	1.33	8.4641	1.4107E-07	7.0534E-05	9.97E-05	4.33E-06
2	TOAB	1.33	11.3653	1.8942E-07	9.4711E-05		
3	TOAB	1.33	12.1935	2.0323E-07	1.0161E-04		
4	TOAB	1.33	12.3220	2.0537E-07	1.0268E-04		

5.4.7 Determination of the Phenoxide Extinction Coefficient

To determine the phenoxide extinction coefficient standard phenol solutions were prepared. First, a stock solutions of phenol (714.3 mg, 7.59 mmol) in 5 M aq. KOH (10 mL, 759 mM) was prepared. An aliquot of this solution (250 μL, 190 μmol) was then diluted with 5 M aq. KOH (10.0 mL final volume, 19.0 mM). Seven different aliquots of the diluted stock solution (400, 350, 300, 250, 200, 150, 100 μL) were then further diluted with 0.1 M aq. KOH (10.0 mL final volume). This second dilution was analyzed by UV-vis spectroscopy and the absorbance readings were plotted against the solution concentration. The extinction coefficient was calculated as ε=2526.

Summary Table to Determine Phenol Extinction Coefficient in Aqueous KOH

$[PhO^-]_{aq.}$ (mol/L)	Wavelength (nm)	Absorbance	Mean Absorbance	Std. Dev. Absorbance
7.600E-04	287.5	1.914		
7.600E-04	287.5	1.939	1.923	0.014
7.600E-04	287.5	1.917		
6.650E-04	287.5	1.677		
6.650E-04	287.5	1.685	1.681	0.004
6.650E-04	287.5	1.681		
5.700E-04	287.5	1.445		
5.700E-04	287.5	1.432	1.440	0.007
5.700E-04	287.5	1.444		
4.750E-04	287.5	1.203		
4.750E-04	287.5	1.202	1.200	0.004
4.750E-04	287.5	1.195		
3.800E-04	287.5	0.952		
3.800E-04	287.5	0.955	0.956	0.004
3.800E-04	287.5	0.960		
2.850E-04	287.5	0.715		
2.850E-04	287.5	0.710	0.713	0.003
2.850E-04	287.5	0.714		
1.900E-04	287.5	0.478		
1.900E-04	287.5	0.480	0.478	0.002
1.900E-04	287.5	0.476		

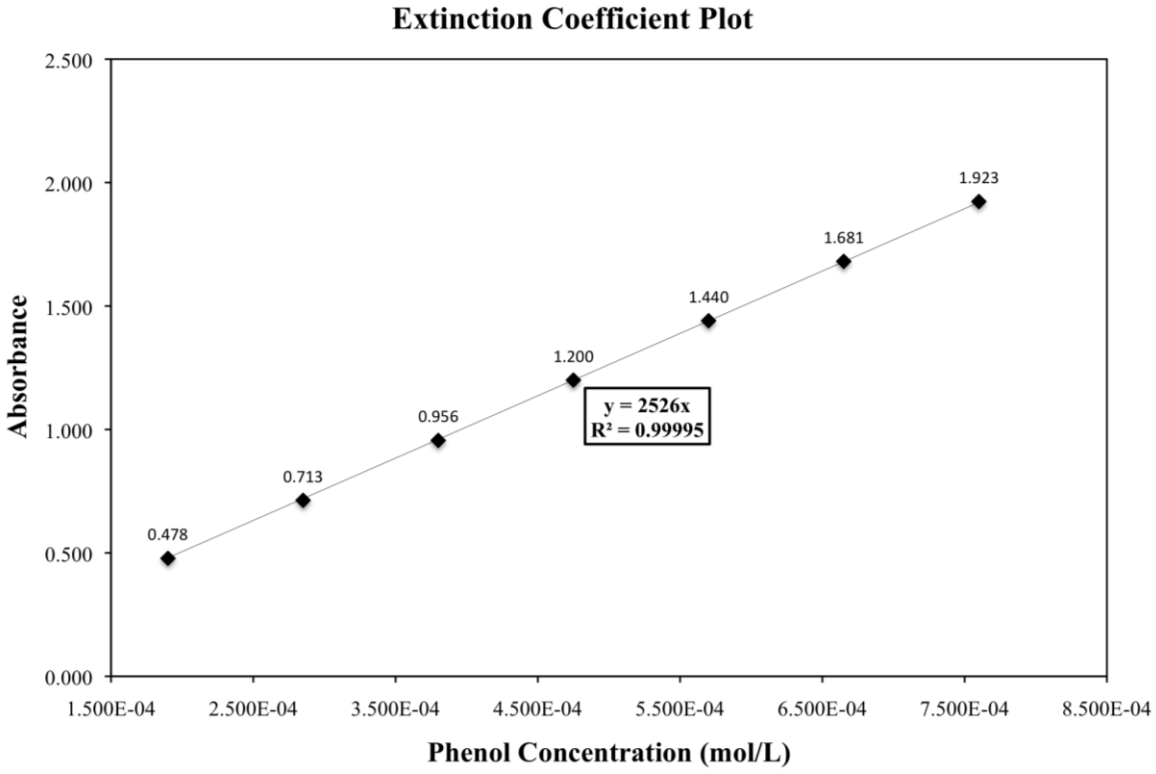
Extinction Coefficient Plot
Absorbance
Phenol Concentration (mol/L)
y = 2526x
R² = 0.99995
0.478
0.713
0.956
1.200
1.440
1.681
1.923
2.500
2.000
1.500
1.000
0.500
0.000
1.500E-04
2.500E-04
3.500E-04
4.500E-04
5.500E-04
6.500E-04
7.500E-04
8.500E-04

5.4.8 UV-vis Spectroscopy Measurements

For the survey conducted with 0.20 equivalents of the quaternary ammonium bromide, a 4 mL dram vial was charged with the respective quaternary ammonium bromide (22.3 to 58.0 mg, 106 μmol) followed by a solution of phenol (50.0 mg, 531 μmol) in 5.0 M aq. KOH (700 μL) and then 2,4-dimethyl-3-pentanone (2.00 mL). A 1.5 cm egg-shaped magnetic stir-bar and a septa screw-cap were then installed. To begin mixing the vial was placed in a 40 °C water bath and the stirring speed was set to maximum (~2000 rpm).

To determine the phenoxide concentration of the aqueous, stirring was ceased and the biphase was allowed to settle over several seconds. After one hour of stirring, a reaction aliquot (25 μL) was taken from the aqueous phase and diluted with additional 5 M aq. KOH (975 uL). From this new solution, another aliquot (200 μL) was taken and diluted with 0.1 M aq. KOH (10.0 mL final volume) in a volumetric flask. This final solution was then transferred to a suitable cuvette for UV-vis spectroscopy. A UV-vis spectrum was collected from 350 to 200 nm and the absorption of interest was observed at 288 to 287 nm.

For the survey conducted with 1.00 equivalents of the quaternary ammonium bromide a similar procedure was employed. Some differences include larger quantities of the quaternary ammonium bromide (81.8 to 290.4 mg, 531 μmol) and a smaller quantity of 2,4-dimethyl-3-pentanone (700 μL).

Based on the initial concentration of the aqueous phenol solution (759 mM), the double dilution procedure as described above would afford a solution with a concentration of 0.380 mM. This leads to a conversion factor of 1997, which was then applied to the concentration determined via UV-vis to afford the effective aqueous concentration in the reaction vial.

(759 mM)*(25.0 μL) = 19.0 μmol

(19 μmol)/(1.00 mL) = 19 mM

(19.0 mM)*(200 μL) = 3.8 μmol

(3.8 μmol)/(10.0 mL) = 0.380 mM

(759 mM)/(0.380 m) = 1997

UV-vis Summary Table with 0.2 equivalents of $R_4N^+Br^-$

Catalyst	Run #	Wavelength (nm)	Absorbance	Mean Absorbance	Std. Dev. Absorbance	Target $[PhO-]_{aq.}$ (mM)	$[PhO-]_{aq.}$ (mM)	Mean $[PhO-]_{aq.}$ (mM)	Std. Dev. $[PhO-]_{aq}$ (mM)	Conversion Factor	Effective $[PhO-]_{aq.}$ (mM)	Mean Effective $[PhO-]_{aq.}$ (mM)	Std. Dev. Effective $[PhO-]_{aq.}$ (mM)	% [PhO-] in organic phase	Mean %	Std. Dev. %
none	1	287.5	0.955			0.380	0.378			1997	755.1			0.5		
none	2	287.5	0.980	0.906	0.015	0.380	0.388	0.383	0.006	1997	774.9	765.2	11.6	-2.1	-0.82	1.19
none	3	287.5	0.981			0.380	0.388			1997	775.7			-2.2		
none	4	287.5	0.955			0.380	0.378			1997	755.1			0.5		
TEAB	1	287.5	0.957			0.380	0.379			1997	756.7			0.3		
TEAB	2	287.5	0.957	0.952	0.006	0.380	0.379	0.377	0.003	1997	756.7	752.4	5.0	0.3	0.87	0.57
TEAB	3	287.5	0.946			0.380	0.375			1997	748.0			1.4		
TEAB	4	287.5	0.946			0.380	0.375			1997	748.0			1.4		
TPAB	1	287.5	0.152			0.380	0.060			1997	120.2			84.2		
TPAB	2	287.5	0.150	0.151	0.001	0.380	0.059	0.060	0.001	1997	118.6	119.0	1.0	84.4	84.32	0.13
TPAB	3	287.5	0.151			0.380	0.060			1997	119.4			84.3		
TPAB	4	287.5	0.149			0.380	0.059			1997	117.8			84.5		
TBAB	1	287.5	0.180			0.380	0.071			1997	142.3			81.2		
TBAB	2	287.5	0.180	0.180	0.001	0.380	0.071	0.071	0.000	1997	142.3	142.1	1.0	81.2	81.27	0.13
TBAB	3	287.5	0.178			0.380	0.070			1997	140.7			81.5		
TBAB	4	287.5	0.181			0.380	0.072			1997	143.1			81.1		
THAB	1	287.5	0.183			0.380	0.072			1997	144.7			80.9		
THAB	2	287.5	0.179	0.181	0.002	0.380	0.071	0.071	0.001	1997	141.5	142.7	1.9	81.4	81.20	0.25
THAB	3	287.5	0.178			0.380	0.070			1997	140.7			81.5		
THAB	4	287.5	0.182			0.380	0.072			1997	143.9			81.0		
TOAB	1	287.5	0.168			0.380	0.067			1997	132.8			82.5		
TOAB	2	287.5	0.165	0.167	0.002	0.380	0.065	0.066	0.001	1997	130.5	132.1	1.4	82.8	82.60	0.19
TOAB	3	287.5	0.166			0.380	0.066			1997	131.3			82.7		
TOAB	4	287.5	0.169			0.380	0.067			1997	133.6			82.4		

In the control study (no catalyst) a minor increase in aqueous phenol concentration was observed. This was assumed to be the result of some water from the initial aqueous solution partitioning into the organic phase after mixing. The remained UV-vis values collected *were not* normalized to account for this small change in concentration.

UV-vis Summary Table with 1.0 equivalents of $R_4N^+Br^-$

Catalyst	R=	Wavelength (nm)	Absorbance	Mean Absorbance	Std. Dev. Absorbance	Target $[PhO^-]_{aq.}$ (mM)	$[PhO^-]_{aq.}$ (mM)	Mean $[PhO^-]_{aq.}$ (mM)	Std. Dev. $[PhO^-]_{aq.}$ (mM)	Conversion Factor	Effective $[PhO^-]_{aq.}$ (mM)	Mean Effective $[PhO^-]_{aq.}$ (mM)	% $[PhO^-]$ in organic phase	Mean %	Std. Dev. %
TMAB	1	287.5	0.918	0.906	0.011	0.380	0.363	0.359	0.005	1997	725.9	716.6	4.4	5.59	1.19
TMAB	1	287.5	0.898			0.380	0.356			1997	710.1		6.4		
TMAB	1	287.5	0.914			0.380	0.362			1997	722.7		4.8		
TMAB	1	287.5	0.895			0.380	0.354			1997	707.7		6.8		
TEAB	2	287.5	0.876	0.869	0.005	0.380	0.347	0.344	0.002	1997	692.7	687.1	8.7	9.47	0.57
TEAB	2	287.5	0.867			0.380	0.343			1997	685.6		9.7		
TEAB	2	287.5	0.870			0.380	0.344			1997	687.9		9.4		
TEAB	2	287.5	0.863			0.380	0.342			1997	682.4		10.1		
TPAB	3	287.5	0.152	0.151	0.001	0.380	0.060	0.060	0.001	1997	120.2	119.4	84.2	84.27	0.13
TPAB	3	287.5	0.150			0.380	0.059			1997	118.6		84.4		
TPAB	3	287.5	0.151			0.380	0.060			1997	119.4		84.3		
TPAB	3	287.5	0.149			0.380	0.059			1997	117.8		84.5		
TBAB	4	287.5	0.180	0.180	0.001	0.380	0.071	0.071	0.000	1997	142.3	142.1	81.2	81.27	0.13
TBAB	4	287.5	0.180			0.380	0.071			1997	142.3		81.2		
TBAB	4	287.5	0.178			0.380	0.070			1997	140.7		81.5		
TBAB	4	287.5	0.181			0.380	0.072			1997	143.1		81.1		
THAB	6	287.5	0.183	0.181	0.002	0.380	0.072	0.071	0.001	1997	144.7	142.7	80.9	81.20	0.25
THAB	6	287.5	0.179			0.380	0.071			1997	141.5		81.4		
THAB	6	287.5	0.178			0.380	0.070			1997	140.7		81.5		
THAB	6	287.5	0.182			0.380	0.072			1997	143.9		81.0		
TOAB	8	287.5	0.168	0.167	0.002	0.380	0.067	0.066	0.001	1997	132.8	132.1	82.5	82.60	0.19
TOAB	8	287.5	0.165			0.380	0.065			1997	130.5		82.8		
TOAB	8	287.5	0.166			0.380	0.066			1997	131.3		82.7		
TOAB	8	287.5	0.169			0.380	0.067			1997	133.6		82.4		
							Third	**Liquid**	**Phase**						
TPAB	3	287.5	2.060	2.049	0.022	0.380	0.816	0.811	0.009	1997	1628.9	1620.5	114.6	113.50	6.05
TPAB	3	287.5	2.064			0.380	0.817			1997	1632.1		115.0		
TPAB	3	287.5	1.939			0.380	0.768			1997	1533.2		102.0		
TPAB	3	287.5	2.024			0.380	0.801			1997	1600.4		110.9		

5.4.9 Determination of Response Factors for Benzyl Phenyl Ether and Phenol

Response factors for benzyl phenyl ether and phenol were determined for GC method 2. Five different stoichiometric ratios of phenol, benzyl phenyl ether, and biphenyl (1:1:1, 2:2:1, 3:3:1, 1:1:2, 1:1:3 by mass, respectively) were examined. All standard solutions were prepared in acetonitrile with a final volume of 1.0 mL. Each unique ratio of components was prepared in triplicate. Each vial was also tested individually in triplicate to ensure that the any error associated with the instrument detector was minimal.

The response factor for phenol was calculated as 2.4676, and the response factor for benzyl phenyl ether was 0.9428 with respect to the biphenyl internal standard. The summary table and plot are shown below.

Summary Data Table for Benzyl Phenyl Ether and Phenol Response Factors

Vial #	Inj #	PhOH (mg)	BnOPh (mg)	Ph_2 (mg)	PhOH (µmol)	BnOPh (µmol)	Ph_2 (µmol)	PhOH (Area)	BnOPh (Area)	Ph_2 (Area)	BnOPh Response Factor	Instrument Std. Dev.	PhOH Response Factor	Instrument Std. Dev.
1	1	0.5	0.5	0.5	5.31	2.71	3.24	39157.4	55448.2	63425.3	0.9574		2.6541	
1	2	0.5	0.5	0.5	5.31	2.71	3.24	41130.0	56732.5	64595.4	0.9530	0.0037	2.5734	0.0444
1	3	0.5	0.5	0.5	5.31	2.71	3.24	41350.0	57396.3	65153.0	0.9501		2.5818	
2	1	0.5	0.5	0.5	5.31	2.71	3.24	41951.2	56917.4	64738.9	0.9520		2.5286	
2	2	0.5	0.5	0.5	5.31	2.71	3.24	42292.8	57942.6	65496.3	0.9461	0.0035	2.5376	0.0049
2	3	0.5	0.5	0.5	5.31	2.71	3.24	42141.1	57580.7	65058.5	0.9457		2.5297	
3	1	0.5	0.5	0.5	5.31	2.71	3.24	42417.1	58049.1	65184.8	0.9399		2.5181	
3	2	0.5	0.5	0.5	5.31	2.71	3.24	44012.1	59197.3	66688.4	0.9429	0.0019	2.4828	0.0212
3	3	0.5	0.5	0.5	5.31	2.71	3.24	44469.7	59724.2	67305.6	0.9433		2.4800	
1	1	1.0	1.0	0.5	10.63	5.43	3.24	91358.5	117621.0	67438.4	0.9598		2.4191	
1	2	1.0	1.0	0.5	10.63	5.43	3.24	90349.4	117209.0	67090.3	0.9582	0.0008	2.4335	0.0120
1	3	1.0	1.0	0.5	10.63	5.43	3.24	89138.2	115981.0	66447.7	0.9591		2.4429	
2	1	1.0	1.0	0.5	10.63	5.43	3.24	91632.5	122364.0	68343.9	0.9350		2.4442	
2	2	1.0	1.0	0.5	10.63	5.43	3.24	90289.4	121350.0	67427.4	0.9302	0.0027	2.4473	0.0073
2	3	1.0	1.0	0.5	10.63	5.43	3.24	92116.8	123061.0	68402.0	0.9305		2.4335	
3	1	1.0	1.0	0.5	10.63	5.43	3.24	90225.2	120531.0	67203.6	0.9334		2.4410	
3	2	1.0	1.0	0.5	10.63	5.43	3.24	89787.6	120848.0	67223.3	0.9312	0.0012	2.4536	0.0067
3	3	1.0	1.0	0.5	10.63	5.43	3.24	92646.1	124132.0	69073.8	0.9315		2.4433	
1	1	1.5	1.5	0.5	15.94	8.14	3.24	140660.0	184708.0	68769.8	0.9349		2.4033	
1	2	1.5	1.5	0.5	15.94	8.14	3.24	141323.0	185709.0	69051.2	0.9337	0.0007	2.4018	0.0017
1	3	1.5	1.5	0.5	15.94	8.14	3.24	135892.0	178630.0	66493.6	0.9347		2.4053	
2	1	1.5	1.5	0.5	15.94	8.14	3.24	138861.0	182372.0	68005.9	0.9364		2.4074	
2	2	1.5	1.5	0.5	15.94	8.14	3.24	137956.0	181427.0	67924.8	0.9401	0.0026	2.4203	0.0072
2	3	1.5	1.5	0.5	15.94	8.14	3.24	137335.0	180295.0	67595.7	0.9414		2.4195	
3	1	1.5	1.5	0.5	15.94	8.14	3.24	160551.0	213260.0	79919.1	0.9410		2.4469	
3	2	1.5	1.5	0.5	15.94	8.14	3.24	155416.0	205936.0	77230.5	0.9417	0.0015	2.4428	0.0050
3	3	1.5	1.5	0.5	15.94	8.14	3.24	159526.0	211751.0	79598.5	0.9439		2.4528	

Summary Data Table for Benzyl Phenyl Ether and Phenol Response Factors, cont.

1	1	0.5	0.5	1.0	5.31	2.71	6.48	44782.8	60006.2	134812.0	0.9402		2.4663	
1	2	0.5	0.5	1.0	5.31	2.71	6.48	44292.2	59530.7	133689.0	0.9399	0.0023	2.4729	0.0043
1	3	0.5	0.5	1.0	5.31	2.71	6.48	42729.1	57208.1	129046.0	0.9440		2.4743	
2	1	0.5	0.5	1.0	5.31	2.71	6.48	52927.9	72000.3	160498.0	0.9329		2.4844	
2	2	0.5	0.5	1.0	5.31	2.71	6.48	52492.3	71497.9	159526.0	0.9338	0.0009	2.4898	0.0094
2	3	0.5	0.5	1.0	5.31	2.71	6.48	52902.8	71463.1	159593.0	0.9346		2.4716	
3	1	0.5	0.5	1.0	5.31	2.71	6.48	44690.9	60664.5	136390.0	0.9409		2.5003	
3	2	0.5	0.5	1.0	5.31	2.71	6.48	45148.4	61050.4	137221.0	0.9407	0.0011	2.4901	0.0052
3	3	0.5	0.5	1.0	5.31	2.71	6.48	45043.3	60922.3	137229.0	0.9427		2.4960	
1	1	0.5	0.5	1.5	5.31	2.71	9.73	45772.3	60772.7	210734.0	0.9675		2.5146	
1	2	0.5	0.5	1.5	5.31	2.71	9.73	44355.9	59247.9	204912.0	0.9650	0.0022	2.5232	0.0092
1	3	0.5	0.5	1.5	5.31	2.71	9.73	44404.8	58993.9	203642.0	0.9631		2.5048	
2	1	0.5	0.5	1.5	5.31	2.71	9.73	43887.3	59437.2	201101.0	0.9440		2.5028	
2	2	0.5	0.5	1.5	5.31	2.71	9.73	45881.5	62011.0	210747.0	0.9482	0.0041	2.5088	0.0032
2	3	0.5	0.5	1.5	5.31	2.71	9.73	44909.5	61106.6	205866.0	0.9400		2.5037	
3	1	0.5	0.5	1.5	5.31	2.71	9.73	42523.2	58717.0	198147.0	0.9415		2.5451	
3	2	0.5	0.5	1.5	5.31	2.71	9.73	44316.5	60388.7	204469.0	0.9447	0.0048	2.5200	0.0125
3	3	0.5	0.5	1.5	5.31	2.71	9.73	44342.7	61325.1	205574.0	0.9353		2.5322	

Benzyl Phenyl Ether and Phenol Response Factor Plot

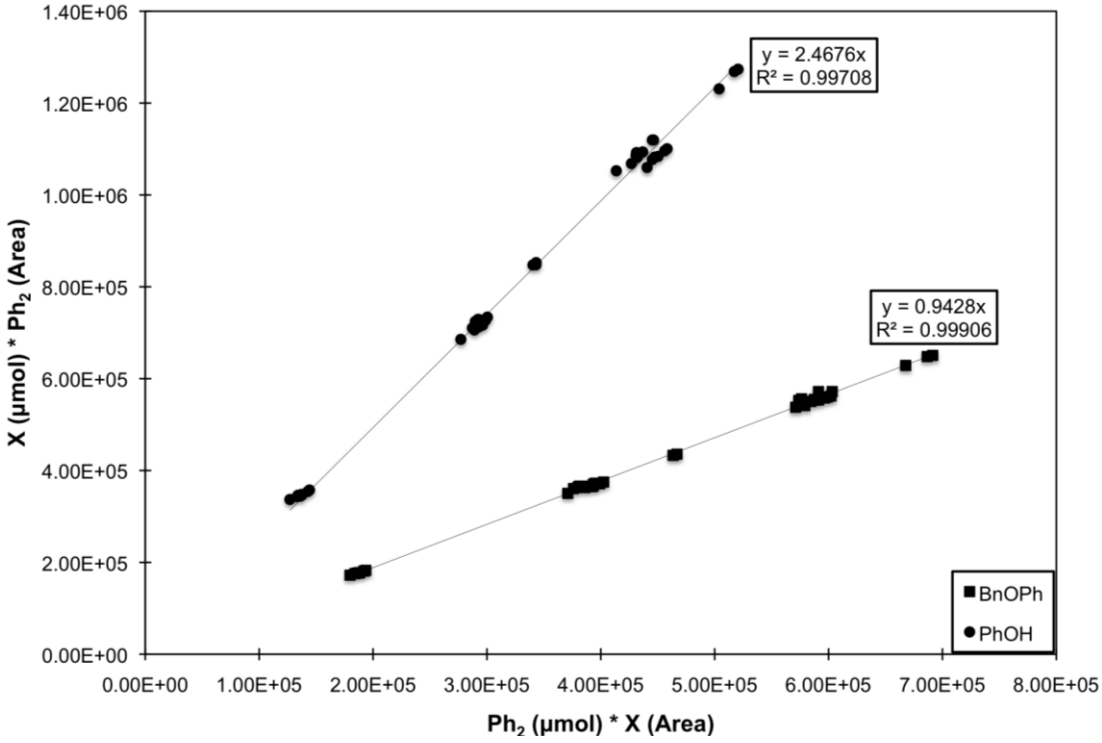

5.4.10 Benzyl Bromide Titration of the Organic Phase

To a 4 mL dram vial was charged the appropriate quaternary ammonium bromide (8.2 to 29.6 mg, 53.1 umol). To this vial, a solution of biphenyl (8.2 mg, 53.1 umol) in 2,4-dimethyl-3-pentanone (2.00 mL, 26.6 mM) was added followed by a solution of phenol (50.0 mg, 531 umol) in 5 M aq. KOH (700 uL). A 1.5 cm egg-shaped magnetic stir-bar and a septa screw-cap were then installed. To begin mixing the vial was placed in a 40 °C water bath and the stirring speed was set to maximum (~2000 rpm). The vial was stirred vigorously for one hour.

To analyze the organic phase, stirring was ceased and the biphase was allowed to settle over several seconds. A reaction aliquot (100 μL) was taken from the organic phase and quickly injected into a small vial containing a solution of benzyl bromide (10.0 mg, 5.85 μmol) in acetonitrile (1.00 mL). The quenched solution was allowed to sit overnight (>12 hours). This solution was analyzed directly via gas chromatography (GC Method 2).

Summary Table for Benzyl Bromide Titration Data

Catalyst	Run #	PhOH (Area)	Ph_2 (Area)	BnOPh (Area)	PhOH (µmol)	Ph_2 (µmol)	BnOPh (µmol)	% PhOH	Mean % PhOH	Std. Dev. % PhOH	% BnOPh	Mean % BnOPh	Std. Dev. % BnOPh	% PhOH + % BnOPH	Mean (% PhOH + % BnOPh)	Std. Dev. (% PhOH + % BnOPh)
TMAB	1	0.00000E+00	4.51207E+04	0.00000E+00	0.00	53.10	0.00	0.00			0.00			0.00		
TMAB	2	0.00000E+00	4.44911E+04	0.00000E+00	0.00	53.10	0.00	0.00	**0.10**	**0.17**	0.00	**0.00**	**0.00**	0.00	**0.10**	**0.17**
TMAB	3	5.41190E+02	4.58240E+04	0.00000E+00	1.55	53.10	0.00	0.29			0.00			0.29		
TEAB	1	0.00000E+00	4.49796E+04	0.00000E+00	0.00	53.10	0.00	0.00			0.00			0.00		
TEAB	2	7.47601E+02	4.53088E+04	0.00000E+00	2.16	53.10	0.00	0.41	**0.26**	**0.23**	0.00	**0.00**	**0.00**	0.41	**0.26**	**0.23**
TEAB	3	6.96186E+02	4.50351E+04	0.00000E+00	2.03	53.10	0.00	0.38			0.00			0.38		
TPAB	1	1.98958E+03	4.64946E+04	1.44779E+03	5.61	53.10	1.56	1.06			0.29			1.35		
TPAB	2	1.92605E+03	4.64721E+04	1.37126E+03	5.43	53.10	1.48	1.02	**1.03**	**0.02**	0.28	**0.28**	**0.01**	1.30	**1.32**	**0.03**
TPAB	3	1.89130E+03	4.55121E+04	1.34741E+03	5.45	53.10	1.48	1.03			0.28			1.30		
TBAB	1	1.21391E+04	4.46383E+04	4.42429E+04	35.63	53.10	49.62	6.71			9.34			16.05		
TBAB	2	1.33858E+04	4.72479E+04	4.64583E+04	37.12	53.10	49.23	6.99			9.27			16.26		
TBAB	3	1.27760E+04	4.65350E+04	4.48905E+04	35.97	53.10	48.29	6.77			9.09			15.87		
TBAB	4	1.33845E+04	4.87735E+04	4.88785E+04	35.96	53.10	50.17	6.77	**6.78**	**0.11**	9.45	**9.35**	**0.15**	16.22	**16.13**	**0.15**
TBAB	5	1.26740E+04	4.65496E+04	4.70446E+04	35.68	53.10	50.60	6.72			9.53			16.25		
TBAB	6	1.30583E+04	4.80559E+04	4.79518E+04	35.60	53.10	49.95	6.71			9.41			16.11		
THAB	1	8.24774E+03	4.61568E+04	7.34046E+04	23.41	53.10	79.62	4.41			14.99			19.40		
THAB	2	9.17470E+03	4.49123E+04	6.81226E+04	26.77	53.10	75.93	5.04			14.30			19.34		
THAB	3	1.07727E+04	4.62675E+04	6.83286E+04	30.51	53.10	73.93	5.75			13.92			19.67		
THAB	4	8.28168E+03	4.79174E+04	7.18287E+04	22.65	53.10	75.04	4.26	**4.92**	**0.67**	14.13	**14.13**	**0.53**	18.40	**19.04**	**0.53**
THAB	5	8.56936E+03	4.83448E+04	7.19967E+04	23.23	53.10	74.56	4.37			14.04			18.41		
THAB	6	1.12643E+04	4.90706E+04	6.96011E+04	30.08	53.10	71.01	5.66			13.37			19.04		
TOAB	1	4.35283E+03	4.54573E+04	7.96443E+04	12.55	53.10	87.71	2.36			16.52			18.88		
TOAB	2	4.72829E+03	4.69690E+04	8.24716E+04	13.19	53.10	87.90	2.48			16.55			19.04		
TOAB	3	4.12302E+03	4.66054E+04	8.42662E+04	11.59	53.10	90.52	2.18	**2.30**	**0.15**	17.05	**16.77**	**0.23**	19.23	**19.07**	**0.15**
TOAB	4	4.10766E+03	4.79866E+04	8.57615E+04	11.22	53.10	89.47	2.11			16.85			18.96		
TOAB	5	4.57867E+03	4.81476E+04	8.61550E+04	12.46	53.10	89.58	2.35			16.87			19.22		

5.4.11 Potassium Titration

As described previously in general procedure H, 1.0 mL of the organic phase was transferred to a PTFE digestion test tube containing benzyl bromide (200 uL). The resulting mixture was mixed briefly by swirling, capped with a rubber stopper, and the contents were allowed to sit overnight. To this solution, H_2O (1.0 mL) and then concentrated nitric acid (6.0 mL) were added and the entire mixture was digested in a microwave oven (ramp to 1200 watts over 40 m, hold for 20 m, cool down over 30 m, max pressure 60 bar).

The resulting solution was then diluted to a final volume of 25.0 mL with H_2O and then analyzed directly by ICP-OES.

CHAPTER 6: *References*

(1) Starks, C. M.; Liotta, C. L.; Halpern, M. Phase Transfer Catalysis: Industrial Perspective. In *Phase Transfer Catalysis Fundamentals, Applications, and Industrial Perspectives*, Chapman & Hall, New York, 1994, p 1.

(2) Mathias, L.; Vaidya, R. A., *J. Am. Chem. Soc.* **1986**, *108*, 1093-1094.

(3) Starks, C. M.; Liotta, C. L.; Halpern, M. Phase Transfer Catalysis: Industrial Perspective. In *Phase Transfer Catalysis Fundamentals, Applications, and Industrial Perspectives*, Chapman & Hall, New York, 1994, p 626.

(4) The scope of this work will primarily address the chemical structure of the catalyst. The numerous factors which can affect process optimization (e.g. temperature, viscosity, impellor geometry, etc.) will not be covered.

(5) Maruoka, K. *Asymmetric Phase Transfer Catalysis*: Wiley-VCH Verlag GmbH & Co. KGaA: Weinheim, 2008.

(6) Starks, C. M. *J. Am. Chem. Soc.* **1971**, *93*, 195-199.

(7) Alan, J. R. *Quaternary Ammonium Salts: Their Use in Phase-Transfer Catalyzed Reactions*, Academic Press, San Diego, 2001.

(8) Sheldon, R. A. *Stud. Sur. Sci. Catal.* **1991**, *66*, 573-594.

(9) Sheldon, R. A. *Chemtech* **1991**, *21*, 566.

(10) Starks, C. M.; Liotta, C. L.; Halpern, M. Phase-Transfer Catalyst: Fundamentals II. In *Phase Transfer Catalysis Fundamentals, Applications, and Industrial Perspectives*, Chapman & Hall, New York, 1994, pp. 48-122.

(11) Rabinovitz, M; Cohen, Y.; Halpern, M. *Angew. Chem. Int. Ed.* **1986**, *25*, 960-970.

(12) Dockx, J. *Synthesis* **1973**, 441-456.

(13) Mąkosza, M.; Chesnokov, A. *Tetrahedron* **2008**, *64*, 5925-5932.

(14) Mąkosza, M. *Pure Appl. Chem.* **1975**, *43*, 439-462.

(15) Landini, D.; Maia, A.; Montanari, F. *Chem. Commun.* **1977**, 112-113.

(16) Starks, C. M.; Liotta, C. L.; Halpern, M. Phase Transfer Catalysis: Industrial Perspective. In *Phase Transfer Catalysis Fundamentals, Applications, and Industrial Perspectives*, Chapman & Hall, New York, 1994, p 90.

(17) O'Donnell, M. J. *Aldrichimica Acta* **2001**, *34*, 3-15.

(18) Maruoka, K.; Ooi, T. *Chem. Rev.* **2003**, *103*, 3013-3028.

(19) O'Donnell, M. J. *Acc. Chem. Res.* **2004**, *37*, 506-517.

(20) Lygo, B.; Andrews, B. I. *Acc. Chem. Res.* **2004**, *37*, 518-525.

(21) O'Donnell, M. J. "Asymmetric Phase-Transfer Reactions," In *Catalytic Asymmetric Synthesis,* 2nd Ed.; Ojima, I.; Wiley-VCH: New York, 2000.

(22) Ooi, T.; Maruoka, K. *Angew. Chem. Int. Ed.* **2007**, *46*, 4222-4266.

(23) Maruoka, K. *Org. Process, Res. Dev.* **2008**, *12*, 679-697.

(24) Jew. S.-S.; Park, H.-G. *Chem. Commun.* **2009**, 7090-7103.

(25) Hiyama, T.; Mishima, T.; Sawada, H.; Nozaki, H. *J. Am. Chem. Soc.* **1975**, *97*, 1626-1627.

(26) Fiaud, J.-C. *Tetrahedron Lett.* **1975**, *16*, 3495-3496.

(27) Saigo, K.; Koda, H.; Nohira, H. *Bull. Chem. Soc. Jpn.* **1979**, *52*, 3119-3120.

(28) Juliá, S; Ginebreda, A.; Guixer, J.; Tomás, A. *Tetrahedron Lett.* **1980**, *21*, 3709-3712.

(29) Kaufman, T.S.; Rúveda, E. A. *Angew. Chem. Int. Ed.* **2005**, *44*, 854-885.

(30) Song, C. E. *Cinchona Alkaloids in Synthesis and Catalysis: Ligands, Immobilization and Organocatalysis*, Wiley-VCH, Weinheim, 2009.

(31) Kacprzak, K.; Gawronski, J. *Synthesis* **2001**, 961-998.

(32) Hentges, S. G.; Sharpless, K. B. *J. Am. Chem. Soc.* **1980**, *102*, 4263-4265.

(33) Kolb, H. C.; VanNieuwenhze, M. S.; Sharpless, K. B. *Chem. Rev.* **1994**, *94*, 2483 and references therein.

(34) Marcelli, T.; Hiemstra, H. *Synthesis* **2010**, 1229-1279.

(35) Yoon, T. P.; Jacobsen, E. N. *Science* **2003**, *299*, 1691-1693.

(36) Ooi, T.; Kameda, M.; Maruoka, K. *J. Am. Chem. Soc.* **1999**, *121*, 6519-6520.

(37) Maruoka, K. *J. Fluor. Chem.* **2001**, *112*, 95-99.

(38) Ooi, T.; Kameda, M.; Maruoka, K. *J. Am. Chem. Soc.* **2003**, *125*, 5139-5151.

(39) Kitamura, M.; Shirakawa, S.; Maruoka, K. *Angew. Chem. Int. Ed.* **2005**, *44*, 1549-1551.

(40) Lygo, B; Allbutt, B.; James, S. R. *Tetrahedron Lett.* **2003**, *44*, 5629-5632.

(41) Shibuguchi, T.; Fukuta, Y.; Akachi, Y.; Sekine, A.; Ohshima, T.; Shibasaki, M. *Tetrahedron Lett.* **2002**, *43*, 9539-9543.

(42) Ohshima, T.; Shibuguchi, T.; Fukuta, Y.; Shibasaki, M. *Tetrahedron* **2004**, *60*, 7743-7754.

(43) Rueffer, M. E.; Fort, L. K.; MacFarland, D. K. *Tetrahedron: Asymmetry* **2004**, *15*, 3297-3300.

(44) Kowtoniuk, W. E.; MacFarland, D. K.; Grover, G. N. *Tetrahedron Lett.* **2005**, *46*, 5703-5705.

(45) Sasai, H. Jpn. Kokai Tokkyo Koho JP2003335780, **2003.**

(46) Maruoka, K. *Asymmetric Phase Transfer Catalysis*; Wiley-VCH Verlag GmbH & Co. KGaA: Weinheim, 2008.

(47) Kacprzak, K.; Gawronski, J. *Synthesis* **2001**, 961-998.

(48) Jew, S.-S.; Park, H.-G. *Chem Commun.* **2009**, *46*, 7090-7103.

(49) Dolling, U.-H.; Davis, P.; Grabowski, E. J. J. *J. Am. Chem. Soc.* **1984**, *106*, 446-447.

(50) Hughes, D. L.; Dolling, U. H.; Ryan, K. M.; Schoenewaldt, E. F.; Grabowski, E. J. J. *J. Org. Chem.* **1987**, *52*, 4745-4752.

(51) O'Donnell, M. J.; Bennett, W. D.; Wu, S. *J. Am. Chem. Soc.* **1989**, *111*, 2353-2355.

(52) O'Donnell, M. J.; Bennett, W. D.; Bruder, W. A.; Jacobsen, W. N.; Knuth, K.; LeClef, B.; Polt, R. L.; Bordwell, F. G.; Mrozack, S. R.; Cripe, T. A. *J. Am. Chem. Soc.* **1988**, *110*, 8520-8525.

(53) O'Donnell, M. J.; Wu, S.; Huffman, J. C. *Tetrahedron* **1994**, *50*, 4507-4518.

(54) Lygo, B.; Wainwright, P. G. *Tetrahedron Lett.* **1997**, *38*, 8595-8598.

(55) Corey, E. J.; Xu, F.; Noe, M. C. *J. Am. Chem. Soc.* **1997**, *119*, 12414-12415.

(56) Corey, E. J.; Bo, Y.; Busch-Peterson, J. *J. Am. Chem. Soc.* **1998**, *120*, 13000-13001.

(57) Lygo, B.; Crosby, J.; Lowdon, T. R.; Wainwright, P. G. *Tetrahedron* **2001**, *57*, 2391-2402.

(58) Jew, S.-S.; Jeong, B.-S.; Yoo, M.-S.; Huh, H.; Park, H.-G. *Chem. Commun.* **2001**, 1244-1245.

(59) Park, H.-G.; Jeong, B.-S.; Yoo, M.-S.; Park, M.-K.; Huh, H.; Jew, S.-S. *Tetrahedron Lett.*, **2001**, *42*, 4645-4648.

(60) Jew, S.-S.; Yoo, M.-S.; Jeong, B.-S.; Park, I. L.; Park, H.-G. *Org. Lett.* **2002**, *4*, 4245-4248.

(61) Yoo, M.-S.; Jeong, B.-S.; Lee, J.-H.; Park, H.-G.; Jew, S.-S. *Org. Lett.* **2005**, *7*, 1129-1131.

(62) Dunitz, J. D. *ChemBioChem* **2004**, *5*, 614-621.

(63) Dehmlow, E. V.; Düttmann, S.; B. Neumann; Stammler, H.-G. *Eur. J. Org. Chem.* **2002**, 2087.

(64) Taggi, A. E.; Hafez, A. M.; Wack, H.; Young, B.; Ferraris, D.; Lectka, T. *J. Am. Chem. Soc.* **2002**, *124*, 6626-6635.

(65) Franz, M. H.; Röper, S.; Wartchow, R.; Hoffmann, H. M. R. *J. Org. Chem.* **2004**, *69*, 2983-2991.

(66) Bucher, C.; Sparr, C.; Schweizer, W. B.; Gilmour, R. *Chem. Eur. J.* **2009**, *15*, 7637-7647.

(67) Hudlický, M. *Org. React.* **1988**, *35*, 513-637 and references therein.

(68) Somekh, L.; Shanzer, A. *J. Am. Chem. Soc.* **1982**, *104*, 5836-5837.

(69) Stenberg, V. I.; Travecedo, E. F. *J. Org. Chem.* **1970**, *35*, 4131-4136.

(70) Barton, D. H. R.; McCombie, S. W. *J. Chem. Soc. Perkin Trans. 1* **1975**, 1574-1585.

(71) R. Barton, D. H.; Jaszberenyi, J. Cs. *Tetrahedron Lett.* **1989**, *30*, 2619-2622.

(72) Parker, A. J. *Chem. Rev.* **1969**, *69*, 1-32.

(73) Denmark, S. E.; Gould, N. D.; Wolf, L. M. *J. Org. Chem.* **2011**, *76*, 4260-4336.

(74) Only minor changes in initial alkylation rate were observed for stirring speeds above 1500 rpm.

(75) Catalyst **1d** (Corey's catalyst) afforded **2** with er 98:2, $[\alpha]_D$ – 198.6 (c = 2.0, CH_2Cl_2). Previous literature report found $[\alpha]_D$-191.4 (c = 2.0 CH_2Cl_2, See Reference 55 and 56).

(76) Lee, J.-H.; Yoo, M.-S.; Jung, J.-H.; Jew, S.-S.; Park, H.-G.; Jeong; B.-S. *Tetrahedron* **2007**, *63*, 7906-7915.

(77) Lipkowitz, K. B.; Cavanaugh, M. W.; Brian, B.; O'Donnell, M. J. *J. Org. Chem.* **1991**, *56*, 5181-5192.

(78) Qi, J.; Beeler, A. B.; Zhang, Q.; Porco Jr. J. A., *J. Am. Chem. Soc.* **2010**, *132*, 13642-13644.

(79) Nakai, T.; Mikami, K. *Chem. Rev.* **1986**, *86*, 885-902.

(80) Nakai, T.; Mikami, K. *Org. React.* **1994**, *46*, 105-209.

(81) Vogel, C. *Synthesis* **1997**, 497-505.

(82) Mikami, K.; Nakai, T. *Synthesis* **1991**, 594-604.

(83) Woodward, R. B.; Hoffman, R. *The Conservation of Orbital Symmetry*, Verlag Chemie, GmbH, Weinheim, 1971, p. 114.

(84) Roth, W. R.; Konig, J.; Stein, K. *Chem. Ber.* **1970**, *103*, 426-439.

(85) Rhoads, S. J.; Raulins, N. R. *Org. React.* **1975**, *22*, 1-252.

(86) Ziegler, F. E. *Chem. Rev.* **1988**, *88*, 1423-1452.

(87) Castro, A. M. M. *Chem. Rev.* **2004**, *104*, 2939-3002.

(88) Wilson, S. R. *Org. React.* **1993**, *43*, 93-250.

(89) Paquette, L. A. *Angew. Chem. Int. Ed.* **1990**, *29*, 609-626.

(90) Sommelet, M. A. *Compt. Rend.* **1937**, *205*, 56-58.

(91) Kantor, S. W., Hauser, C. R. *J. Am. Chem. Soc.* **1951**, *73*, 4122-4131.

(92) Baldwin, J. E.; Hackler, R. E.; Kelly, D. P. *J. Chem. Soc., Chem. Commun.* **1968**, 537-538.

(93) Wittig, G.; Löhmann, L. *Justus Leibigs Ann. Chem.* **1942**, *550*, 260-268.

(94) Wittig, G. *Angew. Chem.* **1954**, *66*, 10-17.

(95) Cast, J.; Stevens, T. S.; Holmes, J. *J. Chem. Soc.* **1960**, 3521-3527.

(96) Rautenstrauch, V. *J. Chem. Soc., Chem. Commun.* **1970**, 4.

(97) Mikami, K.; Taya, S.; Nakai, T.; Fujita, Y. *J. Org. Chem.* **1981**, *46*, 5447-5449.

(98) Mikami, K.; Kishi, N.; Nakai, T.; Fujita, Y. *Tetrahedron* **1986**, *42*, 2911-2918.

(99) Nakai, T; Mikami, K.; Fujita, Y. *J. Am. Chem. Soc.* **1981**, *103*, 6492-6494.

(100) Still, W. C.; Mitra, A. *J. Am. Chem. Soc.* **1978**, *100*, 1927-1928.

(101) Nakai, T.; Mikami, K.; Taya, S.; Kimura, Y.; Mimura, T. *Tetrahedron Lett.* **1981**, *22*, 69-72.

(102) Mikami, K.; Takahashi, O.; Kasuga, T.; Nakai, T. *Chem. Lett.* **1985**, 1729-1732.

(103) Marshall, J. A.; Lebreton, J. *Tetrahedron Lett.* **1987**, *28*, 3323-3326.

(104) Marshall, J. A.; Lebreton, J. *J. Am. Chem. Soc.* **1988**, *110*, 2925-2931.

(105) Marshall, J. A.; Wang, X. *J. Org. Chem.* **1992**, *57*, 2747-2750.

(106) Kang, J.; Cho, W. O.; Cho, H. G.; Oh, H. J. *Bull. Korean Chem. Soc.* **1994**, *15*, 732-739.

(107) Manabe, S. *Chem. Commun.* **1997**, 737-738.

(108) Gibson, S. E.; Ham, P.; Jefferson, G. R. *Chem. Commun.* **1998**, 123-124.

(109) Tomooka, K.; Komine, N.; Nakai, T. *Tetrahedron Lett.* **1998**, *39*, 5513-5516.

(110) Kawasaki, T.; Kimachi, T. *Tetrahedron* **1999**, *55*, 6847-6862.

(111) Tomooka, K.; Komine, N.; Nakai, T. *Chirality* **2000**, 505-509.

(112) Kitamura, M.; Hirokawa, Y.; Maezaki, N. *Chem. Eur. J.* **2009**, *15*, 9911-9917.

(113) Yamamoto, Y.; Oda, J.; Inouye, Y. *Tetrahedron Lett.* **1979**, *19*, 2411-2414.

(114) Halpern, M.; Yonowich-Weiss, M.; Sasson, Y.; Rabinovitz, M. *Tetrahedron Lett.* **1981**, *22*, 703-704.

(115) Halpern, M.; Sasson, Y.; Rabinovitz, M. *J. Org. Chem.* **1983**, *48*, 1022-1025.

(116) Jones, R. A. Formation of C-C Bonds. *Quaternary Ammonium Salts, Their Use in Phase-Transfer Catalysis*; Best Synthetic Methods; Academic Press: New York, 2001, 229-302.

(117) Mąkosza, M. *Pure Appl. Chem.* **1975**, *43*, 439-462.

(118) Mąkosza, M.; Białecka, E. *Tetrahedron Lett.* **1977**, *18*, 183-186.

(119) Cazes, B.; Julia, S. *Synth. Commun.* **1977**, *7*, 113-117.

(120) Cazes, B.; Julia, S. *Synth. Commun.* **1977**, *7*, 273-281.

(121) Cazes, B.; Julia, S. *Bull. Soc. Chim. Fr.* **1977**, 931-935.

(122) Dermer, O. C. *Chem. Rev.* **1934**, *14*, 385-430.

(123) Feuer, H.; Hooz, J.; The Chemistry of the Ether Linkage: Methods of formation of the ether linkage. In *The Chemistry of Functional Groups*; Patai, S.; Wiley: New York, 1967, 445-498.

(124) Patai, S. Editor. In *Chemistry of the Hydroxyl Group*; Patai, S.; Wiley: New York, 1971, 454.

(125) McIntosh, J. M. *Can. J. Chem.* **1977**, *55*, 4200-4205.

(126) Cazes, B.; Julia, S. *Synth. Commun.* **1977**, *7*, 113-117.

(127) Cazes, B.; Julia, S. *Synth. Commun.* **1977**, *7*, 273-281.

(128) Iwanami, K.; Oriyama, T. *Chem. Lett.* **2004**, *33*, 1324-1325.

(129) Mantilli, L.; Gerard, D.; Torche, S.; Besnard, C.; Mazet, C. *Angew. Chem. Int. Ed.* **2009**, *48*, 5143-5147.

(130) Tsunoda, T.; Suzuki, M.; Noyori, R. *Tetrahedron Lett.* **1980**, *21*, 1357-1358.

(131) Utimoto, K.; Wakabayashi, Y.; Shishiyama, Y.; Inoue, M.; Nozaki, H. *Tetrahedron Lett.* **1981**, *22*, 4279-4280.

(132) For synthesis of diazo precursor see: Breslow, R.; Yuan, C. *J. Am. Chem. Soc.* **1958**, *80*, 5991-5994.

(133) For reactivity of diazo compounds see: Davies, H. M. L.; Antoulinakis, E. G. *Org. React.* **2001**, *57*, 1-326.

(134) Enantiomeric ratio was determined by chiral stationary phase supercritical fluid chromatography (CSP-SFC) on a Chiralpak OJ column. Retention times, 3.1 mins. (major), 4.3 mins. (minor).

(135) Takahashi, O.; Saka, T.; Mikami, K.; Nakai, T. *Chem. Lett.* **1986**, 1599-1602.

(136) Mikami, K.; Takahashi, O.; Tabei, T.; Nakai, T. *Tetrahedron Lett.* **1986**, *27*, 4511-4514.

(137) Starks, C. M.; Liotta, C. L.; Halpern, M. "Phase-Transfer Catalysis Reaction with Strong Bases," In *Phase Transfer Catalysis Fundamentals, Applications, and Industrial Perspectives*, Chapman & Hall, New York, 1994, p 383-451.

(138) Parker, A. *Chem. Rev.* **1969**, *69*, 1.

(139) Yang, H.-M.; Wu, H.-S. *Catal. Rev.* **2003**, *45*, 463-540.

(140) Brändström, A. "Principles of Phase-Transfer Catalysis by Quaternary Ammonium Salts." In *Advances in Physical Organic Chemistry*, Academic Press, London, 1977, 267-330.

(141) Landini, D.; Maia, A.; Montanari, F. *J. Chem. Soc. Chem. Commun.* **1977**, 112-113.

(142) Mąkosza, M.; Białecka, E. *Tetrahedron Lett.* **1977**, *18*, 183-186.

(143) Solaro, R.; D'Antone, S.; Chiellini, E. *J. Org. Chem.* **1980**, *45*, 4179-4183.

(144) Rabinowitz, M.; Cohen, Y.; Halpern, M. *Angew. Chem. Int. Ed.* **1986**, *25*, 960-970.

(145) Mason, D.; Magdassi, S.; Sasson, Y. *J. Org. Chem.* **1990**, *55*, 2714-2717.

(146) Sawarkar, C. S.; Juvekar, V. A. *Ind. Eng. Chem. Res.* **1996**, *35*, 2581-2589.

(147) Yang, H.-M.; Wu, H.-S. *Catal. Rev.* **2003**, *45*, 463-540.

(148) Yadav, G. D.; Desai, N. M. *Org. Proc. Res. Dev.* **2005**, *9*, 749-756.

(149) Alan, J. R. "Formation of C-O Bonds." In *Quaternary Ammonium Salts: Their Use in Phase-Transfer Catalyzed Reactions*, Academic Press, San Diego, 2001, 69-118.

(150) McKillop, A.; Fiaud, J. C.; Hug, R. P. *Tetrahedron* **1974**, *30*, 1379-1382.

(151) Wang, M.-L.; Yang, H.-M. *Ind. Eng. Chem. Res.* **1990**, *29*, 522-526.

(152) Wang, M.-L.; Yang, H.-M. *Chem. Eng. Sci.* **1991**, *46*, 619-627.

(153) *Synthetic and Natural Phenols,* Tyman, J. H. P., Ed.; Elsevier, Amsterdam, 1996; Vol. 52.

(154) Bordwell, F. G.; McCallum, R. J.; Olmstead, W. N. *J. Org. Chem*. **1984**, *49*, 1424-1427.

(155) Hammet, L. P. *Physical Organic Chemistry: Reaction Rates, Equilibria, and Mechanisms*, McGraw-Hill, New York, 1970.

(156) Taft, R. W. Chapter 13. In *Steric Effects in Organic Chemistry*, Newman, M. S., Ed., Wiley, New York, 1956.

(157) Hine, J. S. *The Structural Effects on Equilibria in Organic Chemistry*, Wiley, New York, 1975.

(158) Ugelstad, J.; Ellingsen, T.; Berge, A. *Acta. Chim. Scand.* **1966**, 1593-1598.

(159) Conway, B. E.; Verrall, R. E.; Desnoyers, J. E. *Trans. Faraday Soc.* **1966**, *62*, 2738-2748.

(160) Pauling, L. *The Nature of the Chemical Bond and the Structure of Molecules and Crystals; an Introduction to Modern Stuctural Chemistry*, 3rd Ed., Cornell University Press, Ithaca, NY, 1960.

(161) Starks, C. M.; Liotta, C. L.; Halpern, M, Phase-Transfer Catalysis: Fundamentals II. In *Phase Transfer Catalysis Fundamentals, Applications, and Industrial Perspectives*, Chapman & Hall, New York, 1994, p 85.

(162) Minot, C.; Trong, N. A. *Tetrahedron Lett.* **1975**, *18*, 3905-3908.

(163) Landini, D.; Maia, A.; Montanari, F. *J. Am. Chem. Soc.* **1978**, *100*, 2796-2801.

(164) Landini, D.; Maia, A. *Gazz. Chim. Ital.* **1993**, *123*, 19-24.

(165) Maia, A. *Pure & Appl. Chem.* **1995**, *67*, 697-702.

(166) Herriott, A. W.; Picker, D. *J. Am. Chem. Soc.* **1975**, *97*, 2345-2349.

(167) Landini, D.; Maia, A. *J. Mol. Catal. A* **2003**, *204-205*, 235-243.

(168) Nielsen, M. F.; Hammerich, O. *Acta Chem. Scand.* **1989**, *43*, 269-274.

(169) Goddard, R.; Herzog, H. M.; Reetz, M. T. *Tetrahedron* **2002**, *58*, 7847-7850.

(170) Generated from Cambridge Structural Database (CCDC-184571) with Mercury™ software, version 2.4.6.

(171) Landini, D.; Maia, A.; Rampoldi, A. *J. Org. Chem.* **1986**, *51*, 3187-3191.

(172) Pochapsky, T. C.; Stone, P. C. *J. Am. Chem. Soc.* **1990**, *112*, 6714-6715.

(173) Pochapsky, T. C.; Stone, P. C.; Pochapsky, S. S. *J. Am. Chem. Soc.* **1991**, *113*, 1460-1462.

(174) Gould, N. D., An Investigation of Phase Transfer Catalysis Employing Quantitative Structure-Activity Relationships, Ph. D. Thesis, University of Illinois at Urbana-Champaign, IL, 2011.

(175) Harlow, G. A.; Noble, C. M.; Wild, G. E. A. *Anal. Chem*. **1956**, *28*, 787-791.

(176) Abrams, I. M.; Millar, J. R. *React Funct. Polymers*. **1997**, *35*, 7-22.

(177) For titration data, see the Experimental Section.

(178) The solubility of DIPK in H2O at 20 °C is 45.5 mM
Section 5: Aqueous Solubility and Henry's Law Constants of Organic Compounds. CRC *Handbook of Chemistry and Physics*. Ed. 92, 2011-2012.

(179) For sodium and potassium homo-hydrogen bonded phenoxide complex synthesis, see the Experimental Section.

(180) For the homogeneous alkylation rates, see the Experimental Section.

(181) The background alkylation rate was found to be $2.99*10^{-8}$ $mol*L^{-1}*s^{-1}$.

(182) The effective phenoxide concentration of the TLP was calculated at 1620 mM, the starting aqueous phase concentration was 759 mM.

(183) Dehmlow, E. V.; Dehmlow, S. S. *Phase Transfer Catalysis*, 2nd Ed., Verlag Chemie, Weinheim, 1983, p. 13.

(184) Nelson, K. V.; Benjamin, I. *J. Phys. Chem. C* **2011**, *115*, 2290-2296.

(185) Dehmlow, E. V.; Thieser, R.; Sasson, Y.; Pross, E. *Tetrahedron* **1985**, *41*, 2927-2932.

(186) Zerda, J.; Sasson, Y. *J. Chem. Soc. Perkin Trans. II* **1987**, 1147-1151.

(187) Sawada, K.; Sohara, T. *J. Chem. Soc. Faraday Trans.* **1995**, *91*, 643-647.

(188) Sawada, K.; Takahashi, E.; Horie, T.; Satoh, K. *Monatsh. Chem.* **2001**, *132*, 1439-1450.

(189) Odashima, K.; Ito, T.; Tohda, K.; Umezawa, Y. *Chem. Pharm. Bull.* **1998**, *46*, 1248-1253.

(190) Wang, D.-H.; Weng, H.-S. *Chem. Eng. Sci.* **1988**, *43*, 2019-2024.

(191) Mason, D.; Magdassi, S.; Sasson, Y. *J. Org. Chem.* **1991**, *56*, 7229-7232.

(192) Wang, D.-H.; Weng, H.-S. *Chem. Eng. Sci.* **1995**, *50*, 3477-3486.

(193) Mąkosza, M.; Kryłowa, I. *Tetrahedron* **1999**, *55*, 6395-6402.

(194) Langhals, H.; Saulich, S. *Chem. Eur. J.* **2002**, *8*, 5630-5643.

(195) Dixon, E. A.; Fischer, A.; Robinson, F. P. *Can. J. Chem*. **1981**, *59*, 2629-2641.

(196) Pickard, P. L.; Tolbert, T. L. *Org. Syn. Coll,* **1973**, *5*, 520.

(197) Dutton, P. L.; Lichtenstein, B. R.; Cerda, J. F.; Koder, R. L. *Chem. Comm.* **2009**, 168-170.

(198) Lee, I.; Oh, H. K.; Ha, J. S.; Sung, D. D. *J. Org. Chem.* **2004**, *69*, 8219-8223.

(199) Zhang, R.; Kang, K.-D.; Shan, G.; Hammock, B. D. *Tetrahedron Lett.* **2003**, *44*, 4331-4334.

(200) Iwanami, K.; Oriyama, T. *Chem. Lett.* **2004**, *33*, 1324-1325.

(201) Mantilli, L.; Gérard, D.; Torche, S.; Besnard, C.; Mazet, C. *Angew. Chem. Int. Ed.* **2009**, *48*, 5143-5147.

(202) This procedure was later improved and it was found that refluxing for 1 h with 1.2 equivalents of *n*-BuLi and triethylphosphonoacetate afforded the same ratio of **20**:**21** but with no trace acetophenone.